

**TOPICS IN
STEREOCHEMISTRY**

VOLUME 9

A WILEY-INTERSCIENCE SERIES

ADVISORY BOARD

STEPHEN J. ANGYAL, *University of New South Wales, Sydney, Australia*

JOHN C. BAILAR, Jr., *University of Illinois, Urbana, Illinois*

GIANCARLO BERTI, *University of Pisa, Pisa, Italy*

DAVID GINSBURG, *Technion, Israel Institute of Technology, Haifa, Israel*

WILLIAM KLYNE, *Westfield College, University of London, London, England*

KURT MISLOW, *Princeton University, Princeton, New Jersey*

SAN-ICHIRO MIZUSHIMA, *Japan Academy, Tokyo, Japan*

GUY OURISSON, *University of Strasbourg, Strasbourg, France*

VLADIMIR PRELOG, *Eidgenössische Technische Hochschule, Zurich,
Switzerland*

HANS WYNBERG, *University of Groningen, Groningen, The Netherlands*

TOPICS IN
STEREOCHEMISTRY

EDITORS

NORMAN L. ALLINGER

*Professor of Chemistry
University of Georgia
Athens, Georgia*

ERNEST L. ELIEL

*Professor of Chemistry
University of North Carolina
Chapel Hill, North Carolina*

VOLUME 9

AN INTERSCIENCE® PUBLICATION

JOHN WILEY & SONS

New York • London • Sydney • Toronto

An Interscience © Publication

Copyright © 1976, by John Wiley & Sons, Inc.

All rights reserved. Published simultaneously in Canada.

No part of this book may be reproduced by any means, nor transmitted, nor translated into a machine language without the written permission of the publisher.

Library of Congress Catalog Card Number: 67-43943

ISBN 0-471-02472-4

Printed in the United States of America.

10 9 8 7 6 5 4 3 2 1

To the 1975 Nobel Laureates in Chemistry

John W. Cornforth

and

Vladimir Prelog

INTRODUCTION TO THE SERIES

During the last decade several texts in the areas of stereochemistry and conformational analysis have been published, including *Stereochemistry of Carbon Compounds* (Eliel, McGraw-Hill, 1962) and *Conformational Analysis* (Eliel, Allinger, Angyal, and Morrison, Interscience, 1965). While the writing of these books was stimulated by the high level of research activity in the area of stereochemistry, it has, in turn, spurred further activity. As a result, many of the details found in these texts are already inadequate or out of date, although the student of stereochemistry and conformational analysis may still learn the basic concepts of the subject from them.

For both human and economic reasons, standard textbooks can be revised only at infrequent intervals. Yet the spate of periodical publications in the field of stereochemistry is such that it is an almost hopeless task for anyone to update himself by reading all the original literature. The present series is designed to bridge the resulting gap.

If that were its only purpose, this series would have been called "Advances (or "Recent Advances") in Stereochemistry." It must be remembered, however, that the above-mentioned texts were themselves not treatises and did not aim at an exhaustive treatment of the field. Thus the present series has a second purpose, namely to deal in greater detail with some of the topics summarized in the standard texts. It is for this reason that we have selected the title *Topics in Stereochemistry*.

The series is intended for the advanced student, the teacher, and the active researcher. A background of the basic knowledge in the field of stereochemistry is assumed. Each chapter is written by an expert in the field and, hopefully, covers its subject in depth. We have tried to choose topics of fundamental import aimed primarily at an audience of organic chemists but involved frequently with fundamental principles of physical chemistry and molecular physics, and dealing also with certain stereochemical aspects of inorganic chemistry and biochemistry.

It is our intention to bring out future volumes at intervals of one to two years. The Editors will welcome suggestions as to suitable topics.

We are fortunate in having been able to secure the help of an international board of Editorial Advisors who have been of great assistance by suggesting topics and authors for several articles and by helping us avoid duplication of

topics appearing in other, related monograph series. We are grateful to the Editorial Advisors for this assistance, but the Editors and Authors alone must assume the responsibility for any shortcomings of *Topics in Stereochemistry*.

N. L. Allinger
E. L. Eliel

February 1976

PREFACE

Volume IX of *Topics in Stereochemistry* begins with a chapter, written as a postscript to the 1974 Le Bel-van't Hoff centennial, entitled "The Foundations of Classical Stereochemistry." In it, S. F. Mason gives a brief history of chemical thinking leading to the famous work by van't Hoff and Le Bel as well as Werner.

When *Conformational Analysis* was published in 1965, it was possible to discuss the relationship between mass spectrometry and the stereochemistry of organic molecules in one paragraph. It was suggested then that "mass spectrometry may be of very considerable future use in conformational analysis." The second chapter, by Mark M. Green, outlines some of that "future use" which has, in fact, taken place in the intervening ten years. There is no question now but that a number of kinds of stereochemical problems are susceptible to attack by means of mass spectrometry.

The single experimental technique which has contributed the most to stereochemical knowledge in the last 15 years or so has, without question, been nmr spectroscopy. Not only are the number and types of systems studied constantly being increased, but also the development of new and expanded nmr techniques for such studies continues unabated. In Chapter 3, Otmar Hofer discusses the "Lanthanide Induced Shift Technique in Conformational Analysis." This is a technique which has given a whole new dimension to proton magnetic resonance through the spreading out of the chemical shift range available. In addition, it appears to have a very powerful quantitative potential for the determination of structure in solution. One might well ask if this technique can play the role for structural chemistry in solution that X-ray crystallography has played in the crystalline state.

Macrocyclic rings have long presented an intriguing puzzle to the stereochemist. The variety of conformations available to rings containing more than six members, and the pathways by which one conformation is converted to another, form the subject matter for the chapter by Johannes Dale. Although the situation in medium and large rings is complex, the conformational transformations can be broken down into stepwise changes that are reasonable and understandable. Nmr has been the key experimental tool in this area.

The final chapter is concerned with the crystal structures of steroids. With X-ray data becoming easily and abundantly available, they play an increasingly important role in the understanding of stereochemistry. There are now some 150 X-ray structures of steroids known; here, W. L. Duax presents a detailed

and systematic summary of this large body of information. Interpretation of how the variation in structural parameters is related to the overall nature of a number of steroid molecules becomes possible as a result of such systematization.

The editors are delighted that the second Nobel Prize in chemistry during the span of existence of this series has been awarded for work centered on stereochemistry, and we respectfully dedicate this volume to J. W. Cornforth and V. Prelog, the 1975 Nobel Laureates in chemistry.

NORMAN L. ALLINGER
ERNEST L. ELIEL

*January 1976
Athens, Georgia
Chapel Hill, North Carolina*

CONTENTS

THE FOUNDATIONS OF CLASSICAL STEREOCHEMISTRY

*by Stephen F. Mason, Chemistry Department, King's College,
London, England* 1

MASS SPECTROMETRY AND THE STEREOCHEMISTRY OF ORGANIC MOLECULES

*by Mark M. Green, Department of Chemistry, Michigan State
University, East Lansing, Michigan.* 35

THE LANTHANIDE INDUCED SHIFT TECHNIQUE: APPLICATIONS IN CONFORMATIONAL ANALYSIS

*by Otmar Hofer, Lehrkanzel für Organische Chemie der Universität
Wien, Vienna, Austria* 111

MULTISTEP CONFORMATIONAL INTERCONVERSION MECHANISMS

*by Johannes Dale, Kjemisk Institutt, Universitetet i Oslo,
Oslo, Norway* 199

CRYSTAL STRUCTURES OF STERIODS

*by W. L. Duax, C. M. Weeks, and D. C. Rohrer, Molecular
Biophysics Department, Medical Foundation of Buffalo Research
Laboratories, Buffalo, New York.* 271

SUBJECT INDEX 385

CUMULATION INDEX, VOLUMES 1-9 397

**TOPICS IN
STEREOCHEMISTRY**

VOLUME 9

A WILEY-INTERSCIENCE SERIES

THE FOUNDATIONS OF CLASSICAL STEREOCHEMISTRY

STEPHEN F. MASON

*Chemistry Department,
King's College, London, U.K.*

I.	Introduction	1
II.	Inorganic Principles and Procedures	2
III.	Organic Radicals	7
IV.	Type Theory	10
V.	Structural Theory	16
VI.	Molecular Dissymmetry	21
VII.	Chemistry in Space	24
VIII.	Conclusion	27

I. INTRODUCTION

According to the providential view of history, in which events are the outcome of 'the contingent and the unforeseen' (1), the progress of science depends upon the casual chance of genius which appears adventitiously, like Gargantua from Gargamelle's ear (2), to solve the problems of each period. As the historical heirs of the alchemists, who saw all-pervasive analogies between the macrocosm and the microcosm (3), chemists well appreciate the ubiquity of a macroscopic, as well as the microscopic, uncertainty principle, but nonetheless know from experience that some scientific innovations are 'in the air,' and that their discovery in broad outline, if not in detail, is attended by a near-certain inevitability, while other innovations are doomed to delay and even frustration by the principle of unripe time (4).

Historically the innovations that are 'in the air' are often characterized by multiple discovery and by wide acceptance from the outset or after only minor delays. Both of the main stages in the development of classical stereochemistry are characterized by these criteria. The work of van't Hoff and Le Bel, whose seminal papers appeared 100 years ago, was independent and simultaneous, as was that of Kekulé and Scott Couper in 1858 (5). Both van't Hoff and Kekulé had a keen appreciation of ripe and unripe time. Referring to his 1858 work,

Kekule observed in 1890 (6), "As a young Privatdozent at Heidelberg I put these ideas down on paper and showed this work to two of my closest friends. Both of them shook their heads doubtfully. I thought that either my theory was not yet ripe, or the time not yet ripe for it, and put my manuscript away in a drawer." For his Utrecht doctorate van't Hoff submitted in 1874 a straightforward exercise in normal science (7), "a routine dissertation on cyanacetic and malonic acids" (8), and wisely withheld his theoretical pamphlet on chemistry in space. His younger contemporary, Arrhenius, was less fortunate and, floating the idea of the incomplete dissociation of electrolytes in his Uppsala doctoral dissertation, he was awarded a fourth class Ph.D. in 1884. But for the then-commanding influence of Ostwald, Arrhenius would have been precluded from an academic career (9).

Where patronage is absent a notable innovation due to an isolated worker may appear so egregious that it remains ineffective for an extended period and even may await rediscovery, like the *berthollides* and the concept of mass action of Claude Berthollet (1748-1822). Avogadro's hypothesis (1811), which underpinned the atomic valencies and molecular weights required for the structural theory of the 1860s, was largely neglected for half a century. Similarly, Pasteur's concept of molecular dissymmetry, based on his work with the tartrates (1848-1860), made only a minor contribution in 1874 to the stereochemical theory of van't Hoff, although it influenced Le Bel more profoundly.

Towards the end of the nineteenth century, when organic stereochemical theory was well established, the earlier work of Pasteur became more generally known and appreciated. From that time dates the hagiographical tradition that Pasteur was the 'founder of stereochemistry,' as Crum Brown put it in 1897 (10) and Robert Robinson (1886-1975), on the occasion of the van't Hoff - Le Bel centenary, in 1974 (11). Pasteur might have been the founder of stereochemistry had he continued to work in the chemical field after 1860 and to support one or more of the main thrusts of chemical thinking. But he did not as, among other things, the following reconstruction of the development of classical stereochemistry endeavours to show.

II. INORGANIC PRINCIPLES AND PROCEDURES

In its early formative period each branch of the chemical sciences has experienced the domination of an inaugural mandarin who gives the subject an identity and an autonomy by bringing together, and intergrating to a degree, previously separated, or only loosely associated, principles and practices. Jöns Jacob Berzelius (1779-1848) endeavored to lay down the form and organize the content of mineral chemistry for some 40 years

through the six volumes of his Handbook, published from 1808, by way of his students, and above all through his annual reports on the progress of chemistry and mineralogy (1822-1848), in which he described and commented upon, favorably or otherwise, the chemical studies of the past year. The inaugurating pontiffs of organic and of physical chemistry, Justus Liebig (1803-1873) and Wilhelm Ostwald (1853-1923), respectively, exercised a similar, though lesser, command over their individual fields, again by way of their students and control of a periodical publication, Liebig through his *Annalen* from 1832 and Ostwald through the *Zeitschrift für physikalische Chemie* from its foundation in 1887.

The influence of Liebig and, more particularly, that of Ostwald was inevitably less substantial than that of Berzelius on account of the sheer growth and proliferation of chemical science over the years that separated their respective ascendancies. Liebig never completely assimilated the organic chemistry of his French contemporaries, and he turned increasingly to agricultural and physiological chemistry from about 1840. Ostwald similarly failed to come to terms with developments in statistical mechanics and, founding his *Annalen der Naturphilosophie* in 1901, turned to the consolations of philosophy. Of the three inaugural mandarins only Berzelius remained steadfastly a chemist to the end of his days, attempting in his later years to assimilate the new developments in organic chemistry into the inorganic model he had constructed in his youth and prime.

Berzelius based his conception of a research program for the chemical sciences on the developments in pneumatic chemistry, mineral analysis, and electrolysis, which culminated in the new gas laws, stoichiometry, electrochemical concepts, and Daltonian atomic theory of the first decade of the nineteenth century. The field of chemical studies was defined by the law of constant proportions. Berthollet lost the extended dispute of 1800-1808 with Joseph Proust (1754-1826) on the question of constancy of composition, and the *berthollide* substances were banished from chemical science for the following century. Only the *daltonides* with constant composition were recognized as distinct compounds whose elementary composition and interconversions were eligible for chemical investigation.

Initially doubts were expressed whether any organic materials lay within the province of chemistry, but in 1814 Berzelius showed by combustion analysis that a number of simple organic substances satisfied the demarcation criterion of constant elementary proportions (12). A sharp distinction was drawn, however, between *organic* substances, which satisfied the criterion, and *organized* matter, like the proteins, glutens, and gums, which apparently did not (13). The organic substances admitted to the chemical fold exemplified to a more marked and varied degree than inorganic compounds the law of multiple proportions proposed by John Dalton (1766-1828) in 1804. Multi-

ple proportions gave Dalton's atomic theory of 1808 its rationale, and the compounds exemplifying the law raised for the first time the problem of molecular structure. Dalton himself drew schematic structural formulae of the simple hydrides and oxides (14) and even of such complex substances as albumen and gelatin which he depicted as isomers of C_2H_2NO (15) (Fig. 1). For some 30 years Dalton employed ball-and-pin atomic models for teaching purposes (15). However, these formulae and models led to no new practicable expectations during Dalton's lifetime, and many workers preferred to use equivalents rather than atomic weights in the 1820-1860 period.

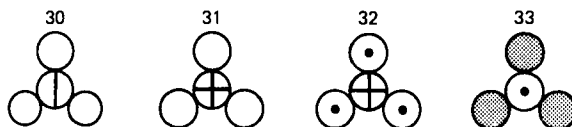
Binary



Ternary



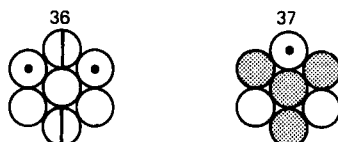
Quaternary



Quinquenary and Sertenary



Septenary



21. An atom of water or steam, composed of 1 of oxygen and 1 of hydrogen retained in physical contact by a strong affinity, and supposed to be surrounded by a common atmos-

phere of heat; its relative weight=	8
22. An atom of ammonia, composed of 1 of azote and 1 of hydrogen	6
23. An atom of nitrous gas, composed of 1 of azote and 1 of oxygen	12
24. An atom of olefiant gas, composed of 1 of carbone and 1 of hydrogen	6
25. An atom of carbonic oxide composed of 1 of carbone and 1 of oxygen	12
26. An atom of nitrous oxide, 2 azote + 1 oxygen	17
27. An atom of nitric acid, 1 azote + 2 oxygen	19
28. An atom of carbonic acid, 1 carbone + 2 oxygen	19
29. An atom of carburetted hydrogen, 1 carbone + 2 hydrogen	7
30. An atom of oxynitric acid, 1 azote + 3 oxygen	26
31. An atom of sulphuric acid, 1 sulphur + 3 oxygen	34
32. An atom of sulphuretted hydrogen, 1 sulphur + 3 hydrogen	16
33. An atom of alcohol, 3 carbone + 1 hydrogen	16
34. An atom of nitrous acid, 1 nitric acid + 1 nitrous gas	31
35. An atom of acetous acid, 2 carbone + 2 water	26
36. An atom of nitrate of ammonia, 1 nitric acid + 1 ammonia + 1 water	33
37. An atom of sugar, 1 alcohol + 1 carbonic acid	35

Fig. 1. The formulation of molecular structure by John Dalton, *A New System of Chemical Philosophy*, (1808).

William Wollaston (1766-1828) was initially an enthusiastic supporter of Dalton's atomic theory, and in 1808 he accounted in structural terms for the multiple proportions he had found in the oxalate, binoxalate, and quadroxalate of potash, proposing that the second and the third of these were made up, respectively, of a symmetrical linear and tetrahedral array of oxalate around the potash (16). The corresponding trisoxalate, he felt, could not exist, owing to an inherent instability of an equatorial triangle of oxalates around the potash without polar groups to sustain the structure (16). By 1814 Wollaston had become disenchanted with the atomic theory on the ground that there appeared to be no criterion for distinguishing the multiple proportion of AB and AB₂ from that of A₂B and AB (17).

Reverting to the use of chemical equivalents, Wollaston introduced a chemical slide rule with a logarithmic scale of equivalent weights based on $O = 10$. The chemical slide rule was much in vogue for the following 30 years or so, although neither Wollaston nor the users of the rule appear to have appreciated that both equivalent and atomic weights were circumscribed by the same ambiguity. It was felt that there should be a unique equivalent for each element, and even Dumas wondered which of the two possible values he should take as the equivalent of copper (18).

A resolution of the multiple-proportion ambiguity had been available from 1811 in the hypothesis of Amedeo Avogadro (1776-1856), deduced from the law of combining volumes discovered in 1808 by Gay-Lussac (1778-1850) in the light of Dalton's atomic theory (19). The hypothesis required the known elementary gases to be diatomic, and homoatomic molecules were forbidden species in the Daltonian and Berzelian theory. Newton had accounted for Boyle's law in terms of an R^{-1} force law of repulsion between stationary particles in a gas. The repulsive force between gas particles was identified with Lavoisier's imponderable material of heat, the element caloric, by Gay-Lussac and Dalton, who independently rediscovered Charles' law in 1801. The expansion of gases on heating was due to the augmentation of the envelope of caloric surrounding each gaseous atom. However, the repulsive forces obtained only between the atoms of the same elementary species for, as Dalton's law of partial pressures (1801) showed, each gas was effectively a vacuum to every other gas. Heteroatomic molecules were allowed species, for there could be no repulsive forces between different elementary atoms, but homoatomic molecules were forbidden, and Avogadro's hypothesis could not be sustained.

The same conclusion emerged from the electrochemical theory of chemical combination based on the electrolytic decomposition of the alkalis and alkaline earths (1807-1808) by Humphry Davy (1778-1829). Davy and Berzelius saw chemical combination as the converse of electrolysis. The electrical charges that atoms lost on combination were restored in the electrolytic process. The atoms of each elementary species were charged in a dipolar sense with both positive and negative electricity to varying degrees; except for the most electronegative element, oxygen, the atoms of which were wholly negatively charged. From oxygen the electrochemical series stretched through the halogens and the other nonmetals to first the noble and then the base metals, the series terminating with the most electropositive element, potassium, in which the polarity was substantially biased with positive charge. Owing to the dipolar character of the atomic charge, each element might combine with a more electronegative or a more electropositive member of the series, giving a compound with a net electronegative or net

electropositive character, respectively, and such binary, but not necessarily diatomic, compounds of the elements underwent further charge-mediated dualistic combinations, as in salt formation from an acid and a base, and then the combination of the salt with water to form the salt-hydrate. In the Berzelian theory electrical charge took over the role played by caloric in Dalton's scheme, and the former had the advantage of providing an attractive force for heteroatomic combinations, but like the latter it regarded homoatomic molecules as forbidden species, owing to the electrical repulsion between like atoms.

Although Berzelius rejected Avogadro's hypothesis, he accepted the more restricted 1808 view of Gay-Lussac that the same volumes of the elementary gases at a given temperature and pressure contain the same number of atoms. On this basis Berzelius formulated such molecules as water and ammonia in modern terms, whereas the chemists who reverted to equivalent weights generally regarded these compounds as diatomic. To Gay-Lussac's hypothesis, Berzelius added in 1819 the law of isomorphism, due to Eilhard Mitscherlich (1794-1863), and made some use of the atomic heat rule proposed in 1819 by Pierre Dulong (1785-1838) and Alexis Petit (1791-1820). With these guides Berzelius was able to obtain by 1826 a set of atomic weights that are close to modern values, with the notable exceptions of silver and the alkali metals, where the oxides were formulated as diatomic, contrary to the indications of the atomic heat rule.

III. ORGANIC RADICALS

Appointed at the age of 21 as assistant professor at Giessen in 1824 and full professor in the following year, Liebig saw mineral chemistry as a near-perfected system of theoretical principles and practical procedures with the authenticated organic substances as a minor but promising addendum. His perception was partly shared by Berzelius and by Jean Baptiste Dumas (1800-1884), although their interests in different ways were wider. Liebig's single-minded devotion to the organic substances led him to develop simple and reliable methods of combustion analysis and for the isolation, degradation, and synthesis of new compounds. His near-messianic teaching and publicity for his chosen field attracted a remarkable number of doctoral students, as many as 65 being registered with Liebig in 1843 (20).

In the realm of theory Liebig remained largely within the conceptual framework prescribed by Berzelius, as did Dumas until the late 1830s. In 1837 Liebig and Dumas published a joint paper (21) in which they affirmed organic chemistry to be the chemistry of complex radicals, inorganic chemistry that of simple

radicals, the elements: "otherwise the laws of combination, the laws governing reactions are the same in the two branches of the science." The work of Liebig with Friedrich Wöhler (1800-1882) on benzoyl derivatives appeared to be paradigmatic of this view, and Berzelius added the congratulatory note that the work marked the "dawning of a new day in vegetable chemistry" at the end of their paper (22). In the chloride, amide, and acid the benzoyl group seemed to play the same role as hydrogen or other electropositive elements, but, unlike the latter, it could not be isolated.

The challenge was apparently met by Robert Bunsen (1811-1899) who, in his work on the cacodyl derivatives 1837-1843 (23), isolated tetramethyl diarsine, $(\text{CH}_3)_2\text{AsAs}(\text{CH}_3)_2$, which he and most of the German chemists, together with Berzelius, regarded as the cacodyl radical, $(\text{CH}_3)_2\text{As}$. As with homoatomic elementary molecules, the dimers of organic radicals were forbidden species on polarity grounds. Describing the work in his annual report for 1845 Berzelius wrote; "The research is a foundation stone of the theory of compound radicals of which Cacodyl is the only one whose properties correspond in every particular with those of the simple radicals" (24).

In the last year of Berzelius' life two general routes to the apparent radicals were discovered in Bunsen's Marburg laboratory, one by Hermann Kolbe (1818-1884) and the other by Edward Frankland (1825-1899), whom Kolbe had met while working with Playfair in London during 1845. Kolbe, a pupil of Wöhler, applied the electrochemical procedure of Wöhler's teacher, Berzelius, to the organic acids and their salts, obtaining thereby a range of what he took to be organic radicals (25). Frankland, by heating alkyl halides with zinc in a sealed tube, obtained a mixture of gases, which he thought contained the alkyl radical, and a spontaneously inflammable liquid zinc alkyl, which generated more of the supposed radical on treatment with water (26). In his memorial lecture of 1851 Heinrich Rose observed that; "it is to be regretted that Berzelius was not spared to see how many of his hypothetical radicals were actually prepared, and that in so short a time after his death" (27).

Following up his discovery of the zinc alkyls, Frankland investigated the reactions of the organometalloid compounds in detail with the expectation "that the chemical relations of the metal to oxygen, chlorine, sulphur, etc. would remain unchanged" (28). But he found that the 'saturation capacity' of a given metalloid was invariably reduced in the corresponding organo derivative. Arsenic itself has a maximum saturation capacity of five equivalents of oxygen, whereas that of cacodyl was only three (Fig. 2). From this and analogous examples Frankland (28) drew three principal conclusions. Firstly, organic radicals played not only their traditional electropositive role but also assumed an electronegative role in taking the place of

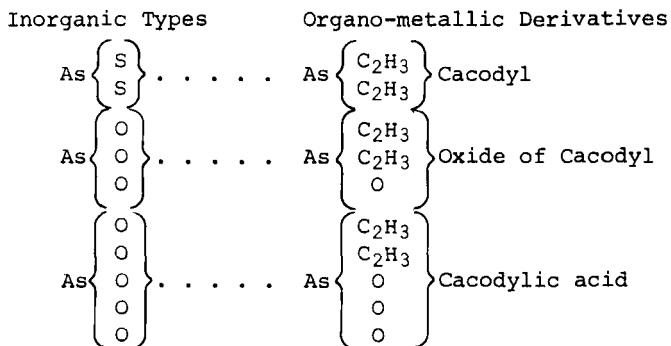


Fig. 2. Frankland's comparison (1852) between the inorganic and organic derivatives of arsenic (O = 8, C = 6).

one or more equivalents of oxygen in an organometallic compound. Secondly, the nitrogen, phosphorus, arsenic, and antimony group of elements form compounds containing three or five equivalents of other elements or radicals, these numbers expressing "the combining power of the attracting element." Thirdly Frankland perceived that; "The formation and examination of the organo-metallic bodies promise to assist in effecting a fusion of the two theories which have so long divided the opinions of the chemists, and which have too hastily been considered irreconcilable; for whilst it is evident that certain types of series of compounds exist, it is equally clear that the nature of the body derived from the original type is essentially dependent upon the electrochemical character of its single atoms, and not merely on the relative position of these atoms" (28).

The two theories to which Frankland referred in his classical paper on valency of 1852 were that of radicals and that of types. These two theories were the ground of much Teutonic-Gallic contention throughout the 1840s and the early 1850s. In the radical theory all chemical combinations were regarded as essentially binary and the characteristics of a compound appeared to derive basically from the properties and powers of the two constituent radicals which might be monatomic, as was often the case in mineral chemistry, or polyatomic, as obtained generally in organic chemistry. The radical theory was rooted in the ancient alchemical tradition that all finite entities were generated by the interaction and union of two opposed but complementary materialized forces. These polarised principles were the Yin and the Yang of the Chinese alchemists and, in the Arabic-European alchemical tradition, they were comprehended as the fiery and active male principle of Sulphur and the more passive but potent female principle of Mercury. While the eighteenth century advances in analytical and pneumatic chemistry attenuated the dominion of binary polarity principles, the

latter were substantially reinforced by subsequent electrochemical discoveries and, in the realm of ideology, by the concurrent rise of the German school of *Naturphilosophie* wherein the alchemical dialectic of the interplay of complementary polarities was generalized into a *Weltanschauung*. Although Berzelius, like Liebig, was much opposed to the philosophical idealism of the *Naturphilosophen*, who poured scorn on the English term "philosophical instruments" for scientific apparatus, he was nonetheless influenced by their concepts in his dualistic theory of chemical combination. A compound, in the dualistic theory, appeared to be invariably the outcome of a binary union between an electropositive and an electronegative radical, simple or complex, and the properties of that compound were a function of the electrochemical characteristics of its two constituents.

IV. TYPE THEORY

The second of the theories to which Frankland referred in 1852, the theory of types, was due largely to the French chemists, Jean Baptiste Dumas (1800-1884), Auguste Laurent (1808-1853), and Charles Gerhardt (1816-1856), the latter two acting as assistants to Dumas in 1831 and 1838 respectively. In contrast to the dualistic radical theory, which was dominant in Germany and Scandinavia until the 1860s, the French theory of types was unitary and morphological, referring the properties of a compound to the overall shape or form of the molecule. The electrochemical nature of the constituent atoms or atomic groupings were regarded as of little or even, in extreme cases, of no consequence for molecular properties in the type theory, the geometric arrangement of the atoms in the molecule being the prime determinant of the characteristics of a compound. While the particular arrangement of the atoms in given molecule was unknown, and might remain inaccessible to purely chemical procedures, a guide was provided through the physical or geometric supposition that the shape of a molecule is reflected in the morphology of the corresponding crystal. Whereas the radical theory had its origins in electrochemistry and the dualistic view of chemical combination, going back from Berzelius to Lavoisier and beyond to the alchemists; the provenance of the type theory lay in crystallography and the ancient microcosm-macrocosm analogy, the theory being augmented by the classificatory schemes designed to accommodate the plethora of organic compounds discovered in the 1820s (29, 30).

The contribution of French scientists to early electrochemistry had not been notable, but with Romé de l'Isle (1736-1790) and, more particularly, René Just Haüy (1743-1822) mineralogy and crystallography passed from a classificatory to an analytical stage. Haüy found that the various morphological

forms of calcium carbonate crystals cleaved to a common rhomboid form, and he supposed that if division were continued down to the ultimate limit the individual molecules of calcium carbonate would be found to have the same rhomboidal shape (31). From the old and enduring theme that analogies mutually obtain between the microscopic and the macroscopic (3), Häuy held that generally the morphology of cleavage crystal units and the forms of the constituent molecules are 'images of each other' (32). Behind the diversity of crystal morphologies there were a limited and small number of irreducible molecular geometries, Häuy thought, based upon the regular polyhedra. These he termed 'primitive forms,' and they were regarded as the nuclei or building blocks of the large number of diverse crystal morphologies, or 'secondary forms,' found in nature.

Mitscherlich's law of isomorphism appeared to support Häuy's view, which served as one of the starting points for the theory of types. As Mitscherlich put it; "The same number of atoms combine in the same manner to produce the same crystalline form; this same crystalline form is independent of the chemical nature of the atoms and is uniquely determined by their relative position" (33). In a critique of the Berzelian dualistic theory, A.E. Baudrimont (1806-1880) argued in 1833 that the principal guide to the number and arrangement of atoms in a molecule was the morphology of the corresponding crystal, since chemical reactions involve the movement of atoms and so can never indicate the disposition of the atoms in a combination. The extraction of a compound from a combination through a reaction does not mean that the compound preexisted in the combination (34).

The second starting point for the theory of types was the study of the halogen substitution reactions of organic compounds (35). From 1833 Dumas and his students investigated the reactions of chlorine with turpentine, alcohol, and acetic acid, finding one equivalent of hydrogen chloride evolved for each equivalent of hydrogen replaced by chlorine in the organic substrate. In these reactions the electropositive element, hydrogen, was replaced by the electronegative element, chlorine, but the product and starting material had similar properties: "chlorinated vinegar is still an acid, like ordinary vinegar; its acid power is not changed" (36). It appeared that chemical properties depended upon the number and type of arrangement of atoms in a molecule rather than the particular electrical character of the atoms, and in 1839 Dumas announced the theory that; "in organic chemistry there exist TYPES which are conserved even when, in place of the hydrogen they contain, equal volumes of chlorine, bromine or iodine are introduced" (36). Chlorine substitution is analogous to isomorphic replacement in crystals, Dumas noted: "in organic chemistry the theory of substitutions plays the same role as isomorphism in inorganic chemistry" (36). In the case of

the isomorphous crystals, KMnO_4 and KClO_4 , for example, electropositive manganese was replaced by electronegative chlorine.

Liebig accepted the replacement of hydrogen by chlorine in organic compounds as empirically established from the outset, but without special theoretical significance. Initially Berzelius held that "an element so eminently electronegative as chlorine can never enter an organic radical; this idea is contrary to the first principles of chemistry" (37). However, when Dumas' assistant Melsens transformed trichloroacetic acid reductively to acetic acid in 1842 (38), Berzelius accepted the analogy between the two acids and reformulated them as binary combinations of an inert 'copula' group and an acidic functional group.

Developing the type theory, Dumas in 1840 hazarded the conjecture that "in an organic compound all the elements can be successively displaced and replaced by others," including the carbon (39). The response of the Berzelian school was immediate, and Wöhler wrote his well-known satirical paper under the pseudonym, 'Swindler,' on the successive chlorination of manganoous acetate to Cl_{24} , which retained all of the properties of the starting material. Written for the private amusement of Berzelius and Liebig, the latter published the paper in his *Annalen*, embellished with a footnote reporting how fashionable garments spun from Cl_{24} had become in London (40).

A further contribution to the development of the theory of types was a partial appreciation of Avogadro's hypothesis in France, where it was generally attributed to Ampère who had proposed a similar hypothesis, published in 1814. Gaudin (1804-1880), a pupil of both Ampère and Dumas, explained in 1833 the apparently anomalous vapor densities of mercury, phosphorus, and sulphur, determined by Dumas in 1826, in terms of monatomic, tetratomic, and hexatomic elementary molecules, respectively, and gave volume diagrams illustrating with Dalton's symbols the combination of the diatomic elementary gases to give HCl , H_2O , and NH_3 in accord with Avogadro's hypothesis (41).

Although little more attention was paid to Gaudin immediately than to Avogadro, the French organic chemists, particularly Laurent and Gerhardt in the later stages of their work, adopted vapor densities as the 'sole guide' for the determination of molecular weights, and, by 1853, the year of Laurent's death, they had a set of atomic weights and organic molecular formulas implicitly based on Avogadro's hypothesis. In contrast Liebig held that "the specific gravity of alcohol vapor cannot be looked upon as any evidence of its constitution... On the contrary, I believe the very circumstance that ether and water vapor unite in equal volumes, and without condensation, is evidence in favor of the view that this compound, alcohol, is a hydrate of ether" (42). As early as 1821 Avogadro had formulated ethyl alcohol as $\text{C}_2\text{H}_6\text{O}$ and diethyl ether as $\text{C}_4\text{H}_{10}\text{O}$ from vapor

density determinations on the basis of his hypothesis (43).

Dumas in 1831 directed Laurent to the study of the chlorination of naphthalene, and in subsequent posts Laurent extended the investigation for a doctorate, which was awarded in 1837. He discovered two general reactions of naphthalene: firstly, substitution, in which a hydrogen atom is replaced by a halogen atom or nitro group with the elimination of a molecule of the hydrohalide or water, and secondly, addition of one or more halogen molecules. The substitution products he found to be relatively inert, whereas the addition products readily eliminated one or more molecules of hydrohalide with alkali to give the corresponding substitution product (44).

Laurent had studied crystallography at the École des Mines, and the substitution reactions of naphthalene and other hydrocarbons not unnaturally appeared to him to be closely analogous to the process of isomorphous replacement, particularly when he found that naphthalene and a number of its substituted derivatives formed isomorphous crystals (45). Pressing the crystallographic analogy even more closely, Laurent took over Häuy's theory of crystal nuclei or 'primitive forms,' supposing that naphthalene and other hydrocarbons had a polyhedral structure with a carbon atom at each apex and a hydrogen atom at each edge. The hydrocarbons were "fundamental nuclei" and substitution reactions gave "derived nuclei" in which the halogen or other substituent not only took the place of the displaced hydrogen but also played the same structural role of sustaining an edge of the polyhedron. In addition reactions the adduct was attached to a face of the polyhedron and remained reactive, playing no structural role. Oxygen in an organic compound is acidic only when it is 'outside the nucleus'; inside it has a structural role and becomes relatively inert (46).

Laurent freely confessed that he had no idea what particular or general polyhedral atomic structure corresponded to any given hydrocarbon; "it is impossible to know this arrangement, but we may nevertheless ascertain whether in any particular body it is the same as in some other body" (47). Thus chlorostrychnine is poisonous, optically active, and isomorphous with strychnine, so that the two compounds must have the same basic structure (48), "although I cannot say.... what the arrangement really is" (49). In contrast to his colleague, Gerhardt, Laurent stood for the view that, while it is impossible to deduce unequivocal structures from reactions, it is possible to deduce discriminatory reactions from two or more hypothetical structures. He assigned a dimeric formula to Bunsen's cacodyl radical, and in 1846 predicted that the "alcohol radical" would similarly be bound to be dimeric "if it is capable of existing" (50). Further, it should be possible to discriminate between the possibility that Bunsen's cacodyl is a simple dimer or a more complex structure produced by a fundamental atomic rearrangement. In the

former case the reaction with chlorine would produce the substitution product, cacodyl chloride, whereas in the latter case chlorine would give an addition product of the new fundamental nucleus (51).

The English translator of Laurent's posthumous *Chemical Method*, William Odling (1829-1921), believed "the generalities of Laurent to be in our day as important as those of Lavoisier were in his" (52), and August Kekulé (1829-1896), breaking away from the profound German distrust of French theory, offered to translate the work into German. In *Chemical Method* Laurent depicted his polyhedral nuclei schematically by polygons, and the page in which benzoyl chloride and ammonia were represented as hexagons (Fig. 3) ["the atoms are arranged so as to form

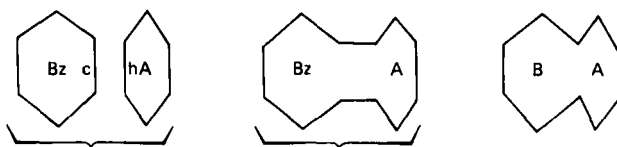


Fig. 3. The representation by Laurent (1853) of the reaction between benzoyl chloride and ammonia to give benzamide, quoted by Kekulé in 1858.

hexagonal figures" (53)] was specifically referred to by Kekulé in his classical paper (54) of 1858.

The early work of Gerhardt was devoted to the classification of organic compounds which, he held, "form an immense scale, whose upper extreme is occupied by brain matter and other more complex substances, while at the lower end we find carbonic acid, water, and ammonia...There is an infinite number of steps between these two extremes" (55). From antiquity biological classification had been dominated by the thematic image of the world as populated by a Great Chain of Being (56) which extended down into the inorganic domain. For Gerhardt organic substances were the missing links in the great chain between the inorganic and the lower forms of life. The scale of organic substances consisted of the homologous series formed by the successive additions of a methylene group to a fundamental residue, producing a constant incremental increase in boiling point and molecular weight. The rank of a substance in the scale was measured by the number of equivalents of carbon in the compound, and from the properties of one homolog those of other members of the series could be predicted (30).

Isomeric substances such as alcohols and ethers were not distinguished in his early scheme, and Gerhardt turned to rational formulas for a differentiation. The molecular formulas currently available for a given compound varied with the basis adopted, the atomic theory, the theory of volumes, or the theory of equivalents, and Gerhardt endeavored to bring these into

coincidence. Most organic molecular weights were taken as four times the relative vapor density, giving the 'four-volume' formulas, which agreed with the analysis of the silver salts of organic acids employing the atomic weight of silver given by Berzelius on the assumption that the oxide is AgO. Gerhardt perceived that a degree of consistency could be achieved by halving the current organic molecular weights to give the 'two volume' formulas and by formulating the oxides of silver and the alkali metals as M_2O . He also halved the atomic weights of other metals by failing to make a consistent use of the atomic heat rule, although this did not affect his organic formulations (57).

With the new set of atomic and molecular weights, Gerhardt reformulated organic molecules in 'two volume' terms and evolved a new classification scheme in 1853 based on four inorganic types, water, ammonia, hydrogen chloride, and hydrogen (58). Gerhardt used the water type in 1843 (57) in formulating the metal oxides as M_2O , and Laurent represented alcohol and ether as water types in 1846 (50), but the first proof of this contention was provided by the ether and, more particularly, the mixed-ether synthesis of Alexander Williamson (1824-1904) in 1851 (59). Gerhardt added the acids and acid anhydrides to the water type with his analogous mixed-anhydride synthesis of 1853 (58). The ammonia type was due to August Hofmann (1818-1892), who reported the synthesis of primary, secondary, and tertiary amines in 1849 (60) following the preparation of primary amines by Adolph Wurtz (1817-1884) earlier in the same year (61).

Gerhardt added the hydrogen chloride and hydrogen types to complete his 'unitary system' or new type theory. All hydrocar-

Type	Ethyl derivative	Benzoyl derivative
$O \begin{Bmatrix} H \\ H \end{Bmatrix}$	$O \begin{Bmatrix} C_2H_5 \\ H \end{Bmatrix}$	$O \begin{Bmatrix} C_7H_5O \\ H \end{Bmatrix}$
water	alcohol	benzoic acid
$\begin{Bmatrix} H \\ Cl \end{Bmatrix}$	$\begin{Bmatrix} C_2H_5 \\ Cl \end{Bmatrix}$	$\begin{Bmatrix} C_7H_5O \\ Cl \end{Bmatrix}$
hydrochloric acid	ethyl chloride	benzoyl chloride
$N \begin{Bmatrix} H \\ H \\ H \end{Bmatrix}$	$N \begin{Bmatrix} C_2H_5 \\ H \\ H \end{Bmatrix}$	$N \begin{Bmatrix} C_7H_5O \\ H \\ H \end{Bmatrix}$
ammonia	ethylamine	benzamide
$\begin{Bmatrix} H \\ H \end{Bmatrix}$	$\begin{Bmatrix} C_2H_5 \\ H \end{Bmatrix}$	$\begin{Bmatrix} C_7H_5O \\ H \end{Bmatrix}$
hydrogen	ethyl hydride	benzaldehyde

Fig. 4. Gerhardt's four types and their derivatives (1853).

bonds were hydrogen types, all halides and pseudohalides were hydrogen chloride types, while the sulfides and selenides were included with the oxygen derivatives in the water type, and the phosphides and arsenides were placed with nitrogen derivatives in the ammonia type (Fig. 4).

Gerhardt ostensibly maintained the positivist view, to which Laurent was opposed, that constitutional organic formulas were merely expressions of chemical reactions, and that there might be as many rational formulas for a given compound as there were distinct types of reaction, none of these formulas having a unique or absolute status. Implicitly, however, Gerhardt adopted the principle of Laurent that reactions may be predicted from a possibly hypothetical structure in synthesizing the mixed acid anhydrides, once these were viewed as water types. Williamson, who had in fact expressly predicted the existence of the acid anhydrides from the water type in 1851, took the realist view that formulas "may be used as an actual image of what we rationally suppose to be the arrangement of constituent atoms in a compound, as an orrery is an image of what we conclude to be the arrangement of our planetary system" (59).

Williamson and other British chemists of the period took a more literal view of chemical formulas than did the French, and implicitly they worked on the procedural assumption that the molecular structure of a compound is not profoundly changed during a reaction, in general. Laurent viewed the relationship between the fundamental and the derived nuclei in the same light, and van't Hoff (62) subsequently defined the procedure as the structural 'principle of inertia' of carbon compounds. Wheland more aptly describes the procedure as the 'principle of minimum structural change' (63).

V. STRUCTURAL THEORY

Although the new type theory was dismissed as 'a French invention' by Wittstein in Munich, Liebig wrote in 1853 to his former student, Gerhardt, that "it is very strange that the two theories, formerly quite opposed, are now combined in one" (64), restating the view expressed more tentatively by Frankland in the previous year from his studies of the organometallic series (28). As yet, however, the radical and the type theories were not wholly united. Liebig's pupil, Kekulé who studied with Gerhardt and others in Paris before working in London during 1854-1855, saw himself in 1890 as the one who had stood at the confluence of the radical and the type streams of chemical progress (6), although the influence of the type theory is the more evident in his early work.

In London Kekulé became acquainted with Williamson and with Odling. The latter added the marsh-gas type to Gerhardt's set in

1855 (65). It was in London too that, on the top of an omnibus, Kekulé experienced the first of his two recorded chemical visions of carbon chains in action (6). The second, which gave him the benzene structure, was revealed in his study at Ghent, to which he moved in 1858 after a brief spell in Heidelberg (6).

Neither Kekulé nor Scott Couper (1831-1892) in their classical papers (5) of 1858 refer to Odling in connection with the marsh-gas type and the tetravalency of carbon, but both added to that basis the crucial hypothesis that carbon "enters into chemical union with itself" (66). Kekulé worked towards a concept of molecular architecture largely within the type theory tradition, holding with Gerhardt that "Rational formulas are reaction formulas and can be nothing else... Every formula, therefore, that expresses certain metamorphoses of a compound is *rational*; among the different rational formulas, however, that one is the *most rational* which simultaneously expresses the largest number of metamorphoses" (54) (Figure 5).

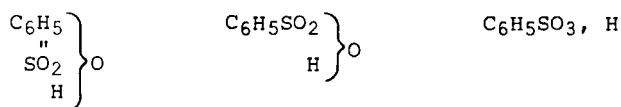


Fig. 5. The three possible rational formulae of benzene sulphononic acid discussed by Kekulé in 1858 (O = 16, C = 12, S = 32).

Kekulé went beyond Gerhardt, however, in affirming that "I regard it as necessary and, in the present state of chemical knowledge, in as many cases as possible, to explain the properties of chemical compounds by going back to the elements themselves which compose these compounds. I no longer regard it as the chief problem of the time, to prove the presence of atomic groups which, on the strength of certain properties, may be regarded as radicals, and in this way to refer compounds to a few types, which can hardly have any significance beyond that of mere pattern formulas" (54).

Couper, with a Scottish common-sense realism more pungent than that of the Englishman, Williamson, felt that the theory of types should be "combated on metaphysical grounds" of general principle, for Gerhardt "is led not to explain bodies according to their composition and inherent properties but to think it necessary to restrict chemical science to the arrangement of bodies according to their decomposition, and to deny the possibility of our comprehending their molecular constitution" (66). While Kekulé continued with the traditional bracketed type-formulas for a period, Couper moved more directly to the formulation of molecular structures (66) (Fig. 6). These were,

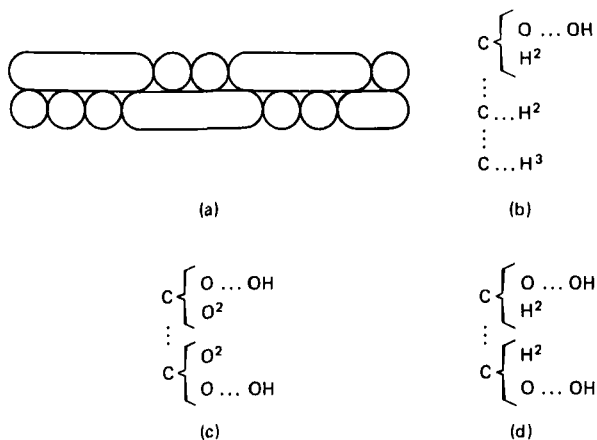


Fig. 6. The graphic formulas of 1-propanol due to (a) Kekulé (1865) and (b) Scott Couper (1858), together with the latter's representation of (c) oxalic acid and (d) glycol, based on O^2 and $O \dots O = 16$, i.e. $O = 8$.

however, relatively uninfluential, owing largely to Couper's breakdown in 1859, following his return to Edinburgh from Paris the previous year. Crum Brown (1838-1922), who depicted molecular structures by graphic formulas in his Edinburgh thesis of 1861 and in subsequent publications (67), may have developed these from Couper's formulations (Fig. 7). Alexander Butlerov

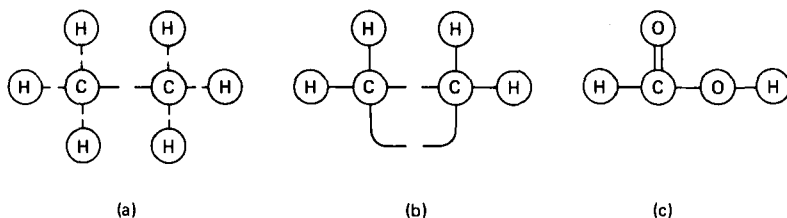


Fig. 7. The 1864 graphic formulae of Crum Brown for (a) ethane, (b) ethylene, and (c) formic acid.

(1828-1886), who worked with Couper under Wurtz in Paris during 1857, referred to both Kekulé and Couper in connection with the tetratomicity of carbon in 1859 (68) and two years later restated the realist position that "only one rational formula is possible for each compound, and when the general laws governing the dependence of chemical properties on chemical structure have been

derived, this formula will express all of these properties" (69).

In the late 1850s chemistry still lacked a generally accepted unambiguous method for the determination of atomic and molecular weights and of atomic valencies. Kekulé and others felt that the problem might be clarified, if not solved, by an international conference on the topics involved, and an organizing committee of 45 well-known chemists issued a general invitation in July, 1860, to a congress in Karlsruhe held in the following September (70). The conference secretary, Wurtz, recorded the names of 127 members of the congress (70). No firm conclusions were reached in Karlsruhe, although Stanislaw Cannizzaro (1826-1910) in his address emphasised the significance of Avogadro's hypothesis and of the work of Gaudin and Avogadro himself based on it. At the end of the meeting, copies of Cannizzaro's *Sketch of a course of Chemical Philosophy* (71) were distributed to the congress members, in which the Avogadro-Cannizzaro method for the determination of atomic and molecular weights was described. The younger chemists in particular found the arguments in the pamphlet convincing. As Lothar Meyer (1830-1895) put it, "It was as though the scales fell from my eyes" (70).

With a general consensus on atomic valencies and molecular weights, organic structural chemistry went ahead with more assurance and less contention, except perhaps for the irascible Kolbe. The field of aromatic chemistry, in which Laurent had derived the concept of fundamental and derived nuclei and the principle of predicting the outcome of reactions from postulated structures, saw the first major triumph of that principle. From 1865 Kekulé employed the same term: "In all aromatic substances a common nucleus may be assumed: it is the closed chain C_6A_6 (in which A denotes an unsaturated affinity)" (72). The hexagonal structure for the benzene nucleus indicated the possibility of one mono- and three disubstituted derivatives, while trisubstitution would result in three isomers for the $C_6H_3X_3$ case but in six for the $C_6H_3X_2Y$ case (72) (Fig. 8). There were possibilities other than the hexagonal structure for benzene, Kekulé noted: "A problem of this kind might at first sight appear quite insoluble; but I nevertheless believe that experiment will furnish a solution. It is only necessary to prepare, by methods as varied as can be devised, as great a number of substitution products of benzene as possible; to compare them very carefully with regard to isomerism, to count the observed modifications; and especially, to endeavor to trace the cause of their difference to their mode of formation. When all this is done we shall be in a position to solve the problem" (72).

The research program outlined by Kekulé was implemented and extended notably by his former assistant, Wilhelm Körner (1839-1925), who in so doing prepared 126 new benzene derivatives (73). Following up Kekulé's prediction of 1866 (72), Körner

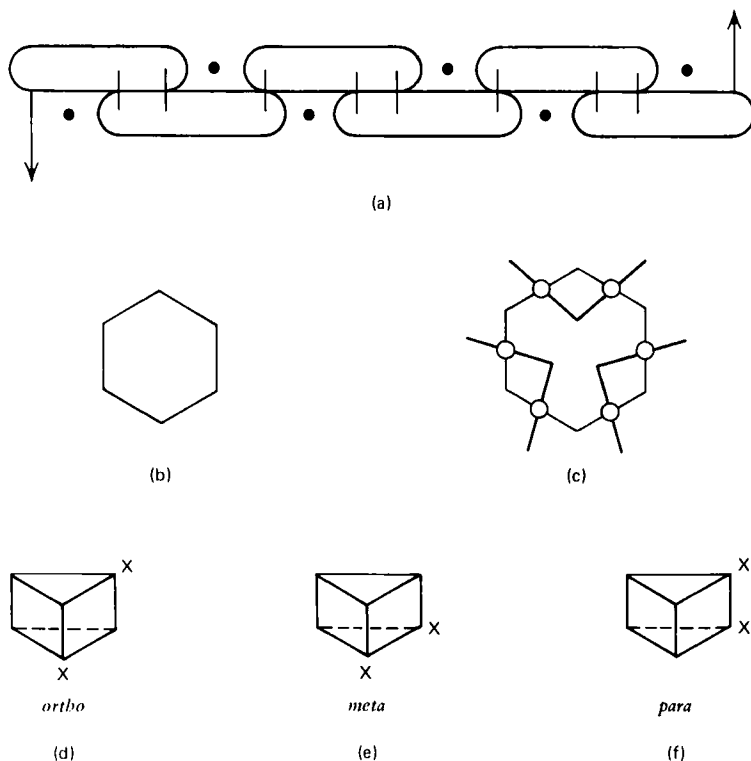


Fig. 8. Representations of benzene by Kekulé (a) initially and (b) later in 1865, and (c) in 1866; and Ladenburg's trigonal prism formulation of (d) an *ortho*-, (e) a *meta*-, and (f) a *para*-disubstituted benzene derivative.

identified the *ortho*, *meta*, and *para* isomers of dibromobenzene by nitration, obtaining two, three, and one dibromonitrobenzene, respectively, from these isomers (73). Another of Kekulé's students, Albert Ladenburg (1842-1911) showed that only one isomer of pentachlorobenzene could be isolated and that all six hydrogen atoms in benzene are equivalent (74). Ladenburg held that two *ortho* isomers were to be expected from the hexagonal benzene structure with alternating single and double carbon-carbon bonds, and proposed a trigonal prism benzene structure from which the expectations of geometrical isomers agreed with those derived for a regular hexagon (74). To meet this objection, Kekulé proposed his theory of atomic oscillations in benzene which produced an equivalence between the 1:2 and 1:6 positions on a time average (75). Subsequently LeBel and van't Hoff pointed out that there would be two *ortho* isomers in the

trigonal prism structure and that these would be optically active (76).

VI. MOLECULAR DISSYMMETRY

The investigation of optical activity was due largely to physicists and crystallographers, mainly French, during the first half of the nineteenth century. For the chemists of the period optical activity presented yet another, and a particularly perplexing, case of isomerism, notably in the example of (+)-tartaric acid and the inactive paratartaric or racemic acid. Malus in Paris discovered the polarisation of light by reflection (1809), and, on propagating white polarized light along the optic axis of a quartz crystal, Arago observed a range of colours on vewing the crystal through a rotatable plate of calcite (1811). Their colleague, Jean Baptiste Biot (1774-1862), distinguished two effects, firstly, the rotation of the plane of polarisation of monochromatic light by the crystal and, secondly, the dispersion of that rotation, α , with respect to wavelength, λ , according to the approximate relation, $\alpha = K/\lambda^2$ (Biot's law). Biot discovered the optical activity of liquid terpenes in 1815 (77) and subsequently that of aqueous solutions of sucrose and tartaric acid, showing that optical activity is a property of submicroscopic molecules as well as macroscopic crystal structures.

Initially Biot attempted to provide a physical explanation for optical activity in terms of Newton's theory of rectangular photons, light corpuscles with different 'sides,' but became reconciled to the new theory of light as a vibration transverse to the direction of propagation in an all-pervading luminiferous ether, due notably to Augustin Fresnel (1788-1827). Fresnel viewed rectilinear polarization as a superposition of left- and right-circular polarization, optical activity resulting from circular birefringence. From the model Fresnel deduced in 1824 that optically active molecules have a helical form or are arranged helically in a crystal: "There are certain refracting media, such as quartz in the direction of its axis, turpentine, essence of lemon, etc., which have the property of not transmitting with the same velocity circular vibrations from right to left and those from left to right. This may result from a peculiar constitution of the refracting medium or of its molecules, which produces a difference between the directions right-to-left and left-to-right; such, for instance, would be a helicoidal arrangement of the molecules of the medium, which would present inverse properties according as these helices were dextrogyrate or laevogyrate" (78).

The crystallographer, Haüy, had noted the hemidral faces of quartz crystals and distinguished the two enantiomorphous types, while Biot had found that some quartz crystals were levorotatory

and others dextrorotatory. The polymath, John Herschel (1792-1871), correlated these two observations in 1822, showing that quartz crystals of one morphological class are dextrorotary while those of the other class are levorotatory (79). Herschel's correlation was probably known to Fresnel and other French workers, as Herschel with Brewster and Babbage was much concerned with the introduction of French physics into Britain and maintained a wide continental correspondence.

Pursuing his investigation of isomorphism, Mitscherlich discovered in 1844 that, while all other salts of tartaric acid and racemic acid had different forms, the sodium ammonium salts appeared to be isomorphic and identical in all respects except optical activity. At the time Louis Pasteur (1822-1895) was at the École Normale as Balard's assistant, studying crystallography with Haüy's former student, Delafosse, and with Laurent, repeating the 1841 work of de La Provostaye on the crystal forms of the tartrates and racemates. Herschel's correlation suggested to Pasteur that Mitscherlich's observation might be incomplete, and he showed that this was indeed the case by hand sorting the crystals of sodium ammonium racemate into two enantiomorphous types with opposite optical activities (80). Biot was astonished and obliged Pasteur to repeat the work in Biot's own laboratory (81). The implication of the result for Pasteur was based on the theme, abiding and potent in France, of mutual analogy between the macroscopic and the microscopic: the individual molecules of (+)- and (-)-tartaric acid have mirror-image morphologies like the corresponding crystal forms.

Pasteur extended his work on the tartrates, and his concept of dissymmetry, at Strasbourg (1848-1854) and Lille before returning to the École Normale as Director in 1857. In 1853 he published the method of resolving optical isomers by fractional crystallization of their diastereoisomers, and prepared *m*-tartaric acid, together with the (-)-isomer, by heating cinchonine (+)-tartrate at 170°C (82). From this work Pasteur concluded that all chiral substances should exhibit four modifications: the (+)- and (-)-isomers, the externally compensated 1:1 compound or racemate, and the internally compensated or 'untwisted' and achiral *meso* form. Synthetic organic chemistry, he believed, would prepare only the achiral *meso* form. Finally, in 1858, by which time he had become almost entirely preoccupied with microbiological studies, he showed that a mould, probably *Penicillium glaucum*, grew selectively in a solution of ammonium hydrogen racemate to which a little phosphate had been added, consuming the (+)-tartrate and leaving the (-)-isomer (83).

From his studies Pasteur early built up a theory of cosmic dissymmetry: "The universe is a dissymmetrical whole...for, if the whole of the bodies which compose the solar system were placed before a mirror, moving with their individual movements, the image in the mirror could not be superposed to the reality.

Even the movement of solar life is dissymmetrical. A luminous ray never strikes in a straight line the leaf where vegetable life creates organic matter. Terrestrial magnetism, the opposition which exists between north and south poles in a magnet, that offered us by the two electricities, positive and negative, are but resultants from dissymmetric actions and movements" (84). Following up the theory, Pasteur at Strasbourg attempted to grow crystals in a magnetic field to induce enantiomorphism, and at Lille employed a clockwork-driven heliostat to reproduce for plants a mirror-image world where the sun rose in the west and set in the east (81). However the plants continued to produce their customary isomers, and the crystals could not be induced to change their usual growth habits.

His crystallographic and microbiological studies, together with his theory of cosmic dissymmetry, led Pasteur to suppose that molecular dissymmetry was the primary demarcation criterion between chemistry and life. Optical activity, he observed in his 1860 lectures, "forms perhaps the only sharply defined boundary which can at the present day be drawn between the chemistry of dead and living nature" (85). Pasteur held that not even racemates could be prepared synthetically from the elements, although they could be obtained from achiral precursors with a vital origin. The best that synthesis could accomplish was the *détordu meso* form. When Dessaignes reported the preparation of aspartic acid by the action of heat on ammonium fumarate (86) Pasteur was incredulous and visited Dessaignes in Vendome to examine his product. It was inactive, and so too was the malic acid prepared from it, and Pasteur concluded that Dessaignes' product was an untwisted *meso* form. It could not be the racemate, "for in that case not only would *one* active body have been made from an inactive one, but there would have been *two* such prepared, one dextro- and the other levo-rotatory" (85).

Pasteur was even more astonished in 1860 when Perkin and Duppa (87) obtained tartaric acid from succinic acid, following Simpson's synthesis of the latter from ethylene in the previous year (88). Pasteur resolved a sample of the synthetic tartaric acid sent to him by Perkin, proving that it was the racemic acid and that two optical isomers had indeed been synthesised from an optically inactive compound. However, Pasteur declined to modify his demarcation criterion. The initiatory 1874 stereochemical papers by van't Hoff (89) and Le Bel (90) were greeted by Pasteur reiterating his view in the following year that "in science there does not exist a single example at present of an inactive substance which can be transformed into an active compound by our laboratory reactions" (91).

Pasteur was never greatly concerned with the internal development of the chemical science of his time, with the radical and type theories, with the debates on atoms, volumes, and equivalents, with the structure theory of Kekulé and the stereo-

chemistry of Le Bel and van't Hoff. His reaction to main-stream chemistry was often the negative one of defending his criterion for vitalism against the encroachments of organic synthesis. Pasteur's contributions to microbiology were so monumental that, after the assimilation of the new stereochemistry, it was felt that his contributions to chemistry too were more than merely suggestive, and that he out-ranked Kekulé, Le Bel, and van't Hoff as the 'Founder of Stereochemistry' (10, 11).

VI. CHEMISTRY IN SPACE

Although Kekulé had been a student of architecture at Giessen before turning to chemistry under the inspiration of Liebig's teaching, his structural insights were largely two dimensional and confined mainly to aromatic substances. The isomerism of open-chain unsaturated compounds long remained a problem for Kekulé. Initially in 1860-1863 he suggested (92) that where two affinity units of carbon are not saturated there is a kind of hiatus or gap, and the two carbon atoms are "some-how pressed together." Both maleic and fumaric acid are derived from succinic acid by the loss of two hydrogen atoms from carbon, and the two isomers differ in that the two hydrogens are lost from the same carbon atom in the more reactive maleic acid but from adjacent carbon atoms, which then became bound by two affinity units, in the less reactive fumaric acid (92).

The problem of isomerism in saturated open-chain compounds was first studied systematically, although largely theoretically, by Butlerov who drew up in 1863 tables of possible isomers based on the structural theory (93). The corresponding experimental thrust came notably from Johannes Wislicenus (1835-1902) whose early work at Zürich centred on the lactic acids (94). By 1869 Wislicenus had distinguished three isomers; the optically inactive lactic acid from sour milk, the optically active sarcolactic acid from animal tissues, and the 'ethylidene lactic acid' he had prepared by hydrolyzing ethylene cyanohydrin. He concluded: "Thus is given the first certainly proved case in which the number of isomers exceeds the number of possible structures. Facts like these compel us to explain different isomeric compounds with the same structural formula by different positions of their atoms in space, and to seek for definite representations of these" (95). "Present formulae can do no more than represent a picture of the compound in one plane," Wislicenus noted, and in 1873 he again emphasized the need for three-dimensional structural models.

The challenge was taken up by van't Hoff (1852-1911) while still a graduate student at Utrecht in 1873. After a visit to Bonn, where he found Kekulé rather remote, he moved on to Wurtz's laboratory in Paris and met Le Bel (1847-1930), returning to Utrecht in mid-1874 to publish his pamphlet on chemistry in space (89) in the autumn and defend his doctoral thesis at the

end of the year. Quite independently and apparently without contact with van't Hoff on the subject, Le Bel published in the same year his paper on the relation between organic structures and optical activity (90). Later van't Hoff observed "That shortly before this we had been working together in Wurtz's laboratory was purely fortuitous; we never exchanged a word about the tetrahedron there, though perhaps both of us cherished the idea in secret. To me it had occurred the year before, in Utrecht, after reading Wislicenus's paper on lactic acid...Le Bel's starting point was the researches of Pasteur, mine those of Kekulé...My conception is...a continuation of Kekulé's law of the quadrivalence of carbon, with the added hypothesis that the four valencies are directed towards the corners of a tetrahedron, at the center of which is the carbon atom" (Fig. 9) (96).

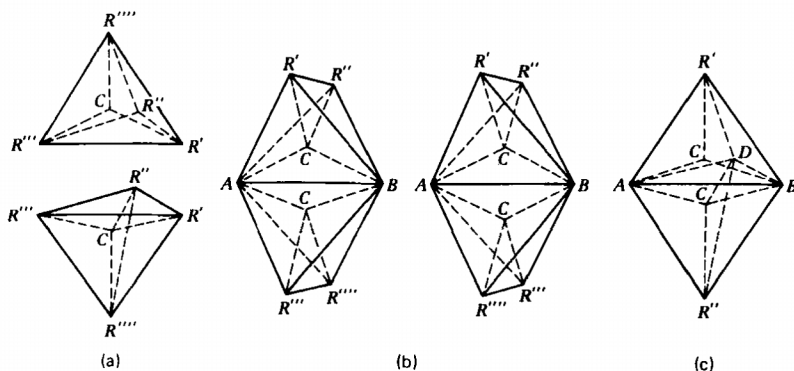


Fig. 9. The representation by van't Hoff in 1874 of (a) the optical isomers resulting from an asymmetric carbon atom, (b) the geometric isomers of an olefin arising from two tetrahedra sharing the common edge AB, and (c) the linear triple bond array formed by two tetrahedra sharing the common face ABD.

Wislicenus immediately accepted the new theory and contributed an introduction to the German edition (1877) of van't Hoff's book, *Chemistry in Space* (97), which elicited a cool response from Kekulé (98) and a choleric attack on Wislicenus, Le Bel, and especially van't Hoff by Kolbe from his editorial chair of the *Journal für praktische Chemie* (99). Kolbe had been outstanding, both as a teacher and experimentalist. In addition to the 'Kolbe reaction' and the 'Kolbe synthesis' he was the first to synthesize an organic compound, acetic acid, from an inorganic basis, despite Berthelot's later claims. From about 1850, however, the severity of Kolbe's attacks on fellow organic chemists came to provide a rough measure of the historical significance of the latter's theoretical innovations. In 1881,

when stereochemical theory was gaining wide acceptance, Kolbe reviewed the history of organic theory in the following terms: "The classificatory type theory of Gerhardt and Kekulé was succeeded by the paper chemistry which is called structural chemistry, which...many young chemists pursue thinking that they are gaining insights into the spatial arrangement of atoms as they draw their drawings and paint their pictures. But in fact they have brought chemistry not a step forward by these means; rather, this is a reversion to the old Naturphilosophie...It was of course much easier to prepare a few new compounds from some substance or other, in order to assign these to the type that was apparently appropriate...rather than investigating the chemical constitution of a compound in Berzelius' sense of the term, that is, examining the nature of the more intimate components and the functions that these fulfil" (100).

By 1880 Kolbe stood alone for the bygone age of the radical theory. Contrary to Kolbe's assertion, the stereochemical theory was fecund with insights and testable expectations, particularly the more structurally based van't Hoff version. Both Le Bel and van't Hoff rationalized the known cases of optical isomers containing an asymmetric carbon atom in terms of a tetrahedral array of the carbon valencies, but it was van't Hoff who predicted the 2^n isomers of a compound containing n different asymmetric carbon atoms, and the *cis* and *trans* isomerism of 1,2-disubstituted olefins, thereby illuminating the still-enigmatic isomerism of maleic and fumaric acid and analogous cases. As late as 1880 Kekulé explained the isomerism by supposing that fumaric was a polymer of maleic acid (101). The optical activity of 1,3-disubstituted allenes and the general alternation of geometric with optical isomerism in the cumulene series with an odd and even number of double bonds, respectively, were further predictions made by van't Hoff, together with the linearity of the acetylenes (97).

The approach of Le Bel, deriving from Pasteur's concept of molecular dissymmetry as the basis of optical activity, was less rich in testable expectations. In 1874 Le Bel supposed that olefins might be either planar or antipolar and that, in the latter case, the 1,2-derivatives would be resolvable into optical isomers (90). Le Bel adopted Ladenburg's trigonal prism structure for benzene and pointed out that, for homodisubstitution, one resolvable and two inactive isomers would result (90). "Mr. Kekulé's hexagon" was adopted for an analysis of cyclohexane derivatives on the assumption of a planar ring (90). The novel predictions specific to Le Bel were that the optical isomers obtained from a symmetrical precursor would be produced generally in a 1:1 ratio, but that the ratio could be changed by the use of an optically active catalyst in a thermal reaction, or by employing circularly polarized light in a photochemical reaction (90). In 1874 circular dichroism was as yet unknown for

homogeneous solutions, and the first unambiguous dissymmetric photolyses were accomplished more than half a century later (102).

The French preoccupation with the mutual analogies between crystal morphology and molecular form led Le Bel in 1892 to the disastrous conclusion that the valencies of carbon are not tetrahedrally disposed but form an array of square pyramidal or lower symmetry (103). He discovered that the crystals of carbon tetrabromide and carbon tetraiodide are biaxial and monoclinic, whereas isotropic cubic crystals were expected, from the macroscopic-microscopic analogy, for a tetrahedral molecular symmetry. Thereupon Le Bel revived his nonplanar model for ethylene and vainly attempted the resolution of citraconic and mesaconic acid (103). Whereas Pasteur had been fortunate in crystallizing sodium ammonium racemate below 27°C, above which the racemate crystallizes as such, and so had obtained both the *d*- and *l*-crystals, Le Bel was correspondingly unfortunate in crystallizing carbon tetrabromide below 47°C, above which this substance crystallizes in cubic form. While for Pasteur the morphological analogy between the molecule and the corresponding crystal had proved to be fruitful and rewarding, for Le Bel, enmeshed by the analogy at the point of its breakdown, it was catastrophic and led him to a model at variance with the wealth of structural evidence which had accumulated since his seminal paper of 1874.

VIII. CONCLUSION

In so far as any branch of chemistry ever has a unique progenitor, the 'founder of stereochemistry' was not so much Pasteur as his teacher, Laurent. From Laurent, Pasteur derived the concept that chemical compounds are "molecular edifices" with an architecture mirrored in the corresponding crystal morphology (104). From Laurent, Kekulé obtained both the structural concept of the aromatic nucleus, perhaps even the particular hexagonal benzene form, and the insight that, while unambiguous rational structures cannot be derived from reactions, the outcome of reactions can be deduced, and can thereby discriminate between, possible rational structures. It was an insight pursued into two-dimensional detail by Kekulé in decucing the possible isomeric products of the substitution reactions of hexagonal benzene, and extended to the third dimension by van't Hoff in predicting the optical and geometrical isomerism of organic compounds containing asymmetric carbon atoms or multiple bonds.

The third major articulation of Laurent's chemical methodology in the development of classical stereochemistry came with the first renaissance of inorganic chemistry. Even during

the lifetime of Berzelius it was perceived that organic chemistry was fast becoming the dominant branch of the science. As early as 1835 Dumas wrote, "The future progress of general chemistry will be due to the application of the laws observed in organic chemistry...and far from limiting myself to taking the rules of mineral chemistry to carry into organic chemistry, I think that one day, and perhaps soon, organic chemistry will give rules to mineral chemistry" (105). Dumas himself gave an impetus to this trend. In 1851, lecturing at the British Association meeting in Ipswich, Dumas conjectured that related inorganic elements, such as the alkali metals or the alkaline earths, were in reality homologs since they differed by a constant increment or increments in equivalent weight, just like the members of a homologous organic series (106).

Kekulé and his students saw organic chain structures as the models upon which inorganic graphic formulas should be based, writing for, e.g., perchloric acid, H-O-O-O-O-Cl . Blomstrand (1826-1897) and Jørgensen (1837-1914) took up these organically based formulations of inorganic compounds and extended them to the transition-metal complexes, viewing such compounds as $[\text{Co}(\text{NH}_3)_6]\text{Cl}_3$ as made up of a chain or chains of NH_3 groups, like the CH_2 groups of an organic chain (Fig. 10).

The autonomy of inorganic chemistry was reasserted by Alfred Werner (1866-1919), who emancipated the chemistry of coordination compounds from the trivial and unproductive organic analogies that had dominated it for half a century by reverting to the fundamental chemical methodology of Laurent. Of the probable regular geometries for the hexacoordinate complexes, the possible isomerisms of substitution products had been predicted for the hexagon by Kekulé and for the trigonal prism by Ladenburg. Werner deduced the outcome for the substitution reactions of an octahedral array of ligands around the metal ion, predicting only two geometric isomers for homo-disubstitution, the *cis* and the *trans*, and two optical isomers for tris-chelate complexes, such as those from ethylenediamine. By exploring experimentally the isomeric complexes formed by a given transition metal ion with two distinct ligands, and by optical resolutions of chelated metal complexes, Werner established between 1893 and 1914 the octahedral geometry of the 6-coordinate compounds and the square-planar structure of the 4-coordinate complexes studied (107).

The final defense of Pasteur's demarcation criterion between chemistry and life lay in the view, adopted by Francis Japp (1848-1925) and other organic chemists who shared Pasteur's theology and metaphysics, that one or more carbon atoms were essential for optical activity (108). Most of the terrestrial carbon had participated in the vital processes of a living organism at some stage in its history and carried the imprint of the experience, albeit in a form that defied definition. Up

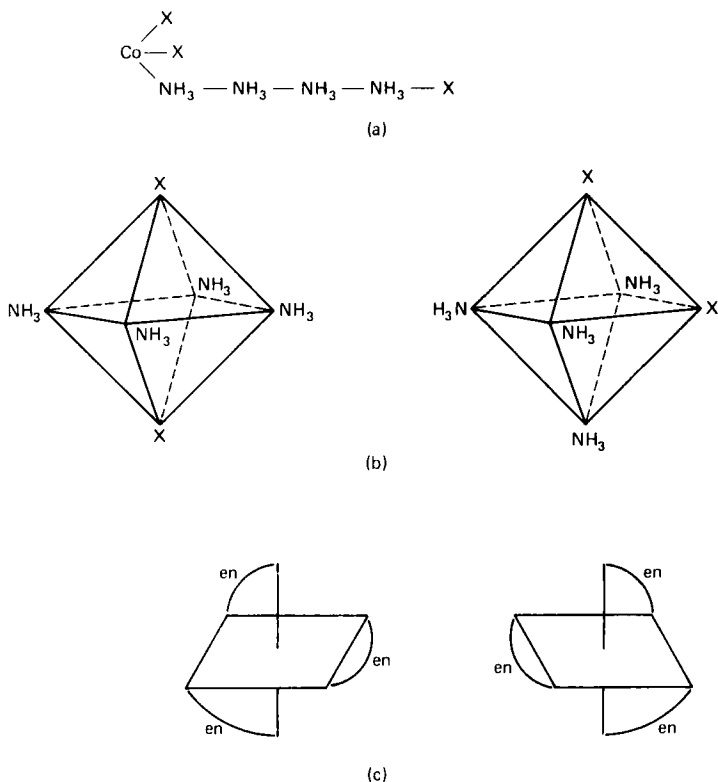


Fig. 10. The structural formulations (a) by Jörgensen (1877) of the bis-acidotetrammine cobalt(III) complexes, (b) by Werner (1893) of the *trans* and *cis* isomers of bis-acido-tetrammine metal complexes, and (c) of the optical isomers of tris-ethylenediamine complexes by Werner (1911).

to 1914 all of Werner's chiral metal complexes had contained carbon, and their optical activity was ascribed to that carbon rather than the asymmetric metal ion or the dissymmetry of the complex as a whole. By resolving a purely inorganic tris-chelate complex, the dodecammine hexa- μ -hydroxo-tetra cobalt(III) ion, $[\text{Co}(\text{OH})_2\text{Co}(\text{NH}_3)_4]_3^{6+}$, Werner disposed of the vitalist contention that organic carbon is the essential concomitant of optical activity (109). With this *tour de force* the rationale for a primary science of specifically *organic* stereochemistry was dispelled. As Wurtz had put it half a century earlier, "there is but one chemistry" (110, 111).

REFERENCES

1. H.A.L. Fisher, *A History of Europe*, Eyre and Spottiswode, London, Vol. 1, part vii, 1935.
2. F. Rabelais, *Works*, translated by T. Urquhart, Bohn, London, Vol. 1, p. 118, 1849.
3. C.P. Conger, *Theories of Microcosms and Microcosms in the History of Philosophy*, Columbia U.P., New York, 1922.
4. F.M. Cornford, *Microcosmographia Academica*, Bowes and Bowes, London, 6th edit. p. 24, 1964.
5. O.T. Benfey ed., *Classics in the Theory of Chemical Combination*, Dover, New York, Papers 5-9, pp. 110-171, 1963.
6. A. Kekulé, *Chem. Ber.*, 23, 1302 (1890); translated by F.R. Japp, 'Kekulé Memorial Lecture,' *J. Chem. Soc.*, 73, 97 (1898).
7. T. S. Kuhn, *The Structure of Scientific Revolutions*, 2nd edit., University of Chicago, 1970.
8. J.R. Partington, *A History of Chemistry*, Macmillan, London, Vol. 4, p. 656, 1964.
9. J.R. Partington, *A History of Chemistry*, Macmillan, London, Vol. 4, p. 673, 1964.
10. A. Crum Brown, "Pasteur as the Founder of Stereochemistry," *Revue Française d'Edimbourg*, 211 (1897).
11. R. Robinson, *Tetrahedron*, 30, 1477 (1974).
12. J.J. Berzelius, *Ann. Phil.*, 4, 323 and 401 (1814).
13. J.H. Brooke, *Ambix*, 15, 84 (1968); *Brit. J. Hist. Sci.*, 5, 363 (1971); *Stud. Hist. Phil. Sci.*, 4, 47 (1973).
14. J. Dalton, *A New System of Chemical Philosophy*, 1808, Citadel Press edit., p. 164, 1964.
15. W.V. Farrar, *John Dalton and the Progress of Science*, D.S.L. Cardwell (ed.), Manchester U.P., p. 290, 1968.
16. W.H. Wollaston, *Phil. Trans.*, 98, 96 (1808); Alembic Club Reprint No.2, Edinburgh (1899).
17. W.H. Wollaston, *Phil. Trans.*, 104, 1 (1814).
18. D.C. Goodman, *Hist. Stud. Phys. Sci.*, 1, 37 (1969).
19. L.R.A.C. Avogadro, *J. Phys.*, 73, 58 (1811); Alembic Club Reprint No. 4, Edinburgh (1899).
20. J.B. Morrell, *Ambix*, 19, 1 (1972).
21. J.B. Dumas and J. Liebig, *Compt. Rend.*, 5, 567 (1837).
22. J. Liebig and F. Wöhler, *Ann.*, 3, 249 (1832); Ref. 5, paper 1.
23. R.W. Bunsen, *Ann. Phys. (Leipzig)*, 40, 219 (1837); *Ann.*, 46, 1 (1843).
24. J.J. Berzelius, *Jahrsberichte*, 24, 640 (1845).
25. A.W.H. Kolbe, *J. Prakt. Chem.*, 42, 311 (1847); *Ann.*, 69, 257 (1849); Alembic Club Reprint, No. 15, Edinburgh (1948).
26. E. Frankland, *J. Chem. Soc.*, 2, 263 and 297 (1849).

27. J.R. Partington, *A History of Chemistry*, Macmillan, London, Vol. 4, p. 508, 1964.
28. E. Frankland, *Phil. Trans.*, 142, 417 (1852); *J. Chem. Soc.*, 6, 57 (1854); Ref. 5, paper 4.
29. S.C. Kapoor, *Ambix*, 16, 1 (1969); *Isis*, 60, 477 (1969).
30. N.W. Fisher, *Ambix*, 20, 106 and 209 (1973); *Ambix*, 21, 29 (1974).
31. J.G. Burke, *Origins of the Science of Crystals*, University of California, Berkeley, 1966.
32. R.J. Haüy, *Tableau Comparatif des Résultats de la Cristallographie et de l'Analyse Chimique relativement à la Classification des Minéraux*, Paris, p. xvii, 1809.
33. E. Mitscherlich, *Ann. Chim. Phys.*, 19, 419 (1821).
34. A.E. Baudrimont, *Introduction à l'Étude de la Chimie par la Théorie Atomique*, Paris, pp. 26 and 50, 1833.
35. J.H. Brooke, *Stud. Hist. Phil. Sci.*, 4, 47 (1973).
36. J.B. Dumas, *Compt. Rend.*, 8, 609 (1839).
37. J.J. Berzelius, *Ann Chim.*, 67, 303 (1838).
38. L.H.F. Melsens, *Compt. Rend.*, 14, 114 (1842).
39. J.B. Dumas, *Compt. Rend.*, 10, 149 (1840).
40. S.C.H. Windler (F. Wöhler), *Ann.*, 33, 308 (1840); translated by H.B. Friedman, *J. Chem. Educ.*, 7, 633 (1930); reprinted in G.W. Wheland, *Advanced Organic Chemistry*, 2nd edit., Wiley, New York p. 678, 1949.
41. M.A.A. Gaudin, *Ann Chim.*, 52, 113 (1833).
42. J. Liebig, *Ann.*, 9, 1 (1834).
43. A. Avogadro, *Mem. Roy. Acad. Torino*, 26, 440 (1821).
44. A. Laurent, *Ann. Chim.*, 59, 376 (1835).
45. A. Laurent, *Comt. Rend.*, 11, 876 (1840); *Compt. Rend.*, 14, 818 (1842); *Compt. Rend.*, 15, 350 (1842).
46. A. Laurent, *Ann. Chim.*, 61, 125 (1836).
47. A. Laurent, *Chemical Method*, translated by W. Odling, Cavendish Society, London, p. 324, 1855.
48. A. Laurent, *Chemical Method*, translated by W. Odling, Cavendish Society, London, p. 203, 1855.
49. A. Laurent, *Chemical Method*, translated by W. Odling, Cavendish Society, London, p. 325, 1855.
50. A. Laurent, *Ann. Chim.*, 18, 266 (1846).
51. A. Laurent, *Chemical Method*, translated by W. Odling, Cavendish Society, London, p. 340, 1855.
52. A. Laurent, *Chemical Method*, translated by W. Odling, Cavendish Society, London, p. viii, 1855; reprinted in Ref. 5, paper 2, p. 43.
53. A. Laurent, *Chemical Method*, translated by W. Odling, Cavendish Society, London, p. 337, 1855.
54. A. Kekulé, *Ann.*, 106, 129 (1858); translated by O.T. Benfey, Ref. 5, paper 5.
55. C.F. Gerhardt, *Rev. Sci.*, 10, 145 (1842); translated in Ref. 30.

56. A.O. Lovejoy, *The Great Chain of Being*, Harvard U. P., Cambridge, 1950.
57. C.F. Gerhardt, *Ann. Chim. Phys.*, [3] 7, 129 (1843); *Ann. Chim. Phys.*, [3] 8, 238 (1843).
58. C.F. Gerhardt, *Ann. Chim.*, 37, 285 (1853).
59. A.W. Williamson, *Chem. Gazette*, 9, 334 (1851); Ref. 3, paper 3.
60. A.W. Hofmann, *Compt. Rend.*, 29, 184 (1849).
61. C.A. Wurtz, *Compt. Rend.*, 28, 223 (1849).
62. J.H. van't Hoff, *Ansichten über die organische Chemie*, Brunswich, p. 658, 1878-1881.
63. G.W. Wheland, *Advanced Organic Chemistry*, 2nd edit., Wiley, New York pp. 95-99, 1949.
64. J.R. Partington, *A History of Chemistry*, Macmillan, London, Vol. 4, p. 460, 1964.
65. W. Odling, *Proc. Roy. Inst.*, 2, 63 (1855), *Phil. Mag.*, 16, 37 (1858).
66. A. Scott Couper, *Phil. Mag.*, 16, 104 (1858); *Compt. Rend.*, 46, 1157 (1858); Alembic Club Reprint No. 21 (1953); Ref 5, papers 6 and 7.
67. A. Crum Brown, *Trans. Roy. Soc. Edinburgh*, 23, 707 (1864).
68. A. M. Butlerov, *Ann.*, 110, 51 (1859).
69. A. M. Butlerov, *Z. Chem.*, 4, 549 (1861).
70. C. De Milt, *Chymia*, 1, 153 (1948).
71. S. Cannizzaro, *Nuovo Cimento*, 7, 321 (1858); translated in Alembic Club Reprint, No. 18, Edinburgh (1910).
72. A. Kekulé, *Bull. Soc. Chim. France*, [2] 3, 98 (1865); *Ann.*, 137, 129 (1866); translated by F.R. Japp, *J. Chem. Soc.*, 73, 97 (1898).
73. W. Körner, *Gazzetta*, 4, 305 (1874).
74. A. Ladenburg, *Chem. Ber.*, 5, 322 (1872); *Chem. Ber.*, 7, 1684 (1874).
75. A. Kekulé, *Ann.*, 162, 77 (1872).
76. J.H. van't Hoff, *Chem. Ber.*, 9, 1881 (1876).
77. J.B. Biot, *Bull. Soc. Philomath., Paris*, 190 (1815).
78. A. Fresnel, *Bull. Soc. Philomath., Paris*, 157 (1824); translated by T.M. Lowry, *Optical Rotatory Power*, Longmans, Green, London, p. 19, 1935.
79. J. Herschel, *Trans. Camb. Phil. Soc.*, 1, 43 (1822).
80. L. Pasteur, *Compt. Rend.*, 28, 477 (1849); 29, 297 and 433 (1849).
81. P. Frankland, Pasteur Memorial Lecture, *Memorial Lectures 1893-1900*, Chemical Society, London, p. 683, 1901.
82. L. Pasteur, *Compt. Rend.*, 36, 973 (1853); *Compt. Rend.*, 37, 162 (1853).
83. L. Pasteur, *Compt. Rend.*, 46, 615 (1858); *Compt. Rend.*, 51, 298 (1860).
84. R. Vallery-Radot, *Life of Pasteur*, translated by R.L. Devonshire, Dover, New York, p. 72, 1960.
85. L. Pasteur, *Researches on Molecular Dissymmetry* (two

- lectures given to the Chemical Society of Paris, 1860), Alembic Club Reprint, No. 14, Edinburgh (1948).
86. V. Dessaignes, *Compt. Rend.*, 31, 432, (1850).
 87. W.H. Perkin and B.F. Duppa, *Chem. News*, 244 (1860); *J. Chem. Soc.*, 13, 102 (1861).
 88. M. Simpson, *Proc. Roy. Soc.*, 10, 574 (1859).
 89. J.H. van't Hoff, *Arch. Néeland. Sci. Exact. Nat.*, 9, 445 (1874); Ref. 5, paper 8.
 90. J.A. Le Bel, *Bull. Soc. Chim. France*, [2] 22, 337 (1874); Ref. 5, paper 9.
 91. L. Pasteur, *Compt. Rend.*, 81, 128 (1875).
 92. A. Kekulé, *Z. Chem.*, 3, 643 (1860); *Z. Chem.*, 4, 257 (1861); *Z. Chem.*, 6, 9 (1863).
 93. A.M. Butlerov, *Bull. Soc. Chim. France*, 5, 582 (1863).
 94. W.H. Perkin, Jr., Wislicenus Memorial Lecture, *Memorial Lectures 1901-13*, Chemical Society, London pp. 59-92, 1914.
 95. J. Wislicenus, *Chem Ber.*, 2, 550 and 619 (1869); *Ann.*, 166, 3 (1873); 167, 302 (1873).
 96. J. Walker, van't Hoff Memorial Lecture, *Memorial Lectures 1901-13*, Vol. 2, Chemical Society, London, pp. 256-271, 1914.
 97. J.H. van't Hoff, *Chemistry in Space*, translated by J.E. Marsh, Oxford U.P., 1891; *The Arrangement of Atoms in Space*, translated by A. Eiloart, London, 1898.
 98. R. Anschütz, *August Kekulé*, Berlin, Verlag Chemie Vol.2. p. 912, 1929.
 99. H. Kolbe, *J. Prakt. Chem.*, 15, 473 (1877); translated by G.W. Wheland, *Advanced Organic Chemistry*, 2nd edit., Wiley, New York p. 132, 1949.
 100. H. Kolbe, *J. Prakt. Chem.*, 23, 305 and 353 (1881); translated in Ref. 30.
 101. R. Anschütz, *August Kekulé*, Berlin, Verlag Chemie, Vol. 1, p. 490, 1929.
 102. T.M. Lowry, *Optical Rotatory Power*, Longmans, Green, London p. 412, 1935.
 103. J.A. Le Bel, *Bull. Soc. Chim. Fr.*, [3] 7, 613 (1892); *Bull. Soc. Chim. Fr.*, [3] 11, 292 (1894).
 104. R. Vallery-Radot, *Life of Pasteur*, translated by R.L. Devonshire, Dover, New York, p. 33, 1960.
 105. J.B. Dumas, *J. Pharm.*, 5, 80 (1835).
 106. J.R. Partington, *A History of Chemistry*, Macmillan, London, Vol. 4, p. 884, 1964.
 107. G.B. Kauffman, *Classics in Coordination Chemistry*, Dover, New York 1968; translation of A. Werner, *Z. Anorg. Chem.*, 3, 267 (1893); *Z. Phys. Chem.*, 12, 35 (1893); *Z. Phys. Chem.*, 14, 506 (1894); *Chem. Ber.*, 40, 4817 (1907); *Chem. Ber.*, 44, 1887 (1911); *Chem. Ber.*, 47, 3087 (1914).
 108. F.R. Japp, *Stereochemistry and Vitalism*, British Association for the Advancement of Science Report, pp. 813-

- 828, 1898.
109. G.B. Kauffman, *Classics in Coordination Chemistry*, Dover, New York, paper 6, 1968.
 110. A. Wurtz, *A. History of Chemical Theory*, translated by Henry Watts, Macmullan, London, p. 3. 1869.
 111. A detailed and useful history of stereochemistry to the midtwentieth century is provided by C.A. Russell, *The History of Valency*, Leicester University Press, 1971.

MASS SPECTROMETRY AND THE STEREOCHEMISTRY
OF ORGANIC MOLECULES

MARK M. GREEN

*Department of Chemistry, Michigan State University,
East Lansing, Michigan*

- I. Foundation 36
 - A. Background 36
 - B. The Structures of Reacting Molecular Ions 37
 - C. Ion Intensity and Kinetics Following Electron Impact 38
 - D. The Extrapolation of Accessible Phase Conformational Analysis to Molecular Ions 41
- II. Stereoisomeric Dependence in the Electron Impact Induced (EI) Rearrangements of Alcohols and Alcohol Derivatives 45
 - A. Alcohols and the Elimination of Water 45
 - B. Steroid, Terpene and Related Alcohols 53
 - C. Polyalcohols and Ethers 61
 - D. Sugars and Related Molecules 65
- III. Stereoisomeric Dependence in the Electron Impact Induced Rearrangements of Carbonyl Compounds 68
 - A. Spatially Dependent EI Rearrangements of Carbonyl Compounds 68
 - B. Fragmentations of Carbonyl Compounds Involving the Spatial Integrity of Double Bonds 76
- IV. Stereoisomeric Dependence in Electron Impact Induced Apparent Electrocyclic Fragmentations 80
 - A. Hydrogen Rearrangements and the Retro-Diels-Alder Reaction (RDA) 80
 - B. The Electron Impact Induced Retro-Diels-Alder Reaction and the Question of Orbital Symmetry 83
- V. Stereoisomeric Dependence in Electron Impact Induced Bond Cleavage Reactions 87
 - A. Hydrocarbons and the Meyerson-Weitkamp

Hypothesis for Stereoisomeric Effects	87
B. Bicyclic Molecules and Related Examples	91
C. Heterocyclic Molecules	93
D. Other Examples	97
E. Final Notes	99

I. FOUNDATION

A. Background

Mass spectrometers allow chemical observations, in the gas phase, in states of controlled intermolecular interactions. Because this chemistry must inevitably depend on structure, and because stereochemistry is an excellent source of structural and mechanistic information, it is not surprising that geometrical questions were asked early in the study of the behavior of organic molecules in mass spectrometers.

A classic case in point is the finding by Field and Franklin (1) that the three carbonium ions represented in Figure 1 were formed from their bromides with differing

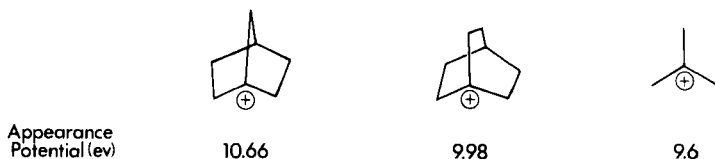


Fig. 1. Dependence of appearance potential on molecular geometry.

appearance potentials. They noted the correlation between these potentials and the geometric constraints of forming a planar array in the bicyclic systems (1,2). The first observations of the dependence of the electron impact (EI) fragmentation pattern on stereoisomerism came shortly thereafter (3-6).

Early studies of the mass spectra of a series of epimeric alcohols and acetates (4) led to the postulate (7,8) that stereoisomeric effects in mass spectrometry may arise from the relative energies of the epimers and, as well, that stereoisomeric differences may be emphasized (8) by "facilitation of a rearrangement process in one of the isomers due to a favorable configuration, holding the two atoms or groups involved in close proximity, while keeping them apart in the other isomer." Rearrangement reactions in mass spectrometers, as elsewhere, involve bond making and bond breaking (9).

D'Or, Momigny, and Natalis in the same year (10) reviewed their results on the EI fragmentation of geometrical isomers. For these cyclic and olefinic diastereomers that underwent simple cleavage reactions (9), they postulated that the excess internal energy of the less stable (ΔH) isomer would be available, after ionization, to drive the decomposition and thus lead to diminished intensity of the molecular ion from the less stable epimer of a pair.

These early ideas sparked other observations, and by 1968 there were numerous examples of stereoisomeric dependence of the mass spectra of organic molecules. This research was collected and critically sorted out by Meyerson and Weitkamp (11). Their general conclusions, which have been borne out and amplified by the studies reported herein, were succinctly stated in the paper's abstract (Fig. 2).

Abstract—The unimolecular reactions that give rise to mass spectra are controlled by spatial relationships and energy considerations. In molecules that contain a heteroatom, elimination reactions, involving bond-making as well as breaking, are often prominent, e.g. loss of water from alcohols. The ease of such reactions depends on spatial relationships in the molecule, and the resultant ion intensities in the spectra of geometric isomers can consequently be correlated with differences in geometry and hence furnish a basis for assigning structures. Processes that do not involve bond-making do not have such rigorous geometric requirements, but depend rather on attainment of a transition state defined in terms of a minimum energy content. Common product ions from stereoisomeric hydrocarbons seem often to arise via a common transition state. When this condition holds, the difference between the enthalpies of the isomers is reflected in the relative appearance potentials and—though the cause-and-effect relationship here is less direct and more readily obscured by other factors—relative intensities of the common product derived from the isomers. In both classes of processes, the spectra of stereoisomers can be simplified and made more distinctive by lowering source temperature and ionizing voltage.

Fig. 2. Abstract from the S. Meyerson and A. W. Weitkamp 1968 review (11).

B. The Structures of Reacting Molecular Ions

Mass spectra are most often overtly different for stereoisomers. It would be useful to discuss and interpret this stereochemistry in the framework of the principles of accessible phase conformational analysis (12). The

validity of this approach is directly dependent on the degree of structural correspondence between molecules encountered in an accessible phase and in mass spectrometers.

The problem is complicated because the ions of interest here are not only short lived, 10^{-6} sec or less, but are present at low pressure as well, in the range of 10^{-6} mm. Although a large literature exists directed toward the elucidation of the structure of these gaseous molecular ions, Bentley and Johnstone (13) have correctly pointed out that "All of the methods used to investigate ion structures in organic mass spectrometry involve comparisons amongst ions and except for atoms and a few simple molecules no ion structures have been absolutely determined." Others (14) have stressed that present studies directed toward molecular ion structure in mass spectrometers yield no information on the nonbonding properties that are central to conformational analysis.

The work reviewed in this chapter demonstrates that a coherent framework for the stereochemical observations in mass spectrometers may be achieved by applying the principles of conformational analysis (12). This success, even in the absence of more direct approaches to structural information lends strong support to the view (15-18) that for at least those molecular ions under scrutiny here, there is close correspondence in structure to their neutral precursors.

For this reason the structures of the reacting molecular ions discussed will be presented as if the removal of an electron to furnish the relaxed ionized state were not a major perturbation on the overall arrangements of the atoms. This hypothesis is simple and highly useful. After a discussion of the relationship between ion intensity and kinetics, immediately below, there is presented a number of EI studies of stereoisomers (Sect. I-D) which lend strong support to this point of view.

C. Ion Intensity and Kinetics Following Electron Impact

The intensity at any m/e value in the mass spectrum is directly proportional to the number of ions of that mass to charge ratio impinging on the detector. This concentration of ions is a function of a large number of variables which are not completely defined.

At this time it is hypothesized that a neutral molecule is vertically promoted to the ionized state on electron bombardment, that is, in a time so short that there is no atomic movement. The ion lifetime under normal operating conditions is believed to be many orders of magnitude longer than the time necessary for equilibration to take place completely among the available energy states of the ion. The

detected ions are isolated and undergo no collisions after ionization until they hit the detector. The ion energy, or that energy left to the ion above the ionization energy (ionization potential), is a complex function of the structure and the energetic state of the molecule prior to ionization. The function that defines the probability of internalizing energy E is known as the $P(E)$, and these values are accessible in some cases by photoelectron spectroscopy.

In general, the molecular ions of a complex organic molecule will be produced with energies varying from zero (ionization without excess energy transfer from the 70 eV electron beam to the molecule) to about 10 eV over the ionization potential. The various fragmentations possible are characterized by rate constants which are a function of this range of molecular ion energy. The qualitative form of the equation relating unimolecular rate constant to ion energy is shown below (eq. [1]). E and E_0 are, respectively, the internal energy of the ion and the activation energy for the fragmentation.

$$k = \gamma \left(\frac{E - E_0}{E} \right)^m \quad [1]$$

The exponential term is taken to the power m , which is related to the effective number of oscillators among which the energy is distributed. The preexponential term γ is key, since it is very different for the two general classes of reactions observed in mass spectrometers. For simple cleavages, or bond breaking, γ will be of the order of magnitude of a vibration, ca. 10^{13} sec^{-1} . For any process (e.g. rearrangement) involving restrictions in the motions of the molecule as a prerequisite to reaction, this γ term may change considerably, e.g., from 10^{13} sec^{-1} to 10^9 sec^{-1} .

For rearrangement fragmentations on electron impact (EI), the energy of activation (E_0) will usually be less than for simple cleavages. Model calculations and inspection of eq. [1] show that for an ion of high internal energy ($E \gg E_0$), cleavage reactions will predominate, while for ions of low internal energy ($E \approx E_0$), rearrangement reactions will be most competitive. This expectation is well borne out by experiment (19,20).

These ideas are important with regard to the effect of stereoisomerism on mass spectra. The molecular ion intensity at the detector depends on the ease of fragmentation of these ions, and this in turn depends on the range of internal energies for an array of molecular ions [$P(E)$] and the modes of unimolecular reactions open to each ion. Under any conditions molecular ions that remain intact long enough to traverse the focusing fields are those of lowest internal energy. The depletion of the molecular ion intensity will be

most effective when processes of low activation energy are available, since these fragmentations are accessible to the lowest energy ions. It follows that molecular ion intensity is very sensitive to the availability of rearrangement reactions, and that ease of rearrangement will act to diminish the molecular ion intensity. This is, of course, also true for extremely facile (low E_0) cleavages, for example, loss of $\text{Br}\cdot$ from tertiary butyl bromide. In that case no molecular ion is observed (1,2). The ease of rearrangement will depend on the proximity of the groups necessary for bonding, and this in turn depends on the geometry or steric disposition of the molecular ion.

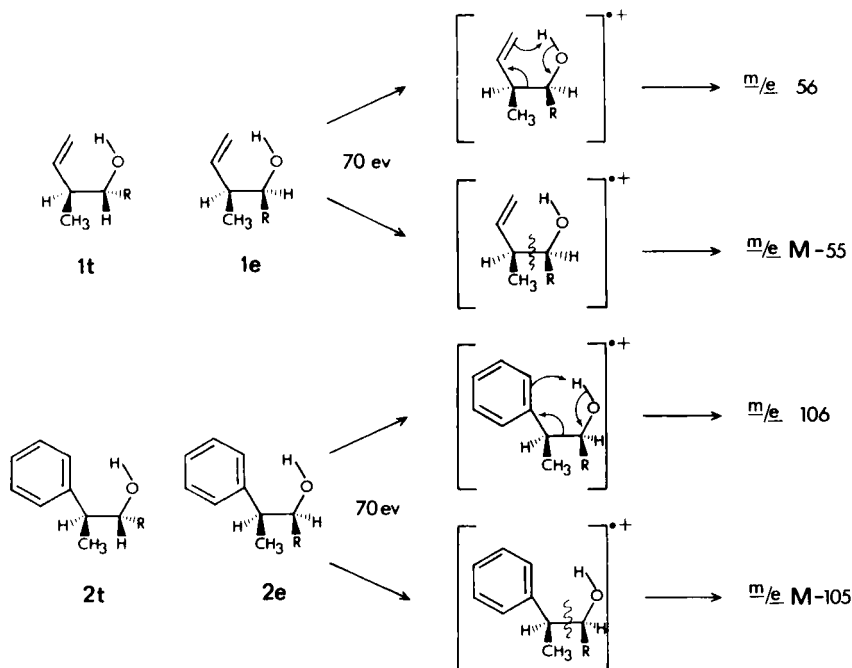
It follows from the above discussion that possible rearrangement fragmentations will cause molecular ion intensity to be heavily a function of molecular ion geometry. In other words, for isomeric substances, where the $P(E)$ functions and available modes of decomposition are closely similar, the relative intensities of the stereoisomeric molecular ions will reflect the ability of these ions to undergo rearrangement fragmentation. Molecular ions with available elimination reactions of lowest E_0 and fastest γ will exhibit reduced molecular ion intensity over *isomeric* molecular ions.

The intensity of a fragment ion is a still more complex problem (21). This intensity depends not only on the rate of formation of the ion but on its rate of further fragmentation as well. The ions may be produced with a range of energies, and this range will certainly affect the number of ions which reach the detector. Nevertheless, ions arising via rearrangement are produced, as discussed above, predominantly from low-energy parents. It follows that such rearrangement ions will have less available energy for further fragmentation than ions produced via high-energy pathways. Thus the ion intensity for rearrangement fragments will reflect more the ease of their creation than of their destruction. This will be the case at 70 eV, and more so at lower beam energies. As seen below from the results reported, higher intensity of rearrangement ion is always consistent with structural features easing rearrangement.

Although ideally one would like to have in hand the absolute unimolecular rate constants for fragmentation from a molecular ion of known energy, these rates are not directly accessible from the mass spectrum as routinely taken. Present research is directed toward gathering these numbers (22). In the absence of these data, the comparisons *within sets of stereoisomers* of relative intensities (percent of total ionization), of fragment ions or molecular ions constitute defensible methods for gaining insight into relative molecular ion reactivity. As will be shown, this reactivity certainly reflects molecular geometry.

D. The Extrapolation of Accessible Phase Conformational Analysis to Molecular Ions

Supported by deuterium labeling and the observation of metastable ions, the following mechanism has been proposed for two major fragments from the alcohols shown in Figure 3



	m/e 56/ m/e M-55		m/e 106/ m/e M-105	
R	1t	1e	2t	2e
CH ₃	1.01	.98	3.71	3.33
C ₂ H ₅	1.32	1.28	4.88	4.55
(CH ₃) ₂ CH	.98	.91	4.44	4.00
(CH ₃) ₃ C	.65	.64	3.28	3.18

Fig. 3. Relative ratios of cleavage and rearrangement. Compounds studied on an Atlas CH-4 mass spectrometer at 220°C and 70 eV.

(16). The quantitative competition between rearrangement and cleavage was determined as a function of both stereochemistry, i.e., 1t versus 1e and 2t versus 2e, and substitution (varying R) and these results are presented as well.

The numbers in each series (1 and 2) are ratios of

rearrangement to cleavage. In every case the threo compounds *1t* and *2t* find greater ease of rearrangement. In addition, the smaller R groups in each series show greater propensity for rearrangement from either isomer. These results are entirely consistent with a higher energy state for rearrangement when the necessary eclipsing interactions in the hydrogen-transfer transition state are emphasized. The latter problem will be larger in the erythro isomers and with large R groups as well. The differences are notable when one considers that the conditions of reaction are bombardment with 70 V electrons in a high vacuum container with walls at 220°C.

In a study under less energetic conditions of temperature and beam energy, the diastereotopic hydrogens on C-4 of 2-pentyl chloride (Fig. 4) (17) were shown to be trans-

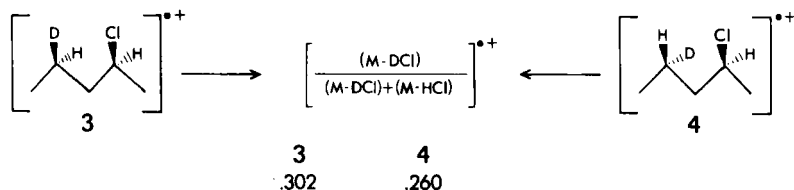


Fig. 4. Stereochemical dependence for elimination of HCl from 2-chloropentane. Data taken at 10 eV and 30°C on a CEC-103 spectrometer.

ferred unequally for loss of HCl from the molecular ion. The analogous alcohol showed preference for the same diastereotopic deuterium atom as in 3. Whatever may be the conformational basis for this effect, the conformational sensitivity was used to support proposals of identical mechanism for 1,3 elimination of H₂O and HCl. Significantly, if the transfer step of hydrogen to X in 3 forms a 1,3-dimethylcyclopentane-like transition state, the stereoselectivity is in line with the greater known stability of the cis epimer (17). As will be seen below this proposal finds support in systems with direct thermal analogs.

Brown and co-workers studied an unusual *EI* 1,2 elimination of water and methanol from 5 through 8 in Figure 5 (23). The system is well chosen in terms of the clear-cut conformational predictions for elimination from a state avoiding phenyl-phenyl eclipsing.

The results (Fig. 5) obtained at threshold voltages and a source temperature of 80°C are precisely in line with these conformational prerequisites. In both loss of water and loss of methanol, 7 and 8 exhibit increased loss of ROD.

Similar conformational studies on the elimination of

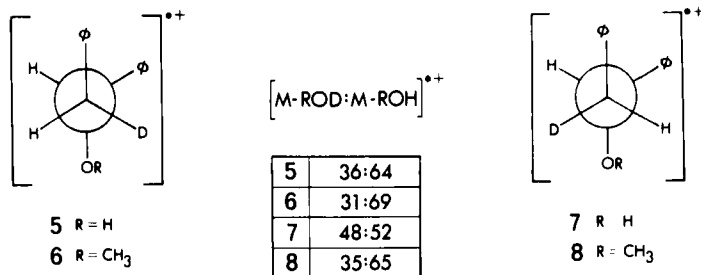


Fig. 5. Elimination of water and methanol under electron impact. Data taken on an Atlas CH-4B mass spectrometer at 10 eV and 80°C.

acetic acid from acyclic acetate molecular ions (18,24) yield increased insight (Fig. 6) since pyrolytic analogs exist. Deuterium labeling was used to identify the diastereotopic hydrogens H_a and H_b .

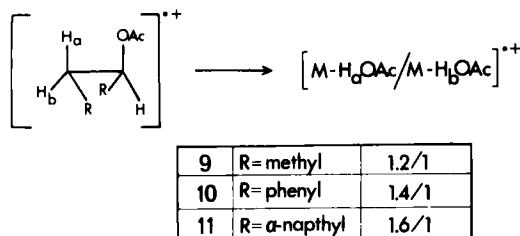


Fig. 6. Stereochemical dependence for elimination of acetic acid. Data taken from a MS-902 mass spectrometer at 15 eV and 135°C.

Although the stereoselectivities were expectedly not quantitatively identical to the pyrolytic system (25), the results fit into the conformational scheme for cis elimination in which these pyrolyses are framed. It is neat that the relative difference between loss of H_a OAc and H_b OAc increases as the size of R increases from methyl through α-naphthyl.

Research on an entirely different rearrangement, the 1,4 elimination of water from acyclic alcohol molecular ions, reinforces these proposals of conformational correspondence.

Alcohol molecular ions, when possible, eliminate water through loss of a C-4 hydrogen (26,27). Alkoxy radicals show identical regioselectivity for intramolecular hydrogen

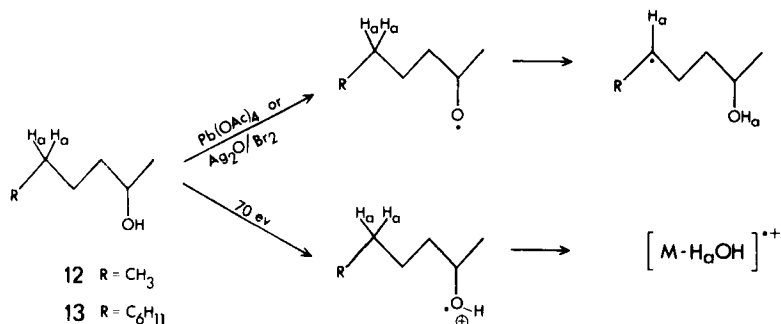


Fig. 7. Putative correspondence of alkoxy radicals and alcohol molecular ions.

transfer from carbon to oxygen (Figure 7).

In the alcohol shown in Figure 7, the methylene hydrogens in focus are diastereotopic by internal comparison. This fact was used as a handle by which to compare the conformational prerequisites for hydrogen abstraction in the two reactions. The results of studies on the deuterium-labeled diastereomers are shown in Figure 8 (28,18).

		k_a/k_b		
		M-H ₂ O	Pb(OAc) ₄	Ag ₂ O/Br ₂
12	methyl	1.10	1.23	1.19
13	cyclohexyl	1.19	1.32	1.29

Fig. 8. Comparative stereoselectivity for alkoxy radicals and alcohol molecular ions (see Figure 7). The final products of the Pb(OAc)₄ and the Ag₂O/Br₂ reactions were the cis and trans 2,5-dimethyltetrahydrofurans. Mass spectral results from an MS-902 mass spectrometer at ca. 100°C and 70 eV.

The data (18) showing corresponding preference for H_a and increasing stereoselectivity from methyl to cyclohexyl speak well for the hypothesis of structural correspondence.

II. STEREOISOMERIC DEPENDENCE IN THE ELECTRON IMPACT INDUCED (EI) REARRANGEMENTS OF ALCOHOLS AND ALCOHOL DERIVATIVES

A. Alcohols and the EI Elimination of Water

As discussed above (Figs. 7 and 8), the EI elimination of water from open chain alcohols exactly parallels the regioselectivity and stereoselectivity for intramolecular hydrogen abstraction of alkoxy radicals (29,30). As is seen (Fig. 9) the regioselectivity for loss of water from cyclohexanol is lower (31).

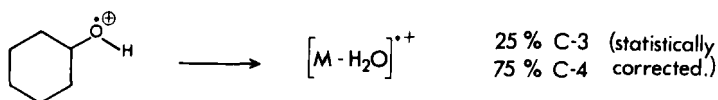


Fig. 9. Elimination of water from cyclohexanol. CEC-103 mass spectrometer at 70 eV and ca. 125°C. Relative ratio from C-3 and C-4. There is an additional loss of ca. 5% from C-2.

The EI behavior of cyclohexanol and related molecules has received a great deal of attention. Early work (32) on 1,4-cyclohexanediol demonstrated that the cis and trans isomers chose unique pathways for elimination of water (Fig. 10).

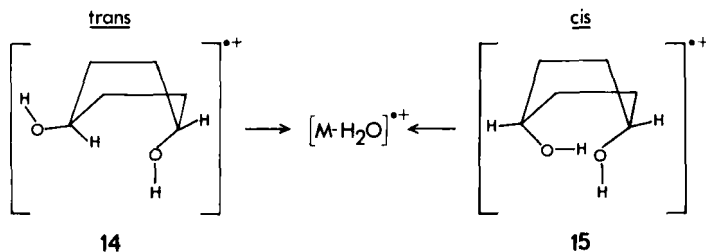


Fig. 10. Mechanism for water loss from the stereoisomers of 1,4-cyclohexanediol.

The trans isomer molecular ion eliminates water eight times more effectively than its cis isomer as measured by the relative percentages of total ionization for M-18. This suggests that the elimination of water takes place from an unrearranged, ring intact, molecular ion. This important conclusion is now known to be true for a large number of systems.

A key study (33,34) was carried out on the *cis*- and *trans*-4-*t*-butylcyclohexanols. Utilizing photoionization and emphasizing the deleterious effects of high temperature on the mass spectra of alcohols, it was demonstrated that the loss of water from *trans*-4-*t*-butylcyclohexanol yielded the base peak while the comparable elimination from the *cis* isomer is vanishingly small (Fig. 11). Photoionization (35) is not a prerequisite for these observations since EI results on these materials and other related molecules give similar stereospecificity (36). Later work with deuterium labeling (37,38) demonstrated that the *cis* C-4 hydrogen is lost as shown in Figure 11.

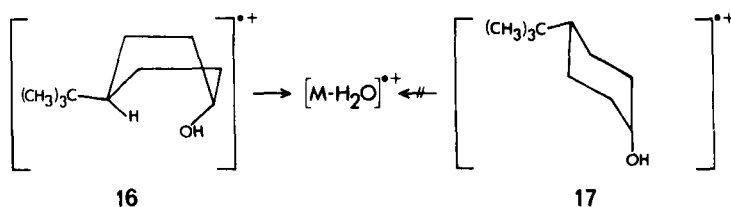


Fig. 11. Photoionization (21.2 eV) at room temperature on the stereoisomers of 4-*tert*.-butylcyclohexanol (34).

In line with this the deuterium labeling of the C-4 diastereotopic hydrogens in cyclohexanol demonstrated that the 1,4 EI elimination of water is at least 80% stereospecific (Fig. 12) (37,39). In contrast, the less favored 1,3 elimin-

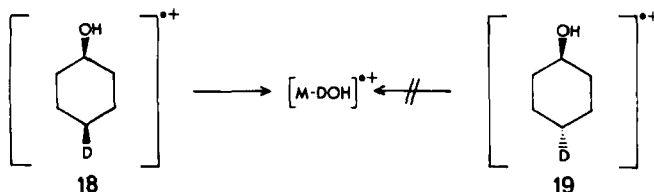


Fig. 12. Stereospecificity of 1,4 loss of water; each deuterated isomer exhibits loss of H_2O as well; results from an MS-902 and a CEC-103 mass spectrometer at 70 eV and threshold voltage.

ation from C-3,5 (Fig. 9) is nonstereospecific (Fig. 13) (37,40).

The differing stereospecificities for 1,4 and 1,3 elimination were hypothesized (37) to follow from the closer distance of approach between the hydroxyl group and the

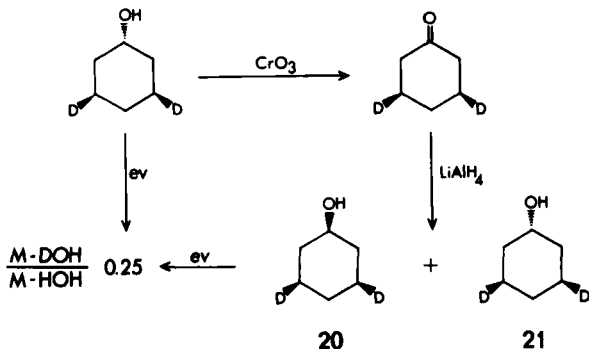


Fig. 13. Stereospecificity for 1,3 loss of water.

C-4 hydrogen over the C-3,5 hydrogens. The longer distance for abstraction from C-3,5, in requiring a higher energy of activation, would give the competitive α -cleavage greater chance for intervention. The α -cleavage process would, in opening the ring, scramble the diastereotopic hydrogens on C-3 or C-5. This cleavage is a major route to fragmentation in EI ionized alcohols and alkoxy radicals (37). In support of this hypothesis the loss of DOH from 3,5-d₂-cyclohexanol has a 0.8 eV higher appearance potential than loss of H₂O. In the 4,4-d₂-cyclohexanol the appearance potential for loss of DOH is now lower than that for H₂O by 0.5 eV (37).

It follows from this proposal that increasing ease of abstraction of the C-3,5 hydrogens would lead to increased competition with α -cleavages and thereby to the observation of stereospecificity for 1,3 loss of water. As seen below, this stereospecificity has been found to be the case for 3-alkyl-substituted cyclohexanols wherein the C-3 hydrogen, now tertiary, may be abstracted with a lower energy of activation than in cyclohexanol.

These results, combined with regioselectivities for elimination of HX from RX (X=Cl, Br, F, SH) compounds of varied structure led to the idea that the abstracted hydrogen needs to be both spatially accessible and within certain maximum allowable distances (37,41). The proposal of 1.8 Å for the ($\text{O}_H^+ \text{H}^-$) distance for abstraction of secondary hydrogen in ionized alcohols (for elimination of water) significantly matches independent proposals for the same distance for hydrogen abstraction by alkoxy radicals (42) and EI ionized ketones (43).

The effect of distance between abstracted hydrogen and hydroxyl oxygen is nicely emphasized by MacLeod and co-workers' studies on the isomers of bicyclo[3.3.1]nonanols (Fig. 14) (44).

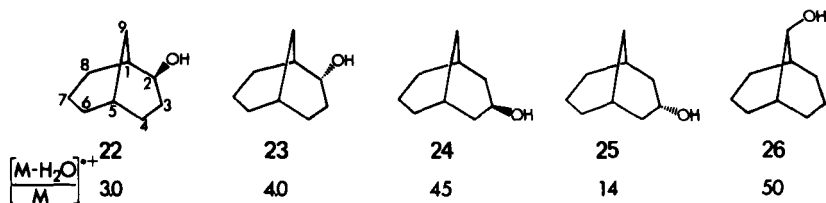


Fig. 14. Water loss intensity from 3,3,1 bicyclic alcohols. Data taken from an MS-902 mass spectrometer at 12 eV and 150°C.

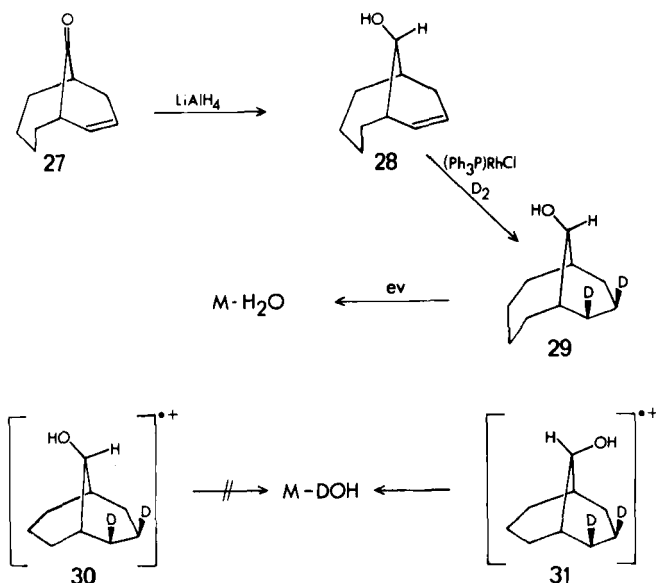


Fig. 15. Assignment of configuration to 27 by mass spectrometry (see Figure 14.)

The ease of elimination of water as measured by the ratio $[M-H_2O/M]^+$ was connected by the authors (44) to the availability of abstractable hydrogens within 1.8 Å. Deuterium incorporation shows that in the 3-exo alcohol, loss of water occurs predominantly from C-9; in the 3-endo, this loss is found overwhelmingly from C-6,7,8; in the 9-alcohol loss occurs from C-3 of the synbridge. The 2-endo alcohol was not labeled at C-7. Significantly, the 2-exo alcohol (Fig. 14) allows no hydrogen to approach within less than 2.5 Å to the hydroxyl oxygen. In the 3-exo and endo and the

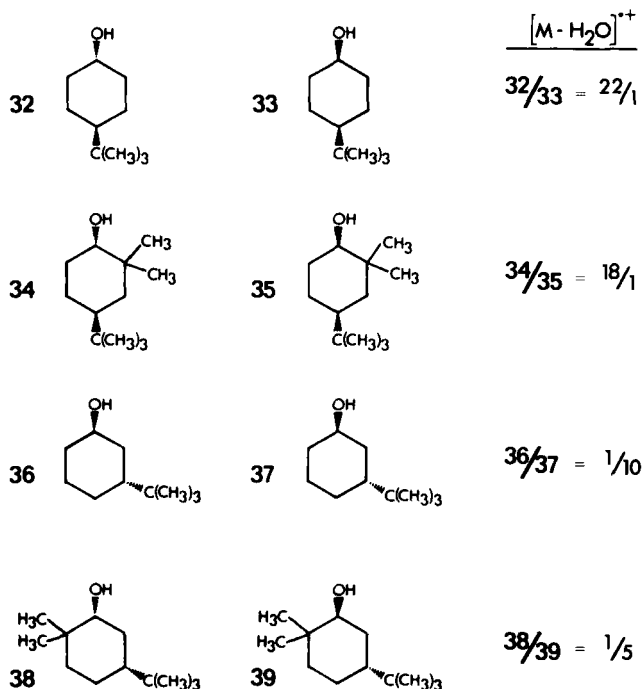


Fig. 16. Loss of water from various tertiary butyl-substituted cyclohexanols. Percent of total ionization above m/e 24 ($\Sigma_{24} m-18$). Data taken on an MCH-1303 mass spectrometer at 70 eV by direct inlet. Temperature not specified.

9 alcohols, at least two hydrogens, shown by labeling to be eliminated, may approach within 1.8 Å. This careful study (44) (Fig. 14) allowed the authors to assign the configuration at C-10 to the closely-related bicyclic alcohol produced by lithium aluminum hydride reduction of 2-bicyclo[4.3.1]-decen-10-one (27) (Fig. 15) (45).

The 10-alcohol in the [4.3.1] system, syn to the 3-bridge, could not be obtained as reduction gave only the epimeric alcohol syn to the larger bridge (Fig. 15).

The absence of loss of heavy water from 29 demonstrates that the hydroxyl group faces away from the unsaturated bridge in the precursor 28. That the unobtainable syn alcohol in the [4.3.1] system would yield loss of heavy water is strongly suggested by the results on 30 and 31.

Further insights into these phenomena arise from results on tertiary butyl-substituted cyclohexanols (Fig. 16).

An important point to be derived from these data (Fig. 16) is that energetic parameters are not determinant. There

is no correlation between elimination and axial or equatorial hydroxyl groups. Moreover, the molecular sets, 32/33 and 34/35, with available and unavailable tertiary hydrogens at C-4 (six-membered ring-transition state for elimination) exhibit the greatest differences. This is consistent with the results found for cyclohexanol (37). Further, *gem*-dimethyl substitution, weakening the bond to the carbinol center and thus enhancing the stereoisomerically destructive α -cleavage, decreases the stereoselectivity. The differences in the 3-*t*-butyl substituted alcohols, 36/37 and 38/39, strongly suggest that 1,3 elimination of tertiary hydrogens occurs stereospecifically, in contrast to unsubstituted cyclohexanol (46). Similar general conclusions may be drawn from Russian work (Fig. 17) on 4-methoxy-3-*t*-butyl substituted cyclohexanols (47).

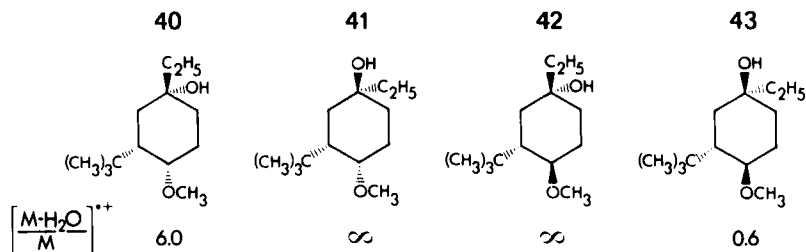


Fig. 17. Elimination of water demonstrating dependency on the 4-substituent. See Figure 16 for instrumental conditions.

Alcohols 41 and 42 with access (through the boat conformation) to the available hydrogen at the carbon bearing the methoxy group eliminate water readily. The ease of elimination of water from 40 over 43 almost certainly arises via abstraction of the activated hydrogens on the methoxyl group as will be well supported by research to be discussed below. Russell (48) has discussed ease of hydrogen abstraction by free radicals. Substitution by electron withdrawing groups decreases the bond dissociation energy thereby giving increased propensity for transfer of hydrogen atoms.

Related research on 3- and 4-substituted cyclohexanols (Fig. 18) (49) indicates that the presence of competitive cleavages and rearrangements will preempt the loss of water in less attractive situations (i.e., 33, 35, 36, 38, 43). In *cis*- and *trans*-4-methylcyclohexanol, although a C-4 tertiary hydrogen is available only in the *trans* isomer, the $[M-H_2O/M]^{++}$ ratio for *trans* to *cis* is only 13/1. The ratio obtained under the same conditions for 32/33 (Fig. 16) is 340/1 (Fig. 18). The rapid loss of the tertiary butyl group from 33 ($M-C_4H_9$ or $C_4H_9^+$) was proposed (49) as providing

$$\left[\text{M} \cdot \text{H}_2\text{O} / \text{M} \right]^{++}, \quad \frac{\text{trans}}{\text{cis}}$$

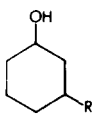
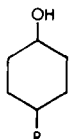
R	CH ₃	C ₂ H ₅	(CH ₃) ₂ CH	(CH ₃) ₃ C
	1.0	1.1	2.0	3.6
	13	5.0	1.3	340

Fig. 18. Stereoselectivity for water loss. Data taken from an Atlas CH-4 mass spectrometer at 70 eV and <70°C.

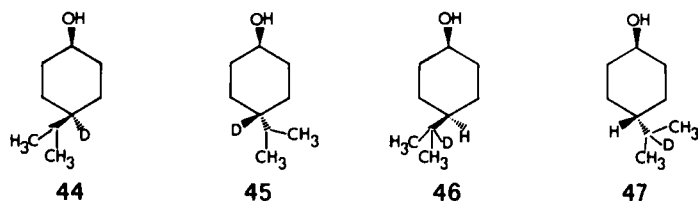
preemptive competition to the slower 1,3 available elimination.

The strange decrease from ethyl to isopropyl in the 4-substituted cases led to the suggestion (49) that 1,5 elimination from the isopropyl group in the *cis* compound could compensate for 1,4 elimination of the available tertiary hydrogen in the *trans*-4-isopropylcyclohexanol. This would act to decrease the observed difference in elimination of water from the isomeric *cis*- and *trans*-4-isopropylcyclohexanol. Brown and co-workers (50) have shown that loss of water may occur through seven-membered ring-transition states (1,5) when the hydrogens transferred are accessible and activated. Studies cited above (32) on the 1,4-cyclohexane-diol stereoisomers demonstrated elimination of water through a seven-membered transition state.

Deuteration (51) of the tertiary hydrogens at C-4 and on the pendant isopropyl group did reveal that the *cis*- and *trans*-4-isopropylcyclohexanol isomers eliminate water in the hypothesized (49) highly stereospecific manner (Fig. 19).

It is clear from the results in Figure 19 that proximity of approach of the hydroxyl group and the isopropyl group in the *cis* isomer allows loss of the available hydrogen. These interactions were presumed to occur through boat (or flexible form) intermediates. Reactions through unstable conformations of cyclohexane are well documented in accessible phase reactions (52), and thus proposals of highly energetic molecular ions are not necessary.

These ideas of elimination of water occurring in competition with other fragmentations and via the abstraction of

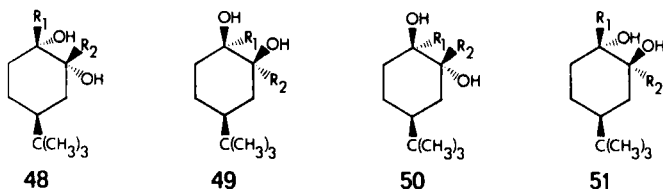


	%M-DOH	%M-HOH
44	13	87
45	81	19
46	82	18
47	17	83

Fig. 19. Stereoselectivity for water loss revealed by deuterium labeling; CEC-103 mass spectrometer at 70 eV and 130°C.

hydrogens that can be brought within bonding distance are supported by a general study on *t*-butylcyclohexanediols (Fig. 20) (53). The decrease in elimination of water and the absence of stereochemical dependence for 48-51 ($R=CH_3$) is in line with increased α -cleavage (C-1, C-2) of the tetra-substituted bond. Such weakening of this bond will act to preempt loss of water by making other cleavage processes more competitive. Further, only in 48 does the tertiary hydrogen on C-4 become available to *both* hydroxyl groups through 1,4 and 1,3 abstraction.

These ideas find further support in a wide range of alcohols discussed below.



$[M \cdot H_2O/M]^+ (12\text{eV})$	48	49	50	51	
	9.75	0.28	0.02	0.87	$R_1=R_2=H$
	.04	.04	.04	.04	$R_1=CH_3, R_2=H$

Fig. 20. Effect of geminal substitution on elimination of water. For $R_1=H, R_2=CH_3$; $R_1=R_2=CH_3$ there occurred no water elimination. From an MS-902 mass spectrometer at 70 eV and 80°C.

B. Steroid, Terpene, and Related Alcohols

The large literature on the mass spectra of compounds of these classes has shown that it is typical to observe stereoisomeric dependence in the spectra. This work, including general papers on the mass spectrometry of these compounds, has appeared in review (54) without stereochemical emphasis.

Klein and Djerassi studied the mass spectra of the 3 α and 3 β alcohols of 5 β -cholane (55). Significantly, the 3 α alcohol, which bears an equatorial hydroxyl group, eliminates water on EI (12 eV) to give an M-18 ion three times more intense than that observed for the axial 3 β alcohol. They noted the potential elimination of the C-9 tertiary hydrogen, which would be available only in the 3 α alcohol. Such a 1,5 abstraction would parallel the situation in *cis*-4-isopropylcyclohexanol (51). Their results on the C-9 deuterated 5 β -cholan-3 α - and 3 β -ols are presented in Fig. 21. For the 3 α alcohol, about 80% of the loss of water appeared as loss

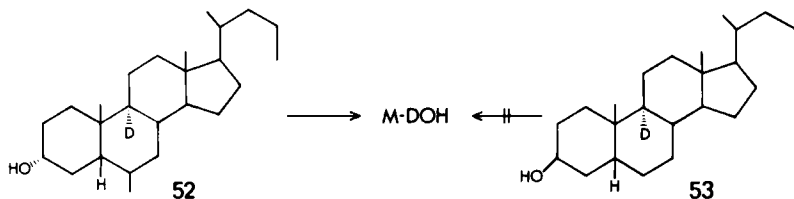


Fig. 21. Stereosepcific water elimination from a 5 β sterol. Data at various beam energies on the MS-9 mass spectrometer at 180°C by direct inlet.

of heavy water (M-19), while the 3 β isomer exhibited only elimination of water (M-18). Models show that the C-9 tertiary hydrogen may be brought within 0.4 Å of the 3-hydroxyl group in the boat conformation of ring A.

Many exemplary studies demonstrating the principle of proximity for bonding have been carried out at the USSR Academy of Sciences. This work has been critically discussed by Meyerson and Weitkamp (11) and Budzikiewicz (56). The observations of a wide spectrum of structural types are exceedingly useful. The mass spectral results on elimination of water from the methyl ethers of 14-hydroxy-*D*-homoestrones (54-57) and isoestrone (58, 59) are presented in Fig. 22 (56, 57).

Dreiding models show that the C-9 tertiary, benzylic hydrogen may be brought, without undue strain, within 2 Å of the abstracting hydroxyl oxygen atom in all cases where

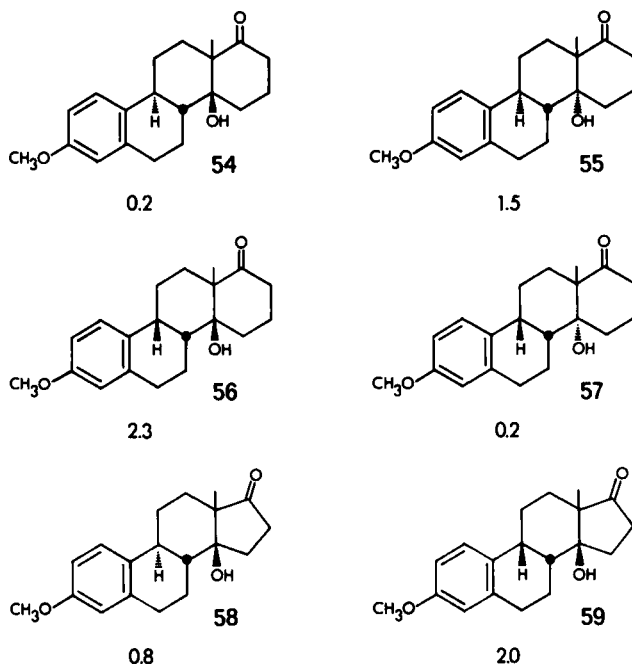


Fig. 22. Elimination of water from homoeestrone stereoisomers. Direct inlet at 70 eV on an MX-1303 mass spectrometer; the numbers are the ion intensity ratios for M-H₂O/M.

this hydrogen is *cis* (55, 56, 59) to the hydroxyl group. The C-9 hydrogen in the *trans* isomers (54, 57, 58) is not accessible without prior ring rupture. The ease of spatial accessibility of this rather activated hydrogen is certainly reflected in the greater propensity for water loss (Fig. 22). An attempt at deuterium labeling, although with poor incorporation, nevertheless demonstrated (57) greater loss of heavy water ($M-19$) in 55 (9,11 d_2) and 56 (9,11 d_2) over 54 (9,11 d_2) and 57 (9,11 d_2). The molecules deuterated at C-8 gave molecular ions that in no case eliminated DOH (57).

The 11-hydroxy- and 16-hydroxyprogesterone (60-63) stereoisomers provide another molecular set demonstrating these proximity effects (Fig. 23) (58).

Models show that the hydroxyl group in 61 cannot approach the secondary hydrogens at C-1 within 2 Å and that the 1,4 related C-14 hydrogen is available only through the impossible C-ring boat. The hydroxyl group in 63 may abstract hydrogen only from the methyl group. Both compounds (61 and 63) show little loss of water. In contrast, both ring

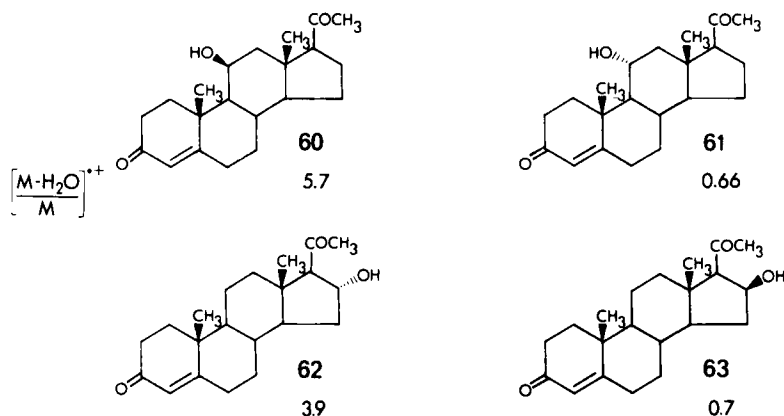


Fig. 23. Water loss from progesterones. Mass spectra by direct inlet on an MX-1303 mass spectrometer at 145-165°C at 70 eV.

juncture methyl groups in 60 are within bonding distance (1.4 Å) without conformational change. The intense loss of water from the molecular ion of 62 is remarkable if it involves the C-14 tertiary hydrogen. The distance in the relaxed Dreiding model is >3Å. The speculative correlation flowing from the data of Figures 22 and 23 is supported by the addition of further studies on bile acids. These interesting molecular templates (Fig. 24) provide a useful

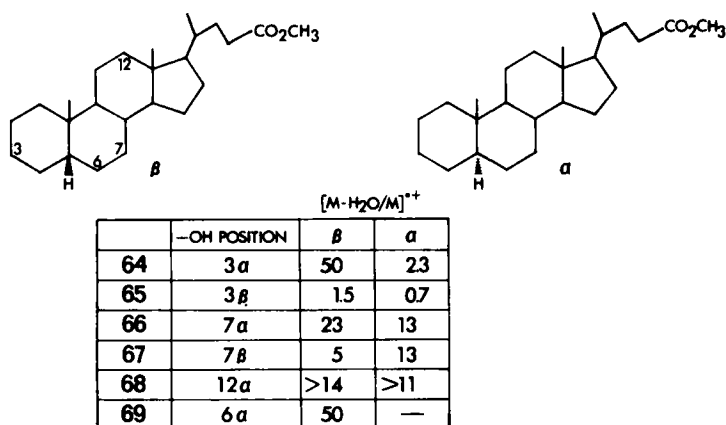


Fig. 24. Stereoisomeric dependency for water elimination from bile acids. Mass spectra on an LKB 9000; temperature and voltage not specified.

test of predictability of the propensity for EI elimination of water (59).

The speculative correlation that flows from the data of Figures 22 and 23 is supported by the addition of further studies on bile acids. These interesting molecular templates (Fig. 24) provide a useful test of predictability of the propensity for EI elimination of water (59).

The two configurations exhibiting the highest ratio of $[M-H_2O/M]^+$ are the 3 α and 6 α alcohols of the 5 β cholanolic acids (64 β and 69 β). The former molecule is directly analogous to 5 β -cholan-3 α -ol studied by Klein and Djerassi (55). As they round, the 3 α alcohol loses water on EI by abstraction of the C-9 tertiary hydrogen while the 3 β epimer has no such possibility. The 6 α -alcohol molecular ion is also well disposed for elimination. Models show that the twist-boat conformation of ring B (rings A and C, chair) is relatively free of eclipsing interactions and the 6 α -hydroxyl group is within 1.6 Å of the C-1 and C-3 α hydrogens. These abstractable hydrogen atoms are also related 1,4 (six-membered ring for transfer) to the hydroxyl group. The 1,4 relationship for elimination is highly favored in both cyclic and acyclic model alcohols (26, 27, 37). A less distinct situation exists for loss of water from the 7 α alcohol (66 β) in the 5 β cholanolic acid. The all-chair conformation allows this hydroxyl group to approach within 1.6 Å of the C-4 α hydrogen. This abstraction is related through a six-membered ring as for 69 β above. Significantly, 69 β eliminates water on EI with twice the relative intensity of $[M-H_2O/M]^+$ and has available two similarly related carbon-bound hydrogens (see above). Similar conjecture serves for analysis of the other isomers as well, and models show reasonable consistency with the ease of elimination of water. The system clearly calls for further scrutiny by deuterium labeling. It seems very likely that studies of detail will reveal that the positions of hydrogen abstraction are conformationally sensible.

An apt demonstration of this regioselectivity for elimination of water is found in studies (60) of 3 β ,12 α ,17 β -trihydroxy-5 α -androsterane (70) and the 12 β isomer (71) pictured in Figure 25.

In both 70 and 71 the ion for elimination of water on EI is intense. Nevertheless, the molecular ion from 70 is absent from the spectrum while 71 yields a low-intensity molecular ion. These results imply that 70 has available a lower energy pathway for decomposition than does its 12 β isomer. Indeed, 70 exhibits only two major ions, $M-H_2O$ and $M-H_2O-CH_3$, while the $M-H_2O$ ion from 71 fragments to eliminate a methyl radical to only a small extent. The ready loss of a methyl radical from the $M-H_2O$ ion derived

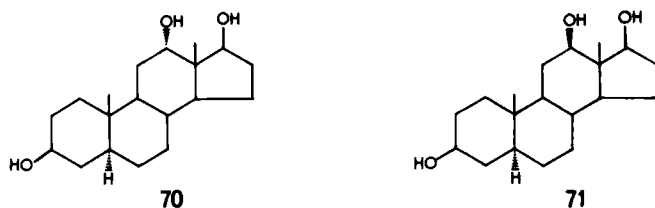


Fig. 25. Androstane isomers studied for water elimination. Measured on an Atlas-CH-4 mass spectrometer at 70 eV and 80°C.

from 70 and a lower molecular ion intensity from 70 both find ready explanation in potential loss of the accessible 17 α activated hydrogen. This hydrogen of reduced bond energy (48) provides a radical site adjacent to the C-18 methyl group, enhancing its loss, and providing as well a low-energy pathway for water elimination. This will reduce the intensity of M^+ from 70. Although the C-18 methyl group was not labeled, the 17 α -hydrogen was substituted by deuterium in both 70 and 71. The former sterol (70) eliminates DOH, while the 12 β epimer does not (60).

Karliner, Budzikiewicz, and Djerassi have uncovered stereospecificity for EI elimination of water from the C-3 epimers of cholestan-3-ol (61). Their case is unique in that elimination of water occurs only after loss of a methyl radical from the molecular ion. Figure 26 presents their findings. The percentages are the fraction of water loss appearing as heavy water. Again, as in the androstanes (60), an activated (i.e., bond weakened) hydrogen is sterically accessible in a 1,3 relationship to the hydroxyl group. The significance of the fact that the cholestanol study involved elimination from an overall even-electron ion is not presently apparent.

Further evidence for the EI steric sensibility of sterols and related fused rings comes from the findings by Fenselau and Robinson (62) that steroid diols capable of

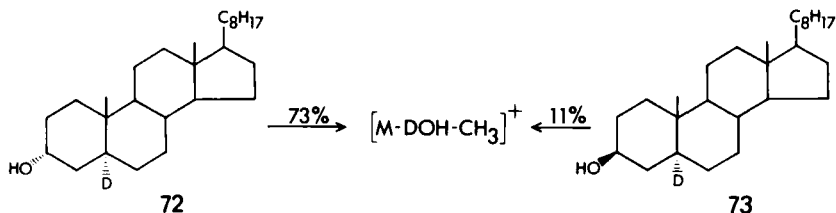
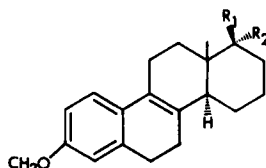


Fig. 26. Unusual water elimination from an even electron ion. Data taken on a CEC-21-103C spectrometer at 70 eV and direct inlet.

internal hydrogen bonding in solution exhibit EI loss of dideuterium oxide from the deuterium exchanged diols.

This predictability is manifested in understanding the relative ratios of $[M-18/M]^+$ from the mass spectra of various 3-methoxy-17-alkyl- $\Delta^{1,3,5(10),8D}$ -homoestratetraen-17-ols (74-77, Fig. 27) (63).



	R ₁	R ₂	$[M-18/M]^+$
74	OH	CH ₃	0.4
75	CH ₃	OH	3.2
76	OH	C ₂ H ₅	0.2
77	C ₂ H ₅	OH	2.3

Fig. 27. Stereoselectivity for water loss from homoestratetraenols. Spectra taken on an MX-1303 mass spectrometer at 70 eV by direct inlet at 100°C.

Dreiding models show that the hydroxyl group in 75 and 77 may approach within 1.8 Å of the tertiary allylic hydrogen at C-14, and further, that this may occur in the chair conformation of ring D. This attractive hydrogen is unavailable to the β alcohols in any conformation. The prediction of increased water elimination from the molecular ions of 75 and 77 is in line with the facts (Fig. 27) (63). Similar findings were obtained on the analogous five-membered D-rings of 74-77 (64). Early success in the observation of stereoisomeric dependence of the mass spectra of sterols led this Russian group to presciently conclude (63) that "The results obtained permit a new approach to the determination of the configuration of steroid and possibly other cyclic alcohols by means of mass spectrometry."

In a series of sixteen pairs of diterpene epimers studied by Enzell, Wahlberg, and Gunnarsson (65) these principles were applied to relating the relative EI elimination of water to the configurations of these materials. Certain of their data are reproduced in Figure 28.

Although the foundations of the stereoselectivities observed (65) for compounds 78-83 may only be revealed by necessary labeling experiments, one can already see the return on earlier investments on model systems. Thus both 78 α and 79 α allow the hydroxyl group to approach well within 1.6 Å of the C-5 hydrogen in the boat conformation of ring A. This proximity to the C-5 tertiary hydrogen is denied to the β epimers. This situation parallels that for the isomers of 4-*t*-butylcyclohexanol where high stereospecificity was observed for EI loss of water (33, 34). The hydroxyl group of the β -isomer has available only more costly carbon-hydrogen

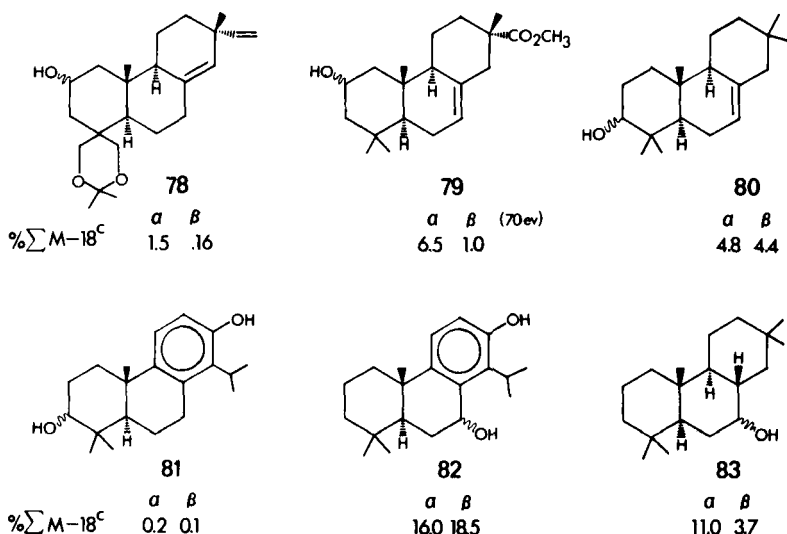


Fig. 28. Water elimination from diterpene epimers. Mass spectra taken on an LKB 9000 by direct inlet and source temperature 270°C. α and β refer to the configuration of the hydroxyl group (α , down; β , up). The numbers are expressed as percent of total ionization; the M^{+} intensity was not given; the numbers here are the average of values given in the original paper (65).

bonds to break to form a molecule of water for elimination. It seems significant that substitution (80 and 81 α,β) adjacent to the carbon bearing hydroxyl group has been seen before to substantially reduce or eliminate stereoisomeric dependence for EI water loss (Figs. 16 and 20) and this is found for 79 α,β compared to 80 α,β and 81 α,β . In addition, in both 80 α and 81 β the C-5 tertiary hydrogen is now related in a less favorable 1,3 position to the hydroxyl function. This allows more energetic routes of the β alcohols to compete more effectively and thus reduce the stereochemical effects.

Series 81 and 82 offer a significant contrast. In both 82 α and 82 β the hydroxyl oxygen may approach to within 1.4 Å (Dreiding Model) of the tertiary benzylic hydrogen on the pendant isopropyl group. The increase in EI loss of water between these constitutional isomeric sets is a startling demonstration of the importance of this proximity.

The isomeric difference in 83 may be ascribed to the two 1,3 related tertiary hydrogens in the isomer unavailable in 83 β . Model studies on 3-*t*-butylcyclohexanol discussed above (Fig. 16) demonstrated that 1,3 tertiary hydrogen availa-

bility leads to large isomeric effects on EI elimination of water. The lower activation energy (E_0 in eq. [1], Sect. I-C) for rearrangement by abstraction of the bond-weakened tertiary hydrogens is nicely reflected in the reduced molecular ion intensity for 83α (Fig. 29). This is a general phenomenon.

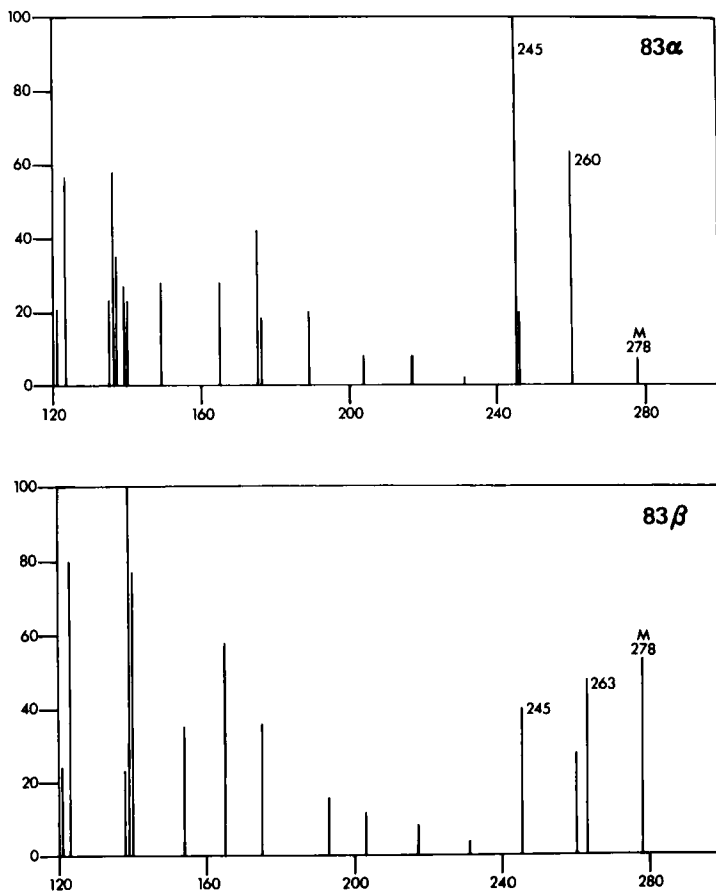


Fig. 29. Mass spectra showing relationship of water loss to molecular ion intensity (see Figure 28). Spectra taken at 70 eV.

Similar arguments regarding the other isomeric sets studied (65) may effectively rationalize the observations. Although the qualitative principles seem established, the detailed validity of these arguments must await more focused experiments. Such experiments are also awaited to elucidate other stereoisomeric effects on sterol mass spectra (66).

C. Polyalcohols and Ethers

Although there is an infinite difference in the EI loss of water from the stereoisomers of *cis*- and *trans*-4-*t*-butylcyclohexanol (33, 34), the methyl ethers of these isomers show difference measured under the same conditions that are less distinct (67). The *trans* isomer continues to find less energetic routes to elimination, methanol in this case, while the *cis* isomer exhibits a substantial ion intensity at $[M-CH_3-OH]^+$ as well (Fig. 30).

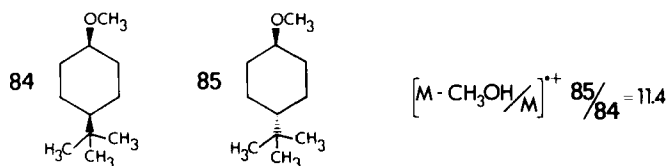


Fig. 30. Stereoselectivity for elimination of methanol. Photoionization at room temperature on an MS-9 mass spectrometer.

These results (67) may be interpreted as demonstrating, first, that the proximal effects for rearrangement loss of water are in force in the related ethers. Second, the reduced stereospecificity for EI elimination of methanol is consistent with studies on cyclohexyl methyl ether and cyclohexyl chloride. Klein and Smith (68) found for cyclohexyl methyl ether that the 1,3 EI elimination of methanol is enhanced over the EI 1,3 elimination of water from cyclohexanol. Whereas the ether exhibits 66% of abstracted hydrogen from C-3 and C-5 of the ring, the alcohol shows only 41%. The increased availability of 1,3 hydrogens in the *cis*-4-*t*-butylcyclohexyl methyl ether opens a competitive route for elimination of methanol from the less-favored isomer. Significantly, increased EI 1,3 elimination of HCl from cyclohexyl chloride was shown to involve only the ring hydrogens *cis* to the pendant chlorine, while EI 1,3 elimination of water involved both geminal diastereotopic hydrogens on C(3) and C(5). This result suggests ring rupture and thereby higher energy of activation. The demonstrated increased ease of EI 1,3 elimination of HCl is reflected in no observable difference for EI loss of HCl between *cis*- and *trans*-4-*t*-butylcyclohexyl chloride (37). It was proposed the *trans* isomer eliminated HCl via the C-4 tertiary hydrogen, while the *cis* isomer has available the now accessible C-3,5 hydrogens. This increased abstraction of hydrogen through larger distances (i.e., models show a hydrogen on C-4 may approach a group located on C-1 closer than a

hydrogen on C-3) has been quantitatively related to the size of the abstracting atom (37, 41). Significantly, the O-H bond distance in R-O-H is longer than that for H₂O (69), in line with these ideas that ethereal oxygen has a longer reach than hydroxyl oxygen.

The symmetrical 1,3,5-trimethoxycyclohexane epimers (70) provide a demonstration of this ease for 1,3 elimination and as well introduce a rearrangement unique to dimethyl ethers. As exhibited in Figure 31, the fragmentation pathways

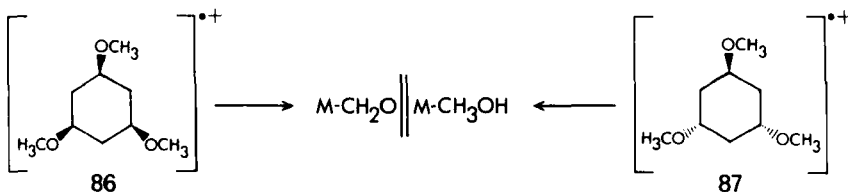
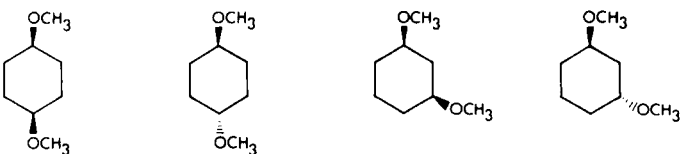


Fig. 31. Spatial dependency for rearrangements of ethers. 70 eV and 150°C on an MS-9 mass spectrometer.

lead *trans*-1,3,5-trimethoxycyclohexane (87) to eliminate CH₃OH under electron impact while the *cis* isomer uniquely pushes out CH₂O. Deuterium labeling showed that 90% of the CH₃OH lost from 87 involved the axial methoxy group and, as expected, that the elements of CH₂O from the molecular ion of 86 involve a methoxyl methyl group. These findings are consistent with a favorable 1-3 abstraction of hydrogen to the axial methoxyl group in 87. In 86, on the other hand, where no EI loss of CH₃OH is observed, these hydrogens are inaccessible. Significantly, the loss of CH₂O takes precedence over the structurally possible but inactive 1,4 elimination of methanol. The authors (70) propose that hydrogen transfer from one ethereal methyl group to a *cis* ethereal oxygen in the molecular ion of 86 is the fount of this rearrangement loss of CH₂O. Hydrogen transfer of this type finds support in studies of other ethers (71).

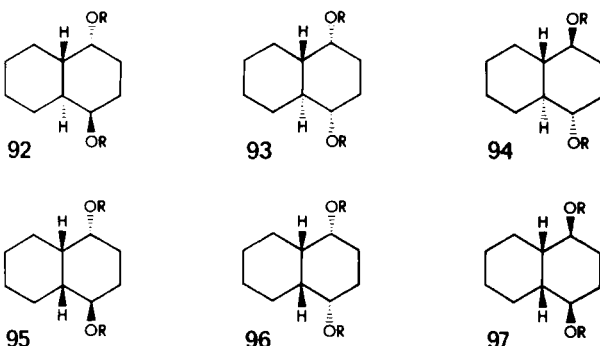
EI measurements on 1,3-dimethoxycyclohexane and 1,4-dimethoxycyclohexane isomers (70) nicely demonstrate (Fig. 32) the proximity effects necessary for observation of the [M-CH₂O]^{•+} and [M-CH₃OH]^{•+} ions. The *trans* isomers in both the 1,4 and 1,3 series (89 and 91) allow bonding interactions between one of the methyl ether groupings and an activated ring-bound hydrogen. This geometry, which obviously enhances loss of CH₃OH, simultaneously does not allow the pendant ether groups to approach each other. Loss of CH₂O from the *trans* molecular ions (89 and 91) is hardly observed (Fig. 32).

Stereoisomeric dependence data from the mass spectra of various 1,4-decalindiols and their methyl ethers (72)



	88	89	90	91
$\% \Sigma_{39}$				
$M-CH_3OH$	5.8	13.9	6.3	14.0
$M-CH_2O$	7.2	0.2	2.4	<0.1

Fig. 32. Isomeric dependence for loss of formaldehyde and methanol. Numbers are the percent of total ionization for the designated ions, i.e., $[M-CH_3OH]^+$ measured as specified in Figure 31.



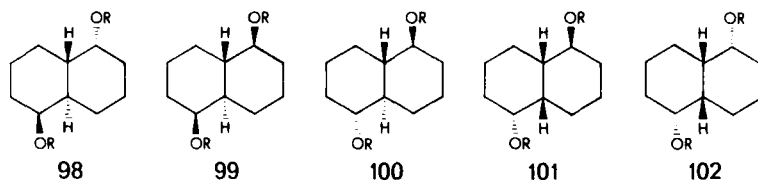
	R	92	93	94	95	96	97
$M-H_2O$	H	8.8	1.8	9.8	7.4	1.8	2.0
$M-D_2O$	D	0.3	1.7	0.3	0.4	1.4	1.3
$M-CH_2O$	CH_3	0.2	0.8	0.2	0.2	0.6	1.2
$M-CH_3OH$	CH_3	5.1	2.6	5.9	3.9	1.8	3.0

Fig. 33. Rearrangement as a function of stereochemistry in decalins. All data presented as percent of total ionization ($\% \Sigma_{39}$); mass spectra taken on an Atlas SM-1B and an Atlas CH-4 at 70 eV and 150°C.

are presented in Figure 33.

There is already gratifying stereosensitivity even in these first-generation observations. The molecular ions, with $R=H$, of 92, 94, and 95 exhibit enhanced elimination of water over the other epimers. These three molecules are unique in allowing one hydroxyl group access to the bond weakened (73)

(i.e., activated for abstraction) carbinol-bound hydrogen. Consistent with the less specific demands for methanol loss (68), these same materials with $R = CH_3$ exhibit decreased elimination compared to the epimeric diethers (93, 96, 97, $R = CH_3$). Further, the alcohols 93, 96, 97 ($R = H$) in which the 1,4 alcohol functions are related cis, exhibit decreased EI loss of water, and that water which is lost is shown by deuterium labeling to involve interaction of the diol functions: $M-D_2O$ in 93, 96, 97 ($R=D$). These results are entirely consistent with the observations on cyclohexane-1,4-diol (32). In that epimeric set, the trans isomer shows facile elimination of water on EI while the decreased banishment of water from the cis isomer arises by loss of D_2O from the dideuterated diol. The cis methyl ethers, 93, 96, 97, ($R = CH_3$), in the related observations show enhanced EI elimination of CH_2O , which is again consistent with the proposed hydrogen transfer from one methoxyl group to another (71). Recent work from the same laboratory (74) on decalin-1,5-diols and dimethyl ethers provide another example (Fig. 34).



	98	99	100	101	102	
$M-H_2O$	4.3	3.3	3.0	4.2	4.9	$R = H$
$M-CH_3OH$	1.6	1.4	1.5	1.8	1.5	$R = CH_3$
$M-CH_2O$	0	0	0	1.3	10.0	$R = CH_3$

Fig. 34. Rearrangement from isomeric decalins. Mass spectra were taken on a MAT-CH-4 mass spectrometer at 70 eV and 150°C. The numbers are the percent of total ionization above m/e 39.

The measurements on the isomers 98-102 with $R = H$ and CH_3 are instructive in that only elimination of CH_2O shows overt dependence on stereoisomerism. This follows from the nature of this fragmentation, which requires interaction of the two functional groups. This interaction is only possible without rearrangement or bond cleavages of the decalin framework in 102, $R = CH_3$. Following from all the results presented above on these and related molecules, it is extremely likely that the elimination of CH_3OH and H_2O from the other isomeric molecular ions occur both regio- and stereospecifically. In the absence of deuterium labeling, these effects will not be

revealed when various more-or-less equivalent hydrogens are available for elimination (51).

In the isomers of monobenzyl monotrimethylsilyl-1,4-cyclohexandiol, the rearrangement reactions are easily perceived since they give rise to stereoisomerically unique fragmentations involving the interaction of the formally remote groupings (75). One of these processes that stands tall among many differences between the mass spectra of the cis and trans isomers (103 and 104, Fig. 35) is the elimina-

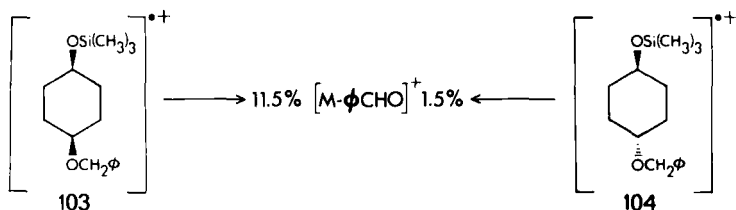


Fig. 35. Isomeric dependence for functional group interactions in 1,4 diethers. Percentages of the total ionization at 12 eV taken on an MS-902 mass spectrometer at 200°C.

tion of the elements of benzaldehyde, $M-C_7H_6O$, from the molecular ion of the cis isomer. Labeling experiments show that a single benzylic hydrogen is retained in the loss of C_7H_6O . It is reasonable and consistent with observations on the methyl ethers discussed above (70) to propose that a boat or twist boat conformation of the molecular ion of only 103 allows transfer of a benzylic hydrogen to the silyloxy group.

D. Sugars and Related Molecules

A number of workers have studied the stereoisomeric dependence of rearrangements in the mass spectra of glycols, sugars, sugar derivatives, and their models (76). This research shows that there is invariable but small dependence of the fragmentation fingerprint on stereochemistry. The foundations of these phenomena remain unresolved. In certain cases, EI reactions of derivatized saccharides are extremely sensitive to configuration (77, 78). These latter effects, which have been ascribed to steric crowding, are exemplified by the mass spectra of the various sets of epimeric benzylidene acetals (105-110) reproduced in Figure 36 and the trifluoroacetylated adenosine isomers (111-114) reproduced in Figure 37. In spite of these clear suggestions (Figs. 36 and 37) of the sensitivity of mass spectrometry to saccharide derivative stereochemistry, and although mass spectrometry is widely

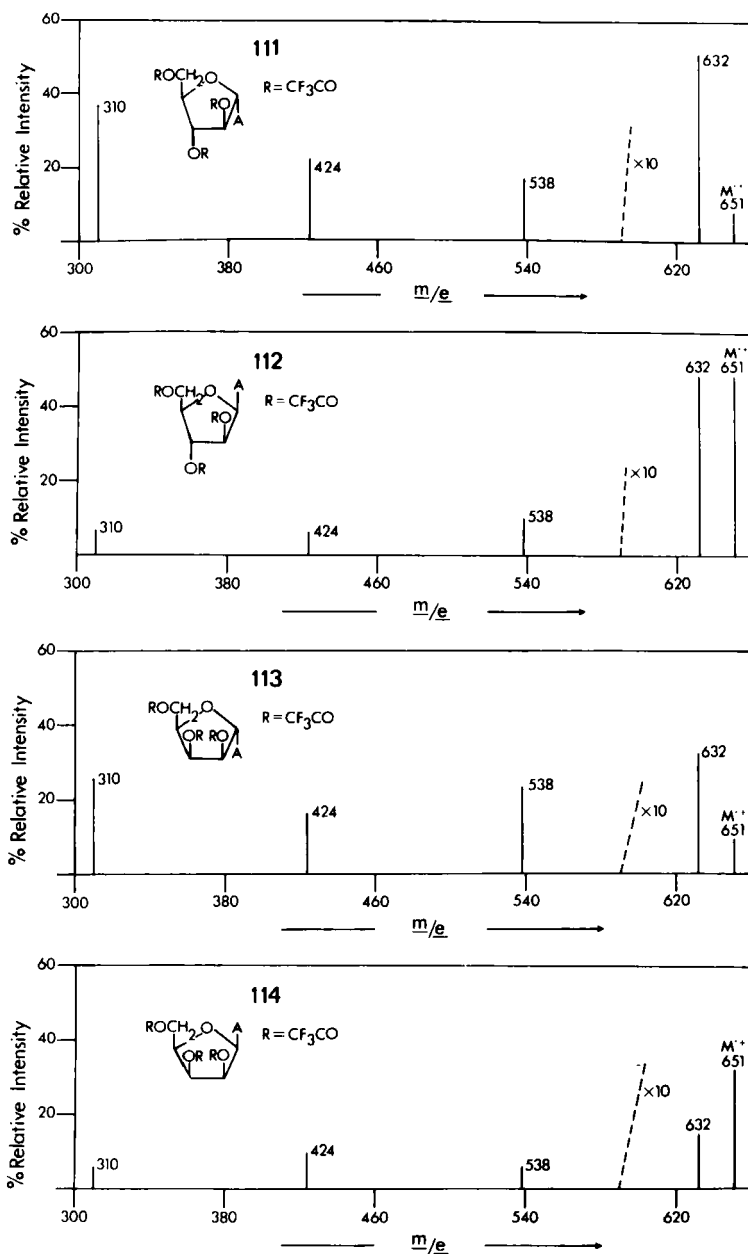


Fig. 37. Mass spectra of trifluoroacetylated adenosine isomers. Spectra measured on an LKB-9000 mass spectrometer by direct inlet at 70 eV and 250°C. Various m/e values correspond to elemental losses as follows: M^+ (651); $(M-F)^+$ (632); $(M-CF_3CO_2)^+$ (358); $M-(CF_3CO_2H + CF_3CO_2)^+$ (424); $M-2CF_3CO_2H + CF_3CO_2)^+$ (310).

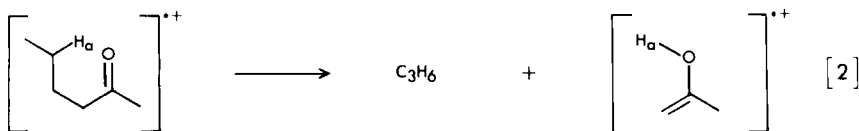
used in structural work on sugars (79), the technique has not been exploited to gain configurational information on these molecules.

In an alternative approach, DeJongh and Biemann converted saccharide stereoisomers to constitutionally isomeric isopropylidene derivatives (80). The latter materials could easily be distinguished by mass spectrometry, thereby secondarily distinguishing their precursor stereoisomers. Pattern recognition has been proposed as a way of consistently distinguishing the mass spectra of stereoisomeric sugars (81). This technique does not require understanding of the fundamental relationship between saccharide structure and the chemistry observed on electron impact. This relationship is the key to progress in this area.

III. STEREOISOMERIC DEPENDENCE IN THE ELECTRON IMPACT INDUCED (EI) REARRANGEMENTS OF CARBONYL COMPOUNDS

A. Spatially Dependent EI Rearrangements of Carbonyl Compounds

The electron-impact-induced gamma-hydrogen transfer to carbonyl oxygen followed by beta-bond cleavage (eq. [2]) has been named in honor of one of its early investigators, F.W. McLafferty. A review has appeared (82).



The allowable distance between the transferred hydrogen (H_a , eq. [2]) and the carbonyl group has been suggested to be less than 1.8 Å, on the basis of studies of steroid ketones by Djerassi and co-workers (83). The maximum allowable angle between the plane of the carbonyl group and that of the transferred hydrogen has been suggested to be about 50 deg., based on studies of medium ring ketones (84).

This research (83, 84) on the spatial dependence for hydrogen transfer has not involved the direct observation of the McLafferty rearrangement but rather the observation of secondary fragmentations postulated as deriving from the McLafferty rearrangement. In addition to this obscuring factor, the molecules studied involve (83, 84) many structural changes in addition to that focused on, i.e., distance and angle between the carbonyl group and the potentially abstracted hydrogen. These widely variable structural parameters and their affect on fragmentation are illunderstood,

leaving one assigning McLafferty rearrangement propensities to factors somewhat arbitrarily chosen. This research, although weak in making general and extrapolatable assignments of quantitative distances and angles, nevertheless is extremely useful in leaving no doubt that these spatial factors are heavy determinants in the possibility for hydrogen rearrangement to carbonyl groups under electron impact. This spatial dependence must give rise to stereoisomeric dependence on these and related EI rearrangements. This has been observed.

Thomas and Willhalm (85) early found that the mass spectra of the exo and endo acetyl- and formylnorbornanes (115-120) were first, widely different (Fig. 38) and second,

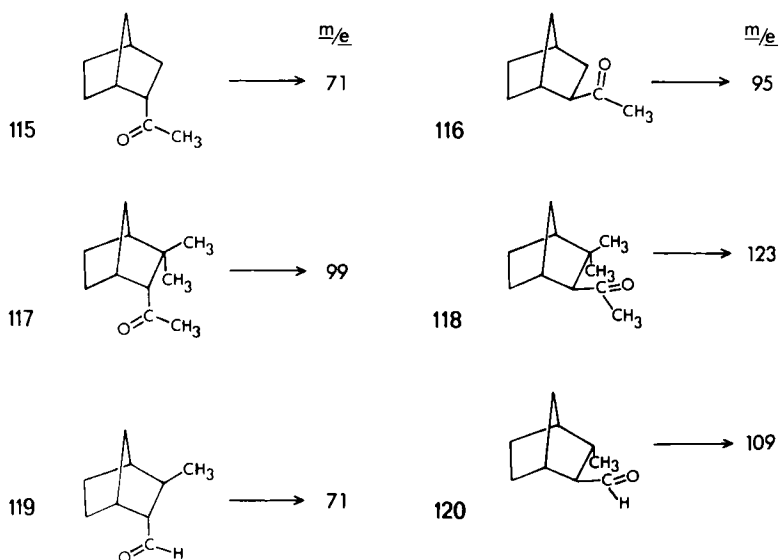


Fig. 38. Stereoisomeric dependence for rearrangement in bicyclic ketones. The ions designated are the most intense peaks (m/e) in each mass spectrum.

interpretable, if viewed as spatially dependent McLafferty rearrangements (Fig. 39).

In each case, (Fig. 38) the ion intensity at the alternative m/e position is minor for each epimeric set. Clearly there is a driving force for rearrangement uniquely at work in the endo isomers 115, 117, and 119. The exo compounds exhibit expulsion of the acyl grouping (Fig. 39). As will be seen below, the loss of R_3CO from the molecular ions of the exo compounds appears to be one example of a general pheno-

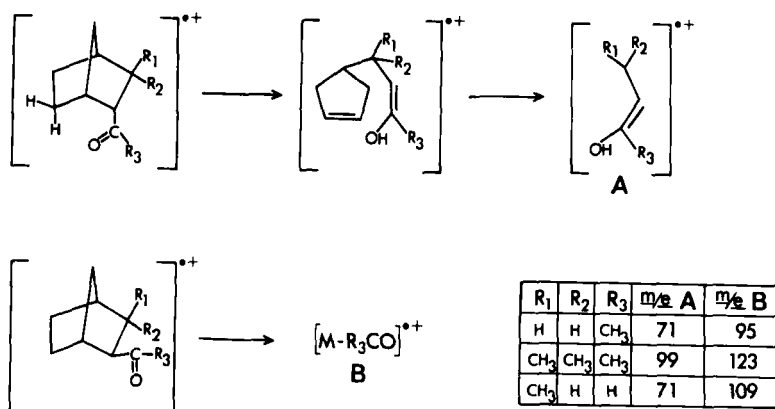


Fig. 39. Possible ion structures for the rearrangement ions of Figure 38.

menon studied in detail in the norbornyl bromides. The elimination of the C₅ fragment in the exo series, leaving an ion with the elements of [A]^{•+}, was not confirmed, since labelling experiments at the position of proposed hydrogen transfer were not carried out. Nevertheless the differential observations for exo and endo isomers are striking and entirely consistent with the spatial accessibility for 1,4 hydrogen transfer for rearrangement only in the endo compounds. In line with Djerassi's view (83), the C₆ endo hydrogen is ca. 1.2 Å from the carbonyl oxygen, while the syn hydrogen on the one-carbon bridge also related 1,4 to the exo carbonyl grouping is 2 Å away.

The 5α and 5β epimers of 4,4-dimethyl-6-androstanone (121, 122, Fig. 40) undergo a rearrangement involving loss of ring A (86). This was seen by the authors as an example of the McLafferty rearrangement. Their proposal (Fig. 40) is independently identical to that hypothesized by Thomas and Willhalm (85) for the rearrangements observed in 115-120.

Deuterium labeling of the gem dimethyl groups showed that the transferred hydrogen was largely from the methyl groups in both epimers 121 and 122, although the transfer was not clean. The spectra are striking in comparison since the m/e 219 ion in 122 takes the lion's share of the fragmentation (Σ₂₈ 20.8%), while the ion of the same m/e value in 121 is one of many intense peaks in the spectrum (Σ₂₈ 3.8%). Significantly, in line with an easy low energy rearrangement, the 5β compound 122 molecular ion intensity is less than one third of that of 121.

Dreiding models show that the ring-intact all-chair

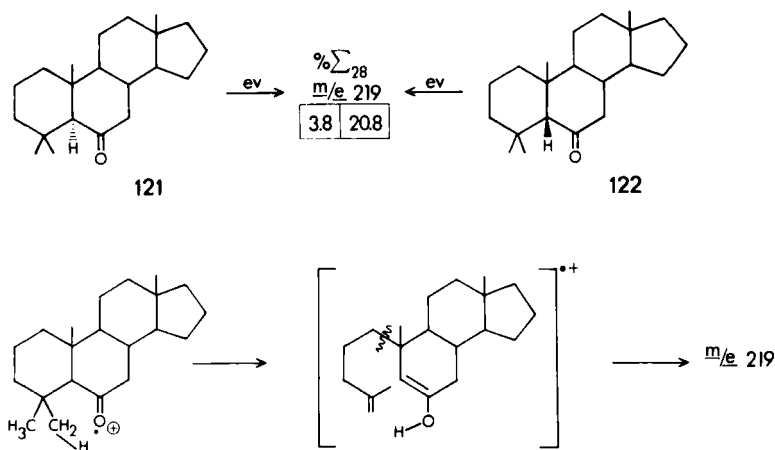


Fig. 40. Stereoisomeric dependence for rearrangement in 5 α and 5 β , 6-ketosteroids. Measured on an Atlas CH-4 mass spectrometer at 70 eV and 200°C; percent of total ionization from m/e 28 to the molecular ion.

conformations (rings A and B) of **121** and **122** allow the carbonyl group to approach within 1.6 Å of the hydrogens on the C-4 α methyl group. The apparent ease of rearrangement in **122** over **121**, although subject to quite reasonable conformational proposals, is a subject for further experiments.

Other examples of stereoisomeric dependence for proposed rearrangement of hydrogen to carbonyl (87, 88) demonstrate that proximity of hydrogen is the key. In particular, the later reference (88) is rich in stereoisomerically dependent fragments involving proposed and likely regiospecific hydrogen rearrangements. The various hypotheses (88) were not further supported by deuterium labeling. These stereoisomers are exhibited in Figure 41 (88).

The EI elimination of methanol and methoxy radical by **123** and **124** wane and wax with the former preferentially cleaving $(M-OCH_3)^{+}$ while the latter exhibits a more intense ion at $(M-CH_2OH)^{+}$. This behavior may be postulated as arising from the accessibility of the C-9 (bridge) tertiary hydrogen only in **124**. Significantly, in the related stereoisomers **125** and **126** there is no cleavage to yield $(M-OCH_3)^{+}$, but rather both compounds eliminate the elements of methanol on electron impact, **125** with far greater facility. In each case the benzylic (**125**) or tertiary hydrogen (**126**) is accessible to the carbonyl group (within 1.6 Å) in the intact molecular ion. The carboxylic acids **127** and **128** in contrast show mutually exclusive EI elimination of the elements of HCO_2H

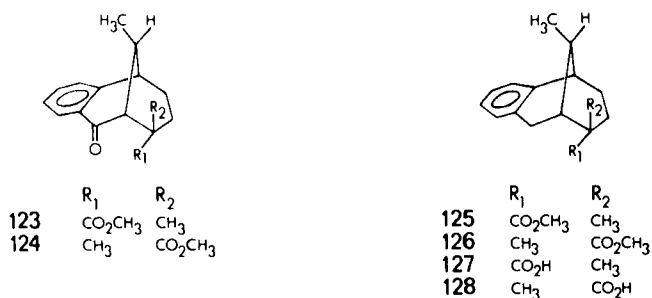


Fig. 41. Bicyclic isomers studied for the epimeric dependence of their mass spectra (88).

and CO_2H , respectively. Whatever may be the ultimate sources of this behavior, it is likely that the presence of the benzylic endo hydrogen within 1.6 \AA of the carbonyl group is important to this difference. It is precisely this access of a carboxyl grouping to a benzylic hydrogen in gibberellins and related compounds that is the foundation of a mass spectral approach for assignment of stereochemistry in these molecules (89).

The various gibberellins studied by Gray and Pryce (89) are represented in Figure 42.

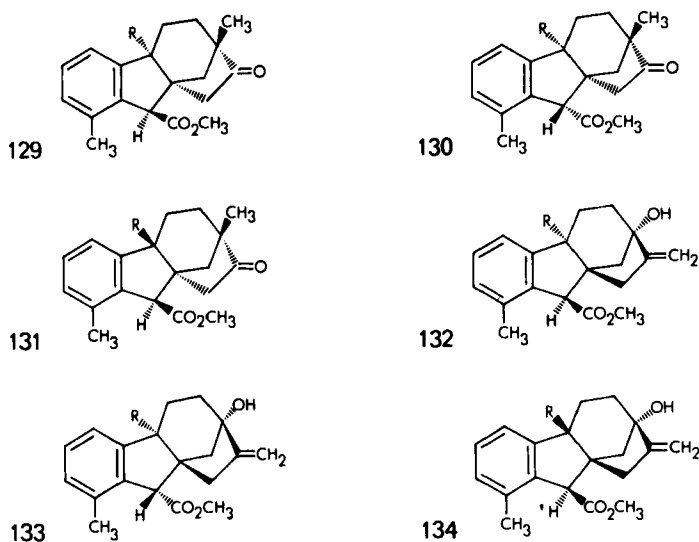


Fig. 42. Gibberellin isomers studied by mass spectrometry. In each case $R=H$ or D .

The mass spectra of the epimers, taken at 250°C and 70 eV, are distinct. The most intense ion in the spectra of 130 (R=H), 131 (R=H), 133 (R=H), and 134 (R=H) appears at m/e 138, and is shown by high resolution mass spectrometry (89) to correspond to the EI loss of the elements of the carbomethoxyl group plus a single hydrogen. The spectra of the other isomers 129 (R = H) and 132 (R = H) are more complicated, show a higher intensity molecular ion, and exhibit in both cases an ion at m/e 139 of higher intensity than that at m/e 138. This ion (m/e 139) involves the loss from the molecular ion of only the elements of the carbomethoxyl group. Substitution of deuterium for hydrogen in all cases (R=D) causes at least 80% of the hydrogen atom involved in the formation of m/e 138 to be replaced by deuterium, i.e., $[M-C_2H_3O_2D]^+ \cdot$ instead of $[M-C_2H_4O_2]^+ \cdot$.

It is clear that the EI elimination of the benzylic tertiary hydrogen cis to the pendant carbomethoxyl group in 130, 131, 133, and 134 (all R = H) is responsible for the intense ion of m/e 138. The first point of interest is the exceptional distance between the carbomethoxyl group and this hydrogen which is $>2 \text{ \AA}$ in the relaxed Dreiding model. This appears to be another example in which decreased bond strength for the eliminated hydrogen allows a longer distance between the heteroatom and the hydrogen in the abstraction step. The stereoisomerically dependent elimination of $C_2H_4O_2$ from the molecular ions allowed the assignment of configuration (89) to two unknown molecules of this structural type (Fig. 43).

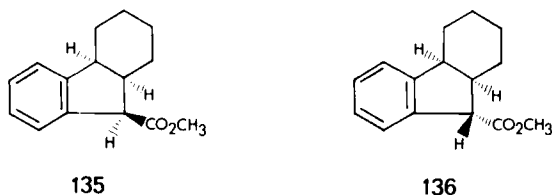


Fig. 43. Molecular configurations assigned by mass spectrometry (89).

The two materials, 135 and 136, were known to be epimeric at the carbon bearing the carbomethoxyl group. One of the unassigned stereoisomers gave a mass spectrum, under the same conditions as for compounds 129-134, in which the most intense ion appeared at m/e 171. The other exhibited a slightly less intense ion of m/e 170. The two fragments correspond to $[M-C_2H_3O_2]^+ \cdot$ and $[M-C_2H_4O_2]^+ \cdot$, respectively, and, therefore, the molecule giving rise to the most intense ion m/e 170 was assigned structure 136 (Fig. 43) (89).

Lansbury and his co-workers (90) have utilized a similar phenomenon to assign configuration to the epimeric synthetic intermediates 137 and 138 (Fig. 44).

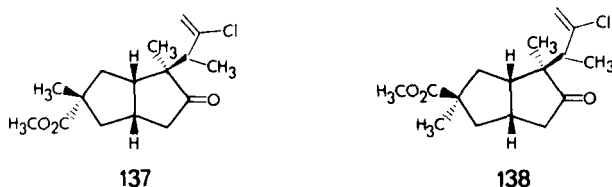


Fig. 44. Configurations assigned by mass spectrometry (90).

The two stereoisomers of unassigned configuration were known to be epimeric at the carbon bearing the carbomethoxyl group (137 and 138). The stereoisomers were distinct in all their spectral properties including the mass spectra. Only the last distinction allowed assignment of stereochemistry. Both isomeric molecular ions lost the elements of the chlorinated side chain to yield $[M-C_4H_5Cl]^+$ ions. This fragment ion went on to eliminate CH_3OH from only one of the isomers. The two materials were deuterated at the open methylene group adjacent to the carbonyl function and the isomer that exhibited an ion for loss of CH_3OH now lost CH_3OD . Molecular structure 137 was therefore assigned to the material that lost CH_3OH . As the structural representation shows (Fig. 44), only in this isomer (137) will the carbomethoxyl group have access to the abstracted hydrogen. This ion subsequently expels a molecule of carbon monoxide, thereby completing the total elimination of the carbomethoxyl group plus one hydrogen. This loss of carbon monoxide in a second step offers a clue to the unusual but proposed (88, 89) elimination of the entire carbomethoxyl or carboxyl groups plus one hydrogen in 130, 131, 133, 134, and 127, respectively (Fig. 41 and 42). In each case there is no evidence offered to preclude the more satisfying elimination of the elements of methanol or water, respectively, followed by loss of carbon monoxide. The stereochemical arguments are unaffected by the stepwise or concerted nature of the fragmentation.

There is in this work the question of the abstraction from the methylene group adjacent to the carbonyl function in the endo carbomethoxyl group versus the formally available syn tertiary hydrogens in the exo isomer. The latter elimination, which does not occur, would involve transfer through a six-membered ring, while that observed involves formal hydrogen transfer through a seven-membered ring. Interestingly, models indicate that the ring breathing or bellows motion that brings the endo carbomethoxyl group well within 2 Å

of the eliminated hydrogen is subject to greater flexibility than the motion that brings the tertiary syn hydrogens to the equivalent position in the exo carbomethoxyl group. Whatever may be the fundamental source of this distinction, these workers (90) found the elimination of ROH to be predominant for the endo isomers depicted in Fig. 45, and thus general for these fused molecules. They did not comment on the exo isomers in that series (Fig. 45).

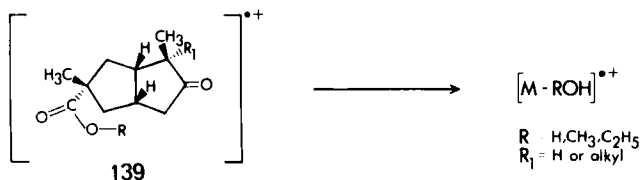


Fig. 45. Stereospecific loss of ROH from the Lansbury and Wang endo stereoisomers (90).

Mandelbaum and his co-workers, consistent with Lansbury (90), had earlier demonstrated (91) that the EI elimination of the elements of methanol from carbomethoxyl groups are not limited to six-membered rings, but may proceed through apparent five- or seven-membered transition states if the distances are appropriate. The molecules under consideration and the ion abundances for loss of CH_3OH and CH_3O^{\bullet} are portrayed in Figure 46.

Both the endo (140) and trans (142) series show easy

n	$[M-CH_3O]^+$	$[M-CH_3OH]^{\dagger}$	$[M-CH_3O]^+$	$[M-CH_3OH]^{\dagger}$	$[M-CH_3O]^+$	$[M-CH_3OH]^{\dagger}$
1	1.1	4.6	2.1	0.4	2.0	5.5
2	1.1	8.0	2.2	0.6	0.5	10.4
3	0.8	6.7	1.4	0.3	1.2	12.2
4	1.3	7.1	0.9	0.2	1.7	12.1

Fig. 46. Elimination of methanol or methoxyl radical from stereoisomeric diesters. Data taken on an Atlas CH-4 mass spectrometer by direct inlet at 70 eV. Data reported as percent of total ionization ($\% \Sigma_{40}$).

EI elimination of the elements of methanol $[M-CH_3OH]^+$ for all values of n . This result is reversed in the exo isomers (141) where the cleavage loss of the methoxy group from the molecular ion waxes over the rearrangement process.

Extensive deuterium labeling (91) revealed the foundation for this stereoisomeric dependence. The endo series (140) molecular ions lost the elements of methanol by abstraction of hydrogen from the allylic methylene group through an apparent seven-membered ring-transition state or intermediate. This process is not possible for the exo series (141). Further, the trans diesters (142) carried out the rearrangement via specific abstraction of the hydrogen on the carbon bearing the vicinal carbomethoxyl group and from no other position. This involves a five-membered ring transition for abstraction. Models indicate that the hydrogens on the allylic methylene may be brought to well within 2 Å of the oxygen bearing the methyl group in the endo series diesters (140). The absence of elimination from the tertiary allylic hydrogen in the trans diesters (142) and the only slight elimination in the exo epimers (141) is notable and inexplicable.

As seen below (Section IIIB), cleavage of the methoxyl group which is most competitive in the exo series (141), is a general interactive phenomenon for cis dicarboxyl groups when rearrangement paths are less available.

B. Fragmentations of Carbonyl Compounds Involving the Spatial Integrity of Double Bonds

There is a body of evidence strongly suggesting spatial integrity of double bonds in a wide range of olefinic carbonyl compounds under electron impact. These facts are presented below starting with a study in Israel on the 3,4-diethylmuconates exhibited in Figure 47 (92).

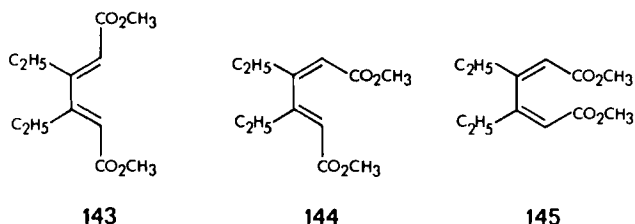


Fig. 47. Mass spectra of stereoisomeric diesters taken on an Altas CH-4 mass spectrometer by direct inlet at 70 eV (92).

The most intense ion in the mass spectra of all three materials appears at m/e 167. This corresponds to the loss

of one of the carbomethoxyl groups. The fact that the intensity of this ion moves from 15-36% to a remarkable 44% of the total ionization ($\Sigma_{40}^{\%}$) in 143, 144, and 145, respectively, suggested to the authors (92) that the process was assisted by the remaining carbomethoxyl group. In support of this proposal they (92) noted the thermal transformation (93) exhibited in Figure 48. This proposal suggests that the

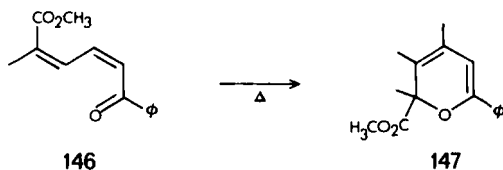


Fig. 48. Thermal reaction as a possible analog for the behavior of 144 and 145 (Fig. 47).

geometry of the double bonds guides the fragmentation. In line with this view, only the molecular ion of 143 exhibits loss of the elements of methanol ($[M-CH_3OH]^+$). The other stereoisomers, either without access to the allylic methylene group, i.e., 145, or with access to the facile competitive rearrangement to m/e 167, i.e., 144 and 145, show only loss of the methoxyl group from their molecular ions.

Examples of cis-trans dependency on the EI fragmentation of vicinal olefinic and cyclic dicarboxylic acids and their derivatives are now commonplace. A consistent picture is seen in the mass spectra of the dicarboxylic acids featured in Figure 49 (94). Only from the molecular ions of 149, 150, 152, and 153 is carbon dioxide eliminated. This loss of 44

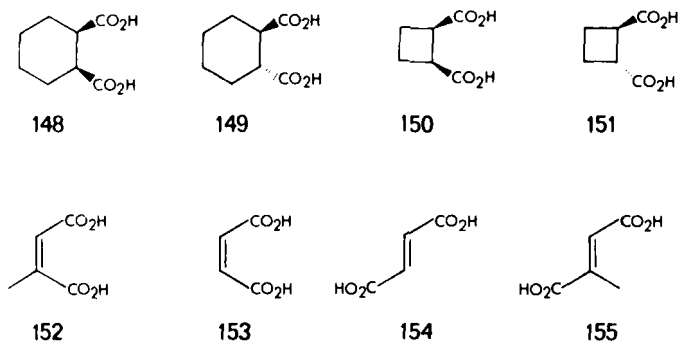


Fig. 49. Mass spectra of stereoisomeric diacids measured on a Hitachi RMU-6D mass spectrometer at 70 eV.

mass units is vanishingly small or unobserved in the alternate stereoisomers 148, 151, 154, and 155. The interaction of the adjacent carboxyl functions as the driving force for the elimination of CO_2 is well supported by the fact that phthalic acid is the only isomer of the three benzene dicarboxylic acids that fragments to eliminate CO_2 (94, 95). Although the precise atomic and electronic motions for this dicarboxylic acid participation remains a subject for speculation, an attractive mechanism (94) would involve the transfer of a hydroxylic hydrogen through a seven-membered ring-transition state to one of the oxygen atoms of the adjacent carboxyl group. Decarboxylation would then involve homolytic cleavage of the vinyl bond to yield a vinyl radical. This mechanistic format and the intermediacy of vinyl and phenyl radicals is precedented (96).

Stereoisomeric dependence is, as well, readily observed (152-155) in the mass spectra of 1,2-dicarboxylic esters of *cis* olefins (97, 98).

A very pretty demonstration of double-bond steric integrity follows from Meyerson's convincing mechanism for the apparently inexplicable loss of R^\bullet from Δ^2 -unsaturated esters 156 (99) (Fig 50). This proposed process (99) queues

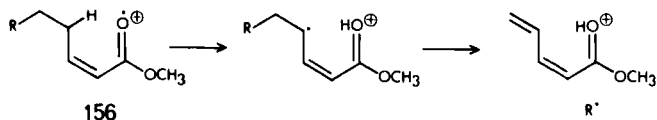


Fig. 50. A mechanistic proposal for loss of R^\bullet from unsaturated ketones.

up with the stepwise nature of the photochemical analog (100) and further explains the ready loss of Cl^\bullet only from 3-chloroalkanoates (157) and not from the structurally isomeric 2- and 4-chloroalkanoates (99) (Fig. 51).

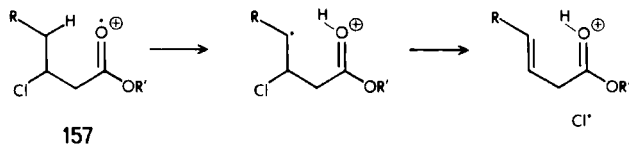


Fig. 51. A mechanistic proposal for loss of Cl^\bullet from certain chloroketones.

Consistent with both this mechanism and substantial double bond steric integrity is the fact, pointed out by

Meyerson (99), that methyl *cis*-2-octadecenoate on EI gives rise to the base peak at m/e 113 $[M-R]^+$, while the *trans* epimer shows much reduced intensity at m/e 113 (Fig. 52)

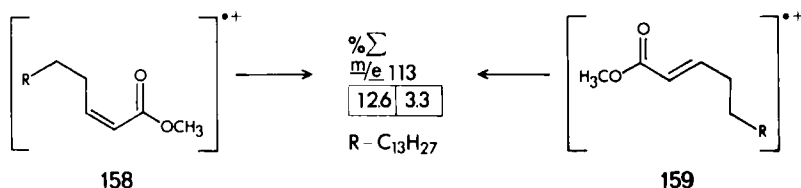


Fig. 52. Stereoisomeric dependence for loss of R° from *cis* and *trans* fatty esters. Data taken at 70 eV and 200°C on a mass spectrometer constructed by R. Ryhage.

(101). The term *substantial integrity* used above is certainly in need of clarification by techniques accessible in the present day state of the art (15, 22).

The unique pathways for fragmentation of the double bond stereoisomers of the α -ionones are certainly due to the accessibility for hydrogen rearrangement of the carbonyl group in the *cis* but not the *trans* isomer (Fig. 53) (102). The



Fig. 53. α -Ionones studied by mass spectrometry. Spectra measured at high and low voltage on a Varian-MAT 711 mass spectrometer at 125°C.

molecular ion of 160 fragments with loss of C_4H_8 [presumed from the ring (102)], which may be seen as an example of the well characterized EI retro-Diels-Alder (RDA) reaction (103, Section IV). In the 161 molecular ion, on the other hand, the carbonyl group may roam over the ring in the isolated gas phase ion radical. The authors proposed, but did not support, a variety of rationales involving hydrogen transfer to the acyl grouping of the 161 molecular ion (102). No more than a trace of RDA fragmentation ion is observed in the mass spectrum of 161.

In general it seems very likely that when the stereoisomerism of double bonds is key to allowing or disallowing favorable rearrangements (bond forming reactions), one can expect high dependency of the fragmentation processes on the

configuration about the double bond. The other side of this picture is seen in the results of the Swedish group (101) on other double-bond stereoisomers of unsaturated fatty acids where little overt dependence is observed. The same reason explains the very similar mass spectra observed for the cis,trans isomers of otherwise unfunctionalized olefins (11, 104).

IV. STEREOISOMERIC DEPENDENCE IN ELECTRON IMPACT INDUCED (EI) APPARENT ELECTROCYCLIC FRAGMENTATIONS

A. Hydrogen Rearrangements and the Retro-Diels-Alder Reaction (RDA)

In a series of molecules related to the dicarbomethoxy esters discussed above (91) (Fig. 46), Deutsch and Mandelbaum found (105) that the RDA fragmentation (103) of the adducts of *p*-benzoquinone and bi-1-cycloalkenyls occurs with an unusual transfer of two hydrogens. This EI reaction (105) is exemplified in Figure 54.

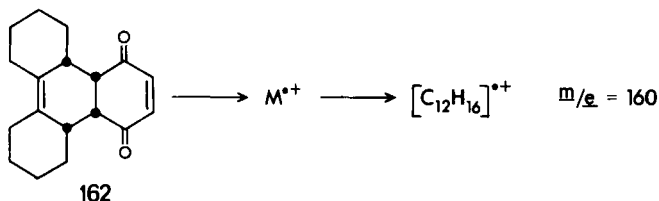
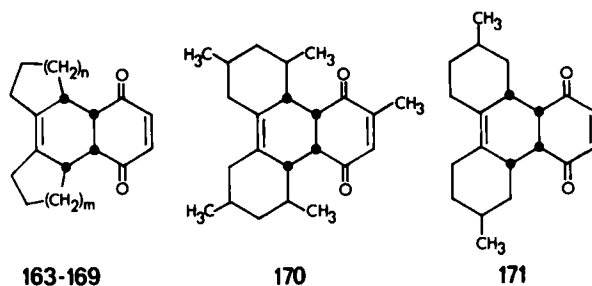


Fig. 54. Example of an RDA-2 reaction (105). Spectra taken at 70 eV on an Atlas CH-4 mass spectrometer. The RDA-2 ion gives the most intense ion in the spectrum.

This ion fragment (*m/e* 160) corresponds to loss of the quinone moiety with two hydrogens transferred to it from the bicyclohexenyl moiety. The normal RDA fragmentation would have yielded an ion at *m/e* 162.

There are a number of points of interest about this fragmentation. Extensive labeling (105) demonstrated that the two hydrogens are lost one each from the two allylic methylene groups, both in 162 and in its analog with five-membered rings (163). This is precisely the position from which hydrogen is abstracted in the related carbomethoxy esters in Figure 46 (91) and suggests that the carbonyl groups are involved in the hydrogen transfer. As in that rearrangement (91), the dione moiety (162) is related endo to the remainder of the molecule.

The fragmentation intensity is markedly dependent on the size of the rings in the bicycloalkenyl component. These data are presented in Figure 55 (106).

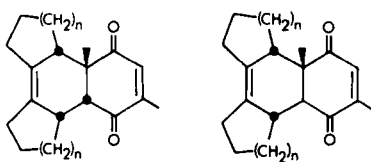


	n	m	% Σ_{40}
163	1	1	25.6
164	1	2	21.5
165	3	3	2.9
166	4	4	1.3
167	1	3	13.4
168	1	4	5.4
169	2	4	2.3
170	—	—	9.4
171	—	—	13.5

Fig. 55. Ring size dependency for RDA-2 reaction (see Figure 54). The data presented are the percent of total ionization ($\% \Sigma_{40}$) for the RDA fragmentation minus two hydrogens as depicted in Figure 54 for 162.

Inspection of models caused the authors to propose that the allylic hydrogens, known to be abstracted in 162 and 163 (105, 106), became less sterically accessible to the carbonyl groups. They presumed that the carbonyl oxygen is the terminus of transfer. This may or may not be the case in these molecules, although it is in line with the rearrangements in the esters (91) (Fig. 46). In the latter molecules the *site* of abstraction was also a function of ring size (91). The regioselectivity for hydrogen abstraction was not determined in the RDA-2 fragmentation except for 162 and 163. Whatever may be the ultimate source of this phenomenon, it is clear (Fig. 55) that there is a marked dependence for the observation of this fragmentation on ring size. The compared data (Fig. 55) for 170 and 171 versus that for 166 is especially convincing.

There is also a heavy dependency on the stereoisomerism at the ring juncture between the dione and dicycloalkenyl components. As may be seen in Figure 56, the RDA-2 fragmen-



n	172	173
1	204	09
2	128	03
3	14	05

Fig. 56. Stereoisomeric dependence for the RDA-2 fragmentation (see Figure 54). Numbers are the $\% \Sigma_{40}$ for the RDA-2 fragmentation.

tation exhibits a highly stereospecific *cis* requirement in these related molecules (107).

Mandelbaum and his co-workers (107) concluded that the RDA-2 fragmentation in these molecules is a concerted electrocyclic process with stereochemical requirements paralleling the thermal Diels-Alder reaction. As will be seen immediately following, these workers have uncovered a large number of related fragmentations which show this stereospecificity. Nevertheless, this RDA-2 fragmentation is unique in the feature of double hydrogen transfer. Models show that both carbonyl groups cannot simultaneously approach the allylic methylene hydrogens, and thus at least in the intact molecular ion, the double-transfer step cannot be concerted to the carbonyl groups. In addition, the geometry of the *trans* compounds (173) does not allow any portion of the enedione moiety to approach the sites for hydrogen abstraction. Thus, the *trans* isomers (173), independent of the requirements of the fragmentation step, are constructed so as not to allow the prerequisite hydrogen transfers. Related studies exist (109, 110).

The RDA-2 fragmentation does not occur in the saturated analog (174) and is substantially repressed in the aromatic analog (175). These compounds and the percent of total ionization for the RDA-2 fragment are shown in Figure 57 (108). These materials (174 and 175) easily undergo normal RDA reaction on electron impact (103) to yield ions that have the elemental composition of the diene and enes from which 174 and 175 were thermally constructed. The characteristics of this reaction in these and related molecules is part of the subject of the next section.

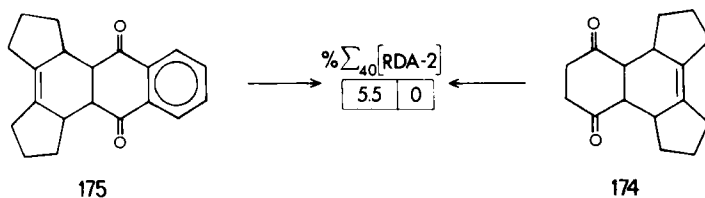
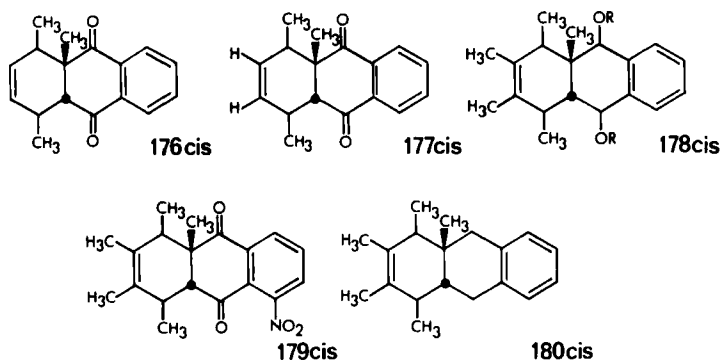


Fig. 57. Structural dependence for the RDA-2 fragmentation (see Figure 54). The ring juncture stereochemistry is *cis*.

B. The Electron Impact Induced Retro-Diels-Alder Reaction and the Question of Orbital Symmetry

Mandelbaum and Bel have studied the stereoisomeric dependence for the EI RDA fragmentation (103) in the isomers shown in Figure 58 (107, 111).

There is a clear requirement for cis stereochemistry at the critical ring juncture. This geometric prerequisite is also in force in the related ketones presented in Figure 59 (107).



		$[RDA \text{ ion}/M]^{*+}$	
		cis	trans
R = H R = COC_6H_5	176	4.0	.01
	177	1.6	.05
	178	3.1	.16
	178	200	.1
	179	4.5	.01
	180	8.1	.3

Fig. 58. Stereoisomeric and structural dependence for the RDA fragmentation. Only cis isomers are shown (see Figure 54).

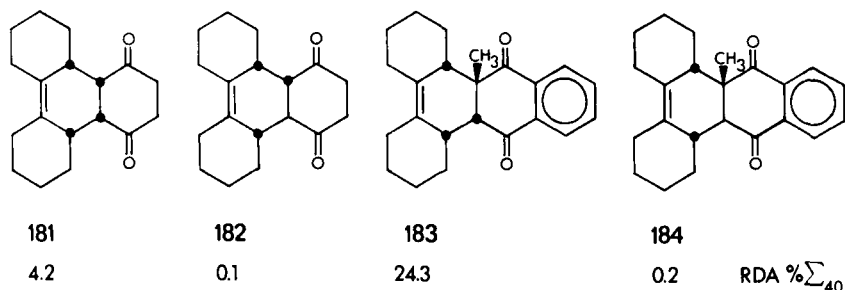


Fig. 59. Mass spectral results on the RDA reaction (see Figure 54); measured from the mass spectra published in the microfilm edition (107).

The highly specific demand for *cis* stereochemistry at the critical ring fusion for the EI-RDA reaction in this fragmentation is notprecedented. Early observations demonstrated that both stereoidal olefins and fused ring models showed abundant RDA fragment ions for *trans* fused compounds (103, 112). In addition, others have demonstrated that the molecular ions of olefins undergo extensive rearrangement processes which scramble hydrogen atoms (113, 114, 115). These rearrangements precede RDA reaction in at least one of these systems (115). Such goings on would provide a ready mechanism for epimerization and seem consistent with the previously observed absence of *cis* stereospecificity even if this were an orbital requirement. Indeed, the elimination of the elements of ethylene from tetralin, which is a formal analog of the RDA reaction, has been shown to occur following extensive rearrangement (116). Determination of the rate constants for hydrogen scrambling in cyclohexene has been accomplished via field ionization kinetics (FIK) (117). These results (117) show that scrambling is complete within 10^{-9} sec. after ionization, and demonstrate that the loss of C_2H_4 from the field ionization produced molecular ion of 3,6-tetradeuterocyclohexene occurs only in the shortest lived ions. This observation is consistent with the lack of observed stereospecificity for RDA fragmentation (112-116) since hydrogen migration would likely epimerize the ring juncture in the precursor *cis* and *trans* molecular ions. The determination of the stereospecificity for RDA cleavage using FIK (22, 117) would make an important contribution to this area.

With regard to the fundamental nature of the RDA fragmentation the results of Smith and Thornton (118) (Fig. 60) have been quoted by others (107, 111) to support a concerted mechanism. They find that the RDA cleavage product ion is formed preferentially from the side chain component. Their

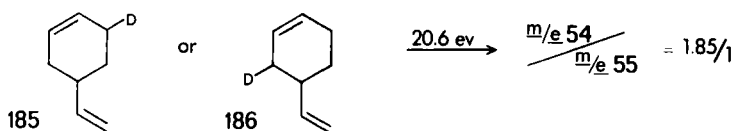


Fig. 60. Experiment to determine the structural source of the charged fragment in the RDA reaction. Electron voltage determined using argon to standardize the scale. 185 and 186 gave the same result.

data do not demand a concerted process. Staley and Reichard (119) have found that the natures of the RDA fragmentations from the molecular ions of the double bond isomers 187 and 188 (Fig. 61) are different. Both materials exhibit ions at



Fig. 61. Diastereomers which give rise to different RDA reactions as observed in their mass spectra. Spectra taken at 70 eV on an LKB 9000 mass spectrometer.

m/e 56 and 94 in their spectra. These ions correspond to the two fragments from RDA reaction with charge retention on one or the other component. The ratio of m/e 94:56 is 30.3 for 188 and 49.2 for 187. These data do not argue for or against any mechanism for EI RDA fragmentation. As the authors proposed (119), the results find a possible explanation in the more effective charge stabilization by the easier planarity of unsaturated charged fragment, m/e 94. This ion carries the elements of the stereoisomerically dependent double bond.

Hammerum and Djerassi (120), drawing attention to the interesting questions of stereospecificity for the EI RDA fragmentation, published their results on the two configurationally assigned decalin olefins in Figure 62. Under the conditions of their measurements, there seems to be little stereoisomeric dependence in this EI fragmentation.

Nevertheless, the results of the work at the Technion (Figs. 58 and 59) discussed above, unequivocally demonstrate

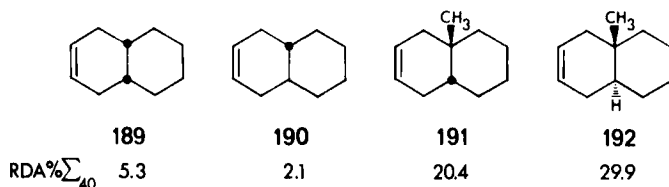


Fig. 62. Molecules exhibiting no clean dependence on stereoisomerism for the RDA reaction. Measured at 70 eV on an MS-9 mass spectrometer.

that overwhelming dependence on configuration is the case in the EI RDA fragmentation from the molecules studied. This work (107, 111) is unique in the sense that the molecules studied (176-184) are ornamented by oxygen and aromatic functionality, while the observations of stereochemical independence (103, 112, 120) were made on less or unfunctionalized olefins. It seems likely that this is a significant difference with regard to these observations, since the burden of the missing electron must be displaced from the site of fragmentation in the aromatic and ketone olefins. How these structural effects and the necessarily dependent charge distributions (the large difference in stereospecificity between 178 R=H and R=COC₆H₅ [Fig. 58] may be seen as an example of the proposed charge displacement) relate to the RDA reaction and to the hydrogen scrambling that likely obscures the stereochemistry in simple olefins is unknown. The stereochemistry of these electrocyclic formal analogs is a potential key element for extending orbital symmetry arguments (121) to these gaseous cation radicals formed by electron impact. In this regard there has been put forth a claim (122) that the molecular ions of *cis*- and *trans*-3,4-cyclobut-1-enedicarboxylic acids are in equilibrium with the dienes formed by disrotatory electrocyclic motions. This, if so, would be allowed in the Woodward-Hoffman sense (121) for the first excited state. The results on the stereospecific RDA reactions discussed above are consistent with the molecular motions demanded by a thermal highest occupied molecular orbital (HOMO).

Williams and Hvistendahl have found high kinetic energy release for metastable ions in the 1,2 loss of H₂ from various mass spectral ions (123). This finding suggests that the reverse reaction, i.e., 1,2 addition of hydrogen to these radical ions, is energetically costly. The thermal HOMO would make this process of suprafacial 1,2 addition of hydrogen to a π bond unfavorable. The mass spectra of carotenoids (124) are understandable in terms of thermally allowed electrocyclic rearrangement, although the critical experi-

ments to sort out the thermal from the electron impact reactions now veil the conclusions.

In related work on the stereochemistry of a putative electrocyclic fragment, Baird and Reese (125a) found that the isomers of 1-bromo-2,3-dimethylcyclopropane and 1,1-dibromo-2,3-dimethylcyclopropane fragment on EI to eliminate a bromine atom. Significantly, they showed that the stereoisomers of each set which lose bromide anion most readily (125) also exhibit the highest ratio of $[M-Br/M]^+$ on electron impact.

This finding is in line with expectation for the steric effects following disrotatory opening of the 2,3-cyclopropane bond leading to an allyl carbonium ion. This is the behavior found in the solvolyses of related tosylates and predicted for a thermal HOMO symmetry controlled process (126). This system is worthy of much further study.

Esters seem to be yet another class of molecules which maintain the same HOMO in the precursor neutral and the EI cation radical. Thus Winnik makes a persuasive case, in a review on methanol loss from the molecular cation radicals of methyl esters (125b), that hydrogen is transferred from carbon to carbonyl oxygen and that this itinerant hydrogen atom does not transfer further via a direct 1,3 process to the oxygen bonded to methyl. This behavior is in line with orbital symmetry requirements in which the HOMO is unchanged on ionization by electron impact.

V. STEREOISOMERIC DEPENDENCE IN ELECTRON IMPACT INDUCED BOND CLEAVAGE REACTIONS

A. Hydrocarbons and the Meyerson-Weitkamp Hypothesis

As has been discussed in Sect. I-C above, molecular-ion intensity is primarily and reversely related to the availability of low energy of activation fragmentations (20). Such fragmentations are most often rearrangement reactions, and thus ease of a rearrangement will generally be revealed by low-intensity molecular ions. There is no such parallel expectation for the cleavage or simple bond breaking fragmentations available to saturated hydrocarbons. The latter decompose on electron impact primarily by high energy of activation cleavages. There is, therefore, no straightforward theoretical expectation of a correlation of molecular ion intensity with the structure or enthalpy of the neutral precursors of these molecules. This will also be the case for other molecular ions which decompose primarily by non-rearrangement, high energy of activation pathways. There are, of course, certain simple bond-breaking pathways that involve

low energies of activation, and these materials will exhibit reduced or even absent (1,2) molecular ion intensity.

There is, in line with these ideas, no general experimental correlation of molecular ion intensity with the relative stability or heats of formation of stereoisomers (3, 10, 127). Meyerson and Weitkamp have discussed (11) the attempts to force this correlation. In a subsequent paper (128), they demonstrate that for a wide range of hydrocarbon diastereomers, all with methyl substituents, the intensity for the ion formed on loss of methyl radical from the molecular ions is always greater for the more stable (enthalpy) stereoisomer of each set of constitutionally equivalent isomers. Meyerson and Weitkamp proposed that the epimers lose methyl radical to form identical fragment ions that differ in energy by virtue of the enthalpic memory of their precursor molecular ion stereoisomers. The extra energy thereby in the $[M-CH_3]^+$ ion from the higher enthalpic isomer (less stable) is available to speed the rate of its further fragmentation.

If the energy distributions among the molecular ions of the compared stereoisomers were closely similar, where closely similar means that the difference is small compared to the enthalpic difference between the epimers, one could comfortably understand the correlation. The energy imparted to molecular ions is nonrestorable since the ions are isolated after ionization. If the two stereoisomeric molecular ions form identical $[M-CH_3]^+$ ions, as the authors propose (128), the higher enthalpic isomer will do so with an energy of activation which is lower. The strain of this molecular ion brings it closer to the product $[M-CH_3]^+$ ion. Therefore, the $[M-CH_3]^+$ ion from the more enthalpic epimer will have an energy residue which is less depleted, i.e., is greater, and the $[M-CH_3]^+$ ion from this less stable epimer will fragment further faster and yield a lower intensity $[M-CH_3]^+$ ion. These questions of the distribution of molecular ion energy for stereoisomers and the related question of stereoisomeric ionization potential are of increasing interest (129, 130).

The central idea (128) of forming structurally identical ions by fragmentation from two isomers of differing initial enthalpy would require that the appearance potentials for these processes be different by exactly the $\Delta\Delta H$ for the two isomers. This must be so in principle since the appearance potential is a measure of a state function, i.e., the thermochemical difference between the precursor neutrals and the ionic and neutral fragments. In practice, these numbers as determined in mass spectrometers are uncertain due to experimental difficulties as well as excess energy involved in the formation and observation of the ionic fragments (131). Natalis has pioneered these measurements on stereoisomers (132). Jalonen and Pihlaja, in a recent review (133),

have collected these data and added studies of their own demonstrating that there is excellent agreement in a number of stereoisomers between the appearance potential differences for a common fragmentation and the $\Delta\Delta H$ between the compared stereoisomers. These workers have pointed out (133) that the experimental uncertainties and excess-energy terms that normally obscure these measurements (131) are most likely to become cancelable terms when comparing isomers. Thus if two stereoisomers fragment to yield a common ion designated A^+ and A_1^+ , respectively, it follows that $AP([A_1]^+) - AP([A]^+) = \Delta H_f(M_1) - \Delta H_f(M)$. The compared isomers are M_1 and M , and AP is the appearance potential. There even seem to be a number of cases in which the difference in ionization potentials between two stereoisomers reflects the $\Delta\Delta H_f$ between them (133, 134). This could only be the case for a vertical ionization when the initially produced molecular ions are relieved of the source of the differential strain or stabilization as a consequence of ionization (134). An exemplary portion of Meyerson and Weitkamp's data is presented in Figure 63.

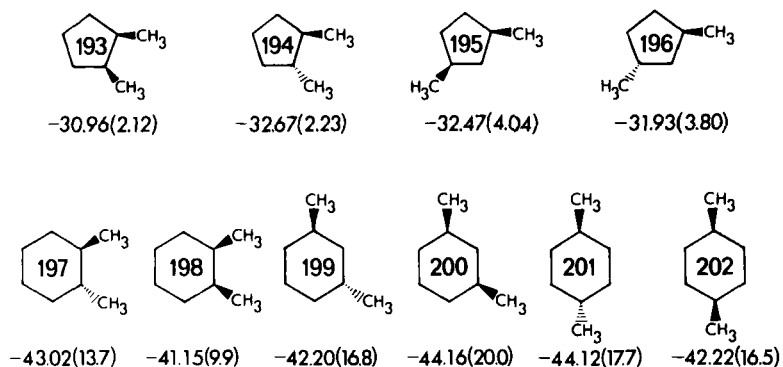
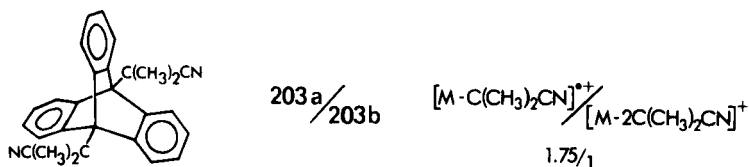


Fig. 63. Mass spectral results on diastereomers giving support to the Meyerson-Weitkamp hypothesis. See (128); data taken from various literature sources by the authors; averages are shown here; the numbers refer to the structure above as ΔH_f ($\% \Sigma - [M-CH_3]^+$).

A potential further test of the Meyerson-Weitkamp model (128) is provided by the mass spectra of the two atropisomers 203a and 203b (Fig. 64) studied by Iwamura (135). Both stereoisomers (Fig. 64) fragment to lose the essential structural atropisomeric feature, thereby reasonably forming identical ions. The ion intensities for loss of the cyano-methylethyl bridgehead functions were published as ratios for 203a and 203b (135).



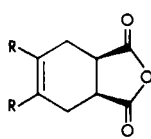
203 a m.p. 365-366 °C

203 b m.p. 503-508 °C

Fig. 64. Atropisomers exhibiting different mass spectra. Spectra taken on a Hitachi RMU6 mass spectrometer by direct inlet at 150°C and 70 eV.

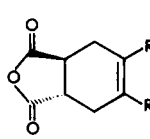
The data in Figure 64 show that the $[M - C(CH_3)_2CN]^{*+}$ ion from **203a** suffers less subsequent fragmentation to the $[M - 2C(CH_3)_2CN]^+$ ion than its epimer **203b**. Equilibration (136) shows that **203a** is favored over **203b** by 65:35. Nevertheless, because this is exactly what is predicted from the entropy difference alone if **203a** is the d,l pair (the other isomer would be meso), the system is an inadequate test of the hypothesis until the enthalpic difference is measured.

Karpati and Mandelbaum (137) studied the mass spectra of the *cis*- and *trans*-1,2,3,6-tetrahydrophthalic anhydrides **204** and **205** (Fig. 65). The large difference in elimination of



204

	$[M - CO/M]^{*+}$	
R	cis	trans
H	26.0	.06
CH ₃	5.1	.03



205

Fig. 65. Stereoisomerically dependent mass spectra supporting the Meyerson-Weitkamp hypothesis. Data taken from an Atlas CH-4 mass spectrometer via direct inlet at 70 eV and ambient temperature.

carbon monoxide was presented by the authors as ratios of $[M - CO]^{*+}/M^{*+}$.

Equilibration of the isomers at 200°C gives about 80% of the *cis* isomer (137, 138). If the enthalpic term is in the direction of the favored **204**, the greater intensity of the $[M - CO]^{*+}$ ion from the molecular ion of **204** would be consistent with the Meyerson-Weitkamp hypothesis (128). It is difficult to see the entire difference, though, as arising from

the subsequent fragmentation of the $[M-CO]^+\cdot$ ion from 205. The critical experiment of lowering the beam energy and thereby decreasing subsequent fragmentation of the $[M-CO]^+\cdot$ ion was not carried out (137). Other observations (139) on hydrocarbons may be related to these effects (128).

B. Bicyclic Molecules and Related Examples

Exo and endo norbornyl bromides offer an example in which the intensity ratio of the $[M-Br]^+/[M]^+\cdot$ ions is greater from the more stable exo norbornyl bromide (140). Although this is consistent with the Meyerson-Weitkamp model for further subsequent fragmentation for the $[M-Br]^+$ ion from the endo norbornyl bromide molecular ion, the increased ratio of the $[M-Br]^+/M^+\cdot$ ion from the exo bromide is maintained at low ionizing energies where further fragmentation is repressed (141). Thomas and Willhalm had earlier (85) noted the increased ion intensity for loss of the acetyl group from exo over endo acetylnorbornanes (Fig. 38 and 39).

The question of the relationship between these EI phenomena (85, 140, 141) and the much discussed character of the norbornyl cation (142) is not without interest. In this regard, Dimmel and Seipenbusch have uncovered an unusual stereoisomeric dependence in exo and endo borneols (143). Their results are compiled in Figure 66.

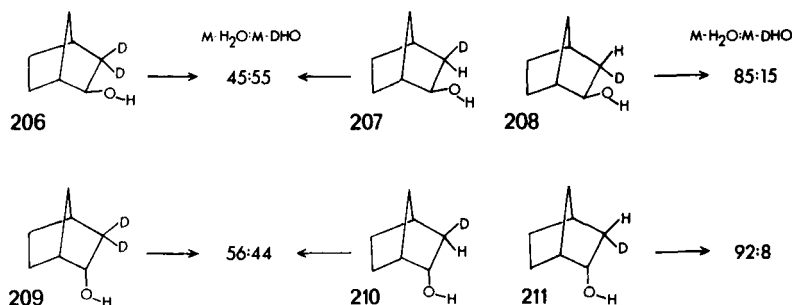


Fig. 66. Deuterium labeling results on exo and endo norborneols. Arrows symbolize EI on a CEC-103C mass spectrometer at 70 eV and 245°C; numbers are the percentage loss of H_2O and HDO .

The loss of heavy water from the molecular ions of 206 and 209 is highly unusual, since elimination of water normally does not occur 1,2 (26, 27, 37). The results for 207 and 208 caused the authors (143) to hypothesize that hydroxyl radical is eliminated leading to an ion of proposed norbornyl cation structure. This latter species, on elimination of a

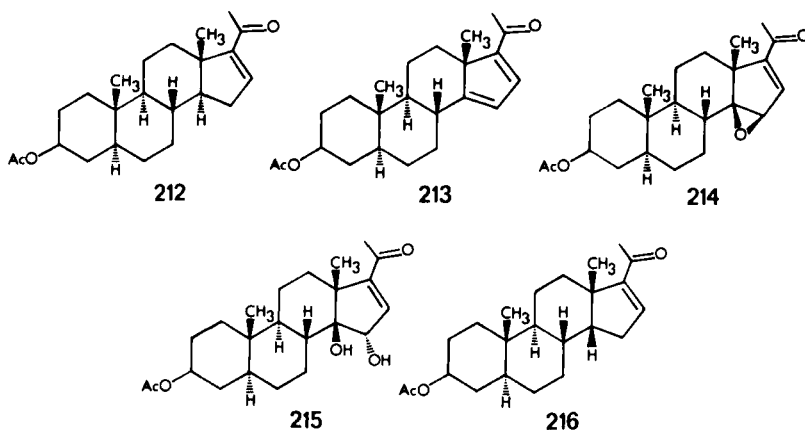
hydrogen atom, would complete the formal loss of the elements of water. Experimentally this view finds support in the fact that both 207 and 210 eliminate the exo deuterium atom, while this loss from the endo position in the molecular ions of 208 and 211 is much smaller (Fig. 66). This behavior is analogous to that observed in accessible phase studies where movement toward and away from the norbornyl 2-bridge occurs preferentially from the exo face (144). In addition, these workers point out that hydroxyl groups bonded to potentially stable cation centers, and with unavailable hydrogen for elimination via 1,4 and 1,3 states, show preceded loss of hydroxy radicals (143). For example, loss of hydroxyl radical leads to a more intense ion than that for loss of water from the molecular ion of 2-butanol (145). Robbiani and Seibl (146) have investigated the mass spectra of the same molecules (Fig. 66). Their results confirm the experimental observations (143). They, as well, found metastable ions for loss of water from the heavy and light borneols and isoborneols. This observation normally calls for a single-step mechanism, in conflict with the Dimmel and Seipenbusch mechanism (143). There are, though, a number of examples of EI two-step processes which lead to the observation of apparent metastables for a single-step mechanism (147).

In contrast to the borneol and isoborneol EI behavior, the norborneol system is subject to much more extensive rearrangement randomization prior to fragmentation (148). The published mass spectra of epimeric 7-substituted norbornenes show great overt dependence on stereoisomerism (149). These have not been explored beyond their observation.

The loss of the acetyl side chain at C-17 from Δ^{16} steroids has been proposed to occur via methyl migration from the adjacent tertiary center (150). The proposal was offered to account for the unusual observation of loss (formally) of a vinyl-bonded group on EI. Inspection of models and consideration of the orbital geometries leads to the conclusion that the methyl transfer would be best when the dihedral angle between the double bond and C-13; C-18 tertiary carbon-to-methyl bond is 90 deg. and this is closely the case in Dreiding models of Δ^{16} steroids with a trans-C/D ring juncture. Fehlhauer, Lenoir, and Welzel (151) have studied the ease of formation for this $[M-43]^+$ ion in five systems in which this dihedral angle is systematically varied (Fig. 67).

It is easy to criticize this work, and one could generate arguments in which differing structural features in each molecule offer an array of mechanisms affecting the ion intensity for the loss of the acetyl group. The differing behavior, though, of the stereoisomers 212 and 216, and the steady correlation with bond angle for loss of the acetyl group leaves the authors' proposal (151) as the most satisfying and comfortable hypothesis

for explaining these data (Fig. 67) and, as well, supporting the original idea of methyl transfer (150).



	DIHEDRAL ANGLE	% $\sum_{40} M \cdot C_2H_5O$
212	90°	6.7
213	110°	3.5
214	120°	1.6
215	140°	.13
216	140°	.17

Fig. 67. Proposed dependence on C-18 methyl to D-ring double bond dihedral angle for loss of C_2H_5O . Spectra taken on an Atlas CH-4 mass spectrometer at 70 eV by direct inlet; the dihedral angle is taken from the publication (151); see the text.

C. Heterocyclic Molecules

In the mass spectrum of deuterated methyl-20-conanine (152), there appears a highly stereospecific loss of a methyl radical. The results are presented in Figure 68. The alkaloids 217 and 218 are diastereomers by virtue of the labeling of the α and β methyl groups at C-20. The results, therefore, reveal the favorable driving force for cleavage loss of the α -methyl group of the disatereotopic *gem*-dimethyl function in the unlabeled molecule. Although the dependence of selectivity on R is a subject for speculation, the favorable loss of the α or *exo* grouping is sterically sensible because *exo* approach in condensed phase to the heterocyclic ring is highly favored as shown in Figure 69

The structure of 219 with participation of the nonbonding electrons on nitrogen could be envisioned as a model for the

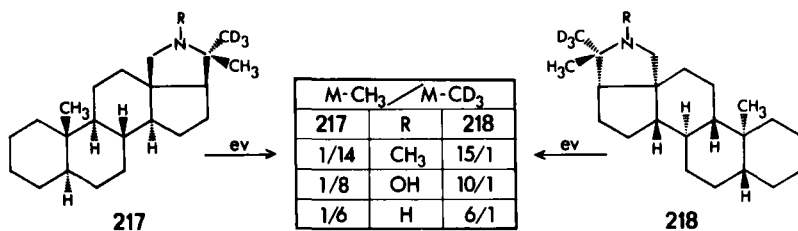


Fig. 68. High stereoselectivity for loss of methyl radical from conanine cation radical. Measured on an MS-9 mass spectrometer by direct inlet at 70 eV.

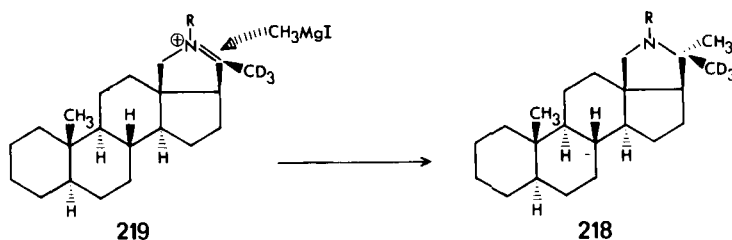


Fig. 69. Demonstration of favored approach to the exo face.

[M-methyl]⁺ ion in the mass spectrometer and movement toward and, therefore, away from the exo face is more facile. This is in direct analogy to the behavior of the well investigated norbornyl system (140, 141, 144).

This conformational approach finds general support in the mass spectrometry of the stereoisomeric β -lactams (153) presented in Figure 70.

Inspection of the data (153) reproduced in Figure 70 demonstrates first, that in each case the ion A is preferentially formed from the molecular ion of the cis isomers (220 series) over the trans isomers. Second, this preference grows as R increases in bulk. Third, and especially for the cis isomers (220 series), the intensity of ion A grows at the expense of competitive ion B. As is seen from the general structure in Figure 70, the cleavage of the ring to yield ions A and B is such that only ion A would immediately relieve the strain of the juxtaposed cis R and phenyl groups. This would be true if these cleavages to ions A and B take place from an unrearranged molecular ion of structure comparable to its accessible phase precursor. The steric sensibility of the results certainly supports this view. Others have utilized steric effects to explain the cleavage of stereoisomeric small rings (154-156). The credibility of their conclusions draws sustenance from the work discussed above (153).

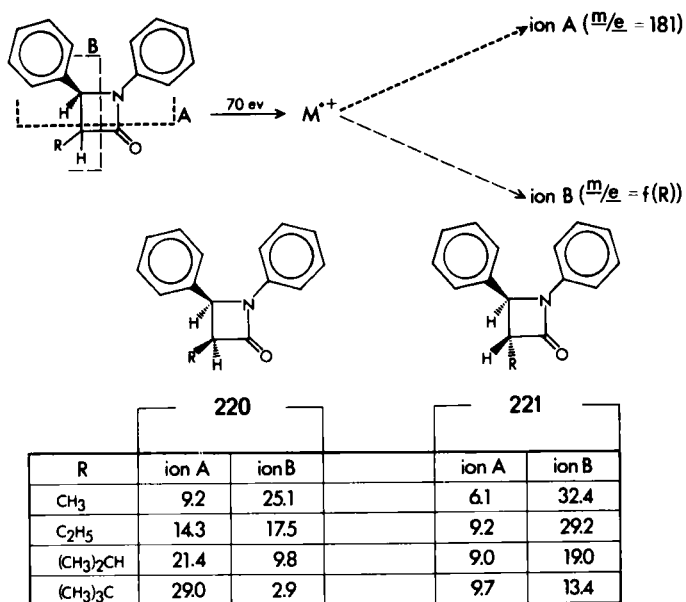
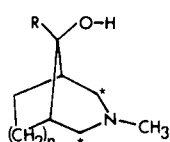
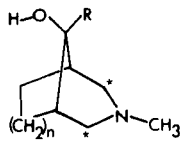


Fig. 70. Stereoisomeric dependence in the fragmentation of a four-membered ring. Spectra taken at 70 eV on an AEI MS-9 mass spectrometer at 180°C. The numbers, which are highly temperature dependent, are the percent of total ionization (%Σ₂₈).

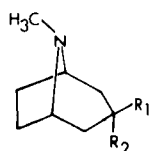
This newly lowered threshold for credibility stands as well for proposals of a strain-dependent driving force for loss of a hydrogen atom from the molecular ions of various epimeric azabicycloalkanes (157). The mass spectra of a series of heterocycles first demonstrated that $[M-1]^+$ fragmentation was common for structures such as 222 and 223 but not for 224 (Fig. 71). In addition, deuterium labeling at the bridgehead carbons, and at the one carbon bridge, gave rise to no ion at m/e $M-2$. In line with the known behavior for β cleavage of amines, which is exemplified in methyl conanine (152) (Fig. 68), they (157) reasonably concluded that the hydrogen arose from the starred (*) carbons in 222 and 223. In a series of fourteen heterocycles of variable n and differing R groups, (Fig. 71) the epimers (222 and 223) with the larger group facing the heterocyclic bridge always exhibited significantly more intense $[M-1]^+$ ions. They (157) saw this as relief of the 1,3 nonbonded interaction but did not investigate the phenomenon further. Strain arguments have served to rationalize stereoisomeric dependence in the mass spectra of 6-aza-bicyclo[3,2,1]octanes (158) and quinolines (159) and perhaps oxindole alkaloids (160).



222

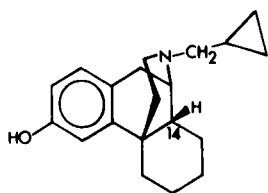


223

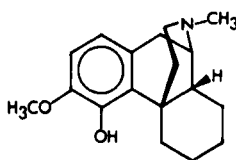


224

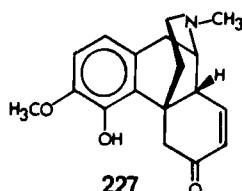
Fig. 71. Stereoisomeric azabicycloalkanes studied by mass spectrometry.



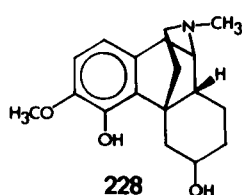
225



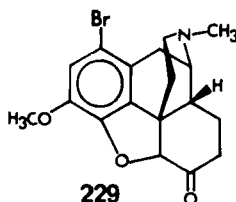
226



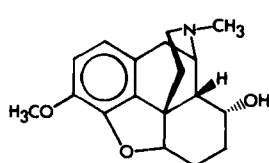
227



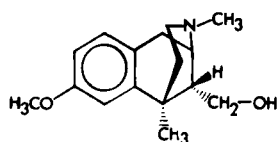
228



229



230



231

<i>cis</i> isomer	$m/e(44+R)$	$\% \sum_{40}^{cis} / trans$
225	99	11.5
226	59	29.0
227	59	50.0
228	59	18.0
229	59	5.0
230	59	3.2
231	59	23

Fig. 72. Stereoisomeric dependence for formation at m/e (44 + R) from morphine derivatives. See the text. Spectra taken on an Atlas CH-4 mass spectrometer at 70 eV; only *cis* isomers shown.

In a stereoisomeric mass spectral study of morphine derivatives, Mandelbaum and Ginsburg (161) have uncovered a highly stereoselective fragmentation apparently unrelated to the strain arguments made above. All isomers in the series with a *cis* junc-

ture of rings B and C and a hydrogen at C-14 exhibit an intense fragment ion at an m/e of $(44 + R)$ where R is bonded to nitrogen. Their results (161) are presented in Figure 72.

The authors (161) ascribed this effect to a mechanism involving migration of the C-14 hydrogen only available in the *cis* isomers shown (225-231), to the departing nitrogen fragment. Others had proposed similar mechanisms in these molecular types (162). These proximity-for-bonding effects have also been proposed as the foundation for the overt stereochemistry of the molecular ions of *N*-tosyl-3-aza-7-carbomethoxybicyclo[3,3,1]-nonanes (163) and matridine (164) isomers.

D. Other Examples

Although stereoisomeric dependence founded on proximity effects for rearrangement are encountered most commonly in carbonyl compounds, alcohols, and related molecules discussed extensively above, there are unusual cases in saturated steroids (165) and phenyltetraline (166).

In another effort involving proximity effects, the EI elimination of CH_3SOH from the R and S enantiomers of 3 β -hydroxy-20-thia-17 α - and β -5-pregnene oxides (17 α and β methylsulfoxides) was found to parallel the pyrolyses (167). The R configuration at sulfur in the 17 α molecule exhibited the most intense elimination ion. Moldowan, in a contradictory report (168), has studied the EI elimination of RSOH from sulfoxides and suggested that the configurational stability of the sulfoxide is lost on ionization. The elimination of RSOH from dialkyl sulfoxides appears to be a true electron impact process (169). tion of RSOH from dialkyl sulfoxides appears to be a true electron impact process (169).

In an entirely different area, Schulten and Beckey (170) found that the isomers of aldrin diol eliminate water unequally by field desorption mass spectrometry (171)(Fig. 73).

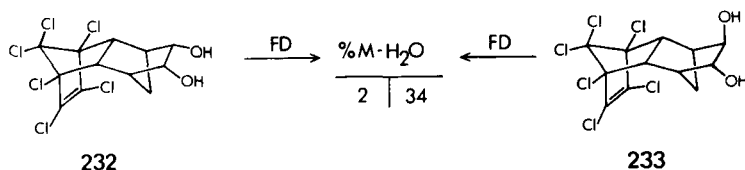


Fig. 73. Field desorption spectra of aldrin diol measured on a CEC-110B mass spectrometer; numbers are the percentage of the molecular ion.

Here, as is predictable on the basis of extensive studies by electron impact, the compound with proximal hydroxyl group and tertiary hydrogen (233) eliminates water most readily.

Stereochemical phenomena have been uncovered in chemical ionization mass spectrometry (172). In one extensive study, Longevialle, Milne, and Fales (173) showed that 5 α -pregnanes substituted with hydroxyl and amino groups on ring A exhibit loss of water from the $[M + H]^+$ ion only when there is no intra-molecular H-bonding. Occurance of the latter was demonstrated by infrared spectrometry (173). A portion of their results are shown in Figure 74.

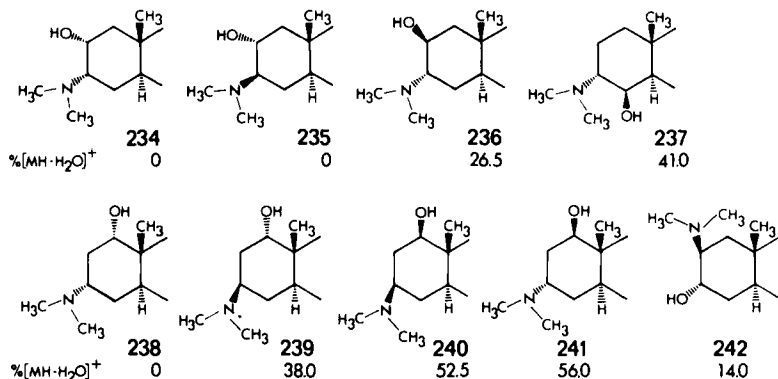


Fig. 74. Isobutane is the reagent gas (contributes H^+) in the chemical ionization spectra of ring A substituted 5 α -pregnanes. Spectra measured on an MS-9 modified mass spectrometer; only ring A (see the text) is shown. The % $[MH - H_2O]^+$ is the percent of the total ions observed.

In 234, 235, and 238 infrared measurements (ir) show no free O-H stretching vibration (173). In 237, 239, 240, and 241 all the O-H absorption in the ir is free of H-bonding. Compounds 236 and 242 exhibit both free and H-bonded hydroxyl groups (173). The reduced intensity of the $[MH - H_2O]^+$ ion in 236 and 242 was convincingly suggested to arise from that portion of the $[MH]^+$ ions that were free of H-bonding. These workers proposed (173) that H-bonding stabilized the protonated ions, and acted to place the ionizing proton intermediate between the nitrogen and oxygen. This would raise the energy of activation for loss of water. There exist other studies, of a preliminary nature, on stereoisomeric dependence in chemical ionization mass spectrometry (174).

Ion cyclotron resonance (icr), which, like chemical ionization, involves intermolecular interactions (175), has also been shown to be sensitive to the expected (176) differential reactivity of diastereomers. Bursey and his co-workers have found the $C_6H_9O_3$ positive ion, formed from a neutral 2,3-butanedione molecule colliding with a molecular ion of 2,3-butanedione, is an effective reagent for acetylating oxygen compounds under icr

conditions. This transfer of acetyl cation appears to be sensitive to steric effects (177) in a manner predictable by applying accessible phase structural considerations (178, 179). Other ionic studies of stereochemical interest exist (180, 181). In one of these studies (181), chloride anion was shown to displace bromide anion from *cis*- and *trans*-4-hydroxycyclohexyl bromide with ca. 90% inversion of configuration. Assignment of configuration to the neutral chloride products followed from the different overt mass spectra of the epimers (181).

E. Final Notes

(1). The chemistry observed in mass spectrometers is heavily dependent on stereoisomerism. This fact in combination with the extreme sensitivity and wide structural applicability of mass spectrometers should make these instruments highly suitable for stereochemical research. In this regard, the potential stereoanalytical utilization of mass spectrometers, recognized some time ago (182), is, with necessary mechanistic underpinnings, just now of beginning importance in solving difficult configurational problems (45, 89, 90, 181, 183). The use of spatially dependent rearrangement reactions (37, 51) for this purpose is especially satisfying because the principle involved is identical to traditional methods of configurational assignment (184).

(2). The various techniques of mass spectrometry allow chemical observations in the gas phase at pressures varying from high vacuum to nearly 1 atmosphere. The resultant reacting media vary from states of unimolecular kinetics in the absence of *all* intermolecular perturbation to states of heavy intermolecular contact and multimolecular kinetics. It follows from this variability that these instruments can be utilized to yield information on intermolecular phenomena such as, for example, solvation. A seminal example is seen in mass spectrometric studies of alcohols where it has been demonstrated that the relative acidities of a range of alcohols in the gas phase are reversed from the acidities in solution. This has led to new insights allowing discrimination between previously confused intrinsic molecular properties and solvative effects (185). The literature reviewed in this chapter shows that stereochemical questions offer a great deal of information on the fleeting species under view in mass spectrometers (186). This information takes two general and dependent forms. First, the stereochemical results may be seen as bridges connecting the structures of the molecules in mass spectrometers to the more directly observed structures of molecules in accessible and familiar environments. This will, and in fact has begun, to act to raise the certainty of structural assignments in mass spectrometers where this information is

available (15, 18). Second, as the structural assignments for reacting molecules in mass spectrometers grow more certain, then stereochemical theory will allow answers to mechanistic questions concerning the effects of structure on reactivity under the unique conditions of stress and molecular isolation encountered in mass spectrometers.

These molecules certainly cast a beautiful three dimensional shadow on our senses.

ACKNOWLEDGEMENT

I want to thank Harold Hart and Robert Botto of this department, and Sy Meyerson of American Oil Company for critically reading the entire manuscript and Denise Aldridge and Kitty Beard for their secretarial assistance. Diane Mitchell prepared all of the Figures. Special thanks go to my colleagues here at Michigan State University for providing a friendly and stimulating atmosphere in which to prepare this chapter and to the National Institute for General Medical Sciences for long supporting my interests in this area.

I am grateful to my wife Janet for a helpful interchange of ideas during the preparation of this chapter and to R. G. Cooks, A. L. Burlingame, Peter Brown, J. K. MacLeod, M. M. Bursey, P. Lansbury, C. B. Reese, D. R. Dimmel, C. E. Brion, W. J. Richter, H. Schwarz, Z. (V. I.) Zaretskii, F. W. McLafferty, C. Djerassi, S. I. Goldberg and N. S. Wulfson for helpful advice and information.

I am grateful as well to Asher Mandelbaum of the Technion for sending a preprint of his own chapter on the same subject to appear in, Handbook of Stereochemistry, Edited by H. Kagan, Georg Thieme Verlag, Stuttgart, 1975 (in press).

REFERENCES

1. F. H. Field and J. L. Franklin, *J. Chem. Phys.*, 21, 550 (1953).
2. F. H. Field and J. L. Franklin, *Electron Impact Phenomena*, Academic, New York, pp. 237-238, 1957.
3. J. Momigny and P. Natalis, *Bull. Soc. Chim. Belges*, 66, 26 (1957).
4. K. Biemann and J. Seibl, *J. Amer. Chem. Soc.*, 81, 3149 (1959).
5. J. H. Beynon, R. A. Saunders, and A. E. Williams, *Appl. Spectrosc.*, 14, 95 (1960).
6. H. Budzikiewicz and C. Djerassi, *J. Amer. Chem. Soc.*, 84, 1430 (1962).
7. K. Biemann, *Mass Spectrometry, Organic Chemical Applications*, McGraw-Hill, New York, pp. 144-151, 1962.
8. K. Biemann, in *Mass Spectrometry of Organic Ions*, F.W. McLafferty, Ed., Academic, New York, p. 591ff, 1963.

9. F. W. McLafferty, *Interpretation of Mass Spectra*, 2nd edit., Benjamin, New York, p. 40ff, 1973.
10. L. D'Or, J. Momigny, and P. Natalis, *Advances in Mass Spectrometry*, Vol. 2, MacMillan, London, p. 370ff, 1963.
11. S. Meyerson and A. W. Weitkamp, *Org. Mass Spectrom.*, 1, 659 (1968).
12. E. L. Eliel, N. L. Allinger, S. J. Angyal and G. A. Morrison, *Conformational Analysis*, Wiley-Interscience, New York, 1965.
13. T. W. Bentley and R. A. W. Johnstone, *Advan. Phys. Org. Chem.*, 8, 151 (1970).
14. R. G. Cooks, M. Bertrand, J. H. Beynon, M. E. Rennekamp, and D. W. Setser, *J. Amer. Chem. Soc.*, 95, 1732 (1973).
15. R. G. Cooks, J. H. Beynon, R. M. Caprioli, and G. R. Lester, *Metastable Ions*, Elsevier, New York, p. 206ff, 1973.
16. H. E. Audier, H. Felkin, M. Fétizon, and W. Vetter, *Bull. Soc. Chim. France*, 1965, 3236.
17. M. M. Green, *J. Amer. Chem. Soc.*, 90, 3872 (1968), and subsequent papers.
18. M. M. Green, J. M. Moldowan, and J. G. McGrew II, *J. Org. Chem.*, 39, 2166 (1974).
19. See Ref. 2, p. 53ff.; Ref. 9, p. 203ff.; Ref. 15, p. 217ff.
20. D. H. Williams and I. Howe, *Principles of Organic Mass Spectrometry*, McGraw-Hill, New York, p. 12ff, 1972.
21. D. J. McAdoo, P. F. Bente III, M. L. Gross, and F. W. McLafferty, *Org. Mass Spectrom.*, 9, 525 (1974).
22. P. J. Derrick, A. M. Falick, and A. L. Burlingame, *J. Amer. Chem. Soc.*, 95, 437 (1973); P. J. Derrick and A. L. Burlingame, *Account Chem. Res.*, 7, 328 (1974); see also Ref. 15, Chap. 4, p. 89ff. P. J. Derrick, J. L. Holmes, R. P. Morgan, *J. Amer. Chem. Soc.*, 97, 4936 (1975).
23. M. E. Munk, C. L. Kulkarni, C. L. Lee and P. Brown, *Tetrahedron Lett.*, 1970, 1377.
24. M. M. Green, J. M. Moldowan, D. J. Hart, and J. M. Krakower, *J. Amer. Chem. Soc.*, 92, 3491 (1970). See also F. Bohlmann, T. Friedrich, C. Köppel and H. Schwarz, *Org. Mass Spectrometry*, 10, 158 (1975); G. Eadon, P. Gold and E. Bacon, *J. Amer. Chem. Soc.*, 97, 5184 (1975).
25. C. H. DePuy and R. W. King, *Chem Rev.*, 60, 431, (1960); G. G. Smith and F. W. Kelly, *Progr. Phys. Org. Chem.*, 8, 75 (1971); D. Y. Curtin and D. B. Kellom, *J. Amer. Chem. Soc.*, 75, 6011 (1953); P. S. Skell and W. L. Hall, *ibid.*, 86, 1557 (1964).
26. W. Benz and K. Biemann, *J. Amer. Chem. Soc.*, 86, 2375 (1964).
27. S. Meyerson and L. C. Leitch, *J. Amer. Chem. Soc.*, 86, 2555 (1964).
28. M. M. Green, J. G. McGrew II, and J. M. Moldowan, *J. Amer. Chem Soc.*, 93, 6700 (1971).

29. M. Akhtar, *Advan. Photochem.*, 2, 263 (1964).
30. M. Lj. Mihailovic^V and Z. Cekovic^V, *Synthesis*, 209 (1970).
31. H. Budzikiewicz, Z. Pelah, and C. Djerassi, *Monatsh. Chem.*, 95, 158 (1964).
32. C. G. MacDonald, J. S. Shannon, and G. Sugowdz, *Tetrahedron Lett.*, 1963, 807.
33. C. E. Brion, *Anal. Chem.*, 37, 1706 (1965).
34. C. E. Brion and L. D. Hall, *J. Amer. Chem. Soc.*, 88, 3661 (1966).
35. B. M. Johnson and J. W. Taylor, *Int. J. Mass Spectrosc. Ion Phys.*, 10, 1, 1972/1973.
36. L. Dolejš and V. Hanuš^V, *Coll. Czech. Chem. Commun.*, 33, 332 (1968).
37. M. M. Green, R. J. Cook, J. M. Schwab, and R. B. Roy, *J. Amer. Chem. Soc.*, 92, 3076 (1970). M. M. Green, D. Bafus and J. L. Franklin, *Org. Mass Spectrom.*, 10, 679 (1975).
38. Z. M. Akhtar, C. E. Brion, and L. D. Hall, *Org. Mass Spectrom.*, 7, 647 (1973); Z. M. Akhtar, Ph.D. thesis, Department of Chemistry, Univ. of British Columbia, Canada, 1972.
39. M. M. Green and J. Schwab, *Tetrahedron Lett.*, 1968, 2955.
40. M. M. Green and R. J. Cook, *J. Amer. Chem. Soc.*, 91, 2129 (1969).
41. W. Benz, *Massenspektrometrie Organischer Verbindungen*, Akademische Verlagsgesellschaft, p. 142ff, 1969.
42. K. Heusler and J. Kalvoda, *Angew. Chem. Int. Edit. Engl.*, 3, 525 (1964); J. W. Wilt, *Free Radicals Vol. I.*, J. K. Kochi, Ed. Wiley-Interscience, New York, p. 387, 1973.
43. H. Budzikiewicz, C. Djerassi, and D. H. Williams, *Mass Spectrometry of Organic Compounds*, Holden-Day, San Francisco, p. 157, 1967.
44. J. K. MacLeod, M. Vegar, and R. J. Wells, *Recent Developments in Mass Spectroscopy*, K. Ogata and T. Hayakawa, Eds., Univ. of Tokyo Press, pp. 1197-1202, 1970; J. Cable, J. K. MacLeod, M. R. Vegar, and R. J. Wells, *Org. Mass Spectrom.*, 7, 1137 (1973).
45. J. K. MacLeod and R. J. Wells, *J. Amer. Chem. Soc.*, 95, 2387 (1973).
46. Further evidence is found in, I. Wahlberg, K. Karlsson and C. R. Enzell, *Org. Mass Spectrometry*, 10, 162 (1975).
47. V. S. Bul'fson, V. I. Zaretskii, V. G. Zaikin, A. A. Akhrem, A. V. Kamernitskii and A. M. Prokhoda, *Izv. Akad. Nauk SSSR, Ser. Khim. Nauk*, 1968, 770; translation, 1968(4), 801-807.
48. G. A. Russell, in *Free Radicals, Vol. I.*, J. K. Kochi, Ed., Wiley-Interscience, New York, Chap. 7, 1973.
49. M. M. Green, R. J. Cook, W. Rayle, E. Walton, and M. F. Grostic, *J. Chem. Soc. Commun.*, 1969, 81.
50. P. Brown, A. H. Albert, and G. R. Pettit, *J. Amer. Chem.*

- Soc.*, 92, 3212 (1970).
51. M. M. Green and R. B. Roy, *J. Amer. Chem. Soc.*, 92, 6368 (1970).
 52. D. S. Noyce and B. N. Batian, *J. Amer. Chem. Soc.*, 82, 1246 (1960).
 53. R. F. J. Cole, J. M. Coxon, M. P. Hortshorn, and G. R. Little, *Aust. J. Chem.*, 26, 1277 (1973).
 54. G. R. Waller, Ed., *Biochemical Applications of Mass Spectrometry*, Wiley-Interscience, New York, Chap. 10, 11, and 13 and references therein, 1972.
 55. H. Klein and C. Djerassi, *Chem. Ber.*, 106, 1897 (1973). See also M. Ende and G. Spiteller, *Org. Mass Spectrometry*, 10, 200 (1975).
 56. G. R. Waller, Ed., *Biochemical Applications of Mass Spectrometry*, Wiley-Interscience, New York, p. 261, 1972.
 57. N. S. Wulfson, V. I. Zaretskii, V. L. Sadovskaya, A. V. Zakharychev, S. N. Ananchenko, and I. V. Torgov, *Tetrahedron*, 23, 3667 (1967).
 58. V. I. Zaretskii, N. S. Wulfson, V. G. Zaikin, L. M. Kogan, N. E. Voishvillo, and I. V. Torgov, *Tetrahedron*, 22, 1399 (1966).
 59. W. H. Elliott, in *Biochemical Applications of Mass Spectrometry*, G. R. Waller, Ed., Wiley-Interscience, New York, Chapter 11, p. 291ff, 1972.
 60. E. Zietz and G. Spiteller, *Tetrahedron*, 30, 585 (1974).
 61. J. Karliner, H. Budzikiewicz, and C. Djerassi, *J. Org. Chem.*, 31, 710 (1966).
 62. C. C. Fenselau and C. H. Robinson, *J. Amer. Chem. Soc.*, 93, 3070 (1971). See also: S. Gaunitz, H. Schwarz and F. Bohlmann, *Tetrahedron*, 31, 185 (1975).
 63. V. I. Zaretskii, N. S. Wulfson, V. G. Zaikin, S. N. Ananchenko, V. N. Leonov, and I. V. Torgov, *Tetrahedron*, 21, 2469 (1965).
 64. V. I. Zaretskii, N. S. Wulfson, V. G. Zaikin, V. N. Leonov, and I. V. Torgov, *Tetrahedron*, 24, 2339 (1968).
 65. C. R. Enzell, I. Wahlberg, and L-E Gunnarsson, *Org. Mass Spectrom.*, 9, 372, (1974); see also A. F. Thomas and B. Willhalm, *J. Chem. Soc.*, B, 1966 219; F. Bohlmann, C. Köppel and H. Schwarz, *Chem. Ber.*, 107, 2905 (1974).
 66. H. -W. Fehlbauer, D. Lenoir, and R. Tschesche, in *Advances in Mass Spectrometry*, Vol. 4, E. Kindrick, Ed. Elsevier New York, pp. 183-191, 1968; J. F. Templeton and C. W. Wie, *Can. J. Chem.*, 52, 517 (1974); A. C. Coxon and J. F. Stoddart, *J. Chem. Soc. Chem. Commun.*, 1974 537.
 67. Z. M. Akhtar, C. E. Brion, and L. D. Hall, *Org. Mass Spectrom.*, 8, 189 (1974).
 68. G. W. Klein and V. F. Smith, Jr., *J. Org. Chem.*, 35 52 (1970).
 69. A. J. Gordon and R. A. Ford, *The Chemists Companion*,

- Wiley-Interscience, New York, p. 107, 1972.
70. J. Winkler and H-F Grützmacher, *Org. Mass Spectrom.*, 3, 1139 (1970). A recent review has appeared: H.-F. Grützmacher, *Suomen Kemistilehti*, 46, 50 (1973). See also H.-F. Grützmacher and R. Asche, *Chem. Ber.*, 108, 2080 (1975).
 71. A. P. Bruins and N. M. M. Nibbering, *Tetrahedron*, 30, 493 (1974).
 72. H.-F. Grützmacher and K.-H. Fechner, *Org. Mass Spectrom.*, 7, 573 (1973).
 73. R. H. Martin, F. W. Lampe, and R. W. Taft, *J. Amer. Chem. Soc.*, 88, 1353 (1966).
 74. H.-F. Grützmacher and K.-H. Fechner, *J. Amer. Chem. Soc.*, 9, 152 (1974).
 75. P. D. Woodgate, R. T. Gray, and C. Djerassi, *Org. Mass Spectrom.*, 4, 257 (1970). See also: M. Machmout-Claeys, P. DeClercq and M. Vanderwalle, *ibid.*, 9, 1182 (1974).
 76. S. Sasaki, Y. Itagaki, H. Abe, K. Nakanishi, T. Suga, T. Shishihou, and T. Matsuura, *Org. Mass Spectrom.*, 1, 61 (1968); G. Peterson, O. Samuelson, K. Anjou, and E. V. Sydow, *Acta Chem. Scand.*, 21, 1251 (1967); H.-F. Grützmacher and K. H. Fechner, *Tetrahedron*, 27, 5011 (1971); A. Buchs, *Helv. Chem. Acta*, 51, 688 (1968); G. A. Singy and A. Buchs, *ibid.*, 54, 537 (1971); A. Buchs and E. Charollais, *ibid.*, 56, 207 (1973); G. A. Singy and A. Buchs, *ibid.*, 57, 1158 (1974); A. Buchs, A. Glangetas, and J. M. J. Tronchet, *ibid.*, 57, 1333 (1974).
 77. O. S. Chizhov, L. S. Golovkina, and N. S. Wulfson, *Carbohydr. Res.*, 6, 143 (1968).
 78. W. A. König, K. Zech, R. Uhmman, and W. Voelter, *Chem. Ber.*, 105, 262 (1972).
 79. T. Radford and D. C. DeJongh, in *Biochemical Applications of Mass Spectrometry*, G. R. Waller, Ed., Wiley-Interscience, New York, Chap. 12, 1972.
 80. D. C. DeJongh and K. Biemann, *J. Amer. Chem. Soc.*, 86, 67 (1964).
 81. J. Vink, W. Heerma, J. P. Kamerling, and J. F. G. Vliegthart, *Org. Mass Spectrom.*, 9, 536 (1974).
 82. D. G. I. Kingston, J. T. Bursey, and M. M. Bursey, *Chem. Rev.*, 74, 215 (1974).
 83. C. Djerassi, *Pure Appl. Chem.*, 9, 159 (1964).
 84. J. D. Henion and D. G. I. Kingston, *J. Amer. Chem. Soc.*, 96, 2532 (1974).
 85. A. F. Thomas and B. Willhalm, *Helv. Chem. Acta*, 50, 826 (1967).
 86. H. E. Audier, M. Fétizon, and P. Foy, *Bull. Soc. Chim. France*, 1967, 1271.
 87. E. Lund, H. Budzikiewicz, J. M. Wilson, and C. Djerassi, *J. Amer. Chem. Soc.*, 85, 941 (1963); T. A. Eggelte and

- N. M. M. Nibbering, *J. Chem. Soc., Perkin II*, 1974, 605.
88. I. Lengyel and V. R. Ghatak, *Advances in Mass Spectrometry*, Vol. 6, A. R. West, Ed., Applied Science, Essex, England, p. 47ff, 1974.
89. R. T. Gray and R. J. Pryce, *J. Chem. Soc., Perkin II*, 1974, 955.
90. N. Y. Wang, Ph.D. thesis, State University of New York at Buffalo, 1972; P. T. Lansbury, N. Y. Wang, and J. E. Rhodes, *Tetrahedron Lett.*, 1829 (1971).
91. J. Deutsch and A. Mandelbaum, *J. Amer. Chem. Soc.*, 92, 4288 (1970); A. Mandelbaum, J. Deutsch, A. Karpatis, and I. Merksammer, *Advances in Mass Spectrometry*, Vol. 5, Elsevier, Amsterdam, pp. 672-675, 1970. S. Weinstein, E. Gil-Av, J. H. Leftin, E. C. Levy and A. Mandelbaum, *Org. Mass Spectrometry*, 9, 774 (1974).
92. E. Gil-Av, J. H. Leftin, A. Mandelbaum, and S. Weinstein, *Org. Mass Spectrom.*, 4, 475 (1970).
93. P. Schiess and H. L. Chia, *Helv. Chim. Acta*, 53, 485 (1970).
94. F. Benoit, J. L. Holmes, and N. S. Isaacs, *Helv. Chim. Acta*, 2, 591 (1969); F. Benoit and J. L. Holmes, *ibid.*, 6, 541 (1972).
95. H. Budzikiewicz, C. Djerassi, and D. H. Williams, *Mass Spectrometry of Organic Compounds*, Holden-Day, p. 221, 1967.
96. H. Fischer, in *Free Radicals*, Vol. II, J. K. Kochi, Ed., Wiley-Interscience, New York, Chap. 19 and references therein, 1973; M. J. Perkins, *ibid.*, Vol. I, Chap. 16 and references therein.
97. J. H. Bowie, D. H. Williams, P. Madsen, G. Schroll, and S.-O. Lawesson, *Tetrahedron*, 23, 305 (1967).
98. S. Meyerson, P. J. Ihrig, and T. L. Hunter, *J. Org. Chem.*, 36, 995 (1971).
99. S. Meyerson, *Int. J. Mass Spectrom. Ion Phys.*, 1, 309 (1968). See also: W. J. Richter and A. L. Burlingame, *Recent Developments in Mass Spectroscopy*, Ed. By K. Ogata and T. Hayakawa, Univ. of Tokyo Press, 1970, p. 1227.
100. P. J. Wagner, *J. Amer. Chem. Soc.*, 89, 5898, (1967).
101. R. Ryhage, S. Stållberg-Stenhagen, and E. Stenhagen, *Ark. Kemi*, 18, 179 (1961).
102. A. van Wageningen, H. Cerfontion, and N. M. M. Nibbering, *Recueil*, 93, 43 (1974).
103. H. Budzikiewicz, J. I. Brauman, and C. Djerassi, *Tetrahedron*, 21, 1855 (1965).
104. P. Natalis, in *Mass Spectrometry*, R. I. Reed, Ed., Academic, New York, p. 379ff, 1965.
105. J. Deutsch and A. Mandelbaum, *J. Amer. Chem. Soc.*, 91, 4809 (1969).
106. J. Deutsch and A. Mandelbaum, *J. Chem. Soc., B*, 1971, 886.

107. A. Karpati, A. Rave, J. Deutsch, and A. Mandelbaum, *J. Amer. Chem. Soc.*, 95, 4244 (1973).
108. J. Deutsch and A. Mandelbaum, *Org. Mass Spectrom.*, 5, 53 (1971).
109. T. Lesman and J. Deutsch, *Org. Mass Spectrom.*, 7, 1321 (1973).
110. R. Grubbs, Ph.D. thesis, Columbia University, Part III, 1968.
111. A. Mandelbaum and P. Bel, *Advances in Mass Spectrometry*, Vol. 6, A. R. West, Ed., Applied Science, Essex, England, pp. 25-29, 1974.
112. H. Audier, M. Fétizon, and W. Vetter, *Bull. Soc. Chim. France*, 1964, 1971.
113. B. J. Millard and D. F. Shaw, *J. Chem. Soc., B*, 1966, 664.
114. B. Willhalm and A. F. Thomas, *Helv. Chim. Acta*, 50, 383 (1967).
115. T. H. Kinstle and R. E. Stark, *J. Org. Chem.*, 32, 1318 (1967).
116. H. F. Grutzmacher and M. Puschmann, *Chem. Ber.*, 104, 2079 (1971).
117. P. J. Derrick, A. M. Falick, and A. L. Burlingaine, *J. Amer. Chem. Soc.*, 94, 6794 (1972).
118. E. P. Smith and E. R. Thornton, *J. Amer. Chem. Soc.*, 89, 5079 (1967).
119. S. W. Staley and D. W. Reichard, *J. Amer. Chem. Soc.*, 90, 816 (1968).
120. S. Hammerum and C. Djerassi, *J. Amer. Chem. Soc.*, 95, 5806 (1973), and Ref. 3 therein.
121. R. B. Woodward and R. Hoffmann, *The Conservation of Orbital Symmetry*, Academic, New York, 1970.
122. M. K. Hoffman, M. M. Bursey, and R. E. K. Winter, *J. Amer. Chem. Soc.*, 92, 727 (1970). See also: R. A. W. Johnstone and S. D. Ward, *J. Chem. Soc. (C)*, 1968, 1805; M. J. Bishop and I. Fleming, *ibid.*, 1969, 1712; A. Mandelbaum, S. Weinstein, E. Gil-Av and J. H. Leftin, *Org. Mass Spectrom.*, 10, 842 (1975).
123. D. H. Williams and G. Hvistendahl, *J. Amer. Chem. Soc.*, 6753 (1974); *ibid.*, 6755 (1974).
124. G. W. Francis, *Acta Chem. Scand.*, 26, 1443 (1972); G. W. Francis, S. Norgard, and S. Liaaen-Jensen, *ibid.*, B28, 244 (1974); J. E. Johansen, A. Eidem, and S. Liaaen-Jensen, *ibid.*, B28, 385 (1974).
125. a M. S. Baird and C. B. Reese, *Tetrahedron Lett.*, 1969, 2117; b M. A. Winnik, *Org. Mass Spectrometry*, 9, 920 (1974).
126. P. Von R. Schleyer, G. W. VanDine, V. Schöllkopf, and J. Paust, *J. Amer. Chem. Soc.*, 88, 2868 (1966).
127. P. Natalis, *Bull. Soc. Chim. Belges*, 75, 668 (1966).
128. S. Meyerson and A. W. Weitkamp, *Org. Mass Spectrom.*, 2, 603 (1969).

129. M. J. S. Dewar and S. D. Worley, *J. Chem. Phys.*, 50, 654 (1969).
130. R. Botter, F. Menes, Y. Gounelle, J. M. Pechine, and D. Solgadi, *Int. J. Mass Spectrom. Ion Phys.*, 1973, 188; C. E. Brion, J. S. H. Farmer, R. E. Pincock, and W. B. Stewart, *Org. Mass Spectrom.*, 4, 587 (1970).
131. G. R. Waller, Ed., *Biochemical Applications of Mass Spectrometry*, Wiley-Interscience, New York, Chap. 4, 1974; A. G. Harrison, in *Topics in Organic Mass Spectrometry*, A. L. Burlingame, Ed., Wiley-Interscience, New York, p. 121ff, 1970.
132. L. D'Or, J. Momigny, and P. Natalis, *Advances in Mass Spectrometry*, vol. 2, MacMillan, London, p. 370ff, 1963; P. Natalis and J. L. Franklin, *Bull. Soc. Chim. Belges*, 75, 328 (1966); see also V. I. Zaretskii, V. L. Sadovskaya, N. S. Wulfson, V. F. Sizoy, and V. G. Merimson, *Org. Mass Spectrom.*, 5, 1179 (1971) and previous papers.
133. J. Jalonen and K. Pihlaja, *Org. Mass Spectrom.*, 7, 1203 (1973); see also: Z. V. I. Zaretskii and L. Kelner, *Tetrahedron*, 31, 85 (1975).
134. K. Pihlaja, J. Jalonen, and D. M. Jordon, *Advances in Mass Spectrometry*, Vol. 6, A. R. West, Ed., Applied Science Essex, England, p. 105ff and references therein, 1974.
135. H. Iwamura, *Tetrahedron Lett.*, 1973 4575.
136. H. Iwamura, *J. Chem. Soc., Chem. Commun.*, 1973 232.
137. A. Karpati and A. Mandelbaum, *Org. Mass Spectrom.*, 5, 1345 (1971).
138. Reference 6 of 137; J. N. Nazarov, and V. F. Kuckarov, *Chem. Abstr.*, 49, 5329 (1955).
139. M. C. Hamming and G. W. Keen, *Int. J. Mass Spectrom. Ion Phys.*, 3, Appl 1-4 (1969).
140. D. C. DeJongh and S. R. Shrader, *J. Amer. Chem. Soc.*, 88, 3881 (1966).
141. D. C. DeJongh, S. R. Shrader, R. G. Isakson, N. A. LeBel, and J. H. Beynon, *Org. Mass Spectrom.*, 2, 919 (1969).
142. D. G. Farnum and A. D. Wolf, *J. Amer. Chem. Soc.*, 96, 5166 (1974) and references therein.
143. D. R. Dimmel and J. M. Seipenbusch, *J. Amer. Chem. Soc.*, 94, 6211 (1972).
144. T. T. Tidwell, *J. Amer. Chem. Soc.*, 92, 1448 (1970); see also H. C. Brown, *Acc. Chem. Res.*, 6, 377 (1973) and references therein.
145. F. W. McLafferty, *Anal. Chem.*, 34, 2 (1962).
146. R. Robbiani and J. Seibl, *Org. Mass Spectrom.*, 7, 1153 (1973).
147. K. R. Jennings, *J. Chem. Soc., Chem. Commun.*, 1966, 283; E. Caspi, J. Wicha and A. Mandelbaum, *ibid.*, 1967, 1161; J. Seibl, *Helv. Chim. Acta*, 50, 263 (1967). S. Meyerson,

- R. W. Vander Haar and E. K. Fields, *J. Org. Chem.*, 37, 4114 (1972).
148. J. L. Holmes and D. McGillivray, *Org. Mass Spectrom.*, 7, 559 (1973); see also P. H. Chen, W. F. Kuhn, D. C. Kleinfelter, and J. M. Miller, Jr., *Org. Mass Spectrom.*, 6, 785 (1972).
149. K. G. Das, M. S. B. Nayar, and C. A. Chinchwadkar, *Org. Mass Spectrom.*, 3, 303 (1970).
150. L. Tökes and C. Djerassi, *Steroids*, 6, 493 (1965).
151. H.-W. Fehlhaber, D. Lenoir and P. Welzel, *Advances in Mass Spectrometry*, Vol. 5, A. Quayle, Ed., Elsevier, Amsterdam, p. 689, 1971.
152. P. Longevialle, J. P. Alazard, and X. Lusinchi, *Org. Mass Spectrom.*, 9, 480 (1974).
153. H. E. Audier, M. Fétizon, H. B. Kagan, and J. L. Luche, *Bull. Soc. Chim. France*, 1967, 2297.
154. D. A. Bak and K. Conrow, *J. Org. Chem.*, 31, 3608 (1966).
155. J.-L. Imbach, E. Doomes, N. H. Cromwell, H. E. Baumgarten, and R. G. Parker, *J. Org. Chem.*, 32, 3123 (1967).
156. M. L. Gross and C. L. Wilkins, *Tetrahedron Lett.*, 1969, 3875.
157. W. M. Bryant III, A. L. Burlingame, H. O. House, C. G. Pitt, and B. A. Tefertiller, *J. Org. Chem.*, 31, 3120 (1966).
158. R. Furstoss, A. Heumann, B. Waegell, and J. Gore, *Org. Mass Spectrom.*, 6, 1207 (1972).
159. V. G. Zaikin, N. S. Wulfson, V. I. Zaretskii, A. A. Bakaev, A. A. Akhrem, L. I. Ukhova, and N. F. Uskova, *Org. Mass Spectrom.*, 2, 1257 (1969); N. S. Wulfson, A. A. Bakaev, V. G. Zaikin, A. A. Akhrem, L. I. Ukhova, A. P. Marochin, and G. V. Bludova, *ibid.*, 6, 533 (1972).
160. M. Shamma and K. F. Foley, *J. Org. Chem.*, 32, 4141 (1967).
161. A. Mandelbaum and D. Ginsburg, *Tetrahedron Lett.*, 1965, 2479.
162. H. Nakata, Y. Hirata, A. Tatematsu, H. Tada, and Y. K. Sawa, *Tetrahedron Lett.*, 1965, 829.
163. A. W. J. D. Dekkers, N. M. M. Nibbering, and W. N. Speckamp, *Tetrahedron*, 28, 1829 (1972).
164. N. S. Wulfson, Z. S. Ziyavidinova, and V. G. Zaikin, *Org. Mass Spectrom.*, For earlier work on alkaloids see K. Biemann, P. Bommer, A. L. Burlingame and W. J. McMurray, *J. Amer. Chem. Soc.*, 86, 4624 (1964).
165. L. Tökes and B. A. Amos, *J. Org. Chem.*, 37, 4421 (1972).
166. M. L. Gross, C. L. Wilkins, and T. G. Regulski, *Org. Mass Spectrom.*, 5, 99 (1971).
167. R. M. Dodson, P. J. Cahill, and V. C. Nelson, *J. Chem. Soc., Chem. Commun.*, 1968, 620.
168. J. M. Moldowan, Ph.D. thesis, University of Michigan, 1972.

169. J. H. Bowie, D. H. Williams, S. O. Lawesson, J. Ø. Madsen, C. Nolde, and G. Schroll, *Tetrahedron*, 1966, 3515.
170. H.-R. Schulten and H. D. Beckey, *J. Agr. Food Chem.*, 21, 372 (1973). W. D. Lehmann and H. D. Beckey, *Org. Mass Spectrometry*, 9, 1086 (1974); S. Caccamese, G. Montaudo and M. Przybylski, *ibid.* 9, 1114 (1974).
171. H. D. Beckey, *Field Ionization Mass Spectrometry*, Pergamon, New York, 1971.
172. F. H. Field, *Acc. Chem. Res.*, 1, 42 (1968).
173. P. Longevialle, G. W. A. Milne, and H. M. Fales, *J. Amer. Chem. Soc.*, 95, 6666 (1973).
174. W. C. Agosta, D. V. Bowen, R. A. Cormier, and F. H. Field, *J. Org. Chem.*, 39, 1752 (1974) and references therein; T. J. Odiorne, D. J. Harvey, and P. Vouros, *J. Org. Chem.*, 38, 4274 (1973); J. Winkler and F. W. McLafferty, *Tetrahedron*, 30, 2971 (1974).
175. J. D. Baldeschwieler and S. S. Woodgate, *Acc. Chem. Res.*, 4, 114 (1971); J. L. Beauchamp, *Annu. Rev. Phys. Chem.*, 22, 527 (1971).
176. K. Mislow, *Introduction to Stereochemistry*, Benjamin, New York, p. 67, 1965.
177. S. A. Benezra and M. M. Bursey, *J. Amer. Chem. Soc.*, 94, 1024 (1972).
178. M. M. Bursey and M. K. Hoffman, *Can. J. Chem.*, 49, 3395 (1971).
179. M. M. Bursey, J.-I. Kao, J.-L. Henion, C. E. Parker, and T.-I. S. Huang, *Anal. Chem.*, 46, 1709 (1974).
180. J. K. Kim, M. C. Findlay, W. G. Henderson, and M. C. Caserio, *J. Amer. Chem. Soc.*, 95, 2184 (1973).
181. C. A. Lieder and J. I. Brauman, *J. Amer. Chem. Soc.*, 96, 4028 (1974); C. A. Lieder and J. I. Brauman, *Int. J. Mass Spec. and Ion Phys.*, 16, 307 (1975).
182. E. L. Eliel, N. L. Allinger, S. J. Angyal and G. A. Morrison, *Conformational Analysis*, Interscience Publ., N. Y., 1965, p. 187-188; See section IA herein and associated references.
183. M. M. Green and J. L. Martin, *Twenty-Third Annual Conference on Mass Spectrometry and Allied Topics*, May 25-30, 1975, Houston, Texas, American Society for Mass Spectrometry Publ., paper 0-10.
184. E. L. Eliel, *Stereochemistry of Carbon Compounds*, McGraw-Hill Publ., N. Y., 1962, p. 185-186.
185. J. I. Brauman and L. K. Blair, *J. Amer. Chem. Soc.*, 92, 5986 (1970); A recent paper with leading references is L. Radom, *Aust. J. Chem.* 28, 1 (1975). See also R. T. Morrison and R. N. Boyd, *Organic Chemistry*, 3rd Edition, Allyn and Bacon, Boston, 1973, p. 526.
186. R. C. Dougherty, *Topics in Current Chemistry*, 10, 93 (1973); M. J. S. Dewar and R. C. Dougherty, *The PMO Theory*

of Organic Chemistry, Plenum/Rosetta Edition, N.Y., 1975, Ch. 7; Metastable ion behavior shows insightful stereo-isomeric dependence. See: K. C. Kim, J. H. Beynon and R. G. Cooks, *J. Chem. Phys.*, 61, 1305 (1974)/K. C. Kim and R. G. Cooks, *J. Org. Chem.*, 40, 511 (1975).

THE LANTHANIDE INDUCED SHIFT TECHNIQUE: APPLICATIONS
IN CONFORMATIONAL ANALYSIS

OTMAR HOFER

*Lehrkanzel für Organische Chemie der
Universität Wien, Vienna, AUSTRIA*

- I. Introduction 111
- II. Theory and Computational Techniques 113
 - A. Paramagnetic Shift 113
 - B. The McConnell-Robertson Equation for an Axially Symmetrical Dipolar Field 115
 - 1. Contact Shifts 117
 - 2. Nonaxial Contributions to Dipolar Shifts 121
 - C. Computational Approaches 122
 - 1. General Procedures 123
 - 2. Agreement Factor and Significance Testing 126
 - 3. Orientation of the Principal Magnetic Axis 131
 - 4. Simple Distance Relationships 132
- III. Experimental Techniques 133
 - A. Reagent 133
 - B. Substrate and Functionality 139
 - C. Extraction of LIS Parameters from Experiment; "Bound" or "Limiting" Shifts; Complexation Constant and Stoichiometry 143
- IV. Stereochemical Applications of LIS Values 153
 - A. Identification of Isomers 155
 - B. Conformational Analysis 158
 - 1. Conformational Changes Introduced by Shift Reagents - Yes or No 158
 - 2. Torsion about Single Bonds not Incorporated in a Cyclic System 162
 - 3. Conformations of Cyclic Systems 179

I. INTRODUCTION

The discovery by Hinckley (1) that large isotropic chemical shifts are produced in the pmr spectrum of cholesterol without concomitant undesirable line broadening when tris(dipivalomethanato)europium(III)dipyridinate, $\text{Eu}(\text{dpm})_3(\text{py})_2$, is added to the

solution of this substrate triggered rapid development in what has become an important specialized area of nmr spectroscopy. Attempts were soon made to improve the shift reagents [the metal (2,3) as well as the ligand (4,5)] and to explore the applicability of the new method to a variety of functional organic molecules. The technique was then extended to other nuclei than ^1H ; ^{13}C lanthanide induced shifts, especially, proved to furnish valuable complementary information, and the method was applied to less common nuclei (^{14}N , ^{19}F , ^{31}P) as well.

From the very beginning there was interest in the quantitative interpretation of the observed phenomenon. In the first attempt in this direction a pure dipolar shift mechanism was assumed, which led (in its simplest form) to a r^{-3} dependency of the induced shifts, r representing the distance from the observed proton to the metal ion. This approach was modified by several authors but soon it was demonstrated that angle dependency could not be ignored since shifts in the "wrong" direction were found (6), the r^{-n} method failing not just with respect to magnitude but with respect to sign as well. Later on, the methods for interpreting the numerical values of lanthanide induced shifts (LIS) became more and more sophisticated through use of elaborate computer programs for the necessary extensive calculations. The model underlying these calculations has often been questioned, but the apparent success of the LIS method is impressive enough to make it into one of the most powerful tools in conformational analysis, especially for organic molecules in solution.

Determination of molecular topology by LIS is more general than use of the nuclear Overhauser effect (NOE) where the maximal distance for a detectable effect is limited to about 3.5 Å. There is almost no distance limit in the case of LIS, even in large molecules (the effect is still observable at 10 Å or more). The two techniques, in fact, complement each other. A third, not yet fully exploited complementary technique, related to the LIS method, should be mentioned here. This is the use of relaxation reagents (7), which are chemically equal to shift reagents, but carry a different lanthanide ion, (Gd(III)) which produces no shifts but, instead, broadening of signals caused by enhanced relaxation rates. The point of interest is that the lanthanide induced relaxation (LIR) is proportional to r^{-6} and no angular dependency is to be expected, thus allowing simple calculation of the distance: observed nucleus to Gd(III).

The most interesting and fascinating applications of lanthanide shift reagents (LSR) take advantage of the numerical value of the LIS. This quantitative aspect is our major concern in this Chapter. Nevertheless, the qualitative use of LSR just for simplification of nmr spectra is of tremendous help for interpretation of the line pattern. This was demonstrated most impressively by Sanders and Williams (4), who obtained a first-order spectrum for *n*-hexanol in the presence of $\text{Eu}(\text{dpm})_3$. The dramatic shifts induced by LSR are different for each of the nuclei in a molecule, and virtually all accidental coincidences

of resonance signals are removed. This improvement of resolution cannot be matched by any other methods enhancing the magnetic field. Aromatic-solvent-induced shift (ASIS) is a much less powerful method, and the construction of stronger magnets to increase the primary, external homogeneous magnetic field is limited and very costly. Adding a "pinch of lanthanide chelate" (8), in contrast, is inexpensive and highly efficient, the lanthanide ion producing an additional secondary, internal anisotropic magnetic field.

Utilization of the resulting high resolution includes such applications as determination of ratios of diastereomers by means of LSR, determination of enantiomeric purity using chiral LSR, and, most important, analysis of nmr spectra is in general greatly simplified because the spin-spin couplings are reduced in order. The latter point is of special interest for conformational analysis in that it allows torsional angles to be deduced by relationships such as the Karplus equation. Since these applications are extensions of already well known tools in stereochemistry, they are not treated explicitly in this report; recent detailed reviews are available (9, 10).

In the following pages the theory of LIS will be presented, and the simplifications assumed in the calculations of LIS are indicated. Evidence for the justification of the computational approaches is presented, including arguments, pro as well as con. The precautions to be taken in the experimental techniques for obtaining reliable values for the parameters to be extracted from experiment will be discussed in the light of theoretical considerations. Finally, there is extensive comment on stereochemical information obtained for a variety of organic molecules by the LIS method. The literature up to December 1974 is covered, and the examples concerning conformational analysis should offer a representative survey of compounds studied so far.

II. THEORY AND COMPUTATIONAL TECHNIQUES

Incorporation of a paramagnetic metal ion into a substrate molecule by means of some kind of complexation or chelation modifies the external homogeneous magnetic field, at least in the close vicinity of the metal ion. When calculating the induced additional chemical shifts one has to reason carefully whenever simplifications are made, which is usually the case. We discuss here what kinds of effects are to be expected and what types of approaches in computation are the most effective with regard to accuracy as well as simplicity.

A. Paramagnetic Shift

The lanthanide induced shift (LIS) value is defined as the difference between the resonance frequencies of a substrate (S) and the shift of the adduct (lanthanide reagent - substrate, LS):

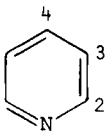
$$\Delta = \nu_{LS} - \nu_S \quad [1]$$

Δ is the observed induced shift, and since it represents the average of the signal for complexed and uncomplexed substrate (fast exchange of L and S with LS occurs on the nmr time scale), Δ is proportional to the concentration of reagent (L) in solution. Thus a plot of Δ versus concentration of LSR is a straight line passing through zero (see Sect. III-C). In cases where only the relative induced shifts for the different nuclei of a substrate are of interest, the Δ values can stand alone; otherwise they need some specifications: units of ppm or Hz; molar ratio of reagent to substrate (L_0/S_0) present in solution (in most cases authors give Δ for $L_0/S_0 = 1:1$, usually obtained by extrapolation); and of course experimental information about reagent, solvent, temperature, and instrument used.

When a paramagnetic shift reagent is used, this Δ is called the "paramagnetic shift", implying that the diamagnetic component (11, 12) on complex formation is negligible.

Few authors worry about the diamagnetic component of the observed shift (11, 12), and this simplification seems to be justified. A simple test to assess this (minor) effect is to measure the shift obtained with a chemically similar diamagnetic ion, in this case, lanthanum(III). When using Eu(dpm)_3 as a paramagnetic shift reagent it is possible to gain information on the diamagnetic component by comparing the shifts adding La(dpm)_3 in a second experiment. The diamagnetic shift effects are usually very small if detectable at all. In the most extreme cases they amount to about 2% of the observed paramagnetic shift. Table 1 illustrates this for pyridine as substrate, and some additional examples are given below.

Table 1. Paramagnetic, Eu(dpm)_3 , and Diamagnetic, La(dpm)_3 , Shifts for Pyridine

LSR	LIS (ppm)			
	H-2	H-3	H-4	
Eu(dpm)_3	25.9	9.0	8.2	
La(dpm)_3	-0.28	0.02	-0.06	
% Diamagn.	1.08%	0.22%	0.73%	

The La(dpm)_3 -induced shifts for ethanol compared to those of Eu(dpm)_3 are 2% for the OH and 0.12% for CH; for *exo-exo*-2,3-camphanediol, 2% (protons at C-2 and C-3), 0% (CH_3); for diethylamine no diamagnetic shifts are observed. (12).

Since the diamagnetic shifts are small we confine further

considerations to the highly dominant paramagnetic shifts.

B. The McConnell-Robertson Equation for an Axially Symmetrical Dipolar Field

For a metal possessing unpaired electrons the paramagnetic shift (Δ_{para}) has two components: the dipolar or pseudocontact term and the Fermi contact term. The first describes all magnetic-dipolar types of interactions, the latter accounts for possible spin-delocalisation within the complex. The first effect acts through space and can be formulated as a dipolar magnetic field, the latter acts through the bonds and represents a polarisation caused by a partially covalent bond between substrate and lanthanide reagent.

$$\Delta_{\text{para}} = \Delta_{\text{dip}} + \Delta_{\text{contact}} \quad [2]$$

We discuss Δ_{dip} first; Δ_{contact} is treated in Sect. II-B-1. To calculate the dipolar- or pseudocontact-term one assumes a dipolar magnetic field. The origin of the field is thought to be represented by the position of the lanthanide ion in the complex (point dipole) with coordinates 0,0,0 in Figure 1. Now the dipolar shift can be expressed (13) as a function of the internal coordinates of the nucleus under consideration: r is the length of a vector joining the paramagnetic center and the nucleus, θ is the angle between this vector and the z -magnetic axis, and ω is the angle which the projection of \vec{r} into the xy -plane makes with the x magnetic axis (Fig. 1.). The equation for this dipolar shift in its most general form is (9,13-15)

$$\Delta_{\text{dip}} = K_{\text{ax}} \left(\frac{3 \cos^2 \theta - 1}{r^3} \right) + K_{\text{nonax}} \left(\frac{\sin^2 \theta \cos 2\omega}{r^3} \right) \quad [3]$$

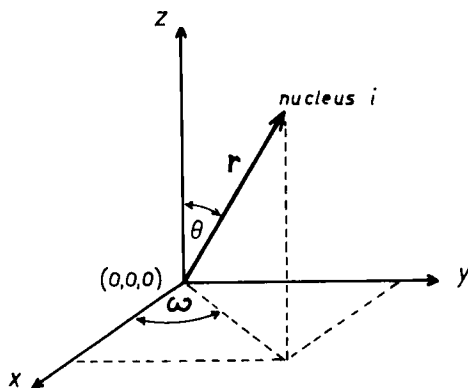


Fig. 1. Definition of the parameters for the dipolar shift equation [3]-[6]; the lanthanide ion is at the origin of the coordinate system.

The expressions in the brackets are called the "geometric factors"; they are dependent on the geometry of the complex formed but independent of the lanthanide itself (except in so far as the metalloorganic molecule used as a shift reagent may influence the substrate geometry significantly).

The constants K_{ax} and K_{nonax} are functions of the magnetic anisotropy of the complex, determined by the electronic properties of the lanthanide in magnitude and sign (see Sect. III-A). In the case of most common relaxation phenomena (13,16) (where the tumbling time of the complex is much greater than the electron spin relaxation time) these constants may be expressed as functions of the three principal molecular magnetic susceptibilities χ_x , χ_y , χ_z (17), corresponding to the x , y , and z axes in Figure 1. (N , Avogadro number):

$$K_{ax} = -\frac{1}{3N} (\chi_z - \frac{1}{2} \chi_x - \frac{1}{2} \chi_y) \quad [4]$$

$$K_{nonax} = -\frac{1}{2N} (\chi_x - \chi_y) \quad [5]$$

A special case is given for an axially symmetrical field where $\chi_z = \chi_{\parallel}$ and $\chi_x = \chi_y = \chi_{\perp}$. Then K_{nonax} becomes zero, and the nonaxial term in eq. [3] vanishes. Equation [3] reduces to eq. [6]. Equation [6] is valid for all i observed resonances of a substrate.

$$\Delta_i = K \frac{3 \cos^2 \theta_i - 1}{r_i^3} \quad [6]$$

Equation [6] is the McConnell-Robertson equation (18) for an axially symmetrical dipolar magnetic field (point dipole). It is used in most calculations of LIS values. K is treated as an adjustable scaling factor to match the experimental to the geometrical factor $(3 \cos^2 \theta - 1)/r^3$. Δ_i is characteristic for a particular nucleus i ; θ_i and r_i depend on the geometry of the complex and can be calculated from an appropriate model of the complex for every nucleus i ; K is characteristic for the entire complex and therefore equal for all i nuclei within the adduct. If one knows the topology of the complex (geometry of the substrate and position of the lanthanide ion), then the observed induced shifts should be proportional to the calculated geometrical factor (details for computational approaches in Sect. II-C).

It is a characteristic feature of the geometrical factor that for $\theta = 54.7$ deg. the sign of the shift is inverted. Figure 2 illustrates the geometrical effect on the LIS.

In the following paragraphs we justify the neglect of contact shifts and of the nonaxial term of the dipolar shifts.

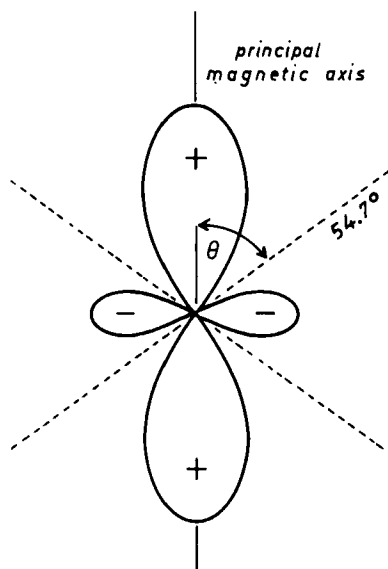


Fig. 2. The dipolar, axially symmetric field (point dipole); positive lobes signify induced downfield shifts, negative lobes upfield shifts for Eu(III); the reverse is true for Pr(III).

1. Contact Shifts

Returning to eq. [2], we see that in order to calculate the paramagnetic shift we need to know something about the contact contribution. Unfortunately the mathematical treatment of contact shifts is as yet rather uncertain, and the only choice we have to calculate Δ_{para} is to keep the contribution of Δ_{contact} as low as possible. This means the condition $\Delta_{\text{contact}} \ll \Delta_{\text{dip}}$ should hold, a point that has to be examined more closely.

There is a lot of evidence that the contact shift contribution for ^1H resonances is rather small. This was demonstrated by calculation of the LIS on the basis of the complete pseudo-contact eq. [3] plus eqs. [4] and [5] using information on the geometry of the complex gained by X-ray crystallography (15). The experimental shifts could be reproduced very well with no need for contact corrections (Table 2). The magnetic anisotropies assumed in these calculations agree with single-crystal anisotropy data (19).

The contact interaction is restricted to protons close to the coordination site, since the "through-bond" interaction

Table 2. LIS Values for All Protons of the $\text{Eu}(\text{dpm})_3$ (pyridine) $_2$ Complex

Proton LIS in ppm	Δ_{obsd}	Δ_{calcd} , eqs. [3]-[5] ^a	Δ_{calcd} , eq. [6] ^b
LSR			
methine	-8.77	-8.69	-7.27
<i>t</i> -butyl	-3.08	-2.29	-3.16
Substrate			
ortho H	15.48	15.65	15.89
meta H	5.47	5.72	6.35
para H	5.07	4.72	5.43
<i>RC</i>		0.047	0.094

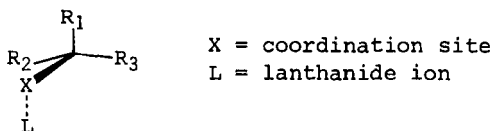
^aComputational result for the complete dipolar shift model.

^bComputational result for the McConnell-Robertson equation; *K* is fixed independently of solid state susceptibility data; the principal magnetic axis, in disagreement with X-ray data, is taken along the Eu-N line (see Sect. II-C-3).

RC is the agreement factor (see Sect. II-C-2).

decreases rapidly and vanishes beyond three or four bonds even in systems where substantial contact contributions are found (e.g., for all nuclei other than ^1H).

There is still another reason why no large contact shifts are expected for protons. There is evidence (8,20,21) that contact shifts should be largest when the metal ion and the observed nucleus are situated in the transoid arrangement.



If any of the substituents R_1 , R_2 , or R_3 is ^1H it will *not* assume position R_1 because the transoid arrangement provides the favored site for the bulkiest substituent (as far away as possible from the bulky lanthanide shift reagent) or, stating it the other way around, the LSR will preferentially orient itself in such a way that steric interference is minimal.

Thus, while ^1H contact shifts cannot be excluded a priori, they should represent a rather small contribution to the observed paramagnetic shift.

Some authors have found ^1H contact shifts up to about 10%

of the still dominant pseudocontact contribution for some of the lanthanides (22-25). The derivation of this value is not very secure. Usually it is based on differences in the induced shift ratios with respect to a series of different lanthanides. The shift ratios for all protons in a particular substrate for different lanthanides (L_1 und L_2) should represent a constant factor; the geometrical factor in [6] cancels out:

$$\frac{\Delta_z(L_1)}{\Delta_z(L_2)} = \frac{K(L_1)}{K(L_2)} = \text{const.}$$

Deviations from this simple relationship were interpreted as being due to different contact contributions for the different lanthanides. However, this computational approach suffers from lack of knowledge of details in the geometry of the complex (since even small differences in the position of the lanthanide ions relative to the substrate might invalidate the assumed cancellation of the geometrical factors) and from neglect of the nonaxial term (which neglect introduces additional uncertainty).

It was found that (especially for ^{13}C) the LIS values derived using $\text{Yb}(\text{dpm})_3$ fit better than the ones derived from $\text{Eu}(\text{dpm})_3$ to the values calculated using eq. [6].

In Figure 3 computational estimates of contact shifts of the system 3-fluoropyridine - $\text{Eu}(\text{dpm})_3$ are shown (22):

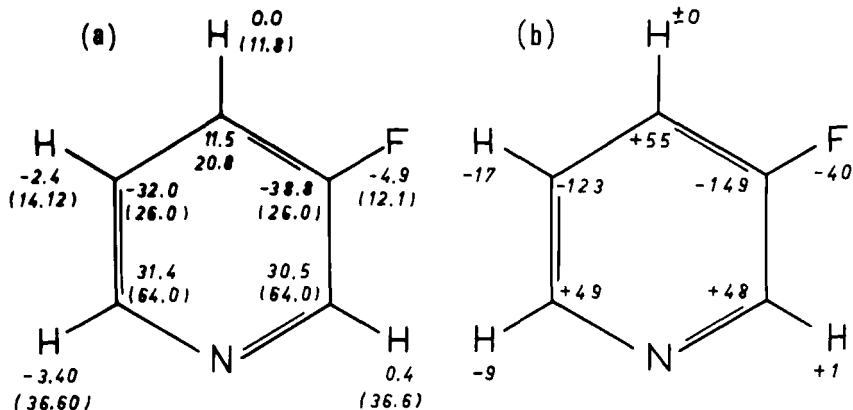


Fig. 3. (a) Estimated contact shifts, in ppm, for 3-fluoropyridine, $\text{Eu}(\text{dpm})_3$, scaled to yield best fit for the observed proton LIS; computed dipolar shifts in brackets; the sum of both is the observed LIS value; (b) contact/dipolar ratio, in percent (the corresponding values for 3-fluoropyridine, $\text{Yb}(\text{dpm})_3$, are between -6 and +6%, for protons as well as carbon atoms).

The contact shifts in Figure 3 might be overestimated on the grounds discussed above. With the complete dipolar eq. [3]

used by Cramer (15) a perfect fit was obtained for the system pyridine - Eu(dpm)₃ without any need for contact interaction for protons (Table 2). In this case one could argue that overcorrection for the nonaxial term overshadowed any contact deviations. The general dilemma here is that the failure of a simplified model is attributed to one particular aspect of the simplification only. At any rate, ¹H contact shift contributions might exist on a very low level for protons in the α or β position to the coordinating functional group.

While one may argue about the reliability of the values for proton contact shifts, the magnitude of the values for ¹³C and ¹⁹F are rather convincing. For all nuclei other than ¹H, both pseudocontact and contact shifts are to be expected: ¹³C (22, 24-28), ¹⁹F (22, 29, 30), ³¹P (31, 32), and ¹⁴N (33). Close to the coordination center, the contact interactions for these nuclei are rather large. Highly dominating dipolar shifts cannot be assumed safely when the nucleus (C,F,P,N) under consideration is not at a distance of at least four bonds.

Estimation of the contact contribution to the induced shifts might disclose regularities which might in turn be exploited to derive stereochemical conclusions (20,21). The sign alteration which is observed for the ¹³C contact contribution along the carbon chain in pyridine was interpreted as spin delocalisation in the σ-bond molecular framework. INDO calculations (34) appropriately simulate the change in sign of the contact contribution along the carbon chain (Table 3). It may be seen from Table 3

Table 3. Induced Chemical Shifts for Pyridine, Eu(dpm)₃; Calculated LIS on the Basis of eq. [6]

Position	Proton LIS		Carbon LIS		¹³ C diff.	Relative diff. ^a	Relative diff. calcd. ^b
	Δ _{obsd}	Δ _{calcd}	Δ _{obsd}	Δ _{calcd}			
α	31.02	31.10	90.0	67.78	22.22	1.00	1.00
β	10.68	10.59	-0.88	24.33	-25.21	-1.13	-0.58
γ	9.71	9.33	30.22	18.73	11.49	0.52	0.34

^aStandardized on α-carbon "difference shift" = 1.00.

^bBased on INDO calculation.

that the ¹H LIS are reproduced very well, emphasizing that the proton contact shifts are obviously negligible despite the quite sizable contact shifts for carbon. Similar good agreement for the proton LIS of quinoline and isoquinoline is reported; there seems to be no detectable contact contribution in these cases

(47).

The carbon "difference shifts" (expected minus experimental value, whereby the model for the geometry of the complex is derived from proton LIS data) are clearly a measure for the contact shifts of carbon. To keep this contribution low one should choose reagents with lanthanides exhibiting a small "difference shift" as compared to shifts calculated on the basis of results for the purely pseudocontact shifting protons in the substrate molecule. For $\text{Yb}(\text{dpm})_3$, for instance, small contact contributions are reported (35) (see Sect. III-A), and for a series of aliphatic alcohols an even better correlation of observed and calculated induced shifts was obtained for ^{13}C than for the ^1H data (26) when the necessary precautions were taken. The contact "contamination" of the LIS seems to be more disturbing for easily polarizable molecules like pyridine (34).

The following points should be stressed again concerning neglect of corrections for contact interaction:

1. ^1H contact shifts may be neglected; there is no real hard evidence for sizable contact "contamination".
2. ^{13}C contact shifts can be substantial, but can be safely neglected for nuclei that are at least four bonds distant from the coordinating atom; the situation is improved using the proper lanthanide ion (the four bonds "for safety" may be reduced to three or even two in favorable cases); scaling the ^1H results seems to be an appropriate measure for estimating contact contributions.
3. other nuclei (F,P,N,O) are of less importance and less explored; the four-bond distance rule of thumb should hold, however.

2. Nonaxial Contributions to Dipolar Shifts

The nonaxial term in the pseudocontact shift equation vanishes for complexes of threefold or higher symmetry only (36). Almost all calculations available [an exception is found in (15)] are executed with the assumption that the complexes have, at least effectively, axial symmetry and the McConnell-Robertson equation [6] can be used. The obvious success of this approach is rather puzzling if one checks with results obtained by X-ray structural determinations of some of the complexes. For $\text{Eu}(\text{dpm})_3 \cdot (\text{pyridine})_2$ (37) [which is of special interest because $\text{Eu}(\text{dpm})_3$ is one of the most often used reagents and the pyridine adduct was the first LSR used by Hinckley who started the LIS-boom] Cramer and Seff found no axial symmetry (37). Similar results are reported by Horrocks et al. (38) for $\text{Ho}(\text{dpm})_3 \cdot (4\text{-picoline})_2$. One might argue that these findings in the solid state are not pertinent to the situation in solution where 1:1 (7-coordinated) complexes are often known to dominate (see Sect. III-C). However,

in those cases of 7-coordinated geometry where X-ray data are available, there are again substantial deviations from axial symmetry: $\text{Eu(dpm)}_3 \cdot (3,3\text{-dimethylthietane-1-oxide})$ (39), $\text{Lu(dpm)}_3 \cdot (3\text{-picoline})$ (40), and $\text{Eu(dpm)}_3 \cdot (\text{dimethylsulfoxide})$ (41).

All available X-ray evidence indicates that the simple approach [6] should not hold, but all nmr-solution experiments show the contrary. (See Table 2, where the neglect of the nonaxial term gives only a slightly worse fit, and see Sect. IV-B-3 for the LIS analysis of $3,3\text{-dimethylthietane-1-oxide}$).

One possibility is to assume free rotation (or an n -fold barrier, $n \geq 3$) about an axis passing through the lanthanide ion (42), the axis of rotation becoming the "effective" principal magnetic axis. This model encounters difficulties even with modestly bulky substituents, because in most LSR-S complexes there would occur a close approach of atoms of the LSR with those of the substrate thus hindering rotation. Another model was put forward by Horrocks that accounts for the features shown in solution and for the findings concerning the solid state (43):

The main assumption is that the LSR-S complex in solution cannot be described by a single geometry but exists as an ensemble of many rapidly interconverting geometrical isomers of either 7- or 8-coordinated complexes (types LS or LS_2). None of these have to be of axial symmetry. Two additional reasonable assumptions are necessary: (a) thirty or more individual forms are taking part in the dynamic equilibrium, and (b) the substrate exhibits a statistical bias to lie in proximity to an extremum susceptibility axis (axis of maximum or minimum susceptibility) with deviations up to 45 deg. allowed. Calculation of 30 - 50 randomly chosen geometrical isomers by means of the complete pseudocontact eq. [3] and averaging of the computed shifts yielded almost the same values as the result of a simple approach neglecting the nonaxial term in eq. [3]. The use of eq. [6] seems adequate, therefore, as demonstrated for two representative substrates, cyclohexanol and isoquinoline (43).

The most important consequences from the model outlined above are (a) a model assuming an "effective" axial symmetry is justified; (b) the results obtained by this model are independent of adduct stoichiometry.

C. Computational Approaches

In the previous sections (II-A and II-B) we have tried to give an outline of all necessary assumptions leading to the McConnell-Robertson eq. [6], which represents the focal point of all common computational approaches (8,26,44-46,48-61,65). We have shown that axial symmetry can be used to describe LSR-S adducts but one question, namely, as to the orientation of the principal magnetic axis in the complex (this is discussed in Sect. II-C-3) still remains unanswered.

The following listing gives a summary of all the assumptions usually adopted for the calculation of LIS:

1. The lanthanide reagent-substrate complex can be described by a single set of coordinates (which may represent the average of a multitude of rapidly interconverting geometrical isomers) (Sect. II-B-2).
2. "Apparent" axial symmetry of the adduct in solution (the nonaxial term in [3] is eliminated, and eq. [6] is sufficient for mathematical treatment) (Sect. II-B-2).
3. The diamagnetic shift upon addition of LSR to the substrate solution is negligible (Sect. II-A).
4. Contact interactions are negligible (a safe assumption for ^1H , not valid for other nuclei when close to the coordination site) (Sect. II-B-1).
5. The principal ("effective") magnetic axis passes through the lanthanide ion and the coordination center of the substrate (Sect. II-C-3).

1. General Procedures

Numerous procedures for simulating LIS are described in the literature (8,26,44-46,48-61,65). The general procedure outlined here follows the method of Willcott III, Lenkinski, and Davis (44), which is well documented and tested and is representative of others as well. Differences with other references in the various steps of the procedure will be noted.

The geometry of the substrate is described with respect to an internal Cartesian coordinate system (Fig. 4a).

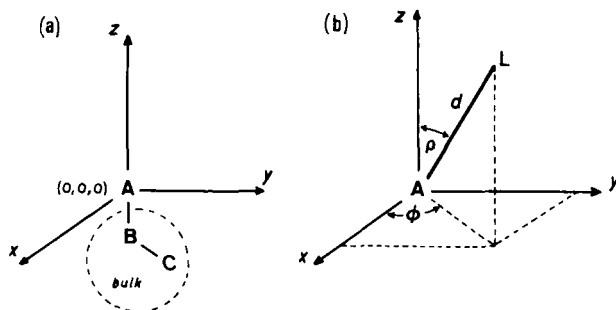


Fig. 4. Basic coordinate parameters for computation of LIS values; (a) Cartesian coordinate system, used for the atoms of the substrate molecule; the coordinating atom (A) of the substrate is at the origin; (b) Polar coordinates, used for positioning the lanthanide ion (L); in the common approach $L \rightarrow A$ is the principal magnetic axis (see Fig. 2).

The coordinates are sometimes taken from X-ray diffraction results (available in a few cases only), but more usually standard bond lengths and bond angles are used. For freely rotating single bonds all possible conformations have to be checked. The proposed geometry of the substrate can be derived from molecular models (for instance, Dreiding) or, better, by using a computer program converting the well-known internal coordinates of a molecule (bond lengths, bond angles, dihedral angles) into Cartesian coordinates (for instance, COORD or similar programs available at the Quantum Chemistry Program Exchange, QCPE, Bloomington, Indiana). Usually the X-ray derived geometry and standard geometry do not differ enough to change the results of the LIS analysis significantly (51), since eq. [6] represents a comparatively "soft" function of distance and angle. This is an advantage in many cases (estimated coordinates for the substrate may be used). On the other hand, it is a disadvantage when no clear cut decision between two closely related substrate geometries is possible (see Sect. II-C-2).

The coordination center of the substrate A (Fig. 4a) is placed at the origin of the coordinate system, the bond A-B defines the negative z axis, the xy plane is defined by the plane of atoms ABC. (For a keto group, A= oxygen, B= keto carbon, and C= any of the next carbons; for a sulfoxide, A= oxygen, B= sulfur, and C= any one of the atoms attached to sulfur).

In the course of calculating the optimal lanthanide ion position (for optimal matching of the experimental LIS data) the substrate coordinates are kept constant and the lanthanide ion is allowed to move, its coordinates changing incrementally. Most commonly the position of the lanthanide ion is described (Fig. 4b) by the distance between the coordinating atom A and the lanthanide ion L (distance d), the angle made by the vectors A→L and B→A [colatitude angle ρ (44)] (the vector B→A is equal to the positive z axis in our case) and the angle measured from the x axis to the projection of vector \vec{d} into the xy plane (azimuthal angle ϕ). Most authors prefer these polar coordinates for the lanthanide ion because they offer immediate information on the interesting data of coordination geometry, namely, the distance from the coordination center to the metal and the colatitude ρ , which should be comparable within a row of compounds of the same functionality for coordination.

Changing ρ and ϕ corresponds to a movement of the lanthanide ion over the surface of a sphere of radius d ; for constant d and ϕ the movement corresponds to a circle described on the surface of the sphere. In the program PDIGM (44) all positions for L are screened varying d , ρ , and ϕ in incremental steps.

For each lanthanide position the variable term $(3 \cos^2 \theta_i - 1)/r_i^3$ in the McConnell-Robertson eq. [6] is evaluated for all i nuclei (corresponding to i experimental LIS values); r_i is the distance between the lanthanide ion and the i th nucleus, and θ_i is the angle made by the vector corresponding to r_i and the prin-

cipal magnetic axis of the complex (which is assumed to be represented by the vector lanthanide ion - coordination center).

The calculated geometrical factors are then scaled by a least squares fit against the observed induced shifts $\Delta\sigma_i$, since the experimental induced shifts are proportional to the geometrical factor and the proportionality constant K is not known (eq. [6]).

After this scaling, the calculated LIS values may be compared to the experimental ones. Each particular lanthanide position will yield a particular good or bad fit (characterized by an error function, which will be discussed separately in the next section). The lanthanide position yielding the best fit is regarded the best possible one for the particular substrate geometry presumed in this calculation. The next step, then, is to change the topology of the substrate (e.g., to assume different conformations), again positioning the lanthanide ion for best fit. Now the best fits for the different substrate geometries can be compared to decide which one would yield the best overall fit (see Sect. II-C-2). For a decision between isomers, only a few structures have to be tested; for a decision concerning the conformation of a substrate, many proposals will have to be tested (the infinite number of possible conformations are approximated by incremental changes of rotational angles). The final best fit corresponds to an optimal arrangement of all nuclei (giving LIS values) with respect to the lanthanide ion, restricted by chemical considerations (coordination site and reasonable bond lengths and angles).

Modifications of this procedure include:

1. x , y , and z axes in the Cartesian coordinate system are chosen differently, which is a trivial modification.
2. The lanthanide ion is placed in the origin of the coordinate system, and the substrate is moved incrementally [program PSEUDO (45)].
3. The error function is minimized in an iterative manner in successive cycles [programs CHMSHIFT (8,65), LISHIFT (48)].
4. Equation [6] is expanded in a Taylor series, and an iterative error minimization is employed (46, 51).

The outcome of the final lanthanide ion position in iterative programs may depend on the choice of the initial position, since local minima in the error function often occur. A global search (complete search of all possibilities) avoids this danger. The simplicity of eq. [6] allows many computations of values in reasonable computing time, and the global search with the program PDIGM (44) needs computing times in the order of minutes (1-10 min, depending on the options used, on the number of LIS values to be considered, and last but not least, on the computer available).

2. Agreement Factor and Significance Testing

There are a lot of individual error functions, to be found in the relevant literature, which are used to assess the correspondence between the observed and calculated LIS; some are listed here (n is the total number of observed nuclei for the particular substrate which is examined):

$$\text{error} = \left[\frac{\sum_i (\Delta_i^{\text{obs}} - \Delta_i^{\text{calc}})^2}{n} \right]^{1/2} \quad (\text{Ref. 58})$$

$$= \frac{\left[\frac{\sum_i (\Delta_i^{\text{obs}} - \Delta_i^{\text{calc}})^2}{n} \right]^{1/2}}{\text{average shift}} \quad (57)$$

$$= \left[\frac{\sum_i (\Delta_i^{\text{obs}} - \Delta_i^{\text{calc}})^2}{n} \right]^{1/2} \quad (59)$$

Other authors report correlation coefficients taken from a plot of Δ_{obs} versus Δ_{calc} (26,65).

The most useful error function is the one chosen by Willcott III, Lenkinski, and Davis, as is demonstrated in the following.

The agreement factor R is defined by

$$R = \left[\frac{\sum_i (\Delta_i^{\text{obs}} - \Delta_i^{\text{calc}})^2 w_i}{\sum_i (\Delta_i^{\text{obs}})^2 w_i} \right]^{1/2} \quad [7] \quad (44,61)$$

(Other expressions used for R in the literature include crystallographic disagreement factor, reliability factor, Hamilton agreement factor, or simply R factor.)

This form of an error function is suited to statistical interpretation, which is treated extensively by Hamilton in (62). Similar procedures of significance testing are used in the evaluation of X-ray data for structural determinations and should prove useful in the LIS method also (62).

In eq. [7] weighting factors (w_i) are introduced; $w_i = 1$ for every signal yielding a LIS value, usually. Use of weighting factors is advantageous for symmetrical molecules, or more generally for any molecule where one observed nmr-resonance signal corresponds to two or more nuclei placed at different sites in the coordinate system. The calculated LIS values have to be averaged in these cases, and it is desirable to weight the single contributions so as to keep the weights equal for each signal rather than for the total number of nuclei producing the signal.

For instance, in pyridine the two o and the two m protons must be averaged since only one LIS value each for o and m protons is obtained. When no averaging is done, the lanthanide ion is forced artificially into the symmetry plane bisecting the pyridine molecule adopting either one of the two equivalent

positions above or below the pyridine ring; averaging corresponds to a model allowing for four equally populated lanthanide ion positions (Fig. 5).

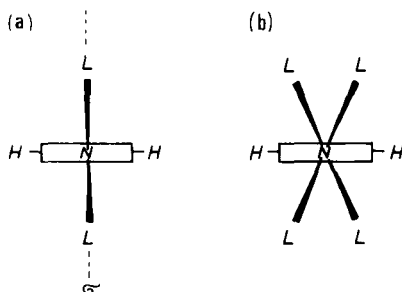
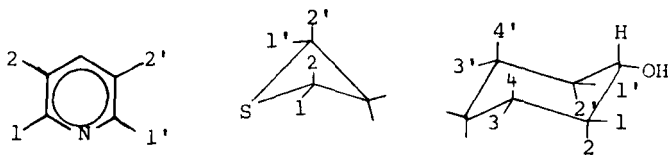


Fig. 5. Possible lanthanide ion positions (L) for a computational model allowing no averaging of LIS of symmetrically positioned nuclei (a); averaging allowed (b); the pyridine molecule is viewed from the front of the flat ring.

Similar examples, where averaging is necessary, are all types of symmetrical cyclic compounds:



For groups that are rotating freely and therefore exhibit just one signal for several protons, similar problems arise. The most common example for this is the methyl group. One can assume three individual protons and calculate their individual LIS values for the staggered position of the methyl group, then averaging the three calculated LIS values and weighting the three individual protons with a weight of 0.33 each. (In (51) the free rotation of a methyl group is accounted for by calculating 100 protons oriented along a circle and averaging, but this seems a rather extreme procedure; see Sect. IV-B-2, example f). The other approach used quite frequently is simpler (Fig. 6).

Since the three protons of a methyl group are rather close together, they can be treated as one proton in a positionally averaged site in the coordinate system. We have found that the error thereby introduced is negligible except in cases where the methyl is close to the coordination site and, therefore, close to the lanthanide ion (this depends on the characteristics of eq. [6]). Roberts (8) points out the nonequivalence of the two

approaches; but the simplification introduced by position averaging usually does not change results.

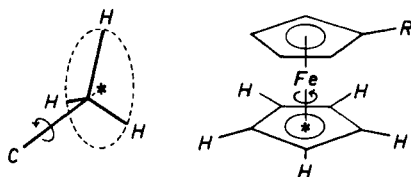


Fig. 6. Positional averaging of the methyl protons and the protons of the heterocyclopentadienyl ring in a ferrocene derivative; the average H position is indicated by an asterisk.

Figure 6 shows a similar problem caused by rotational freedom of the (hetero)-cyclopentadienyl ring in a ferrocene derivative. Here positional averaging is not likely to yield reasonable results because the error introduced by representing five rather distant protons by one proton in the center of the hetero-ring seems too grave. Nevertheless, even here such a simplification would not lead to a wrong conformation with respect to rotation about the single bond cyclopentadienyl - R (Fig. 6.; see also Fig. 28, see Sect. IV-B-2). But the results obtained by calculating for five individual protons with averaging and weighting of 0.2 for each one, yield more significant differences for the proposed trial conformations of the compound investigated.

The application of the agreement factor, corresponding to the least squares fit of a model, in assessment of reliability of hypotheses has been studied extensively by Hamilton (62). His statistical considerations (62) apply to the agreement factor R defined by eq. [7] as well (44,61). One reason for preferring the R factor introduced by Willcott III and Davis (44,61) in the LIS method to other error functions is the possibility it provides for making the statistical R factor ratio test. Several authors have already used the agreement factor for characterization of the goodness of fit (45, 48, 50, 52-54, 158). The value of R is zero for perfect fit; up to 0.10 may be regarded to represent a good fit; agreement factors of about 0.04 correspond to agreement within usual experimental errors. In (158) an additional measure of reliability [$\psi^2 = (1-r^2)n/(n-2)$] is used together with the R factor.

For each proposed geometry (conformers, isomers) of the substrate one obtains an individual best R value for an optimal LSR-S arrangement, the geometry exhibiting the smallest R factor being the most probable one. The confidence level at which one model can be rejected in favor of another is determined by the R factor ratio. Generally each individual geometry R factor, (R_1) can be tested against any other (R_2) by simply taking the ratio R_1/R_2 (for $R_1 > R_2$) or R_2/R_1 (for $R_2 > R_1$). This ratio cor-

responds to a particular confidence level that can be taken from Table 4. Table 4 lists the values of the ratios necessary for

Table 4. R Factor Ratios for N Degrees of Freedom for Decisions of One-dimensional Hypotheses on Particular Confidence Levels (in percent)

N	50% ^a	75%	90%	95%	97.5%	99%	99.5%
1	1.41	2.61	6.39	12.75	25.47	63.67	100.00
2	1.16	1.51	2.29	3.20	4.50	7.09	10.01
3	1.09	1.29	1.69	2.09	2.61	3.52	4.42
4	1.07	1.21	1.46	1.71	2.01	2.51	2.97
5	1.05	1.16	1.35	1.52	1.73	2.06	2.36
6	1.04	1.13	1.28	1.41	1.57	1.81	2.03
7	1.04	1.11	1.23	1.34	1.47	1.66	1.82
8	1.03	1.09	1.20	1.29	1.40	1.55	1.68
9	1.03	1.08	1.17	1.25	1.34	1.47	1.59
10	1.02	1.07	1.15	1.22	1.30	1.42	1.51

^aThat means no decision is possible.

certain confidence levels for different degrees of freedom for the case of a one-dimensional hypothesis (62) (i.e., a yes-or-no decision between two possibilities).

For use of Table 4 we have to know how many degrees of freedom are characteristic of the problem under investigation. The number of parameters varied in the calculation of the LIS are four: three parameters to define the position of the lanthanide ion and one parameter to scale the calculated geometrical factor to the observed LIS. At least four LIS data should be available for proper adjustment of the lanthanide ion position. This condition may be excessively stringent because small molecules with, say, three (or even two) protons may yield quite a reasonable metal position (135). This is possible because an additional restriction is imposed by allowing only one particular coordination site. In the most rigorous statistical treatment (61) we need at least five signals giving well defined LIS to apply the R factor ratio test. The number of degrees of freedom is then one, and a ratio R_1/R_2 of 6.39 would be needed to reject the R_1 geometry (large R) at a 90% confidence level in favor of the R_2 geometry (small R) (or the other way around, there is only a 10% confidence level for the R_1 geometry). When we have six LIS values for the significance testing of proposed geometries we need only a ratio of 2.29 for the same confidence level ($6-4=2$

degrees of freedom). This example demonstrates the desirability for as many LIS values as possible (^1H and ^{13}C) and hopefully a distinct minimum agreement factor for a particular geometry proposed.

In treating conformational problems one has to test numerous (strictly speaking, an infinite number of) slightly changed geometries (conformations), each yielding an individual R factor for the optimal LSR-S arrangement of that particular conformation. The conformation showing the minimum R is tested against all others. Numerous examples are given in Sect. IV-B.

One important fact should be mentioned at this point concerning the graphical representation of the goodness of fit (represented for instance by the R factor) versus continuous geometrical changes in substrate geometry. The minima of R factors in plots used to illustrate locating the best fit are to be understood as reliability maxima, and *not* as energy minima. For examples of plots of R_θ or R_θ/R_{\min} versus the angle of rotation θ about single bonds see Sect. IV-B-2, Figures 19, 20, and 28-30.

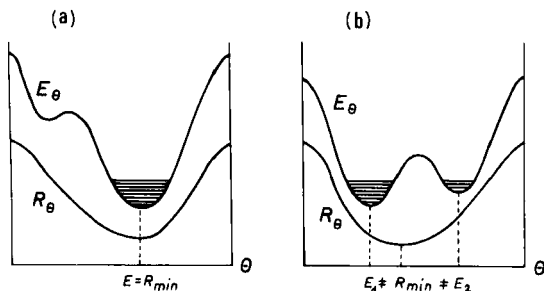


Fig. 7. Idealized plots of conformational energy (E_θ) and agreement factor (R_θ) versus torsional angle about a single bond (θ); energy diagram and reliability factor diagram: (a) only one conformer is populated, (b) two conformers are populated.

The pattern of the R_θ versus θ curve does not necessarily reflect the pattern of the curve E_θ versus θ (Fig. 7). R minima and energy minima will very often coincide (case a in Fig. 7), but this is not necessarily so. In particular, when several low-energy conformers are present in solution the R minimum may represent an average determined by the population of these conformations according to the Boltzmann distribution (case b in Fig. 7). It is interesting that an analogous case is found in situations of strong disorder in X-ray crystal structure data (e.g., 49a). Here the originally determined X-ray structure refined to an unreasonable geometry; later the structure turned out to reflect two superimposed conformational isomers.

For cases where a single highly preferred conformation is

present in solution, a good fit should be possible; the results can be compared to structure determinations by means of the X-ray diffraction technique. One is tempted to call the LIS technique the "X-ray method for the dissolved state". Parallels include the use of the crystallographic R factor in the LIS method as well as the use of structure plot programs by several authors (48,49); ORTEP - type (Oak ridge thermal ellipsoid plot), giving a stereoscopic view of the molecular structure determined. However, this analogy may reflect excessive enthusiasm. By way of additional information about computational reliability, one may observe the following characteristic features of the calculation:

1. Structural proposals giving an $R > 0.1$ are not likely to be correct.

2. Significant changes for the R factor should be observed when the lanthanide position is changed within a particular substrate geometry; this criterion is used in a more quantitative way in the significance test where several substrate geometries, each with an optimally arranged lanthanide ion, are tested against each other; for certain locations in space near the lanthanide ion eq. [6] is unfortunately a rather soft function (8). Possible pitfalls are pointed out in (8) and (158).

3. Finding a minimum value for R at an unreasonable lanthanide position, for instance closer than 2 Å to, or further than 3.5 Å from the coordination center indicates an accidentally good but incorrect fit.

3. Orientation of the Principal Magnetic Axis

There has been some concern about the orientation of the magnetic axes in the calculation of LIS for LSR-S adducts. Most workers in this field have assumed the principal magnetic axis to coincide with the orientation of the bond from the lanthanide ion (L) to the coordinating atom (A) (Fig. 8), and the apparent success of this procedure has been taken to justify it.

To account for cases in which this assumption might not be true it was proposed to introduce an additional angle made by the magnetic axis and the vector $A \rightarrow L$ (63). Later it was pointed out that at least two additional angles are needed to define the orientation of the magnetic axis relatively to the A-L bond and the substrate molecule (64): ϕ , defined by the angle made by the principal magnetic axis and the vector $A \rightarrow L$ (Fig. 8), and ω , representing the rotation of the principal magnetic axis about the L-A bond out of the zy plane. ω is not well defined when ϕ is close to zero.

In principle, this implies two additional parameters in the usual fit procedure. However, calculations by Roberts et al. (8, 65) using this approach for some representative molecules showed that the deviations of the effective magnetic axis from the usu-

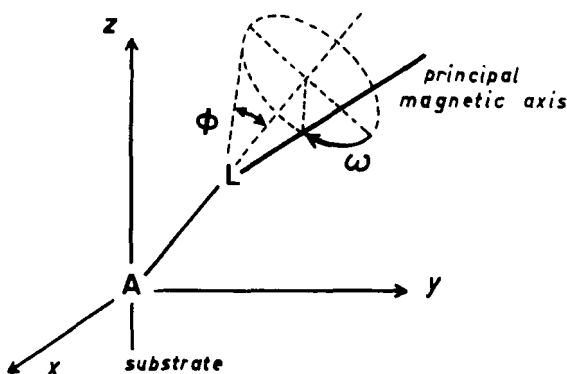


Fig. 8. Defining the additional parameters ϕ and ω , when the principal magnetic axis is not assumed to coincide with the L-A line (see Fig. 4).

ally assumed orientation (A-L) are not substantial. ϕ s of 0.04 - 2.4 deg. were found for borneol and isoborneol. Ammon et al. (51) found maximal deviations of 2 deg. and no significant improvement of the fit with the use of two additional adjustable parameters.

The simplification concerning the orientation of the effective principal magnetic axis thus seems justified.

4. Simple Distance Relationships

The earliest correlations of LIS values with substrate geometry were made using simple distance relationships, neglecting the angular term in the McConnell-Robertson eq. [6] (1,66-70). The LIS values are then proportional to r^{-3} . The distance r from the lanthanide ion to the nucleus under consideration had to be estimated from models assuming a reasonable position for the reagent in the complex. This method was modified by substituting for r the distance from the coordination center to the nucleus (r'). In that case the r'^{-3} dependence no longer holds but a proportionality factor of ca. $r'^{-2.2}$ was found; the exponent -2.2 reflects the artificially reduced distance parameter.

Usually log - log plots were used, in which case straight lines result independently of the magnitude of the exponent (plot of $\log \Delta$ versus $\log r$ or r').

The McConnell-Robertson eq. [6] written in logarithmic form illustrates these findings.

$$\log \Delta = -3 \log r + \log (3 \cos^2 \theta - 1) + \log K$$

If one takes the angular term as constant, the plot $\log \Delta$

versus $\log r$ will be a straight line with slope -3. With r' (*vide supra*) slopes of about -2.2 are obtained.

This method can work only for regions of θ where the expression $(3 \cos^2 \theta - 1)$ is not very sensitive to changes in θ , which is the case from 0 to 40 deg. At 54.7 deg. inversion of sign occurs, resulting in "wrong" shifts when the nucleus under consideration is situated in the region θ between 54.7 and 90 deg. (see Fig. 2). This demonstrates the inadequacy of the simple distance dependence for LIS analysis, and this method should, therefore, be used only for simple stereochemical questions (deciding between two stereoisomers, for instance), but never for subtle conformational problems.

III. EXPERIMENTAL TECHNIQUES

In this part the conditions for obtaining reliable experimental data for LIS are discussed including considerations of theoretical aspects.

A. Reagents

The properties of a lanthanide shift reagent (LSR) are determined by the two components of which it consists: the metal ion and the ligand.

For some purposes the inorganic salts of lanthanides are used, e.g., for polar organic substrates in aqueous solution which are of special interest in biological systems (50,71,72). However, in most relevant papers metalloorganic LSRs are employed.

Let us first focus on the influence of the lanthanide ion, keeping the organic ligand constant. Horrocks et al. (14) have studied the shifting power of the complete lanthanide series in the system $\text{Ln}(\text{dpm})_3$, $\text{Ln} = \text{Pr, Nd, Sm, Eu, Gd, Tb, Dy, Ho, Er, Tm, and Yb}$, for representative substrates (*n*-hexanol, 4-picoline-*N*-oxide, and 4-vinylpyridine). For all substrates studied the relative shifting abilities of the single lanthanide ions were quite consistent, which is to be expected when the shifts are dominantly of dipolar origin. In an isostructural series, $\Delta\epsilon_i$ is proportional to K , which in turn depends on the magnetic properties of the metal alone (eq. [6]), provided dipolar or pseudocontact interactions are solely responsible for the shifts. The results are shown in Figure 9.

Pr and Eu exhibit the largest shifting power for the lanthanides of relatively low atomic number: Pr upfield and Eu downfield. The shifts produced by the "higher" lanthanides are larger (Dy causing the largest upfield and Tm the largest downfield displacements), but the exploitation of the higher lanthanides is hampered by severe broadening of the signals upon

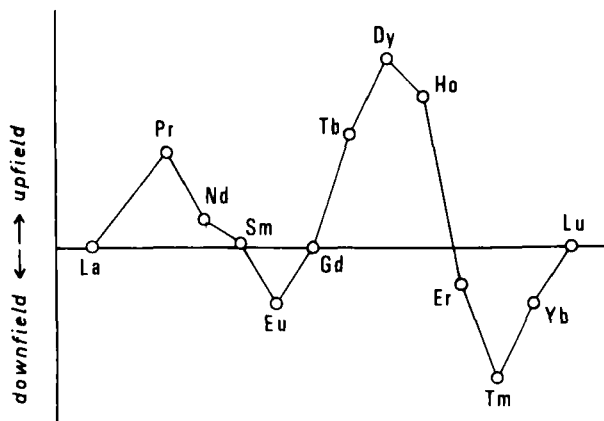


Fig. 9. Relative LIS for a typical dipolar-shifted nucleus in the region $-54.7 < \theta < +54.7$ deg. for different lanthanide ions.

addition of the reagent so that the exact signal position can no longer be determined with the necessary accuracy. This means the lanthanides of greatest interest for shifting experiments are Pr and Eu.

For praseodymium reagents less accurate LIS values are reported in (51) as compared to europium reagents. Praseodymium reagents seem to exhibit a greater tendency to dimerize in solution [$\text{Ln}(\text{dpm})_3$ reagents in general have a dimeric structure in the solid state (73)]. Partial dimerization of LSR cannot be excluded even in dilute solution; both monomeric (6-coordinated) and dimeric species (which are 7-coordinated) for $\text{Eu}(\text{dpm})_3$ and $\text{Pr}(\text{dpm})_3$ have been observed in solution (74). At low concentrations of the reagent (a higher concentration of substrate is used) the dimeric form of the LSR is supposed to break up when coordinating to the substrate, preferably forming adducts of 1:1 stoichiometry (which are again 7-coordinated, symbolized by LS), but 1:2 adducts as well (LS_2 , 8-coordinated). There is some evidence now that Pr-shift reagents coordinate to some degree in the dimeric form. The corresponding complexes, LSR-substrate, are then of the types L_2S (one lanthanide ion 7-, the other one 8-coordinated) and L_2S_2 (both lanthanides 8-coordinated). In these complexes two lanthanide ions are close to one substrate molecule, and two dipolar fields are superimposed. This gives rise to less good agreement with eq. [6] and distances which are too low in the fit. This is exactly what is reported in (51) with the conclusion that Δ_{Pr} data are intrinsically less accurate than Δ_{Eu} data (the dpm ligand was used in these experiments).

Interesting facts concerning the tendency of lanthanide

ions for contact interaction (of special interest for ^{13}C - LIS, Sect. II-B-1) are pointed out in (35) and (22). As can be seen from Table 5 Eu(III) produces the highest contact shifts for carbon resonances.

Table 5. *R* Factors for LIS Simulation and Estimates of Contact Contributions of the System Isoquinoline- $\text{Ln}(\text{dpm})_3$

$\text{Ln} =$	Eu	Nd	Er	Tb	Ho	Pr	Dy	Yb
$R(^1\text{H})^a$	0.030	0.048	0.011	0.015	0.013	0.020	0.018	0.014
$R(^1\text{H}, ^{13}\text{C})^b$	0.477	0.468	0.176	0.269	0.333	0.116	0.300	0.040
$\Delta(\text{contact})^c$	0.8	0.7	0.25	0.21	0.19	0.15	0.13	0.05
$\Delta(\text{dipole})$								

^aProton LIS simulated.

^bProton and carbon LIS simulated.

^cThe ratio contact/dipolar contributions to the observed LIS represents an average for the carbons of the *N*-ring of isoquinoline.

According to Table 5, the lanthanide of choice for ^{13}C -LIS is, therefore, Yb(III), despite some line broadening; but Pr(III) is not bad either. Eu(III) should be avoided in ^{13}C LIS; ApSimon et al. (28), for instance, observed in a LIS study of monofunctional keto and hydroxy steroids substantial contact shifts for the carbonyl and hydroxyl carbons, as well as the alpha carbons, with $\text{Pr}(\text{fod})_3$; with $\text{Eu}(\text{fod})_3$ the beta carbons suffered contact interaction in addition.

Gadolinium does not produce any shifts (each *f* orbital is singly occupied), but its broadening abilities are remarkable. This has prompted some authors to use Gd(III) complexes for relaxation reagents, since the width of a resonance signal in nmr is reciprocally related to the average length of time a nucleus stays in a particular spin state. This relaxation time is changed by a paramagnetic ion nearby, and the r^{-6} dependence can be used to determine the distance from the relaxing nucleus to the lanthanide ion. This technique [not necessarily using lanthanide ions but other paramagnetic ions as well (7)] complements the information gained by the LIS technique [Literature: Gd (75,76), Ho (50), Cr, Fe, and general considerations (7)].

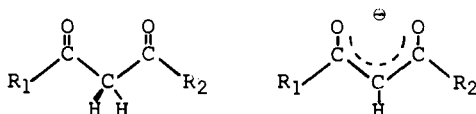
Since this paper deals with LIS only, we confine ourselves to Eu(III) (for ^1H), Pr(III) (for ^1H and ^{13}C), and Yb(III) (for ^{13}C LIS).

Now let us consider the ligands attached to the lanthanide ion. For most organic-chemical systems, one is usually confined

to solutions in organic solvents; and thus there is need for metalloorganic lanthanide shift reagents that are as soluble as possible in the solvents most common in nmr spectroscopy, namely, CDCl_3 and CCl_4 . Most LIS work has been and is done in these solvents.

Since LSR-substrate adducts are fast exchanging species of the type LS and LS_2 , the observed shifts in the nmr spectra represent the concentration-weighted averages of all S, LS, and LS_2 molecules. The LIS will be the larger, the more of the complexed form of the substrate is present in solution. In the complexing mechanism the LSR acts as a Lewis acid; high Lewis acidity of the LSR will increase the degree of complexation to basic substrates, but steric requirements of either reagent or substrate will influence the complexation constant and thus the obtainable LIS. One possible means of influencing complex formation is to vary the ligand of the shift reagent.

Organic anions reported to be able to solubilize lanthanide(III) ions in nonpolar organic solvents are practically all derived from 1,3-diketo compounds.



The first reagent to attract the attention of organic chemists was $\text{Eu}(\text{dpm})_3(\text{pyridine})_2$ (1). $\text{Eu}(\text{dpm})_3$ was demonstrated (4) to exhibit better shifting abilities than the dipyridine adduct, since, presumably, pyridine competes with the substrate for coordination. The situation is similar with $\text{Eu}(\text{fod})_3$ which is ordinarily obtained as monohydrate; when dried over P_4O_{10} in vacuo the (now anhydrous) reagent shows shifting abilities, improved by a factor of about two, since water no longer competes with the substrate (41).

$\text{Eu}(\text{dpm})_3$ is still one of the most widely used LSR despite the introduction of reagents of increased solubility and acidity. For the most frequently used LSR and the usual abbreviations for the organic anions see Figure 10.

To obtain LSRs with improved solubility and coordination properties, partially fluorinated ligands were introduced (5,41). A LSR that has gained or even surpassed the popularity of $\text{Eu}(\text{dpm})_3$ is $\text{Eu}(\text{fod})_3$ which is superior to $\text{Eu}(\text{dpm})_3$, especially with weakly basic substrates where a strongly Lewis acidic reagent is needed to obtain adequate complexation of the substrate. In such cases the greater solubility of $\text{Ln}(\text{fod})_3$ reagents is of importance also, since higher concentration of LSR increases the observed shift displacements.

Improved interaction between fluorinated LSR and substrate

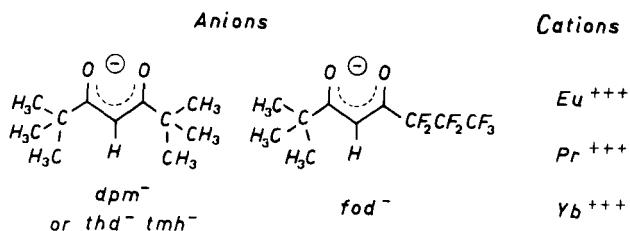


Fig. 10. Most frequently used lanthanide shift reagents; all combinations of the organic anions *dpm* = dipivalomethanato (= *thd* = *tmh* = 2,2,6,6-tetramethyl-3,5-heptanedionato) and *fod* = 1,1,1,2,2,3,3-heptafluoro-7,7-dimethyl-4,6-octanedionato, and the cations *Eu*(III) (for ¹H-LIS), *Pr*(III) (for ¹H and ¹³C), and *Yb*(III) (for ¹³C).

was independently demonstrated by studies using gas chromatography (77) (a column is loaded with LSR, and the substrate passed through; the retention time allows conclusions concerning the complexation of the substrate to the LSR).

*Eu(fod)*₃ usually produces larger LIS than *Eu(dpm)*₃, but this need not always be true as was pointed out in (78).

An argument in favor of *dpm*⁻ is that the *t*-butyl resonance of the reagent is found upfield of the TMS signal and does not interfere with substrate signals; the *t*-butyl resonance of *fod*⁻ remains in the δ[~] 1.7 shift region and may cover up aliphatic substrate protons.

There is still another reason for favoring *Ln(dpm)*₃ over *Ln(fod)*₃, at least if the basicity of the substrate allows one to obtain reasonable shifts with *Ln(dpm)*₃. Many substrates of interest possess more than one functionality, and very often one of these is substantially more strongly basic than the others. In such cases *Ln(dpm)*₃ may still yield an easily interpretable, well defined complex, whereas the stronger Lewis acid *Ln(fod)*₃ might yield a mixture of complexes, the reagent interacting with a multitude of strong and weak basic sites in the substrate.

A related effect is demonstrated quite impressively in the following example (79). In this study of 3-aryl-1,3,5,5-tetramethylcyclohexanols a different pattern of LIS values for aryl = *o*-methoxyphenyl was found as compared to aryl = *m*-methoxyphenyl, *p*-methoxyphenyl, or phenyl when *Eu(fod)*₃ was used as reagent; when *Eu(dpm)*₃ was used this difference was not observed. This suggests that the system 3-*o*-methoxyphenyl-1,3,5,5-tetramethylcyclohexanol - *Eu(fod)*₃ shows uniquely anomalous behavior. Anticipating some of the results of the LIS method discussed in

part IV, the anomaly can be interpreted in terms of aryl rotation (illustrated in Fig. 11). The systems 1 and 3 (3 possess-

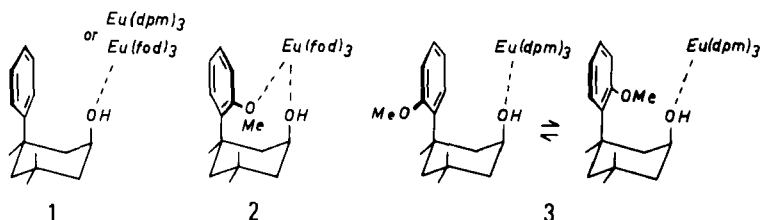


Fig. 11. Perspective structures of some 3-aryl-1,3,5,5-tetramethylcyclohexanol - Ln(III) complexes.

ing two low energy rotamers) show a very similar orientation of the aryl ring with respect to the cyclohexane ring, corresponding to minimum steric interaction. In system 2 [Eu(fod)₃ as reagent] the aromatic ring is rotated towards the hydroxy group thus allowing the stronger Lewis acid Eu(fod)₃ to form a bidentate complex. The LIS value for the aromatic methoxy protons in complex 2 is 1.40 ppm, for complex 3, 0.39 (the other protons in 2 and 3 do not differ so much and for all other LIS the values for 3 are larger than the ones for 2). The LIS values for the methoxy protons of the corresponding *m*- and *p*-methoxyphenyl compounds with Eu(fod)₃ as reagent are -1.54 and -1.70, respectively. This proves that it is not simply a second LSR that is coordinated in 2, since such coordination would show up in the *m*- and *p*-methoxylated species also, causing a LIS value of positive sign in these compounds (direct coordination to a methoxy group always produces a sizable positive displacement of the chemical shifts for the methoxy protons). All observed LIS find a rationale in the assumption that a change of conformation is initiated by interaction of the substrate with Eu(fod)₃. This change of conformation of substrate caused by the reagents is a matter of great concern when using LSR for determination of substrate conformation. Clearly, a weakly interacting LSR might be somewhat less likely to introduce unwanted conformational changes in the substrate than a strongly complexing one.

Beta-diketonate chelates other than the quite bulky ones described above do not yield satisfactory shifts (80a). In complexes with less bulky substituents there seems to exist no preferred orientation of the substrate molecule within the complex, and thus quantitative evaluation of the LIS is hampered.

If one needs a reagent with almost unlimited solubility and high shifting power Ln(dfhd)₃ might be of interest (80b) (see Fig. 12). This reagent is highly acidic, and the lack of aliphatic protons in the substituents is an additional bonus.

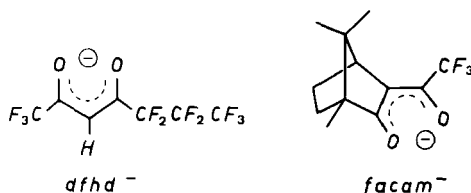


Fig. 12. Structure of anions for LSR used for special LIS problems; dfhd = 1,1,1,5,5,6,6,7,7,7-decafluoro-2,4-heptanedione (extreme solubility in CDCl_3 or CCl_4) and facam = 3-trifluoroacetyl-*d*-camphorato (most frequently used chiral anion in LSR).

For maximum resolution a "typical" ratio of 260 mg $\text{Eu}(\text{dfhd})_3$ to 20 mg *n*-heptanol in 0.5 ml CCl_4 is reported in (41), a first-order spectrum being readily obtained at this ratio.

For the special LIS technique of determining the enantiomeric purity of chiral compounds, a series of chiral LSR have been created, the most popular being " $\text{Eu}(\text{facam})_3$ " [(81) and references cited therein] (see Fig. 12).

The following comparison of the two most often used LSR ligands summarizes their relative advantages and disadvantages:

<u>dpm</u>			<u>fod</u>
good solubility in organic solvents	(+)	(+)(+)	excellent solubility in organic solvents, therefore, high concentrations possible (good resolution)
good complexing with strong bases	(+)	(+)	good complexing with strong bases as substrates
less complexation with weak bases	(-)	(+)	good complexation even with weak bases
<i>t</i> -butyl of the reagent very close to TMS (in most cases upfield)	(+)(+)	(-)	<i>t</i> -butyl of the LSR may obscure aliphatic protons of the substrate
less likely to influence substrate conformation	(+)	(-)	more prone to conformational interference with substrate
unstable with weak acids (phenols and carbonic acids)	(-)	(+)	stable with weak acids

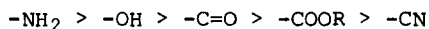
B. Substrate and Functionality

The extent of the lanthanide shift induced upon addition of a particular amount of reagent is strongly influenced by the com-

plexation constant. Since the LSRs are Lewis acids the complex binding constant of the adduct is a function of substrate basicity and, of course, steric effects, which play an important role also.

In (83) an almost linear correlation between basicity of substrates (seven different *p*-substituted anilines) and LIS values [for *o* and *m* protons, with $\text{Eu}(\text{dpm})_3$] is reported. This does not hold true any more when molecules of different steric requirement are compared. In (84) the observations are discussed within the framework of HSAB (hard-and-soft acid-and-base) theory: the LSR are hard acids, and interaction is better with hard than with soft bases.

For the most common functionalities an order of basicity may be given (80) (decreasing affinity to usual LSRs):



This order is useful as a rule of thumb only. Tertiary alcohols, for instance, coordinate more poorly than ketones (137). The etheral function $-\text{O}-$ can show very different behavior from case to case; so the aryllic methoxy coordinates poorly to LSRs (compare sect. IV-B-3, example e) but the ether oxygen incorporated in small rings are very efficient in complexing (see Sect. IV-B-3, example c).

Coordination takes place with all kinds of bases (Lewis bases), including a number of organic molecules of less common functionality: sulfoxides (85), sulfites (86), sulfines (87), *N*-oxides (23), *N*-nitroso compounds (88), azoxy compounds (89), carboxylic acids ($-\text{COO}^-$), and phenols (ArO^-) (41,90), the last two with $\text{Ln}(\text{fod})_3$ or other highly acidic LSRs only, $\text{Ln}(\text{dpm})_3$ being unstable with acidic substrates (41,90).

An attempt to obtain LIS with cations as substrates has been reported (91). Cyanine dyes, quinolinium, and quaternary ammonium salts (Lewis acids!) in CDCl_3 with $\text{Eu}(\text{fod})_3$ yielded induced shifts that were lower than the usual values for Lewis bases, but were sufficient to simplify the nmr spectra. Contact ion pairs were assumed, the substrate anion complexing with $\text{Eu}(\text{III})$ directly. The cation - $\text{Eu}(\text{fod})_3$ interaction is then a consequence of contact ion pairing of substrate cation to substrate anion. Another possibility for inducing shifts in cations is to use diamagnetically active anions, for instance, the tetraphenylborate ion (92). Though this case is far off our main topic, it does show a possible extension of the induced-shift method, at least if only simplification of spectra is desired.

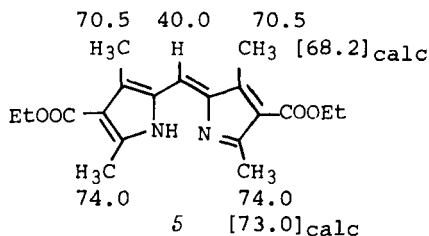
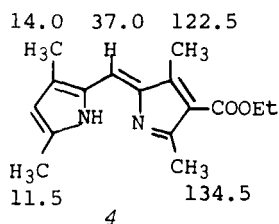
The relative shifting (and complexing) abilities of functional groups can be determined by nmr, either by intermolecular (external) or intramolecular (internal) competition experiments; the former is done with a mixture of substrates (93),

the latter with a substrate containing more than one function. This latter case is of great interest in practical terms, since one frequently has to deal with polyfunctional substrates.

Double or higher complexation in polyfunctional molecules shows up in the absolute shift values observed [large LIS, if the different centers of complexation have comparable coordination binding constants, the induced shifts of the two or more Ln(III) being additive] or in a bend in the Δ versus LSR-concentration slope (at low LSR concentration the strongest basic function is dominant, when the strongest base site approaches saturation, the other(s) start to coordinate LSR too).

Some illustrative examples are discussed in the following.

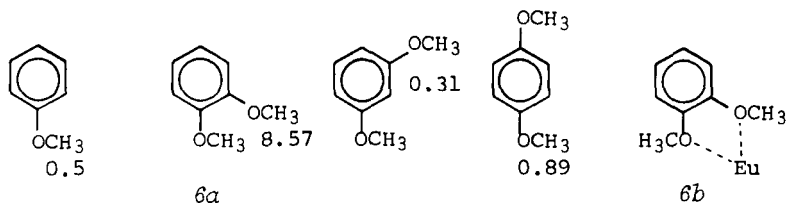
Compound 5 represents a case where the functions are not just comparable but identical. Therefore the Δ versus LSR concentration slope is a straight line. The LIS values are given in formulas 4 and 5 for a molar ratio of Eu(dpm)₃: substrate of 0.3 (CDCl₃).



Since this is far from saturation, the two functionalities in 5 compete for the reagent molecules and on the basis of the corresponding monofunctional compound 4, the LIS for the methyl groups in 5 would be expected to be $(14.0 + 122.5)/2 = 68.2$ and $(11.5 + 134.5)/2 = 73.0$, respectively. The observed values of 70.5 and 74.0 Hz are very close to the predicted values (94).

The additivity of LIS can be exploited to determine complex populations in polyfunctional compounds by use of the LIS values of monofunctional standard model compounds (95).

Distinct nonadditivity indicates some special effects. In the series methoxy-, *o*-, *m*-, *p*-dimethoxybenzene a remarkable increase in the LIS (ratio LSR:S = 1:1, ppm) is observed for the methoxyl groups in the ortho isomer only.



Clearly, **6a** forms a strongly bound bidentate complex (**6b**). It was found (95) that the *o*-dimethoxy arrangement in **6a** appears to have about twice the affinity for $\text{Eu}(\text{fod})_3$ as an aromatic ester group. (An isolated methoxy function coordinates poorly compared to the ester group.)

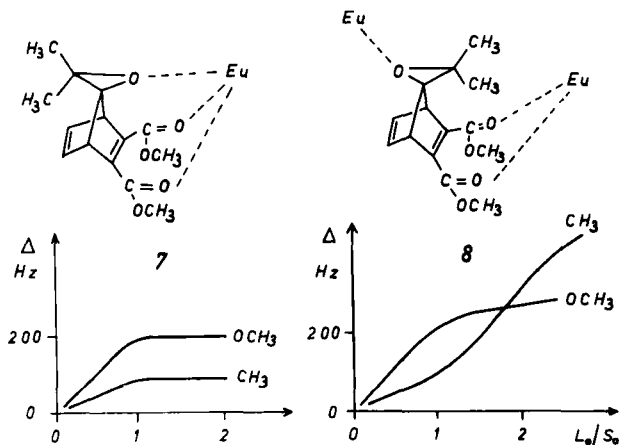


Fig. 13. Δ versus L_0/S_0 plots for **7** and **8**, showing that **7** forms a tridentate (9-coordinated) complex, whereas **8** incorporates a second $\text{Eu}(\text{III})$ at higher $\text{Eu}(\text{fod})_3$ concentrations.

Another interesting example (96) is illustrated in Figure 13, which shows the Δ versus L_0/S_0 (molar ratio LSR:substrate in solution) plots for substrate **7** and **8**. In substrate **8** a second $\text{Eu}(\text{III})$ is incorporated at higher LSR concentrations, whereas the LIS for **7** remain virtually unchanged after incorporation of one lanthanide ion. This is due to formation of a tridentate (9-coordinated) complex in **7**, which represents a rather rare case. The stereochemistry (syn or anti) can be deduced, in this special case, from such simple considerations concerning the mode of complexing alone (96).

All these examples demonstrate the special problems arising with polyfunctional substrate molecules. If the main purpose of a LIS experiment is the elucidation of stereochemistry, and especially of conformation, of the substrate, then well-defined complex geometry is necessary. The simplest way to make the case clear cut is to use a model compound with one, and only one, strongly Lewis-basic functionality. If additional atoms with free electron pairs cannot be avoided, as, for instance, in the dipyrromethene system (formulas **4** and **5**) (94), then the LIS of the system without the dominating basic group should be checked for reference under equal conditions. Fortunately, for dipyrromethenes lacking the strongly coordinating carboethoxy group, no detectable LIS are observed under the experimental conditions

employed for 4 and 5 (*vide supra*).

Future developments in the computational approach will include extension of the calculations to polyfunctional molecules (60).

C. Extraction of LIS Parameters from Experiment; "Bound" or "Limiting" Shifts; Complexation Constant and Stoichiometry

Determination of relative LIS values by plotting Δ versus the ratio molar concentration of reagent: substrate (plots of Δ vs L_0/S_0 ; Fig. 14) would seem to be a reliable and rather easy

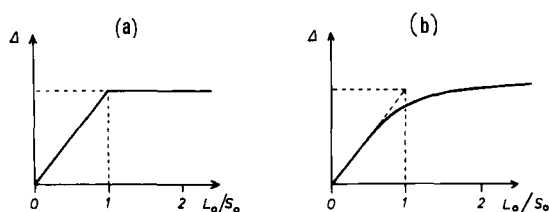


Fig. 14. (a) Ideal and (b) typical Δ versus L_0/S_0 plot; in (b) the plot should represent a straight line up to $L_0/S_0 \sim 0.5$ allowing extrapolation of the Δ value for the 1:1 complex; S_0 is kept constant, L_0 is varied in the experiment.

procedure. However, it has been shown that the values obtained for the slope (at low LSR concentrations) differ for different substrate concentrations despite equal L_0/S_0 ratios (97); this finding and the nonlinearity of the plot at L_0/S_0 ratios higher than ~ 0.5 require explanation.

For strong Lewis-base substrates (e.g., amines, alcohols) one can assume that at high concentrations of LSR a value for the LIS is obtained which does not change upon further addition of reagent, since no more lanthanide ions can be incorporated into the complex, all coordination sites being saturated. In the ideal case of a well defined 1:1 complex, a very sharp bend should show up in the plot (Fig. 14). However, this is almost never true, thus indicating that a simple, one-step, 1:1 equilibrium is not, in fact, the only one involved. Besides the species L, S, and LS, the species LS_2 (1:2 stoichiometry) will be present in solution, also (see Sect. III-A). Another factor complicating matters is self-association of the reagents especially at high concentrations (74) (see Sect. III-A). This adds the species L_2 , L_2S , and L_2S_2 to the previously mentioned ones, LS, LS_2 and, of course, L and S alone. Nevertheless, almost all methods to obtain the intrinsic parameters of the reagent - substrate equilibrium are based on the assumption of a 1:1 complex. The values given in the literature are usually the extrapolated induced shift

values for a molar concentration ratio reagent:substrate = 1:1, taken from the linear part of the plot Δ versus L_0/S_0 (Fig. 14). We show in the following that this slope depends on the substrate concentration and on the binding constant of the complex formed for weakly Lewis-basic functional substrates.

A trivial reason for deviation of the straight line in the plot Δ versus L_0/S_0 at very low LSR concentration should be mentioned at this point. Deviations of this type usually indicate either some kind of impurity in the reagent or the presence of a "scavenger" in the substrate solution (usually traces of water) which binds the reagent.

Methods to extract the intrinsic LIS parameters even for mixtures have been reported (98). We will, however, confine ourselves to "simple" systems that are controversial enough, for reasons to be discussed. Somewhat paradoxically, the controversy is fueled by the rather fortunate circumstance, that good and interpretable LIS data can be obtained by methods assuming rather different mechanisms and using different analytical (mathematical) methods.

The equilibrium for a 1:1 complex can be formulated in the following manner:



The species of interest in solution are the shift reagent L, the substrate S, and the coordination product LS. The observed lanthanide-induced shift Δ for any particular nucleus is an average of the shifts for the complexed substrate and the uncomplexed one in the case of rapid exchange on the nmr time scale [only a few cases are known where, at low temperatures, the peaks for complexed and uncomplexed substrate show up separately in the nmr spectrum (15, 99)], determined by the concentration of S and LS in solution.

$$\Delta = \frac{x}{S_0} \Delta_1 \quad [9]$$

Where x is the concentration of the LS complex; S_0 is the total concentration of the substrate (in complexed and uncomplexed form); x/S_0 is, therefore, the fraction of the complexed form, LS, of the substrate; and Δ_1 is the induced shift of a particular nucleus for the case that the substrate is completely bound to the reagent [e.g., "bound chemical shift" (100); since this is the upper limit for the LIS of the complex LS, another proposal is to call this intrinsic parameter "limiting shift" (101)], $\Delta = \Delta_1$ for the pure LS complex.

The second characteristic parameter for the system [8] is the equilibrium binding constant:

$$K_1 = \frac{LS}{L \cdot S} = \frac{x}{(L_0 - x)(S_0 - x)} \quad [10]$$

L , S , and LS are used in this and the following equations to denote the concentrations of lanthanide reagent, substrate, and complex, respectively, at the equilibrium; L_0 is the total concentration of the reagent (bound to the substrate and free); S_0 and x are as defined above. S_0 and L_0 are determined by the experimental conditions chosen.

By extraction of x from eq. [10] and substituting x in eq. [9] one obtains an expression where Δ is a function of Δ_1 , K_1 , S_0 , and L_0 . An iterative trial guess method can be used to computer fit the experimental Δ to particular values of Δ_1 and K_1 . This is too complicated to be done by hand.

Reasonable simplifications in the mathematical treatment are often introduced to allow manual (graphical) evaluation of the experimental results. The experiments in turn are then restricted to particular conditions in accordance with the mathematical framework chosen.

One experimental restriction to simplify matters is to use low reagent concentrations:

$$S_0 \gg L_0$$

in which case x will be small too (x is the LS concentration)

$$S_0 \gg x$$

Upon introducing this condition, eq. [10] becomes

$$K_1 = \frac{x}{(L_0 - x) S_0} = \frac{x}{L_0 S_0 - x S_0}$$

extracting x ,

$$x = \frac{K_1 L_0 S_0}{1 + S_0 K_1}$$

and substituting in Δ (eq. [9]) yields

$$\Delta = \frac{K_1 L_0 \Delta_1}{1 + S_0 K_1} \quad [11]$$

Eqs. [10] and [11] are the basic equations for the two most important approaches to obtain intrinsic LIS parameters.

Approach 1. Δ versus L_0/S_0 plot at constant S_0 . The most-used graphical method is the one where the substrate concentration S_0 is kept constant and the reagent concentration L_0 is varied (the condition $S_0 \gg L_0$ remaining valid). In practice,

a nmr sample of the substrate is prepared, and the nmr spectra are recorded for various concentrations of the reagent, which is added incrementally. The slope of the plot Δ versus L_O/S_O is assumed to give a measure of the "bound" or "limiting" shift.

To check the validity of this assumption we have to consider two limiting cases:

1. Strong binding of the substrate to the reagent: this means $K_1 S_O \gg 1$ in [11], then [11] becomes

$$\Delta = \frac{K_1 L_O \Delta_1}{S_O K_1}$$

or

$$\Delta = \Delta_1 \frac{L_O}{S_O} \quad [12]$$

Equation [12] corresponds to a straight line for the plot Δ versus L_O/S_O passing through the origin, with slope equal to the bound chemical shift Δ_1 . For high S_O ($S_O \gg L_O$) and good complexing (a large value for K_1) this method will yield correct results.

2. Weak binding of the substrate to the reagent: this means $K_1 S_O \ll 1$ in [11], then [11] becomes

$$\Delta = K_1 L_O \Delta_1$$

or

$$\Delta = K_1 S_O \Delta_1 \frac{L_O}{S_O} \quad [13]$$

Equation [13], too, corresponds to a straight line in the plot of Δ versus L_O/S_O , but the slope is not equal to Δ_1 any more. It is also dependent on the substrate concentration and the binding constant of the complex formed.

Taking the Δ versus L_O/S_O plot at several different substrate concentrations helps one to decide if the slope can be regarded as the limiting shift or not. But even for case 2, where the slopes for the individual nuclei are not equal to Δ_1 , the relative values should still be proportional to Δ_1 . Since in the McConnell-Robertson eq. [6] only the relative values are of importance, the LIS can be used in either case as the slopes of the plot discussed.

Approach 2. Plot of S_O versus $1/\Delta$ at constant L_O . This approach was introduced by Armitage (97, 100). It offers the bonus that values for Δ_1 and K_1 are obtained as well. Some recent authors seem to favor this method over the older approach 1 (48, 101a).

We write eq. [10] in the following form

$$K_1 = \frac{x}{L_0 S_0 - S_0 x - L_0 x + x^2}$$

We have assumed $S_0 \gg L_0$; therefore, x (concentration of LS) will be low and x^2 will be very small, therefore, negligible.

Rearranging eq. [9] to extract x ($x = \Delta S_0 / \Delta_1$) and substituting in K_1 ,

$$K_1 = \frac{\Delta}{\Delta_1 L_0 - \Delta \cdot S_0 - L_0 \Delta}$$

rearranging to extract S_0 yields

$$S_0 = \Delta_1 L_0 \left(\frac{1}{\Delta} \right) - \left(L_0 + \frac{1}{K_1} \right) \quad [14]$$

Equation [14] predicts a straight S_0 versus $1/\Delta$ plot with a slope of $L_0 \Delta_1$ and a y intercept of $-(L_0 + 1/K_1)$, thus yielding values for both intrinsic parameters Δ_1 and K_1 . A typical (idealized) plot is shown in Figure 15. The separate lines for

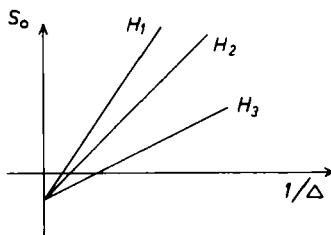


Fig. 15. Idealized S_0 versus $1/\Delta$ plot for three nuclei of a particular substrate; at low L_0 concentrations a straight line is expected; L_0 is kept constant, S_0 is varied in the experiment.

all protons converge to the same intercept, which corresponds to a consistent value of K_1 obtained from any one of the protons. For $K_1 > 100$ the y intercept is so small that only a lower limit for K_1 can be given. This is the case if $\text{Eu}(\text{fod})_3$ is used in the examples shown in Table 6. The binding constants for $\text{Eu}(\text{dpm})_3$ in these examples are much smaller. Interestingly enough, the values for the bound chemical shifts do not differ very much, evidencing that the induced shifts for the "pure" complexes are mainly dependant on the lanthanide ion and to a lesser degree on the ligand of the reagent.

All previously derived equations ([8] - [14]) are valid for a "one step - 1:1 binding model". To account for the expected 1:2 complexing, also, the equations can be modified easily for the assumption of a "one step - 1:2 binding model"

Table 6. Δ_1 and K_1 Values Evaluated by Means of a S_0 versus $1/\Delta$ Plot at Small L_0 with L_0 Constant; Two Examples

	Δ_1	K_1	Δ_1	K_1
$ \begin{array}{c} \text{CH}_3 \\ \\ \text{H}_3\text{C}-\text{C}-\text{CH}_2-\text{OH} \\ \\ \text{CH}_3 \\ \begin{array}{cc} 1 & \\ 2 & \end{array} \end{array} $				
Neopentyl Alcohol				
	<u>Eu(dpm)₃</u>		<u>Eu(fod)₃</u>	
H-1	19.7	9.7	20.8	≥100
H-2	7.6	9.8	8.3	≥100
$ \begin{array}{ccccc} \text{H}_3\text{C}-\text{CH}_2-\text{CH}_2-\text{NH}_2 \\ \begin{array}{ccccc} 3 & & 2 & & 1 \end{array} \end{array} $				
<i>n</i> -Propylamine				
	<u>Eu(dpm)₃</u>		<u>Eu(fod)₃</u>	
H-1	12.8	32.1	19.0	≥100
H-2	7.7	32.9	12.7	≥100
H-3	4.1	37.8	6.6	≥100

of the type, $L + 2S \leftrightarrow LS_2$. The formulas hold in a similar form and the plot to be evaluated is then S_0^2 versus S_0 ($1/\Delta$). Thus the system norcamphor - Eu(fod)₃ in CCl₄ yields (105) a straight line in the S_0 versus $1/\Delta$ plot (treatment as a 1:1 system); in CDCl₃ a one-step 1:2 system seemed to be the appropriate model, since no straight line was obtained in the S_0 versus $1/\Delta$ plot but a S_0^2 versus S_0/Δ plot did fit very well. The mechanism proposed (105) is interesting and indicates what kind of complications may occur. The authors (105) propose a 2:2 stoichiometry (instead of the apparent 1:1) in CCl₄, with two ligand oxygens bridging the complex, so that after adding two substrate molecules a coordination number of eight is obtained (complex of type L_2S_2). The more polar CDCl₃ would cleave the dimer and a second norcamphor molecule would occupy the vacant eighth coordination site of the Eu(III).

The assumption of purely 1:1 (or purely 1:2) complexing seems rather artificial. Both modes of complexing have been

proved by independant methods, and both have to be accounted for in an analytical approach.

The following summary represents a cross-section of all kinds of evidence available concerning the stoichiometry of LSR-substrate complexes:

1. Low-temperature nmr (99, 102, 103): the exchange is slowed down so that the resonances of complexed and free substrate can be observed separately, thus allowing determination of the composition of the complex directly. This method will only work with strongly interacting combinations of LSR and substrate, a weakly bonded complex will not "freeze." Strong interaction favors 1:2 complexing, so this method in most cases observed supports the LS_2 type.

2. X-ray structure determination: both 1:1 complexes (39-41) and 1:2 complexes (37, 38, 41) have been observed in the solid state (see Sect. II-B-2).

3. Analytical methods like the Δ versus L_0/S_0 plot or the S_0 versus $1/\Delta$ plot should show deviations from the straight line if the assumptions made concerning stoichiometry are wrong. Shapiro et al. (101) have demonstrated that the common analytical procedures used in evaluating LIS data are too insensitive to decide between the possible mechanisms of complexation (*vide infra*). In most cases, the simple relationships outlined in approaches 1 and 2 yield straight lines despite the simplifying assumptions. Shapiro and Johnston (101) obtained an improved fit for a two-step mechanism involving both LS and LS_2 type complexes. Their model is discussed extensively below.

4. A sensitive analytical method for obtaining information concerning the composition of the complex is offered by the "Job plot" used by Roth et al. (104). The concentration of the complex is plotted against the molar fraction of substrate present in solution, keeping $S_0 + L_0 = \text{constant}$; a 1:1 complex is indicated by a maximum of the curve at a molar fraction of $S_0 = 0.5$; deviations are evidence for some kind of complication. The Job plot in Figure 16 indicates 1:1 stoichiometry for *t*-butyl alcohol [$\text{Eu}(\text{fod})_3$, CCl_4 , and CDCl_3] but not for *t*-butylamine (same experimental conditions) where some mixtures of complex species cause displacement of the maximum in the plot.

5. By electronic spectroscopy both 1:1 and/or 1:2 complexing was found for a variety of alcohols in CCl_4 solution (114), either by studying the effect of added substrate on the intensity of absorption bands of lanthanide ions (114a), or by observing the circular dichroism of Ln(III) bands upon complexation to optically active substrate (114b).

Altogether we can say that the numerous pieces of evidence, although not too convincing and unambiguous in many cases, imply that both LS and LS_2 complexes are to be expected in general. Most experiments are executed at small reagent concentrations

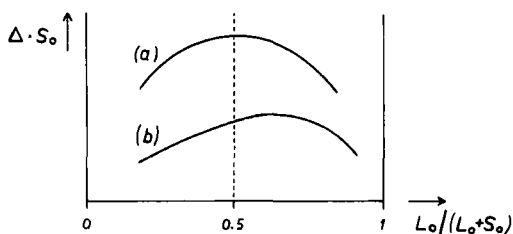


Fig. 16. Job plots for $\text{Eu}(\text{fod})_3$ complexes with *tert*-butyl alcohol (a) and *tert*-butylamine (b); ΔS_0 is taken as a measure for the concentration of the complex; $S_0 + L_0 = \text{constant}$.

relative to the substrate concentration. This should increase the importance of the LS_2 species but suppress complex species of the type L_2S .

A two-step mechanism should provide a reasonable model for the equilibria involved in the complex mechanism (101).



By analogy with eq. [9], the actually observed induced shift for a particular nucleus Δ can be expressed in terms of the molar concentration of the LS species (x), with the individual shift (limiting shift or bound chemical shift) Δ_1 for this complex, and in terms of molar concentration of the LS_2 species (y) with Δ_2 (which is defined in analogy to Δ_1).

$$\Delta = \frac{1}{S_0} (x \Delta_1 + 2y \Delta_2) \quad [16]$$

K_1 and K_2 are defined as follows (derived from the equilibria [15])

$$K_1 = \frac{\text{LS}}{\text{L} \cdot \text{S}} = \frac{x}{(S_0 - x - 2y)(L_0 - x - y)} \quad [17]$$

$$K_2 = \frac{\text{LS}_2}{\text{LS} \cdot \text{S}} = \frac{y}{x(S_0 - x - 2y)} \quad [18]$$

In principle, x and y can be extracted from eqns. [17] and [18] and substituted in [16] to solve this four-parameter problem for Δ_1 , Δ_2 and K_1 , K_2 . This was done by an iterative computer-fit procedure for the system 3-(*p*-chlorophenyl)-3,5,5-trimethylcyclohexanone - $\text{Eu}(\text{fod})_3$ in CCl_4 . The fit by the two-step mechanism is much better than for the assumption of a one-step equilibrium. Nevertheless, evaluation of the LIS data by the comparatively simple plot methods of approach 1 (plot Δ vs

L_0/S_0) and approach 2 (S_0 vs $1/\Delta$) yielded straight lines allowing one to extract Δ_1 and K_1 also. Δ_1 and K_1 corresponding to the 1:1 model without further approximations were calculated as well (entry "two parameter computer fit" in Table 7); this corresponds to the complete solution of the system eqs. [9] and [10]. In Table 7 the results are summarized for all procedures discussed so far. Inspection of the table shows that the relative LIS values are comparable for all methods (the values are normalized for easier comparison in the last five rows). This is rather fortunate and suggests (101) that for structural determinations the observed LIS may be used and determination of limiting or bound chemical shifts may not be necessary. The important result of these exacting studies (100, 101) is that LIS values at small L_0/S_0 ratios ($0 \leq L_0/S_0 \leq 0.4$) are simply proportional to Δ_1 as well as Δ_2 ; in the most extreme case, the LIS values at a single (low) concentration of reagent can be used for structural determinations, but this procedure is not recommended. For reliable values any of the linear relationship-plot methods can be used safely, since the slope is not based on just one experiment (three to six points are recommended).

Matters are different for the absolute values of Δ_1 and K_1 . These depend decisively on the mechanism assumed in deriving their values. Within a series of experiments (and employing the same procedure for extracting Δ_1 and K_1) the values doubtlessly represent a measure for the bound shifts and the complex binding affinity. Δ_1 and K_1 derived by different analytical methods cannot be compared for reliable conclusions.

It is interesting that the validity of the graphical plot methods can be derived for the two-step mechanism with the same assumptions as was done for the one-step mechanism in eqs. [8]-[14]. The condition $S_0 \gg L_0$ may be valid; then eqns. [16], [17], and [18] assume the following form when $2y\Delta_2 \gg x\Delta_1$ is assumed for [16] and $S_0 \gg x$, $S_0 \gg 2y$ is assumed for [17] and [18]:

$$\Delta = \frac{2y\Delta_2}{S_0} \quad [19]$$

$$K_1 = \frac{x}{S_0 (L_0 - x - y)} \quad [20]$$

$$K_2 = \frac{y}{x S_0} \quad [21]$$

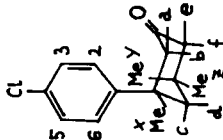
Equation [21] upon rearrangement is

$$y = x S_0 K_2$$

Equation [20] upon rearrangement is

$$K_1 S_0 L_0 - K_1 S_0 x - K_1 S_0 y = x$$

Table 7. Treatment of Experimental LIS Data by Different Methods (Shifts in ppm, Eu(fod)₃, CCl₄)

<div></div>		Two-Step Approach for 1:2 Complexing $K_1 = 222 \pm 15$ $K_2 = 63 \pm 4.3$ Four-Parameter Computer Fit to eq. [16]+[17]+[18]	One-Step Approach for 1:1 Complexing $K_1 = 99 \pm 12$ Two-Parameter Computer Fit Method to eqs. [9]+[10] eq. [14]	Simple Plot Δ vs. L_0/S_0 ; No K_1 is Obtained	Entries I-V Scaled for Convenient Comparison of the Relative Values; $I' = 0.447 \times I$, $II' = II$, $III' = 0.5 \times III$, $IV' =$ $0.5 \times IV$, $V' = 0.5 \times V$	
Protons	Δ_1 I	Δ_2 II	Δ_1 III	Δ_1 IV	Δ V	I' II' III' IV' V'
Me. x	4.40	1.84	3.92	3.70	3.74	1.97 1.84 1.96 1.85 1.87
Me y	6.49	2.90	5.80	5.80	5.80	2.90 2.90 2.90 2.90 2.90
Me z	4.12	1.70	3.68	3.40	3.48	1.84 1.70 1.84 1.70 1.74
H a	17.52	7.00	15.63	14.04	14.40	7.83 7.00 7.82 7.02 7.20
H b	14.56	5.87	12.98	11.76	12.06	6.51 5.87 6.49 5.88 6.03
H c	5.53	2.35	4.93	4.68	4.76	2.47 2.35 2.47 2.34 2.38
H d	6.20	2.53	5.53	5.08	5.18	2.77 2.53 2.76 2.54 2.59
H e	16.90	7.09	15.08	14.22	14.40	7.55 7.09 7.54 7.11 7.20
H f	14.85	6.09	13.24	12.20	12.44	6.64 6.08 6.62 6.10 6.22
H ₃ , H ₅	1.09	0.66	1.01	1.32	1.24	0.49 0.66 0.51 0.66 0.62
H ₂ , H ₆	7.73	3.46	6.92	6.96	6.88	3.46 3.46 3.46 3.48 3.44

Equation [21] substituted in [20] is

$$K_1 S_O L_O - K_1 S_O x - K_1 S_O x S_O K_2 = x \quad [22]$$

Now x , extracted from [22] is

$$x = \frac{K_1 S_O L_O}{1 + K_1 S_O + K_1 K_2 S_O^2} \quad [23]$$

Equation [23] substituted in [21] becomes

$$y = \frac{K_1 K_2 S_O^2 L_O}{1 + K_1 S_O + K_1 K_2 S_O^2} \quad [24]$$

and eq. [24] substituted in [19] becomes

$$\Delta = \frac{2\Delta_2}{S_O} \frac{K_1 K_2 S_O^2 L_O}{1 + K_1 S_O + K_1 K_2 S_O^2}$$

Now the assumption $S_O^2 K_1 K_2 \gg 1$ or $K_1 S_O$ is introduced, yielding

$$\Delta = 2\Delta_2 \frac{K_1 K_2 S_O L_O}{K_1 K_2 S_O^2}$$

rearranged becomes

$$\Delta = 2\Delta_2 \left(\frac{L_O}{S_O} \right) \quad [25]$$

and rearranged again becomes

$$S_O = 2\Delta_2 L_O \left(\frac{1}{\Delta} \right) \quad [26]$$

Comparison of eqns. [25] and [26] with [12] and [14], respectively, demonstrates that for both complexation models (1:1, one step, and 1:2, two steps) the plots Δ versus L_O/S_O and S_O versus $1/\Delta$ yield straight lines, the Δ_1 in [12] and [14] being equal to $2\Delta_2$ in [25] and [26] (compare with the results listed in Table 7).

IV. STEREOCHEMICAL APPLICATIONS OF LIS VALUES

Generally, the use of LSR might be (somewhat arbitrarily) divided into two categories:

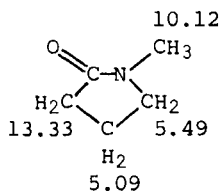
1. Simplification of spectra: one wants to separate all accidentally coinciding resonances.
2. Utilization of the numerical LIS parameters: in most

cases the bound or limiting shifts or simply relative LIS values, in a few cases the binding constant of the complex.

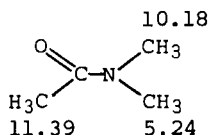
1. Typical uses include the determination of optical purity of enantiomers (106, 107, 81, 82); recently used for the correlation of configuration in closely related compounds [(108) and references therein]; the manifestation of a secondary isotope effect (109), in this case the separation of resonances of deuterated and undeuterated compound is not due to the differences in the geometrical factor but in the complex binding constant (deuterium substitution near the coordinating functionality increases the basicity of the substrate); for simplified interpretation of nmr spectra of complicated systems, e.g., polymer molecules (110); for separating out the different proton signals for C-H heteronuclear double-resonance experiments, thus extending this technique of ^{13}C resonance assignment to otherwise inaccessible nuclei (111); and, last not least, the extraction of coupling constants from simplified low-order spectra.

2. This invariably involves some correlation of the topology of molecules with the experimental LIS data, e.g., in problems concerned with isomerism and conformation. Since the LIS values have to be assigned to particular nuclei an additional bonus is the assignment of resonances of the undoped spectra. Unidentified resonances will match experimental data well if assigned to the correct nuclei, so in cases where assignments cannot be made with certainty a reordering of the dubious assignments may improve the fit. An algorithm for automatic sorting of signals is reported (112), and most computational approaches (computing programs) allow for groups of unidentified signals which are assigned by the computational fit (for instance two vinyl, or three methyl resonances within a molecule).

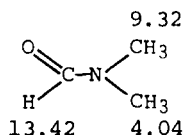
An example where assignments can be made easily on grounds of LIS data is shown below for tertiary amides (113) (9-11); here a model compound is used for a fixed *cis-N*-methyl group (9). The results agree with previous findings; the LIS are given in ppm extrapolated for a 1:1 complex with $\text{Eu}(\text{fod})_3$ in CCl_4 .



9



10



11

In some cases the assignment of resonances may constitute the main task, especially in ^{13}C nmr spectroscopy (111, 115).

We focus on the quantitative use of LIS (type 2) but, in this section, also discuss the utilization of coupling constants, not only because of its relevance to conformational problems but also because a comparison of coupling constant data for undoped and doped spectra allows an estimation of (unwanted) changes in conformation of the substrate introduced by the interaction with the lanthanide shift reagent.

A. Identification of Isomers

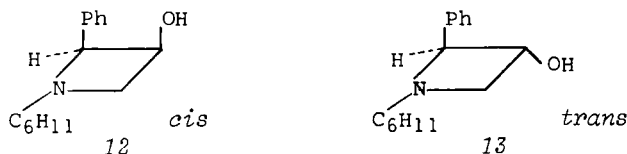
LIS methods have been used for determination of positional isomers in a few cases (30, 89, 116) when other methods have failed.

The true domain of LIS concerning isomerism, however, lies in deciding between structures related as *cis-trans*, *syn-anti*, *E-Z*, *exo-endo*, and other types of diastereoisomers.

Identification of isomers was one of the first broadly used applications of LIS, since in most cases a simple $\log \Delta$ versus $\log r$ plot (Sect. II-C-4) permitted a crude estimation of substrate topology. In some cases the result is obvious at first glance; nevertheless, the reliability of the results is greatly enhanced by a full treatment, taking account of distance as well as angle dependence.

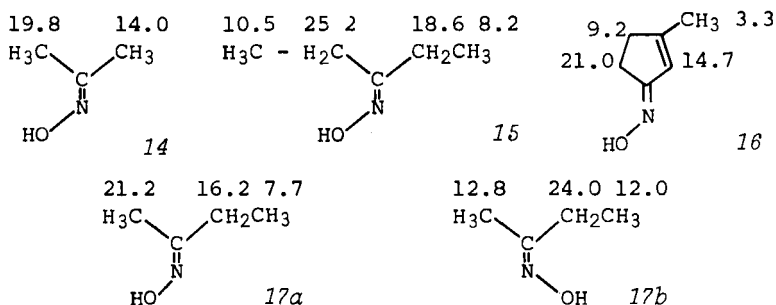
The examples given here are considered representative for problems of this type.

1. A typical example for configurational assignment is that of *cis*- and *trans*-3-hydroxy-1-cyclohexyl-2-phenylazetidine (12 and 13) (117).



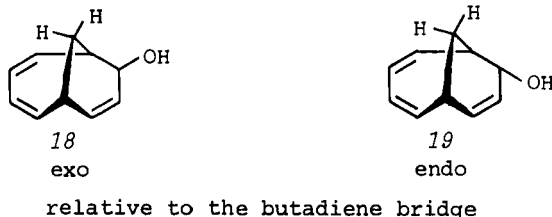
The phenyl protons in the *cis* isomer (12) are shifted downfield upon addition of $\text{Eu}(\text{dpm})_3$ (in CDCl_3) more strongly than those in the *trans* isomer (13) and vice versa for the proton at carbon-2. A check with 3-cyano-1-cyclohexyl-2-phenylazetidine showed that the pmr spectrum was unaffected by addition of $\text{Eu}(\text{dpm})_3$ in the concentration range of interest, thus demonstrating that the dominant coordination site is the hydroxyl group.

2. The following oximes (14-17) are representative of a number of compounds studied (68h). Eu(dpm)₃, CCl₄, LIS in ppm:



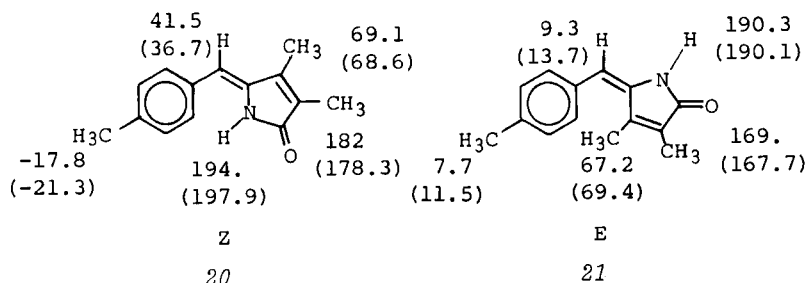
A plot on a log-log scale for the obtained LIS values versus either the estimated distance from Eu to proton or from O to proton, taken from molecular models (Sect. II-C-4) yielded straight lines for a series of syn and anti oximes, including the illustrative compounds shown above.

3. Willcott III and Oth (69) in the course of their research isolated 7-hydroxybicyclo[4.3.1]deca-2,4,8-triene and a stereochemical question arose: is the hydroxyl group exo (18) or endo (19) to the butadiene bridge?



Analysis of the shift data (plot log Δ vs log r , r =distance O...H) favored the exo arrangement for the compound in question; the conformation of the six-membered ring could be deduced from coupling constants favoring the half-chair conformation of the cyclohexene ring.

4. The last example of this type discussed demonstrates the superiority of a quantitative treatment of LIS data for problems of isomerism. In this example the log Δ versus log r relationship would fail, because induced shifts of opposite sign to the usual direction are observed (negative sign in the LIS values given below indicate upfield shifts, the usual shifts for Eu(III) reagents are downfield). The reagent used was Eu(dpm)₃ in CDCl₃, the LIS values are given in Hz for a concentration ratio LSR:substrate = 0.33:1, (118), calculated Δ s are in brackets.



The LIS values of the protons of the Δ^3 -pyrrolin-2-one ring do not depend on *Z* or *E* configuration but those of the methine proton and the *p*-tolyl protons do. An additional complication is the rotational freedom of the aromatic ring. Fortunately the position of the *p*-methyl is not subject to change caused by rotation and the methine proton of the bridge plus the methyl protons of the aromatic ring are ideally suited to prove either *Z* or *E* configuration for a particular isomer. Five resonance signals can be utilized in the computation [program PDIGM (44)]; therefore, the significance test can be applied for one degree of freedom; the results are listed in Table 8.

Table 8. Results of Computer Simulation of the LIS Data for 20 and 21 (Eu(dpm)₃, CDCl₃), Including Significance Testing

	<i>Z</i> (20)	<i>E</i> (21)
Computed positional parameters for the lanthanide ion ^a	2.7 Å 50.0 deg. 246.0 deg.	3.1 Å 50.0 deg. 222.0 deg.
<i>R</i> factors for assignment ^b		
Correct	0.029	0.024
Incorrect	0.12	0.14
<i>R</i> factor ratios: $\frac{R(\text{correct})}{R(\text{incorrect})}$	4.14	5.83
Degrees of freedom	1	1
Reliability of the better hypothesis	~83%	~89%

^aThe pyrrolinone ring is kept at the same coordinates for the calculation of either *Z* or *E*; the parameters found indicate comparable positions of Eu(III) in both compounds.

^bFive protons were utilized in the calculations (see text).

B. Conformational Analysis

Conformational analysis is the most thrilling aspect of the LIS technique because a wealth of information concerning the conformation of molecules in solution can be gained. However, there are some complications to be mentioned in brief at this point which are discussed in more detail for specific cases later.

Important questions are:

1. Is it feasible to assume an average conformation of the substrate in the complex that oscillates only a little about a singular representative conformation?

2. Or is the calculated average conformation instead an average of two (or more) dominant conformations?

Usually the fit is bad if the assumptions made for the geometry of the substrate are wrong, but it might happen that a minimum R value is found for a "wrong" structure that even passes the significance test. This is one reason for using all accessible techniques for gaining information, e.g., NOE measurements, lanthanide relaxation reagents, theoretical quantum chemical model calculations, decoupling experiments, coupling constants, etc.

3. If a singular structure is found to present by far the best model for a LIS fit, another crucial question arises: Is the conformation derived from a LSR-substrate complex valid only for this complex or does it represent the structure of the pure substrate as well?

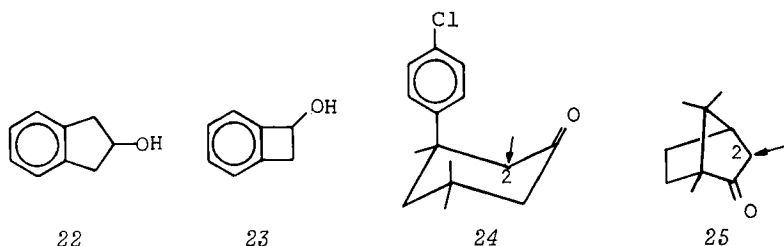
Problems of this type are treated in the next Section.

1. Conformational Changes Introduced by Shift Reagents — Yes or No

Gross changes in substrate conformation are not expected to be induced by the weak coordination of a lanthanide ion to the substrate molecule, especially when the coordination site is well accessible by the Ln(III) on steric grounds. If, however, the binding LSR-to-substrate is greatly facilitated by minor changes in the conformation (see Sect. III-A), it might happen that the conformation will change to allow for better binding.

A method well suited to investigate these problems is to observe the coupling constants for the complexed and uncomplexed substrate. This has been done in a few cases. Unfortunately, the evidence that changes in coupling constants are due to conformational changes is sometimes inconclusive since other causes may be responsible. The aromatic coupling constants of compounds 22 and 23 have been investigated by high-resolution nmr spectroscopy (220 MHz for 22 and 300 MHz for 23) and upon addition of Eu(dpm)₃ at 60 MHz. Iterative computer-fit analysis (LAOCN-3) yielded

different coupling constants for the doped spectra. The authors (119) suggest caution in deriving conclusions from aromatic coupling constants for complexed substrates; yet the aliphatic couplings that are much closer to the coordination site seem to remain unchanged by $\text{Eu}(\text{dpm})_3$.



For compound 24 the observed geminal couplings (for instance, of the protons at C-2) increase proportionally to the amount of shift reagent added [from -13.72 to -14.38 for $\text{Eu}(\text{dpm})_3$:substrate ratios of 0:1 to 1:1; from -13.72 to -14.89 for $\text{Eu}(\text{fod})_3$]. The effect seems to be due to some kind of substituent effect ("substitution" meaning binding of a Lewis acid to the substrate) rather than to a change in conformation. Indeed, the C-2 protons of camphor (25), which is not conformationally mobile, show exactly the same change in coupling. The effect is larger for $\text{Eu}(\text{fod})_3$, which is the stronger Lewis acid (120).

Another case where the coupling of complexed and uncomplexed substrate was thoroughly checked is represented by substituted bicyclo[3.3.1]nonanes (compounds 62 and 63). No change of couplings and, therefore, no conformational changes were detectable (121).

An example where the conformation seems to be changed is reported in (26). The conformations for all 18 possible six-carbon aliphatic alcohols were determined, and in four cases couplings of doped and undoped spectra could be recorded. In three cases no change in the couplings were detectable, but for 3,3-dimethyl-1-butanol changes in the coupling pattern of the α and β protons were observed in presence of even small quantities of $\text{Eu}(\text{dpm})_3$. This was explained by an equilibrium shift between anti and gauche forms favoring the anti conformer in the complexed alcohol (Fig. 17). The equilibrium was estimated to shift from anti : gauche about 75 : 25 to > 90% anti. This means that the *t*-butyl group is removed from the vicinity of the coordination site.

Another quite sensitive equilibrium was reported (122) for 3,3'-disubstituted diphenylsulfines (27).

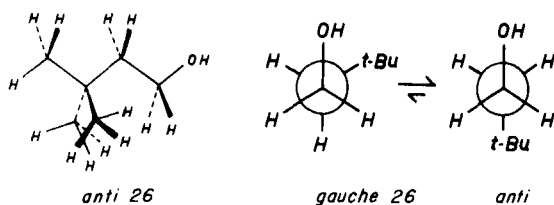
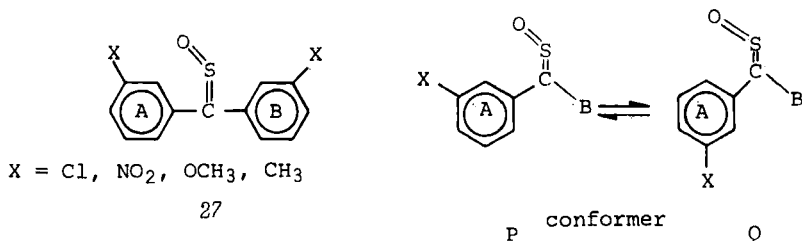


Fig. 17. gauche - anti Equilibrium for 3,3-dimethyl-1-butanol (26).



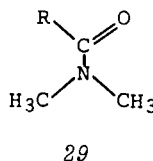
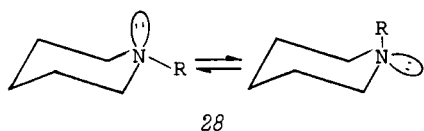
Upon addition of $\text{Eu}(\text{dpm})_3$ the equilibrium shifts to the right side (e.g., favoring Q); the substituent X in conformer Q does not interfere with $\text{Eu}(\text{III})$ coordinated to $=\text{S}=\text{O}$. This effect cannot be due to change of polarity of solvent, since the less polar molecule Q is favored despite the increase of medium polarity when the reagent is added. Typical values in these experiments are: for $\text{X} = \text{Cl}$ in CCl_4 , conformer P (uncomplexed) = 45%, P (complexed) = 29%; for $\text{X} = \text{CH}_3$ in CCl_4 , P (uncomplexed) = 72%, P (complexed) = 45%. In this example relative LIS values were used for the analysis of the conformational equilibria.

Similar effects are observed in equilibria of six-membered ring systems if the coordination site is involved in a (possible) conformational change. For instance, in the equilibrium of 1-methylcyclohexanol [-OH axial or equatorial; see Sect. IV-B-3, example (e)] the conformer with -OH equatorial is favored when $\text{Eu}(\text{dpm})_3$ is added. In cyclohexanones the determination of conformational equilibria is consistent with the results obtained by other than the LIS method [see Sect. IV-B-3, example (d)]. Here the keto part in the molecule represents a rigid structure, and the $\text{Eu}(\text{III})$ bound to it is not significantly involved in the conformation of the substrate.

For the special ring system of alkyl-substituted 1,3,2-dioxaphosphoran-2-one a sizable effect of a shift in equilibrium was observed (123) by analysis of coupling constants in the absence and presence of $\text{Eu}(\text{fod})_3$. A steric dependence is not consistent with the findings for this system; there might be an electronic interaction involving the phosphoryl oxygen that causes the abnormal effect.

Another example indicating the limits of the induced shift method (as well as of other methods) is the question of axial or equatorial preference of the lone pair in piperidine and derivatives (28). This is a matter of much controversy (124-126) which involves a number of current methods of conformational analysis. Paramagnetic shift data could not provide hard evidence either; Refs. (125) and (126) contradict each other. Since the reagent [Cobalt(II)acetylacetonate, $\text{Co}(\text{AA})_2$, was used in the experiments] complexes in piperidines exactly at the conformationally most sensitive center in the molecule, no unambiguous results can be expected in these experiments.

So far we have used paramagnetic shift data and coupling constants to point out possible complications in substrate conformation or conformational equilibria caused by interaction with shift reagents. Another parameter obtainable by nmr may be included in these considerations, namely free energies of activation.



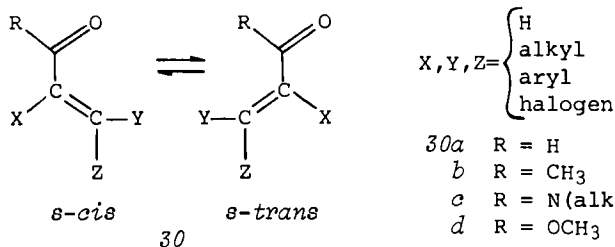
Free-energy barriers to rotation, ΔG^* , have been determined for complexed and uncomplexed amides, $\text{R}=\text{alkyl}$ in 29 (127). No remarkable differences in activation energy were found for complexed and uncomplexed *N,N*-dimethylamides at very low $\text{Eu}(\text{fod})_3$ concentrations (which sufficed to increase the separation of the diastereotopic *N*-methyl signals, thus facilitating analysis of the spectra). For trimethyl carbamate ($\text{R}=\text{OCH}_3$ in 29) the free-energy barriers of rotation were determined at higher $\text{Eu}(\text{fod})_3$ concentrations as well, and a substantial increase of ΔG^* for rotation about the C-N bond was found when the amide was bound to the reagent (128). The values found are: $\Delta G^* = 15.5$ kcal/mol for the pure substrate; and $\Delta G^* = 18.0$ kcal/mol extrapolated to the 1:1 complex. This increase of ΔG^* in the complexed substrate does not necessarily mean that ΔG^0 for equilibrium changes too [Sect. IV-B-3, example (f)].

In this section we may have overemphasized cases where some perturbation of properties of the substrates were found to be caused by interactions with the shift reagent; in what follows many successful applications of the LIS technique will be presented, and the results in general agree very well with known results whenever comparison is possible. In most cases the conformation of a substrate seems not to be influenced by complexing to a LSR. In some particular cases this might not be true, e.g., when steric hindrance for complex formation can be readily

decreased by conformational equilibration between low-energy forms and the free energy of activation is low, also. If the coordination site itself is the key to conformational changes in the molecule, one has to be very careful in the interpretation of LIS experiments [Sect. IV-B-3, example (e)]. On the other hand, if the coordination site is incorporated in a rigid part of the molecule and the conformational problem is somewhat distant from that site, a change of conformation induced by the LSR can be safely excluded.

2. Torsion about Single Bonds not Incorporated in a Cyclic System

a. α, β -Unsaturated keto compounds have been studied thoroughly by several groups: aldehydes *30a* (53, 54, 129), ketones *30b* (53, 54, 68a), amides *30c* (53, 54, 130), and esters *30d* (53, 131).



Earlier calculations used simple r dependence of the LIS and assumed either one or the other of the (planar) rigid structures (*s-cis* or *s-trans*) to be the one exclusively present in solution, i.e., the equilibrium *30* was assumed to lie completely to the right or to the left.

The approach of Montaudo et al. (53, 54) is a different one. They simulated the observed LIS values, not by presuming a single conformation to be present (either a planar or a nonplanar form is possible in principle), but by the assumption of an equilibrium between the two planar forms *30*. The population ratio between *s-cis* and *s-trans* forms can be calculated if the McConnell-Robertson eq. [6] is written in the following form:

$$\Delta = K [w_1 G_1 + (1-w_1) G_2]$$

w_1 is the molar fraction of form 1, $(1-w_1)$ the molar fraction of form 2, and G_1 and G_2 the geometrical factors for a particular nucleus for forms 1 or 2, respectively.

For a particular lanthanide ion position, only the values K and w_1 are independent variables, since G_1 and G_2 are fixed for an assumed LSR-substrate arrangement. By this reasoning the con-

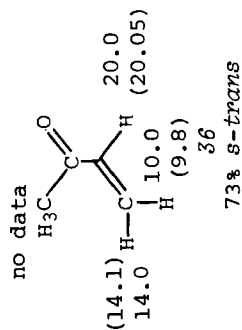
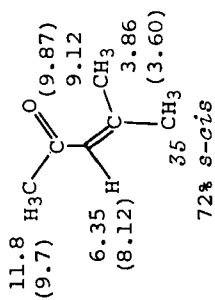
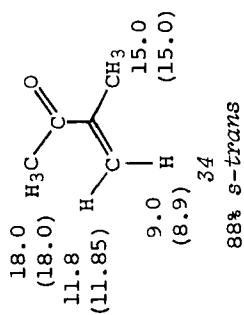
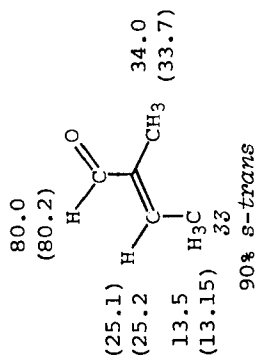
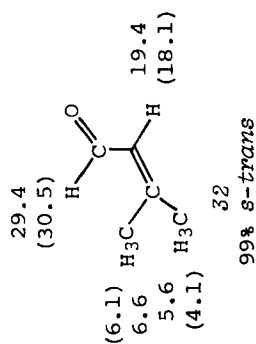
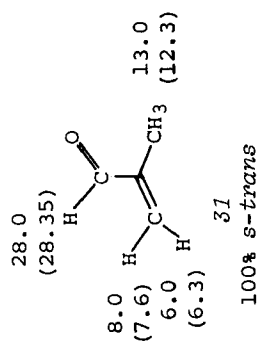
clusion is arrived at (53) that a minimum of three LIS values will yield solutions which are mathematically determined. However, the more rigorous approach applied in (61) would require at least six observations for a two-conformer system to evaluate the statistical reliability of a particular hypothesis: three variables for the Ln(III) position, one scaling factor K , and the additional variable introduced by the population ratio of the two conformers leaving one degree of freedom for significance testing. Nevertheless, the results obtained by the simpler method for some thirty aldehydes, ketones, amides, and esters fit well into the picture already gained by other methods. The population ratios determined are quite reasonable, and the perturbation of the equilibria by the shift reagent Yb(dpm)_3 , Eu(dpm)_3 , or Pr(fod)_3 is not significant. In some sterically hindered cases the planar forms assumed might be idealized, the most stable form being one in which the carbonyl group is actually somewhat rotated out of the C-C double-bond plane, as has been suggested for α,β -unsaturated ketones (132); the decrease of orbital overlap might be more than counterbalanced by avoiding steric crowding.

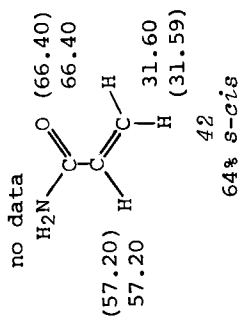
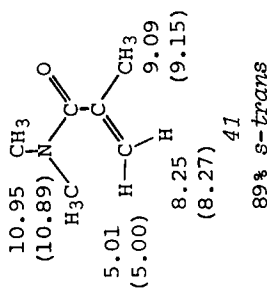
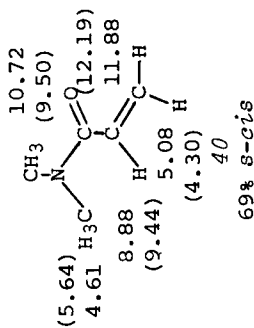
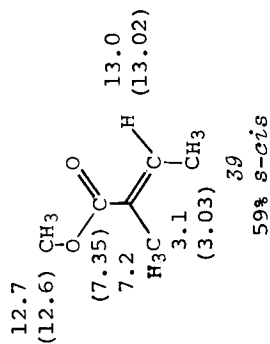
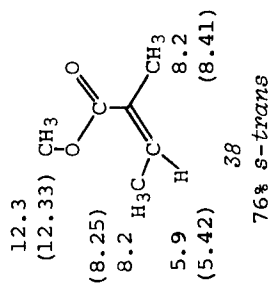
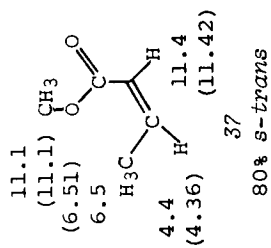
The aldehydes are found to be more or less predominantly in the *s-trans* conformation; and so, generally, are the ketones, but when the α -substituent is hydrogen and the two β -substituents are bulky, the *s-cis* form becomes favored; thus for mesityl oxide (35) 72% *s-cis* was found. To find general trends for preference of *s-cis* or *s-trans* forms for esters (37-39) and amides (40-42) seems, as yet, to be somewhat problematic.

In the scheme below, representative compounds are shown with experimental and (calculated) LIS in ppm (for LSR:substrate = 1:1); the favored conformer is illustrated in each case; the calculated values are for the conformer ratio indicated.

b. Purely aliphatic molecules (alcohols and amines). Comparison of the values of the LIS of the four isomers of butanol (133) leads to important conclusions with respect to conformation. The absolute values of the LIS (extrapolated to 1:1 complex, in ppm, see Fig. 18) show similar values for all compounds for comparably positioned protons; therefore, the lanthanide ion is positioned similarly in the series of compounds, and direct comparison of the LIS values is permissible. The same applies to the corresponding amines (Fig. 18).

Extensive calculations have been performed (26) for all 18 possible six-carbon aliphatic alcohols utilizing ^1H LIS [Eu(dpm)_3] as well as ^{13}C LIS [Yb(dpm)_3]. For preliminary screening of meaningful structures, Dreiding models were used to keep computer time within reasonable limits. For computation an oxygen-lanthanide ion distance of 3 Å and a carbon-oxygen-lanthanide ion angle of 130 deg. were assumed; this was justified by comparison of relevant references for rigid alcohols: borneol $d=$





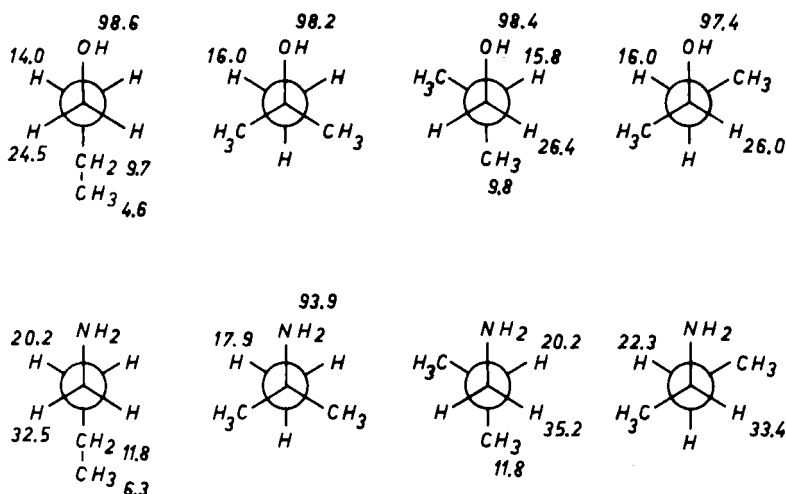


Fig. 18. Lanthanide-induced shifts in ppm downfield for *n*-butanol, *tert*-butanol, isobutanol, *sec*-butanol and *n*-butylamine, *tert*-butylamine, isobutylamine, *sec*-butylamine; Eu(dpm)₃ in CHCl₃ or CDCl₃ at 32°C; extrapolated to 1:1 complex.

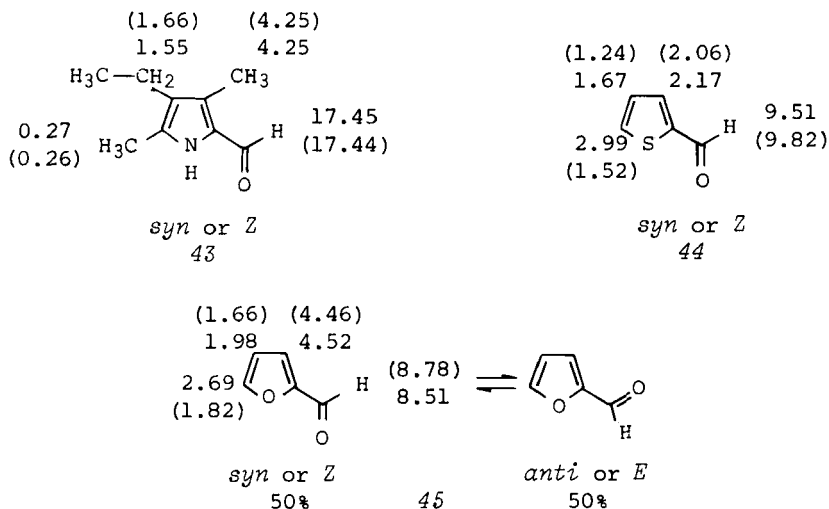
2.4–2.7 Å, $\rho = 129.5$ –133 deg. (65); $d = 3.2$ Å, $\rho = 130$ deg. (44, 61); and adamantan-2-ol $d = 2.3$ Å, $\rho = 139$ deg. (57). The goodness of fit was expressed in terms of a correlation coefficient [Δ (obs) versus Δ (calc)], which was usually better for the results based on ¹³C than on ¹H data; but the results are in all cases virtually the same for both nuclei.

It is somewhat problematic to apply the LIS technique to purely aliphatic systems when no possibility exists to orient the lanthanide ion with respect to some rigid partial structure of the molecule. In some cases the "softness of the function" used (8) to calculate the LIS for particular conformations does not allow one to decide in a straightforward manner between several possible structures. The main purpose for calculations performed on purely aliphatic systems, where all bonds are free to rotate, is to check if the intuitively assumed conformations are, in fact, compatible with the observed LIS.

The situation is better for aliphatic chains attached to a large rigid system [example (k)]; or any of the following examples where one freely rotating group is connected to a larger system; even introduction of a double bond cuts down the multitude of possible conformers drastically; in the previous example (a) rotation was hindered on grounds of the reasonable assumption that orbital overlap of conjugated double bonds retains such bonds in a plane.

c. 2-formylpyrrole, -thiophene, and -furan. These compounds

have been thoroughly investigated by numerous methods (134): nmr studies (coupling, temperature studies, NOE measurement, solvent-induced shifts), X-ray diffraction, ir studies, gas-phase microwave spectroscopy, dipole-moment study, and Kerr-constant determinations. Most of the evidence leads to the conclusion that 2-formylpyrrole and 2-formylthiophene are quite preponderantly in the *syn* (*Z*) arrangement 43 and 44; whereas 2-formylfuran is considered to represent a mixture of both *syn* and *anti* isomers in comparable amounts (45). The results are shown in the formulas below, Δ in ppm, calculated Δ in brackets.



The LIS method can be applied here in a very simple and successful manner. Figure 19 shows the change in the agreement factor for rotation about the single bond of the formyl group. The three curves for 43, 44, and 45 exhibit interesting features. The curves for the substituted 2-pyrrolaldehyde (118) and for 2-thiophenaldehyde (54) show a broad but clear minimum at 180 deg. corresponding to the *syn* form being present in solution. The curve for 2-formylfuran exhibits two very flat minima near $\theta = 60$ and 300 deg. They might correspond to two out-of-plane forms, but an assertion to this effect demands a check of whether a mixture of dominant conformers might not account better for the experimental LIS. In this case (45) a mixture of about equal amounts of *syn* and *anti* (*Z* and *E*) isomers is the better choice, based on external evidence as well as R factor analysis of the LIS fit (53, 54). Decisions of this type are the easier the more LIS values can be obtained for a system.

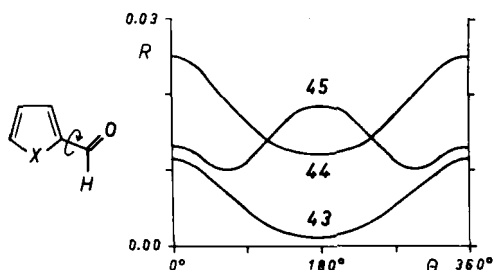


Fig. 19. Plot of the agreement factor R versus the torsional angle θ of the formyl single bond in 3,5-dimethyl-4-ethyl-2-formylpyrrole (43), 2-formylthiophene (44), and 2-formylfuran (45); the starting conformation is shown.

d. *N*-vinyl-1-pyrrolidone. The vinyl group in *N*-vinyl-1-pyrrolidone (Fig. 20) can, in principle, adopt the following conformations: either one of the two planar forms (keto syn or anti to vinyl), all possible rotational conformers about N-C (vinyl), or any mixture of two or more favored conformers. The single minimum at 180 deg. with an excellent agreement factor proves that the anti form is highly predominant (Fig. 20). The experimental values (54) are not accounted for better by any kind of mixture.

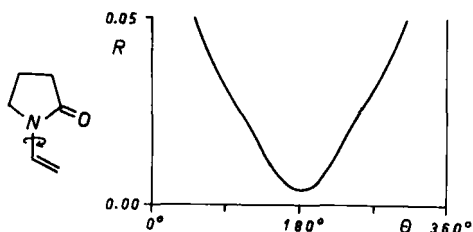


Fig. 20. Plot of the agreement factor R versus the torsional angle θ of the N-C(vinyl) bond in *N*-vinyl-1-pyrrolidone; the starting conformation is shown.

e. *Methoxyxanthenes*. An interesting study of 1-, 2-, 3-, and 4-methoxyxanthone by Willcott III and Davis (135) points out the limits of the LIS method when no additional external information is available. We pick 4-methoxyxanthone for discussion as typical for the series [except for 1-methoxyxanthone which forms a bidentate complex with $\text{Eu}(\text{dpm})_3$; for the three other isomers complexation takes place solely at the keto-oxygen]. ^1H LIS (excluding the methoxy protons) were used to determine the position of the lanthanide ion $[\text{Eu}(\text{dpm})_3, \text{CDCl}_3, \Delta]$ extrapolated to LSR:substrate 1:1, program PDIGM (44), agreement factor less

than 0.01 for the parent compound]. Then the LIS values to be expected for the methoxy protons upon rotation about the ring-oxygen bond are calculated in incremental steps and compared with the actually observed ones (Fig. 21). Figure 21 shows that either a conformer with methoxy 90 deg. out of plane or a 1:1 mixture of the two planar forms (0 and 180 deg.) would account for the experimental value. Based on external evidence that anisoles should have at least twofold rotational barriers, the authors favor the solution in terms of two equally populated planar forms.

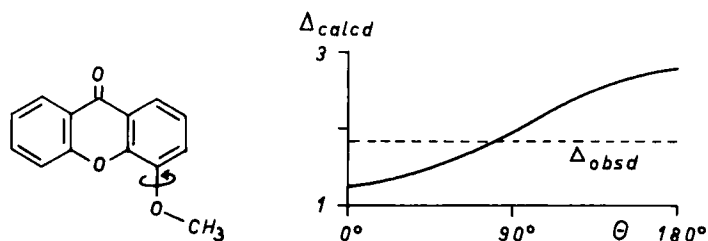


Fig. 21. Plot of calculated lanthanide induced shift for the methoxy group of 4-methoxyxanthone; the starting conformation is shown.

A twofold rotational barrier was found by analysis of the far infrared and Raman spectra of anisole (135a,b). The rotational barrier in anisole is 3.6 kcal/mole in the gas phase. In the liquid state higher values were found. For additional discussion concerning the planarity of anisoles see (135c).

f. *Exo-2-methoxy-3-aza-4-keto-7,8-benzobicyclo [4.2.1] nonene* (48). Compound 48 (Fig. 22) provides a perfect model for

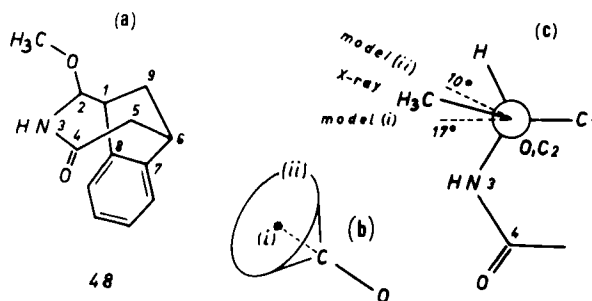


Fig. 22. (a) Perspective structure of 48; (b) Computational models used: (i) positionally averaged central H and (ii) the "100 H circle"; (c) results of models (i) and (ii) compared to the X-ray structure determination illustrated by a Newman projection looking down the O-C-2 bond.

studying the $\text{CH}_3\text{O}-\text{C}$ torsion by means of the LIS method because the rest of the molecule is rigid. The structure of **48** has been determined (**51**) by X-ray diffraction analysis as well as by the LIS technique, using $\text{Eu}(\text{dpm})_3$ and $\text{Pr}(\text{dpm})_3$ as LSRs. The lanthanide ion position was obtained by means of the LIS of the 12 ring protons; an iterative computer fit of the experimental LIS-ratios using the geometry of the substrate determined by X-ray analysis was made. $\text{Eu}(\text{III})$ yielded the significantly better fit (see Sect. III-A), and therefore, the conclusions based on the $\text{Eu}(\text{III})$ shift data are discussed below. With the geometry of the rigid part of the molecule established relative to the $\text{Eu}(\text{III})$ position, the methoxy group was allowed to rotate about the $\text{O}-\text{C}-2$ bond, searching for the position of the methoxy protons yielding the best fit. Two models for the methyl group were used: (i) an "average" proton positioned along the $\text{O}-\text{CH}_3$ vector at a distance of 0.36 \AA from the methyl-C (this is the usual positionally averaged methyl-LIS; $1.09 \cos (180-109.5) = 0.364$, using tetrahedral angles of 109.5 deg. and C-H distances of 1.09 \AA in the calculation) and (ii) a "100 H circle," synthesized by rotating a proton in 3.6 deg. increments about the $\text{H}_3\text{C}-\text{O}$ bond and averaging the calculated shifts for all 100 fictitious positions. (i) corresponds to positional averaging and (ii) to LIS averaging for a representative set of probable positions of the nuclei under consideration.

The position found for the methoxy protons deviates slightly from the one measured in solid state. The best fit for model (i) lies 17.3 deg. off the position determined by X-ray analysis (towards N-3; see Fig. 22), the best fit for model (ii) is located 10 deg. on the opposite side (Fig. 22). Model (ii) allows a better fit than model (i), the "100 H circle" obviously representing the actually freely rotating methyl group better.

The simpler approach of positioning the methyl group so that the protons are staggered with respect to the substituents on the neighboring atom might be physically more meaningful, since a whole circle puts the protons in positions where they never are (see Sect. II-C-2).

g. 3-Arylcyclohexanones (**136**) and 3-arylcyclohexanols (**6b**, **79**, **137**) have been studied extensively by Shapiro *et al.* In most cases the orientation of the aryl residue relative to the cyclohexyl moiety is the expected one (in terms of minimal steric interaction) - for instance in *cis*-3- α -naphthyl-1,3,5,5-tetramethylcyclohexanol (**49**) (Fig. 23). Matters seem to be different for **50** and **51**. The induced shifts for the aromatic protons in *trans*-3- α -naphthyl-1,3,4,4-tetramethylcyclohexanol (**50**) and *cis*-3- β -naphthyl-1,5,5-trimethylcyclohexanol (**51**) exhibit interesting features. Usually $\text{Eu}(\text{III})$ -induced shifts are downfield; however, the LIS of the protons **6** and **7** in **50** and **4**, **5**, **6**, **7**, and especially **8** in **51** are strongly upfield. This is possible only when the aromatic moiety is turned towards the hydroxyl group.

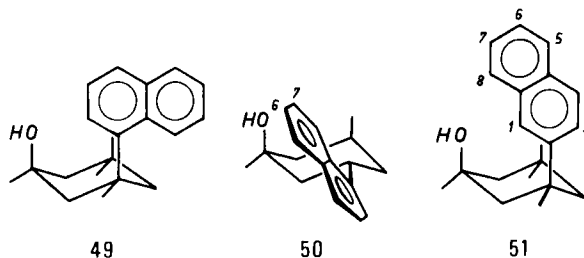


Fig. 23. Perspective structures for compounds 49, 50, and 51.

Figure 23 illustrates the proposed conformations for the aromatic residue of compounds 50 and 51.

These conformations are surprising. If the lanthanide ion were to influence the conformation to some degree, the conformations would be exactly the other way round (aryl turned away from the hydroxyl group). Compounds 50 and 51 assume a rather compact form, and the smaller size of the molecules in solution might be of importance in explaining these results. This effect ("internal pressure" of the solvent) (147) is real, but since it is small (0.2 to 0.3 kcal/mole for solvation in ordinary solvents, relative to the gas phase) it is unlikely to be the full explanation for the conformation found. Hydrogen bonding to the aromatic ring might be of importance too.

h. cis- and trans-2-Benzylcyclohexanol (52a and b) present a case where analysis of coupling constants led to ambiguous results with respect to the C-2-benzyl bond (the phenyl is rotationally free). Either conformation I or II (Fig. 24) accounts for the observed coupling pattern. LIS (Eu(dpm)₃, CDCl₃, log Δ versus log τ plot) allowed a decision in favor of conformation I in both cases (52a and b) (138).

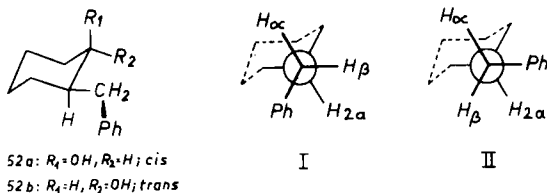


Fig. 24. Possible conformations I and II for the compounds 52a and b.

i. Pyrromethenes and pyrromethenones were studied (94, 139) with respect to torsion about the methine bridge bond, as indicated in Figure 25. In the pyrromethenes 53 and 54 a carbethoxy group was introduced to furnish a good coordination site (the two ring nitrogens do not show any complexation to

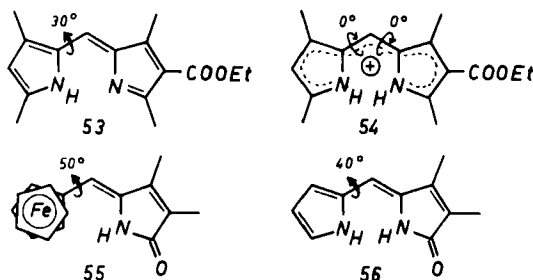


Fig. 25. Structures of the pyrromethenes **53** and **54** and the pyrromethenones **55** and **56**, showing the LIS-determined torsional angles about the methine-bridge single bonds.

Eu(dpm)₃ in the concentration range of interest; this was checked with the corresponding compound lacking the carboxy group). Since no information concerning the rotational preference of the ester C=O was available, the carbon of the ester group was taken as the coordination site in the computation [program PDIGM (44)]; the excellent fit justifies this assumption. The -C(=O)...Eu(III) distance computed in the fit is 3.8 Å for **53**, and 3.7 Å for **54**; the corresponding (-C)=O...Eu(III) distances are, therefore, about 2.6 Å for **53** and 2.5 Å for **54**, which are very reasonable values; the corresponding angles ring-carbon, ester-carbon, Eu(III) are 60 deg. for **53** and 50 deg. for **54** (94).

Figure 26 shows all possibilities of rotation in compound **54**; only rotation about single bonds is considered in the individual quadrants of Figure 26, but the special pyrromethene system allows the bonds in the methine bridge to change single and double bond character by tautomerism.

The best fit was obtained for the conformation corresponding to formula **53** in Figure 25, the pyrrole ring being out of plane by approximately 30 deg. (agreement factor $R = 0.014$) (94).

Things are different for the protonated form **54**. The positive charge is averaged completely over the molecule [the electron distribution in the two Ns is completely averaged as was demonstrated by photoelectron-spectroscopic methods; for **53** two distinct Ns were shown to be present (140)]. As a consequence, simultaneous torsions about both methine bridge bonds have to be considered possible in **54**. The best fit was found for $\psi = \omega = 0$ deg. ($R = 0.013$) indicating an average planar *Z-syn*-conformation for **54**. Figure 27 illustrates the results of the calculations (94).

In the pyrromethenones **55** and **56**, only torsion about the single bond in the methine bridge is possible and, judging from space filling molecular models, necessary. Compound **55** is especially well suited for study of this torsion because the

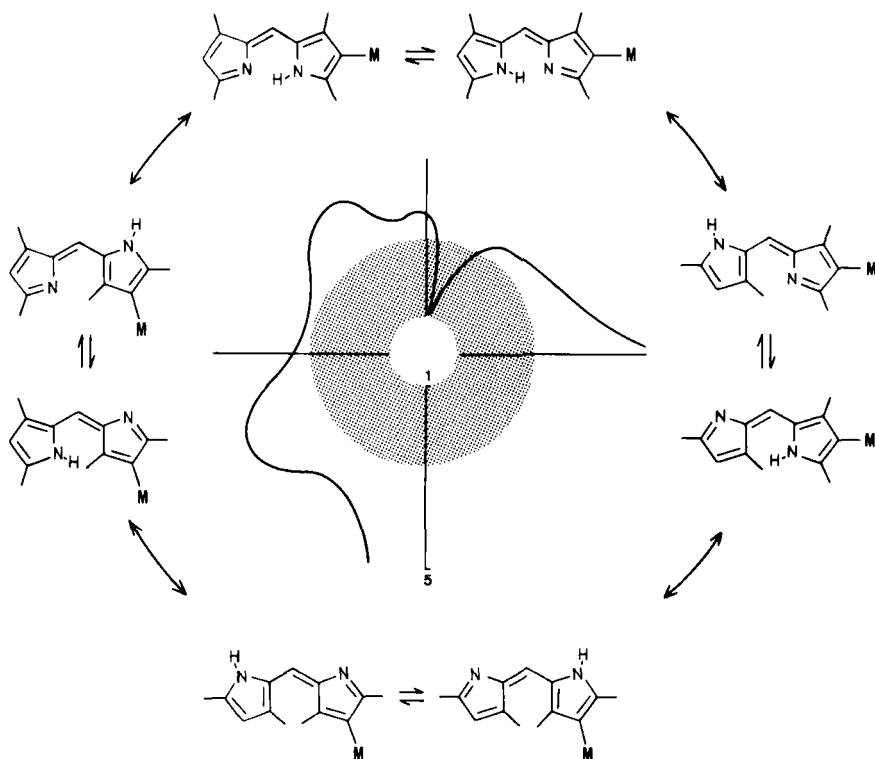


Fig. 26. Plot of R/R_{\min} calculated for all possible tautomer conformations of **53** using a cyclic coordinate system (180 deg. torsion corresponds to 90 deg. in the figure); the shaded area indicates the R/R_{\min} limits within which conformations cannot be rejected at least at the 90% level (similar, but linear plot in Fig. 28); M stands for COOEt.....Eu(dpm)₃. Taken from *Monatsh. Chem.*, 105, 1004 (1974), used by permission from Springer Verlag.

protons of the hetero ring of the ferrocene moiety are far off the axis of rotation and should display great differences in LIS values, even for small torsional angles. In principle the cyclopentadienyl hetero ring could be turned towards the N-H of the pyrromethenone ring (this should be unfavorable on steric grounds) or in the opposite direction (this should be favorable). The best fit was found for a torsional angle of 50 deg. away from the pyrrolinone ring as indicated by the arrow in Figure 25 (defined as positive torsion in Fig. 28). In Figure 28 the computational results are shown for both treatments of the five hetero ring protons giving one experimental LIS value (see Sect. II-C-2). The fit is good for both (R about 0.03) but the

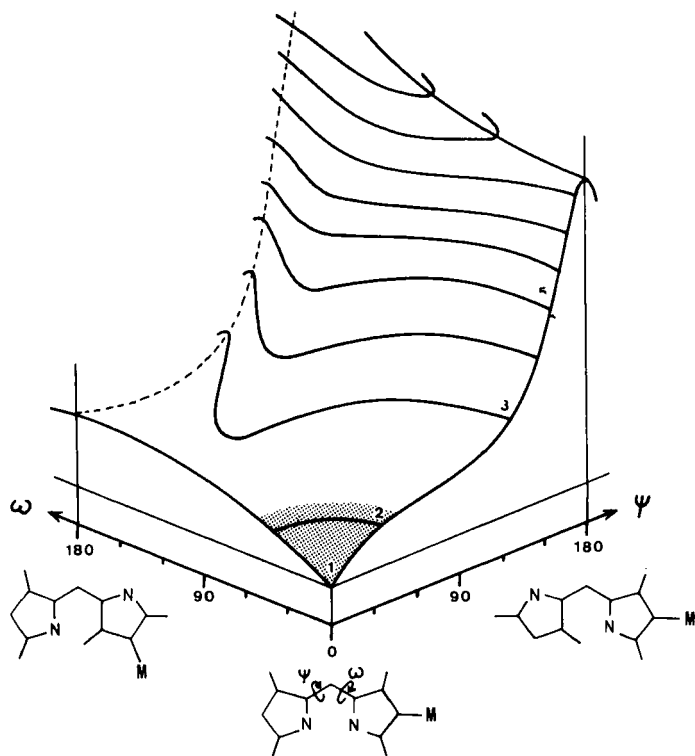


Fig. 27. Three-dimensional plot for R/R_{\min} values (z coordinate and corresponding contour lines in the figure) versus variation of the torsional angles of both methine bridge bonds of 54 (x, y coordinates); the shaded area indicates the 90% confidence level (see Figs. 26 and 28); M has the same meaning as in Figure 26. Taken from *Monatsh. Chem.*, 105, 1004 (1974), used by permission from Springer Verlag.

minimum of R is very flat for positional averaging, thus jeopardizing meaningful significance testing because almost all possible conformers are within the 90% confidence level (dashed line in Fig. 28). Averaging of the calculated LIS for the five hetero ring protons (staggered to the homo ring) and comparison with the experimental shift favors a torsion of 50 ± 15 deg. (118).

For 56 the best fit was found for a torsional angle of ~ 40 deg. ($R = 0.078$), (139).

j. The determination of the structure of the *tetrahalo terpene alcohol* 57 (isolated from the California Sea Hare, *Aplysia Californica*) was described by Willcott III and Davis

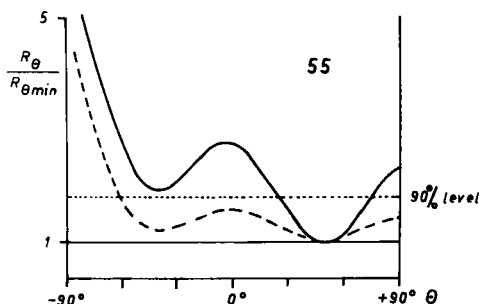
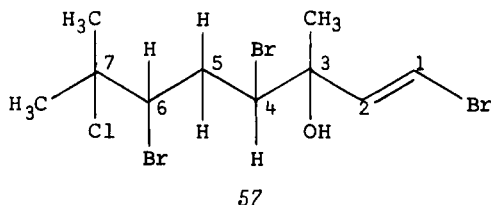
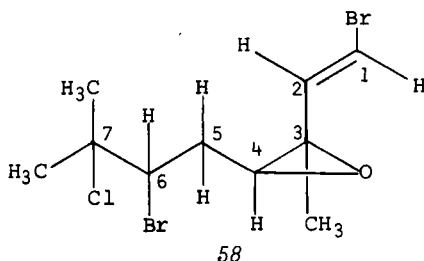


Fig. 28. Plot of R/R_{\min} for torsion about the methine bridge single bond of 55; the sign of the torsional angle is taken to be positive as indicated by the arrow in formula 55 (Fig. 25); 90% confidence level is indicated; two different models for the cyclopentadienyl hetero-ring were used (see text).

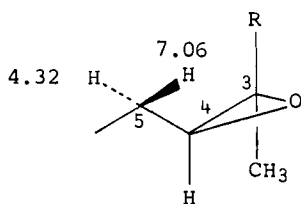
in some detail (135).



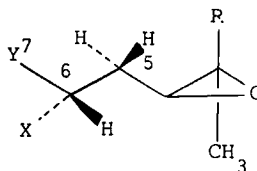
To simplify the problem, the first step was to convert the alcohol to the epoxide 58. The olefinic protons are *trans* (coupling constant) and the proton at C-4 is *cis* to the methyl at C-3 (NOE).



Next epoxide 58 was treated with $\text{Yb}(\text{dpm})_3$ to obtain LIS values. A reasonable Yb position was calculated based on the epoxide ring alone. The two hydrogens at C-5 were located by calculation of a dummy hydrogen which was rotated about the C-4-C-5 bond in small increments; with the additional restriction of tetrahedral angles, two positions were chosen for which the fit, calculated to experimental LIS (program PDIGM (44)), was good.



58a



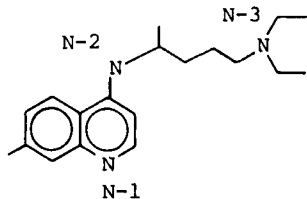
58b

The next step, locating the proton at C-6, turned out to yield two possible positions for one hydrogen. By means of first-order coupling analysis it was obvious that the possibility putting the C-6 proton *anti* to the one with the LIS index 4.32 was the right one (58a).

Now the proton at C-6 is fixed, but as yet there was no decision between the possible positions of -Br and -CCl(CH₃)₂. This decision was again made by calculating the hypothetical LIS of the three staggered rotamers for a geminal dimethyl group for both possible configurations (X = Br, Y = CCl(CH₃)₂, or vice versa in 58b). The experimental LIS for the two geminal methyls at C-7 are 0.66 and 1.05, respectively. The calculated (hypothetical) LIS for X=Br, Y=CCl(CH₃)₂ are 0.66, 0.96, and 1.59 for the three staggered conformers and 3.68, 1.00, and 2.12 for X=CCl(CH₃)₂, Y=Br. Matching of the values 0.66 versus 0.66 and 1.05 versus 0.96 is convincing, and the structure determination is complete.

To summarize the general features in this sophisticated procedure: a rigid partial structure carrying the coordination site is utilized to fix the lanthanide ion position, then the structure is fitted step by step to the experimental LIS, using whatever external evidence is available. The lanthanide ion position can be recorrected for each newly attached group furnishing LIS data during the procedure.

k. *Chloroquine* (an antimalarial) presents a case where the conformation found for the dihydrochloride in the crystal by X-ray structure determination differs substantially from the conformation found for the base in solution using the LIS technique (49).



59

Distance N-1 to N-3:

solid state (X-ray)	14.1 Å
acetone solution 20°C (LIS)	7.4 Å
acetone solution 48°C (LIS)	9.3 Å

The shift reagent $\text{Pr}(\text{dpm})_3$ was found to complex preferentially to the aromatic nitrogen (N-1), the other potential coordination sites [a secondary nitrogen (N-2) and a tertiary one (N-3) in the aliphatic chain] being at least ten times weaker in binding to the LSR. The orientation of the lanthanide ion with respect to the quinoline ring was determined in the first step of the computational procedure, then in the second step the side chain conformation was determined. The procedure used was to vary the dihedral angles along the entire chain in a sequential manner through 360 deg., with restrictions imposed by possible bonding arrangements (bond distances, bond angles). For protons where rotational motion (and/or torsional oscillation) gave rise to averaged LIS values, this was accounted for by corresponding computational averaging of the LIS.

The conformation found [$\text{Pr}(\text{dpm})_3$, acetone solution, best overall least squares fit] at 20°C is a rather compact one, in contrast to the one in the solid state.

The X-ray structure determination was done on the diprotonated form of 59 (N-1 and N-2) (141). In the solid state the aliphatic side chain is directed out of the quinoline plane at a roughly normal angle. The bonds of the backbone of the side chain are oriented in all-*anti* fashion, which is typical for alkanes. The distance N-1 to N-3 that comprises some measure of the compactness of molecule 59 is 14.1 Å in the solid state.

At a temperature of 20°C in acetone solution, the N-1 to N-3 distance for the complexed chloroquine is only 7.39 Å, indicating a rather compact structure with the side chain curled over the plane of the quinoline ring. The backbone bonds adopt a staggered form in solution with the overall net effect amounting to a curling of the side chain over the center of the quinoline ring.

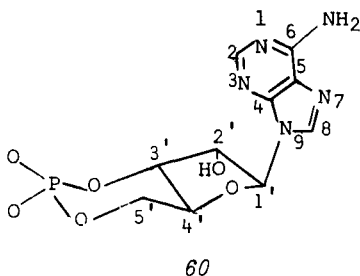
At a temperature of 48°C the structure opens up somewhat by thermal motion, the N-1 to N-3 distance now being 9.33 Å.

The conformations found in solution represent a statistical mixture of various possible conformations. Eight single bonds correspond to 3^8 possible conformations; even when many are sterically forbidden a large number of energetically similar conformers will still be left. The significance of the "average structure" obtained is problematic.

2. The conformation of cyclic β -adenosine-3',5'-phosphate (3',5'-AMP, 60) was determined by Lavalley and Zeltmann (50) in aqueous solution ($\text{Pr}(\text{ClO}_4)_3$, D_2O over a pD range of 2.2-5.3) by means of the LIS technique.

The crystal structure of 3',5'-AMP shows two species in the asymmetric unit (142) that have very different orientations of the purine about the glycosyl bond. One conformation present in the solid state is a rather compact one (purine syn to the phosphate-ribose unit, torsional angle 102 deg.) the other one

is extended (anti arrangement, torsional angle -50 deg.). (The torsional angle is zero when the oxygen of the ribose and C-4 of the base are antiplanar, and the sense of torsion is positive for a clockwise rotation of the ribose unit when viewed in the direction C-1' to N-9.)



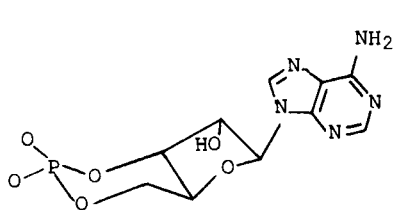
The question of conformation in solution arises, since the two different forms of 3',5'-AMP in the solid state seem to be determined by crystal packing forces. Careful analysis of the LIS data revealed the conformation of 60 to resemble the *syn* conformation of the crystalline state, the torsional angle found being 86 deg. with error limits of ± 22 deg.

The first step to determine the structure via LIS analysis (program MSEARCH; R factor) was to find the position of Pr(III) considering only the ribose unit. Both phosphate oxygens were found to coordinate with the lanthanide ion; the conformation of the ribose unit was found to be consistent with the structure in the solid state (with the phosphate ring in the chair form).

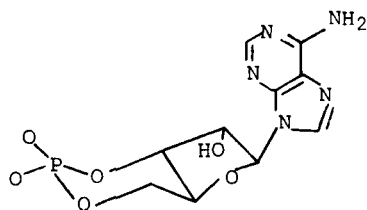
Broadening information with Ho(III) was used as an agreement criterion [based on the r^{-6} relationship (Sect. III-A)] to aid the assignment of resonances.

The next step was to rotate the base about the glycosyl bond and to check the fit for different torsional angles. The best agreement ($R = 0.048$) between calculated and observed shifts was found for a glycosyl torsional angle of 86 ± 22 deg.

The following structural formulas illustrate these findings;



Extended form:
crystalline state

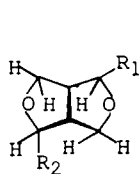


Compact form: crystalline
state and in aqueous solution

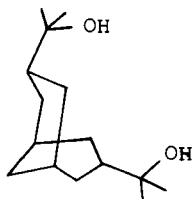
3. Conformations of Cyclic Systems

For problems concerning the conformation of ring systems either one of the following methods may be used: analysis of coupling constants or simulation of the LIS values of the doped spectra. Both kinds of information should be used for conformational evidence, since each supports the other.

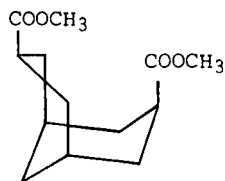
In some cases the LSR-doped low-order nmr spectra were used primarily to extract coupling constants and thereby to derive the conformation; this was done (121, 143) for the cases given below; other examples come from terpene chemistry (144) and from the carbohydrate field (145). Evaluation of the couplings from doped spectra is the method of choice, especially for polyfunctional cyclic systems where computation of LIS is tedious, if at all possible. Since in unfavorable cases the interaction with the reagent might influence the conformation and the coupling constants, some care is advisable; cases are even known where the coupling constants change without conformational perturbation (See Sect. IV-B-1). Extrapolation to a reagent concentration of zero is possible in many cases and prevents errors of this type.



R₁ = 3,4,5-trimethoxyphenyl
R₂ = piperonyl
61



62



63

In 61 (epiaschantin (143), a lignan found in a Formosan medicinal plant, *Hernandia ovigera* Linn.) the two oxolane rings form a rooflike structure with the 3,4,5-trimethoxyphenyl groups in the exo and the piperonyl group in the endo positions.

For 62 (3 α ,7 α -bis-2-(2-hydroxypropyl)bicyclo[3.3.1]nonane) a double twist conformation was found by analysis of coupling constants [Eu(dpm)₃ (121)]. Compound 63 (3 α ,7 α -bicyclo[3.3.1]-nonanedicarboxylic acid dimethyl ester) shows an important contribution of the chair-boat conformation, where both the chair and the boat might be flattened to some extent (121).

In all three cases (61-63) the coupling pattern was not interpretable in the undoped spectra.

We now focus on examples where the LIS values were exploited for determination of conformation in cyclic systems.

Wood et al. (86) used $\text{Eu}(\text{dpm})_3$ -induced shifts in a qualitative way to confirm other conformational evidence (from nmr and dipole moments) for the equilibrium positions in differently substituted trimethylene sulfites.

The following *nine* examples are devoted to conformational problems solved by quantitative use of LIS values, either by comparison with model compounds (which is of particular advantage for studies concerning conformational equilibria, examples d, e, and g.) or by full computer simulation of the relative LIS (for cases where highly favored single conformations rather than equilibrium mixtures are present in solution).

The order of examples is in accordance with increasing ring size.

a. *cis*- and *trans*-1-Cyano-2-vinylcyclobutane (64 and 65)

Willcott III and Davis (135) have investigated 64 and 65 by LIS simulation [program PDIGM (44)]. The LIS values for the cyclobutyl resonances were fitted to several conformations of the cyclobutane ring corresponding to folding of the ring from $+60$ to -60 deg. on either side of the average plane (Fig. 29).

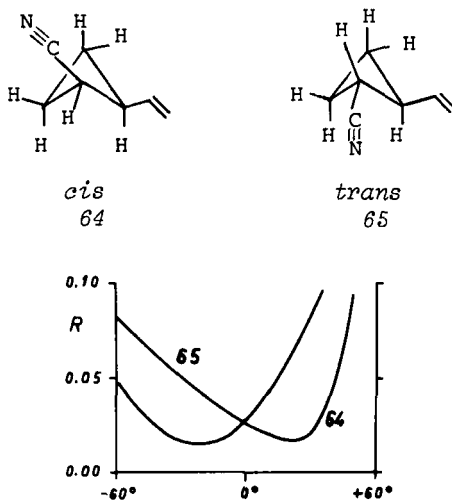


Fig. 29. Plot of the agreement factor R for different angles of folding for 64 and 65; the ring is folded up on either side of the average plane.

The results are illustrated by a plot agreement factor R versus folding of the ring in Figure 29. For the *trans* isomer (65) a folding of -20 ± 5 deg. was found, for the *cis* (64) $+20 \pm 5$ deg.;

this corresponds in either case to a puckering of the cyclobutane ring of about 40 deg. Previous determinations (146) of the topology of the cyclobutane ring are quite comparable with these findings.

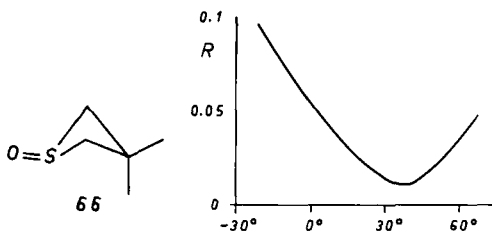


Fig. 30. Plot of the agreement factor R for different angles of puckering of the ring system 66.

b. The system *3,3-dimethylthietane-1-oxide* (66)-Eu(dpm)₃ (Figure 30) has been described in detail by Uebel, Wing, and Andersen (39, 45). The structure of the 1:1 complex was determined by X-ray diffraction, and calculations based on the McConnell-Robertson equation were carried out as well.

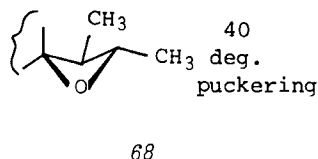
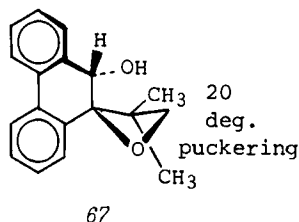
With their program PSEUDO the authors encountered difficulties in matching the experimental LIS data to the geometry derived from X-ray data. It was necessary to include three weighted rotamers about the O-S bond to fit the LIS properly (otherwise the assignment of the two methyl groups came out wrong). Since the assumption of three rotamers introduces two additional variables, this approach appears rather unsatisfactory.

A check of the data (39) with the program PDIGM (44) revealed that the LIS values can be simulated very well assuming only one particular geometry for the entire complex. Figure 30 shows the results (118).

The minimum agreement factor (for ring puckering of 35 deg.) is 0.012, whereas for the reversed (wrong) assignment of the methyl resonances it is 0.043. The calculated LIS values for the two identical C-2 axial and C-2 equatorial protons, respectively, were averaged in the computational procedure to avoid forcing the Eu(III) into the symmetry plane of the molecule (Sect. II-C-2).

The calculation yields an O...Eu distance of 2.5 Å (2.40 Å obtained by X-ray determination) and a puckering of 30-40 deg., which is in excellent agreement with 35 deg. determined by X-ray analysis of the solid complex.

c. The conformations of sterically hindered *oxetane ring systems* were investigated by Farid et al. (57).



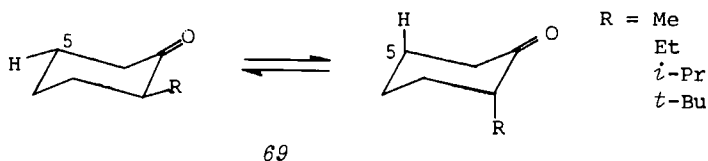
Interestingly enough, in *67* and *68* not the hydroxyl group but the sterically less hindered ether oxygen is the center of coordination for $\text{Eu}(\text{dpm})_3$ (in CCl_4). An angle of 17 deg. between the planes of the two benzene rings was assumed, thus allowing an unstrained structure for the six-carbon ring. Only the puckering of the oxetane ring was varied, and the best fit for differently puckered conformers was calculated allowing the $\text{Eu}(\text{III})$ to assume the optimal position for all proposed conformations.

A puckering of 20 deg. for the geminal 3,3-dimethyl compound (*67*) and 40 deg. for the 2,3-dimethyl compound (*68*) was found. In *68* both methyl groups assume equatorial positions to minimize steric hindrance.

d. The conformational analysis of 2-alkylcyclohexanones (*69*) via the $\text{Eu}(\text{fod})_3$ complex, described by Servis and Bowler (148), is typical for evaluating conformational equilibria by comparison with conformationally "rigid" model compounds.

In principle one could compare the chemical shifts of particular characteristic protons of the lanthanide complex in model compounds with corresponding shifts in the compound under consideration. An easier and more reliable way is to scale the induced shifts internally since chemical shifts of complexes are, in most cases, not reliable enough for basing results on absolute shift values.

In 2-alkylcyclohexanones the C-5 axial and C-5 equatorial protons are well suited to serve as probes for the determination of the equilibrium of interest.



The conformationally rigid model compound chosen is 4-*tert*-butylcyclohexanone, where the LIS values for the C-5 axial and C-5 equatorial protons can be observed in the absence of conformational averaging. As parameters independent of the complex binding constants of all molecules involved, the values

$$\left(\frac{\Delta_{eq}}{\Delta_{ax} + \Delta_{eq}} \right)_{4tBu} = \Delta_e^0 \quad \text{or} \quad \left(\frac{\Delta_{ax}}{\Delta_{ax} + \Delta_{eq}} \right)_{4tBu} = \Delta_a^0$$

are taken to be characteristic for the "pure" axial or equatorial position of the protons at C-5. A necessary assumption is that the lanthanide ion position in the model compound and the compounds under investigation is the same.

The experimental values for 4-*tert*-butylcyclohexanone are $\Delta_e^0 = 0.393$ and $\Delta_a^0 = 0.607$.

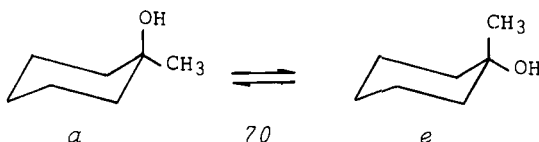
If a similar system is conformationally mobile the value

$\frac{\Delta_{eq}}{(\Delta_{ax} + \Delta_{eq})} = \Delta_e$ for the equatorial positioned proton is an average of Δ_e^0 and Δ_a^0 according to the molar fractions, n_e and n_a present in the equilibrium: $\Delta_e = n_e \Delta_e^0 + (1-n_e) \Delta_a^0$ or $\Delta_a = (1-n_a) \Delta_e^0 + n_a \Delta_a^0$. For 2-methylcyclohexanone for instance a value of 0.415 was obtained for Δ_e ; therefore, $0.415 = 0.393 n_e + 0.607 (1-n_e)$ whence $n_e = 0.897$. This means 89.7% of the protons observed are in an equatorial position, and, therefore, the conformation with the C-2 methyl equatorial (equilibrium 69) is preferred to the same extent, corresponding to a ΔG^0 of -1.33 kcal/mol; this value is, of course, directly valid only for the complexed 2-methylcyclohexanone.

The values found by the LIS method for the equilibria 69 are listed in Table 9 together with the values for similar systems previously determined by other methods.


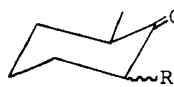
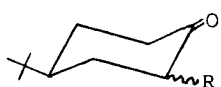
The conformational free-energy differences agree very well. This indicates that the equilibria are not perturbed by interaction with the shift reagent to any appreciable extent.

e. In the case of 1-methylcyclohexanol (70) things are different from example (d) because the coordination site is involved in the conformational changes directly (150).



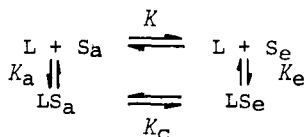
The complete equilibrium pattern, including the complexed and

Table 9. Conformational Free-Energy Differences for 2-Alkylcyclohexanone - Eu(fod)₃ Complexes, Using the LIS Technique, Compared to the Results for 2,6-Dialkylcyclohexanones and 2-Alkyl-4-*t*-butylcyclohexanones, Determined by Base Interconversion of the Equilibria

R	 LIS Method $\Delta G_{31.9}^0$ ^a (148)	  Base Interconversion ΔG_{25}^0 (149a) ΔG_{25}^0 (149b)	
Me	-1.33	-1.82	-1.51
Et	-1.05	-1.21	-1.06
<i>i</i> -Pr	-0.71	-0.56	-0.57
<i>t</i> -Bu	-1.57	-1.52	-1.61

^aThe ΔG^0 values obtained by the LIS method are primarily valid for the equilibrium of the complex LSR-substrate; ΔG^0 in kcal/mol; equilibrium type 69.

uncomplexed species, actually consists of four equilibria with four equilibrium constants (150, 151).



K and K_C are the equilibrium constants for the uncomplexed and complexed substrate molecules, K_a and K_e are the complex binding constants for the substrate with OH axial and OH equatorial, respectively.

The following relationships are obvious from the equilibration scheme (70, Eu(dpm)₃): $K = \frac{n_e}{n_a}$ and $K \cdot K_e = K_a \cdot K_C$. The equilibrium constant for the free substrate (K) is determined by the ratio of the molar fractions of both conformers; the second relationship takes advantage of the cyclic character of the scheme.

In order to solve this conformational problem, Bouquant et al. (150) determined the complex binding constants K_a and K_e (for pure 70a and 70e) with suitable reference compounds, namely, the corresponding 4-*t*-butyl-1-methylcyclohexanols assuming the

conformational equation for averaged properties ($P = n_e P_e + n_a P_a$). The 4-*t*-butyl group is supposed to have no influence on the constants, which seems reasonable because this holding group is far from the coordination center.

The complex binding constant of the conformationally mobile system 70 (K_m) is then an average of K_a and K_e , determined by the molar fractions of 70a and 70e present in solution: $K_m = n_a K_a + (1-n_a) K_e$.

The experimental complexation constants are (in mol^{-1} , at 313°K , $\text{Eu}(\text{dpm})_3$, CHCl_3): $K_m = 95$, $K_e = 124$, $K_a = 70$. Therefore, $95 = 70 n_a + 124 (1-n_a)$ and $n_a = 0.538$, $n_e = (1-n_a) = 0.462$. Now K can be calculated: $K = 0.462/0.538 = 0.86$, which corresponds to a ΔG_{313}^0 of 0.1 kcal/mol.

This compares very well with the results obtained by other methods: 0.2 kcal/mol in aqueous acetic acid (152a) at 298°K and 0.24 kcal/mol in aqueous dioxane (152b).

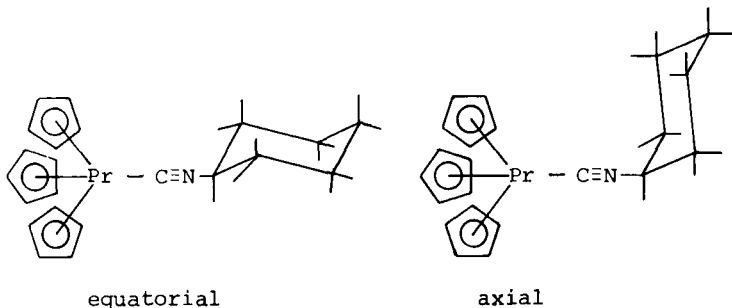
The equilibrium constant for the complexed forms a and e may also be calculated: $K_C = K \frac{K_e}{K_a} = 0.86 \frac{124}{70} = 1.52$ ($\Delta G_{313}^0 = -0.3$ kcal/mol). This means that the equatorial conformation of the hydroxyl group is favored in the complex.

The use of complex binding constants to assess conformational equilibria requires comment.

The constants were determined using the method described in (153); this method is a variation of the ones discussed in Sect. III-C assuming a 1:1 complex and deriving absolute values for K by use of a plot Δ versus $(\Delta/S_0)^{1/2}$ with the experimental condition $S_0 = L_0$.

Since a simple 1:1 complex was assumed, the absolute values for the complex binding constants are not likely to be correct, but fortunately only ratios of the constants enter in the relationships used; and *relative* binding constants, all determined in the same manner, are once again meaningful.

f. The conformational analysis (154) of *tris(cyclopentadienyl)-(cyclohexylisonitrile)-praseodymium(III)* (71) is a very special case because there is a direct covalent bond between the lanthanide(III) and the isonitrile group.

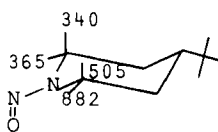


The equilibrium can be determined directly, since the seven proton resonance signals in the widely spread nmr spectrum (resulting from rapid inversion of the ring) at room temperature separate into thirteen signals at -70°C . The lines can be assigned by using the McConnell-Robertson equation, and the ratio of axial to equatorial form can be determined by simply integrating the peaks. The corresponding ΔG° is -0.282 ± 15 kcal/mol at -75°C .

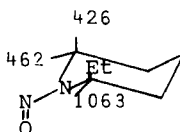
It is interesting to compare this value with those obtained for similarly substituted cyclohexanes. Some values for $\text{C}_6\text{H}_{11}\text{X}$ systems similar to 71 are (155) $\text{X} = -\text{N}\equiv\text{C}$, -0.210 ± 13 at -80°C ; $\text{X} = -\text{C}\equiv\text{N}$, -0.240 ± 13 at -79°C ; $\text{X} = -\text{F}$, -0.276 ± 15 at -86°C ; $\text{X} = -\text{N}=\text{C}=\text{S}$, -0.284 ± 13 at -79°C ; $\text{X} = -\text{C}\equiv\text{CH}$, -0.410 ± 50 at -80°C (kcal/mol).

Interestingly enough, the "bulky" substituent $\text{X} = -\text{N}\equiv\text{C}-\text{Pr}(\text{C}_5\text{H}_5)_3$ acts like a similar substituent of much smaller size. The conclusion to be drawn is that only the $-\text{N}\equiv\text{C}-$ part of the substituent is decisive since the $-\text{Pr}(\text{C}_5\text{H}_5)_3$ part is already too far from the cyclohexane ring to interact sterically; despite the covalent binding, the conformational influence of the lanthanide ligand is negligible.

g. Equilibrium constants for *N*-nitrosopiperidines have been determined (88) using a similar technique as described in example (d). An internal reference shift is used for obtaining induced shift ratios which are independent of the complex binding constant. The 4-*t*-butyl-substituted compound 72 is assumed to represent the conformationally rigid standard compound. From the nine compounds investigated in (88) we pick two to illustrate the calculation.



72



73

Δ values in Hz, $\text{Eu}(\text{fod})_3$, for 1:1 complex extrapolated

The probe proton is taken to be $\text{H}_{2\text{eq}}$, the internal standard ($\text{H}_{6\text{eq}} + \text{H}_{6\text{ax}}$); the following relationship holds: (the index $^{\circ}$ refers to the standard 72)

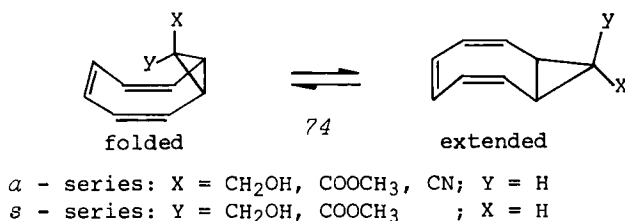
$$\frac{\Delta_{2\text{e}}(\text{obs})}{\Delta_{6\text{e}}(\text{obs}) + \Delta_{6\text{a}}(\text{obs})} = n_{\text{e}} \frac{\Delta_{2\text{e}}^{\circ}}{\Delta_{6\text{e}}^{\circ} + \Delta_{6\text{a}}^{\circ}} + (1-n_{\text{e}}) \frac{\Delta_{2\text{a}}^{\circ}}{\Delta_{6\text{e}}^{\circ} + \Delta_{6\text{a}}^{\circ}}$$

$$\frac{1063}{462 + 426} = n_e \frac{882}{365 + 340} + (1-n_e) \frac{505}{365 + 340}$$

From these equations $n_e = 0.90$, corresponding to a strong preponderance of the conformer with axial ethyl (compound 73).

For the 2-methyl compound (with the nitroso group syn to the methyl group) the result is $n_e = 0.85$, again indicating strong preference for the axial orientation of the methyl group in the complex. This agrees well with the results of other authors for the free substrate (156), based on analysis of chemical shifts and coupling constants.

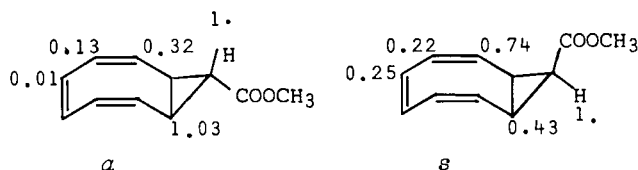
h. Bicyclo[6.1.0]nona-2,4,6-triene derivatives were investigated by Cheer, Rosen, and Uebel (52). In these compounds two conformers are possible: the folded and extended conformations are in equilibrium 74 (in 74 all compounds studied are shown).



Using the LIS method (Eu(dpm)₃ and/or Eu(fod)₃ in CDCl₃, McConnell-Robertson equation, R factor) the authors proved the extended conformation to be the preferred one in all cases. For all five compounds studied the folded form gave a poor fit (high R factors), with the extended conformations allowing significantly superior fits (low R factors). The ratios R factor (folded): R factor (extended) are between 3.8 and 4.9 for the α series and about 14.0 for the s series; this constitutes convincing evidence in favor of the extended conformers in 74. Applying the most rigorous condition for significance testing (see Sect. II-C-3) we have 5-4=1 degree of freedom; the corresponding significance levels for the extended forms are, therefore, about 80% for the α series and about 95% for the s series.

For the *anti*-*p*-bromophenylester (α series; X = COOC₆H₄-*p*-Br; Y = H) the extended conformation was determined to be the one favored in the solid state, too (Ref. 13 in 52).

Two typical examples (one from each series) are shown below; the induced shifts are given relative to the proton geminal to the methyl ester group.



$$R(\text{folded}) = 0.363$$

$$R(\text{extended}) = 0.096$$

$$R \text{ factor ratio} = 3.8$$

80% significance in favor of the extended form

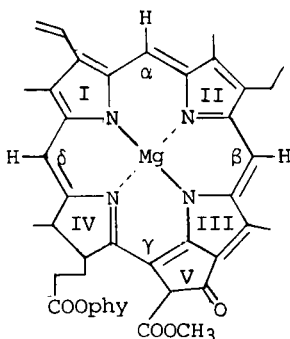
$$R(\text{folded}) = 0.909$$

$$R(\text{extended}) = 0.069$$

$$R \text{ factor ratio} = 14.3$$

95% significance in favor of the extended form

i. An interesting case is the problem of the relative conformation of the two macrocycles in the *chlorophyll a* dimer.



75

chlorophyll a

rings numbered from I to V; meso positioned C are indexed α to δ

Methyl pheophorbide a (76) has two hydrogens instead of Mg and methyl in place of phytyl (phy); methyl bacteriopheophorbide a (77) has, in addition, a saturated ring II.

Trifunac and Katz (48) tested the LIS approach to this type of macrocycle on *methyl pheophorbide a* and *methyl bacteriopheophorbide a*; the geometry of the first one is known from X-ray studies, and a LIS computer fit [Eu(fod)₃, C₆D₆, program LIShift] proved to be in agreement with the X-ray diffraction data (157) of 76 giving an excellent fit of $R = 0.087$.

The fit for 77 is less good ($R = 0.20$) since the geometry derived from the crystal data of 76 was used for 77, despite the expectation that the geometry of the latter must differ slightly because of saturation of ring II. Nevertheless the results indicate that 76 and 77 are of similar structure.

Now let us turn to the chlorophyll a dimer problem.

Chlorophyll a (75) has the tendency to form dimers in solvents like benzene or carbon tetrachloride and oligomers in aliphatic hydrocarbon solvents. This is caused by the donor and acceptor groups present in the molecule: the ring V keto C=O group is the donor, and the central Mg atom can function as acceptor.

Trifunac and Katz (48) demonstrated the dimer to be present in C_6D_6 and CCl_4 by the unusual pattern of the plot Δ versus L_0/S_0 (the spectra are not well resolved and, therefore, do not permit more quantitative study); Figure 31 shows a typical, somewhat idealized, plot.

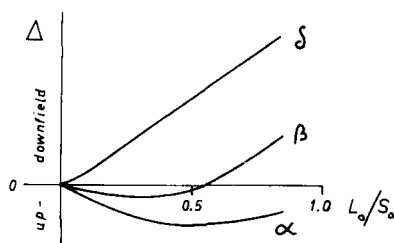


Fig. 31. Observed LIS curves (plot Δ vs. L_0/S_0) for the system chlorophyll a (75), $Eu(fod)_3$ in CCl_4 ; the LIS of the methine protons α , β , and δ are shown.

The methine α and β protons show a shift to higher field up to a L_0/S_0 ratio of about 0.5 (for α) and about 0.3 (for β); at higher concentrations the induced shifts switch to the expected sign again [$Eu(fod)_3$ was used].

At low reagent concentrations there is only one coordination site free in the dimer; at higher LSR concentration the chlorophyll a dimer units are broken apart, thus the slope changes at about $L_0/S_0 \approx 0.5$.

Two opposing shift effects might be responsible for this unusual behavior: (i) the π - π interactions that are dependent on the degree of macrocycle overlap and (ii) the usual lanthanide induced shifts.

A rationalization of the observed effects is that a number of different dimer conformations are present in solution and a more overlapping conformer of the chlorophyll a dimer becomes more favored as the $Eu(fod)_3$ concentration is increased; at higher concentrations ($L_0/S_0 > 0.5$) effect (i) gradually disappears as the dimeric units are successively broken up.

ACKNOWLEDGMENTS

I thank Doz. H. Falk for many helpful discussions and critical reading of the manuscript, and Prof. K. Schlögl for his

stimulating interest in this work.

We thank Prof. R. E. Davis for supplying us with a PDIGM program deck.

Our own research that contributed to this chapter was supported by the Hochschuljubiläumsstiftung der Stadt Wien.

REFERENCES

1. C. C. Hinckley, *J. Amer. Chem. Soc.*, 91, 5160 (1969).
2. J. Briggs, G. H. Frost, F. A. Hart, G. P. Moss, and M. L. Staniforth, *Chem. Commun.*, 1970, 749.
3. D. R. Crump, J. K. M. Sanders, and D. H. Williams, *Tetrahedron Lett.*, 1970, 4419.
4. J. K. M. Sanders and D. H. Williams, *Chem. Commun.*, 1970, 422.
5. R. E. Rondeau and R. E. Sievers, *J. Amer. Chem. Soc.*, 93, 1525, (1971).
6. (a) T. H. Siddall III, *Chem. Commun.*, 1971, 452; (b) B. L. Shapiro, J. R. Hlubucek, G. R. Sullivan, and L. F. Johnson, *J. Amer. Chem. Soc.*, 93, 3281 (1971).
7. G. C. Levy and R. A. Komorski, *J. Amer. Chem. Soc.*, 93, 678, (1971).
8. J. D. Roberts, G. E. Hawkes, J. Husar, A. W. Roberts, and D. W. Roberts, *Tetrahedron*, 30, 1833 (1974).
9. R. v. Ammon and R. D. Fischer, *Angew. Chem.*, 84, 737 (1972); *Angew. Chem., Int. Edit. (Engl.)*, 11, 675 (1972).
10. A. F. Cockerill, G. L. O. Davies, R. C. Harden, and D. M. Rackham, *Chem. Rev.*, 73, 553 (1973).
11. B. Bleaney, C. M. Dobson, B. A. Levine, R. B. Martin, R. J. P. Williams, and A. V. Xavier, *Chem. Commun.*, 1972, 791.
12. J. J. Uebel, C. Pacheco, and R. M. Wing, *Tetrahedron Lett.*, 1973, 4383.
13. W. DeW. Horrocks, Jr., *Inorg Chem.*, 9, 690 (1970).
14. W. DeW. Horrocks, Jr. and J. P. Sipe III, *J. Amer. Chem. Soc.*, 93, 6800 (1971).
15. R. E. Cramer, R. Dubois, and K. Seff, *J. Amer. Chem. Soc.*, 96, 4125 (1974).
16. J. B. Jesson, *J. Chem. Phys.*, 47, 579, 582 (1967).
17. W. DeW. Horrocks, Jr. and E. S. Greenberg, *Inorg. Chem.*, 10, 2190 (1971).
18. H. M. McConnell and R. E. Robertson, *J. Chem. Phys.*, 29, 1361 (1958).
19. W. DeW. Horrocks, Jr. and J. P. Sipe III, *Science*, 177, 994 (1972).
20. I. Morishima, K. Okada, T. Yonezawa, and K. Goto, *J. Amer. Chem. Soc.*, 93, 3922 (1971) and references therein.
21. S. J. Angyal, *Tetrahedron*, 30, 1695 (1974).

22. R. E. Davis and M. R. Willcott III, in *Nuclear Magnetic Resonance Shift Reagents*, R. A. Sievers, Ed., Academic, New York, p. 143, 1973.
23. B. F. G. Johnson, J. Lewis, P. McArdle, and J. R. Norton, *Chem. Commun.*, 1972, 535.
24. (a) K. Tori, Y. Yoshimura, M. Kainosho, and K. Ajisaka, *Tetrahedron Lett.*, 1973, 3127; (b) M. Hirayama, E. Edagawa, and Y. Hanyu, *Chem. Commun.*, 1972, 1343.
25. A. A. Chalmers and K. G. R. Pachler, *Tetrahedron Lett.*, 1972, 4033 (1972).
26. K. L. Williamson, D. R. Clutter, R. Emch, M. Alexander, A. E. Burroughs, C. Chua, and M. E. Bogel, *J. Amer. Chem. Soc.*, 96, 1471 (1974).
27. K. Tori, Y. Yoshimura, M. Kainosho, and K. Ajisaka, *Tetrahedron Lett.*, 1973, 1573.
28. J. W. ApSimon, H. Beierbeck and J. K. Saunders, *Can. J. Chem.*, 51, 3874 (1973).
29. M. Kainosho, K. Ajisaka, and K. Tori, *Chem. Lett.*, 1972, 1061.
30. G. M. Brooke and R. S. Matthews, *Tetrahedron Lett.*, 1973, 3469.
31. J. K. M. Sanders, S. W. Hanson, and D. H. Williams, *J. Amer. Chem. Soc.*, 94, 5325 (1972).
32. J. K. M. Sanders and D. H. Williams, *Tetrahedron Lett.*, 1971, 2813.
33. M. Witanowski, L. Stefaniak, H. Januszewski, and Z. W. Wolkowski, *Tetrahedron Lett.*, 1971, 1653.
34. O. A. Gansow, P. A. Loeffler, R. E. Davis, M. R. Willcott III, and R. E. Lenkinski, *J. Amer. Chem. Soc.*, 95, 3390 (1973).
35. O. A. Gansow, P. A. Loeffler, M. R. Willcott III, and R. E. Lenkinski, *J. Amer. Chem. Soc.*, 95, 3389 (1973).
36. G. N. La Mar, W. DeW. Horrocks, Jr., and L. C. Allen, *J. Chem. Phys.*, 41, 2126 (1964).
37. R. E. Cramer and K. Seff, J. C. S., *Chem. Commun.*, 1972, 400; *Acta Crystallogr.*, B, 28, 3281 (1972).
38. W. DeW. Horrocks, Jr., J. P. Sipe III, and J. R. Luber, *J. Amer. Chem. Soc.*, 93, 5258 (1971).
39. J. J. Uebel and R. M. Wing, *J. Amer. Chem. Soc.*, 94, 8910 (1972).
40. S. J. S. Wasson, D. E. Sands, and W. F. Wagner, *Inorg. Chem.*, 12, 187 (1973).
41. D. S. Dyer, J. A. Cunningham, J. J. Brooks, R. E. Sievers, and R. E. Rondeau, in *Nuclear Magnetic Resonance Shift Reagents*, R. A. Sievers, Ed., Academic, New York p. 21, 1973.
42. J. M. Briggs, G. P. Moss, E. W. Randall, and K. D. Sales, *Chem. Commun.*, 1972, 1180.
43. W. DeW. Horrocks, Jr., *J. Amer. Chem. Soc.*, 96, 3022 (1974).

44. M. R. Willcott III, R. E. Lenkinski, and R. E. Davis, *J. Amer. Chem. Soc.*, 94, 1742 (1972).
45. R. M. Wing, J. J. Uebel, and K. K. Andersen, *J. Amer. Chem. Soc.*, 95, 6046 (1973).
46. (a) J. W. ApSimon and H. Beierbeck, *Tetrahedron Lett.*, 1973, 581; (b) J. W. ApSimon, H. Beierbeck, and J. K. Saunders, *Can. J. Chem.*, 51, 3874 (1973).
47. H. Huber and C. Pascual, *Helv. Chim. Acta*, 54, 913 (1971).
48. A. D. Trifunac and J. J. Katz, *J. Amer. Chem. Soc.*, 96, 5233 (1974).
49. N. S. Angerman, S. S. Danyluk, and T. A. Victor, *J. Amer. Chem. Soc.*, 94, 7137 (1972).
- 49a. J. D. Dunitz, H. Eser, M. Bixon, and S. Lifson, *Helv. Chim. Acta*, 50, 1572 (1967).
50. D. K. Lavalley and A. H. Zeltmann, *J. Amer. Chem. Soc.*, 96, 5552 (1974).
51. H. L. Ammon, P. H. Mazzocchi, W. J. Kopecky, Jr., H. J. Tamburin, and P. H. Watts, Jr., *J. Amer. Chem. Soc.*, 95, 1968 (1973).
52. C. J. Cheer, W. Rosen, and J. J. Uebel, *Tetrahedron Lett.*, 1974, 4045.
53. G. Montaudo, V. Librando, S. Caccamese, and P. Maravigna, *J. Amer. Chem. Soc.*, 95, 6365 (1973).
54. G. Montaudo, S. Caccamese, V. Librando, and P. Maravigna, *Tetrahedron*, 29, 3915 (1973).
55. J. Briggs, F. A. Hart, and G. P. Moss, *Chem. Commun.*, 1970, 1506.
56. I. M. Armitage, L. D. Hall, A. G. Marshall, and L. G. Werbelow, *J. Amer. Chem. Soc.*, 95, 1437 (1973).
57. S. Farid, A. Ateya, and M. Maggio, *Chem. Commun.*, 1971, 1285.
58. P. V. Demarco, B. J. Cerimele, R. W. Crane, and A. L. Thakkar, *Tetrahedron Lett.*, 1972, 3539.
59. T. Heigl and G. K. Mucklow, *Tetrahedron Lett.*, 1973, 649.
60. A. Recca and P. Finocchiaro, *Tetrahedron Lett.*, 1974, 4185.
61. R. E. Davis and M. R. Willcott III, *J. Amer. Chem. Soc.*, 94, 1744 (1972).
62. W. C. Hamilton, *Acta Crystallogr.*, 18, 502 (1965); *Statistics in Physical Science*, Ronald, New York, pp. 157-162, 1964.
63. C. L. Honeybourne, *Tetrahedron Lett.*, 1972, 1095.
64. H. Huber, *Tetrahedron Lett.*, 1972, 3559.
65. G. E. Hawkes, D. Leibfritz, D. W. Roberts, and J. D. Roberts, *J. Amer. Chem. Soc.*, 95, 1659 (1973).
66. P. V. Demarco, T. K. Elzey, R. B. Lewis, and E. Wenkert, *J. Amer. Chem. Soc.*, 92, 5734, 5737 (1970).
67. A. F. Cockerill and D. M. Rackham, *Tetrahedron Lett.*, 1970, 5149, 5153.
68. (a) Z. W. Wolkowski, *Tetrahedron Lett.*, 1971, 821, 825;

- (b) C. Beauté, Z. W. Wolkowski, and N. Thoai, *Tetrahedron Lett.*, 1971, 817.
69. M. R. Willcott and J. F. M. Oth, *Tetrahedron Lett.*, 1971, 1579.
70. W. Walter, R. F. Becker, and J. Thiem, *Tetrahedron Lett.*, 1971, 1971.
71. K. G. Morallee, E. Nieboer, F. J. C. Rossetti, R. J. P. Williams, A. V. Xavier, and R. A. Dwek, *Chem. Commun.*, 1970, 1132.
72. C. R. Jones and D. R. Kearns, *J. Amer. Chem. Soc.*, 96, 3651 (1974).
73. C. S. Erasmus and J. C. A. Boeyens, *Acta Crystallogr.*, B, 26, 1943 (1970).
74. M. K. Archer, D. S. Fell, and R. W. Jotham, *Inorg. Nucl. Chem. Lett.*, 7, 1135 (1971).
75. J. W. Faller and G. N. LaMar, *Tetrahedron Lett.*, 1973, 1381.
76. C. D. Barry, C. M. Dobson, D. A. Sweigart, L. E. Ford, and R. J. P. Williams, in *Nuclear Magnetic Resonance Shift Reagents*, R. A. Sievers, Ed., Academic, New York, p. 173, 1973.
77. B. Feibush, M. F. Richardson, R. E. Sievers, and C. S. Springer, Jr., *J. Amer. Chem. Soc.*, 94, 6717 (1972).
78. B. L. Shapiro, M. D. Johnston, Jr., A. D. Godwin, T. W. Proulx, and M. J. Shapiro, *Tetrahedron Lett.*, 1972, 3233.
79. B. L. Shapiro, M. D. Johnston, Jr., and M. J. Shapiro, *J. Org. Chem.*, 39, 796 (1974).
80. (a) J. K. M. Sanders and D. H. Williams, *J. Amer. Chem. Soc.*, 93, 641 (1971); (b) M. F. Richardson and R. E. Sievers, *Inorg. Chem.*, 10, 498 (1971).
81. (a) H. L. Goering, J. N. Eikenberry, G. S. Koerner, and C. J. Lattimer, *J. Amer. Chem. Soc.*, 96, 1493 (1974); (b) M. D. McCreary, D. W. Lewis, D. L. Wernick, and G. M. Whitesides, *J. Amer. Chem. Soc.*, 96, 1038 (1974); (c) V. Schurig, *Tetrahedron Lett.*, 1972, 3297.
82. (a) H. Falk, W. Fröstl, and K. Schlögl, *Monatsh. Chem.*, 105, 574 (1974); (b) D. J. Pasto and J. K. Borchardt, *Tetrahedron Lett.*, 1973, 2517.
83. L. Ernst and A. Mannschreck, *Tetrahedron Lett.*, 1971, 3023.
84. T. C. Morrill, R. J. Opitz, and R. Mozzer, *Tetrahedron Lett.*, 1973, 3715.
85. (a) K. K. Andersen and J. J. Uebel, *Tetrahedron Lett.*, 1970, 5253; (b) R. R. Fraser and Y. Y. Wigfield, *Chem. Commun.*, 1970, 1471.
86. G. Wood, G. W. Buchanan, and M. H. Miskow, *Can. J. Chem.*, 50, 521 (1972).
87. A. Tangerman and B. Zwanenburg, *Tetrahedron Lett.*, 1973, 79.

88. T. P. Forrest, D. L. Hooper, and S. Ray, *J. Amer. Chem. Soc.*, 96, 4286 (1974).
89. R. E. Rondeau, M. A. Berwick, R. N. Steppel, and M. P. Servé, *J. Amer. Chem. Soc.*, 94, 1096 (1972).
90. K.-T. Liu, M.-F. Hsu, and J.-S. Chen, *Tetrahedron Lett.*, 1974, 2179.
91. R. E. Graves and P. I. Rose, *Chem. Commun.* 1973, 630.
92. G. P. Schiemenz, *Tetrahedron*, 29, 741 (1973).
93. H. Hart and G. M. Love, *Tetrahedron Lett.*, 1971, 625.
94. H. Falk, S. Gergely, and O. Hofer, *Monatsh. Chem.*, 105, 1004 (1974).
95. G. E. Wright and T. Y. Tang Wei, *Tetrahedron*, 29, 3775 (1973).
96. R. Schüttler and R. W. Hoffmann, *Tetrahedron Lett.*, 1973, 5109.
97. I. Armitage, G. Dunsmore, L. D. Hall, and A. G. Marshall, *Chem. Commun.*, 1971, 1281.
98. D. E. Williams, *Tetrahedron Lett.*, 1972, 1345.
99. D. F. Evans and M. Wyatt, *Chem. Commun.*, 1972, 312.
100. I. Armitage, G. Dunsmore, L. D. Hall, and A. G. Marshall, *Can. J. Chem.*, 50, 1972, 2119.
101. B. L. Shapiro and M. D. Johnston, Jr., *J. Amer. Chem. Soc.*, 94, 8185 (1975).
- 101a. J. J. Cawley and D. V. Petrocine, *Org. Magn. Resonance*, 6, 544 (1974).
102. D. F. Evans and M. Wyatt, *Chem. Commun.*, 1973, 339.
103. A. M. Grotens, J. J. M. Backus, F. W. Pijpers, and E. de Boer, *Tetrahedron Lett.*, 1973, 1467.
104. K. Roth, M. Grosse, and D. Rewicki, *Tetrahedron Lett.*, 1972, 435.
105. V. G. Gibb, I. M. Armitage, L. D. Hall, and A. G. Marshall, *J. Amer. Chem. Soc.*, 94, 8919 (1972).
106. G. M. Whitesides and D. W. Lewis, *J. Amer. Chem. Soc.*, 92, 6979 (1970).
107. R. R. Fraser, M. A. Petit, and J. K. Saunders, *Chem. Commun.*, 1971, 1450.
108. G. R. Sullivan, D. Ciavarella, and H. S. Mosher, *J. Org. Chem.*, 39, 2411, and references therein.
109. (a) G. V. Smith, W. A. Boyd, and C. C. Hinckley, *J. Amer. Chem. Soc.*, 93, 6319 (1971); (b) C. C. Hinckley, W. A. Boyd, and G. V. Smith, *Tetrahedron Lett.*, 1972, 879.
110. A. R. Katritzky and A. Smith, *Tetrahedron Lett.*, 1971, 1765.
111. B. Birdsall and J. Feeney, *Chem. Commun.*, 1971, 1473.
112. J. W. ApSimon, H. Beierbeck, and A. Fruchier, *Can. J. Chem.*, 50, 2905 (1972).
113. L. R. Isbrandt and M. T. Rogers, *Chem. Commun.*, 1971, 1378.
114. (a) J. S. Ghotra, F. A. Hart, G. P. Moss, and M. L.

- Staniforth, *Chem. Commun.*, 1973, 113; (b) N. H. Andersen, B. J. Bottino, and S. E. Smith, *Chem Commun.*, 1972, 1193.
115. I. Armitage, J. R. Campbell, and L. D. Hall, *Can. J. Chem.*, 50, 2139 (1972).
116. D. V. C. Awang, A. Vincent, W. L. Wilson, and H. W. Avdovich, *Can. J. Chem.*, 50, 104 (1972).
117. T. Okutani, A. Morimoto, T. Kaneko, and K. Masuda, *Tetrahedron Lett.*, 1971, 1115.
118. H. Falk, S. Gergely, K. Grubmayr, O. Hofer, and F. Neufingerl, unpublished results.
119. T. B. Patrick and P. H. Patrick, *J. Amer. Chem. Soc.*, 94, 6230 (1972).
120. B. L. Shapiro, M. D. Johnston, Jr., and R. L. R. Towns, *J. Amer. Chem. Soc.*, 94, 4381 (1972).
121. J. A. Peters, J. D. Remijnse, A. v. d. Wiele, and H. v. Bekkum, *Tetrahedron Lett.*, 1971, 3065.
122. A. Tangerman and B. Zwanenburg, *Tetrahedron Lett.*, 1973, 5194.
123. K. C. Yee and W. G. Bentrude, *Tetrahedron Lett.*, 1971, 2775.
124. (a) R. A. Y. Jones, A. R. Katritzky, A. C. Richards, R. J. Wyatt, R. J. Bishop, and L. E. Sutton, *J. Chem. Soc., B*, 1970, 122; (b) E. L. Eliel and F. W. Vierhapper, *J. Amer. Chem. Soc.*, 96, 2257 (1974); (c) P. J. Growley, M. J. T. Robinson, and M. G. Ward, *Chem. Commun.*, 1974, 825.
125. T. Yonezawa, I. Morishima, and Y. Ohmori, *J. Amer. Chem. Soc.*, 92, 1267 (1970).
126. I. D. Blackburne, A. R. Katritzky, and Y. Takeuchi, *J. Amer. Chem. Soc.*, 96, 682 (1974).
127. G. Montaudo, P. Maravigna, S. Caccamese, and V. Librando, *J. Org. Chem.*, 39, 2806 (1974).
128. S. R. Tanny, M. Pickering, and C. S. Springer, Jr., *J. Amer. Chem. Soc.*, 95, 6227 (1973).
129. C. Beauté, Z. W. Wolkowski, J. P. Merda, and D. Leländais, *Tetrahedron Lett.*, 1971, 2473.
130. C. Beauté, Z. W. Wolkowski, and N. Thoai, *Chem. Commun.*, 1971, 700.
131. O. Ceder and B. Beijer, *Acta Chem. Scand.*, 26, 2977 (1972).
132. D. D. Faulk and A. Fry, *J. Org. Chem.*, 35, 364 (1970) and references therein.
133. R. B. Lewis and E. Wenkert, in *Nuclear Magnetic Resonance Shift Reagents*, R. A. Siever, Ed., Academic, New York, p. 99, 1973.
134. (a) J. M. Angelelli, A. R. Katritzky, R. F. Pinzelli, and R. D. Topsom, *Tetrahedron*, 28, 2037 (1972); (b) C. L. Cheng, I. G. John, G. L. D. Ritchie, and P. H. Gore, *J. Chem. Soc., Perkin II*, 1974, 1318; (c) K.-M. Marstokk and H. Mollendal, *J. Mol. Struct.*, 23, 93 (1974).
135. M. R. Willcott III, and R. E. Davis, in *Nuclear Magnetic Resonance Shift Reagents*, R. A. Siever, Ed., Academic,

- New York, p. 159, 1973; (a) P. J. D. Park, R. A. Pethrick, and B. H. Thomas, in *Internal Rotation in Molecules*, W. J. Orville-Thomas, Ed., Wiley-Interscience, p. 94, 1974; (b) G. Allen and S. Fewster, *Internal Rotation in Molecules*, W. J. Orville-Thomas, Ed., Wiley-Interscience, pp. 274-5, 1974; (c) N. L. Owen and R. E. Hester, *Spectrochim. Acta*, 25A, 343 (1969).
136. B. L. Shapiro, M. D. Johnston, Jr., and M. J. Shapiro, *Org. Magn. Resonance*, 5, 21 (1973).
137. B. L. Shapiro, M. D. Johnston, Jr., R. L. R. Towns, A. D. Godwin, H. L. Pearce, T. W. Proulx, and M. J. Shapiro, in *Nuclear Magnetic Resonance Shift Reagents*, R. A. Sievers, Ed., Academic, New York, p. 227, 1973.
138. P. Granger, M. M. Claudon, and J. F. Guinet, *Tetrahedron Lett.*, 1971, 4167.
139. H. Falk, K. Grubmayr, U. Herzig, and O. Hofer, *Tetrahedron Lett.*, 1975, 559.
140. H. Falk, O. Hofer, and H. Lehner, *Monatsh. Chem.*, 105, 366 (1974).
141. H. S. Preston and J. M. Stewart, *Chem. Commun.*, 1970, 1142.
142. K. Watenpaugh, J. Dow, L. H. Jensen, and S. Furberg, *Science*, 159, 206 (1968).
143. C. Nishino and T. Mitsui, *Tetrahedron Lett.*, 1973, 335.
144. E. C. Sen and R. A. Jones, *Tetrahedron*, 28, 2871 (1972).
145. D. Horton and J. K. Thomson, *Chem. Commun.*, 1971, 1389.
146. J. B. Lambert and J. D. Roberts, *J. Amer. Chem. Soc.*, 87, 3884 (1965).
147. R. A. Ford and N. L. Allinger, *J. Org. Chem.*, 35, 3178 (1970).
148. K. L. Servis and D. J. Bowler, *J. Amer. Chem. Soc.*, 95, 3392 (1973).
149. (a) B. Rickborn, *J. Amer. Chem. Soc.*, 84, 2414 (1962); (b) N. Allinger and H. Blatter, *J. Amer. Chem. Soc.*, 83, 994 (1961).
150. J. Bouquant, M. Wuilmet, A. Maujeau, and J. Chuche, *Chem. Commun.*, 1974, 778.
151. J. Paul, K. Schlögl, and W. Silhan, *Monatsh. Chem.*, 103, 243 (1972).
152. (a) J. J. Uebel and H. W. Goodwin, *J. Org. Chem.*, 33, 3317 (1968); (b) S. Winstein and N. J. Holness, *J. Amer. Chem. Soc.*, 77, 5562 (1955).
153. J. Bouquant and J. Chuche, *Tetrahedron Lett.*, 1972, 2337.
154. R. v. Ammon, R. D. Fischer, and B. Kanellakopulos, *Chem. Ber.*, 104, 1072 (1971).
155. F. R. Jensen, C. H. Bushweller, and B. H. Beck, *J. Amer. Chem. Soc.*, 91, 344 (1969).
156. (a) R. K. Harris and R. A. Spragg, *J. Mol. Spectrosc.*, 23, 158 (1967); (b) Y. L. Chow and C. J. Colon, *Can. J.*

- Chem.*, 46, 2827 (1968).
157. M. S. Fischer, D. H. Templeton, A. Zalkin, and M. Calvin, *J. Amer. Chem. Soc.*, 93, 2622 (1971).
158. H.-J. Schneider and E. F. Weigand, *Tetrahedron*, 31, 2125 (1975).

MULTISTEP CONFORMATIONAL INTERCONVERSION MECHANISMS

JOHANNES DALE

*Kjemisk Institutt
Universitetet i Oslo, Oslo, Norway*

I.	Introduction	200
II.	Terminology and Graphic Representation	203
III.	Open Chains	204
IV.	Monocyclic Compounds of Saturated Character	206
A.	18-Membered Rings	207
B.	16-Membered Rings	209
C.	15-Membered Rings	213
D.	14-Membered Rings	213
E.	13-Membered Rings	215
F.	12-Membered Rings	217
G.	11-Membered Rings	219
H.	10-Membered Rings	221
I.	9-Membered Rings	225
J.	8-Membered Rings	229
K.	7-Membered Rings	233
L.	6-Membered Rings	236
M.	5-Membered Rings	237
V.	Cyclic Acetylenes	238
VI.	Cyclic Compounds containing cis Double Bonds or Equivalent Units	239
A.	<i>cis</i> -Cyclooctene	240
B.	Cycloheptene	241
C.	Cyclohexene	242
D.	<i>cis,cis</i> -Cyclodeca-1,6-diene	243
E.	<i>cis,cis,cis</i> -Cyclododeca-1,5,9-triene	244
F.	<i>cis,cis</i> -Cycloocta-1,5-diene	246
G.	<i>cis,cis,cis,cis</i> -Cyclododeca-1,4,7,10-tetraene	248
H.	<i>cis,cis,cis</i> -Cyclonona-1,4,7-triene	248
VII.	Cyclic Compounds containing trans Double Bonds or Equivalent Units	250
A.	<i>trans,trans,trans</i> -Cyclododeca-1,5,9-triene	251
B.	<i>trans,trans,trans</i> -Cycloundeca-1,4,8-triene	252
C.	<i>trans,trans</i> -Cyclodeca-1,5-diene	252
D.	<i>trans</i> -Cyclodecene	253
VIII.	Cyclic Compounds Containing Both cis and trans	

Double Bonds	255
A. <i>cis,trans,cis,trans</i> -Cyclododeca-1,4,7,10-tetraene	255
IX. Bicyclic and Multicyclic Compounds	257
A. <i>trans</i> -Decalin	258
B. <i>cis</i> -Decalin	258
C. <i>cis,syn,cis</i> -Perhydroanthracene	259
D. <i>cis</i> - $\Delta^{2,6}$ -Hexalin	261
E. Tricyclo[4.4.4.0 ^{1,6}]tetradecane	261
F. Tricyclo[4.4.4.0 ^{1,6}]tetradeca-3,8,12-triene	262
G. Bicyclo[3.3.3]undecane	263
H. Spiro[5.5]undecane	264
I. Triarylboranes, Triarylmethanes, and Similar Compounds	265

I. INTRODUCTION

Only very simple molecules undergo conformational change by passing over a single well-defined barrier. The best known example is the inversion of ammonia or simple amines (1) to an identical or enantiomeric conformation, which must proceed by total flattening; the barrier top or transition state can be confidently defined as a planar molecule. Likewise, cyclobutane undergoes ring inversion through total flattening of the carbon skeleton (2). The rotation about the partial CN double bond of amides, like formamide, is an example of interconversion of rotational conformers involving a single barrier (3).

The simplest example of a multistep mechanism is the passage of a 1,2-disubstituted ethane (butane; 1,2-dichloroethane) from one *gauche* conformation to the enantiomeric *gauche* conformation (4). The *syn* barrier (0°), being much higher than the *anticlinal* barrier (120°) separating it from the *anti* conformation, the interconversion obviously proceeds most easily in two distinct steps via the intermediate *anti* conformation.* Both the initial, intermediate, and final conformations are here well defined, and the mechanism by which each barrier is passed is essentially a simple rotation about the central bond.

In cyclic compounds of normal ring size the constraints of the ring structure will make the conformational processes more complex. Thus, the chair conformation of cyclohexane is transformed to the inverted chair by passing through an intermediate boat conformation, but although the boat is clearly separate from the initial and final

* That the *anti* conformation is more populated than the *gauche* conformation is irrelevant for this argument.

chairs, it is ill defined geometrically and energetically (boat or twist-boat), as are the barriers (C_2 or C_2') separating it from the chairs (5). Also, the conformational change is not localized in one or a few bonds, but concerns all bonds of the ring skeleton.

In cyclopentane the situation is further complicated by the fact that although nonplanar conformations of specific symmetry can be defined (envelope and twist-envelope), they happen to be extremely close in energy (6). If the twist-envelope is for a moment considered as a conformational minimum, it can exchange the sites of all hydrogens and of all ring atoms by passing repeatedly over envelope barriers to equivalent twist-envelopes. However, the mechanism is really a degenerate molecular vibration (pseudorotation), and individual conformers are not distinguishable spectroscopically (7). This kind of interconversion therefore is not considered here as a multistep mechanism.

The present chapter deals primarily with cases where well-defined conformational minima have been demonstrated to exist, or are with good reasons believed to exist, and where local or partial conformational changes can occur without major accompanying changes elsewhere in the molecule. Open-chain compounds satisfy best these criteria, but are trivial because almost any sequence of changes can occur. Rings of medium and moderately large size are much more interesting since conformational changes can to a large extent be of localized character. Yet, restrictions due to the ring structure limit greatly the type and number of possible changes and the number of populated and intermediate conformations on the multistep interconversion path which has to be followed in order to exchange nonequivalent conformational sites for ring atoms or substituents which are constitutionally equivalent.

The main source of experimental information available to us about conformational processes is dynamic nmr spectroscopy (8). The coalescence at a certain temperature of two or more signals from conformationally different sites for constitutionally equivalent atoms in the same molecule, or in different molecules, yields the rate constant at that temperature for the critical or rate-determining step in the site-exchange process. Whether the process consists of only this step or of a sequence of steps cannot be decided experimentally, and one must rely on a more or less intuitive interpretation. With a knowledge of the geometry and symmetry of the populated conformation(s), available in principle by static nmr spectroscopy below the coalescence temperature or by other spectroscopic methods and diffraction methods, it

is often possible to postulate a mechanism which fits the data. Additional support can be provided by comparison with qualitative, semiquantitative, and quantitative calculations (9) of relative strain energies of conformational minima and lowest barriers between them.

In certain cases partial site exchange is possible over only low barriers, whereas full site exchange requires the passage also over high barriers. Particularly useful information can often be obtained by the combined use of ^1H and ^{13}C nmr spectroscopy in cases when both processes are observed in the ^1H spectrum but only the lower-energy process in the ^{13}C spectrum. The occurrence of several processes may even permit conclusions to be drawn about the symmetry of the stable conformation, since those symmetries may be excluded that are such that a single low-energy process must affect full site exchange.

When two (or several) conformers are populated and observable in the low-temperature spectrum, more extensive conclusions can sometimes be drawn about the interconversion mechanisms. Thus, if the same critical barrier that separates two conformers also hinders full site exchange in one of these conformers, it becomes very likely that its exchange path requires the other as an intermediate. It may even happen that both use each other as intermediates for full exchange.

The simplest situation in dynamic nmr spectroscopy is the degenerate case when a conformer is converted to an equivalent one having the sites for one or several sets of constitutionally identical atoms exchanged. A more complex situation arises when the other conformer is not equivalent and has a higher energy and therefore a lower population (8). In both cases, however, there is thermodynamic equilibrium between the conformers. It is, on the other hand, also possible, when the critical conformational barrier is relatively high, to follow the irreversible conversion of a crystal conformer (less stable in solution) to the equilibrium mixture of more stable conformers in solution by dissolving the crystalline substance at a temperature sufficiently low to give a reasonable lifetime, and then observe its transformation by subsequent heating (10). This is, of course, equivalent to following the isomerization of an unstable configurational isomer, but now performed at low temperature, and is outside the scope of this review.

For further details and a critical discussion of dynamic nmr spectroscopy and strain-energy calculations, as well as an exhaustive literature compilation of applications, the reader is referred to the recent review by Anet and Anet (9).

II. TERMINOLOGY AND GRAPHIC REPRESENTATION

Terminology in connection with conformational processes varies considerably. Very often in the study of cyclic compounds, depending on which nuclei are observed, it may seem natural to describe a process either as an inversion, if the exchange of geminal substituent sites is the observable result, or as a pseudorotation, if the exchange of ring atom sites is observed. However, since the real mechanism is very often the same in both cases, we prefer in this review the terms "inverted" or "pseudorotated" conformation in order to imply that only a particular result of some process is meant. The terms "inversion" and "pseudorotation" will be reserved for the description of actual mechanisms, such as the total flattening halfway in the inversion of amines and the molecular vibration mechanism in the special case of cyclopentane pseudorotation. The word "conformer" is simply an abbreviation of "conformational isomer," while "conformation" is used descriptively for a given molecular species. "Conformer" and "conformation" are also often given the meaning "conformational energy minimum," whereas a "barrier" or "transition state" is never referred to as a conformation; it is the lowest pass between two given minima. The term "torsional barrier" when used in connection with cyclic molecules is an abstraction and refers to the torsional barrier in a given bond when such a bond occurs in a small ethane-like molecule.

The graphic representation of three-dimensional molecular conformations also shows a great variation, and quite different systems are in use for the various types of compounds. For acyclic compounds the Newman projection is widely used but is limited to ethane derivatives; larger molecules are usually represented by some type of perspective drawing. Cyclic compounds of the normal ring size (5-8 ring atoms) are well represented by the familiar side-view perspective drawings, but the larger rings are more clearly represented by bird's eye-view drawings (11). For the following discussions of stepwise conformational changes, it is very important to have graphic representations revealing clearly the symmetry, and it is also advantageous to use the same system for chain molecules, normal rings, and large rings. The two versions of a wedge-type system shown in Figure 1 will handle all molecules of saturated type, either each used in pure form, or mixed. The preferred conformations for cyclohexane, cyclooctane, and cyclodecane are shown as illustrations. If also the torsion-angle sign is added alongside each gauche bond, or anticlinal

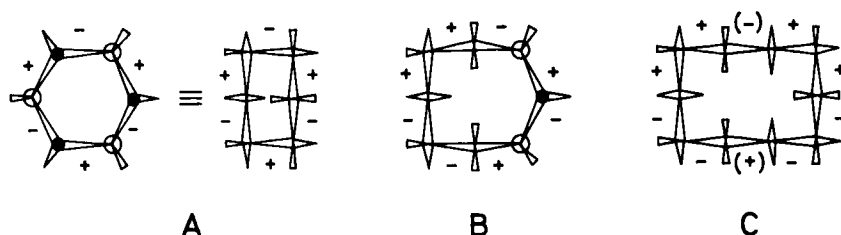


Fig. 1. Wedge-type representation of the preferred conformation of cyclohexane (A), of cyclooctane (B), and of cyclodecane (C). Torsion angle signs are indicated by + and -.

bond in olefins, it becomes particularly easy to follow the stepwise changes on an interconversion path. Anti-bonds will generally not need a marking although they can of course deviate from 180° .

III. OPEN CHAINS

Unbranched saturated-chain molecules in the liquid, in solution, or in the gas are unconstrained, and any interconversion between conformers can occur by a repetition of simple rotations about skeletal bonds over the lower anticlinal barrier (~ 4 kcal/mol for alkanes (11)) without ever needing to pass the higher syn barrier (~ 7 kcal/mol for alkanes (11)). Thus, a monogauche conformer of an n -alkane can be converted to a positionally different monogauche conformer most simply either by passing first to the all-anti conformer, whereafter the new gauche bond is formed, or by forming first the new gauche bond, whereafter the old gauche bond is changed to anti. Certain pathways may, however, be excluded because they involve intermediate conformers of forbiddingly high energy. Thus, a sequence of gauche bonds with alternating sign produces very serious 1,5-interactions (12), although in a sequence of gauche bonds of the same sign the strain energy due to 1,4- interactions is simply additive (12).

As an example, consider the conversion of $\underline{g}^+ \underline{a}$ pentane to the identical $\underline{a} \underline{g}^+$ conformer or to the enantiomeric $\underline{a} \underline{g}^-$ conformer (Fig. 2). For conversion to the $\underline{a} \underline{g}^-$ conformer both two-step paths $\underline{A} \rightarrow \underline{B} \rightarrow \underline{A}'$ and $\underline{A} \rightarrow \underline{C} \rightarrow \underline{A}'$ are probably comparable energetically and involve passage of only anticlinal barriers. The conversion to the $\underline{a} \underline{g}^-$ conformer, on the other hand, can only go via the $\underline{a} \underline{a}^-$ conformer ($\underline{A} \rightarrow \underline{C} \rightarrow \underline{A}'$), since the energy of the $\underline{g}^+ \underline{g}^-$

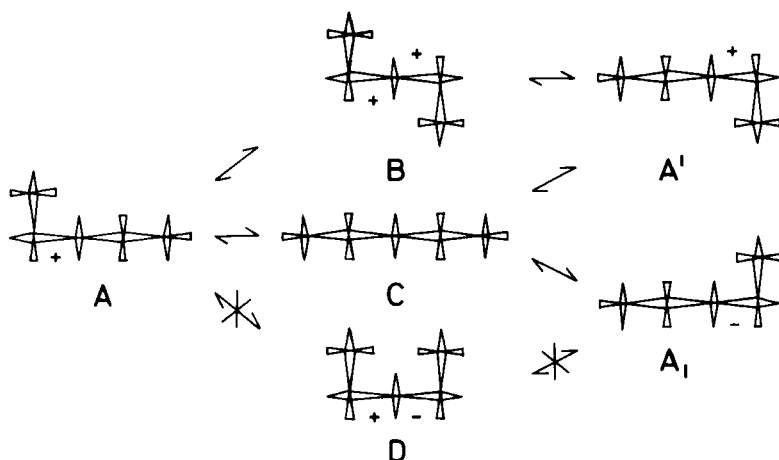


Fig. 2. Interconversion paths for conformers of pentane.

conformer on the other path ($A \leftrightarrow D \leftrightarrow A_1$) is expected to exceed the energy of the anticlinal barriers.

In the crystal lattice all *n*-alkanes are present as the extended all-anti conformer (13). Although this rod-like chain can undergo rotation about its long axis in an expanded crystal phase existing over a short temperature range just below the melting point (13), the rotation does not involve any conformational change. This is understandable in view of the drastic change in overall shape if one or several bonds had been converted from anti to gauche. However, chain molecules carrying substituents at certain points usually crystallize in other conformations (14), for example, in the shape of helices or roughly planar "meanders." Conversion from one folding pattern to a different one may not necessarily involve gross changes in overall shape.

An interesting example of a conformational change taking place in the solid state far below the melting point is provided (15) by meso-bigeranyl tetrahydrochloride (2,6,11,15-tetrachloro-2,6,11,15-tetramethylhexadecane) (Fig. 3). A metastable hexagonal crystalline form (A), m.p. 95°C , is converted to a stable crystalline form (C), m.p. 110°C , even at room temperature, requiring weeks, and more rapidly at higher temperature, the corresponding activation energy being $\Delta G^\ddagger \sim 26$ kcal/mol. The crystal structures (16) show that a migration of two gauche bonds, each by one step along the chain and with change of sign has taken place. If then the gross shape of the molecule is to be maintained all along the conversion,

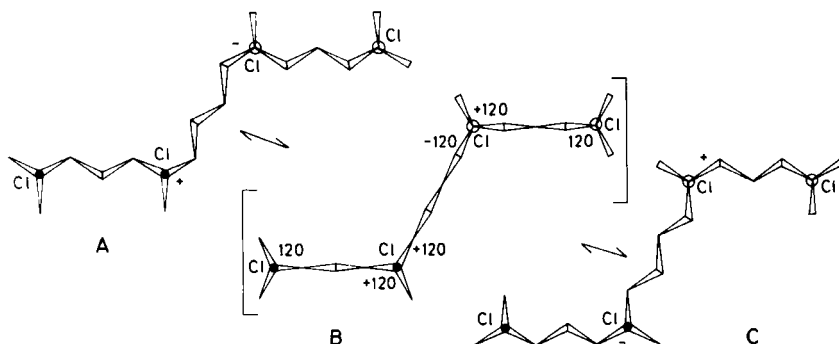


Fig. 3. The conformational change occurring in the solid phase of *meso*-bigeranyl tetrahydrochloride. Hydrogen atoms are not drawn.

the barrier (B) must involve anticlinal eclipsing of altogether six chain bonds. Depending on the severity of the constraints of the crystal lattice, the passage of the six barriers may be more or less synchronous and would alone correspond to most of the activation energy (<24 kcal/mol), but more likely other constraints make up a considerable part.

The corresponding conversion in solution is no doubt of a multistep nature, but the roughly synchronous eclipsing of two bonds occurring at each of the two chain-bonds (Fig. 3) is an "elementary process" that may be of interest also in free molecules where the constraints are looser, for example in large cyclic structures (17). When only one such process occurs locally, the chain ends do change orientation (Fig. 4), and for smaller rings other elementary processes are more efficient in preserving ring shape (see Sec. IV).

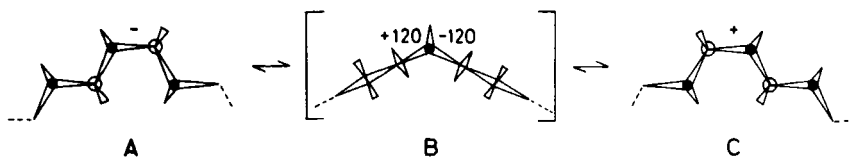


Fig. 4. Elementary process for the migration of a gauche bond by one position with sign change.

IV. MONOCYCLIC COMPOUNDS OF SATURATED CHARACTER

The different types of cyclic compounds having a

saturated ring skeleton are conveniently treated together since the conformational properties depend more on ring size than on whether the ring contains simple substituents (methyl groups, ketonic oxygen) or simple hetero atoms (amine nitrogen, ether oxygen). It is also most natural for the present approach to the analysis of conformational paths to start out with the largest rings where the elementary step processes can to a better approximation occur locally than in smaller and more constrained rings. Also, a sufficiently large saturated ring will in the equilibrium and intermediate conformations to a greater extent be defined by a sequence of clear gauche and anti bonds, and will, therefore, be in relatively deep energy minima separated by the maxima of the barriers; these latter are defined (17) by having at least one completely eclipsed bond.

A. 18-Membered Rings

Cyclooctadecane is the smallest cycloalkane which can have a diamond lattice conformation with isolated gauche bonds (18); it has the torsion-angle sequence a a g⁺a a g⁻a a g⁺a a g⁻a a g⁺a a g⁻ (fig. 5A). Although this is

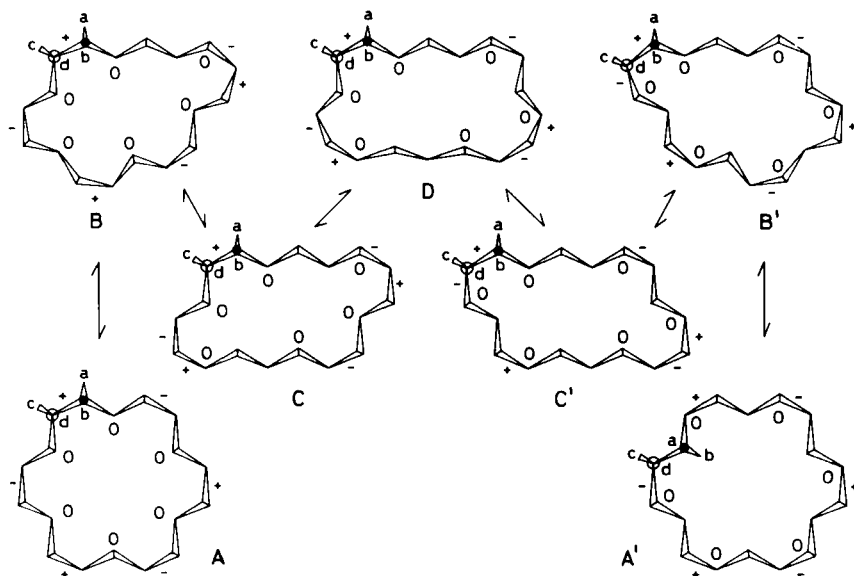


Fig. 5. Six-step interconversion cycle for ring-atom site-exchange in cyclooctadecane and 1,4,7,10,13,16-hexaoxacyclooctadecane (oxygen positions indicated).

probably not the most favored for the hydrocarbon itself (18), the 1,4,7,10,13,16-hexaoxa derivative takes this conformation (19,20) when complexing cations like potassium, rubidium and cesium (Fig. 5A, with oxygen positions indicated). In still larger rings, the conformational feature of isolated gauche bonds may have widespread occurrence since it is found in many types of polymer chains carrying substituents or hetero atoms (14).

For full exchange to occur in this type of ring conformation, a mechanism must be devised that permits migration of a gauche bond to all ring-bond positions, as well as the change of sign of its torsion angle. The elementary process in Figure 4 does move a gauche bond by one position with sign change, but entrains too large geometric changes even for this 18-membered ring. There exists another elementary process (fig. 6) which

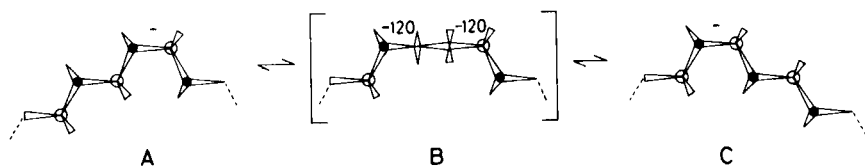


Fig. 6. Elementary process for the migration of a gauche bond by two positions without sign change.

will move a gauche bond by two positions without sign change ($a\ g^- \rightarrow g^-a\ a$) and which requires little geometric change outside the three-bond unit involved (17). The maximum energy for this process is ~ 8 kcal/mol if the two bonds which must pass through an anticlinal torsional barrier are eclipsed synchronously; most likely this is not necessary.

When this elementary process is applied repeatedly to cyclooctadecane in a systematic sequence (fig. 5), an equivalent conformation is obtained with all carbon atoms moved by two positions. A second cycle will lead to full exchange of all carbon sites, but only to partial exchange of hydrogen sites, geminal hydrogens remaining different. Further repetitions of this cycle can never lead to exchange of geminal hydrogen sites. Thus, protons a and c will visit only outer equatorial and inner axial positions, while protons b and d will visit only outer axial and inner equatorial positions. The result is that only the pseudorotated conformers are produced, not the inverted. It is of interest that one of the necessary intermediate conformations (Fig. 5C, with oxygen positions indicated) is identical with the one that the noncomplexing

1,4,7,10,13,16-hexaoxa derivative chooses in the crystalline state (21). In the hydrocarbon this, as well as all other intermediate conformers B and D, must be of relatively high energy because of repulsive 1,5 interactions (g^+g^- sequences).

To produce also inverted conformers of A requires the turning of each gauche bond over a syn barrier in a sequence of six steps. This type of process is, however, accompanied by more severe geometric changes elsewhere in the ring and is therefore expected to have a higher barrier than the path leading to pseudorotated conformers. Only geminal exchange of hydrogens, but no exchange of ring atoms, can result from the high-energy process, but since the low-energy process will be occurring even more rapidly, full exchange should be observed.

The interconversion scheme shown in Figure 5 can of course also be used to effect full carbon exchange in the 1,4,7,10,13,16-hexaoxa derivative, taking the stable noncomplexing conformation C with six different carbon sites as the starting point and running through several six-step cycles $C \rightleftharpoons D \rightleftharpoons C' \rightleftharpoons B' \rightleftharpoons A' \rightleftharpoons B \rightleftharpoons C$. The presence of oxygen atoms will of course make the critical barrier in each cycle different depending mainly on whether the barriers in a cycle involve double eclipsing in COCC fragments or in OCCO fragments.

No change of their nmr spectra with temperature has been reported for these compounds, and no strain-energy calculations are available.

B. 16-Membered Rings

The lowest energy conformation for cyclohexadecane and a series of tetraoxa-derivatives is found both experimentally (22-25) and by strain-energy calculations (11,23) to be of the "square" diamond-lattice type a a g^+g^+a a g^-g^-a a g^+g^+a a g^-g^- shown in Figure 7. It

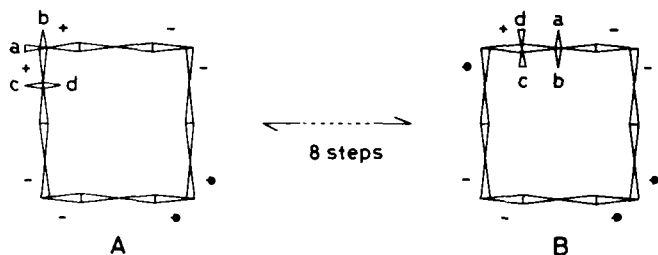


Fig. 7. Initial and final conformation in an eight-step interconversion cycle for partial site exchange in cyclohexadecane based on the elementary process $aa g^+ \rightleftharpoons g^+ aa$.

is briefly designated as [4444] since it is made up of four extended chains or "sides," each with four bonds, joined together at "corners" having adjacent gauche bonds of identical sign. No conformation with isolated gauche bonds is competitive in this ring size (11).

For conformational site exchange the elementary process shown in Figure 6, more completely given here as $a \text{ } g^+g^+ \rightleftharpoons g^+a \text{ } a \text{ } g^+$, is inefficient in this ring. First, two subsequent steps of this process, which are needed to move a corner by two positions, effect here essentially a rotation "through" the ring of the methylene group between the old and the new corner (fig. 8), and some of the eight steps necessary for a

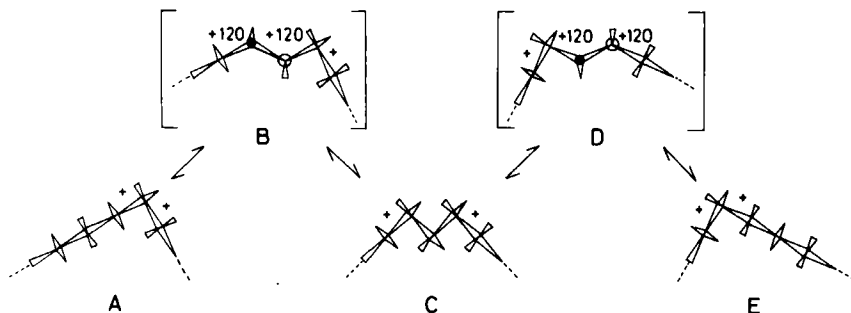


Fig. 8. Elementary two-step process for the migration of a g^+g^+ corner by two positions without sign change.

full cycle (Fig. 7) must be very high in energy in this (and smaller) rings (17). Second, also the seven intermediate conformations are very high in energy (17). Finally, only partial site exchange can be obtained; thus the four corner carbons are exchanged only with the four central "side" carbons after one cycle, and their hydrogens after three cycles, while the eight remaining carbons stay invariant but get their geminal hydrogen sites exchanged after one cycle (Fig. 7).

A much more efficient and less energy demanding process for this type of conformation (17) is the one shown in Figure 9, which moves a g^+g^+ corner by one position with torsion angle signs changed in both bonds. It is true that the transition state, if it is symmetric, has as many as three eclipsed bonds, one of which is even on the higher-energy syn barrier, but if the ring constraints are not too severe, the three bonds need not be fully eclipsed simultaneously. Calculations (17) based on the assumption that the barrier top is reached the moment the bond between the old and the new corner atoms becomes

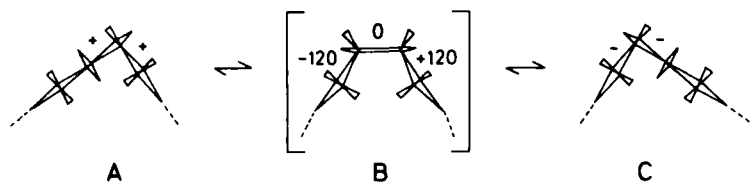


Fig. 9. Elementary process for the migration of a g^+g^+ corner by one position with sign change.

syn-eclipsed, so that a planar four-carbon system can be defined and the energy minimized by adjusting the rest of the molecule, show that one adjacent bond has already gone through the anticlinal eclipsing and the other has not yet become eclipsed. A clear advantage of the process for this ring, and particularly for still smaller rings, is that the outward flattening releases internal hydrogen crowding.

A complete cycle consisting of four such steps, operating once on each corner, can be devised in several different ways, two of which are calculated (17) to be of the lowest energy (Fig. 10). They are seen to lead

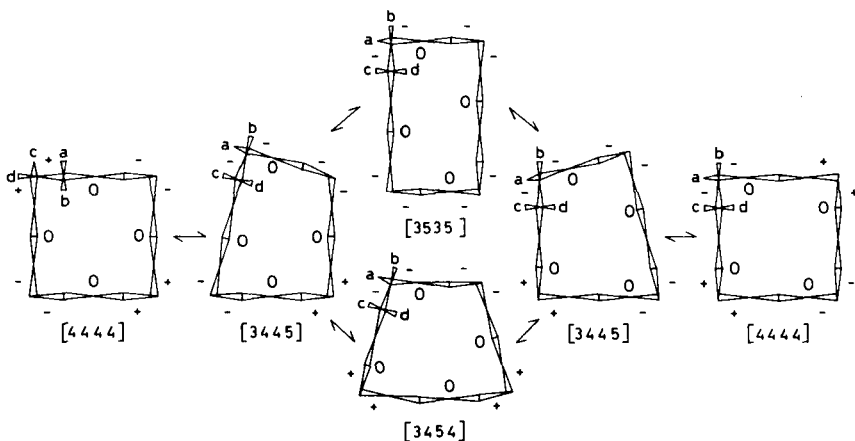


Fig. 10. Four-step interconversion cycles for full site exchange in cyclohexadecane and 1,5,9,13-tetraoxacyclohexadecane (oxygen positions indicated).

not only to full exchange of all carbon atoms if run through systematically three times, but also to full exchange of all hydrogen atoms after six cycles; an inner hydrogen atom stays inner as its carbon moves along one

side, then occupies a corner position (both of which are equivalent), and then becomes outer on the next side. The intermediate conformers are all of quadrangular type and happen to be exactly those of next-lowest calculated energy. The rectangular conformation [3535] is 1.9 kcal/mol higher (23) than [4444], the others (11) about 3 kcal/mol. The barriers have also been calculated by semiquantitative methods (17) that give maximum values of 12-13 kcal/mol (more likely estimates (23) are about 7 kcal/mol), the itinerary via [3454] being favored over that via [3535], and the first step having the critical barrier. Experimentally, a single process is in fact observed (23) for full site exchange with an activation energy of $\Delta G^\ddagger = 6.7$ kcal/mol.

The 1,5,9,13-tetraoxa derivative adopts (22,24) a very much preferred [4444] conformation with all oxygen atoms in central side positions (marked in Fig. 10). The conformational symmetry is thus so close to the constitutional symmetry that the occurrence of the interconversion process in Figure 10 should only be observable as an averaging of inner and outer α hydrogen, four cycles being needed.

The 1,3,9,11-tetraoxa derivative adopts a mixture of [4444] and [3535] conformations (25,26), both having the 1,3-dioxa groupings across corners (Fig.11). The

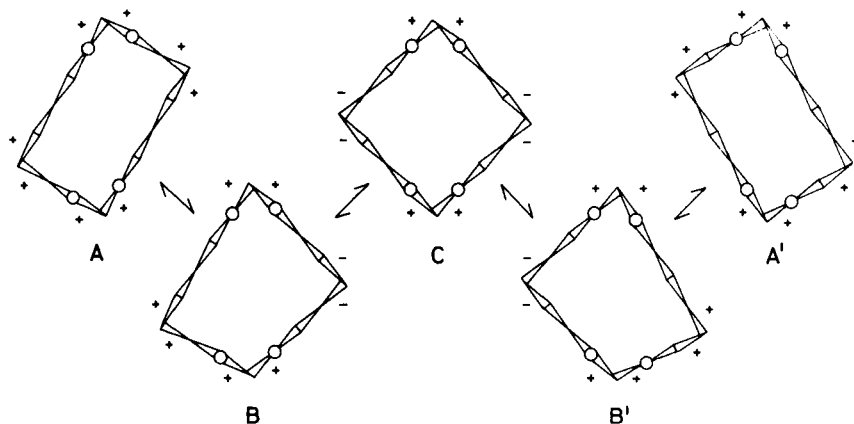


Fig. 11. Partial exchange path for the rectangular conformation of 1,3,9,11-tetraoxacyclohexadecane.

former will again be so close to the constitutional symmetry that the only remaining possible averaging is between inner and outer α and β hydrogens, obtainable after four of the cycles shown in Figure 10. The [3535]

conformation, on the other hand, has a lower symmetry and can undergo partial averaging to obtain the apparent symmetry of the [4444] conformation, which it actually goes through half-way on its interconversion path (Fig. 11). This path consists of four steps with syn eclipsing of only CC bonds. Since syn eclipsing of CO bonds in COCC units are expected to be of higher energy (27), and since also intermediate conformations with the 1,3-dioxa grouping in noncorner positions are of higher energy (28), the full averaging through further steps must require higher energy. A corollary from this analysis is that an intermediate temperature must exist when a mixture of the square and rectangular conformation cannot be seen as separate species in the nmr spectrum even though the geminal exchange is frozen.

The effect of introducing one or more gem-dimethyl substituents will be to raise the critical barrier for full exchange because the syn eclipsing energy in the adjacent and penadjacent ring bonds must increase. On the other hand, partial exchanges not involving eclipsing of these bonds may not be influenced. Simpler examples are given in the discussion of smaller rings.

C. 15-Membered Rings

There is no experimental information about the preferred conformation for cyclopentadecane, but semi-quantitative calculations (11) suggest that a quinquangular conformation [33333] is of lowest energy with several other quinquangular conformations only slightly higher. A great number of interconversion schemes can be devised (17) depending on which conformation is considered for possible exchanges. They are, however, quite involved and interwoven and are not further discussed here since the principles can be better demonstrated on the smaller cycloalkanes.

D. 14-Membered Rings

For cyclotetradecane, both the experimentally observed in solid (29) and in solution (30) and the calculated (11,31) lowest-energy conformation is the "rectangular" [3434] conformation of diamond-lattice type (Fig. 12). Applying the elementary process $a\text{-}g^+g^+ \rightleftharpoons g^-g^-a$ (Fig. 9) in four subsequent steps, one can arrive at the pseudorotated [3434] conformer by several paths, two of which (Fig. 12) have been calculated (31) to involve the lowest barriers. These differ in the identity of the second intermediate conformation. On one path this is equivalent with the

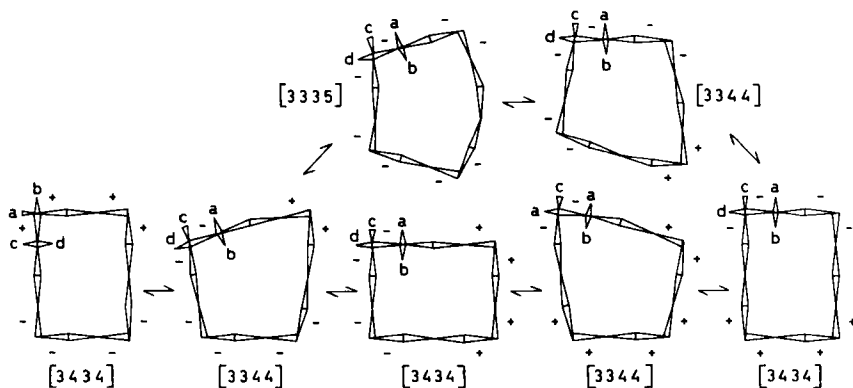


Fig. 12. Four-step interconversion cycles for cyclotetradecane. The upper path led to exchange of only carbon atoms, the lower double cycle to full exchange.

starting conformation, so that we have really a double cycle; on the other it is a strained [3335] conformation of high energy. The calculated (31) heights of all barriers are similar; on the double-cycle path all four are identical (8.0 kcal/mol), on the other the two central barriers are slightly lower (7.3 kcal/mol). Full carbon exchange is obtained already after two (double) cycles on the first path but needs five (single) cycles on the second. Hydrogen atoms will never be exchanged completely on the second path, since one half will always be outer on the long "side" and inner on the short "side," and vice versa for the other half. Also, the locally very similar geminal corner substituents are really different on the [3434] conformation. Passing through the [3434] conformation half-way through each cycle on the first path has the effect of exchanging geminal substituents, and after six double cycles all hydrogen sites are exchanged. Experimentally (30), only one process is indeed seen in both the ^1H and the ^{13}C spectrum with an activation energy of $\Delta G^\ddagger \approx 7$ kcal/mol, and line shapes can only be fitted if the $[3344] \leftrightarrow [3335]$ barrier is lower than the $[3434] \leftrightarrow [3344]$ barrier, in agreement with calculations.

The intermediate conformations in the interconversion schemes (Fig. 12) are identical with the next-lowest calculated conformations for cyclotetradecane (31); [3344] is 1.1 kcal/mol higher, while [3335] is 2.4 kcal/mol higher.

The effect of *gem*-dimethyl substitution is to increase the activation energy for full exchange, not only because the syn eclipsing energy in certain ring bonds is raised,

but also because a methyl group when intraannular on noncorner positions in otherwise low-energy minima will cause transannular repulsion with ring methylene groups or other intraannular methyl groups. Among those bis(*gem*-dimethyl)-substituted derivatives that fit the most stable [3434] conformation in having the substituents on corner positions, neither 1,1,4,4- nor 1,1,5,5-tetramethylcyclotetradecane can undergo partial exchange over unchanged barriers, whereas 1,1,8,8-tetramethyl- (and 1,1--dimethyl-)cyclotetradecane (Fig. 13) should have such an easy process leading to the constitutional symmetry for the ring atoms and substituents in 1 and 8 positions (32). Geminal hydrogens in other positions are thereby not exchanged.

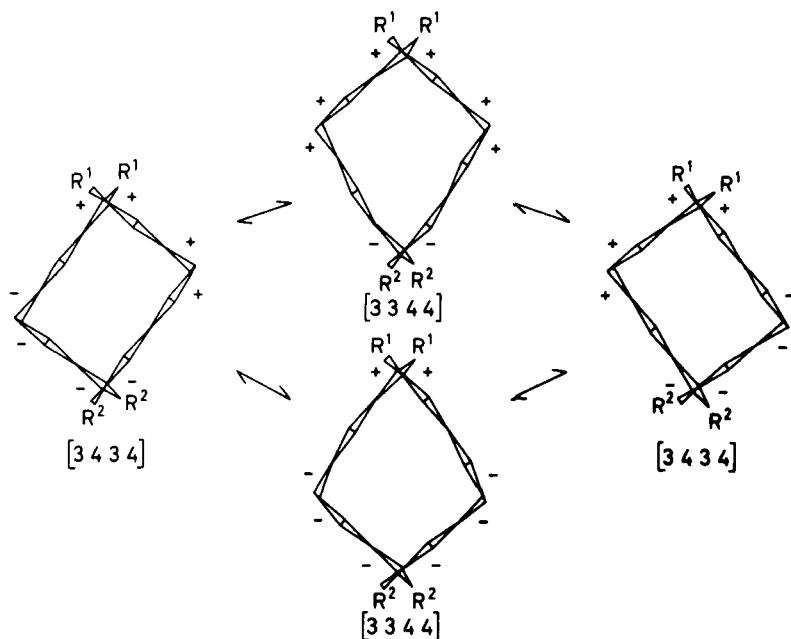


Fig. 13. Low-barrier partial exchange paths for 1,1-dimethylcyclotetradecane ($R^1 = \text{Me}$; $R^2 = \text{H}$) and 1,1,8,8-tetramethylcyclotetradecane ($R^1 = R^2 = \text{Me}$).

E. 13-Membered Rings

Nothing is known experimentally about the preferred conformation of cyclotridecane, but semiquantitative calculations (17) suggest that two conformations of quinquangular type, [12433] and [13333], are lowest, and

that two of triangular type, [355] and [445], are only slightly higher. The interconversion paths to be considered for site exchange depend on which conformation is taken as the starting point; they are numerous and interwoven, and are not discussed further. Dynamic nmr spectroscopy suggests (30) that critical interconversion barriers are lower than ~ 6 kcal/mol.

A close relationship exists (11) between each conformation of triangular type and one or two conformations of quinquangular type having a centrally located one-bond side. Thus when the three sides of a triangular conformation are of comparable length and all interior bonds in these sides are reasonably near anti (torsion angles $\gg 120^\circ$), the triangular is by far lower in energy than the quinquangular. As an example, [445] is calculated (11) to be more than 11 kcal/mol more stable than [12442] (Fig. 14); in fact,

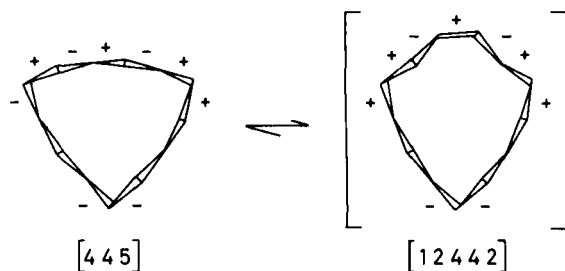


Fig. 14. A conformational pair of cyclotridecane with the triangular partner strongly favored.

the latter should not be considered as a conformation since there is hardly any barrier separating the two, even though three bonds must pass anticlinal torsional barriers in the conversion of one to the other. When, however, one side is clearly longer than the other two in a triangular conformation, so that some of the "interior" bonds are closer to the anticlinal torsional barrier, then the energies of the triangular and quinquangular partners are more similar, but still there is no clear barrier between them. As an example, [12433] is calculated (11) to be about 4 kcal/mol more stable than [346] (Fig 15). Finally when one of the sides in a triangular conformation would have been very long, with several bonds on anticlinal barriers, the related quinquangular conformation is by far the better. The extreme example is here [13333], calculated (11) to be about 7 kcal/mol more stable than [337], which again represents no real conformational minimum (Fig. 16).

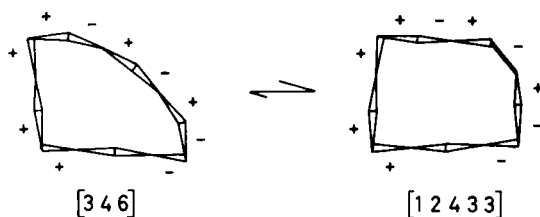


Fig. 15. A conformational pair of cyclotridecane with both partners of comparable energy.

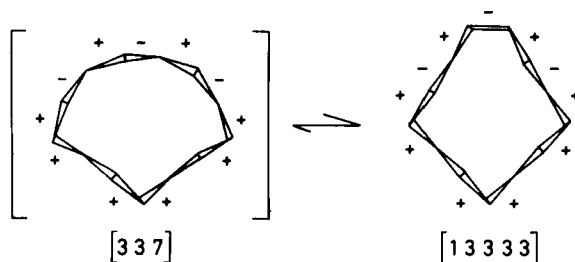


Fig. 16. A conformational pair of cyclotridecane with the quinquangular partner strongly favored.

It will be noted that the three gauche bonds around a one-bond side have torsion-angle signs alternating in exactly the same way as in the corresponding near-anti bonds on the "convex" side of the related triangular conformations. Also on this formal basis, they are, therefore, naturally related and conveniently treated as being of the same family. Interconversion between distinctly different conformers always requires a sign change.

F. 12-Membered Rings

The "square" [3333] conformation, although not of the diamond-lattice type, is distinctly preferred for cyclododecane according to all strain-energy calculations (11), and is also the one observed in the solid (33) and in solution (30). The preferred interconversion path (17) is shown in Figure 17. It involves again the use of the $a^+g^+ \leftrightarrow g^-g^-a$ elementary corner-moving process on all four corners in succession, and leads to the pseudorotated and inverted mirror-image conformation. The second barrier in this cycle is calculated (34) to be higher than the first (8.4 against 7.9 kcal/mol) and hence corresponds to the one observed experimentally (30) both by ^{13}C and ^1H nmr spectroscopy ($\Delta G^\ddagger = 7.3$

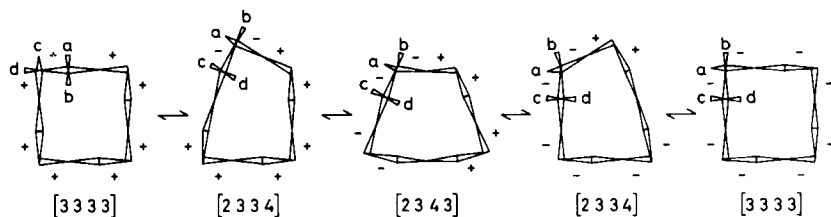


Fig. 17. Four-step interconversion cycle for full site-exchange in cyclododecane.

kcal/mol. In fact, this cycle must lead to full exchange; all carbons are exchanged after two cycles, while four cycles are needed to exchange all hydrogen sites. The necessary intermediate quadrangular conformations happen to be exactly those two calculated (34) to be of next-lowest energy; [2334] is 1.6 kcal/mol and [2343] is 3.0 kcal/mol higher.

Gem-dimethyl substitution leads to no interesting partial exchange processes when the substitution pattern fits the most stable [3333] conformation. Only when this is made impossible and less symmetric ring conformations take over can partial exchanges be observed (32).

The 1,4,7,10-tetraoxa derivative, both as the free molecule and when it complexes lithium and sodium cations, has been shown (27) also to adopt the [3333] conformation with the oxygen atoms in side positions. When the four-step cycle mechanism of Figure 17 is applied to this molecule (Fig. 18), it is readily seen that two different

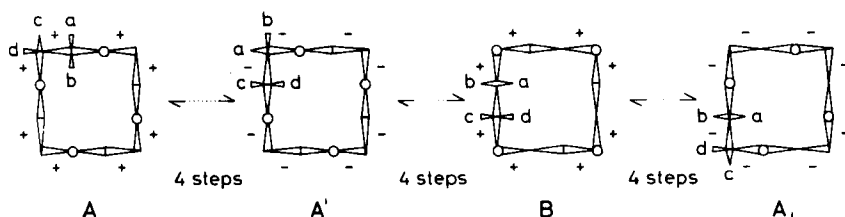


Fig. 18. The three interconversion cycles needed for full site exchange in 1,4,7,10-tetraoxacyclododecane.

types of cycles exist. One of these ($A \rightleftharpoons A'$) involves lower critical barriers, since in all four steps only CC bonds become syn eclipsed. The other ($A' \rightleftharpoons B$ or $B \rightleftharpoons A$) involves higher critical barriers, since in all four steps now only CO bonds become syn eclipsed. Going through the low-barrier cycle once transforms the stable conformation

A to an equivalent A' whereby all carbons become exchanged, but the four types of hydrogen are only exchanged pairwise (*a* with *c*, *b* with *d*). Going through only the high-barrier cycle twice, via the intermediate less stable conformation B, transforms A' to A,, whereby once again all carbons become exchanged, and the hydrogens are now exchanged in different pairs (*a* with *d*, *b* with *c*). At a temperature when this occurs rapidly, of course also the low-barrier process occurs rapidly, and so full exchange must be observed. This agrees perfectly well with the observation (27) that only the low-barrier process is seen in the ^{13}C spectrum and both processes in the ^1H spectrum ($\Delta G^\ddagger = 5.5$ and 6.8 kcal/mol).

A completely analogous situation is expected for cyclododecanone since it is clear from the low-temperature ^1H spectrum (35) that its conformation is unsymmetric with the carbonyl group in a side position. The observation of a single process in ^1H spectroscopy (35) can, therefore, only mean that both types of interconversion cycles have critical barriers of similar heights.

G. 11-Membered Rings

For cycloundecane, the low-temperature nmr spectrum (30) indicates very low conformational barriers. Strain-energy calculations (11,34) show that two triangular conformations, [344] and [335], and two unrelated quinquangular conformations, [12323] and [13223], are lowest and very close in energy (1.2, 0, 0, and 1.5 kcal/mol). The interconversion between the triangular conformations is particularly easy, whereas it is particularly difficult to interconvert directly the quinquangular conformations (17). In fact, the [12323] conformer can more easily change slightly uphill to its triangular partner [236], which by the usual corner-moving steps undergoes full site exchange (17).

Of particular interest is the possibility for the [344] conformation to be converted in one step directly to an equivalent conformation over a low barrier [calculated (34) to have a height of 5.7 kcal/mol] without the necessity to pass through any intermediate conformation (Fig. 19). This step must of course be repeated three times to effect migration of all ring atoms by one step, and so it is really the triple cycle shown in Figure 19 that is to be compared with other cycles for interconversion of triangular conformations. Eleven steps ($3\frac{2}{3}$ cycle) are needed to exchange all carbon atoms, whereas fifteen steps (5 cycles) are needed to exchange all hydrogens.

Energetically, however, it is even more advantageous (34) to pass the still lower barrier (calculated height

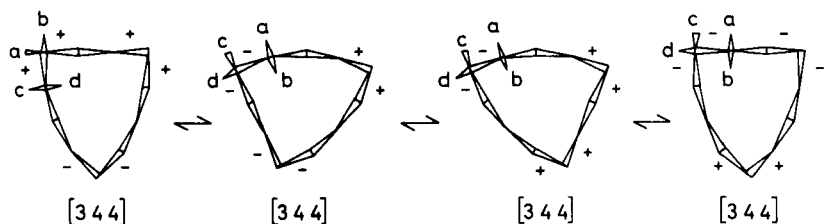


Fig. 19. Triple interconversion cycle involving only the most regular triangular conformation of cycloundecane.

4.2 kcal/mol) for conversion of the [344] conformation to [335]. Thus, by the repeated intermediacy of the [335] conformation, a multistep path can be devised for the full exchange of [344], while, on the other hand, full exchange for [335] is obtained by passing repeatedly through the [344] conformation, and so their most easy interconversion mechanisms are completely interwoven (Fig. 20).

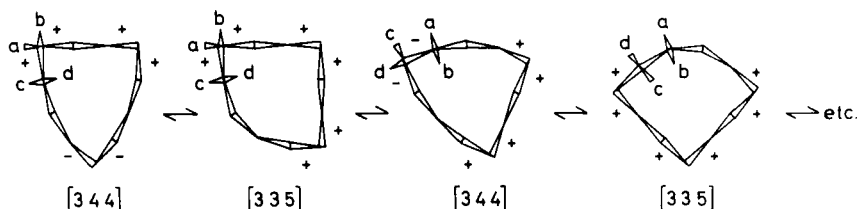


Fig. 20. Lowest-energy interconversion path for triangular conformations of cycloundecane.

Cycloundecanone adopts in the solid (36) a [335] conformation with the carbonyl group unsymmetrically located near the middle of the five-bond side. If this is also the single conformation seen by nmr in solution (35) the observation of two processes in the ^1H spectrum ($\Delta G^\ddagger = 6.0$ and 6.9 kcal/mol) can be nicely explained; a partial averaging process $[335] \rightleftharpoons [344] \rightleftharpoons [344] \rightleftharpoons [335]$ gives the ring skeleton the constitutional symmetry, but in order to obtain geminal exchange, further steps which must bring the carbonyl group into corner positions are required, and more severe transannular hydrogen repulsions will raise the energy of these intermediates and adjoining barriers.

Since *gem*-dimethyl substituents can only occupy corner positions, one or a few ring conformations will become favored when two ring atoms are *gem*-dimethyl

substituted (32). A great variety of situations will arise, illustrated by 1,1,4,4-tetramethylcycloundecane. In the [344] conformation no partial exchange over unchanged barriers can take place. In the [335] conformation, however, the symmetry will be lower (Fig. 21), with four different methyl groups, and a partial exchange can take place over unchanged low barriers via the [344] conformation, whose symmetry it acquires by this averaging (Fig. 21). Thereby the ring carbon skeleton gets the constitutional symmetry, but geminal methyl groups and hydrogens, except the 8-hydrogens, remain different. The chirality of the conformation is preserved during the process.

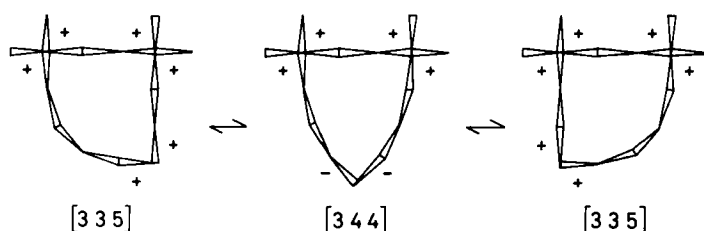


Fig. 21. Low-barrier partial exchange path for 1,1,4,4-tetramethyl cycloundecane.

H. 10-Membered Rings

The lowest-energy conformation for cyclodecane established experimentally for the hydrocarbon in the gas phase (36a) as well as for many crystalline derivatives (37), and also according to most strain-energy calculations (26), is the rectangular [2323] conformation of diamond-lattice type.

Several interconversion paths with retention of symmetry in barriers and intermediates have been discussed (5), but the calculated activation energies are too high compared with experimental values. The path shown in Figure 22 with only unsymmetrical barriers is derived in the usual way by successive corner-moving steps (17,37). As for cyclotetradecane, the initial conformation is reproduced already half-way through the cycle, so that it is really a double cycle with the same barrier in all steps. The calculated (26) barrier height (6.6 kcal/mol) is in excellent agreement with the observed (30) value ($\Delta G^\ddagger = 6$ kcal/mol). Full carbon exchange requires only six steps (1 1/2 cycle), while for full hydrogen exchange four double cycles are needed. The intermediate conformation [2233] is identical with the one that

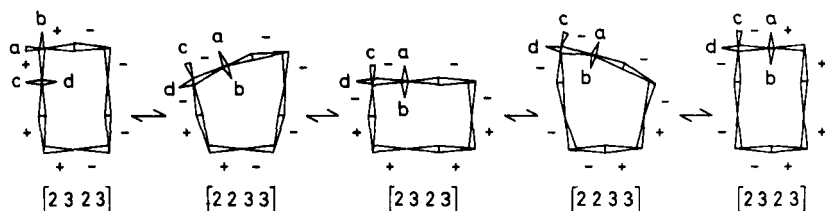


Fig. 22. Double interconversion cycle for full site exchange in cyclodecane.

calculations (26) show to be third lowest in energy (1.3 kcal/mol).

Conformations having one-bond sides, such as [1333], [1324], and [1414], are also competitive in this medium ring; calculated energies are 0.4, 1.6, and 1.5 kcal/mol, respectively (26). The bond arrangement at the one-bond side in these quadrangular conformations is more clearly defined as $g^+g^-g^+$ than in the quinquangular conformations of the larger odd-membered rings discussed so far, but on the basis of the torsion-angle sign sequence, the above conformations may also be called biangular ([1333] = [37]; [1324] = [28]) or nonangular ([1414] = [10]). The migration of a one-bond side with its two corners by one position involves a particular elementary process a $g^+g^-g^+ \rightarrow g^-g^+g^-a$ (Fig. 23), whereby only anticlinal

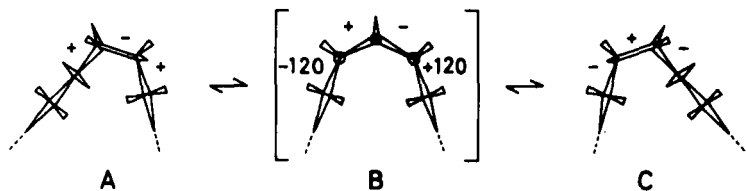


Fig. 23. Elementary process for the migration of a one-bond side by one position.

torsion barriers have to be passed more or less synchronously in two bonds (17). A simple example is the conversion of [1324] to its mirror image over a very low barrier (calculated (26) at 2.6 kcal/mol) of this kind (Fig. 24). This barrier has a higher symmetry than the unsymmetric conformational minima which it separates, in contrast with the more common situation that the first barrier

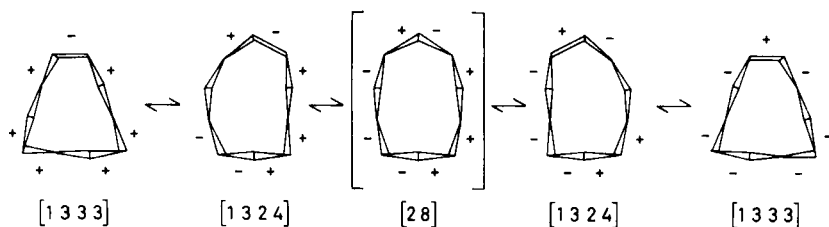


Fig. 24. Low-barrier-partial exchange path within the [28] family of cyclodecane and its use for interconversion in the [37] family.

away from a symmetric minimum is unsymmetric. The path $[1324] \leftrightarrow [28] \leftrightarrow [1324]$ in Figure 24 produces partial averaging, so that even at the lowest temperature the nmr spectrum will correspond to the symmetry of the biangular barrier [28], and so this symbol may well be used to describe a whole family of nmr spectroscopically nondistinguishable conformers. Full ring-atom exchange can be achieved by interconversion through other biangular families like the [37] family, including [1333] (Fig. 24), over a barrier calculated (26) to be 6.3 kcal/mol, but no geminal exchange is possible since a given hydrogen will always be inner on the short side and outer on the long side, or vice versa. Full exchange requires further conversion over a still higher barrier (26) of 7.5 kcal/mol to conformer [2233] of unambiguous quadrangular type on the exchange path given in Figure 22.

The crown- or trans-decalin-like conformation [1414] demonstrates a situation becoming increasingly more common as the ring size gets smaller, that it sometimes may be more economical to perform changes in two or more regions of the ring simultaneously than to pass through two or more steps. The conversion to a pseudorotated equivalent conformation goes over a symmetrical barrier calculated (26) to be 7.5 kcal/mol (Fig. 25), and repetition will exchange all ring atoms but not geminal hydrogens, all inner hydrogens remaining inner and all outer remaining outer. The signs of the torsion angles alternate around the ring and do not change during the process, so that this whole crown-family of minima and barriers may be called nonangular and designated [10]. To obtain also geminal exchange requires the passage over a much higher barrier calculated (26) to be 17 kcal/mol, to the biangular [28] family and from there to any of the two quadrangular conformers on the exchange path shown in Figure 22.

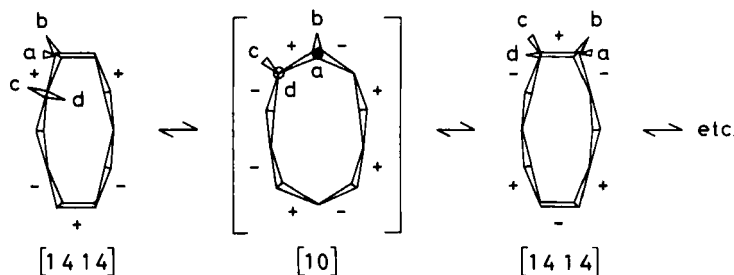


Fig. 25. Interconversion path for ring-atom site exchange within the crown family of cyclodecane.

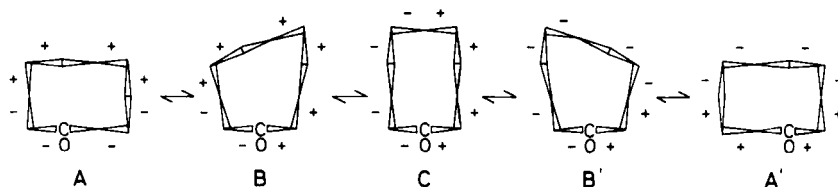


Fig. 26. Low-barrier partial exchange path for cyclodecanone.

Cyclodecanone adopts preferentially the unsymmetric [2323] conformation (A, Fig. 26) where transannular hydrogen repulsions are best relieved (35). A simple passage through the cycle of Figure 22 will give the carbon skeleton an averaged symmetry corresponding to the constitutional symmetry of the intermediate conformation C (Fig. 26). To achieve also geminal hydrogen exchange, further cycles must be run through, whereby the carbonyl group will have to occupy also corner positions. Certain barriers must then be raised because of the more severe transannular hydrogen repulsions. This explains why two processes ($\Delta G^\ddagger = 6.5$ and 7.3 kcal/mol) are seen in ^1H spectroscopy, but only the lower of these in ^{13}C spectroscopy (35).

Among the *gem*-dimethyl substituted derivatives 1,1-dimethyl- and 1,1,6,6-tetramethylcyclodecane should have interesting partial-exchange processes (32) over unchanged barriers (Fig. 27); these are analogous to those shown for corresponding cyclotetradecane derivatives. The constitutional symmetry is thereby acquired by the ring atoms and for the R^1 and R^2 substituents, but not for the remaining geminal hydrogens.

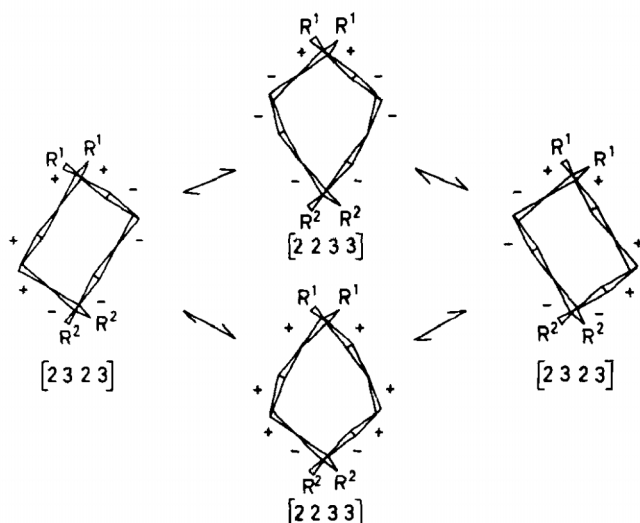


Fig. 27. Low-barrier partial exchange paths for 1,1-dimethylcyclodecane ($R^1 = \text{Me}$; $R^2 = \text{H}$) and 1,1,6,6-tetramethylcyclodecane ($R^1 = R^2 = \text{Me}$).

I. 9-Membered Rings

The lowest calculated conformation (26) and the major one observed (38) for cyclononane is the triangular [333]. Its interconversion path (Fig. 28) provides a good demonstration of the energetic advantage of passing in several steps (here three) with localized changes to the both pseudorotated and inverted mirror-image conformation, instead of more directly with synchronous changes. It also demonstrates the unsymmetric nature of the barrier (A, Fig. 28) in the first conversion step from the symmetric minimum [333] and the symmetric nature of the barrier B between the two equivalent unsymmetric intermediate minima [234]. If the highest possible symmetry were retained during the whole process, all nine ring bonds would become eclipsed simultaneously at the barrier top C, three of them at the high syn torsional barrier, and the required energy would be very high. A two-step path of somewhat lower symmetry has therefore been proposed (5); it goes through an intermediate "conformation" that is identical with the central barrier B of the three-step path, whereby only four bonds must go through eclipsing during the passage over each of the two undefined barriers. This is still too high in energy, and the use finally

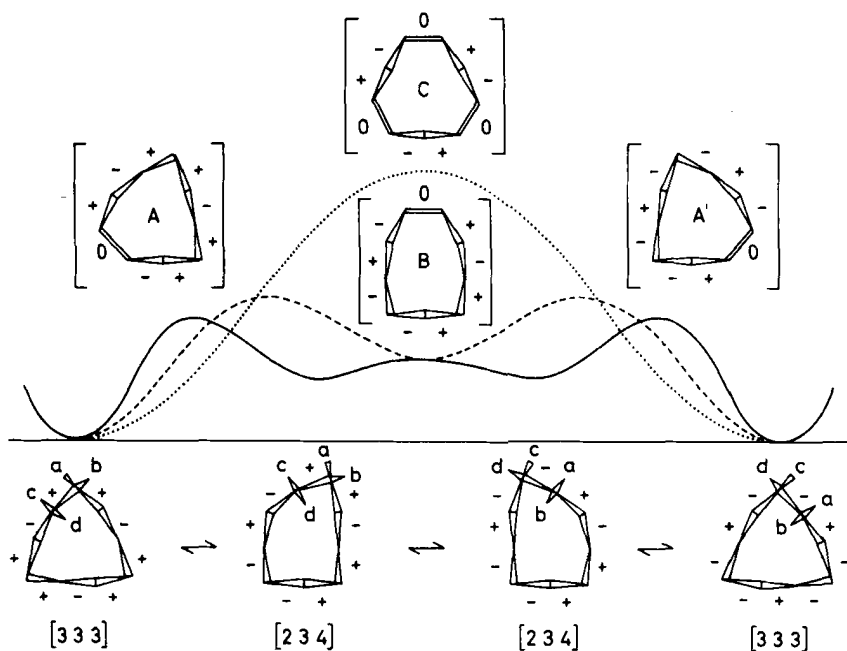


Fig. 28. Interconversion cycles for full site-exchange in the [333] conformations of cyclononane. Dotted line: one-step cycle over the high-symmetric barrier C. Dashed line: two-step cycle over B as intermediate. Full line: three-step cycle over the barriers A, B, and A'. Relative energies are only semi-quantitative.

of the [234] conformation as an intermediate [calculated (26) energy 3.2 kcal/mol] divides the process into three steps (17) each involving the eclipsing of only three bonds, resulting in a calculated (26) critical barrier for the first (and last) step of 6.9 kcal/mol in excellent agreement with the observed (38) barrier for full exchange ($\Delta G^\ddagger = 6.0$ kcal/mol). The central barrier is much lower [calculated (26) at 4.4 kcal/mol]. Two cycles will exchange all carbons and four cycles all hydrogens. The detailed calculations (39) also confirm that the assumption made earlier (17) that the barrier top is reached when the bond between the old and new corner goes exactly through syn eclipsing, is valid for the barriers involved in this cycle and others mentioned below.

A minor conformation of cyclononane in solution, calculated (26) at 1.7 kcal/mol, but nevertheless found

in the crystal structure of derivatives (37), is quin-quangular of type [12222] and also classifiable as triangular [225]; this is often more convenient in discussions of interconversions. The best mechanistic path for full exchange (Fig. 29) goes through the same intermediate conformations [234] as were needed for interconversion of the [333] conformation (Fig. 28). An even lower critical barrier (5.9 kcal/mol) is calculated (26) for this cycle; it occurs in the first and last step. Because of the particular sequence of corner-moving operations and the symmetries involved, one cycle will here move all ring atoms by two positions. As many as eight cycles are, therefore, needed to exchange all carbons, and twelve to exchange all hydrogens.

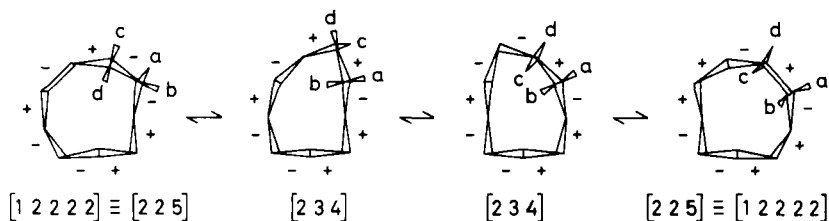


Fig. 29. Three-step interconversion cycle for full site exchange in the [225] conformation of cyclononane.

A fourth conformation, which can be considered either as triangular [144] or as uniangular [9], is also calculated (26) to be of low energy (1.2 kcal/mol) and found in trace amounts in cyclononane solutions (26). It can exchange only over a barrier calculated (26) to be 8.5 kcal/mol, and which is essentially of a $g^+g^+ \leftrightarrow g^-g^-$ type, but much less symmetric (26) than the schematic synchronous process shown in Figure 30. There are also

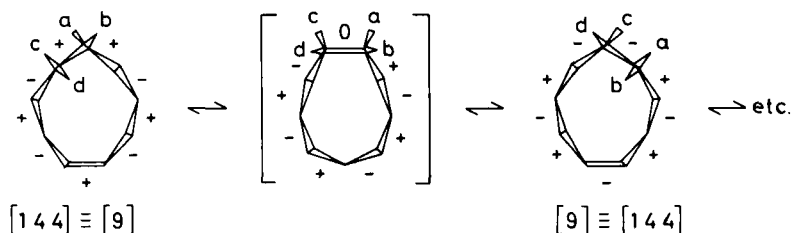


Fig. 30. Interconversion step for full site-exchange in the [9] conformation of cyclononane.

adjustments on the opposite end so that the one-bond side moves by one position over a barrier of a $g^+g^-g^+ \leftrightarrow g^-g^+g^-$ type. By repeating this double step, not only do all carbons migrate to all ring positions, but also geminal exchange is obtained.

Cyclononanone has been shown (40) to take an unsymmetric [12222] conformation in a crystalline $HgCl_2$ complex (A Fig. 31). This conformation is also in accord with the

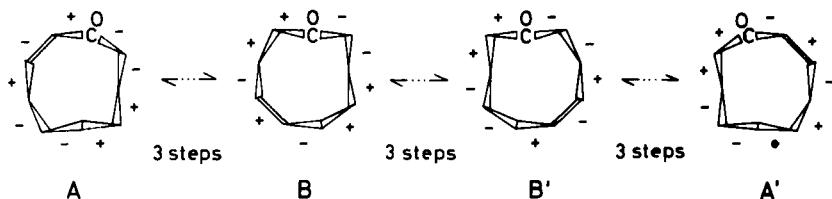


Fig. 31. Low-barrier partial exchange path for cyclononanone.

observation in solution of two processes ($\Delta G^\ddagger = 5.0$ and 6.5 kcal/mol) in dynamic 1H nmr spectroscopy, but only the lower-energy process in ^{13}C spectroscopy (35). Three cycles of the type shown in Figure 29 will take the molecule through two intermediate [12222] conformations (B and B', Fig. 31) to an equivalent conformation A', whereby the carbonyl group will remain all through the process in positions where it relieves transannular hydrogen interactions. The carbon atoms are thereby averaged to the constitutional symmetry. Geminal hydrogen exchange, however, requires further cycles where the carbonyl group must also occupy corner positions, and some of these barriers will be higher due to more severe transannular hydrogen interactions.

The low-temperature nmr spectrum of 1,4,7-trioxacyclononane reveals a single conformation having no symmetry, and two processes ($\Delta G^\ddagger = 7.3$ and 7.9 kcal/mol) are seen both in 1H and ^{13}C spectroscopy (41), the low-barrier process leading to pairwise averaging of six ^{13}C lines before on further heating the three lines coalesce to one. One [12222] conformer and three different [234] conformers satisfy these observations, and a choice can only be based on assumptions about relative heights of critical barriers on various interconversion paths. The original conclusion (41) was that the low-barrier partial averaging was represented by the simple process $B \leftrightarrow C \leftrightarrow B'$ (Fig. 32), but it may also be represented by the three-step process, $A \leftrightarrow B \leftrightarrow C \leftrightarrow B' \leftrightarrow A'$, shown in the same figure.

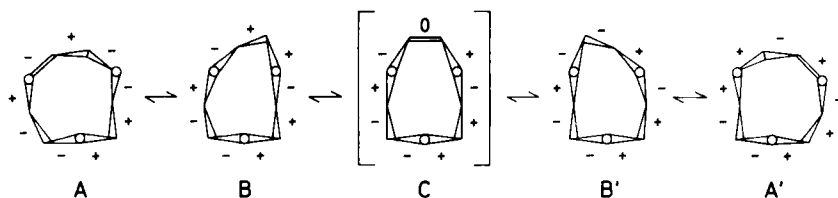


Fig. 32. Low barrier partial exchange path for 1,4,7-trioxacyclononane.

Among *gem*-dimethyl substituted cyclononanes, both the 1,1-dimethyl and 1,1,4,4-tetramethyl derivatives will fit and further favor the lowest [333] conformation. No partial averaging process is possible, and full exchange requires passage over increased barriers. This is in accord with observation (38, 42); the barrier increases from 6 kcal/mol to 9 and 20 kcal/mol, respectively, for these two derivatives. The nonadditivity is easily explained as due to 1,4-methyl-methyl interaction as compared to hydrogen-methyl interaction in the critical barrier of the second cycle of the type shown in Figure 28 when the C_2C_3 bond goes through syn eclipsing.

J. 8-Membered Rings

The dynamics of eight-membered rings has been fully elucidated by Anet and recently reviewed by him (43). Nevertheless, a brief description of interconversion schemes is given here from a somewhat different viewpoint, using terms, symbolism, and graphic presentation of the type introduced for the larger rings. In this and smaller rings even "long" sides will contain only bonds with torsion angles smaller than 120° , and so it is convenient to extend the definition of a "side" to include a sequence of bonds with alternating torsion-angle signs, and call any ring atom between two bonds of the same sign a "corner."

The conformation of lowest energy for cyclooctane, both by strain-energy calculations (44) and established experimentally (45), is not the square diamond-lattice type [2222], but a biangular [26], usually called boat-chair (Fig. 33). Its most easy interconversion requires the intermediacy of another biangular conformation [35], usually called twist-boat-chair, which is only 1.7 kcal/mol higher in energy (44). The nature of the transition state is adequately described as a corner movement with syn eclipsing of one bond, although the exact angle is calculated (44) to be not of 0° but 8° . The

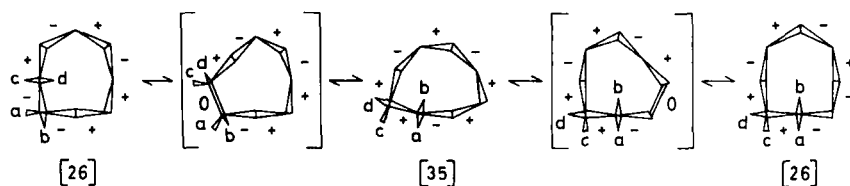


Fig. 33. Two-step interconversion cycle for ring-atom site exchange in the [26] conformation of cyclooctane.

two-step cycle (Fig. 33) with both barriers calculated (44) at 3.3 kcal/mol, and estimated from experimental data (43) at 3.7 kcal/mol, will average all carbon atoms after seven repetitions, but geminal hydrogens will never be exchanged since they stay inner on the two-bond side and outer on the six-bond side, and vice versa. To effect full exchange, formally the [26] conformation might first be distorted to its quadrangular partner [1223] of higher energy and converted by one corner movement to the [2222] conformation, whence it could be taken back in a different direction so as to produce the set of inverted [26] conformations. Calculations show, however, that it is more economical in this ring to perform the conversion in a symmetric fashion (44), which demonstrates that the constraints in this ring are too severe to permit freely any type of localized conformational change. The direct symmetric conversion of [26] to the [2222] conformation, from which it can return to the inverted [26] conformation (Fig. 34), has a calculated barrier (44)

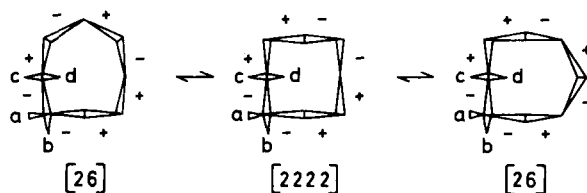


Fig. 34. Two-step interconversion path for geminal site exchange in [26] conformation of cyclooctane.

of 10.7 kcal/mol. A still more favorable process (Fig. 35), with a calculated (44) barrier of 7.5 kcal/mol, in excellent agreement with the observed (46) $\Delta G^\ddagger = 8.1$ kcal/mol, leads from the [35] conformation over a doubly eclipsed symmetric barrier B, usually called chair, directly

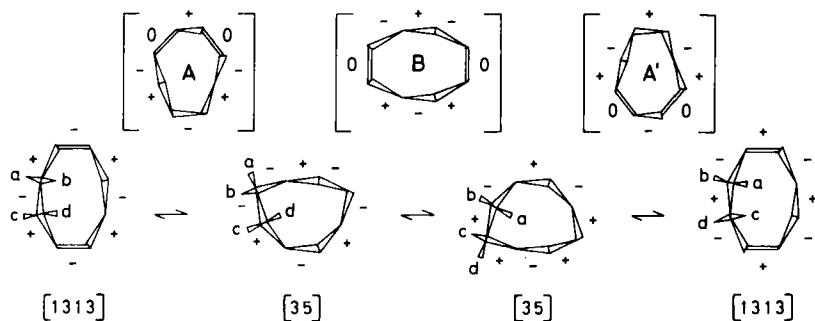


Fig. 35. Interconversion paths for geminal site exchange in the [8] and [35] conformations of cyclooctane.

to the mirror image [35]. Inner hydrogens on the three-bond side remain thereby inner when arriving on the five-bond side, so that full exchange can be obtained.

The next-lowest conformation of cyclooctane is the quadrangular [1313] conformation, usually called twist-chair-chair (Figs. 35 and 36). It is the lowest-energy

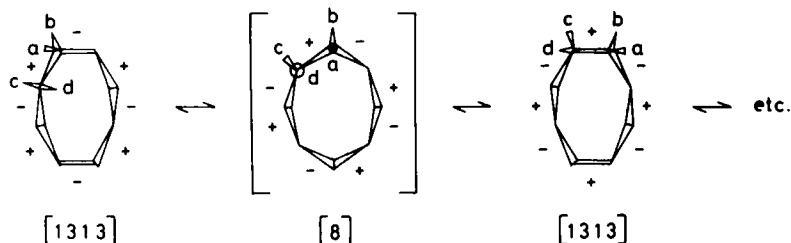


Fig. 36. Interconversion path for ring-atom site exchange in the [8] conformation of cyclooctane.

member of the nonangular [8] family, usually called crown-family. Calculations (44) place it 0.8 kcal/mol higher than [26] and observation 1.7 kcal/mol higher (47). All carbons, but not geminal hydrogens, can be exchanged (44) by passage over very low symmetric double barriers (Fig. 36). To exchange also geminal substituents it is necessary to pass a relatively high symmetrical barrier (A, Fig. 35), calculated (44) at 10.3 kcal/mol, to a [35] conformation maintaining the twofold axis. This then passes over the lower chair barrier B to its mirror image [35] and finally over A' to the inverted [1313] conformation.

The conclusion to be drawn is that if cyclooctane consists of a mixture of [26] and [1313], then the single ^1H nmr signal at high temperature should on gradual cooling, neglecting vicinal coupling, split first into a single line for [26] and a quartet for [1313]; then the single line should also become a quartet, and finally each quartet should be further split into several quartets corresponding to the real symmetry (five and two, respectively). The lowest barrier processes can, however, not be frozen experimentally (47).

Cyclooctanone and oxacyclooctane provide examples of derivatives which among the five different positions for these groups on the [26] conformation, have a particular preference for those where the group can best relieve transannular hydrogen interactions (43). This is illustrated for cyclooctanone by A in Figure 37. By going through

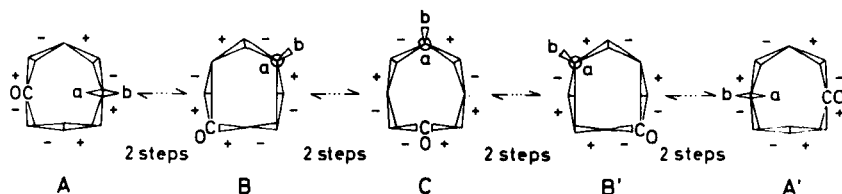


Fig. 37. One of the two interconversion paths for ring-atom site exchange in cyclooctanone ($a=b=\text{H}$), and the exclusive one for 5-*t*-butylcyclooctanone ($a = \text{H}$; $b = t\text{-Bu}$).

four full cycles of the low-energy process shown in Figure 33, the mirror image A' can be reached in two different directions (43). The one shown in Figure 37 is favored for 5-*t*-butylcyclooctanone since the bulky substituent will then remain extraannular in all seven intermediates and all eight barriers, while the other path would make it intraannular on the short side. For cyclooctanone itself the path shown is less favored since the carbonyl group must pass through the corner positions where it can not relieve transannular hydrogen interactions. The averaging produced by any of these two paths gives the carbon skeleton the constitutional symmetry, and, in fact, the observed barrier (43) is higher for the *t*-butyl derivative ($\Delta G^\ddagger = 8.0$ against 6.3 kcal/mol). To exchange also geminal hydrogens (possible only in the unsubstituted ketone) requires the passage over the higher barrier (43) shown in Figure 35 ($\Delta G^\ddagger = 7.5$ kcal/mol).

Similarly, 1,3-dioxacyclooctane strongly prefers to have the 1,3-dioxa group situated across a corner atom (48,49) and so fits the [26] conformation only in the

way shown for A in Figure 38. Constitutional symmetry is obtained for the carbon atoms by running through two cycles of the same low-energy process (Fig. 33) and geminal exchange by using also one of the higher-energy processes $[26] \leftrightarrow [26]'$ (Fig. 34) or $[35] \leftrightarrow [35]'$ (Fig. 35), and, in fact, two processes ($\Delta G^\ddagger = 5.7$ and 7.3 kcal/mol) are observed (49).

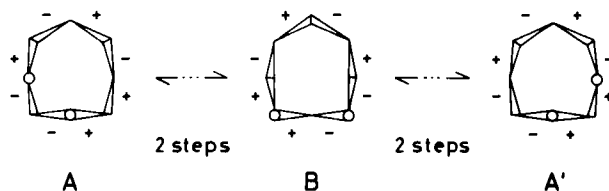


Fig. 38. Interconversion path for ring-atom site exchange in 1,3-dioxacyclooctane.

1,5-Dioxacyclooctane and cyclooctane-1,5-dione should be biased even more strongly and have both functional groups in the preferred positions of the [26] skeleton (similar to A and A' in Fig. 37), as has, in fact, been found to be true for the diketone (50) and a derivative, *cis,trans,cis*-2,4,6,8-tetrabromocyclooctane-1,5-dione (51). For the observed partial exchange of the latter, a symmetric one-step mechanism has been proposed (51), but it is entirely possible also to devise a three-step path based on the mechanisms shown to be favored for other cyclooctane derivatives. Thus, the path, $[26] \leftrightarrow [35] \leftrightarrow [35]' \leftrightarrow [26]'$, will effect the same exchanges, the bromine substituents remaining unhindered during the whole process.

1,3,5,7-Tetraoxacyclooctane shows a single ^1H nmr line at room temperature. On cooling it splits directly into a single line for the [26] family of conformers and one quartet for the [8] family (48,49). This can be taken as an argument that geminal hydrogen exchange in [8] can only take place via conversion (Fig. 35) to the same [35] conformer that is accessible over a lower barrier from [26] (Fig. 33).

K. 7-Membered Rings

Hendrickson's pioneering analysis of the dynamics of cycloheptane (5,6,52,52a) needs no revision, and the common perspective drawings of the conformations involved are satisfactory for visualization. For certain purposes, schemes of the type used with the larger rings nevertheless present some advantages.

The preferred conformation of cycloheptane, usually called twist-chair, can be described as triangular [133] or better as uniangular [7]. By the familiar corner-moving step (Fig. 39) it can pass over a low barrier, usually called chair and calculated (52) to be 1.4 kcal/mol higher, to its mirror image with all carbons moved by one position. Repetition of this step will exchange all carbon sites and also geminal hydrogen sites.

The effect of *gem*-dimethyl substitution has been analyzed (53) on the basis of Hendrickson's "pseudorotation" paths and calculated conformational energies for methyl substituents (54). With reference to the present scheme (Fig. 39), the methyl groups of 1,1-dimethylcycloheptane will prefer the g^+g^+ -corner (or isoclinal) position, but will already in the second step, when the C_2C_3 bond goes through eclipsing, give a strong 1-methyl-4-hydrogen interaction, and this barrier, estimated to be 5.3 kcal/mol, will be decisive for any site exchange.

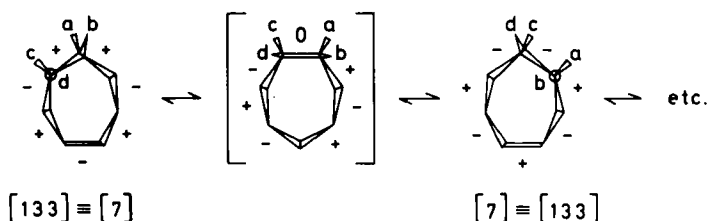


Fig. 39. Interconversion path for full site exchange in the chair conformation of cycloheptane.

Of particular interest is 1,1,4,4-tetramethylcycloheptane (53), since only one *gem*-dimethyl group can occupy the g^+g^+ -corner position. This unsymmetric conformation (A, Fig. 40) can, therefore, undergo partial exchange over medium barriers, but full exchange is hindered

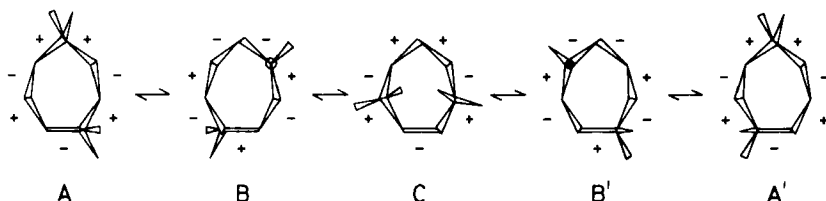


Fig. 40. Low-barrier partial exchange path for 1,1,4,4-tetramethylcycloheptane.

by the very high barrier that arises from 1,4-dimethyl repulsion when in further steps the C_2C_3 bond becomes eclipsed. In the partial exchange $A \leftrightarrow A'$ the ring atoms obtain the constitutional symmetry, like the intermediate conformer C, but geminal methyl groups and hydrogens (except the C-6 hydrogens) are not exchanged, and the mechanism for full exchange has been proposed (53) to go via the so-called boat family.

The energy minimum of the boat family, calculated (52) at 2.4 kcal/mol, may be described as triangular [223] and can be reached over a much higher barrier (Fig. 41).

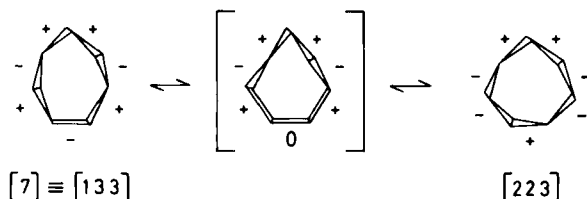


Fig. 41. Interconversion between the chair and boat family of cycloheptane.

In this twist-boat conformation, however, there is so much eclipsing distributed over many bonds, that unsubstituted cycloheptane will interconvert smoothly with itself over a very low boat barrier (calculated (52) to be only 0.3 kcal/mol higher) with substantial simultaneous changes in all bonds of the whole ring. A description in terms of distinct step processes is, therefore, no longer valid, even though the process can be formulated as a series of corner-moving steps (Fig. 42) whereby all carbons migrate now by two positions in each step, and repetition leads to full exchange. The actual mechanism is here no doubt very close to a genuine pseudorotation, that is, a molecular vibration.

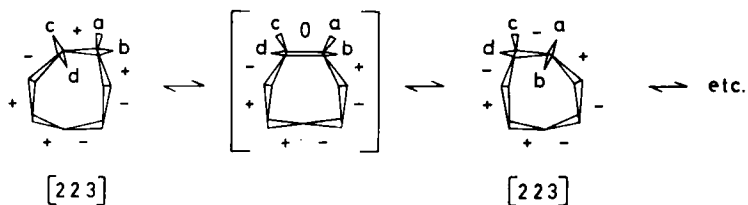


Fig. 42. Interconversion path for full site exchange in the boat conformation of cycloheptane.

L. 6-Membered Rings

The conformational situation in cyclohexane is of course better known and has been more studied (5,6,52, 100,54a) than that of any other ring system. Only a brief outline is given here from the viewpoint employed in the analysis of the larger rings.

The chair form can be considered (Fig. 1) as quadrangular [1212], which disguises its high symmetry, or as nonangular [6]. It is converted (Fig. 43) over a high barrier [$\Delta G^\ddagger = 10.8$ kcal/mol (55)] having four (nearly) coplanar ring atoms to the twist-boat, which is here considered biangular [33], and back again to an inverted chair. All carbons are, of course, already identical in the chair, and the result is simply the exchange of geminal hydrogens (axial \leftrightarrow equatorial).

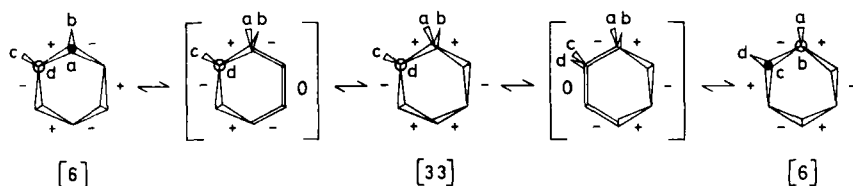


Fig. 43. Interconversion path for geminal site exchange in the chair conformation of cyclohexane.

The twist-boat [33] converts smoothly to itself over a boat-barrier of such a symmetry that two bonds are eclipsed simultaneously (Fig. 44). By repeating

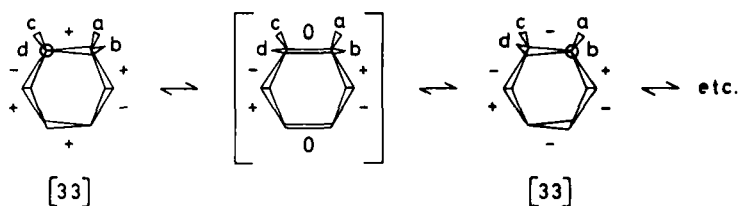


Fig. 44. Interconversion path for full site exchange in the twist-boat conformation of cyclohexane.

this step, all carbons, which are here of two types, and all hydrogens become exchanged. The barrier is only slightly higher (calculated (52, 100, 54a) less than 1 kcal/mol) than the twist-boat, so that this process may perhaps be considered as a genuine pseudor-

otation rather than as a multistep interconversion.

In substituted and hetero derivatives the process in Figure 44 need not have a low barrier, and the exchange may well occur in several steps through distinctly different intermediate twist-boats. In fact, there are cases, such as bis-pentamethylene-*s*-tetrathiane (56), where the [33] conformation is not only populated, but predominant over the [6] conformation, and where one particular twist-boat with the *gem*-dimethyl substituted carbon atoms on the twofold axis is much more stable than other twist-boats. The reason for this preference is that the methyl groups then occupy the two corner positions and that the SS bonds with the highest torsional barrier become fully staggered. Experimentally (56), the [33] \leftrightarrow [33] barrier is found to have a value between \sim 11 kcal/mol, corresponding to a faster process in the spiro-linked cyclohexane rings, and \sim 16 kcal/mol, corresponding to the slower [6] \leftrightarrow [33] interconversion of the tetrathiane ring.

A special type of multistep process must occur in aza-cycloalkanes when a conformational cycle in the ring as such must be combined with inversion at the nitrogen atom to arrive at an equivalent conformation with all sites exchanged. In six-membered rings, the critical barrier is usually (57) hard to define, but can become a clear nitrogen inversion in *N*-chloro derivatives (57) or when the ring is made "flexible" by a carbonyl group (58). However, it is difficult to decide at which point nitrogen inversion takes place, that is, whether the equatorial substituent becomes axial in the chair as a first step and vice versa in the last step, or whether inversion takes place during the stay in the boat family. It is even possible that it is synchronized with the passage of an adjoining bond through syn eclipsing.

M. 5-Membered Rings

For cyclopentane the formal extrapolation from multistep processes in the larger rings suggests that the uniaxial [5] conformation, or twist-envelope, should be considered as the stable form, and that it is converted to itself in a corner-moving step over an envelope barrier (Fig. 45). After five such steps all ring atoms and geminal hydrogens have been exchanged. Of course, in this particular case, the twist-envelope and the "barrier" are so close in energy that the whole process is really a molecular vibration, and we recognize the classic example of pseudorotation (7).

As an attempt to demystify this concept, it may be stressed that the particular situation is a consequence

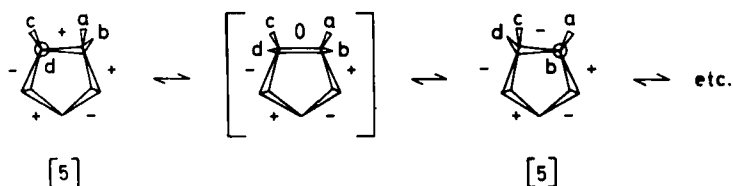


Fig. 45. Interconversion path for full site exchange in cyclopentane.

of accidental closeness in energy and of symmetry degeneracy (all minima are identical and all barriers are identical). In other five-membered rings of lower symmetry, or with another balance between valency angle potentials and torsional potentials, the interconversion process in Figure 45 may well become an ordinary multistep process.

V. CYCLIC ACETYLENES

When a multiple bond is "inserted" into a saturated chain, the simplest conformational situation results when this is a triple bond. The linear geometry of the acetylenic C_4 unit means that, as far as valency angles are concerned, only an extension of a single bond has taken place. On the other hand, there is practically no torsional barrier in the single bonds adjoining the triple bond (59), and the net result is free rotation about the "extended" single bond. In open chains this has of course the consequence that any set of three conformations in a given bond, together defined by an identical anti-gauche sequence in the other CC bonds, becomes replaced by a continuous family of conformations.

In cyclic compounds this is not necessarily so because of the restrictions of the ring. Particularly interesting cases are obtained if two acetylenic groups are introduced diametrically in even-membered cycloalkanes. Thus, cyclotetradeca-1,8-diyne (60) has two conformations, B and C (Fig. 46), directly derivable from two of the best cyclodecane conformations without any change in the saturated parts. Of these, B is the low-temperature crystal conformer, and C is the solution conformer. The conformational process which leads to geminal hydrogen exchange in conformer C (the carbon skeleton of C has already the constitutional symmetry) might have been thought of as a simple flipping of one pentamethylene

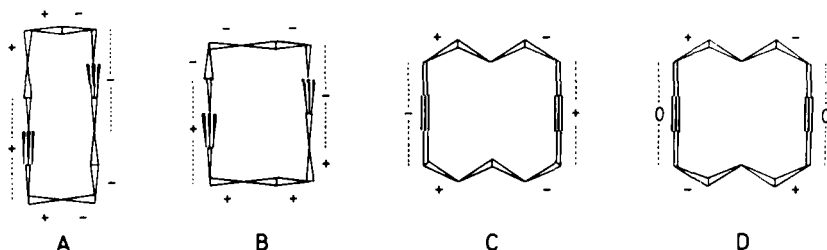


Fig. 46. Conformations of cyclotetradeca-1,8-diyne. A and B are derivable from the [2323] conformation of cyclododecane, C from the [1414] conformation.

chain to give the intermediate conformer D, which by flipping of the other chain would produce the inverted conformer C. This requires, however, the concerted eclipsing of two CC bonds in each step, which would require a much higher energy than the observed (60) barrier ($\Delta G^\ddagger = 5.0$ kcal/mol). By using energetically less expensive steps, each involving syn eclipsing of only one CC bond, it has been possible to devise two different multistep paths to achieve the same result (60). One path is composed of eight steps, and conformation D is one of the intermediates. The other path has ten steps, and conformation A and B occur twice each as intermediates.

VI. CYCLIC COMPOUNDS CONTAINING CIS DOUBLE BONDS OR EQUIVALENT UNITS

The rigid angular C_2 unit of a cis double bond in saturated surroundings is roughly equivalent to an extra CH_2 group (Fig. 47), although valency angles and

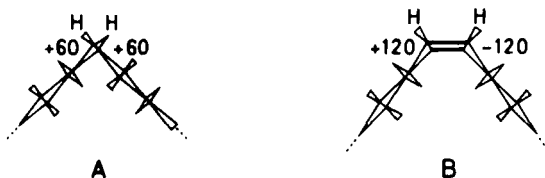


Fig. 47. A stable conformation of the cis double bond in saturated surroundings (B) compared with the CH_2 -group in "corner" position (A).

preferred torsion angles in the adjacent CC single bonds are different (61). This means that molecules like cyclopentene and cyclohexa-1,4-diene have the same conformational degrees of freedom as cyclobutane, and cycloheptene and the cyclooctadienes correspond to cyclohexane. The *cis* double bond unit fits well, of course, the geometry of normal rings, but is also efficient in creating the necessary corners in the larger rings, although the geometry and torsion-angle sign sequence (+ -) of such a corner is different from that of a g^+g^+ -corner in saturated compounds (Fig. 47). The conformational mobility of ring systems is quite differently influenced by the presence of one or more *cis* double bonds, depending on ring size. Thus, in normal rings the *cis* double bond lies so near the mean plane of the ring, that it can flip through the plane in an outward motion even more easily than can a CH_2 group. In larger rings, however, such a flipping may entrain an inward motion of the β -carbon atoms and is more strongly resisted than the corresponding movement of a CH_2 group.

A variety of medium-ring compounds contain in saturated environments two or more *cis* double bonds or groups derivable therefrom, such as the annelated benzo group, or other groups resembling it conformationally, such as the *cis*-amide group. These compounds show interesting exchange processes observable by dynamic nmr spectroscopy, and are treated together in order of increasing relative unsaturation. The conjugated compounds are beyond the scope of this chapter, due to the inherent complexities (tendency towards coplanarity, bond shift and aromaticity effects in annulenes (62), etc.).

A. *cis*-Cyclooctene

The preferred conformation for this olefin (A, Fig. 48) has no element of symmetry (63). On the basis of the sign sequence of the torsion angles it can be defined as uniaxial, with the corner in 4 position. Any exchange process must consist in moving this corner to the 7 position, and this can occur stepwise (Fig. 48) either along the saturated part ($A \leftrightarrow B \leftrightarrow C \leftrightarrow B' \leftrightarrow A'$) or through the double bond ($A \leftrightarrow X \leftrightarrow Y \leftrightarrow X' \leftrightarrow A'$). Both paths lead to the averaged constitutional symmetry for the ring atoms, but only to pair-wise averaging of geminal hydrogens. Thus, the first path exchanges only *cis*-related protons and introduces a plane of symmetry as in the central barrier C ($a = d$; $b = c$), whereas the second path exchanges only *trans*-related protons and introduces an axis of symmetry as in the central barrier

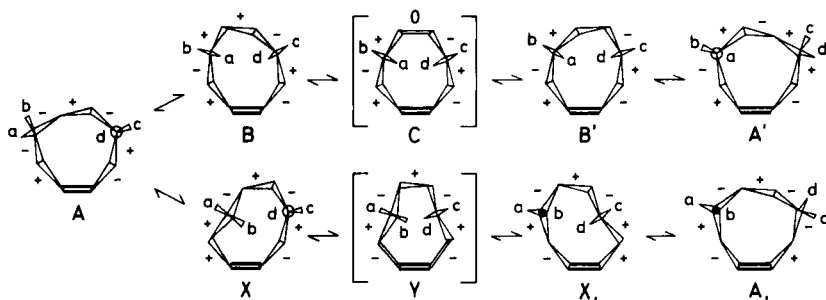


Fig. 48. The two interconversion paths needed for full site exchange in *cis*-cyclooctene.

Y ($a = c$; $b = d$). Only at a temperature when both processes can occur will full geminal exchange be observed by nmr spectroscopy. Experimentally, two processes are indeed seen (63) in the ^1H spectrum (ΔG^\ddagger 5.8 and 8.2 kcal/mol), and the lowest is found (9) to correspond to $A \rightleftharpoons A'$. This suggests that in this ring it is easier to "flip" the double bond ($X \rightleftharpoons Y \rightleftharpoons X'$) than to move the corner along the saturated chain.

In agreement with these mechanisms, only one process is observed (64) in the ^{19}F spectrum of 1-fluorocyclooctene. Both paths (Fig. 48) will exchange the two fluorine sites, and only that of lowest barrier ($A \rightleftharpoons A'$) can, of course, be observed ($\Delta G^\ddagger = 6.1$ kcal/mol). In *cis*-cyclooctene oxide, which has the same type of conformation, the constitution is such that only *cis*-related protons can undergo degenerate exchange, and so, of course, the only observed (65) process ($\Delta G^\ddagger = 8.0$ kcal/mol) must correspond to $A \rightleftharpoons A'$.

B. Cycloheptene

The best conformation for cycloheptene (66) is the chair (A, Fig. 49), definable as nonangular. Since the

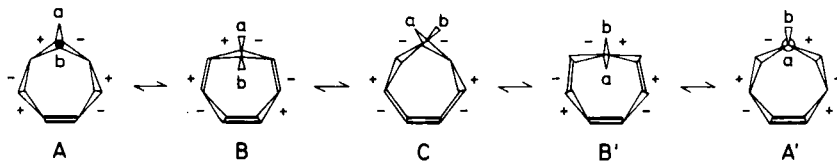


Fig. 49. Interconversion path for geminal site exchange in cycloheptene.

chair has already the constitutional symmetry for the ring skeleton, the only possible process is geminal exchange. As for cyclohexane, it is necessary to pass through the biangular boat (B, Fig. 49), but because of the lower symmetry, one pseudorotation-like step via the twist-boat C is required before passage back to the inverted chair A' can occur by the same mechanism ($B' \leftrightarrow A'$) as in the first step ($A \leftrightarrow B$). According to the strain-energy calculations (66) the cis double bond "flipping" shown in Fig. 49 is of lower energy than the alternative 5-methylene "flipping," and represents the critical barrier (5.2 kcal/mol). The boat is hardly any minimum at all and continues over a low barrier (3.4 kcal/mol) to the twist-boat minimum, which is only 0.6 kcal/mol higher than the chair. Experimentally, the barrier height for cycloheptene (67) agrees well ($\Delta G^\ddagger \sim 5.0$ kcal/mol), but for a variety of benzocycloheptenes (68) it is much higher ($\Delta G^\ddagger = 10\text{--}14$ kcal/mol). This may in part be due to the greater resistance of the benzene ring to the necessary valency angle widening at the double bond during the flipping process, but predominantly to the relief of torsion angle strain in the CC bonds next to the double bond when cycloheptene goes from the chair to the critical barrier; in benzocycloheptene there is no such torsion strain to be relieved (66).

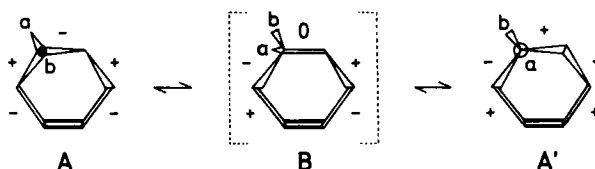


Fig. 50. Interconversion path for geminal site exchange in cyclohexene.

C. Cyclohexene

The half-chair of cyclohexene (A, Fig. 50), definable as uniaxial, is also so symmetric that only geminal exchange can be observed. This goes through the boat B, but it is not quite clear whether the boat represents an intermediate on a two-step path or is the barrier top in a direct conversion. The calculated (66) energy of the boat (6.4 kcal/mol) agrees well with the observed (69) barrier ($\Delta G^\ddagger = 5.4$ kcal/mol).

D. *cis,cis*-Cyclodeca-1,6-diene

This hydrocarbon and a series of 4,9-disubstituted and 4,9-bis-hetero derivatives have been shown (70) by several methods to have a very well defined chair-like conformation (A, Fig. 51) with perfect torsion angles in all bonds and no transannular repulsion. The mechanism by which geminal α -hydrogens are exchanged with relatively high observed activation energies (ranging from 10 to 20 kcal/mol) is, of course, most simply envisaged as a flipping of one double-bond unit to a boat-like conformation B and then a second flipping to the inverted chair A' (Fig. 51).

An interesting correlation between the height of the observed barriers and the torsional barriers in the CX bonds to be expected from simple model compounds (71) gives strictly no clue to the real mechanism, since by any mechanism these bonds must at some point pass through syn eclipsing. It is more significant that the 4,9-dioxa and dithia derivatives are exceptional in that they show lower barriers than expected from this correlation, thus suggesting a transannular interaction involving the 4 and/or the 9 group in the critical barrier (70). Based on a symmetric path of the type shown in Figure 51, it has been proposed (70) that the 4 and 9 groups come very close to each other on the barrier top. A symmetric two-step path seems improbable, however, in a ring of this size and flexibility. Also, there is no compelling reason to accept that the unfavorable boat is necessarily an intermediate conformation.

An analysis of possible multistep paths is best made with the chair drawn as in Figure 52A. If this is to be inverted to A', the four α -CH₂ groups must be turned outwards and to the opposite side in a sequence of four steps. The least expensive elementary process is considered to be the eclipsing of the 3,4 bond, requiring coplanarity of the 2,3,4,5 system, immediately followed by eclipsing of the adjacent 2,3 bond, requiring coplanarity of the 10,1,2,3,4 system. Two torsion angles thereby change sign.

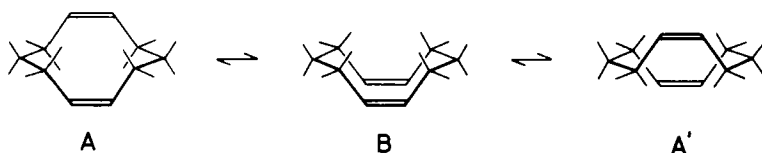


Fig. 51. Interconversion path over symmetric barriers for geminal exchange of α -hydrogen sites in *cis,cis*-cyclodeca-1,6-diene.

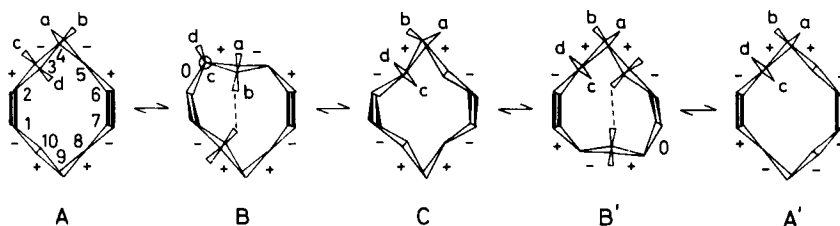


Fig. 52. Interconversion path over unsymmetric barriers for geminal exchange of α -hydrogen sites in *cis,cis*-cyclodeca-1,6-diene. *a* and *b* may also represent lone pairs or a double bond in derivatives. Note that a zero torsion angle value in the 2,3 bond represents a staggered minimum.

The first step to B and the fourth step ($B' \rightarrow A'$) are then uniquely determined by the symmetry of A, whereas for the central intermediate, three different conformations, hence three different processes, must be considered. The one chosen in Figure 52 seems most favorable. This mechanistic path does not go through the boat, but satisfies the criterion that the bulk of the 4 and 9 groups is critical in at least one step, namely the first (and the last) leading from A to B. The transannular interaction is not, however, between these groups, but between one of them and an α -CH₂. Also in conformation B (and B') this interaction remains quite serious.

No quantitative calculations of barriers have been made for this system.

E. *cis,cis,cis*-Cyclododeca-1,5,9-triene

The restrictions of the three rigid *cis*-olefin units in this ring are such that only two conformations can be envisaged, both of which have the CH₂CH₂ units in anti. One of these (A, Fig. 53) has D₃ symmetry and has been

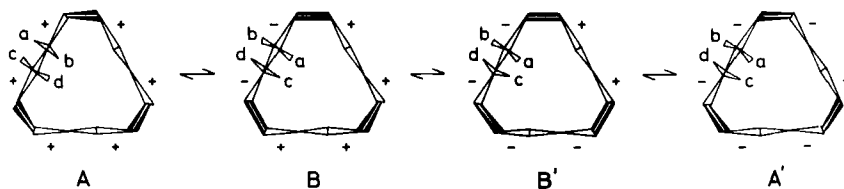


Fig. 53. Interconversion path for geminal site exchange in *cis,cis,cis*-cyclodeca-1,5,9-triene.

referred to (72) as "propeller"; the other (B) has C_2 symmetry and has been referred to (72) as "helix." If the propeller is considered the more stable, its only possible site-exchange process is the geminal exchange of inner and outer methylene hydrogens. The best elementary process seems to be a synchronous rotation of the preserved anti CH_2CH_2 unit about the two adjacent single bonds, whereby one CH_2 group must go "through" the ring, the other making an outward motion (73). At the barrier top not only these four carbons, but also one olefin unit must be roughly coplanar.* One such step leads to a helix conformation B, a second to an equivalent helix B', and a third step to the inverted propeller A' (Fig. 53) with all geminal hydrogens exchanged.

If the helix, which is favored by the presence of a "wrong" ++ conformation around only one of the *cis* double bonds, is considered the more stable, it needs only to interconvert repeatedly with itself using steps of the kind $B \rightarrow B'$ (Fig. 53) in order to achieve full site exchange. After two such steps the three types of methylene carbons are exchanged, and after three further steps also inner and outer methylene hydrogens become exchanged.

The 1H nmr spectrum of *cis,cis,cis*-cyclododeca-1,5,9-triene is in fact temperature dependent (74), but no conclusions could be drawn.

On the other hand, a tris(3,6-dimethylbenzo) derivative (A, Fig. 54) has been studied successfully by dynamic

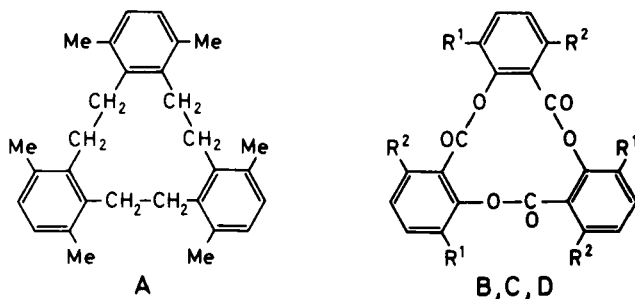


Fig. 54. Tris (3,6-dimethylbenzo)cyclododeca-1,5,9-triene (A), and cyclic trisalicylides (B: $R^1=R^2=Me$; C: $R^1=Me$, $R^2=iPr$; D: $R^1=iPr$, $R^2=Me$).

*Although the motion of a CH_2 group through the ring may seem energy demanding in a 12-membered ring, the other possibility, a rotation about the CH_2CH_2 bond in an outward motion and through syn eclipsing is severely hindered by the rigid *cis* geometry of the double bonds.

nmr spectroscopy (72) and found to be present in the helix conformation exclusively, interconverting over a barrier of $\Delta G^\ddagger = 17.1$ kcal/mol. Strain-energy calculations (72) give 16.7 kcal/mol for the $B \rightleftharpoons B'$ barrier (Fig. 53) and a similar value for the unobserved $A \rightleftharpoons B$ barrier, but these can not be simply related to the triolefin, because of the steric hindrance of the aromatic methyl groups and the lack of torsional barriers in the CC bonds next to the aromatic ring.

A series of cyclic trisalicylides (B,C,D; Fig. 54), where the CH_2CH_2 units are replaced by trans ester units, provide examples of compounds with both helix and propeller conformers populated, the propeller even predominantly, and both barriers can be determined (73). The best direct comparison is the tris-3,6-dimethylsalicylide (B, Fig. 54) where the barrier separating the helix conformers is even lower ($\Delta G^\ddagger = 14$ kcal/mol) than in the hydrocarbon. This supports the proposed mechanism, since the larger carbonyl group turns outward and the ring oxygen, being smaller than a CH_2 group, goes through the ring. The other barrier, separating propeller and helix, is higher ($\Delta G^\ddagger = 18$ kcal/mol). With larger substituents (C and D; Fig. 54) both conformational barriers increase because of steric hindrance (73).

F. *cis,cis*-Cycloocta-1,5-diene

The CH_2CH_2 units of this smaller ring cannot be anti; even in the chair form they are only 120° and thus eclipsed. The favored conformation is a distorted biangular boat (A, Fig. 55) which averages over a boat barrier

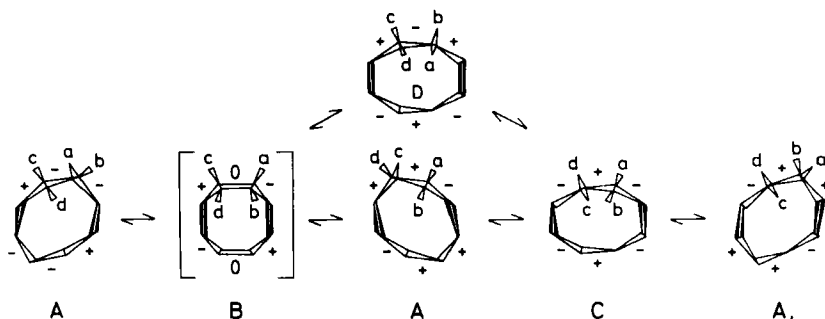


Fig. 55. Interconversion paths for *cis,cis*-cycloocta-1,5-diene.

(B) of only 4.3 kcal/mol with its mirror image (A') to obtain the symmetry of the barrier (75); only *cis*-related

hydrogens are thereby exchanged. A similar pseudorotation-like movement in the opposite direction leads to a twist-boat C, also called skew form, which is an intermediate or barrier to the inverted distorted boat A, (Fig. 55). By this process the carbon sites are again exchanged, but now only *trans*-related hydrogens exchange sites. This may correspond to the higher-energy process ($\Delta G^\ddagger = 4.9$ kcal/mol) seen only (75) in the ^1H nmr spectrum, since full exchange results when both processes occur rapidly. It will be appreciated that both these processes involve the whole ring and, due to the constraints of the ring, have no localized character. The whole path $A' \leftrightarrow A \leftrightarrow A$, shown in Figure 55 has the flavor of boat-cyclohexane "pseudorotation."

An alternative mechanism for geminal exchange is the conversion to the nonpopulated chair conformation of nonangular type (D, Fig. 55) and back again. This process can occur (76) from either of the boat conformers, for example, from B, by bringing six ring carbons ($-\text{C}-\text{C}=\text{C}-\text{C}-\text{C}-$) into coplanarity or from C, by bringing four ring carbons ($=\text{C}-\text{C}-\text{C}-\text{C}=\text{C}$) into coplanarity. The analogy with the cyclohexane boat \leftrightarrow chair transitions is again evident.*

The corresponding dibenzo derivative exists as a mixture of the "pseudorotating" boat (presumably also distorted) and the chair, as seen in the low-temperature nmr spectrum (76,77). The barrier between them can, therefore, be observed and is much higher ($\Delta G^\ddagger = 10.2$ kcal/mol). The barrier to equilibration within the boat family is lower ($\Delta G^\ddagger = 7.5$ kcal/mol) (77). Strain-energy calculations (76, 76a) give similar energies for the chair and the boat minima, 4.7 and 6.8 kcal/mol respectively for the critical "pseudorotation" barrier and 11.5 kcal/mol for the lowest barrier separating these forms from the chair.**

Several hetero analogs have also been studied (78). The replacement of the CH_2CH_2 unit by CH_2S favors the boat and raises both critical barriers. The introduction of one ester group will, of course, stabilize the boat by the planarity of the cis ester, and the barrier between boat and twist-boat is doubled (10 kcal/mol). With two ester groups, as in substituted cyclic disalicylides,

*The former barrier is calculated (76a) to be of slightly lower energy than the pseudorotation barrier C (5.2 against 5.9 kcal/mol), so that either of the two may correspond to the observed higher-energy process (75).

**The increased height of this latter barrier in the dibenzo derivative, as compared with the diene itself, is again rationalized on the basis of torsion-strain release in the barrier of the diene.

this barrier is 18 kcal/mol. The *N*-benzylamide group, with its still stronger requirement for planarity, increases the barrier even more (21 and >27 kcal/mol, respectively).

G. *cis,cis,cis,cis*-Cyclododeca-1,4,7,10-tetraene

The conformational freedom in this ring is severely limited by the rigid *cis*-olefin units. Just four conformations are possible, different only in the up-down relationship between the four CH₂ groups. Of these, the one with up-down alternation is probably the least favored as it has two very close transannular CH₂ interactions. It is also not needed as an intermediate in the interconversion of the remaining three conformations (A, B and C; Fig. 56).

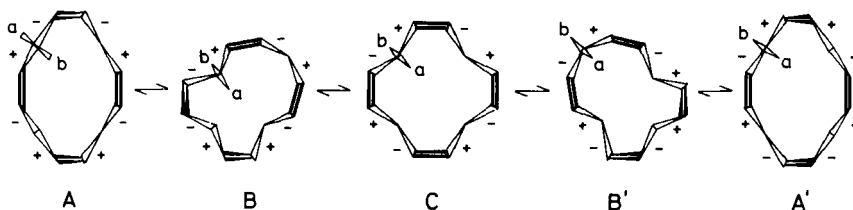


Fig. 56. Interconversion path for geminal site exchange in *cis,cis,cis,cis*-cyclododeca-1,4,7,10-tetraene.

The mechanism of their interconversion is particularly interesting because the outward bending of a CH₂ group is made difficult by the ring geometry imposed by the neighboring *cis* double bonds, whereas, on the other hand, the rotation of a CH₂ group through the ring is surprisingly favored in spite of this being a medium ring.

The tetraene itself is not known, but the corresponding tetrakis(4,5-dimethoxybenzo) derivative (cyclotetraveratrylene) has been studied by nmr (79) and found to take the "sofa" conformation A, with full exchange occurring over a barrier of $\Delta G^\ddagger = 13$ kcal/mol. It has been proposed (79) that the mechanism is a successive rotation of the four CH₂ groups, probably via the "crown" conformation C. This is in accord with the detailed path shown in Figure 56. It is not obvious, however, that the CH₂ groups must necessarily pass through the ring; it may well be so in the second (and third) step, but an outward motion seems more likely in the first (and fourth) step.

H. *cis,cis,cis*-Cyclonona-1,4,7-triene

In this smaller ring the constraints of the *cis*

double bond unit definitely exclude the possibility that the CH_2 groups can be turned "through" the ring. The preferred conformation (80-82) is a crown with all CH_2 groups on one side, all double bonds on the other (A, Fig. 57). The activation free energy for the only

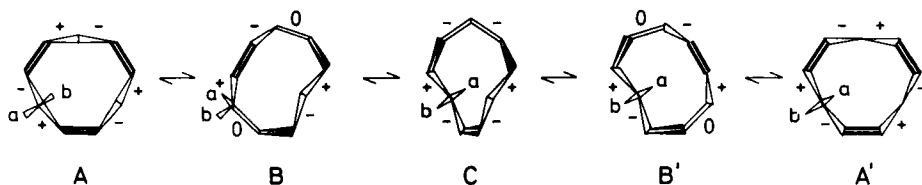


Fig. 57. Interconversion path for geminal site exchange in *cis,cis,cis,cis*-cyclonona-1,4,7-triene.

observable process, geminal hydrogen site exchange, is found (82) by nmr spectroscopy to be 14.5 kcal/mol and represents most probably the passage over the first barrier on the interconversion path shown in Figure 57. Whether the mechanism is a CH_2 flipping or *cis* double-bond flipping is not clear, but in analogy with the related situation in cycloheptene, the latter mechanism has been chosen in Figure 57. The resulting intermediate boat conformation B is then further converted in a pseudorotation-like movement over lower barriers to the twist-form C, thence to a second boat B', and finally to the inverted crown A'. A one-step synchronous ring-flattening inversion of the whole molecule has been favored (81) on the basis of an observed, apparent, very large, negative entropy of activation, but is utterly unlikely.

The aromatic analogs, the tribenzo derivative (83) and the tris(4,5-dimethoxybenzo) derivative (84) (cyclo-triveratrylene), have also the crown conformation, but the barrier for geminal hydrogen exchange becomes unobservable (84) by dynamic nmr spectroscopy up to 200°. A conformationally chiral derivative has even been resolved (85), and two conformationally different alcohols isolated (84), and so the barrier must be higher than 23 kcal/mol. That the barrier is higher than for the triene may again be due to relief of torsional strain in the transition state of the triene, to the smaller ring valency angles at the aromatic nucleus than at the double bond (120 vs 123°), and to the higher resistance to twist of the aromatic nucleus, making the flipping process more symmetric and concerted in several bonds. It may also be of importance that during the flipping of the aromatic group ($A \leftrightarrow B$, Fig. 57) the other two groups come close to each other

across the ring; this then is a reason to exclude the alternative CH_2 flipping mechanism.

The intermediate conformations become populated exclusively when substitution creates steric hindrance in the crown, for example, geminal substitution of one methylene group with methyl and hydroxyl (84). The better conjugation of a carbonyl group with the aromatic nuclei is assumed to be the reason why the monoketone prefers to be exclusively in a rapidly interconverting twist form (84). When the carbonyl group is replaced by an exocyclic methylene group, both crown and twist conformers are populated, and the barrier between them becomes measurable by simple equilibration (84) and is found to remain very high (20-24 kcal/mol). It is, therefore, unlikely that the low-barrier process becoming slow in dynamic nmr spectroscopy at -80 to -90°C in the oxa derivative ($\Delta G^\ddagger = 9$ kcal/mol) is the passage of a crown to the boat to obtain CH_2 exchange (83), but rather the repeated interconversion of boat and twist forms. If the boat (B, Fig. 57) with ether oxygen pointing into the ring is the preferred conformation, all geminal hydrogens will be exchanged after six steps of the type $\text{B} \rightleftharpoons \text{C} \rightleftharpoons \text{B}'$.

Finally, the cyclic tripeptide of sarcosine (86), which has all three *N*-methyleamide groups *cis*, shows a barrier to geminal CH_2 exchange of 20 kcal/mol, and again an interconversion scheme of the type shown in Figure 57 has been proposed (87). That the barrier is also here higher than for the olefin is difficult to understand, because twisting of the amide bond should be more easy. Possibly the resistance to valence angle opening is increased due to the greater size of the NCH_3 and C=O groups as compared with the olefinic CH groups. Also, the trans-annular repulsion referred to in the discussion of the benzo derivatives may play a greater role between two *N*-methyleamide groups than between two *cis* double bonds.

VII. CYCLIC COMPOUNDS CONTAINING TRANS DOUBLE BONDS OR EQUIVALENT UNITS

The rigid C_4 unit of a trans double bond in saturated surroundings is not just an extended single bond like the acetylenic C_4 unit. First of all, the geometry is not linear, and in any scheme for full interconversion the trans double bond has to be rotated about its adjacent single bonds, whereby one carbon makes an outward motion and the other has to pass "through" the ring (Fig. 58). This rotation is, therefore, more or less hindered, depending on the substituents on the double bond. Secondly,

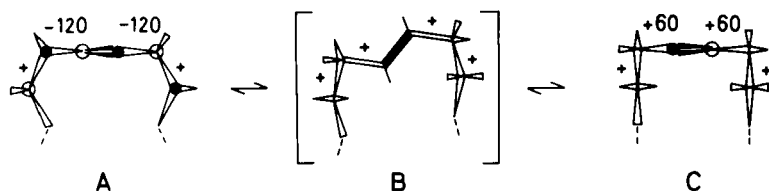


Fig. 58. A stable conformation of the trans double bond in saturated surroundings (A) and an unstable situation (C) resulting from its rotation by 180° .

rotation about adjacent single bonds is not free as in acetylenes, but hindered by well-defined torsional barriers (61) so that the orientation as shown in A (Fig. 58) represents an energy minimum. After 180° rotation the adjacent single bonds will be in eclipsed positions, and the result C is therefore no conformational minimum.

On the other hand, any process in the saturated part of the cyclic chain, which is also necessary for geminal exchange, will lead to the same wrong conformational situation about the trans double bond. Both processes must, therefore, occur to obtain full exchange. If a ring contains one or more trans double bonds, it is sufficient that the rotation of one of these is blocked, and full site exchange or even partial exchange becomes impossible, no matter how mobile the saturated part or the other trans double bonds are.

Since a certain ring size is necessary to incorporate stably a trans double bond in a ring system, and the rotation of this double bond as such should become very easy once a critical ring size is exceeded, it is not surprising that known examples of cyclic *trans*-olefins which show temperature variation of their nmr spectra, are restricted to 10-, 11-, and 12-membered rings.

A. *trans,trans,trans*-Cyclododeca-1,5,9-triene

The crystal conformation of this triolefin (88) is shown in Figure 59A, and it is characterized by having all single bonds correctly staggered. Conversion of the three CH_2CH_2 bonds from g^- to g^+ in three steps of syn eclipsing ($A' \rightarrow B$) can only lead to the unstable conformation B. Also, rotation of all three trans double bonds in three steps ($A \rightarrow B$) can only lead to this same wrong conformation. Both processes must occur in order to observe geminal CH_2 exchange, and the activation energy corresponds to

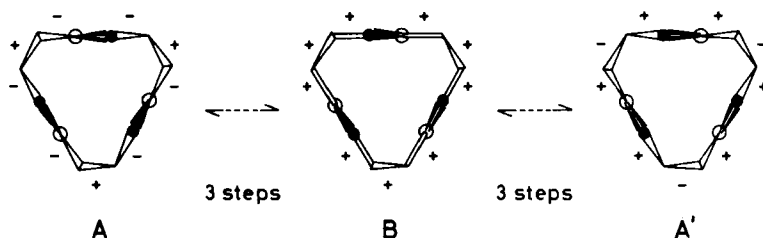


Fig. 59. Interconversion path for geminal site exchange in *trans,trans,trans*-cyclododeca-1,5,9-triene.

that one of the processes which has the highest barrier. The experimental value (89) is so high ($\Delta G^\ddagger \approx 9$ kcal/mol) that it most likely represents a *trans* double bond rotation step.

B. *trans,trans,trans*-Cycloundeca-1,4,8-triene

The crystal structure of the 2,6,6,9-tetramethyl derivative (humulene) shows here a conformation related to that of cyclododeca-1,5,9-triene with only *trans* double bonds (90). Two of these carry one methyl substituent each, but rotation is still possible since the remaining olefinic hydrogen can be the one that is turned "through" the ring. A relatively high activation energy for geminal exchange has been observed ($\Delta G^\ddagger = 10.6$ kcal/mol), and the possible processes involved have been discussed (91).

C. *trans,trans*-Cyclodeca-1,5-diene

The crystal conformation observed (92) for the 1,5-dimethyl-8-isopropylidene derivative (germacratriene) is of type A shown in Figure 60. This may be thought of as derived from the [1333] conformation of cyclodecane by placing the two *trans* double bonds in three-bond sides and rotating both to satisfy the torsion angle requirements in the adjacent single bonds. There are thus no "corner" atoms according to the torsion-angle sign definition, and the conformation may be called nonangular or "crown."

If only one *trans* double bond is rotated, conformation B is obtained; it has two "corners" and may be characterized as biangular. The process (Fig. 60) which exchanges the geminal hydrogens of A must necessarily involve rotation of both double bonds, and B will, therefore, be an intermediate. It is also necessary to move a g^+g^+ corner

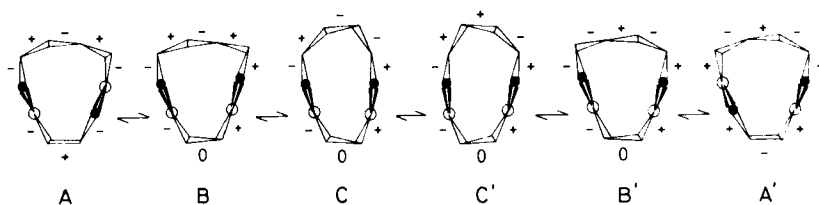


Fig. 60. Interconversion path for full site exchange in *trans,trans*-cyclodeca-1,5-diene.

in the saturated part by three steps over presumably lower barriers through the intermediate conformers C and C' to arrive at the mirror image conformer B', which then by rotation of the second double bond over a high barrier gives the inverted conformer A'.

The temperature variation of the nmr spectrum of 1,5-dimethylcyclodeca-1,5-diene (93) can be explained on this basis. In addition to conformer A (=A'), two other conformers are also seen in the low-temperature spectrum (93). They can be identified as B and B' (which are now different due to the methyl substituents) on the basis of coupling constants and chemical shifts, and they interconvert over a relatively low critical barrier ($\Delta G^\ddagger = 8\text{--}10$ kcal/mol) which must be one of the three barriers on the path $B \rightleftharpoons C \rightleftharpoons C' \rightleftharpoons B'$ (Fig. 60). To interconvert also with A, so as to get full exchange of all the three populated conformers, the passage over a higher barrier ($\Delta G^\ddagger = 15\text{--}17$ kcal/mol) is necessary. This then is the energy required to rotate the *trans* double bond, with the olefinic hydrogen passing through the ring, the methyl group out.

This analysis is in agreement with the original discussion (93), but differs from it in the way the possible conformations are derived and in the detailed mechanism for the interconversion of B with B'.

D. *trans*-Cyclodecene

The crystal conformation of this *trans*-monoolefin (94) as silver nitrate complex (A, Fig. 61) is derivable from the [2323] conformation of cyclodecane by placing the *trans* double bond in a three-bond side and rotating it to obtain correct dihedral angles in the adjacent single bonds (37). The torsion-angle signs define it as biangular [37]. With this high symmetry, only one process should be observable in dynamic ^1H nmr spectroscopy and none in ^{13}C spectroscopy if A is the exclusive conformer in solution. The fact that in addition to a high-barrier

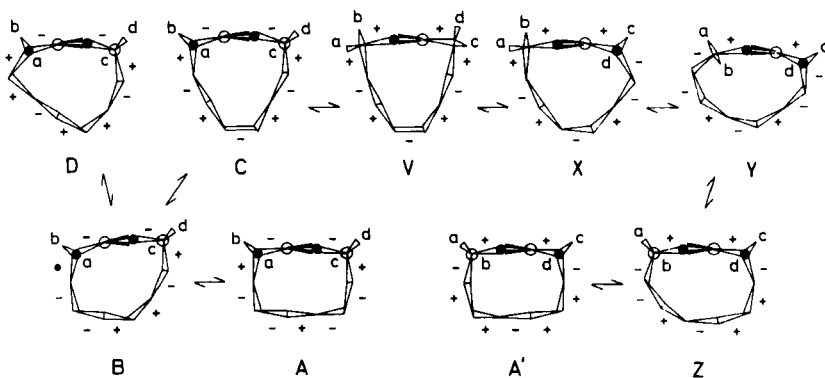


Fig. 61. Interconversion path for *trans*-cyclodecene.

process for geminal exchange ($\Delta G^\ddagger = 12.0$ kcal/mol) also a low-barrier process is observed (95), would, therefore, mean that there is in solution either a single conformation of lower symmetry which by partial averaging over a low barrier acquires the constitutional symmetry for the ring atoms, or that there is a mixture of several conformations. The latter possibility is the more likely, since the 3,3-difluoro derivative (96) shows the same high-barrier process for geminal exchange ($\Delta G^\ddagger = 12.4$ kcal/mol) and a low-barrier process representing the averaging of at least five different conformers, all of which are appreciably populated.

On this basis the interconversion scheme in Figure 61 is proposed. Some of the intermediate conformations (B and C) are of the same biangular type as the crystal conformation (A) in being derivable from low-energy quadrangular cyclodecane conformations (B, or [28], from [2233]; C, or [19], from [1333]). In addition, a fourth conformation of the same type (D, or [37], derived from [1333]) should exist, and has, in fact, been found in the crystal structure of *trans*-5-cyclodecenyl *p*-nitrobenzoate (37), but it is not needed as an intermediate on the interconversion path for A. For the unsymmetric 3,3-difluoro derivative there will be an additional variant of B and of D. All these biangular conformers may be expected to be of low energy, and they can be interconverted by the familiar corner-moving steps, but without effecting geminal exchange. It seems, therefore, highly probable that these are the six conformations that can be populated by 3,3-difluorocyclodecene, five of which are observed in the ^{19}F spectrum (96). They average over low barriers to give the constitutional symmetry for the ring atoms, but one fluorine atom will remain "axial" and have anti coupling

to the olefinic and one aliphatic proton, whereas the other will remain "equatorial" and have only gauche couplings; this is all in accord with the spectra (96).

To achieve geminal exchange, the trans double bond must be rotated through the ring at some point, most likely in the crown-like nonangular conformation C (Fig. 61). The resulting biangular conformation V can then proceed by four successive corner-moving steps to the inverted crystal conformation A'. All these intermediate conformations (V,X,Y,Z) are probably unpopulated, since there is more eclipsing strain in the saturated part.

The important conclusion is now that, contrary to what has been assumed in earlier discussions (95,96), it is not necessary to perform a high-energy rotation of the 6,7-CH₂CH₂ group as such through the ring, only of the rigid double bond.

VIII. CYCLIC COMPOUNDS CONTAINING BOTH CIS AND TRANS DOUBLE BONDS

Examples of nonconjugated cyclic olefins containing both cis and trans double bonds are few, and still fewer have been studied from a conformational point of view. Cyclic peptides, however, can be considered as belonging to this category if the conformational barriers for the ring skeleton are lower than the barrier for cis-trans isomerization of the amide groups. Nevertheless, for simplicity, the olefin case is shown for the general discussion of interconversion mechanisms.

A. *cis,trans,cis,trans*-Cyclododeca-1,4,7,10-tetraene

Since there are only single CH₂ groups between the double bonds, the conformational freedom is restricted to the up or down orientation of these groups. Furthermore, the geometry is such that the two CH₂ groups adjoining a cis double bond must be on the same side, and so the three conformations A, B, and C (Fig. 62) become the most likely. Among these, the crown-like conformation A has the most favorable torsion angles in the single bonds and is indeed the type observed for a series of cyclic tetrapeptides (97,98).

The number of possible interconversion paths is reduced by the restriction that if one CH₂ group is turned in an outward motion over to the other side of the ring, the resulting strain will force the one on the other side of the cis double bond to follow immediately (87). Conformation A can thus be converted in a kind of unsymmetric cis double bond flipping to conformation B,

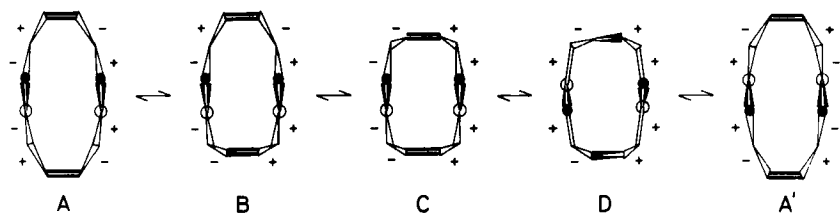


Fig. 62. Interconversion path for geminal site exchange in *cis,trans,cis,trans*-cyclododeca-1,4,7,10-tetraene.

and by a second flipping further to conformation C (Fig. 62). This is, however, how far this type of mechanistic step will take it, and it can only return from these unpopulated conformations to the original one, A. It is necessary also (87) to rotate both trans double bonds as such, one after the other, to proceed further via conformation D to the inverted conformation A'. Strictly, the sequence of *cis* double bond flipping and trans double bond rotation steps may be different from that shown in Figure 62, but this does not alter the argument. If both hydrogens of at least one of the trans double bonds are substituted, the step involving rotation of this bond may become critical and prevent geminal exchange. No hindrance is expected if there remains one olefinic hydrogen on each, since this is then the one which turns through the ring.

The nmr spectrum of cycloglycylsarcosylglycylsarcosyl (98) reveals this type of conformation with both trans positions occupied by the two CONH amide bonds, and the CH₂ exchange occurs (87) over a relatively low barrier ($\Delta G^\ddagger = 13\text{--}14$ kcal/mol). The smaller substituent NH can here pass through the ring with little hindrance. On the other hand, dynamic nmr spectroscopy of both cycloglycyltrisarcosyl (98) and cyclotetrasarcosyl (86) reveal much higher barriers (~ 23 kcal/mol) for CH₂ exchange, in fact, higher than necessary for *cis-trans* isomerization of free amide groups. The smallest substituent on one or both *trans*-amide groups is here C=O, and this is too large to be rotated through the ring. A rotation about the CN partial double bond in an outward motion to the *cis*-configuration and back to the other trans configuration becomes necessary. That this is the mechanism is supported by the fact that *cis-trans* configuration exchange between all four amide groups occurs simultaneously with CH₂ exchange in cyclotetrasarcosyl (86) the only of these compounds where the constitutional symmetry allows

its observation by dynamic nmr spectroscopy.

α -Substituents can only be accommodated in the outer position, hence may alter the population of conformations A, B, and C. Thus, whereas cyclo-glycyl-L-prolyl-glycyl-D-prolyl (99) fits the centrosymmetric conformations A and C, but not the unsymmetric conformation B (Fig. 62), the opposite is true for the L,L isomer (99). Geminal exchange is of course not possible here, but for the L,L isomer two *trans*-amide rotation steps (87,99) will effect exchange with the pseudorotated conformation ($A \leftrightarrow A'$ in Fig. 63), whereby the molecule acquires by averaging the twofold symmetry of the intermediate (unpopulated) conformation B (Fig. 63). The observed activation energy ($\Delta G^\ddagger = 13-15$

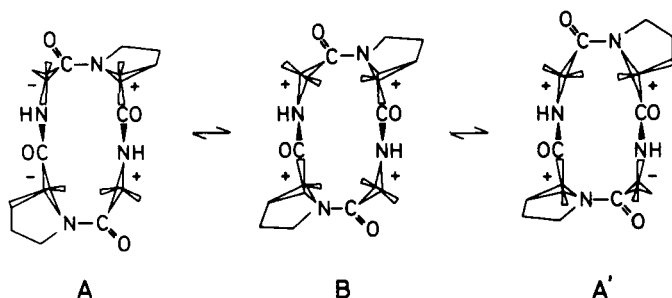


Fig. 63. Interconversion path for cyclo-glycyl-L-prolyl-glycyl-L-prolyl.

kcal/mol) for this process (99) is very similar to that observed for full exchange in cycloglycylsarcosylglycylsarcosyl, and so supports the postulation of *trans*-amide rotation as the critical step on the full interconversion path in Figure 62.

IX. BICYCLIC AND MULTICYCLIC COMPOUNDS

Each ring in a bicyclic (or multicyclic) compound can be considered as substituted by the other ring (or rings). In the same way as a monocyclic compound can obtain geminal site exchange only if substituents occur as geminal pairs of identical groups, similar conditions must be satisfied in order to make geminal site exchange processes possible in bi- and multicyclic compounds.

In the majority of commonly encountered cases this condition is not met. Thus, in *cis*- and *trans*-decalin geminal site exchange is excluded; only ring-atom site exchange can occur if the conformational symmetry is lower

than the constitutional symmetry.

When a ring is substituted by two equivalent bridges between the same two ring atoms, then, of course, geminal exchange can occur, as in the simple flipping of the longest bridge of bicyclo[3,1,1]heptane (100). Multistep mechanisms become possible when all bridges are equal.

Only a limited number of examples of such conformational processes have been observed. They represent such a variation in type that each is treated separately, and no classification in subgroups is attempted.

A. *trans*-Decalin

The strongly favored conformation for this bicyclo[4.4.0]-decane isomer, with both rings in the chair form (101), has already the high symmetry corresponding to the constitutional symmetry for the carbon atoms (A, Fig. 64). This is the real reason why *trans*-decalin behaves differently from *cis*-decalin in dynamic nmr spectroscopy, not a difference in flexibility; it is of course as easy to get one or both rings into the boat form in both isomers.

If *trans*-decalin had the less symmetric boat-boat conformation X (Fig. 64) with carbon atoms of five different

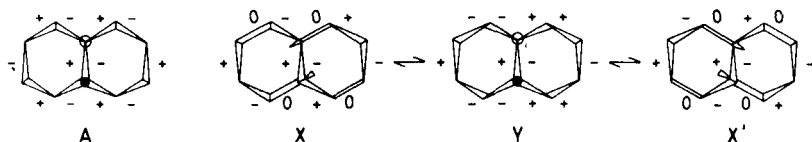


Fig. 64. The chair-chair form (A), and the interconversion path for site exchange in the boat-boat form (X) of *trans*-decalin.

types, it could have passed in two steps to the equivalent boat-boat B' and acquired by such averaging the symmetry of the intermediate twist-twist form Y with carbon atoms of only three different types (as in the chair A). The pseudorotation within each ring is limited by the trans fusion to the process shown in Figure 64, and any change in one ring is concerted with a corresponding change in the other.

B. *cis*-Decalin

The interconversion of the favored chair-chair conformation (A, Fig. 65) to an equivalent one must go through several intermediates (102). Each ring is first

converted from chair to boat, one after the other, and then the boat-boat conformation C pseudorotates to an equivalent boat-boat C' via the symmetric boat-boat D. Finally, the inverted chair-chair is reached in two last steps equivalent to the two first. The carbon skeleton thereby acquires the averaged symmetry corresponding to the central intermediate D, which is also the constitutional symmetry. This process is best seen in the ^{13}C nmr spectrum (103) and has an activation energy of $\Delta G^\ddagger = 12.6$ kcal/mol; it corresponds most probably to the barrier of the second step, $\text{B} \rightleftharpoons \text{C}$ (Fig. 65). The process

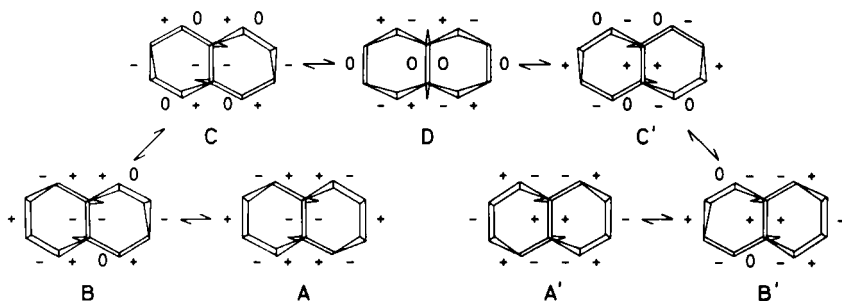


Fig. 65. Interconversion path for site exchange in *cis*-decalin.

is also seen, but much less clearly, in the ^1H spectrum (102); each proton goes from an axial to an equatorial site, and vice versa, although no geminal exchange occurs. The 2,2,7,7-tetramethoxy derivative (104) is very suitable for the determination of the barrier, since the four methoxy signals coalesce to two ($\Delta G^\ddagger = 12.4$ kcal/mol). In the ^{19}F spectrum of the 2,2-difluoroderivative (105) the same process is observed as the coalescence of two AB quartets to one AB quartet ($\Delta G^\ddagger = 12.3$ kcal/mol); the quartets belong to two different conformers present in the ratio 3:1.

Strain-energy calculations (105) of the overall barrier based on this multistep mechanism give a value of 17 kcal/mol. A simple estimate (9) based on adding a cyclohexane barrier (10 kcal/mol) to the energy of a boat conformation B (5 kcal/mol) gives an even better value of 15 kcal/mol.

C. *cis,syn,cis*-Perhydroanthracene

When several cyclohexane rings are fused together, it is sufficient that one of the fusions is trans to

block a conformational exchange process.* The simplest example of an interconvertible doubly *cis*-fused system is *cis, syn, cis*-perhydroanthracene (A, Fig. 66). Its exchange

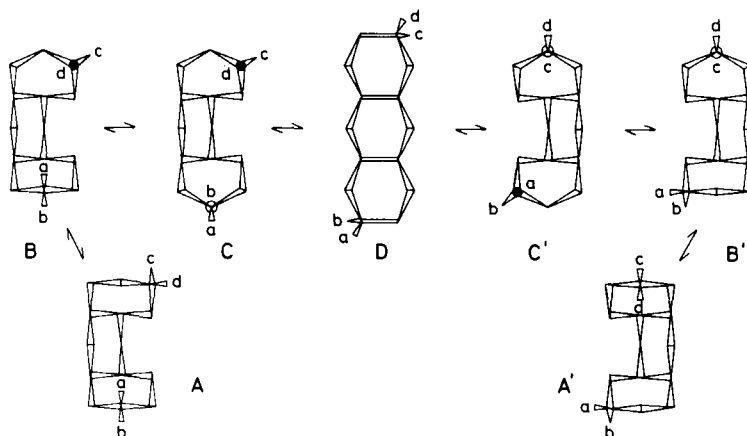


Fig. 66. Interconversion path for site exchange in *cis, syn, cis*-perhydroanthracene.

scheme must involve the conversion of all three rings to boat forms, one after the other, to produce the central intermediate conformation D with full constitutional symmetry, from which the inverted conformation A' can be reached. The sequence of steps is not uniquely given; it is only certain that the middle ring can not be the first to change to the boat form since it is locked by two chairs. The critical barrier for this multistep process has been determined on the 2,2,6,6-tetramethoxy derivative (106), where the four nmr lines corresponding to methoxy positions *a*, *b*, *c*, and *d* (Fig. 66) become averaged to two on heating ($a = d$, $b = c$); the activation energy is surprisingly low ($\Delta G^\ddagger = 11.2$ kcal/mol), probably because 1,3-diaxial strain caused by *a* or *d* in one of the chairs raises the energy of the ground state (106).

*If one ring is large enough to connect the 1,2-diaxial positions of adjacent cyclohexane rings, exchange processes become possible, as observed recently (105a) in *trans, syn, trans*-4,5:9,10-biscyclohexane-1,3,6,8-tetraoxacyclodecane. A twelve-step interconversion scheme, different from the one proposed (105a), can be devised to explain the two observed processes. It employs only the low-energy mechanistic steps of Fig. 22 for the 10-membered ring, but requires conversion of the cyclohexane rings to boat-forms in the critical step of $\Delta G^\ddagger = 11.7$ kcal/mol observed by dynamic nmr.

D. *cis*- $\Delta^{2,6}$ -Hexalin

In contrast with the situation in *cis*-decalin, where passage of the critical barrier and conversion to the boat-boat conformation can occur before the need arises to rotate about the central bond common to both rings (Fig. 65), no conformational change can occur in either of the rings of this particular diolefinic derivative without involving exactly this common central bond (Fig. 67). This is because "inversion" of the favored conformation of cyclohexene (as in both rings of A) implies eclipsing of the single bond opposite to the double bond, and any process in one ring must, therefore, be concerted with the same process in the other ring. The critical barrier should thus have both rings near a boat-like energy maximum (B, Fig. 67).

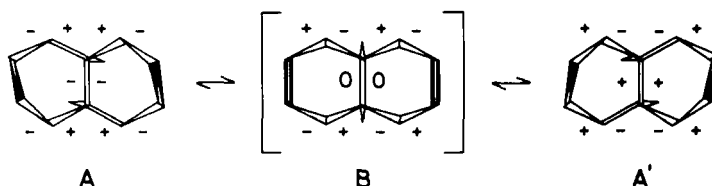


Fig. 67. Interconversion process for site exchange in *cis*- $\Delta^{2,6}$ -hexalin.

It is, therefore, not surprising that the activation energy measured on 9,10-disubstituted derivatives (107) is more than twice as high ($\Delta G^\ddagger = 12-14$ kcal/mol) as for the isolated cyclohexene ring ($\Delta G^\ddagger = 5.3$ kcal/mol). The barrier for *cis*-decalin, for comparison, is only 20% higher than for cyclohexane.

It is likely that the symmetric form B (Fig. 67) represents the barrier top rather than an intermediate between two slightly higher equivalent barriers, and so this is one of the few examples of a large molecule undergoing only a one-step conformational process over a symmetric barrier.

E. Tricyclo[4.4.4.0^{1,6}]tetradecane

Very closely related to *cis*-decalin is this so-called [4.4.4]propellane, which contains actually the *cis*-decalin skeleton three times (Fig. 68). In the same way as both chairs of *cis*-decalin must be converted to boats before the crucial rotation about the common bond ($\underline{g^+} \leftrightarrow \underline{g^-}$) can

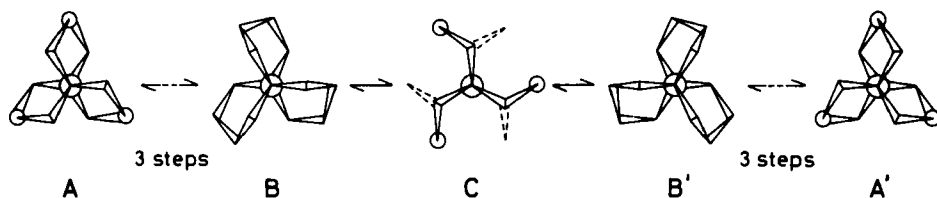


Fig. 68. Interconversion path for site exchange in tricyclo[4.4.4.0^{1,6}]tetradecane.

occur, with concerted pseudorotation in both rings, all three chairs of the propellane (A, Fig. 68) must be converted to boats, one after the other, before rotation about the central bond can occur ($B \leftrightarrow C \leftrightarrow B'$), accompanied by concerted pseudorotation in all three rings. In the resulting mirror image conformation A' only geminal hydrogens have been exchanged, the carbon atoms possessing already in A the constitutional symmetry. The total number of steps in the interconversion scheme is increased only by two as compared with *cis*-decalin.

By the same argument as was used for *cis*-decalin, the critical barrier should occur in the third step, just before reaching conformation B, and its height may be roughly estimated at 20 kcal/mol. The experimental value for the 3,3-difluoro derivative (107) is $\Delta G^\ddagger = 15.7$ kcal/mol, only 50% higher than for cyclohexane, and may be taken as a strong argument for a multi-step mechanism.

The 2,5,7,10,11,14-hexaoxa derivative (108) has a still lower activation energy for geminal exchange ($\Delta G^\ddagger = 12.6$ kcal/mol), which is only 20% higher than for the monocyclic analog, 1,4-dioxan.

F. Tricyclo[4.4.4.0^{1,6}]tetradeca-3,8,12-triene

This triolefinic [4.4.4] propellane derivative is the tricyclic analog of the *cis*-hexalin already discussed. Again, the only possible conformational change in each ring must involve eclipsing of the central bond common to all three rings, and so must be concerted in all three. In agreement with this, the observed activation energy (107) is very high ($\Delta G^\ddagger = 16.7$ kcal/mol), more than three times higher than in the monocyclic compound cyclohexene ($\Delta G^\ddagger = 5.3$ kcal/mol). This is a strong argument for a one-step process as shown in Figure 69 with a B representing the barrier top rather than an intermediate; the central bond is then eclipsed, and all three rings are in boat-forms. The mirror image of the barrier B as shown in Figure 69

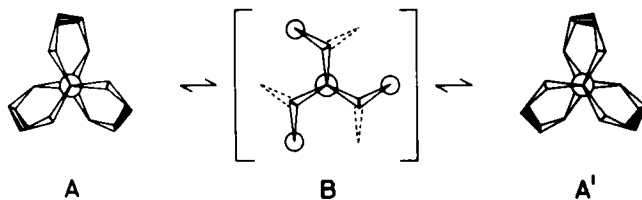


Fig. 69. Interconversion process for site exchange in tricyclo[4.4.4.0^{1,6}]tetradeca-3,8,12-triene.

is of course equally probable, but it suffices to pass through a single one.

G. Bicyclo[3.3.3]undecane

This is the simplest example of a bridged compound undergoing a multistep process.* The stable conformation (110,111) is water-wheel-like (A, Fig. 70), having three eight-membered rings in the [26] conformation. The intermediate conformations (B and B') on its straightforward interconversion path (Fig. 70) have two rings in the less favorable [8] and [2222] conformations.

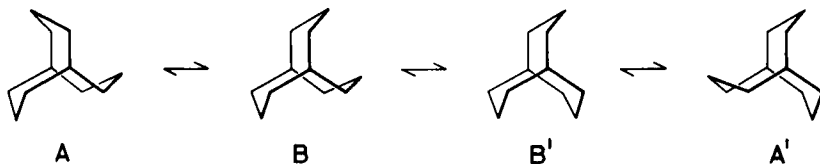


Fig. 70. Interconversion path for site exchange in bicyclo[3.3.3]undecane.

Only the ¹H nmr spectrum can here be temperature dependent, and a barrier of $\Delta G^\ddagger = 11$ kcal/mol is observed (110). Which of the two barriers, $A \rightleftharpoons B$ or $B \rightleftharpoons B'$, is rate determining is difficult to guess.

Also the 1-aza-derivative has the same conformation (112) and shows by dynamic nmr spectroscopy a process with a similar activation energy (111).

*The slightly twisted chiral conformation of bicyclo[2.2.2]octane (109) is forced by the severe restrictions of the ring systems to interconvert with its enantiomer over a single barrier having all three CH₂CH₂ bonds eclipsed.

H. Spiro[5.5]undecane

If both cyclohexane rings in this compound are in the chair conformation, not only are all geminal methylene hydrogens different, but also the 1 and 2 carbons are each split into two different types. Inversion of one ring will average its own geminal hydrogens, and the 1 and 2 carbons of the other ring, but not its own carbons. Rapid inversion in both rings are needed to obtain full exchange. There are all together four equivalent conformers, pairwise identical and mirror images of the other pair. All conformational barriers are, therefore, identical and close to that of cyclohexane.

This is also the case for the 2,4-dioxo derivative (Fig. 71, R=H), and a barrier of $\Delta G^\ddagger = 10.1$ kcal/mol has

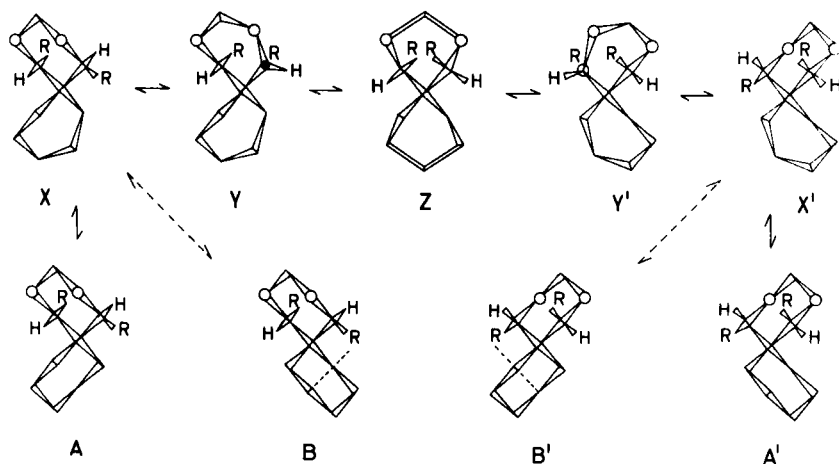


Fig. 71. Interconversion path for site exchange in 2,4-dioxaspiro[5.5]undecane (R = H or Me). When R = H also other paths are competitive. The dotted lines in B and B' indicate steric interaction.

been determined by dynamic nmr spectroscopy (113). This barrier would correspond to any of the four boat-chair transitions of the type $A \rightleftharpoons X$ occurring on each of the paths $A \rightleftharpoons B \rightleftharpoons A'$, $A \rightleftharpoons B' \rightleftharpoons A'$, $B \rightleftharpoons A \rightleftharpoons B'$, or $B \rightleftharpoons A' \rightleftharpoons B'$. That the identical conformers A and A' are here just mirror images of B and B' can only be appreciated on models.

When *trans*-related methyl groups occupy the 1 and 5 positions (Fig. 71, R=Me), conformers A and A' become really different from B and B'. The energies of the latter

conformers, and probably also of the barriers leading to them, are much higher in energy due to the "1,5-pentane" interaction between one methyl group and a CH₂ group of the cyclohexane ring (113). Nevertheless, the observed barrier (113) is only slightly higher ($\Delta G^\ddagger = 11.4$ kcal/mol). The reason is no doubt that after one chair-to-boat transition ($A \leftrightarrow X$) it is not really necessary to proceed to the high-energy conformer B. Instead, a second chair-to-boat transition in the other ring leads to a boat-boat conformer (Y), which can pseudorotate via the twist-twist conformer (Z) to the boat-boat (Y'), and this can finally go further via X' to the conformer A' with all possible site exchanges achieved. This process is thus not correctly described as a concerted ring flipping (113), but rather as a multistep interconversion through the boat-boat family in much the same way as in *cis*-decalin.

I. Triarylboranes, Triarylmethanes, and Similar Compounds

A particular class of multicyclic compounds have a central atom carrying three aromatic substituents and comprises triarylboranes, triarylcarbonium ions, triarylmethanes, triarylsilanes, and triarylgermanes. These have propeller-like conformations, and their conformational freedom is limited to rotation about the pivot bonds, which can occur either through the molecular plane or planes perpendicular to it ("flipping"). Critical barriers have been determined by dynamic nmr spectroscopy, and the possible multistep interconversion mechanisms analysed. This field has been reviewed very recently (114).

ACKNOWLEDGEMENT

I am particularly indebted to Professor F.A.L. Anet, Los Angeles, who permitted me to cite unpublished experimental and theoretical results. Whenever possible, his calculated strain energies have been given exclusively instead of earlier and less reliable published data, including my own.

REFERENCES

1. J.M. Lehn, *Fortsch. Chem. Forsch.*, **15**, 311 (1970).
2. R.M. Moriarty, in *Topics in Stereochemistry*, E.L. Eliel and N.L. Allinger, Eds., Wiley-Interscience, New York, Vol. 8, p. 271, 1974.
3. H. Kessler, *Angew.Chem.*, **82**, 237 (1970); *Angew.Chem. Int.Ed.*, **9**, 219 (1970).

4. E.L. Eliel, N.L. Allinger, S.J. Angyal, and G.A. Morrison, *Conformational Analysis*, Wiley-Interscience, New York, 1965.
5. J.B. Hendrickson, *J. Amer. Chem. Soc.*, **89**, 7047 (1967).
6. J.B. Hendrickson, *J. Amer. Chem. Soc.*, **83**, 4537 (1961).
7. J. Laane, *Quart. Rev.*, **25**, 533 (1971).
8. G. Binsch, in *Topics in Stereochemistry*, E.L. Eliel and N.L. Allinger, Eds., Wiley-Interscience, New York, Vol. 3, p. 97, 1968.
9. F.A.L. Anet and R. Anet, in *Dynamic Nuclear Magnetic Resonance Spectroscopy*, L.M. Jackman and F.A. Cotton, Eds., Academic, New York, p. 543, 1975.
10. K. Titlestad, P. Groth, and J. Dale, *Chem. Commun.*, **1966**, 375.
11. J. Dale, *Acta Chem. Scand.*, **27**, 1115 (1973).
12. A. Abe, R.L. Jernigan, and P.J. Flory, *J. Amer. Chem. Soc.*, **88**, 631 (1966).
13. P.J. Flory and A. Vrij, *J. Amer. Chem. Soc.*, **85**, 3548 (1963).
14. P.J. Flory, *Statistical Mechanics of Chain Molecules*, Wiley-Interscience, New York, 1969.
15. H. Sørum, J. Barstad, and J. Dale, *Acta Chem. Scand.*, **10**, 1663 (1956).
16. F. Mo and H. Sørum, *Acta Cryst.*, **B**, **24**, 605 (1968); and personal communication.
17. J. Dale, *Acta Chem. Scand.*, **27**, 1130 (1973).
18. J. Dale, *Pure Appl. Chem.*, **25**, 469 (1971).
19. P. Groth, *Acta Chem. Scand.*, **25**, 3189 (1971).
20. J.D. Dunitz, M. Dobler, P. Seiler, and R.P. Phizackerley, *Acta Cryst.*, **B**, **30**, 2733 (1974).
21. J.D. Dunitz and P. Seiler, *Acta Cryst.*, **B**, **30**, 2739 (1974).
22. G. Borgen and J. Dale, *Chem. Commun.*, **1970**, 1340.
23. F.A.L. Anet and A.K. Cheng, *J. Amer. Chem. Soc.*, **97**, 2420 (1975).
24. P. Groth, *Acta Chem. Scand.*, **25**, 725 (1971).
25. J. Dale and T. Ekeland, *Acta Chem. Scand.*, **27**, 1519 (1973).
26. F.A.L. Anet and J. Krane, unpublished.
27. F.A.L. Anet, J. Krane, J. Dale, K. Daasvatn, and P.O. Kristiansen, *Acta Chem. Scand.*, **27**, 3395 (1973).
28. J. Dale, *Tetrahedron*, **30**, 1683 (1974).
29. B.A. Newman, unpublished.
30. F.A.L. Anet, A.K. Cheng, and J.J. Wagner, *J. Amer. Chem. Soc.*, **94**, 9250 (1972).
31. F.A.L. Anet and A.K. Cheng, unpublished.
32. J. Dale, *Acta Chem. Scand.*, **27**, 1149 (1973).
33. J.D. Dunitz and H.M.M. Shearer, *Helv. Chim. Acta*, **43**, 18 (1960).

34. F.A.L. Anet and T. Rawdah, unpublished.
35. F.A.L. Anet, A.K. Cheng, and J. Krane, *J. Amer. Chem. Soc.*, **95**, 7877 (1973).
36. P. Groth, *Acta Chem. Scand.*, **A**, **28**, 294 (1974).
- 36a. R.L. Hilderbrandt, J.D. Wieser, and L.K. Montgomery, *J. Amer. Chem. Soc.*, **95**, 8598 (1973).
37. J.D. Dunitz, *Pure Appl. Chem.*, **25**, 495 (1971).
38. F.A.L. Anet and J.J. Wagner, *J. Amer. Chem. Soc.*, **93**, 5266 (1971).
39. S. Rustad and H.M. Seip, *Acta Chem. Scand.*, **A**, **29**, 378 (1975).
40. S.G. Dahl and P. Groth, *Acta Chem. Scand.*, **25**, 1114 (1971).
41. G. Borgen, J. Dale, F.A.L. Anet, and J. Krane, *Chem. Commun.*, 1974, 243.
42. G. Borgen and J. Dale, *Chem. Commun.*, 1970, 1105.
43. F.A.L. Anet, *Fortschr. Chem. Forsch.*, **45**, 169 (1974).
44. F.A.L. Anet and J. Krane, *Tetrahedron Lett.*, 1973, 5029.
45. F.A.L. Anet and M. St. Jacques, *J. Amer. Chem. Soc.*, **88**, 2585, 2586 (1966).
46. F.A.L. Anet and J.S. Hartman, *J. Amer. Chem. Soc.*, **85**, 1204 (1963).
47. F.A.L. Anet and V.J. Basus, *J. Amer. Chem. Soc.*, **95**, 4424 (1973).
48. J. Dale, T. Ekeland, and J. Krane, *J. Amer. Chem. Soc.*, **94**, 1389 (1972).
49. F.A.L. Anet and P.J. Degen, *J. Amer. Chem. Soc.*, **94**, 1390 (1972).
50. F.A.L. Anet, M. St. Jacques, P.M. Henrichs, A.K. Cheng, J. Krane, and L. Wong, *Tetrahedron*, **30**, 1629 (1974).
51. J.E. Heller and A.S. Dreiding, *Helv. Chim. Acta*, **56**, 723 (1973).
52. J.B. Hendrickson, *J. Amer. Chem. Soc.*, **89**, 7036 (1967).
- 52a. D.F. Bocian, H.M. Pickett, T.C. Rounds, and H.L. Strauss, *J. Amer. Chem. Soc.*, **97**, 687 (1975).
53. G. Borgen and J. Dale, *Acta Chem. Scand.*, **26**, 3593 (1972).
54. J.B. Hendrickson, *J. Amer. Chem. Soc.*, **89**, 7043 (1967).
- 54a. H.M. Pickett and H.L. Strauss, *J. Amer. Chem. Soc.*, **92**, 7281 (1970).
55. F.A.L. Anet and A.J.R. Bourn, *J. Amer. Chem. Soc.*, **89**, 760 (1967).
56. C.H. Bushweller, G.V. Rao, and F.A. Bissett, *J. Amer. Chem. Soc.*, **93**, 3058 (1971).
57. J.B. Lambert and W.L. Oliver, *Tetrahedron Lett.*, 1968, 6187.
58. J.M. Lehn and J. Wagner, *Chem. Commun.*, 1970, 414.

59. For a review, see J. Dale, in *Chemistry of Acetylenes*, H.G. Viehe, Ed., Dekker, New York, p. 3, 1969.
60. E. Augdahl, G. Borgen, J. Dale, and J. Krane, *Acta Chem. Scand.*, B, 28, 125 (1974).
61. J. Dale, *Tetrahedron*, 22, 3373 (1966).
62. For a review, see J.F.M. Oth, *Pure Appl. Chem.*, 25, 573 (1971).
63. F.A.L. Anet, in *Conformational Analysis*, G. Chiurdoglu, Ed., Academic, New York, p. 15, 1971.
64. F.J. Weigert and D.R. Strobach, *Org. Magn. Resonance*, 2, 303 (1970).
65. K.L. Servis and E.A. Noe, *J. Amer. Chem. Soc.*, 95, 171 (1973).
66. N.L. Allinger and J.T. Sprague, *J. Amer. Chem. Soc.*, 94, 5734 (1972).
67. M. St. Jacques and C. Vaziri, *Can. J. Chem.*, 49, 1256 (1971).
68. W. Tochtermann, *Fortschr. Chem. Forsch.*, 15, 378 (1970).
69. F.A.L. Anet and M.Z. Haq, *J. Amer. Chem. Soc.*, 87, 3147 (1965).
70. For a review, see B.W. Roberts, J.J. Vollmer, and K.L. Servis, *J. Amer. Chem. Soc.*, 96, 4578 (1974).
71. J. Dale, T. Ekeland, and J. Schaug, *Chem. Commun.*, 1968, 1477.
72. D.J. Brickwood, W.D. Ollis, and J.F. Stoddart, *Chem. Commun.*, 1973, 638.
73. A.P. Downing, W.D. Ollis, and I.O. Sutherland, *J. Chem. Soc., B*, 1970, 24.
74. K.G. Untch and D.J. Martin, *J. Amer. Chem. Soc.*, 87, 3518 (1965).
75. F.A.L. Anet and L. Kozerski, *J. Amer. Chem. Soc.*, 95, 3407 (1973).
76. R. Crossley, A.P. Downing, M. Nógrádi, A. Braga de Oliveira, W.D. Ollis, and I.O. Sutherland, *J. C. S., Perkin I*, 1973, 205.
- 76a. N.L. Allinger and J.T. Sprague, *Tetrahedron*, 31, 21 (1975).
77. D. Montecalvo, M. St. Jacques, and R. Wasylishen, *J. Amer. Chem. Soc.*, 95, 2023 (1973).
78. W.D. Ollis and J.F. Stoddart, *Chem. Commun.*, 1973, 571.
79. J.D. White and B.D. Gesner, *Tetrahedron*, 30, 2273 (1974).
80. P. Radlick and S. Winstein, *J. Amer. Chem. Soc.*, 85, 344 (1963).
81. K.G. Untch and R.J. Kurland, *J. Amer. Chem. Soc.*, 85, 346 (1963).
82. W.R. Roth, *Ann. Chem.*, 671, 10 (1964).
83. T. Sato and K. Uno, *J. C. S. Perkin I*, 1973, 895.

84. R.C. Cookson, B. Halton, and I.D.R. Stevens, *J. Chem. Soc., B*, 1968, 767.
85. A. Lüttringhaus and K.C. Peters, *Angew. Chem.*, 78, 603 (1966); *Angew. Chem., Int. Ed.*, 5, 593 (1966).
86. J. Dale and K. Titlestad, *Chem. Commun.*, 1969, 656.
87. J. Dale and K. Titlestad, *Acta Chem. Scand., B* 29, 353 (1975).
88. G. Allegri and I.W. Bassi, *Atti Acad. Naz. Lincei, Rend. Cl. Sci. Fis. Mat. Nat.*, 38, 72 (1962).
89. J. Dale and D.G.T. Greig, unpublished.
90. A.T. McPhail, R.I. Reed, and G.A. Sim, *Chem. Ind.*, 1964, 976.
91. S. Dev, and J.E. Anderson, V. Cormier, N.P. Damodaran, and J.D. Roberts, *J. Amer. Chem. Soc.*, 90, 1246 (1968).
92. F.H. Allen and D. Rogers, *Chem. Commun.*, 1967, 588.
93. P.S. Wharton, Y.C. Poon, and H.C. Kluender, *J. Org. Chem.*, 38, 735 (1973).
94. P. Ganis and J.D. Dunitz, *Helv. Chim. Acta*, 50, 2379 (1967).
95. G. Binsch and J.D. Roberts, *J. Amer. Chem. Soc.*, 87, 5157 (1965).
96. E.A. Noe, R.C. Wheland, E.S. Glazer, and J.D. Roberts, *J. Amer. Chem. Soc.*, 94, 3488 (1972).
97. P. Groth, *Acta Chem. Scand.*, 24, 780 (1970).
98. J. Dale and K. Titlestad, *Chem. Commun.*, 1970, 1403; *ibid.*, 1972, 255.
99. C.M. Deber, E.T. Fossel, and E.R. Blout, *J. Amer. Chem. Soc.*, 96, 4015 (1974).
100. K.B. Wiberg and R.H. Boyd, *J. Amer. Chem. Soc.*, 94, 8426 (1972).
101. O. Hassel and H. Viervoll, *Acta Chem. Scand.*, 1, 149 (1947).
102. F.R. Jensen and B.H. Beck, *Tetrahedron Lett.*, 1966, 4523.
103. D.K. Dalling, D.M. Grant, and L.F. Johnson, *J. Amer. Chem. Soc.*, 93, 3678 (1971).
104. A. Geens, D. Tavernier, and M. Anteunis, *Chem. Commun.*, 1967, 1088.
105. J.T. Gerig and J.D. Roberts, *J. Amer. Chem. Soc.*, 88, 2791 (1966).
- 105a. T.B. Grindley and W.A. Szarek, *Canad. J. Chem.*, 52, 2566 (1974).
106. F. DePessemier, D. Tavernier, and M. Anteunis, *Chem. Commun.*, 1973, 594.
107. H. Gilboa, J. Altman, and A. Loewenstein, *J. Amer. Chem. Soc.*, 91, 6062 (1969).
108. B. Fuchs, Y. Auerbach, and M. Sprecher, *Tetrahedron Lett.*, 1972, 2267.
109. O. Ermer and J.D. Dunitz, *Helv. Chim. Acta*, 52,

- 1861 (1969).
110. M. Doyle, W. Parker, P.A. Gunn, J. Martin, and D.D. Macnicol, *Tetrahedron Lett.*, 1970, 3619.
111. J.C. Coll, D.R. Crist, M.d.C.G. Barrio, and N.J. Leonard, *J. Amer. Chem. Soc.*, 94, 7092 (1972).
112. A.H.J. Wang, R.J. Missavage, S.R. Byrn, and I.C. Paul, *J. Amer. Chem. Soc.*, 94, 7100 (1972).
113. D. Tavernier, M. Anteunis, and N. Hosten, *Tetrahedron Lett.*, 1973, 75.
114. K. Mislow, D. Gust, P. Finocchiaro, and R.J. Boettcher, *Fortschr. Chem. Forsch.*, 47, 1 (1974).

CRYSTAL STRUCTURES OF STEROIDS

W. L. DUAX, C. M. WEEKS, AND D. C. ROHRER

*Molecular Biophysics Department, Medical Foundation of
Buffalo Research Laboratories, Buffalo, New York*

- I. Introduction 272
 - A. Steroid Function 272
 - B. Steroid Nomenclature 277
 - C. Crystal and Molecular Structures 278
- II. Conformational Analysis 279
 - A. Conformational Flexibility 279
 - B. Quantitative Analysis of Ring Conformation 280
 - 1. Symmetry in Rings 281
 - a. Five-membered rings 282
 - b. Six-membered rings 283
 - 2. Asymmetry Parameters 284
 - C. Overall Conformation 286
 - D. 17 β Side Chain Conformation 287
 - E. Bulky Substituents 288
- III. Intermolecular Forces and Crystal Packing 289
 - A. Chain Formation 289
 - B. Layer Formation 290
 - C. Coil Formation 290
 - D. Crystalline Polymorphs, Multiple Asymmetric Units, and Conformational Isomers 291
- IV. Expected and Observed Geometry 294
 - A. 1,3,5(10)-Estratrienes 302
 - 1. Average Bond Lengths and Angles 302
 - 2. B-Ring Conformation 302
 - 3. Correlated Changes 304
 - 4. Restricted Flexibility 309
 - B. 8 α -Estrenes 310
 - C. 9 β -Estrenes 312
 - D. Δ^4 -3-One Structures 313
 - 1. Average Bond Lengths and Angles 314
 - 2. A-Ring Conformation 315
 - 3. Correlated Changes 318
 - a. Bond lengths, Valency Angles, Torsion Angles 318

b. Other Parameters	321
4. Restricted Flexibility	321
a. Substituent Effect	321
b. Unsaturation	325
E. 9 β ,10 α - Δ^4 -3-One Structures	325
F. 5-Ene Structures	328
G. Saturated Structures	330
1. Average Bonds, Lengths, Angles, Torsion Angles	333
2. Distorted Chair Conformations	333
3. Cyclosubstitutions	333
4. Heterosubstitutions	335
5. Boat and Twist Conformers of Saturated Rings	342
6. Doubled Asymmetric Unit Structures	342
a. 17 β -Hydroxy-5 α -androsten-3-one	345
b. 5 α -Androstan-3,17-dione	347
c. 5-Bromo-6 β ,19-epoxy-3 β -hydroxy-5 α -pregnan-20-one	347
d. (20S)-20-Chloro-5 α -pregnane-3 β ,1 β -diol di- <i>p</i> -bromobenzoate	348
e. 5 α ,17 α ,,-pregna-3 β ,20 α -diol	348
H. D-Ring Conformations	349
V. Side Chain and Substituent Conformations	352
A. Pregnane 17 β Side Chain Conformations	352
B. 17 β -Acetate and Benzoate Substituents	354
C. 3 β -Acetate and Benzoate Substituents	359
D. C(19) Substituents	365
VI. Intermolecular Interactions	366
A. Crystal Packing	366
B. Gross Packing Features	371
C. Hydrogen Bonding Patterns	372
VII. Summary	374

I. INTRODUCTION

A. Steroid Function

The steroids are a group of naturally occurring organic compounds and their synthetic derivatives, all of which are characterized by a basic carbon skeleton or nucleus consisting of three six-membered rings and one five-membered ring (Fig. 1). The most important classes of steroids include (1) the sex hormones, which are responsible for the development and maintenance of primary and secondary sex characteristics; (2) the adrenal cortical hormones, which are essential for maintenance of salt and water balance and carbohydrate metabolism; (3) bile acids present in animal bile and used in chemical synthesis of

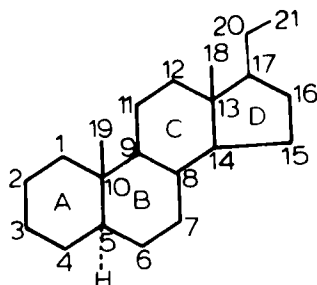


Fig. 1. Basic steroid structure with standard atomic numbering and ring designations.

anti-inflammatory agents; (4) sterol constituents of cell membranes; and (5) cardiogenic agents useful in the treatment of congestive heart failure. In addition to the regulatory functions that steroids perform, they play a significant role in the body responses to emotional and physical stress and disease conditions.

The intimate involvement of steroids in the cause and cure of cancer is illustrated by the therapeutic effect of treating cancer victims with massive quantities of specific steroids and steroid analogues. Regression of breast cancer in women through estrogen, androgen, and corticoid administration, the regression of breast cancer in men through androgen and artificial estrogen administration, and corticosteroid therapy of lymphomas and leukemias are a few of the most common examples of hormonal cancer therapy.

The way in which a given steroid acts in a normal, a carcinogenic, or a carcinostatic process is unquestionably a function of its total structure. The more detailed knowledge we have concerning the structures of individual steroids, the easier it will be to correlate specific structural features with the various steroid functions. Minor changes in the basic steroid make-up totally alter biological function. Compounds as similar as progesterone, cortisol, and aldosterone (Fig. 2) are vital to such dissimilar physiological activities as maintenance of pregnancy, metabolism of proteins, and maintenance of electrolyte balance. There is some overlap in the activities of these steroids, and the question of which compositional or structural differences are associated with each of the functional changes is significant and challenging.

Although a specific biological function can be shown to be directly dependent upon the action of a particular steroid, the exact nature of all molecular level events

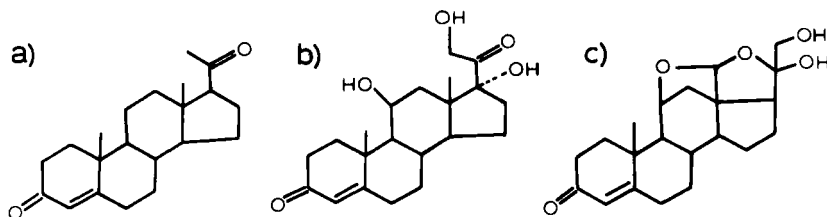


Fig. 2. Three of the most active pregnane derivatives, (a) progesterone, (b) cortisol, and (c) aldosterone, have vastly dissimilar functions resulting from minor substitutional variations.

involved in this structure-function dependence is not fully understood. The complex nature of a single steroid's interactions in the body is suggested by the steroid "life cycle" depicted in Figure 3. This diagram is based upon present knowledge and theory concerning the action of estrogens and glucocorticoids. At any point in the sequence of events including synthesis, transport, target interaction, and degradation, specific structural features of a steroid may be essential for optimum activity. Other steroids or nonsteroidal molecules that share some of these features further complicate the picture by competing in a particular stage of the sequence. Conversely, the steroid of Figure 3 may interact with other proteins, secondary transport, or target molecules, and metabolizing enzymes for which it is not the primary substrate.

It is clear that the functions and activities of steroids are determined by their composition, constitution, configuration, and conformation. *Composition* defines the number and kinds of atoms that make up the molecule and is readily represented by its chemical formula. *Constitution* refers to the connectivity of the molecule and is best illustrated by diagrammatically showing which atoms are bonded to one another. *Molecular configuration* defines the chirality of all asymmetric centers in the molecule. In many instances conventions have been adopted that allow the designation of configuration on connectivity drawings. *Conformation* refers to the total geometric distribution or disposition of the atoms in three dimensions. The molecular conformations of steroids can be approximated by Dreiding models. The concept of compositional and constitutional control of function is readily accepted, and examples of structural isomers having different functions are unnecessary here. Functional dependence upon configuration is illustrated in the case of testosterone, a male sex hormone,

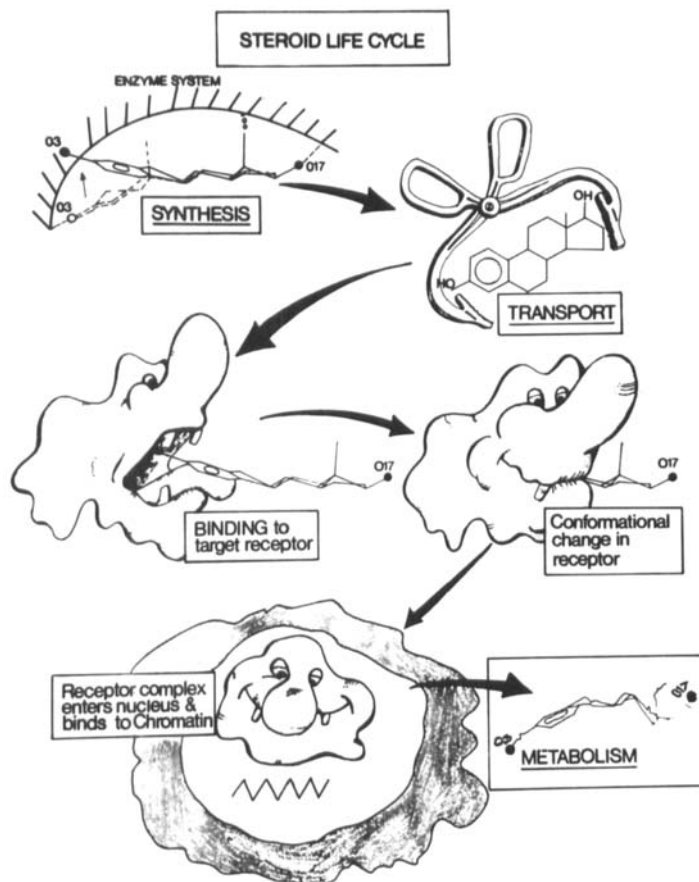


Fig. 3. Natural steroid hormones are involved in a complex series of interactions with proteins that include (a) biogenesis, (b) transport, (c) receptor binding, (d) entry into the cell nucleus, and (e) metabolism.

and its inactive epimer, 17α -hydroxy-4-androsten-3-one (Fig. 4). These molecules are configurational isomers differing only in the stereochemistry at C(17). The β face of a steroid is the surface normally containing the C(18) and C(19) methyl groups, and the α face is the flatter underside of the molecule. As indicated in Figure 4, the 17-hydroxyl in testosterone is β substituted, while the 17-hydroxyl in epitestosterone is α substituted. It is noteworthy that despite the inactivity of epitestosterone the conformations are nearly identical, and the relative locations of hydrogen bond acceptors from the

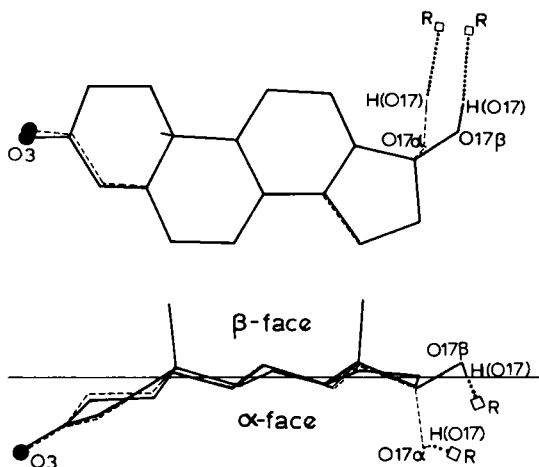


Fig. 4. The configurational difference at the C(17) position in the active androgen testosterone, AN14A, (solid lines) and the inactive steroid epitestosterone, AN35, (dashed lines) controls biological function. The directionality of the hydrogen bonding in each structure as observed in the crystal structures is indicated. R indicates the hydrogen acceptor.

17 α - and 17 β -hydroxyls in the two crystal structures are within 1.5Å of one another. An appreciation of functional dependence upon steroid conformation has only recently emerged. For example, the 17 β side chain of progesterone possesses conformational flexibility, and the orientation of the 20-keto group relative to the bulk of the steroid may determine its interaction with target proteins (Fig. 5).

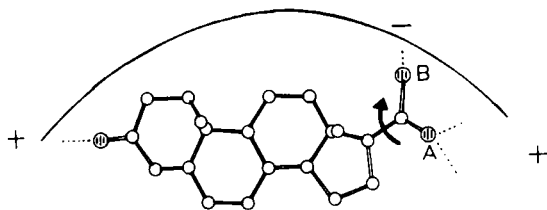


Fig. 5. If simultaneous binding at both ends of the steroid is necessary for interaction with a particular protein, the conformation of the flexible 17 β side chain needed for optimal interaction may be greatly restricted. A conformation having the O(20) atom at position A may be compatible with binding while conformation B is incompatible.

The importance of steroid conformation to *in vitro* reactions is well established. The occurrence of conformational transmission or long range effects (1-5) has been the subject of extensive discussion over the past ten years. Conformational transmission is the term chosen by Barton to define the phenomenon whereby structural modification at one point on the steroid skeleton is found to have a profound effect upon the rate of a specific reaction at some distant point (6). For example, base-catalyzed condensations of benzaldehyde with triterpenes (Fig. 6)

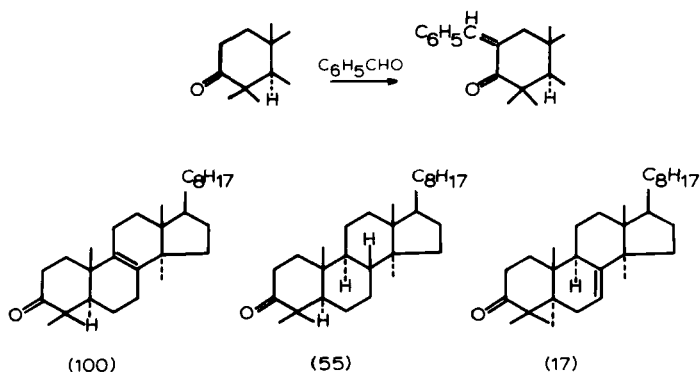


Fig. 6. The rate of benzaldehyde condensation at C(2) in the A ring varies over a five fold range as a function of structural differences at the B/C ring junction. The relative rates of reaction are given in parenthesis. This long range effect observed in steroids was referred to by Barton as *conformational transmission*.

were observed by Barton to be dependent upon substitutions in the steroid at points remote from the reaction site. The relative rates of condensation of lanost-8-en-3-one, lanostanone, and lanost-7-en-3-one were found to be in the ratio 100:55:17. Comparative analysis of conformational data for closely related structures should provide details of the molecular changes that are responsible for conformational transmission.

B. Steroid Nomenclature

Steroid nomenclature has been derived from the structural and functional characteristics of these compounds. Although many of the trivial names that were derived from molecular function or tissue of origin are still in use, adherence to nomenclature based upon structural characteristics

is necessary for rational comparative analysis. Because structural classification followed the development of a trivial nomenclature and because major functional variation accompanies major structural variation, there is a parallel development of the two classification systems as illustrated in Table 1. The nomenclature for steroids has been completely systematized by IUPAC conventions and all steroids can be assigned unique names defining composition, constitution, and configuration (7).

Table 1.
Steroid Classification

Structural	Functional
Estranes	Estrogens
Androstanes	Androgens
Pregnanes	Progestins
	Glucocorticoids
	Mineralocorticoids
Cholanes	Bile acids
Cholestanes	Sterols

C. Crystal and Molecular Structures

X-Ray crystal structure studies have often been conducted in order to determine the configuration of a natural or synthetic product and have even been instrumental in defining steroid composition and constitution. The early work of Bernal, Crowfoot, and Fankuchen (8) played an essential part in determining the connectivity of the steroid backbone. This work showed that the then-accepted structural formula for the steroids (Fig. 7), which had

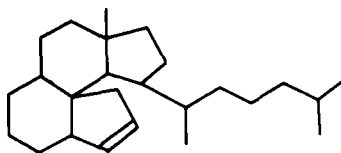


Fig. 7. The connectivity proposed by Windaus and Wieland for cholesterol was shown to be inconsistent with cell dimensions for the crystallized compound.

been proposed by Windaus and Wieland (9), was incorrect inasmuch as compounds having this connectivity would not fit the unit cells that had been determined by X-ray measurements. Full X-ray crystal structure studies provide the most precise and accurate details concerning molecular conformation, the most favored orientation of side chains, and the nature of the primary intermolecular interactions that a specific steroid has with its environment.

The first complete X-ray crystal structure analysis of a steroid (cholesteryl iodide) including determination of atomic coordinates was reported by Carlisle and Crowfoot in 1945 (10). Since that time full crystal structure determinations have been published for 234 steroids. A breakdown of these steroids according to class is presented in Table 2. Only structures for which atomic coordinates have been published, or privately distributed by the authors as of November 1, 1974, are included in this table. These structure determinations provide a wealth of raw material concerning molecular conformation and intermolecular interactions that is ideally suited to analysis of structure-function relationships. In the *Atlas of Steroid Structure* (11) all available data have been collected and subjected to an exhaustive and uniform analysis in order to delineate relative structure.

Table 2.
Steroid Crystal Structure Determinations since 1945,
Distribution According to Steroid Class

Class	Determined	Class	Determined
Estranes	37	Cholestanes	19
Androstanes	75	Steroid alkaloids	11
Pregnanes	59	Ergostanes	11
Cholanes	9	Lanostanes	8
		Cardanolides	4
		Bufanolides	1

II. CONFORMATIONAL ANALYSIS

A. Conformational Flexibility

Steroids having saturated nuclei are relatively inflexible molecules. However, the most active naturally occurring

steroid hormones contain unsaturated bonds in their nuclei and this unsaturation introduces a potential for conformational flexibility. The Δ^4 -3-one A ring of many androgens, progestins, and corticoids is the area of greatest conformational flexibility in these molecules, whereas the B rings are the focal points of conformational flexibility in cholestenes and estrogens. It is reasonable to assume that the conformational flexibility exhibited by these naturally occurring hormones facilitates their highly specific interaction with a variety of proteins including synthesizing enzymes, transport proteins, and target proteins. Furthermore, it is now apparent that additional modification of these hormones (e.g., 9 α -fluoro substitution) may remove or greatly restrict the flexibility and limit the range of molecular interaction of these analogs in the biological setting. The conformational flexibility of steroid molecules observed in the crystallographic data will be discussed in this context. Special attention is given to active hormones and their structural analogs in which some conformational flexibility is observed. In some cases, such as in the progesterone and corticoid 17 β side chains, there is surprisingly little flexibility and these data are also considered.

B. Quantitative Analysis of Ring Conformation

Molecular conformation is most conveniently and precisely characterized by the torsion angles. An excellent discussion of the torsion angle concept in conformational analysis appears in a previous article in this series by Bucourt (12), and the relative conformations of sidechains are discussed in terms of their torsion angles in accordance with Bucourt's presentation.*

In the case of five- and six-membered rings, the endocyclic torsion angles redundantly define the conformation of the ring in question (13). Clearly, if all bond lengths and angles are held constant and closure is required, two endocyclic torsion angles having only one common bond will fully define the conformation of a six-membered ring. Consequently, a two-parameter definition of the conformation of a ring would be a desirable improvement over the six-torsion-angle definition. It has been generally recognized that the symmetry in a ring provides a qualitative

*An analogous geometric relationship relating four atoms that are not contiguous is also being used in steroid analysis. An example of such a *pseudo*-torsion angle is that defined by steroid atoms C(19)-C(10) \cdots C(13)-C(18). Note that the C(10) to C(13) linkage is dotted to indicate that this is not a bond.

means of defining the ring's conformation. A thorough analysis of symmetry in rings of various sizes has been described by Hendrickson (14) and Pitzer and Donath (16). The most widely used quantitative descriptors of ring conformation other than torsion angles are the *pseudo*-rotation parameters (Δ and ϕ) defined by Altona, Geise, and Romers (15). A quantitative evaluation of the conformations of rings of any size from which comparative analysis can be easily made is obtainable from a mathematical combination of torsion angles. This analysis is based upon consideration of approximate symmetry possessed by most rings.

1. Symmetry in Rings

The two types of symmetry that need to be considered in order to define ring conformation are mirror planes perpendicular to the dominant ring plane and twofold axes lying in the ring plane. Either of these symmetry elements may be present at any of the three kinds of locations described below. The location of symmetry in a ring depends on the number of atoms comprising that ring. If there is

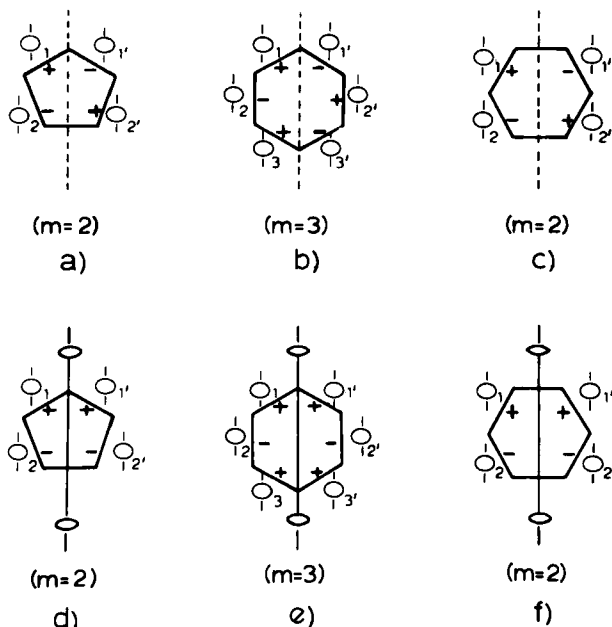


Fig. 8. The signs of the torsion angles in five- and six-membered rings describe the symmetrical positioning of atoms related by the symmetry operation. Torsion angles of atom sequences related by mirrors (---), have opposite signs (a,b,c), whereas torsion angles of atomic sequences related by rotations (ϕ) have the same signs (d,e,f).

an odd number of atoms in the ring, all symmetry elements pass through one ring atom and bisect the opposite bond (Figs. 8a and d). In rings containing an even number of atoms, symmetry elements may pass through two ring atoms located directly across the ring from each other (Figs. 8b and e) or bisect two opposite ring bonds (Figs. 8c and f).

a. *Five-membered rings.* The ten symmetry elements that are potentially possible in five-membered rings consist of five mirror planes (perpendicular to the dominant ring plane) that pass through the ring atoms and the midpoints of the opposite bonds as well as twofold axes passing through each ring atom and the midpoint of the opposite bond. Figure 9 illustrates each of the ideal

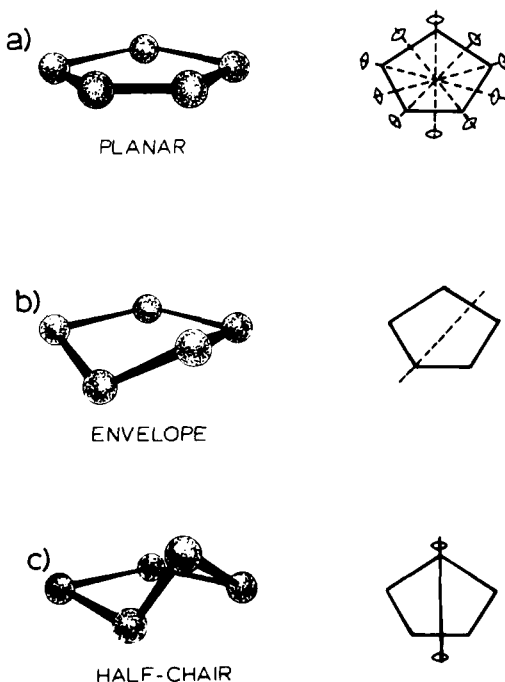


Fig. 9. The three most symmetric conformations observed for five-membered rings have the symmetries indicated at the right.

conformations used to classify five-membered rings and shows the locations of the symmetry elements. The planar ring has the highest symmetry and possesses all ten possible symmetry elements. The ideal envelope conformation has

only a single mirror plane of symmetry passing through the out-of-plane atom, and the ideal half-chair has only a twofold axis of symmetry bisecting the bond between the two out-of-plane atoms.

b. Six-membered rings. Six-membered rings possess twelve potential symmetry elements that must be considered in order to determine the ring's conformation. The two-, three-, and sixfold rotations perpendicular to the dominant plane of the ring are ignored for purposes of this discussion. Figure 10 illustrates the symmetry

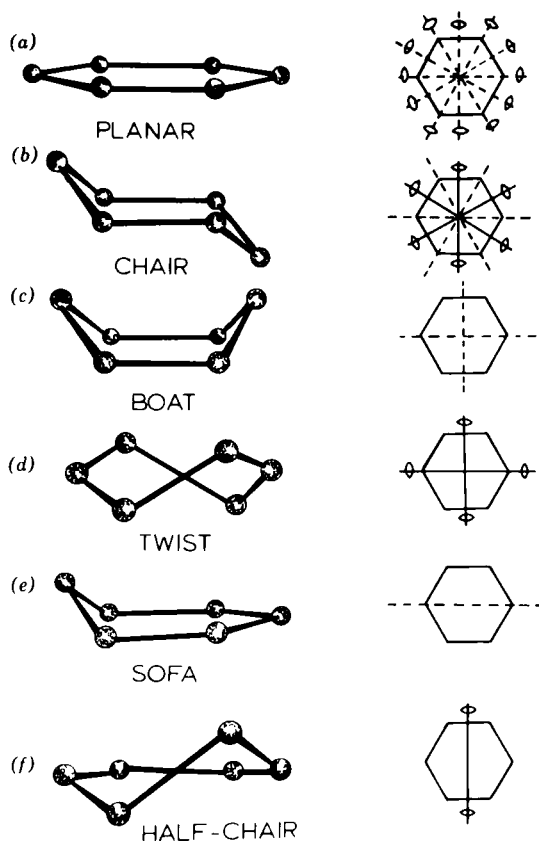


Fig. 10. The most commonly observed conformations of six-membered rings. The mirror and twofold rotational symmetries are indicated on the right.

elements that define the ideal forms of commonly observed conformations. The planar ring is highly symmetric and contains all possible symmetry elements (i.e., a mirror plane and a twofold axis of symmetry at each of the six possible locations). The chair conformation possesses the next highest symmetry, having three mirror planes of symmetry and three twofold axes of symmetry. The boat and twist-boat conformations each have two mutually perpendicular symmetry elements. The sofa and half-chair conformations each have only a single symmetry element.

2. Asymmetry Parameters

Until now a formalism for precise measurement of the degree to which a given ring deviates from ideal symmetry has only been proposed in the case of five-membered rings (15). The asymmetry parameters described here precisely define the conformation of any ring relative to ideal conformations (chair, boat, envelope, etc.) and relative to any other ring of similar composition.

The asymmetry parameters of nonideal systems measure the degree of departure from ideal symmetry (i.e., asymmetry) at any of the possible symmetry locations. Related torsion angles are compared in a way that will result in a value of zero if the symmetry in question is present. Mirror-related torsion angles are inversely related (same magnitude, opposite sign), and such torsion angles are compared by addition. The twofold related torsion angles are directly related (same magnitude and sign) and are compared by subtraction. The root-mean-square synthesis of these individual discrepancies then yields a measure of the ring's deviation from ideal symmetry at the symmetry location in question. The two equations used to calculate the asymmetry parameters are

$$\Delta C_s = \left(\frac{\sum_{i=1}^m (\phi_i + \phi_i^*)^2}{m} \right)^{1/2} \quad [1]$$

and

$$\Delta C_2 = \left(\frac{\sum_{i=1}^m (\phi_i - \phi_i^*)^2}{m} \right)^{1/2} \quad [2]$$

where m is the number of individual comparisons and ϕ_i and ϕ_i' are the symmetry-related torsion angles. Equation [1] is used to calculate mirror-plane asymmetry parameters (ΔC_S). Figures 8a, b, and c illustrate the three types of mirror symmetries. Similarly, eq. [2] is used to calculate the twofold asymmetry parameters (ΔC_2) and Figures 8d, e, and f are examples of the twofold symmetry locations. Although asymmetry parameters are measured in degrees, for convenience the units have been omitted from the legends of graphs in the data presented below.

It is also necessary to define which of the possible locations the asymmetry parameter is describing. Therefore, an atom or bond label must be included with the asymmetry parameter that uniquely fixes the location of the parameter in the ring. The atom label for the lower numbered atom present in the symmetry location or the two-atom label of the bisected bond containing the lowest numbered atom will generally be sufficient to locate the position of the asymmetry parameter uniquely (Fig. 11). In Figure 12 the significance of the magnitudes of the asymmetry parameters is illustrated using a typical steroid ring. The angles depicted (Fig. 12) are between the least-squares plane of the four atoms forming the seat of the chair and the planes of the three atoms forming the back and the legs of the chair. The average value of these angles in undistorted chairs is 131° .

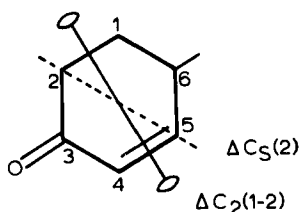


Fig. 11. The nomenclature defining the location of an asymmetry parameter includes the symmetry symbol and the lower numbered atom or bond length intersected by the symmetry element.

The asymmetry parameters of saturated six-membered rings are useful for detecting the nature of distortions brought about by ring junction and substituent strains. In a perfectly symmetric saturated ring in the chair conformation, six asymmetry parameters (three rotations and three mirrors) would have magnitudes of zero. Individual saturated rings in a steroid molecule usually retain some symmetry at the expense of others. The parameters that have

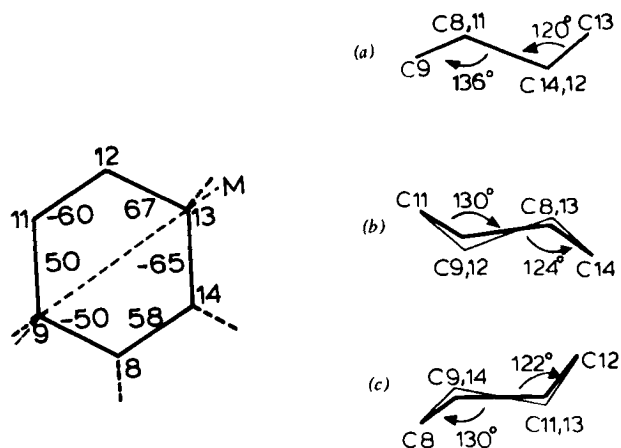


Fig. 12. Distortions typical of saturated six-membered rings are illustrated by the C ring of 17 β -bromoacetoxy-1 β ,2 β -(1',1'-dichloro)-ethylene-5 α -androstan-3-one (AN08), which has excellent mirror symmetry $\Delta C_5(9) = 0.9$ but is seen to be flattened at C(9) and puckered at C(13) as indicated by interplanar angles of 136 and 120 deg., respectively. The ring is shown in the three possible views parallel to lines joining the midpoints of opposite bonds.

larger magnitudes will distinguish symmetry loss due to twist motions from symmetry loss due to flattening or puckering of the rings. If a good mirror is orthogonal to a poor rotation axis, the ring is flattened at one atom and puckered at the opposite atom. If one good rotation axis is retained and it is orthogonal to a poor plane of mirror symmetry, the ring is twisted. The average value of the absolute magnitude of the torsion angles in a ring will distinguish between ring flattening (low average) and puckering (high average).

In the simplest mode of distortion, one of the six symmetries normally present in a six-membered chair will be lost, and a symmetry orthogonal to this will be retained. Since there are six symmetries in each ring, there are eighteen simple modes of distortion conceivable for the A, B, and C rings.

C. Overall Conformation

Because the B/C and C/D ring junctions seldom have cis configurations, the least-squares plane through the atoms of the B, C, and D rings [C(5) \rightarrow C(17)] has been

chosen as a reference element for gross analysis of the steroid conformations (Fig. 13). The distances of functional

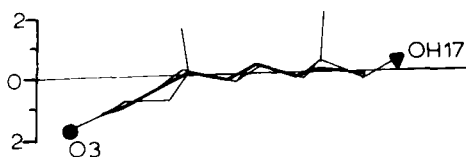
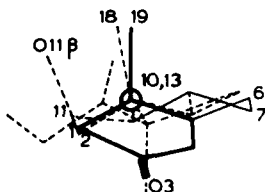


Fig. 13. The least-squares plane of the atoms of the B, C, and D rings of the steroid is used as a reference plane for comparison of relative orientation of functional groups on different steroids. The molecule is conveniently viewed parallel to this plane and perpendicular to the C(8)-C(14) bond. The scale is in Angstrom units in all least-squares planes diagrams.

groups from this plane have been tabulated and analyzed. The angle of inclination of the least-squares plane through the atoms of the A ring and the C(5)-C(17) reference plane has also been compared for related structures. The twist about the length of the steroid is measured in terms of the torsion angles C(1)-C(10)···C(13)-C(18) for estranes, or C(19)-C(10)···C(13)-C(18) for androstanes and pregnanes (Fig. 14).

PR18



PR09

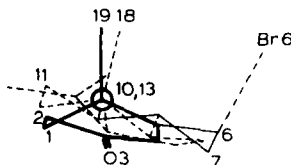


Fig. 14. The twist about the length of many steroids, reflected in the relative orientation of the angular methyl groups, is conveniently viewed in a projection from C(10) to C(13) and measured by the C(19)-C(10)···C(13)-C(18) torsion angle. The steroid conformations in structures having positive and negative values of this parameter are exemplified by PR18 and PR09, respectively.

D. 17 β Sidechain Conformation

Because over 90% of the pregnanes have a 20-keto group, the least-squares plane of atoms C(17), C(20), O(20), and C(21) and its orientation relative to the

C(5)-C(17) reference plane may be used to compare conformational features. The conformation of the side chain is also defined by the C(13)-C(17)-C(20)-O(20) torsion angle (Fig. 15). In structures having a substitution on C(21)

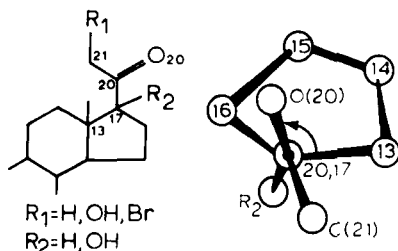


Fig. 15. The conformation of the side chain typical of progestins and corticoids is defined by the C(13)-C(17)-C(20)-O(20) torsion angle.

the relative position of this atom is defined by the O(20)-C(20)-C(21)-R(21) torsion angle. In addition, the conformations of O(20) relative to C(13) and of R(21) relative to O(20) are assigned one of the qualitative descriptors, *synperiplanar*, *synclinal*, *anticlinal*, or *antiperiplanar* in accordance with the definitions of Klyne and Prelog (17) as shown in Figure 16.

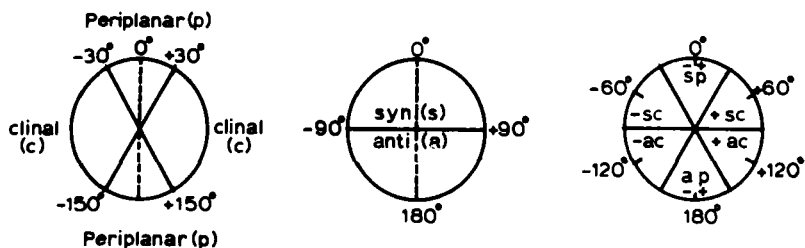


Fig. 16. Nomenclature useful for the qualitative description of the conformation of flexible substituents and sidechains has been outlined by Klyne and Prelog (17).

E. Bulky Substituents

Many of the steroids contain acetates, benzoates, or other bulky substituents. In some cases crystals of a steroid acetate may have been of better quality than crystals of the parent alcohol. The halogenated substituents have usually been added to simplify structure determination. Steroid *p*-bromophenol complexes have occasionally been

prepared that allow the introduction of the heavy atom useful for structure determination without masking a possible functional site on the steroid. Patterns of conformational preference have been observed for these flexible substituents, and the relative conformations of acetate and benzoate substituents are discussed in some detail.

III. INTERMOLECULAR FORCES AND CRYSTAL PACKING

Steroid packing is controlled by molecular conformation and the hydrophilic and hydrophobic nature of molecular surfaces. Although hydrogen bonds are the strongest intermolecular interactions generally observed in steroid crystals, the composite of all other molecular surface interactions may be the most significant factor controlling packing (18). The dominant packing features can be characterized by means of a modified version of packing notation originally outlined by Bernal, Crowfoot, and Fankuchen (8). In this notation the orientation of the steroid thickness (t), width (w), and length (l) relative to the cell sides is recorded, and the number of steroid thicknesses, widths, and lengths present in a unit cell are recorded. The Hodgkin notation provides an easily scanned label useful for detecting isomorphous crystal forms. In the course of this analysis it was discovered that a number of steroid structures had almost identical crystal packings. Without questioning the importance of hydrophobic interactions, it is often convenient to consider the extended crystal structure in terms of the linking of molecules by hydrogen bonds if they are present.

A. Chain Formation

One characteristic pattern observed in steroid packing is the appearance of infinite chains. Head-to-tail hydrogen bonding is commonly observed to bind adjacent links in these chains. The following are among the types of chains commonly observed in steroid crystal structures.

1. Extended chains in which adjacent links are translationally equivalent are usually formed by molecules that are predominantly flat (the 1,3,5(10)-estratriene structures) and have hydrogen bonding groups at the C(3) and C(17) positions. The flat molecules occur less frequently in twisted chains in which adjacent links are related by rotation. In the three crystal forms of estrone the head-to-tail hydrogen-bonded chains are observed in three types of extended chains (Fig. 17).

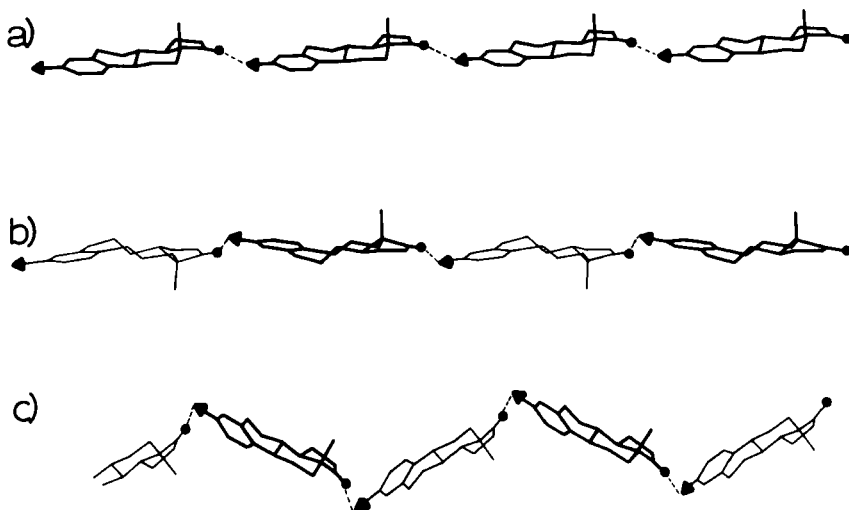


Fig. 17. The three crystal forms of estrone illustrate the variety in appearance of chains of molecules that are head-to-tail hydrogen bonded. In form (a) ES13B and adjacent chain links are translationally related and in forms (b) ES13C and D and (c) ES13A the links are rotationally related.

(2) Twisted chains in which adjacent links are rotationally equivalent more commonly occur in crystals of androstanes having some bowing toward the α face (Fig. 18). The orientation of the length of the steroid relative to the rotation axis will control the appearance of these twist chains.

B. Layer Formation

In general, straight chains and twist chains are packed together to form layers. The packing of the three estrone chains in their respective crystals (Fig. 19) illustrates that the layers are much better defined in those structures having extended chains (19a and 19b) rather than twisted chains (19c).

C. Coil Formation

Chains in which rotationally related steroids are hydrogen bonded and in which the length of the steroid is more nearly perpendicular than parallel to the rotation axis, may also be described as coils. Coils are commonly observed in the crystal packing of Δ^4 -3-one pregnanes in which the A-ring unsaturation and the crowding of the

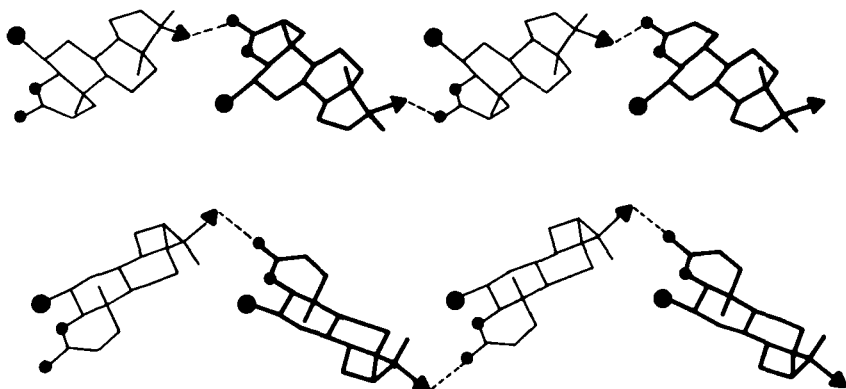


Fig. 18. The twisted chains of head-to-tail hydrogen bonded molecules in 6 α -bromo-17 β -hydroxy-17 α -methyl-4-oxa-5 α -androstane-3-one (AN09) approach a conformation that may be better termed a coil. The chain is shown in two mutually perpendicular views.

β face combine to accentuate the bowing of the molecule that lends itself to coil formation. Two of the most common coil forms are those observed in crystals of cortisol and cortisone. In cortisone the steroid thickness is nearly parallel to the rotation axis, and the C(6)···C(14) edge of the steroid is away from the coil axis (Fig. 20a). In cortisol the steroid width is nearly parallel to the rotation axis and the β face of the steroid is away from the coil axis (Fig. 20b). The uncommon double coil of 6 α -methylprednisolone (Fig. 21) suggests the complexity of the extended structures that can be discerned in the steroid packing patterns. Many structures, particularly pregnanes in which there are a number of potential hydrogen bond donors and acceptors, have interlocking patterns of chains, coils, and layers.

D. Crystalline Polymorphs, Multiple Asymmetric Units, and Conformational Isomers

The existence of polymorphs (different crystal forms of the same molecule) is common among the naturally occurring steroids. The analysis of several crystal forms of the same steroid provides information concerning the flexibility of the observed conformation or the possible existence of conformational isomers.

In many cases a particular crystal form may contain two crystallographically independent molecules. The

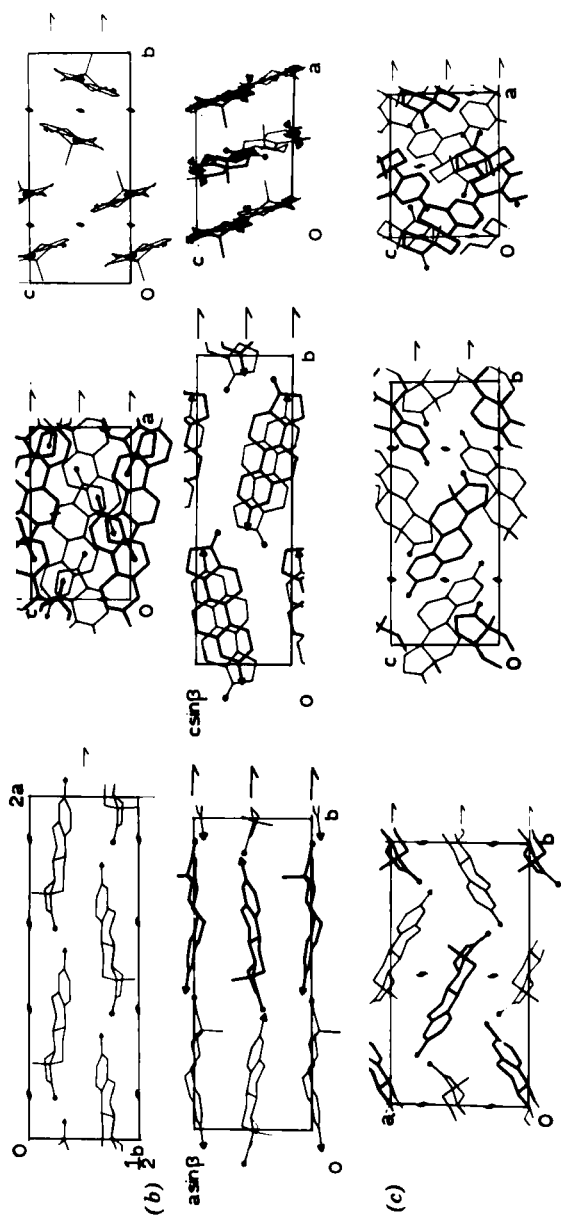


Fig. 19. Layers of estrone molecules are apparent in the crystal packing of the most extended chain forms (a) ES13B and (b) ES13C and D. In contrast, the molecules in the more twisted chains in (c) ES13A do not lie in well defined layers.

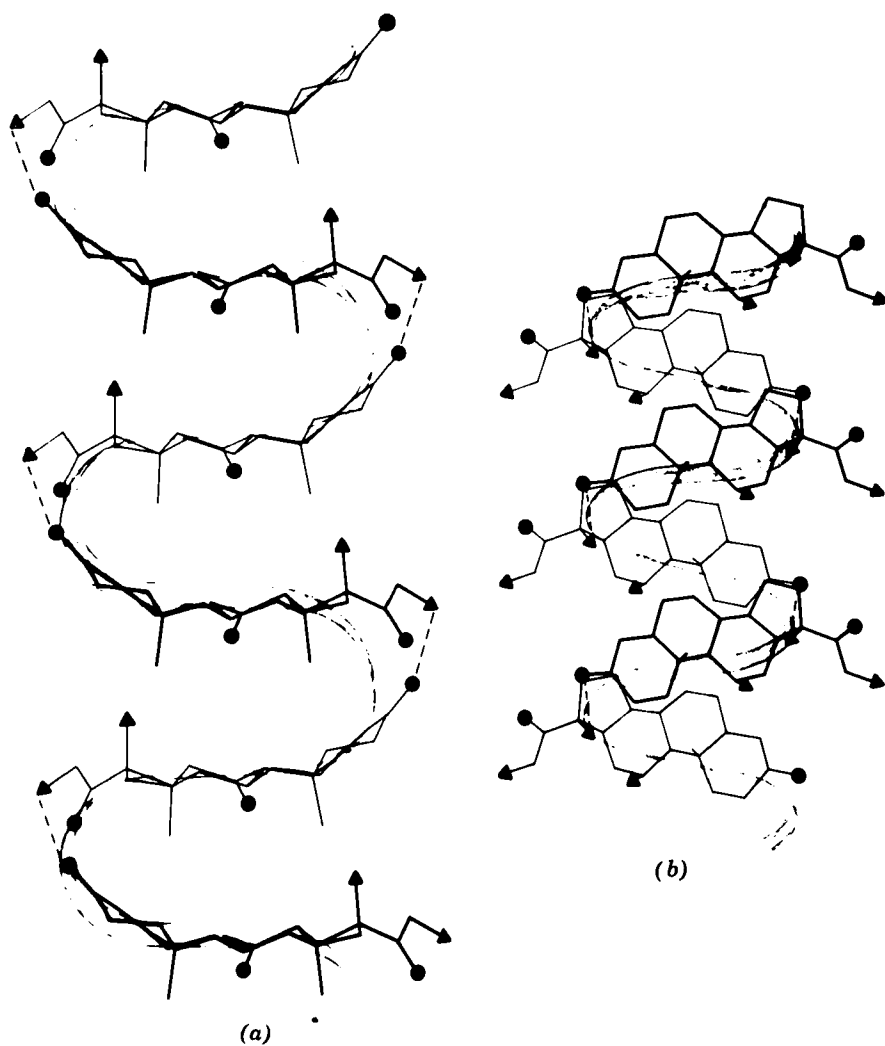


Fig. 20. Two types of molecular coils commonly observed are (a) that in which the dominant molecular plane is perpendicular to the coil axis exemplified by cortisone, PR20, and (b) that in which the width of the steroid molecule is parallel to the coil axis exemplified by cortisol, PR15.

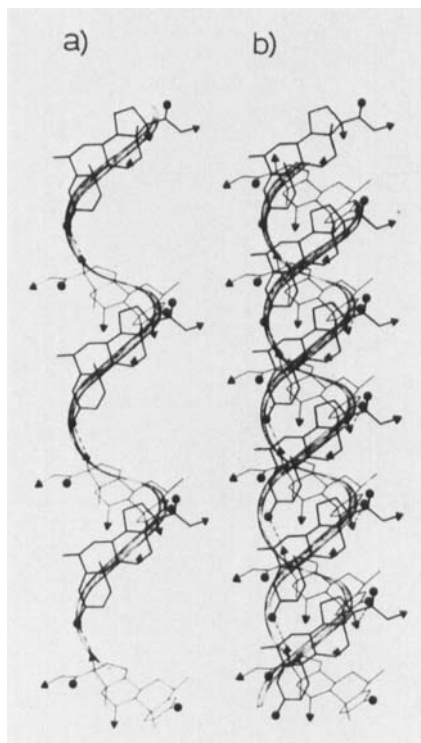


Fig. 21. A double coil of steroids is observed in the structure of 6 α -methylprednisolone, PR23. Individual coils (a) have head to tail hydrogen bonding and two coils related by a rotation axis at their core form a double coil (b).

asymmetric unit of such crystals is said to be doubled, and the crystallographically unique unit may be thought of as containing a dimer. Careful analysis reveals that in most cases the two crystallographically independent molecules are also conformationally distinct. Analysis of the steroid data suggests that the molecules are in fact conformational isomers having a finite barrier to interconversion. The relative population of conformers and the polymorph that is crystallized are determined by the solvent and conditions of crystallization.

IV. EXPECTED AND OBSERVED GEOMETRY

The variation in bonds and angles observed in steroid

crystal structures is a property of these molecules and not merely a result of errors in measurement or artifacts of packing forces. Perhaps the most striking example of the variation of molecular geometry in steroids from theoretical or expected values based upon consideration of simpler systems concerns the valency angles C(8)-C(14)-C(15) and C(14)-C(13)-C(17). The average values of these angles in 91 steroids are 119.3 ± 1.9 deg. and 99.2 ± 2.2 deg., respectively. This severe strain is a result of the fusion of the five- and six-membered rings at the C(13)-C(14) bond. Only three of the C(8)-C(14)-C(15) angles and six of the C(14)-C(13)-C(17) angles in this sample are more than two standard deviations from the average. Conformational differences can be attributed to strain caused by unusual substitution in some cases and regarded as an artifact of an inferior determination in others.

In order to assess the importance of individual variations in molecular geometry and conformations, tabulations of the observed ranges of variation and the average values of geometric parameters in subsets of the steroid data are required. An excellent summary of steroid molecular geometry derived from X-ray data and its comparison to theoretical calculations has recently been published by Romers, Altona, Jacob, and de Graaff (19). The sample analyzed by Romers *et al.* contained 30 estranes, 37 androstanes, 30 pregnanes, and 21 steroids of other classes.

The geometric and conformational analysis presented in the following sections concerns subsets drawn from 42 estrane, 78 androstane, and 64 pregnane structures listed in Table 3. Structural comparisons are made within subsets defined according to the presence of one or a combination of common characteristics. The members of a subset defined according to A-ring constitution may differ greatly in such things as D-ring constitution and the nature of ring junctions. Subsets having a single type of steroid nucleus may differ in substitution on that nucleus. For each subset, the compositional and configurational elements defining the set are stated. The structures comprising a given subset are designated by their code number, and in many cases comments on unusual characteristics of individual members of a subset are included.

The subsets to be discussed include (a) structures having the 1,3,5(10)-estratriene nucleus common to the naturally occurring estrogens (b) structures having Δ^4 -3-one constitution common to active androgens, progestins, and corticoids, (c) 5-ene structures such as cholesterol, (d) saturated structures having all trans ring junctions, and (e) retro steroids (9 β ,10 α).

Table 3.
Estranes, Androstanes, and Pregnanes
Analyzed by X-ray Crystallography

Code No.	IUPAC Name	Ref.
ES01	17 β -Hydroxy-5(10)-estren-3-one	20
ES02	5(10)-estren-17 β -yl-iodoacetate	21
ES03	17 β -Bromoacetoxy-7 α -methyl-4-estren-3-one	22
ES04	17 β - <i>p</i> -Bromobenzenesulfonyloxy-2 β -methyl-4-estren-3-one	23
ES05	1,3,5(10)-Estratriene-3,17 β -diol hemihydrate	24
ES06	1,3,5(10)-Estratriene-3,17 β -diol propanol (1:1)	25
ES07	1,3,5(10)-Estratriene-3,17 β -diol urea (1:1)	26
ES08	4-Bromo-1,3,5(10)-estratriene-3,17 β -diol methanol (1:1)	27
ES09A-C	2,4-Dibromo-1,3,5(10)-estratriene-3,17 β -diol	28
ES10	1,3,5(10)-Estratriene-3,17 β -diol-3- <i>p</i> -bromobenzoate	29
ES11	3-Methoxy-8 β -methyl-1,3,5(10)-estratrien-17 β -yl-bromoacetate	30
ES12	(\pm)-8-Aza-1,3,5(10)-estratriene-3,17 β -diol	31
ES13A-D	3-Hydroxy-1,3,5(10)-estratrien-17-one I, II, III	32a
ES13A	3-Hydroxy-1,3,5(10)-estratrien-17-one II	32b
ES14	4-Bromo-3-hydroxy-1,3,5(10)-estratrien-17-one	33
ES15	(\pm)-3-Hydroxy-8-aza-1,3,5(10)-estratrien-17-one hydrobromide	34
ES16	(\pm)-2,3-Dimethoxy-18-nor-8,13-diaza-1,3,5(10)-estratrien-17-one	35
ES17A,B	1,3,5(10)-Estratriene-3,16 α ,17 β -triol	36
ES18	17-Ethylenedioxy-3-methoxy-6 β ,7 β ,8 β -methylidyne-1,3,5(10)-estratriene	37
ES19	3-Methoxy-8 α -methyl-1,3,5(10),6-estratrien-17 β -yl-bromoacetate	37
ES20	3-Methoxy-7 α ,8 α -methylene-1,3,5(10)-estratrien-17 β -yl bromacetate	38
ES21	(\pm)-3-Methoxy-12-amino-18-nor-11,13-diaza-8 α -estra-1,3,5(10)-trien-17-one hydrobromide	39
ES22	(\pm)-10-Aza-5 β ,9 β -estr-8(14)-ene-3,17-dione	40
ES23	17 β -Acetoxy-9 β ,10 α -estr-4-en-3-one	41

Table 3. (Cont'd)

Code No.	IUPAC Name	Ref.
ES24	(\pm)-3-Methoxy-8-aza-9 β -estra-1,3,5(10)-trien-12-one hydrobromide	42
ES25	3-Methoxy-7-thia-9 β -estra-1,3,5(10),8(14)-tetraen-17 β -yl acetate	43
ES26	(\pm)-3-Methoxy-B-nor-9 β -estra-1,3,5(10)-trien-17-one	44
ES27	(\pm)-18-Acetyl-3-methoxy- <i>D</i> -homo-6-thia-18-aza-9 β -estra-1,3,5(10)-trien-17A-one nitromethane (1:1)	45
ES28A,B	17 α -Bromobenzoyloxy-7,7-dimethyl-8 α ,14 β -estr-4-en-3-one	46
ES29	17 β -Hydroxy-8(9-10 β)abeo-4-estrene-3,9-dione	47
ES30	2-Bromo-11,11-dimethyl-12 β ,17 β -methylene-3,14 α ,17 α ,17A β -tetrahydroxy- <i>D</i> -homo-18-nor-6-oxa-13 α -estra-1,3,5(10),7-tetraen-15-one	48
ES31	11 β -Methoxy-1,3,5(10)-estratriene-3,17-diol acetonitrile (1:1)	49
ES32A,B	9 α ,14 α ,17 α ,17A β -tetramethyl- <i>D</i> -homo-1,3,5(10)-estratrien-17 α -ol	50
ES33	17 β -Acetoxy-14 α -methyl-8 α ,9 β ,10 α ,13 α -estr-4-en-3-one	51
ES34	3,3-Dimethoxy-5 α -estran-17 β -yl <i>p</i> -toluenesulfonate	52
AN01	16 β ,17 β -Dibromo-5 α -androstande	53
AN02	5 α -Androstande-3 α ,17 β -diol	54
AN03	3 α -Bromoacetoxy-5 α -androstande-17-one	55
AN04	3 β -Hydroxy-5 α -androstande-17-one	56
AN05	3 α -Hydroxy-5 α -androstande-17-one	57
AN06A,B	17 β -Hydroxy-5 α -androstande-3-one	58
AN07	17 β -Hydroxy-5 α -androstande-3-one monohydrate	59
AN08	17 β -Bromoacetoxy-1 β ,2 β -(1',1'-dichloroethylene)-5 α -androstande-3-one	60
AN09	6 α -Bromo-17 β -hydroxy-17 α -methyl-4-oxa-5 α -androstande-3-one	61
AN10	5 α -Androstande-3,17-dione	62
AN11A,B	5 α -Androstande-3,17-dione <i>p</i> -bromophenol (1:1)	63
AN12	4 α -Bromo-5 α -androstande-2-ene-1,17-dione	64
AN13A,B	17 β -Hydroxy-4-androstande-3-one	65
AN14A,B	17 β -Hydroxy-4-androstande-3-one monohydrate	66,67
AN15	17 β -Hydroxy-4-androstande-3-one mercuric chloride (2:1)	68
AN16	17 β -Hydroxy-4-androstande-3-one <i>p</i> -	69

Table 3. (Cont'd)

Code No.	IUPAC Name	Ref.
	bromophenol (1:1)	
AN17	17 β - <i>p</i> -Bromobenzoyloxy-4-androsten-3-one	70
AN18	17 β -Trimethylsiloxy-4-androsten-3-one	71
AN19	2,2,6 β -Trichloro-17 β -acetoxy-4-androsten-3-one	72
AN20	17 β -Bromoacetoxy-8 β -methyl-4-androsten-3-one	73
AN21	9 α -Bromo-17 β -hydroxy-17 α -methyl-4-androstene-3,11-dione	74
AN22	17 β -Chloroacetoxy-2 β -acetoxy-4-androsten-3-one methanol (1:1)	75
AN23	2 β ,17 β -Diacetoxy-4-androsten-3-one <i>p</i> -bromophenol (1:1)	75
AN24	4-Androstene-3,17-dione	77
AN25A,B	3 β -Chloro-5-androsten-17 β -ol methanol (2:1)	78
AN26	17 α -Iodo-5-androsten-3 β -yl acetate	79
AN27	3 β - <i>p</i> -Bromobenzoyloxy-5-androsten-17-one	80
AN28	17 β -Hydroxy-1,4-androstadien-3-one <i>p</i> -bromophenol (1:1)	81
AN29	1,4,6-Androstatriene-3,17-dione <i>p</i> -bromophenol (1:1)	82
AN30	5 β -Androstane-3 α ,17 β -diol	83
AN31	3 β ,6 β -Dimethoxy-5,19-cyclo-5 β -androstan-17-one <i>N</i> -acetyl <i>p</i> -bromobenzenesulfonylhydrazone	84
AN32A,B	9-Hydroxy-9 β 10 α -androst-4-ene-3,17-dione	85
AN33	6 α -Fluoro-17 β -acetoxy-6 β -methyl-9 β ,10 α -androst-4-en-3-one	86
AN34	17 β -Bromoacetoxy-9 β ,10 α -androst-4-en-3-one	87
AN35	17 α -Hydroxy-4-androsten-3-one	88
AN36	9 β ,10 α -Androsta-4,6-diene-3,17-dione	89
AN37	6 β -Fluoro-17 β -acetoxy-6 α -methyl-9 β ,10 α -androst-4-en-3-one	90
AN38	3 β - <i>p</i> -Bromobenzoyloxy-13 α -androst-5-en-17-one	91
AN39	(\pm)-17 β -Hydroxy- <i>D</i> -homo-12,18-dinor-8 α ,13 α ,14 β -androst-4-en-3-one	92
AN40	3-Methoxy- <i>AB</i> (10 α)-homo-19-nor-1 (10),2,4-androstatrien-17 β -yl <i>p</i> -bromobenzoate	93
AN41	3 α ,17 β -Diacetoxy-2 β ,16 β -dipiperidino-5 α -androstane dimethylbromide methylene chloride monohydrate (1:1:1)	94
AN42	3 α - <i>p</i> -Bromobenzoyloxy-11 α -hydroxy- <i>C</i> -nor-5 β ,13 α -androstan-11 β ,17 β -carb lactone	95
AN43	2 β -Methoxy-1 β -hydroxy-18-nor-5,8,11,13-androstetetraene-3,7,17-trione-	96

Table 3. (Cont'd)

Code No.	IUPAC Name	Ref.
	(6,5- <i>b</i>)-furan	
AN44	(\pm)-3-Chloro-4,5-seco-13 α -androsta-2,8,14-triene-5,17-dione	97
AN45	3 β ,17 β -Dihydroxy-5 α -androstane monohydrate	98
AN46	1 α ,4 α -Epoxy-A-homo-3-aza-5 β -androstan-16 β -ol hydrobromide methanol (1:1)	99
AN47	2 α -Bromo-3 α -hydroxy-17 α -methyl-5 α ,14 β -androstane	100
AN48	17 β -Benzoyloxy-3-oxo-4-androsten-19-al	101
AN49	17 β -Acetoxy-2,4-dioxa-3-thia-5 α -androstan-3-one	102
AN50	16 α -Bromo-3 β -hydroxy-5-androsten-17-one methanol (1:1)	103
AN51	2 β ,17 β -Diacetoxy-4-androsten-3-one	104
AN52	17 β - <i>p</i> -Bromobenzoyloxy-2,2-dimethyl-5 α -androstan-3-one	105
AN53	5 α -Androst-2-en-17 β -yl chloroacetate	106
AN54	19-Hydroxy-4-androstene-3,17-dione	107
AN55	5-Androstene-3 β ,17 β ,19-triol 17- <i>p</i> -bromobenzoate	108
AN56	17 β -Chloroacetoxy-2 β -acetoxy-4-androsten-3-one	109
AN57	2,4-Dioxa-5 α -androstan-17 β -yl acetate	110
AN58	14 α ,15 α -Epoxy-5 α ,8 β -androstane-3 β ,17 β ,19-triol 3,17-diacetate	111
AN59	17 β -Acetoxy-6 β ,7 β -methylene-4-androsten-3-one	112
AN60	3-Ethylenedioxy-5-androstene-17 β ,19-diol 17-benzoate	113
AN61	3 β -Hydroxy-17-oxo-5-androsten-19-al	114
AN62	(\pm)-4 α ,8,14-trimethyl-18-nor-5 α ,8 α ,14 β -androst-9(11)-ene-3,17-dione	115
AN63	(\pm)-14 β -Androsta-4,8-diene-3,17-dione	116
AN64	2 α ,17 β -Diacetoxy-4-androsten-3-one	117
AN65	(19 <i>R</i>)-19-Methyl-5-androstene-3 β ,17 β ,19-triol	118
AN66	2 α ,3 α -Epithio-5 α -androstan-17 β -yl <i>p</i> -bromobenzoate	119
AN67	14 β -Azido-5 α -androstane	120
AN68	(19 <i>R</i>)-Methoxy-5,19-methyleneoxido-17 β -acetoxy-5 β -androstan-3-one	121
AN69	17 β - <i>p</i> -Toluenesulfonyloxy-5 α -androstan-3-one	122
AN70	4-Androsten-17 β -yl <i>p</i> -bromobenzenesulfonate	123
PR01	16 β -Bromo-3 β ,17 α -dihydroxy-5 α -pregnane-	124

Table 3. (Cont'd)

Code No.	IUPAC Name	Ref.
	11,20-dione	
PR02	16 β -Bromo-3 β -acetoxy-17 α -hydroxy-5 α -pregnane-11,20-dione	125
PR03	21-Bromo-3 β ,17 α -dihydroxy-5 α -pregnane-11,20-dione	126
PR04A,B	5-Bromo-6 β ,19-epoxy-3 β -hydroxy-5 α -pregnan-20-one	127
PR05A,B	(20S)-20-Chloro-5 α -pregnane-3 β ,16 β -diol di- <i>p</i> -bromobenzoate	128
PR06	16 α -Ethyl-16(2)-cyano-16(2),21-cyclo-5 α -pregna-17(20),21-dien-3 β -yl bromoacetate	129
PR07	Trans-21,21-tetrafluoroethylene-5 α -pregn-17(20)-en-3 β ,20-diol 3- <i>p</i> -bromobenzoate 20-acetate	130
PR08	4-Pregnene-3,20-dione	131
PR09	6 β -Bromo-4-pregnene-3,20-dione	132
PR10	15,16-Di (trifluoromethyl)-14 α ,17 α -vinylene-4,15-pregnadiene-3,20-dione	133
PR11	12 α -Bromo-11 β -hydroxy-4-pregnene-3,20-dione	134
PR12	17 α -Hydroxy-4-pregnene-3,20-dione	135
PR13	21-Hydroxy-4-pregnene-3,20-dione	136
PR14	17 α ,21-Dihydroxy-4-pregnene-3,20-dione	137
PR15	11 β ,17 α ,21-Trihydroxy-4-pregnene-3,20-dione methanol (1:1)	138
PR16	6 α -Fluoro-11 β ,17 α ,21-trihydroxy-4-pregnene-3,20-dione	139
PR17	9 α -Fluoro-11 β ,17 α ,21-trihydroxy-4-pregnene-3,20-dione	140
PR18	9 α -Bromo-11 β ,17 α ,21-trihydroxy-4-pregnene-3,20-dione	141
PR19	9 α -Chloro-11 β ,17 α ,21-trihydroxy-4-pregnene-3,20-dione	142
PR20	17 α ,21-Dihydroxy-4-pregnene-3,11,20-trione	143
PR21	21-Acetoxy-17 α -hydroxy-4-pregnene-3,11,20-trione	144
PR22	4-Chloro-17 α ,21 β -dihydroxy-4-pregnene-3,11,20-trione	145
PR23	11 β ,17 α ,21-Trihydroxy-6 α -methyl-1,4-pregnadiene-3,20-dione	146
PR24	21-Bromo-9 α -fluoro-11 β -hydroxy-16 α ,17 α -(22R)-methylphenylmethylenedioxy-4-pregnene-3,20-dione methanol (1:1)	147
PR25	(18 <i>R</i> ,20 <i>S</i>)-18,11-Acetal-20,18-hemiketal of 11 β ,21-dihydroxy-3,20-dioxo-4-	148

Table 3. (Cont'd)

Code No.	IUPAC Name	Ref.
	pregnen-18-al monohydrate	
PR26A,B	16 α -Iodo-3 β -acetoxy-14 α ,17 α -ethylene-5-pregnen-20-one	149
PR27	3 β -Bromoacetoxy-16 α ,17 α ((1' <i>S</i> ,2' <i>S</i>)-1',2'-dichloroethylene)-5-pregnen-20-one	150
PR28	16 α ,20-Tetrafluoroethyleneoxy-5,17(20)-pregnadien-3 β -yl <i>p</i> -bromobenzoate	151
PR29	6 α ,7 α -Difluoromethylene-11 β ,17 α -dihydroxy-21- <i>p</i> -bromobenzoyloxy-16 α -methyl-2,4-pregnadien-20-one (2,3- <i>d</i>)-1'-phenylpyrazole	152
PR30	6 α ,7 α -Difluoromethylene-11 β -hydroxy-16 α ,17 α -isopropylidenedioxy-21- <i>p</i> -bromobenzoyloxy-2,4-pregnadien-20-one (2,3- <i>d</i>)-1'-phenyl-pyrazole butanol (1:1)	153
PR31	9 β ,10 α -Pregna-4,6-diene-3,20-dione	154
PR32	6 α -Methyl-9 β ,10 α -pregn-4-ene-3,20-dione	155
PR33	11 α -Hydroxy-9 β ,10 α -pregn-4-ene-3,20-dione	156
PR34	4-Bromo-9 β ,10 α -pregna-4,6-diene-3,20-dione	157
PR35	(20 <i>R</i>)-20-Bromo-17A β -(<i>N</i> -cyano- <i>N</i> -methylaminomethyl)- <i>D</i> -homo-12,18-dinor-5 α ,13 α -pregnane	158
PR36	7 α -Acetylthio-3-oxo-17 α -pregna-4-ene-21,17 β -carb lactone	159
PR37	17 α -(9'-Oxo-10'-chloridedecanoyloxy)-4-pregnene-3,20-dione	160
PR38	11 β ,21-Dihydroxy-4-pregnene-3,20-dione	161
PR39	3,20-Bis(ethylenedioxy)-9,10-seco-5,7,10(19)-pregnatriene	162
PR40	9 α -Fluoro-11 β ,17 α ,21-trihydroxy-4-pregnene-3,20-dione	163
PR41	3 α ,9 α -Epoxy-18,14 β -(<i>N</i> -methylaminoethyleneoxy)-5 β ,14 β -pregna-7,16-diene-3 β ,11 α ,20-triol 20- <i>p</i> -bromobenzoate	164
PR42	(20 <i>S</i>)-3 α ,9 α -Epoxy-18,14 β -(<i>N</i> -methylaminoethyleneoxy)-5 β ,14 β -pregn-16-ene-3 β ,11 α ,20-triol 3-methyl ether	165
PR43	6-Chloro-21-fluoro-17 α -acetoxy-16-methylene-4,6-pregnadiene-3,20-dione	166
PR44	17 β -Hydroxy-19-nor-17 α -pregna-4,9-dien-20-yne-3,11-dione	167
PR45	3,20-Bis(ethylenedioxy)-5,7-pregnadiene	168
PR46	9 α -Fluoro-11 β -hydroxy-2 α -methyl-4-pregnene-3,20-dione	169
PR47	9 α -Fluoro-11 β ,17 α ,21-trihydroxy-2 α -	170

Table 3. (Cont'd)

Code No.	IUPAC Name	Ref.
	methyl-4-pregnene-3,20-dione	
PR48	19-Nor-5,14-dimethyl-18-aza-5 β ,14 β -pregnane	171
PR49	11 β ,17 α ,21-Trihydroxy-4-pregnene-3,20-dione pyridine (1:1)	172
PR50A,B	9 α -Fluoro-11 β ,17 α ,21-trihydroxy-6 α -methyl-1,4-pregnadiene-3,20-dione	173
PR51	(\pm)-9 α -Methyl-19-nor-4-pregnene-3,20-dione	174
PR52	9 α -Fluoro-11 β ,21-dihydroxy-16 α -methyl-1,4-pregnadiene-3,20-dione	175
PR53A,B	5 α ,17 α -Pregnane-3 β ,20 α -diol	176
PR54	6-Chloro-17 α -acetoxo-1 α ,2 α -methylene-4,6-pregnadiene-3,20-dione	177
PR55	11 β ,16 α ,17 α ,21-Tetrahydroxy-1,4-pregnadiene-3,20-dione	178
PR56	Potassium 17 β -hydroxy-3-oxo-17 α -pregna-4,6-diene-21-carboxylate	179

A. 1,3,5(10)-Estratrienes

1. Average Bond Lengths and Angles

Structures having the 1,3,5(10)-estratriene configuration are of particular interest because they include the natural estrogens and many of their precursors and metabolites. The average bond lengths and angles of seventeen structures having 1,3,5(10)-estratriene composition and all *trans* junctions are given in Figure 22.

The estimator of the standard deviation of the mean of these dimensions is also included in the figure. This parameter is defined as

$$s = \left[n^{-1} (n-1)^{-1} \sum_{i=1}^n (q_i - \bar{q})^2 \right]^{1/2} \quad [3]$$

where n = number of observations and \bar{q} = unweighted average of the measurements q_i .

2. B-Ring Conformation

The principal point of molecular flexibility in this series of steroids is in the B ring. The B-ring conformation is observed to vary over a range extending from a 7 α ,8 β

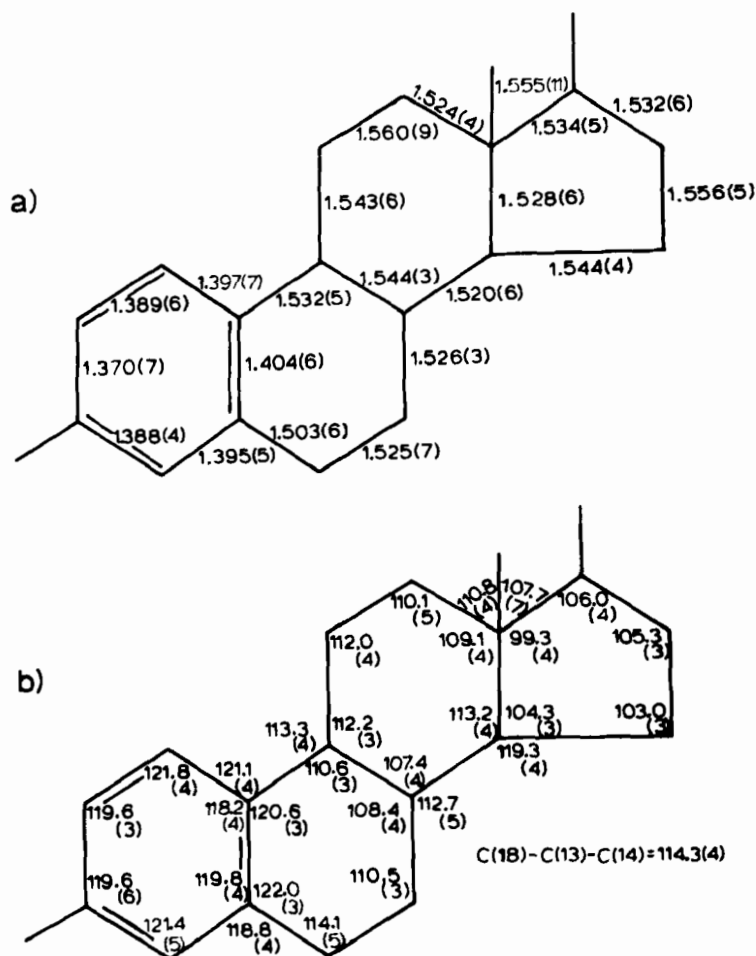


Fig. 22. Average bond lengths (a) and angles (b) for the 1,3,5(10)-estratriene structures ES05, 06, 07, 08, 09A, 09B, 09C, 10, 11, 13A, 13B, 13C, 13D, 14, 17A, 17B, and 31. The estimators of standard deviation are in parenthesis.

half-chair conformation to an 8B sofa conformation. The two crystallographically distinct molecules of estriol exemplify the extremes of this range. In ES17B the B ring is observed in a nearly perfect 7 α ,8B half-chair conformation. The displacements of atoms C(7) and C(8) from the least-squares plane through atoms C(5), C(6), C(9), and C(10) are -0.34 and +0.44 Å, respectively. The

nearly perfect rotation symmetry about a line joining the midpoints of the C(7)-C(8) and C(5)-C(10) bonds is reflected in the small magnitude of the $\Delta C_2(5-10)$ asymmetry parameter (3.5). In ES17A the B ring is observed in an 8β sofa conformation. The displacement of the C(8) atom from the least-squares plane through the remaining five atoms of the B ring is 0.70 Å. The approximate mirror symmetry across a plane intersecting atoms C(8) and C(5) is indicated by the small magnitude of the $\Delta C_s(5)$ asymmetry parameter (4.2). The effect of this B-ring conformational difference upon the orientation of the A ring relative to the bulk of the molecule is illustrated in Figure 23.

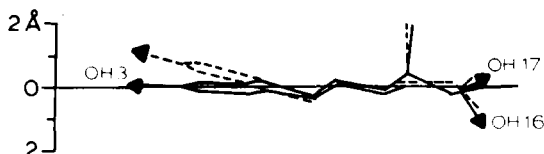


Fig. 23. Superposition of the B-ring sofa (dashed line) and the B-ring half-chair (solid line) conformers of estriol (ES17).

The relative conformations in the B-ring in the 1,3,5(10)-estratriene structures are displayed in a plot of rotation asymmetry $\Delta C_2(5-10)$ versus mirror asymmetry $\Delta C_s(5)$ (Fig. 24). The plot of these B ring asymmetry parameters forms two straight lines that represent the interconversion between a perfect sofa conformation and a perfect half-chair conformation. The clustering of points at each end of the line and the presence of observations at either extreme of the line for molecules of identical constitution (Table 4) and configuration suggests that for many structures the 8β sofa and $7\alpha,8\beta$ half-chair conformers are energy-minimum forms separated by a finite barrier. Crystallization conditions and packing forces may stabilize one conformer or the other (ES13A) or may result in the co-crystallization of both conformers (ES17A and B, ES13C and D, ES09B and C).

3. Correlated Changes

Specific changes in the molecular geometry and conformation of other parts of the steroid can be correlated with the 8β sofa to $7\alpha,8\beta$ half-chair transition. Because some of these changes must be relevant to long-range

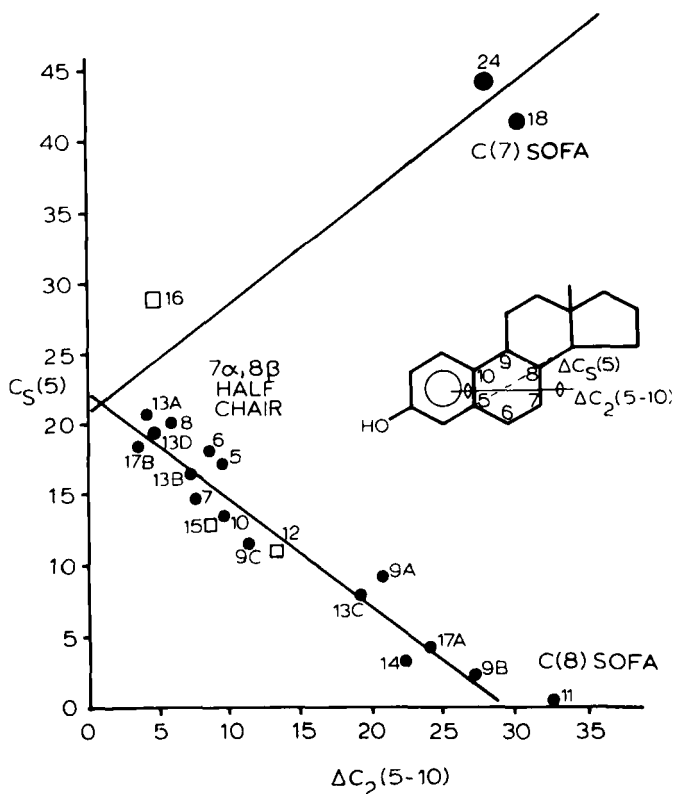


Fig. 24. Correlated variation in principal asymmetry parameters of the B rings in 1,3,5(10)-estratriene structures. The rotational asymmetry parameter $\Delta C_2(5-10)$, is plotted versus the mirror asymmetry parameter, $\Delta C_S(5)$. Three aza-substituted estranes (\square) are also included in the figure.

or conformational transmission effects previously described, the geometry of structures having 8 β sofa B-ring conformations are contrasted with those having 7 α ,8 β half-chair conformations.

The bond lengths, valency angles, and torsion angles for the 8 β sofa subset, I (ES09A, 09B, 11, 13C, 14, 17A), and the 7 α ,8 β half-chair subset, II (ES05, 06, 07, 08, 09C, 10, 13A, 13B, 13D, 17B) were averaged. The averages for corresponding parameters were compared, and Student's *t*-test was applied to determine whether observed differences were significant. The magnitudes of differences in bond lengths and valency angles that were above the 90% level are recorded in Figure 25. The average endocyclic torsion angles in the two conformers are compared in

Table 4.
Conformational Isomers in the
1,3,5(10)-Estratriene Series

Structure	B-Ring Conformation	
	8 β Sofa	7 α ,8 β Half-chair
Estriol	ES17A	ES17B
Estrone	ES13C	ES13A, 13B, 13D
2,4-Dibromoestradiol	ES09B	ES09C
4-Bromo-1,3,5(10)- estratriene	ES14 (17-one)	ES08 (17-ol)

Figure 26. The differences that pass the t -test at the 90% confidence level are designated with an asterisk. It is noteworthy that the magnitudes of the averaged torsion angles of the A ring alternate in sign indicating a slight symmetric puckering of the ring that is significantly enhanced when the B ring has a sofa conformation. Approximate relationships between torsion angles and valency angles in five- and six-membered rings recently derived by Dunitz (13) provide the basis for much of the variation observed here.

The twist about the length of the steroid [C(1)-C(10)···C(13)-C(18)] is a function of the B-ring conformation as illustrated in Figure 27. The subsequent dependence of relative positions of bulky and functional groups distant from the B rings is indicated in Figure 28. The position of the C(18) methyl relative to the least-squares plane of atoms C(5)-C(17) is seen to be correlated with B-ring conformation to a greater degree than is the position of the O(3) atom relative to the same plane (Fig. 28). The crowding of the β face caused by the 8 β -methyl substitution in ES11 is responsible for conformational anomalies evident in this structure. The C(18) distance from the plane is also unusually large in the 4-bromoestrone structure (ES14), but no simple explanation is evident.

The B-ring conformation is also observed to influence the distances between the O(3) and C(18) atoms (Fig. 29a), the predominant symmetry in the C ring (Fig. 29b), and the C(14)-C(8)-C(9)-C(11) torsion angle (Fig. 29c). The variation in these parameters is greater in structures having 7 α ,8 β half-chair B-ring conformations [$\Delta C_2(5-10)$ near 0.0] than in structures having 8 β sofa B-ring conformations. Once again the conformation of the 8 β -

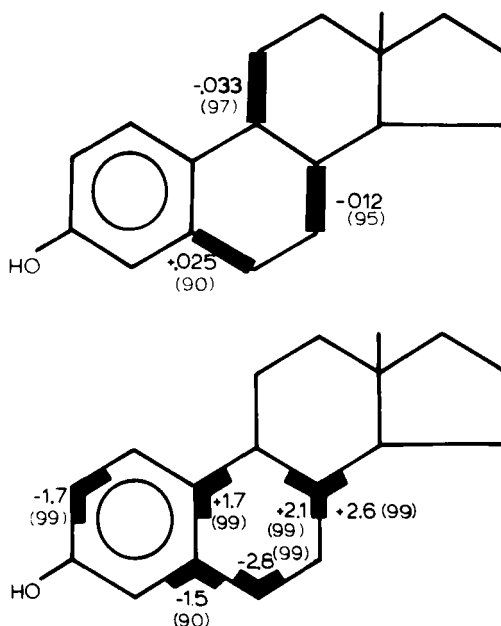


Fig. 25. The bond length and valency angle differences that are correlated with B-ring conformational differences at the 90% significance level or greater. The average magnitudes of parameters in B-ring sofa conformers have been subtracted from the corresponding averages in B-ring half-chair conformers.

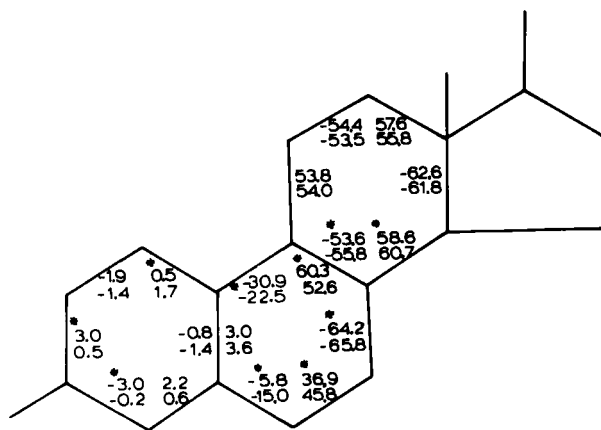


Fig. 26. Comparison of the average torsion angles in the 8 β sofa and the 7 α ,8 β half-chair conformers of 1,3,5(10)-estratriene structures. Differences significant above the 90% level are marked with an asterisk.

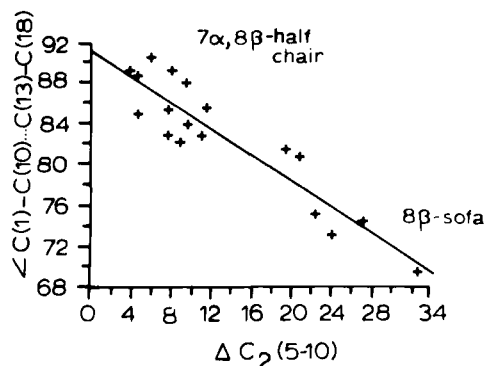


Fig. 27. Correlated variation in the twist about the length of the steroid [$C(1)-C(10) \cdots C(13)-C(18)$] and the B-ring conformation. The points do not deviate appreciably from their least-squares line.

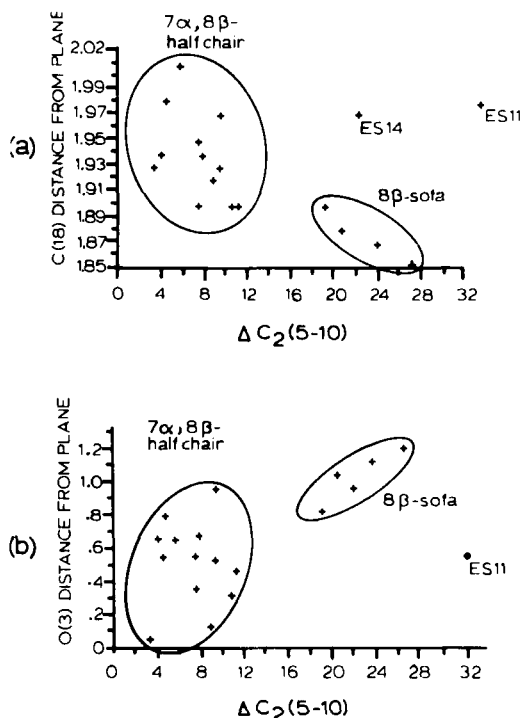


Fig. 28. The distance in Angstroms of (a) the angular methyl carbon atom $C(18)$ and (b) the $O(3)$ substituent from the least-squares plane through atoms $C(5)+C(17)$ as a function of B-ring conformation.

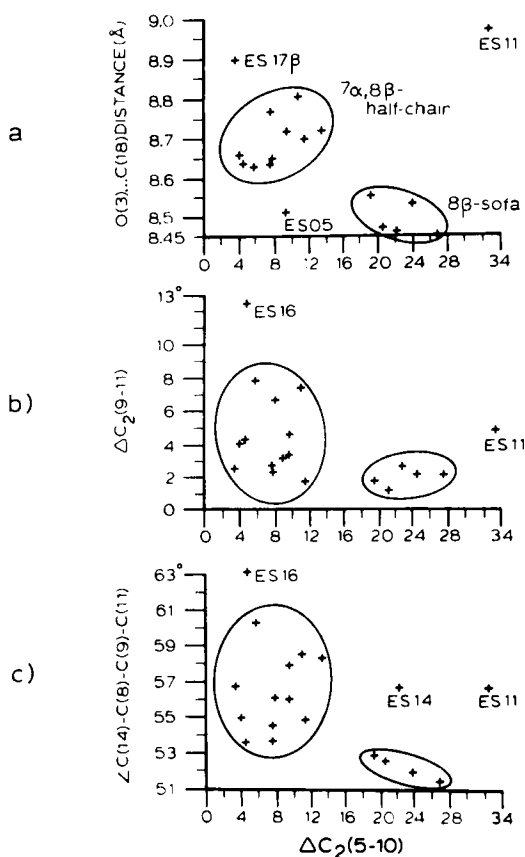


Fig. 29. Correlated variations between the B-ring conformation and (a) the $O(3) \cdots C(18)$ interatomic distance, (b) the symmetry in the C ring, and (c) the $C(14)-C(8)-C(9)-C(11)$ torsion angle.

methyl structure is atypical.

4. Restricted Flexibility

Certain configurations have less flexibility than others. In all three crystal complexes of estradiol (ES05, ES06, and ES07) the conformational variance in the B ring is negligible. Crowding of the steroid nucleus and heterosubstitution may result in the stabilization of a particular conformer. The B-ring conformations in two 8-aza-substituted steroids (ES12 and ES15) are nearly

identical (Fig. 24). The B ring in an 8 β -methyl derivative of the 1,3,5(10)-estratriene nucleus is in one of the most perfect 8 β -sofa conformations thus far observed [$\Delta C_s(5) = 0.5$]. With methylidyne addition to the C(6), C(7) and C(8) atoms, the B ring adopts a 7 α sofa conformation (ES18). This conformation is also observed in an 8-aza-9 β -estrone (ES24). The B rings of the two 5(10)-estrenes (ES01, ES02) have 7 α ,8 β half-chair conformations similar to those observed for 1,3,5(10)-estratrienes. In these steroids the observed A ring conformations are 2 α sofa in the structure having a 3-carbonyl substituent (ES01) and 2 α ,3 β half-chair in the unsubstituted A-ring (ES02) as illustrated in Figure 30.



Fig. 30. A-ring conformations in the 5(10)-estrenes.

B. 8 α -Estrenes

A number of 8 α -estrone derivatives have estrogenic activity comparable to that of estradiol. The striking conformational differences between steroids having 8 α and 8 β configurations are illustrated in Figure 31 in which ORTEP drawings of estradiol (ES05), an 8 α -steroid (ES19), the plant estrogen bromomirestrol (ES30), and the nonsteroidal estrogen, diethylstilbesterol, are compared. The diethylstilbesterol molecule shown in the crystallographically observed form considered by Hospital and Busetta to be the active conformer (180). The artificial estrogen and the plant estrogen are seen to have conformations more closely resembling the 8 α estrogens than estradiol itself. The interatomic distance between the terminal oxygens O(3)···O(17) is commonly regarded as a significant parameter in determining estrogenic function. The O(3)···O(17) distances of the 8 α and 8 β derivatives are not significantly different but the distance is much less than the 12.1 Å distance between the terminal oxygens in diethylstilbesterol (Table 5).

Alternating ± 12 deg. endocyclic torsion angles in the 8 α -substituted structure (ES19) clearly show puckering of the phenolic A ring. In addition to having an 8 α configuration, structure ES28 has a 14 β configuration. The combination of these two unusual configurations reduces the O(3)···O(17) distance to 9.3 Å (Fig. 32).

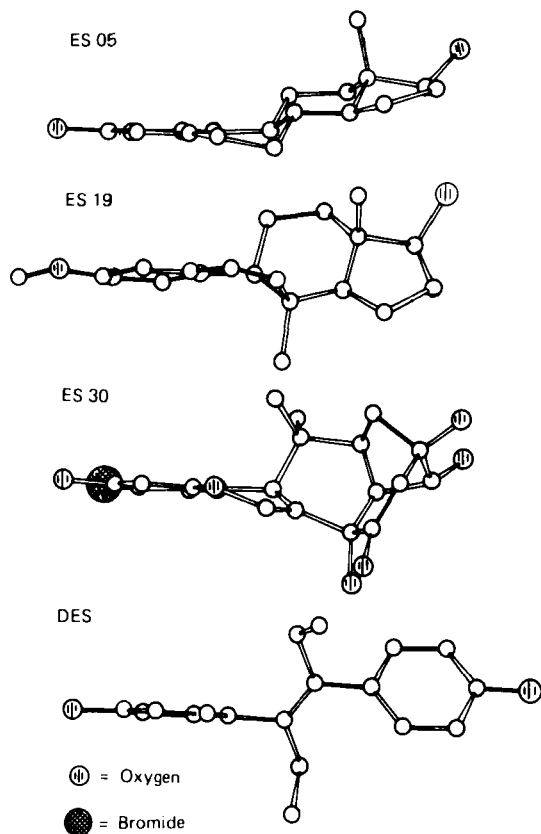


Fig. 31. Comparison of the overall conformations of estradiol (ES05), an 8 α -estrene (ES19), bromomirestrol (ES30) and diethylstilbesterol. ⊖ = oxygen and ● = bromine.

Table 5.
Oxygen-Oxygen Distances in Some Estrogens

Structure	O(3)···O(17) distance (Å)
ES05	10.9
ES06	11.0
ES19	10.7
ES30	10.9
Diethylstilbesterol	12.1

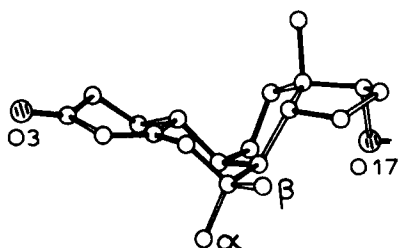


Fig. 32. Overall conformation of the $8\alpha,14\beta$ -estrone (ES28).

C. 9β -Estrones

The overall conformations of six estrones having 9β configurations are compared in Figure 33. Most structures are curved toward the α face, but the degree to which they are curved is altered by configurational differences in the molecules. The most pronounced bend is in ES27, which has the 1,3,5(10)-estratriene configuration and no other unsaturation. The bend in ES26 is less severe

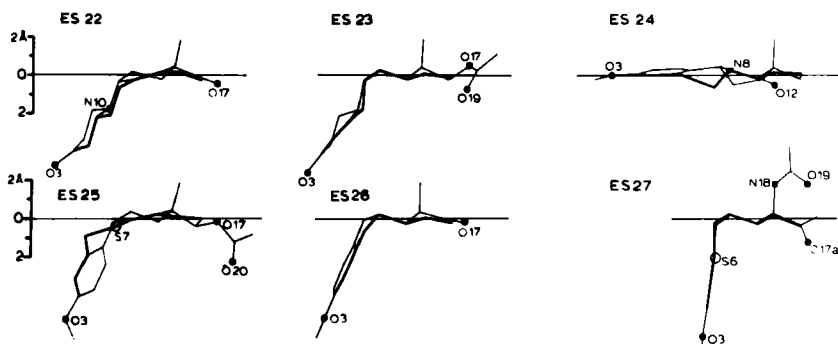


Fig. 33. Relative conformations of six 9β -estrone derivatives, projected parallel to a line joining the midpoints of the C(8)-C(14) and C(11)-C(12) bonds. The horizontal line is the least-squares plane of the atoms of the C and D rings.

because of the five-membered B ring. The 10α -4-en-3-one configuration of ES23 further relaxes the bend toward the α face. Structures ES22 and ES25 each have an 8-14 double bond that draws the B ring up toward the average plane of the C and D rings. While all rings in the ES22

structure have normal conformations, the 6-thia-8-ene configuration in ES25 appears to be responsible for the presence of a boat conformation observed in the B ring of this structure. The most unusual conformation observed in the 9β -estrene series is that of ES24 in which the steroid nucleus is nearly as flat as that in structures having all trans junctions. This variation from the pattern of the other 9β -estrenes is accomplished as a result of the twist conformation of the C ring. It seems likely that this twist conformation must result from the 8-aza substitution or the 12-keto addition or a combination of the two.

D. Δ^4 -3-One Structures

The Δ^4 -3-one structure is common to numerous natural and synthetic androgens, progestins, and corticoids. The presence of the double bond introduces the potential for conformational flexibility that may be vital to the complex sequence of interactions in which an active hormone participates. The Δ^4 -3-one structures for which atomic coordinates are available include structures having additional unsaturation in the nucleus as well as various abnormal junction configurations. However, the largest subset of these structures has no other unsaturation or cis junctions. All Δ^4 -3-one structures are catalogued in Table 6 and subdivided according to differences in the steroid skeleton.

Table 6.
Classification of Δ^4 -3-One Structures

a. Δ^4 -3-one	ESO3, ESO4; AN13A, AN13B, AN14A, AN14B, AN15, AN16, AN17, AN18, AN19, AN20, AN22, AN23, AN24, AN35, AN48, AN51, AN54, AN56, AN64; PRO8, PRO9, PR10, PR11, PR12, PR13, PR14, PR15, PR16, PR17, PR18, PR19, PR24, PR25, PR36, PR37, PR38, PR46, PR47, PR49, PR51
b. Δ^4 -3,11-dione	AN21; PR20, PR21, PR22
c. $\Delta^{1,4}$ -3-one	AN28; PR23, PR50A, PR50B, PR52, PR55
d. $\Delta^{4,6}$ -3-one	AN59; PR43, PR46
e. $\Delta^{1,4,6}$ -3-one	AN29; PR54
f. $9\beta,10\alpha$ - Δ^4 -3-one	ES23, ES35; AN32A, AN32B, AN33, AN34, AN37; PR32, PR33
g. $9\beta,10\alpha$ - $\Delta^{4,6}$ -3-one	AN36; PR31, PR34
h. Other	ES28A, ES28B, ES29; AN39; PR29, PR30

1. Average Bond Lengths and Angles

The average bond lengths and valency angles of the androstanes and pregnanes in categories (a) and (b) in Table 6 are displayed in Figure 34. The magnitudes of average bond lengths between sp^3 carbons are observed to vary from 1.522(3) to 1.567(2) Å. The average magnitudes of the endocyclic valency angles involving sp^3 carbons in the six-membered rings are observed to range from 108.1 to 113.4 deg. indicating a general flattening of the rings.

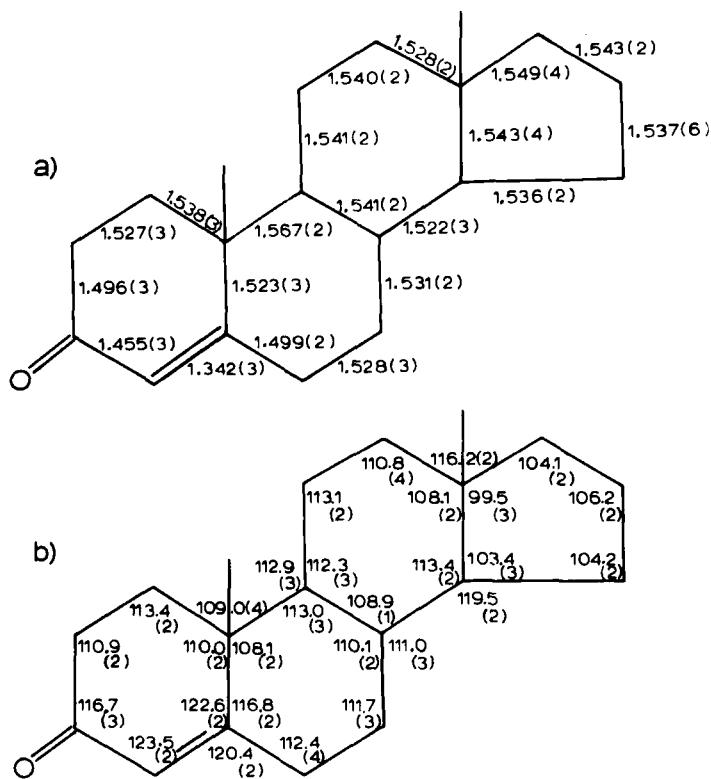


Fig. 34. The average bond lengths (a) and valency angles (b) for the Δ^4 -3-one structure ES03, 04; AN13, 14, 15, 18, 19, 22, 23, 24, 51, 54, 56, 59, 64; PRO8, 09, 10, 11, 12, 13, 14, 15, 16, 17, 18, 19, 20, 21, 22, 25, 36, 37, 38, 46, 47, 49, 51. The estimators of the standard deviations in the averages are given in parentheses.

2. A-Ring Conformation

The A-ring conformations of 37 of the 43 steroids in Table 6 vary from the $1\alpha,2\beta$ half-chair conformation observed in 12α -bromo- 11β -hydroxyprogesterone (PR11, Fig. 35a) to the 1α sofa conformation observed in 6β -bromoprogesterone (PRO9, Fig. 35b). The effect of this A-ring conformational difference upon the orientation of the C(3)-O(3) bond with respect to the steroid nucleus is illustrated in Figure 35c. The relative conformations of the A rings of the structures in Table 6 are displayed in a plot of the rotational asymmetry parameter $\Delta C_2(1-2)$ versus the mirror asymmetry parameter $\Delta C_s(1)$ (Fig. 36a). The A-ring conformations are observed to fall along a straight line tracing the interconversion between the perfect sofa and perfect half-chair conformations.

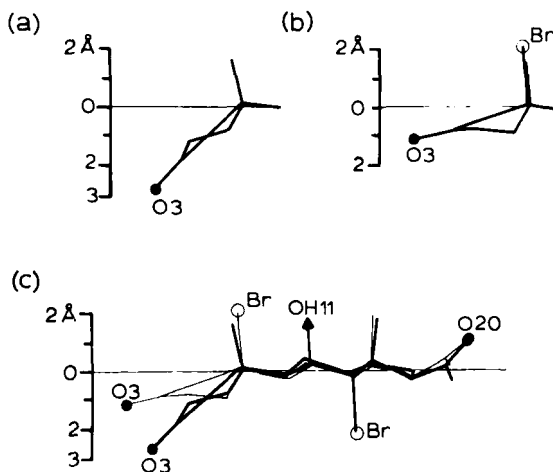


Fig. 35. Δ^4 -3-One A rings (a) in the $1\alpha,2\beta$ half-chair conformation in 12α -bromo- 11β -hydroxyprogesterone (PR11), and (b) in the 1α sofa conformation in 6β -bromoprogesterone (PRO9). The change in relative position of the O(3) atom accompanying the A-ring variation is shown in the superposition diagram (c).

The structures can be subdivided into groups I, II, and III as indicated in Figure 36a. Fourteen of the structures have A-, B-, and C-ring configurations identical to that of testosterone. The A-ring conformations of these structures are observed to fall in the middle range (II) of the pathway of conversion from sofa to half-chair (Fig. 36b). The remaining structures in the sample tend

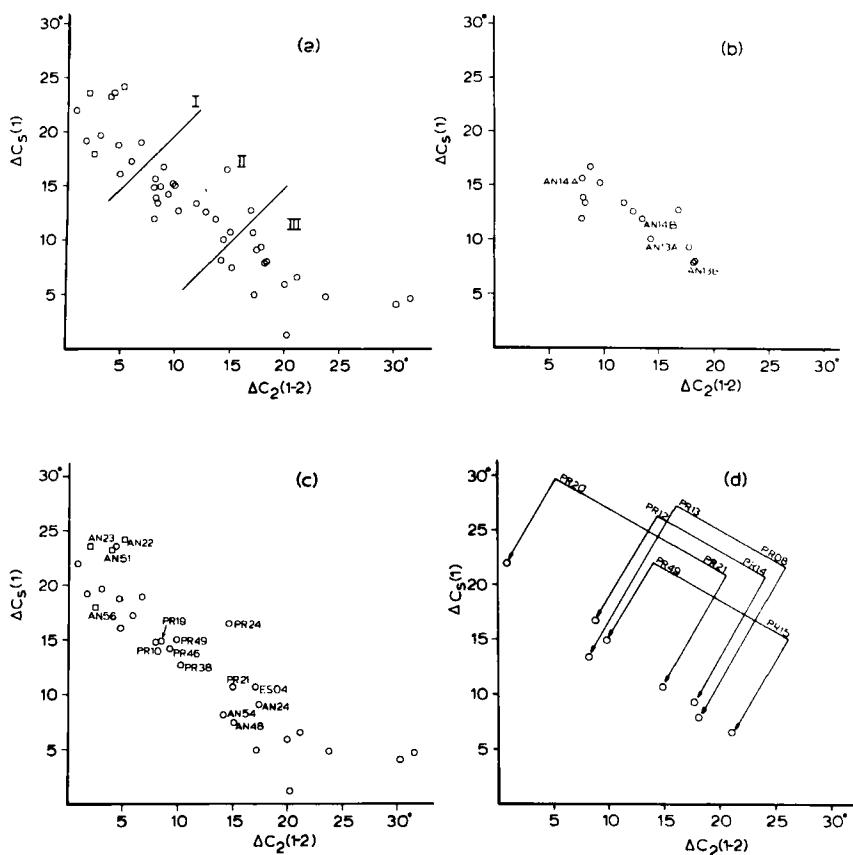


Fig. 36. The relative conformations of Δ^4 -3-one A rings as defined by the rotational asymmetry [$\Delta C_2(1-2)$] and the mirror asymmetry [$\Delta C_s(1)$] of the ideal $1\alpha,2\beta$ half-chair and the 1α sofa conformers, respectively. The graphs include (a) all Δ^4 -3-one structures, (b) structures having the testosterone A, B, and C rings, and (c) structures having further substitution of the testosterone nucleus. Pairs of conformational isomers are shown in the fourth graph (d).

to be grouped on either side of the midpoint of the path of conversion between sofa and half-chair (Fig. 36c).

Upon close inspection it becomes apparent that most of the structures in ranges I and III differ in composition from the structures in range II in a highly specific way. The structures nearest the sofa conformation (range I) and nearest the half-chair conformation (range III) are

those having substituents in the B and C rings. This further crowding of the steroid nucleus appears to remove flexibility from the A ring and hold it nearer one of the ideal symmetry forms. Perhaps the most interesting example of this influence of C-ring substitution on the A-ring conformation is observed in the structures of cortisone (PR20) and cortisone acetate (PR21). The A-ring conformations in these structures are a nearly perfect half-chair and a slightly distorted sofa respectively (Fig. 37). The separation between the cortisone conformations (Fig. 36d) is greater than the separation between the most dissimilar testosterone molecules. The existence of conformational isomers is not as easily demonstrated in the Δ^4 -3-one structures as it was in the 1,3,5(10)-estratriene series where there were numerous examples of cocrystallization of steroids having 8β sofa and $7\alpha,8\beta$ half-chair conformations. Some of the best examples of structures from the Δ^4 -3-one series that have identical or nearly identical configurations and are observed as 2β sofa and $1\alpha,2\beta$ half-chair conformers are collected in Table 7. The separation in the A-ring conformations of these paired structures is shown in Figure 36d.

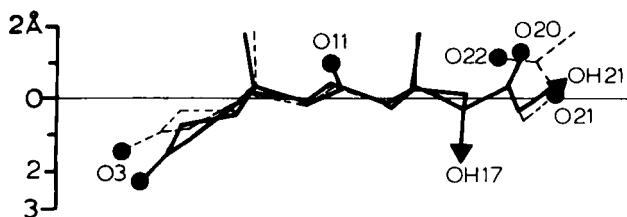


Fig. 37. Superposition of the observed structures of cortisone, PR20, (solid lines) and cortisone acetate, PR21, (dashed lines) illustrating the difference in the A-ring orientation accompanying 1α sofa and $1\alpha,2\beta$ half-chair variation.

Table 7.
Approximate Conformational Isomers in the Δ^4 -3-One Series

1α Sofa	$1\alpha,2\beta$ Half-chair
PR15 cortisol	PR49 cortisol
PR08 progesterone	PR13 21-hydroxyprogesterone
PR14 $17\alpha,21$ -dihydroxyprogesterone	PR12 17α -hydroxyprogesterone
PR21 cortisone acetate	PR20 cortisone

3. *Correlated Changes*

Specific changes in the molecular geometry and conformation of other parts of the steroid can be correlated with the 2β sofa to $1\alpha,2\beta$ half-chair transition.

a. Bond lengths, valency angles, and torsion angles.
Because β -face crowding introduced by the pregnane side chain may have long-range effects comparable to the geometric variations accompanying A-ring sofa to half-chair conversion, the average geometries of the androstanes and pregnanes have been considered separately. The bond lengths and valency angles of the androstane and pregnane subgroups defined in Table 8 have been calculated.

Table 8.
Subsets of Approximate A-Ring Sofa and Half-Chair Conformers
in 4-Androsten-3-one and 4-Pregnen-3-one Structures

	1α Sofa	$1\alpha,2\beta$ Half-chair
Androstanes (AN)	13A, 13B, 14B, 15, 19, 20, 24, 48, 54	14A, 16, 17, 18, 64
Pregnanes (PR)	08, 14, 15, 16, 21, 37	11, 12, 13, 17, 18, 19, 20, 24, 36, 38, 46, 47, 49, 51

The averages of the corresponding parameters in these subgroups were compared, and Student's *t*-test was applied to determine the level of significance. The magnitudes of differences in bonds and angles that were above the 90% level are listed in Table 9.

The parameters showing significant variation between androstenes in which the A rings have sofa conformations and the androstenes in which the A rings have chair conformations are centered about the A/B-ring junction (Table 9a). A comparison of the average geometries of pregnenes in which the A rings have sofa or half-chair conformations also shows significant differences to be in the A and B rings (Table 9b). In contrast to this, a comparison of the bonds and angles of androstenes and pregnenes having A-ring sofa conformations (Table 9c) and of androstenes and pregnenes having A-ring half-chair conformations (Table 9d) shows that significant differences

Table 9.
Bond Length and Valency Angle Differences
Significantly Correlated (>90%)
with Changes in A-Ring Conformation

Parameter	Significance (%)		
a.	AS	AH	
C(6)-C(7)	1.520(8)	1.555(11)	97
C(11)-C(12)	1.545(9)	1.579(15)	94
C(15)-C(16)	1.547(10)	1.576(11)	91
C(10)-C(1)-C(2)	113.9(6)	111.8(4)	96
C(10)-C(5)-C(6)	118.0(3)	116.3(3)	99
C(6)-C(7)-C(8)	111.6(3)	109.9(7)	98
C(9)-C(11)-C(12)	112.4(4)	110.3(11)	93
b.	PS	PH	
	—	—	
c.	AS	PS	
C(13)-C(17)	1.544(8)	1.564(6)	96
C(1)-C(2)-C(3)	110.1(8)	111.9(3)	93
C(10)-C(5)-C(6)	118.0(3)	116.8(3)	96
C(10)-C(9)-C(11)	111.4(8)	113.5(6)	93
C(12)-C(13)-C(17)	115.5(5)	116.8(2)	96
C(16)-C(17)-C(13)	105.4(7)	103.4(4)	94
d.	AH	PH	
C(1)-C(10)	1.559(5)	1.539(6)	91
C(6)-C(7)	1.555(11)	1.529(5)	98
C(11)-C(12)	1.579(15)	1.540(3)	94
C(15)-C(16)	1.576(11)	1.546(4)	99
C(5)-C(6)-C(7)	110.9(8)	113.6(7)	96
C(6)-C(7)-C(8)	109.9(7)	111.9(4)	97
C(10)-C(9)-C(11)	110.7(7)	113.6(5)	99
C(9)-C(11)-C(12)	110.3(11)	113.6(3)	95
C(12)-C(13)-C(17)	115.0(4)	116.5(3)	98
C(16)-C(17)-C(13)	105.6(7)	103.5(2)	99
C(15)-C(16)-C(17)	105.3(4)	106.8(2)	99

AS , androstenes with A-ring sofa;
 AH , androstenes with A-ring half-chair;
 PS , pregnenes with A-ring sofa;
 PH , pregnenes with A-ring half-chair.

occur throughout the molecules. This indicates that conformational variation in rings results in correlated bond and angle changes that are located primarily within that ring or adjacent rings. Substitutions such as the pregnane 17 β side chain have a longer range effect upon bonds and angles. Average bond lengths and angles of the 13 4-androsten-3-ones were compared with corresponding parameters of the 19 4-pregnen-3-ones without considering A-ring conformation. The parameters differing at the 90% level are indicated in Figure 38. Similar differences in the endocyclic torsion angles are indicated in Figure 39.

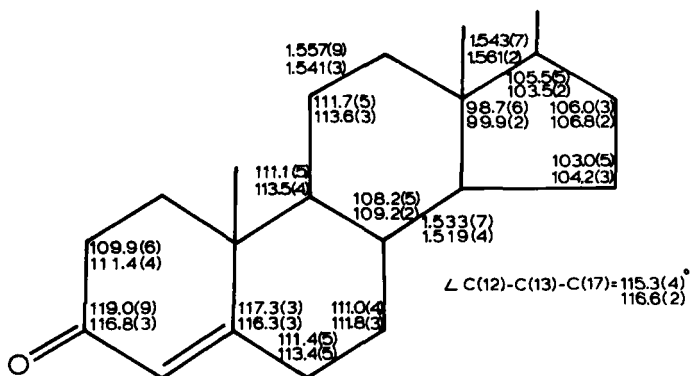


Fig. 38. Bond length and valency angle variations significantly (>90%) correlated with structural differences between 4-androsten-3-ones (top) and 4-pregnen-3-ones (bottom).

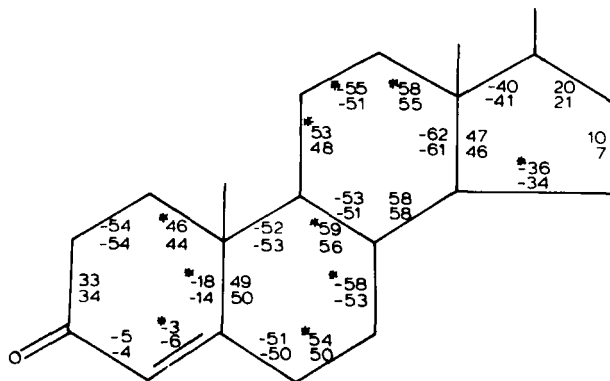


Fig. 39. Average torsion angles in 4-androsten-3-one (top) and 4-pregnen-3-one (bottom) structures. Significant (>90%) differences are marked with asterisks. The estimators of the standard deviation of the average magnitude range from 0.4 to 1.4 deg.

b. Other parameters. The dependence of the distance of the O(3) atom from the least-squares plane through the bulk of the steroid nucleus [C(5)→C(17)] upon the A-ring conformation is illustrated in Figure 40a. The line represents a least-squares fit to the points, and the identities of structures farthest from the line are recorded. In 4-estren-3-ones (ESO3 and ESO4) the absence of the 19-methyl group allows the A ring to arch upward, bringing O(3) closer to the plane of the other rings. Similarly the crowding of the α face by chlorine or bromine substitution at the C(9) position forces the A ring up while the ring still retains a $1\alpha,2\beta$ half-chair conformation. In contrast to this, the crowding of the β face by 8β -methyl addition bows the steroid toward the α face causing a greater deviation of the O(3) atom from the plane than is generally observed in the case of 1α sofa conformers.

The interdependence of adjacent rings is reflected in the correlated variations of A-ring conformation and the B-ring endocyclic torsion angle C(9)–C(10)–C(5)–C(6) (Fig. 40b). The 12 deg. decrease of the C(9)–C(10)–C(5)–C(6) angle closely parallels the half-chair to sofa conformational transition, and the principal exceptions to this dependence involve 19-nor structures (PR51 and ESO3) or 19-aldehyde derivatives (AN48). The C(7)–C(8)–C(9)–C(10) angle increases as the A-ring conformation varies from half-chair to sofa. Variations in the relationships between the angular methyl groups are also correlated with A-ring conformation. Although the distance between atoms C(19) and C(18) is roughly constant, there is a slight decrease in this magnitude as the A-ring varies from half-chair to sofa conformation (Fig. 40c). In addition, the twist about the long axis, as reflected in the C(19)–C(10)···C(13)–C(18) torsion angle, varies from -10 to +12 deg. as the A ring varies from a half-chair to a sofa conformation (Fig. 40d). In most cases, deviations of individual structures from this pattern are related to unusual substitutions in the C or D rings (AN64, PR24, PR25).

4. Restricted Flexibility

The flexibility of the testosterone nucleus can be constrained as a result of additional substitutions or ring unsaturation.

a. Substituent effect. The addition of substituents in the B and C rings is observed to shift the conformation of the A ring toward the ideal sofa and half-chair conformations. 9α -Fluoro- 11β -hydroxy substitution in

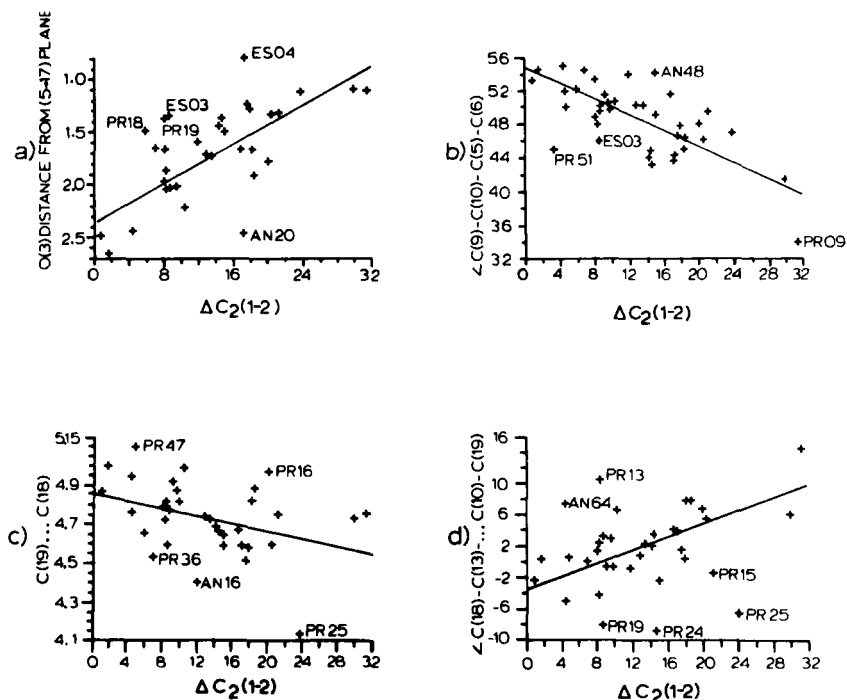


Fig. 40. The A-ring asymmetry parameters, $\Delta C_2(1-2)$, for Δ^4 -3-one steroids are plotted versus (a) the distance of O(3) from the mean plane of atoms C(5)→C(17), (b) the torsion angle C(9)–C(10)–C(5)–C(6), (c) the nonbonded interatomic distance C(19)···C(18), and (d) the twist about the length of the steroid as indicated by the torsion angle C(18)–C(13)···C(10)–C(19). Proceeding from left to right in each graph, the A rings vary in conformation from $1\alpha,2\beta$ half-chair, $\Delta C_2(1-2) = 0$, to 1α sofas, $\Delta C_2(1-2) = 30$. The straight lines are least-squares fits to the observed data, and identities of structures at greatest variance from the line are recorded.

Δ^4 -3-one steroids appears to remove the flexibility of the testosterone nucleus as indicated by the fact that the A ring conformations of PR17, PR46, and PR47 are nearly identical (Fig. 41). Although the A rings in these three structures all have $1\alpha,2\beta$ half-chair conformations, other substituent differences alter the overall conformations of the molecules (Fig. 42). The phenyl-methylene substituent in a fourth 9α -fluoro- Δ^4 -3-one steroid (PR24) is probably responsible for further alteration of the molecular profile.

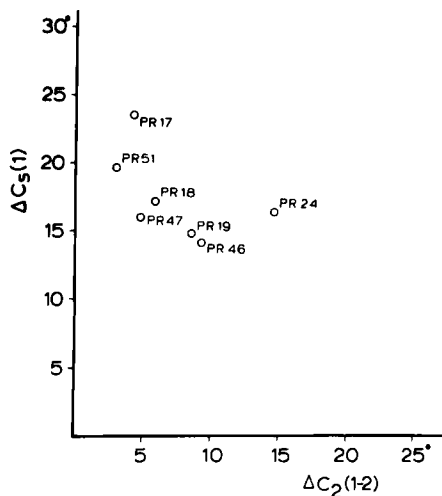


Fig. 41. The Δ^4 -3-one A-ring conformation is influenced by 9 α substitution in a highly specific fashion.

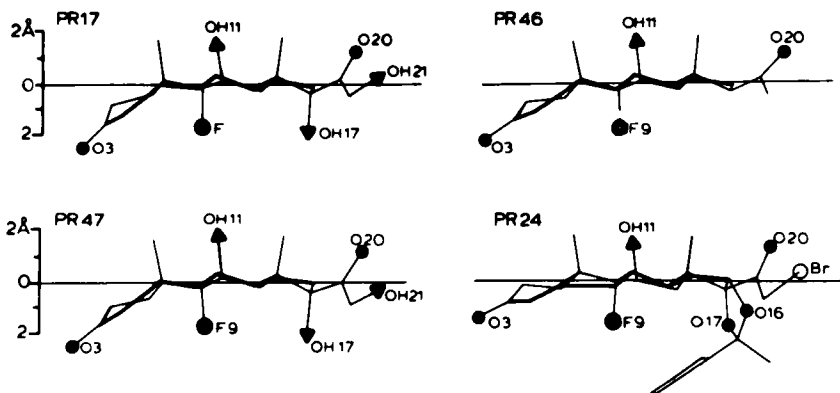


Fig. 42. The overall conformations of four 9 α -fluoro- Δ^4 -3-one derivatives. Despite similar A-ring conformations other substituent variations (2 α -methyl in PR46 and PR47 and 16 α ,17 α -methyl-phenyl-methylenedioxy in PR24) alter the overall conformations.

The 9 α -substituted cortisol series illustrates the complexity of the influence of different substituents at the same site upon overall conformation. The conformational result of electronic and steric effects illustrated

in Figure 43, would be difficult to predict. The A rings in all three halo-substituted cortisols have $1\alpha,2\beta$ half-chair conformations but the size of the larger halogens has the net effect of flattening the molecule so that the sharpest

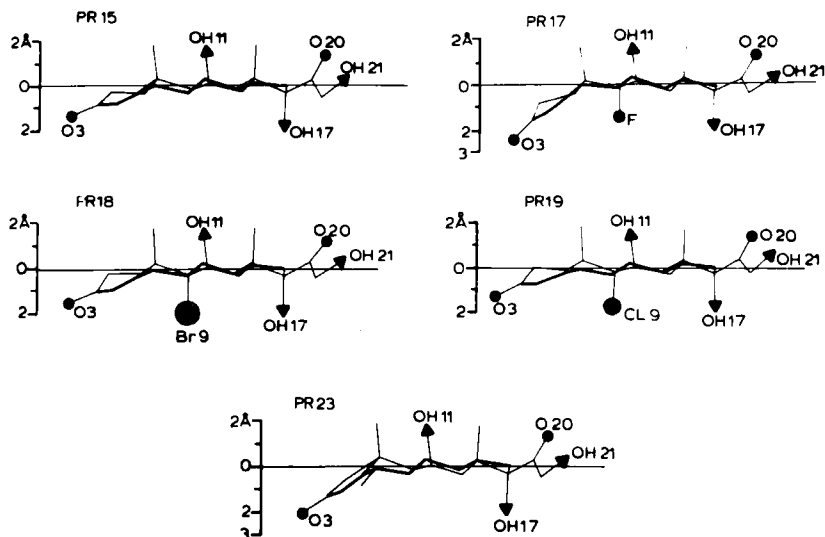


Fig. 43. Cortisol (PR15) and three 9α -halo derivatives (PR17, 18, and 19) illustrate the differences in the location of the O(3) atom relative to the C(5)-C(17) plane. The maximum deviation of O(3) from the plane observed in the 9α -fluoro derivative (PR17) is seen to resemble the bowing caused by the 2,4-diene constitution of 6α -methylprednisolone (PR23).

bowing of the A ring toward the α face is observed in the 9α -fluorocortisol structure. The profile of the 9α -fluorocortisol structure is most similar to that of 6α -methylprednisolone, in which a second double bond in the A ring constrains the ring to bend toward the α face. This observation is of particular significance in view of the enhanced glucocorticoid activity of prednisolone derivatives and 9α fluorocortisol and the likelihood that 9α -fluoro substitution has constrained the more flexible cortisol molecule to the conformation optimal for binding to a particular target protein.

The most unusual Δ^4 -3-one A-ring conformation thus far observed is that found in 2β -acetate derivatives. All four of the Δ^4 -3-one structures that have 2β -acetate substituents (AN22, AN23, AN51, AN56) are observed to have an inverted $1\beta,2\alpha$ half-chair A-ring conformation.

The overall molecular shape of Δ^4 -steroids with normal $1\alpha,2\beta$ half chair A-ring conformations resembles that of 5α -steroids, but the 2β -acetate- Δ^4 -3-one structures resemble 5β -steroids (Fig. 44). It is most probable that the inverted A-ring conformation is adopted to relieve diaxial strain between the 19 -methyl group and the 2β -substituent.

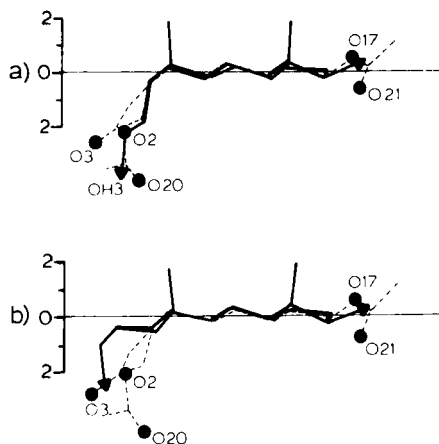


Fig. 44. The conformation observed in four 2β -acetoxy-4-androsten-3-one structures exemplified by AN23 (dashed lines) is contrasted with (a) a 5β -androstane, AN30, and (b) a 5α -androstane, AN02.

b. Unsaturation. Steroids having a 1,4-diene A-ring configuration are of particular interest because of the glucocorticoid activity of many members of this class. Although further unsaturation removes flexibility from the A ring and brings the O(3) atom well below the mean plane of atoms C(5) to C(17), there is still considerable variation in the relative orientation of the carbonyl oxygen (Fig. 45). The distances of the O(3) atoms from the reference plane in these six structures are given in Table 10. The O(3) distances are similar to those in the three 9α -fluoro derivatives.

E. $9\beta,10\alpha$ - Δ^4 -3-One Structures

Projections parallel to a line joining the midpoints of the bonds C(11)-C(12) and C(8)-C(14) of nine Δ^4 -3-one structures having the $9\beta,10\alpha$ configuration are compared in Figure 48. The A-ring conformations of these structures,

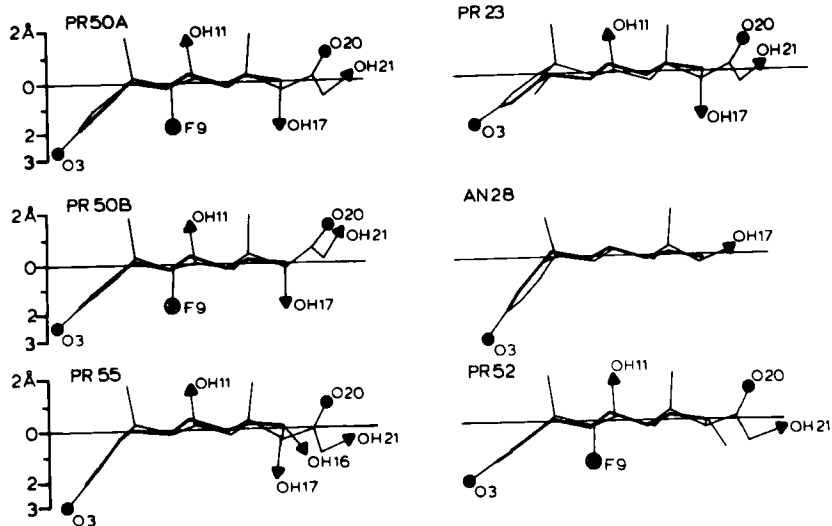


Fig. 45. A-ring orientations in 1,4-diene-3-one steroids depend on the substituents.

Table 10.

Distance of O(3) from the Least-Squares Plane through Atoms C(5)→C(17) for 1,4-Diene-3-one Steroids

Structure	O(3) Distance (Å)
PR23	-1.95
AN28	-3.13
PR50a	-2.63
PR50b	-2.48
PR52	-2.19
PR55	-2.94

Structures having the double-bond sequences 4,6-diene and 1,4,6-triene are also restricted in conformation as illustrated in Figures 46 and 47. The A rings in PR43 and PR56 have nearly identical α -sofa conformations,

indicating that little conformational flexibility remains in the A ring after the addition of the 6-7 double bond. Methylene substitution is comparable to introduction of a double bond as indicated in Figures 46c and 47b.

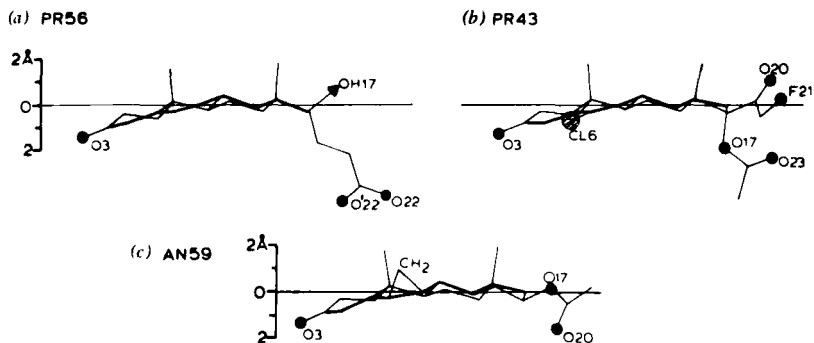


Fig. 46. Conformations of 4,6-diene-3-one steroids illustrate the restrictive influence of conjugated unsaturation. A β -methylene substitution at C(6) and C(7) has a similar net effect upon the A-ring conformation and orientation.

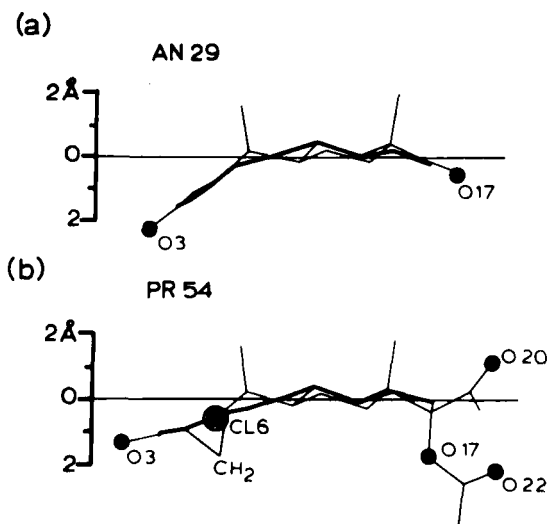


Fig. 47. While the conformations of a 1,4,6-triene-3-one structure and a 4,6-diene-3-one structure having a $1\alpha,2\alpha$ -methylene substituent are similar, the methylene structure has a more nearly planar steroid nucleus.

which range from 1β sofa to $1\beta,2\alpha$ half-chair forms, are displayed in a plot of the rotation asymmetry parameters $\Delta C_2(1-2)$ versus the mirror asymmetry parameters $\Delta C_s(1)$ in Figure 49. Seven of these structures are observed to have unexceptional ring conformations and similar overall conformations. The exceptional structures are AN37 and PR32. The B and C rings in AN37 are observed to be midway between boat and twist conformations, and the B ring in PR32 is observed in a nearly perfect twist. The contrast in conformation between AN33 and AN37 is remarkable considering that the configurational variation is so slight (6α -fluoro, 6β -methyl in AN33 versus 6α -methyl, 6β -fluoro in AN37). It would appear that the diaxial interaction of the 10α - and 6α -methyl groups is sufficient to destabilize B-ring chair conformations in these structures. The 6α -fluoro, 10α -methyl crowding in AN33 is apparently less severe. In the absence of a 6β -substituent, 6α -methyl substitution in a $9\beta,10\alpha$ steroid causes α face crowding that is relieved by the B ring adopting a twist conformation. The further addition of a 6β substituent results in distributing the strain through the B and C rings.

The effect of introducing an additional double bond at C(6)-C(7) is illustrated in Figure 50. In all three structures having $9\beta,10\alpha$ -4,6-diene-3-one constitution the A rings have nearly perfect 1α sofa conformations. The $\Delta C_s(1)$ asymmetry parameters in AN36, PR31, PR32 are 3.3, 1.6, and 4.5 deg., respectively. As previously noted, additional unsaturation in the A and B rings removes flexibility from Δ^4 -3-one structures and stabilizes a particular conformation.

F. 5-Ene Structures

Cholesterol belongs to the class of steroids that contain a 5-6 double bond and an otherwise saturated steroid nucleus. This unsaturation provides the molecule with conformational flexibility in the B ring. There are 15 androstane and pregnane structures having a 5-6 double bond included in the present study. Four of these have a sp^2 hybrid carbon in the C(17) position. AN38 has a 13α configuration, and PR26 and PR27 have additional four- and five-membered rings on the steroid D ring. The average bond lengths and valency angles of the 5-ene structures are displayed in Figure 51.

The conformations of the B rings of the 15 steroids in this subset are equally distributed on either side of an $8\beta,9\alpha$ half chair conformation (Fig. 52). Only one of the structures (PR26B) is more than half way along the

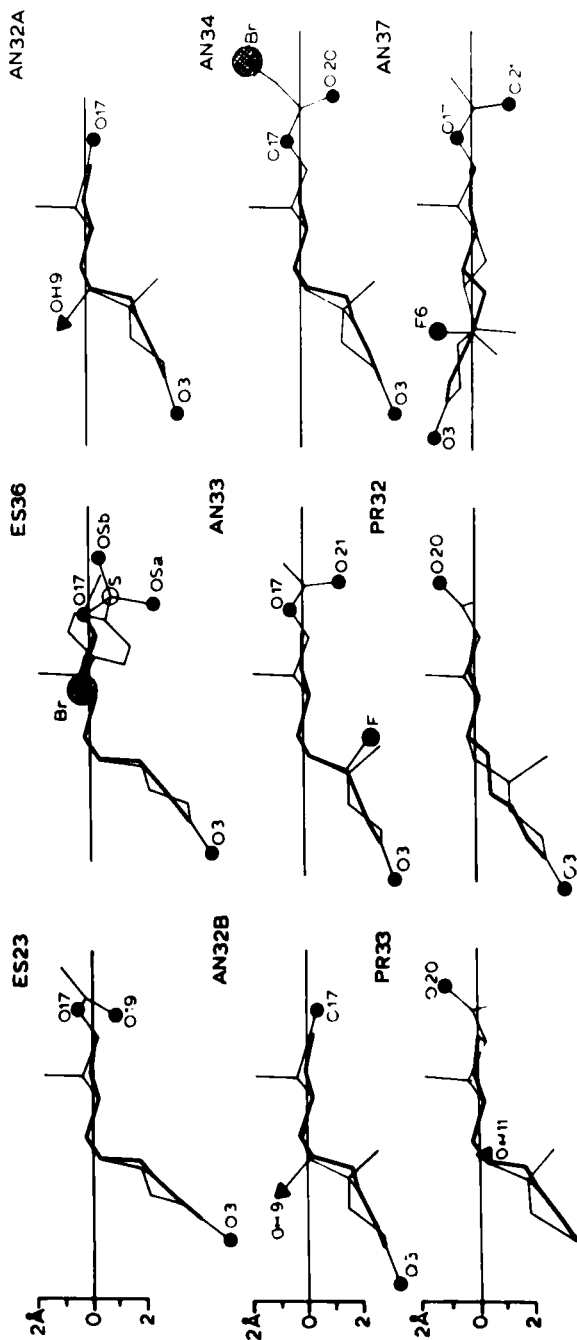


Fig. 48. The conformations of $9\beta,10\alpha-\Delta^4-3$ -one structures. The major conformational changes caused by 6α -methyl substitution are illustrated in the diagrams of PR32 and AN37.

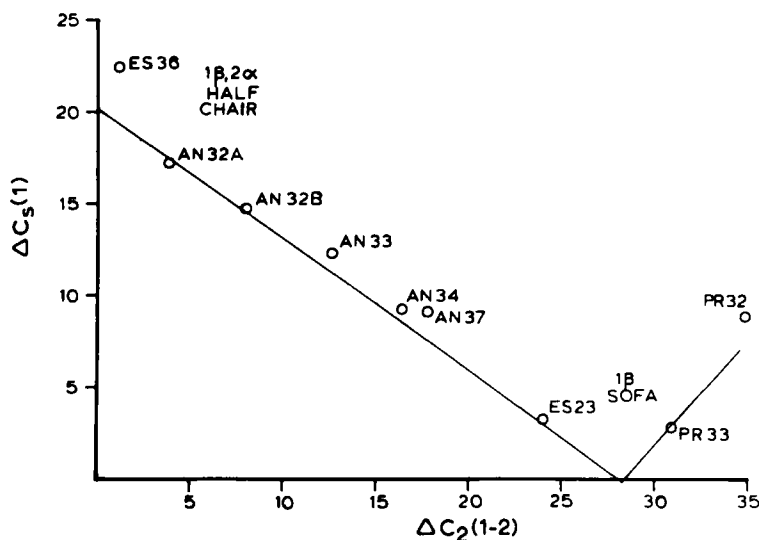


Fig. 49. A-ring conformations of $9\beta,10\alpha-\Delta^4-3$ -one steroids as defined by asymmetry parameters.

path of interconversion to a 9α sofa conformation, and none approaches an 8β sofa conformation. Molecules representative of the extremes of this conformational variation illustrate the significance of the B ring flexibility (Fig. 53). The two 5-ene structures that have crystallized with two molecules in the asymmetric unit exhibit differences in the conformation of the B ring similar to those observed in 1,3,5(10)-estratrienes. Differences in the B rings of the two molecules of PR26 are particularly clear. The B ring in PR26A is in an $8\beta,9\alpha$ half-chair conformation, and that in PR26B is in a distorted 9α sofa conformation. The differences between the two molecules in AN25 are much less pronounced. Variations in the B-ring conformation are observed to be correlated with changes in A-ring conformation (Fig. 54) and the overall twist about the length of the steroid (Fig. 55).

G. Saturated Structures

Thirty-one of the estrane, androstane, and pregnane structures presently in the literature have all-*trans* junctions and no endocyclic double bonds. Generally speaking, these structures have little conformational flexibility. However, ten crystallize with doubled asymmetric units, and the conformational differences in these five

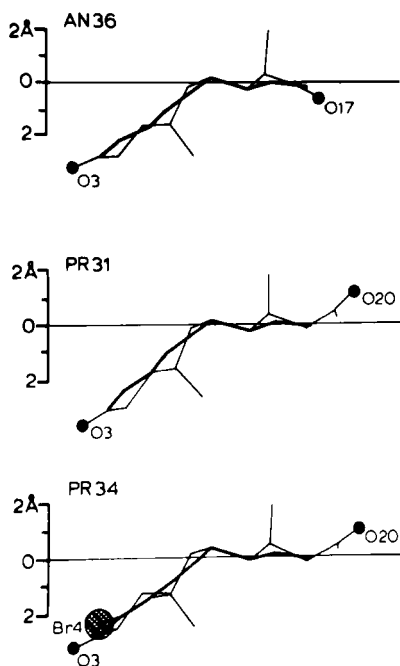


Fig. 50. Restricted flexibility of $9\beta,10\alpha$ -4,6-diene-3-one structures.

Table 11
Saturated 5α Steroids

a. all sp^3 carbons	ES34, ANO1, ANO2, AN41, AN45, PRO4A, PRO4B, PRO5A, PRO5B, PR35A, PR53B
b. 3-keto	ANO6A, ANO6B, ANO7, ANO8, AN52, AN69
c. 17-keto	ANO3, ANO4, ANO5, PRO6, PRO7
d. 3,17-diketo	AN10, AN11A, AN11B
e. 11-keto	PRO1, PRO2, PRO3
f. heterosubstituted	AN09 (4-oxa), AN49 (2,4-dioxa, 3-thia), AN57 (2,4-dioxa)

1. Average Bond Lengths, Angles, Torsion Angles

The average bond lengths, for the B and C rings of 5 α steroids with all-*trans* junctions are recorded in Figure 57. The accuracy of the estimators of standard deviation can be judged by comparing the averages and estimators from this sample of 24 estranes, androstanes, and pregnanes with averages and estimators for the seventeen 5 α steroids in the sample studied by Romers. The two samples have nine members in common. In all cases the averages are within two standard deviations of one another, and in 75% of the cases they are within one standard deviation. The average valency and torsion angles for the 24-compound sample are recorded in Figure 58.

The average A-ring bond lengths, valency angles, and torsion angles for 3 β -hydroxy and 3-keto structures are compared in Figure 59. Differences in the averages that are significant at the 90% level are indicated with asterisks. The average B-ring geometries of Δ^4 -3-one steroids (from Fig. 34) and saturated steroids are contrasted in Figure 60. Similarly, the average bond lengths and angles in C rings for the 1,3,5(10)-estratriene, Δ^4 -3-one, and saturated structures are collected for purposes of comparison in Figure 61.

2. Distorted Chair Conformations

The 29 most distorted chairs in the steroids of the first volume of the *Atlas of Steroid Structure* exhibit only seven of the 18 most probable modes of distortion. Six of the seven involve the loss of rotation symmetry with retention of the orthogonal mirror. The exceptions are nine structures in which the $\Delta C_s(9-11)$ symmetry is retained in the C ring at the expense of $\Delta C_s(8)$ symmetry. Representative examples of the seven distortion modes appear in Figure 62. The asymmetry parameters for the 29 distorted rings are given in Table 12.

3. Cyclosubstitutions

The most significant variation in ring conformations in the all-*trans* structures having no endocyclic unsaturation generally results from cyclosubstitutions (Fig. 63). The sulfur addition at C(2) and C(3) in AN66 has the same effect as double bond addition, and the A ring is observed in a 5 α ,10 β half-chair conformation. Similarly, the methylene bridge across C(5)-C(10) in AN31 leads to 2 β ,3 α half-chair and 7 α ,8 β half-chair conformations for the A

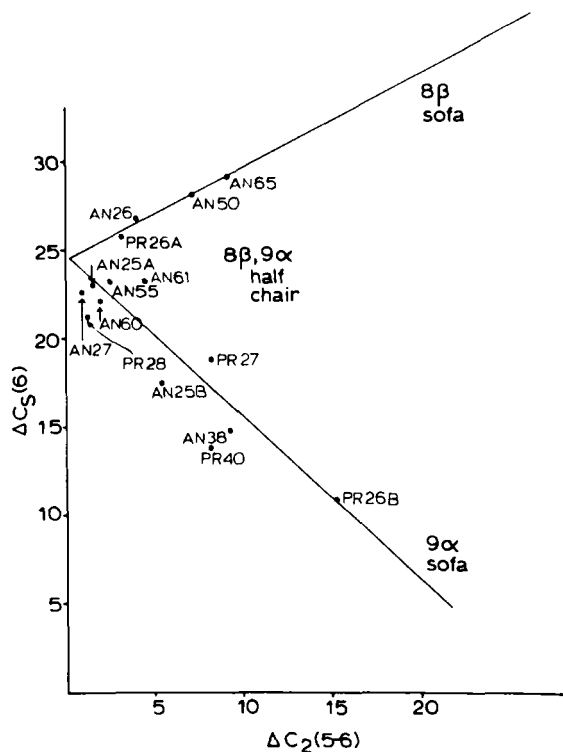


Fig. 52. Asymmetry parameters of 5-ene steroids illustrating conformational variations about the $8\beta, 9\alpha$ half-chair form.

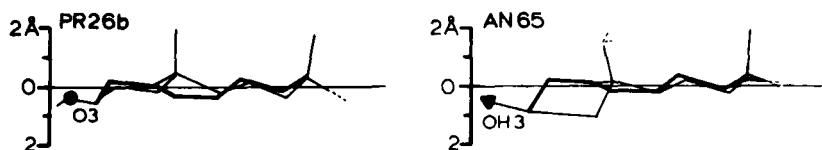


Fig. 53. Extremes of conformational variation in B rings of 5-ene steroids illustrate the impact upon overall molecular conformation.

and B rings, respectively, and the $14\alpha, 15\alpha$ -epoxide in (AN58) flattens the five-membered ring to a perfect 13β sofa. The $1\beta, 2\beta$ -dichloromethylene addition in AN08 produces a distorted $2\alpha, 3\beta$ twist conformation. The effect

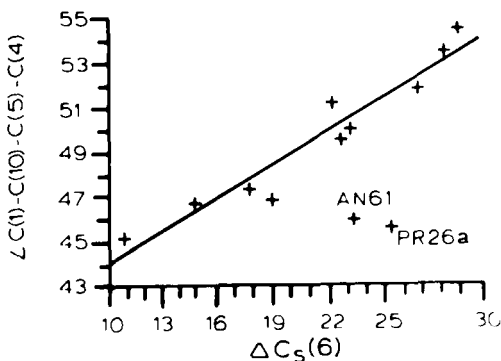


Fig. 54. As the B-ring conformation of 5-ene steroids changes from a 9α sofa to an 8β sofa, going from left to right in the figure, the A ring torsion angle $C(1)-C(10)-C(5)-C(4)$ increases by 10 deg. The labeled points were not included in calculating the least-squares line through the other points.

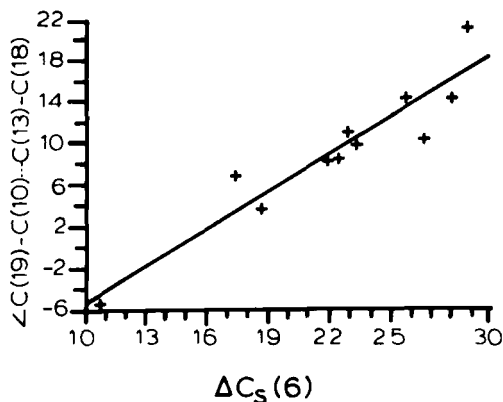


Fig. 55. As the B-ring conformation of 5-ene steroids changes from a 9α sofa to an 8β sofa, going from left to right in the figure the twist about the length of the steroid $[C(19)-C(10)\cdots C(13)-C(18)]$ varies from -6 to +20 deg.

of other cyclosubstitutions is less pronounced (e.g, $6\beta,19$ -epoxide in PR04 and ethyl cyano cyclization in PR06).

4. Heterosubstituted Structures

The three heterosubstituted androstane structures are compared with natural analogues in Figure 64. The

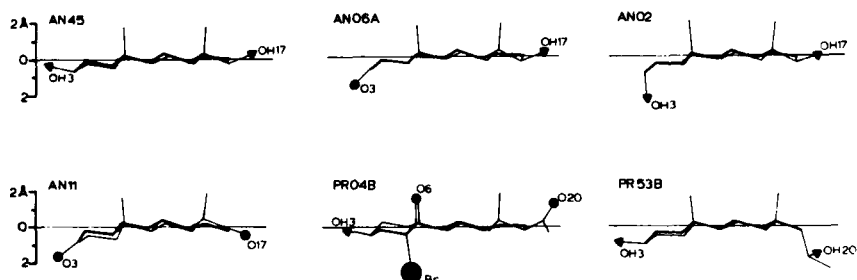


Fig. 56. Typical examples of steroids with all-*trans* junctions and no endocyclic double bonds. The relative orientations of the O(3) atom in 3 β -hydroxy, 3-keto, and 3 α -hydroxy derivatives are illustrated by AN45, AN06A, and AN02, respectively. The relative orientation of the O(17) atom in 17 β -hydroxy and 17-keto derivatives is illustrated by AN06 and AN11, respectively. Finally, the differences in 17 β - and 17 α -pregnane structures are illustrated by PR04B and PR53B.

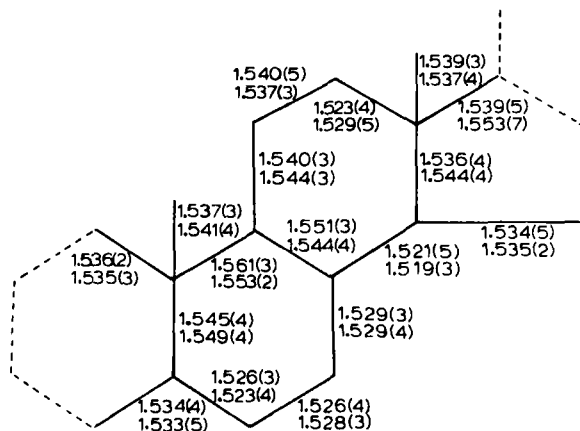


Fig. 57. The average bond lengths in the B, C, and D rings of 5 α steroids having all-*trans* junctions. The averages for the sample, ES34, AN01, AN02, AN03, AN04, AN05, AN06A, AN06B, AN07, AN10, AN11A, AN11B, AN45, AN52, AN69, PR01, PR02, PR03, PR04A, PR04B, PR06, PR07, PR53A, and PR53B, (top) is compared with the averages for a sample of seventeen related structures studied by Romers.

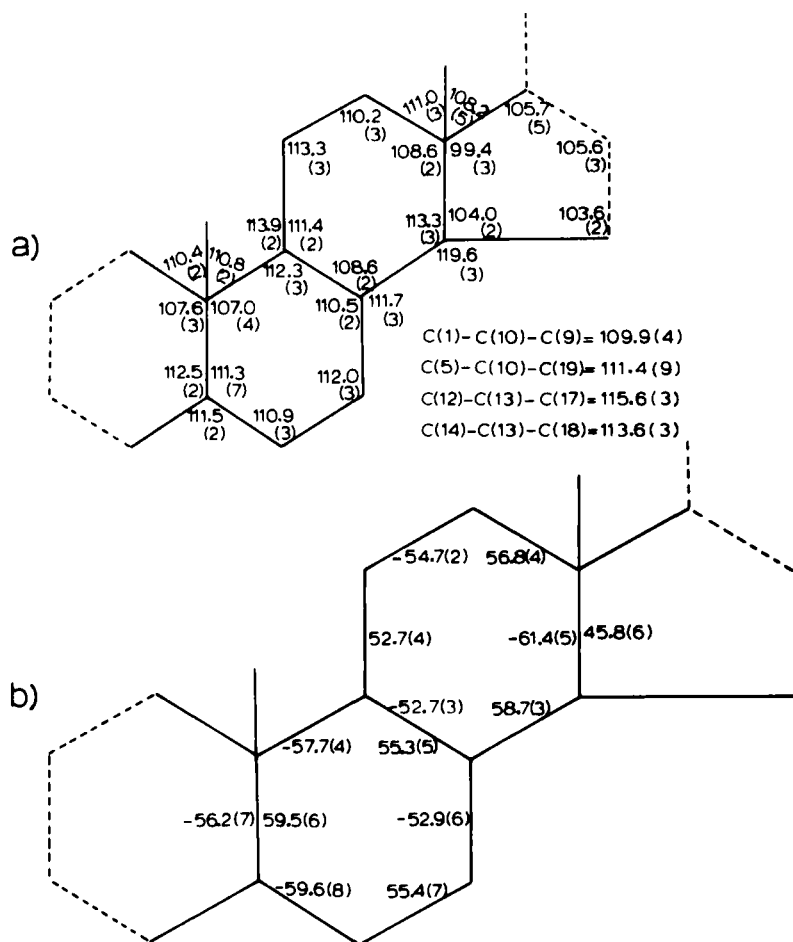


Fig. 58. Average (a) valency angles and (b) torsion angles in the B, C, and D rings of 5α steroids having all-*trans* junctions. The estimators of the standard deviations in the averages are given in parentheses.

A rings of the AN49 and AN57 structures closely resemble the A rings in the ANO5 and ANO1 molecules, respectively. However, the 4-oxa molecule (ANO9) has a $5\alpha,10\beta$ half-chair conformation with atoms C(1), C(2), C(3), O(3), and O(4) being within ± 0.05 Å of coplanarity and is different from ANO7.

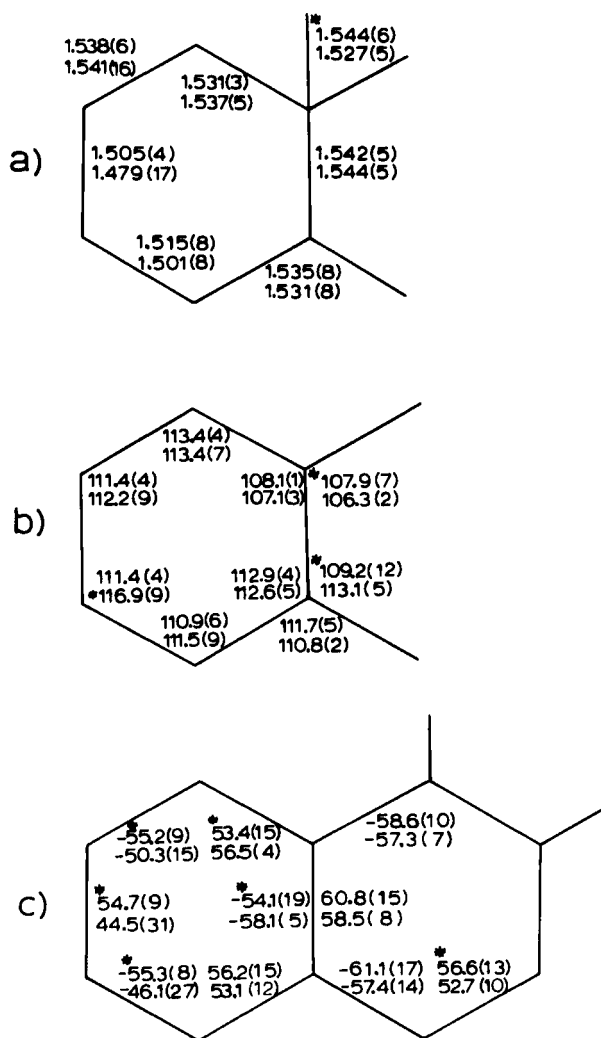


Fig. 59. A comparison of the average (a) bond lengths, (b) valency angles, and (c) torsion angles in A rings having 3 β -hydroxy configurations (above) and 3-keto configurations (below). Estimators of standard deviations are in parentheses and significant (> 90%) differences are flagged.

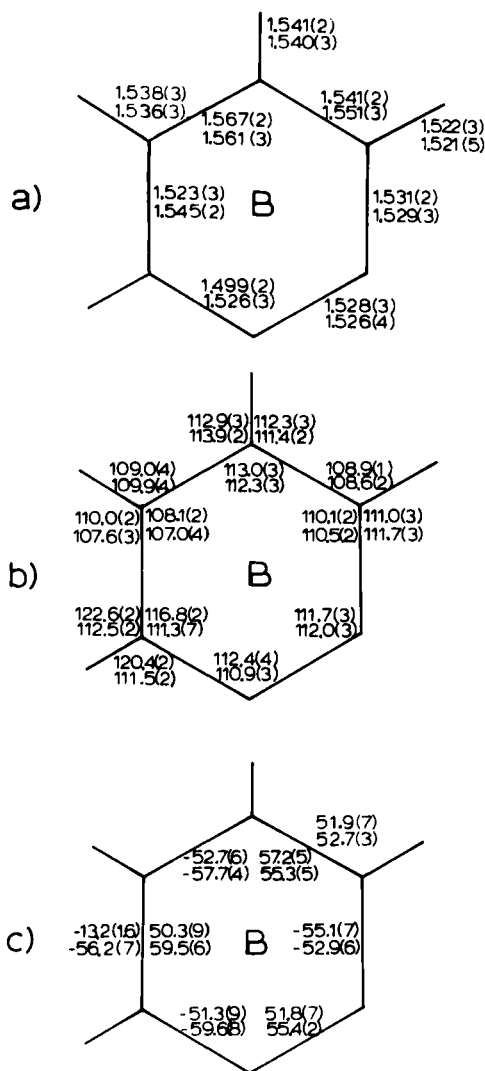


Fig. 60. A comparison of the average (a) bond lengths, (b) valency angles, and (c) torsion angles in the B rings of structures having Δ^4 -3-one constitution (above) and those having saturated A rings (below). Estimators of standard deviations are in parentheses.

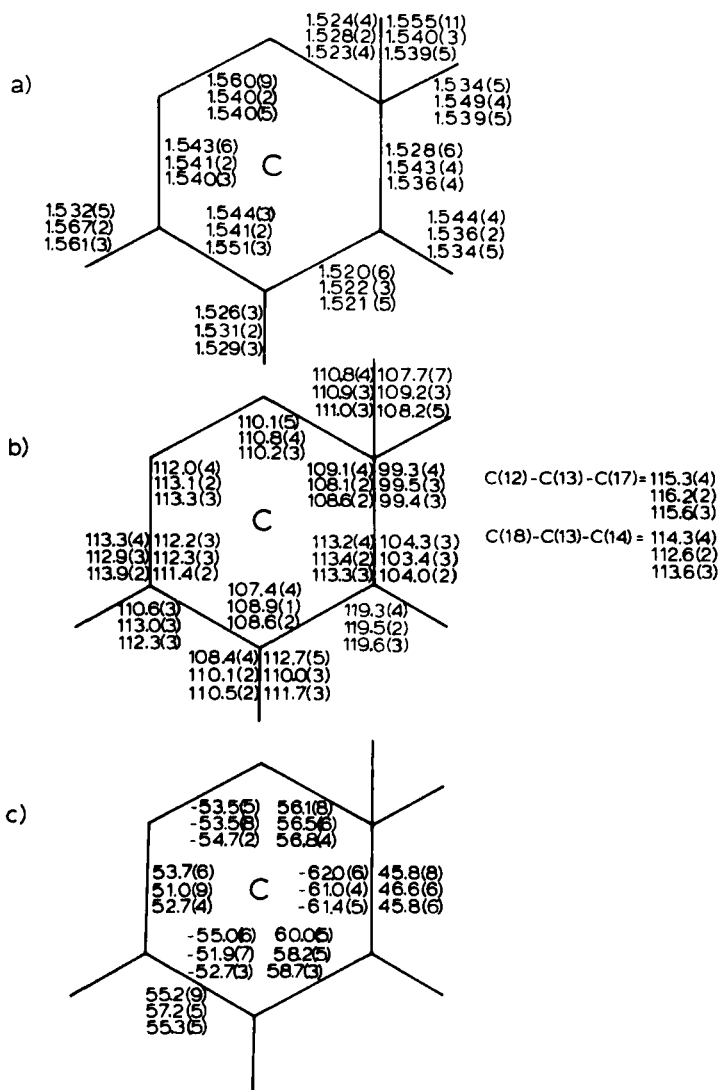


Fig. 61. A comparison of the average (a) bond lengths, (b) valency angles, and (c) torsion angles in C rings of structures having 1,3,5(10)-estratriene (top), Δ^4 -3-one (middle), and saturated (bottom) steroid skeletons. Estimators of standard deviations are in parentheses.

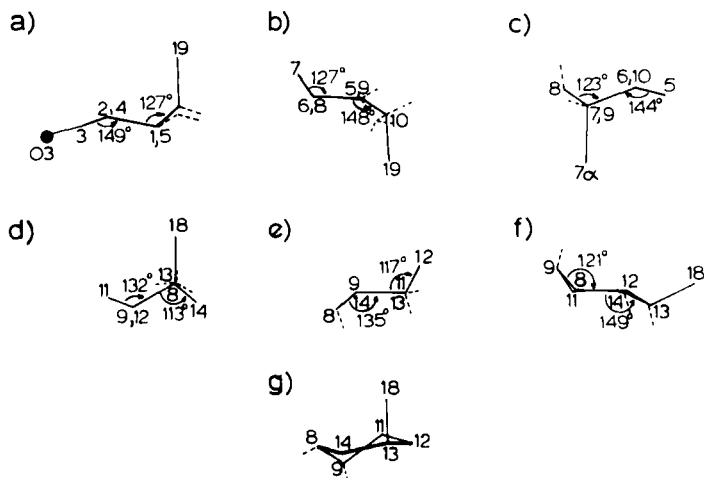


Fig. 62. The seven principal modes of distortion observed for steroid rings in chair conformations are exemplified by (a) $\Delta C_2(1-2)$ distortion in AN10, (b) $\Delta C_2(5-6)$ distortion in PR33, (c) $\Delta C_2(6-7)$ distortion in ES28B, (d) $\Delta C_2(8-9)$ distortion in AN31, (e) $\Delta C_2(9-11)$ distortion in PR25, (f) $\Delta C_2(8-14)$ distortion in ES28B, and (g) $\Delta C_s(8)$ distortion in ES28A. The interplanar angles recorded in the figures are another indication of ring distortion. The average interplanar angle in undistorted rings is 131 deg.

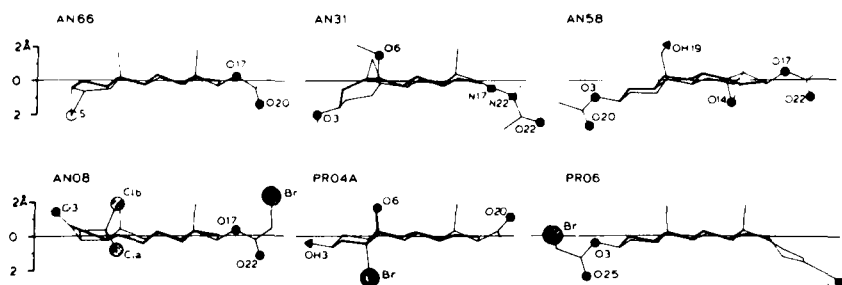


Fig. 63. Conformational variation in cyclo derivatives of steroids with all-*trans* junctions having no endocyclic unsaturation.

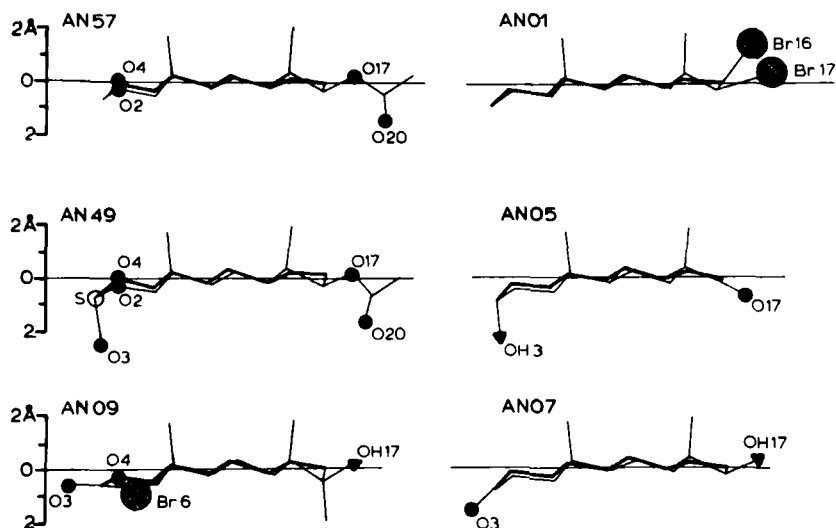


Fig. 64. Comparison of profiles of A-ring heterosubstituted structures with their all carbon analogs.

5. Boat and Twist Conformers of Saturated Rings

In a few of the steroid structures, intramolecular strain introduced by crowding is severe enough to destabilize normal chair conformations and produce rings with boat or twist conformations. The relevant asymmetry parameters for 11 such rings are recorded in Table 13. An ideal boat conformation has two mutually perpendicular mirror planes, and the deviations from symmetry are recorded for six boat conformers. Similarly, an ideal twist conformer has two mutually perpendicular rotation axes, and the deviations from symmetry are recorded for five twist and two distorted twist conformers. The B and C rings in AN37 are observed to be at the midpoint between a perfect boat and perfect twist conformation as indicated by the magnitudes of their asymmetry parameters. Representative boat and twist rings are illustrated in Figure 65.

6. Doubled Asymmetric Unit Structures

The five structures with saturated nuclei having two molecules in the crystallographic asymmetric unit are ANO6, AN11, PRO4, PRO5, and PR53. In addition, ANO7 and AN10 are alternate crystal forms of ANO6 and AN11,

Table 12
Distorted Chair Conformations

Ring	(a) Symmetry Lost	(b) Symmetry Retained	(a) Asymmetry Magnitude	(b) Asymmetry Magnitude	Ave T.A.	Structure
A	ΔC_2 (1-2)	ΔC_s (3)	23.6	3.8	47	AN10
			18.1	3.1	47	AN11B
			17.4	4.7	60	PRO5B
B	ΔC_2 (5-6)	ΔC_s (7)	21.4	4.4	48	PR33
			15.3	5.7	48	ES23
			14.3	4.3	54	ESO3
C	ΔC_2 (6-7)	ΔC_s (5)	25.2	1.7	54	ES28B
			21.5	3.2	46	PRO9
			20.5	4.5	53	ESO4
			15.1	5.1	57	ES28A
	ΔC_2 (8-9)	ΔC_s (11)	18.8	4.9	61	AN31
			17.0	2.8	54	PR29
	ΔC_2 (9-11)	ΔC_s (8)	23.4	0.8	62	PR25
			13.2	5.0	55	PR26B
	ΔC_2 (8-14)	ΔC_s (9)	35.5	7.3	49	ES28B

Table 12 (Con't)

Ring	(a) Symmetry Lost	(b) Symmetry Retained	(a) Asymmetry Magnitude	(b) Asymmetry Magnitude	Ave T.A.	Structure
C	ΔC_2 (8-14)	ΔC_5 (9)	23.1	2.6	49	PR32
			19.8	4.2	51	PR34
			16.6	0.9	58	AN08
			13.5	3.9	52	PR27
	ΔC_s (8)	ΔC_2 (9-11)	12.4	3.5	53	AN25B
			30.3	6.3	47	ES28A
			21.5	1.9	48	PR24
			17.9	4.3	52	AN32B
			15.2	4.3	52	AN36
			15.2	3.8	53	PR31
			15.8	2.9	51	AN32A
			13.5	3.8	52	AN38
			13.2	3.1	53	AN33
			11.9	2.4	55	AN11B

Ave T.A. = the average of the absolute magnitudes of the six endocyclic torsion angles.

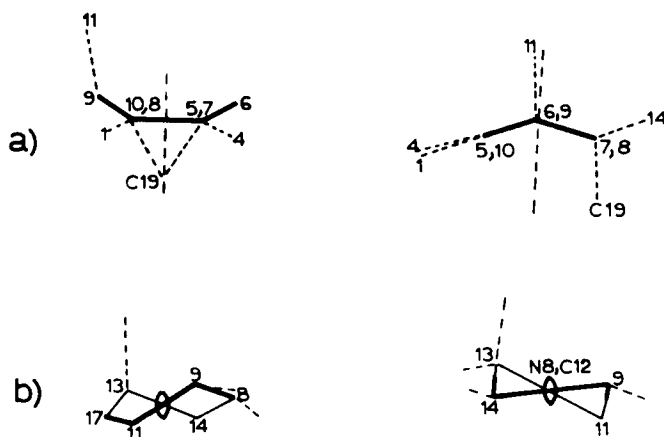


Fig. 65. The B ring of ES20 (a) and the C ring of ES24 (b) provide examples of highly symmetric boat and twist rings, respectively.

respectively. The conformational differences between crystallographically independent observations are not as pronounced in saturated rings as they have been demonstrated to be in the unsaturated rings previously discussed. Nevertheless, there are significant differences between molecules in a doubled asymmetric unit, and, in two cases, a third independent molecule is observed to be nearly identical to one of the pair in the first crystal.

a. 17 β -Hydroxy-5 α -androstane-3-one. Three independent observations of the active androgen 17 β -hydroxy-5 α -androstane-3-one (dihydrotestosterone) are provided in the crystal structures of the hydrated and anhydrous forms. There are significant conformational differences between the two crystallographically independent steroids in the anhydrous form, ANO6. The original investigators cited bond distance variations that include a C(1)-C(2) bond comparison of 1.48 and 1.56 Å. In addition, the dominant symmetries in the A, B, and C rings differ between the independent molecules. The observed conformation of ANO7 has an C ring that is nearly identical to that of ANO6A. The average deviations of corresponding bond distances, valency angles, and torsion angles are 0.02 Å, 0.7 deg. and 0.6 deg., respectively. A similar comparison of the C rings of ANO7 and ANO6B provides average deviations of

Table 13.
Six-Membered Rings in Boat and Twist Conformations

	Relevant Asymmetry Parameters (deg.)	
Boat Conformations		
B ring, ES20	$\Delta C_s(6) \approx 2.8$	$\Delta C_s(5-10) = 1.9$
B ring, ES25	$\Delta C_s(6) = 5.3$	$\Delta C_s(5-10) = 6.4$
B ring, ES30	$\Delta C_s(6) = 2.7$	$\Delta C_s(5-10) = 4.0$
B ring, AN39	$\Delta C_s(7) \approx 8.9$	$\Delta C_s(5-6) = 9.0$
A ring, PR41	$\Delta C_s(3) = 8.7$	$\Delta C_s(4-5) = 6.3$
A ring, PR42	$\Delta' C_s(3) = 14.7$	$\Delta C_s(4-5) = 12.7$
Twist Conformations		
C ring, ES24	$\Delta C_2(8) = 3.7$	$\Delta C_2(9-11) = 2.1$
C ring, ES30	$\Delta C_2(11) = 31.8$	$\Delta C_2(8-9) = 5.4$
A ring, AN08	$\Delta C_2(1) \approx 27.1$	$\Delta C_2(2-3) = 10.4$
A ring, AN41	$\Delta C_2(1) = 10.4$	$\Delta C_2(2-3) = 8.2$
B ring, PR32	$\Delta C_2(5) = 4.4$	$\Delta C_2(6-7) = 2.9$
Midway Between Boat and Twist		
B ring, AN37	$\Delta C_s(7) = 21.8$	$\Delta C_s(5-6) = 19.0$
	$\Delta C_2(6) = 20.2$	$\Delta C_2(5-10) = 22.1$
C ring, AN37	$\Delta C_s(11) = 23.2$	$\Delta C_s(8-9) = 18.6$
	$\Delta C_2(8) = 23.5$	$\Delta C_2(9-11) = 28.0$

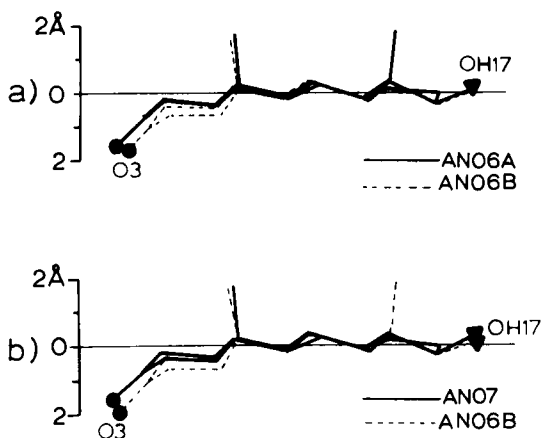


Fig. 66. A comparison of three observations of the conformation of 17 β -hydroxy-5 α -androstan-3-one, AN06A, AN06B, and AN07, illustrates the similarities between AN07 and AN06A and the differences in AN06B.

0.03 Å, 1.7 deg., and 2.7 deg. While overall structures of AN07 and AN06A are entirely superimposable, the C ring difference in AN06B is clearly apparent in the superposition diagram Fig. 66.

b. 5 α -Androstane-3,17-dione. Three independent determinations of molecular conformations of 5 α -androstan-3,17-dione are provided in the crystal structures of the pure steroid and the (1:1) *p*-bromophenol complex. There are significant conformational differences between the two crystallographically independent steroids in the *p*-bromophenol complex. Rings A and C of AN11B have distorted chair conformations, and a pronounced flattening of ring A results in a significant difference in the orientation of oxygen atom O(3) relative to the bulk of the steroid. The conformation of the 5 α -androstan-3,17-dione molecule AN10 is nearly identical to that of AN11B. This similarity is graphically accentuated in the superposition diagram (Fig. 67).

c. 5-Bromo-6 β ,19-epoxy-3 β -hydroxy-5 α -pregnan-20-one. The conformations of the two independent molecules in this crystal structure are similar. Individual ring conformational differences are subtle, but there is a perceptible difference

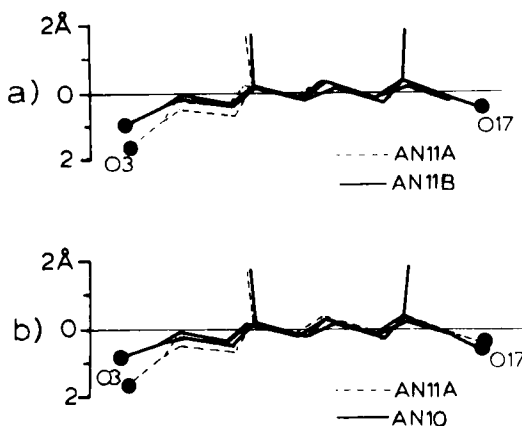


Fig. 67. A comparison of three observations of the conformation of 5 α -androstane-3,17-dione, AN10, AN11A, and AN11B, illustrates the similarities between AN10 and AN11B and the differences in AN11A.

in the twist about the long axis of the steroid nucleus. This is observed in the tilt of the A ring in the C(5) \rightarrow C(17) reference projection and a comparison of the C(9)-C(10) \cdots C(13)-C(18) torsion angles (PRO4A, -15. deg.; PRO4B, -19.8 deg.). A more pronounced difference is observed in the 17 β side chain orientation involving a 9.6 deg. rotation about the C(17)-C(20) bond.

d. (20S)-20-Chloro-5 α -pregnane-3 β ,16 β -diol di-*p*-bromobenzoate. The bromobenzoate conformations differ in the two molecules by 14 and 3 deg. rotations about the C(3)-O(3) and C(16)-O(16) bonds, respectively. The 17 β side chain conformations are nearly identical. While the A and B rings of PRO5A have normal chair conformations, the A ring in PRO5B is significantly distorted and the B ring is highly symmetric.

e. 5 α ,17 α -Pregnane-3 β ,20 α -diol. The conformations of the C and D rings in the two crystallographically independent molecules differ significantly. One D ring has a 14 α envelope conformation ($\Delta = 4.6$ deg., $\phi_m = 46.1$), and the other has a 13 β ,14 α half-chair conformation. The differences in the C and D rings are discussed in detail in the careful study by Romers, de Graaff, Hoogenboom, and Rutten (176).

H. D-Ring Conformation

The pseudorotation parameters Δ and ϕ_m have gained wide acceptance for use in evaluating D-ring conformation. A complete discussion of their evaluation and use in steroid analysis has been given by Altona, Geise, and Romers (15).

Standard torsional angles, Δ and ϕ_m values, and the asymmetry parameters for the symmetrical 14α envelope, $13\beta, 14\alpha$ half-chair, and 13β envelope conformations observed in the structures of ES14, ES23, and ES17A are given in Table 14. The conformations of these D-rings are illustrated in Figure 68. A plot of Δ versus ϕ_m for all five-membered D rings of estrane, androstane, and pregnane structures currently available illustrates the distribution of observed conformations (Fig. 69).

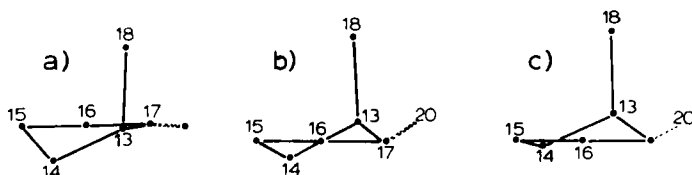


Fig. 68. The symmetric D-ring conformations 14α -envelope, $13\beta, 14\alpha$ half-chair, and 13β envelope are found in the structures of (a) ES14, (b) ES23, and (c) ES17A, respectively.

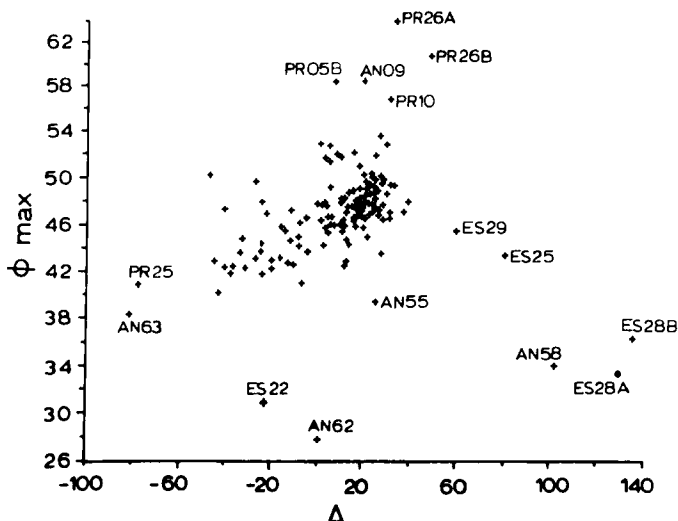


Fig. 69. The distribution of pseudorotation parameters for 165 D rings. Δ values for ideal forms are given in Table 14.

Table 14.
Observed D-Ring Conformations That Approximate Ideal Forms

	14 α Envelope, ES14 (deg.)	13 β ,14 α Half-chair, ES23 (deg.)	13 β Envelope, ES17A (deg.)
Torsion Angles			
C(17)-C(13)-C(14)-C(15)	39.8	47.7	48.2
C(13)-C(14)-C(15)-C(16)	-41.1	-38.2	-32.3
C(14)-C(15)-C(16)-C(17)	25.1	13.4	2.7
C(15)-C(16)-C(17)-C(13)	-1.9	16.2	27.8
C(14)-C(13)-C(17)-C(16)	-23.5	-38.3	-46.0
Asymmetry Parameters			
$\Delta C_s(13)$	32.5	16.9	3.5
$\Delta C_s(14)$	1.4	18.9	32.6
$\Delta C_2(13-14)$	22.7	2.0	20.2
Pseudorotation Parameter			
Δ	-39.9	2.3	29.3
ϕ_{\max}	42.4	47.7	49.8

Of the 34 structures having conformations intermediate between 13 β ,14 α half-chair ($\Delta=0$ deg.) and 14 α envelope ($\Delta=-3.50$ deg.) forms, 24 are so constrained as a result of sp^2 hybridization at C(17). Of the remaining ten structures, PR35A, PR53B, and PR56 have 17 α -pregnane side chains, ES26 has a 17 α -iodine substituent, PR27 and PR30 have 16 α substituents, and ES18 has a 17-spiro configuration.

D Rings having all- sp^3 hybrid carbons usually have conformations intermediate between 13 β ,14 α half-chairs ($\Delta=0$ deg.) and 13 β envelopes ($\Delta = 35$ deg.). The 120 structures shown in this range in Figure 69 include 17 β -ol estranes and androstanes; 17 β -acetate, benzoate, and benzene-sulfonyloxy derivatives; and 17 β -pregnane structures. Correlation between D-ring conformations and the nature of this 17 β substitution is apparent in Figure 70.

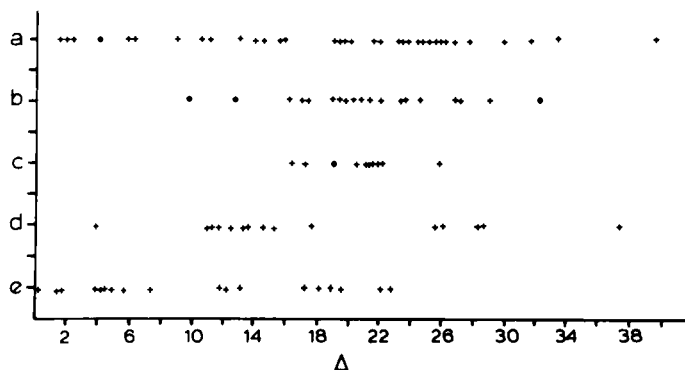


Fig. 70. Observed ranges of D-ring conformations differ for (a) 17 β -acetate, benzoate, and benzenesulfonyloxy structures, (b) 17 β -hydroxy androstane, (c) 17 β -hydroxy estrane, (d) 17 α ,21-dihydroxy progesterone, and (e) other 17 β -progesterone derivatives.

The D rings of steroids having 17 β -acetate and benzoate substituents are observed to cover the entire range of conformations from 13 β ,14 α half-chairs to 13 β envelopes. The 17 β -hydroxy-androstane D-ring conformations are observed to extend over the middle of this range, and the 17 β -hydroxy-estrane conformations cover a smaller part of the range. A slightly different dependence is noted in the pregnane structures. The distribution for 17 α ,21-dihydroxy-progesterone derivatives is shifted significantly toward the 13 β sofa conformation.

V. SIDE CHAIN AND SUBSTITUENT CONFORMATIONS

A. Pregnane 17β Side Chain Conformation

Although Dreiding models suggest freedom of rotation for the pregnane 17β side chain, crystallographic findings demonstrate that rotation is hindered and that deviation from a single conformation is highly restricted. Because the sidechain of the naturally occurring progestins and corticoids has a 20-keto substituent, this side chain composition is often encountered in crystallographic studies, and 41 of the 60 pregnanes have a 20-keto substituent. Thirty-six structures having a saturated D ring, a 20-keto function, and no constraint upon the side chain or D ring imposed by addition of bridges to or within the D ring are listed in Table 15. The nature of the substituents at positions 17α and 21 and selected geometric parameters defining the D-ring and side chain conformations are also given in this table. The existence of structural data on 22 structures with a 17α -hydroxyl group, 14 structures without a 17α -hydroxyl, 17 structures with a 21-hydroxyl, three with a 21-halogen or other bulky group, and 16 with a 21-hydrogen atom allows the exploration of dependence of side chain conformation upon substitutions.

In 35 of the 36 structures, the 20-keto bonds are plus clinal with respect to the C(13)-C(17) bonds (Fig. 71).

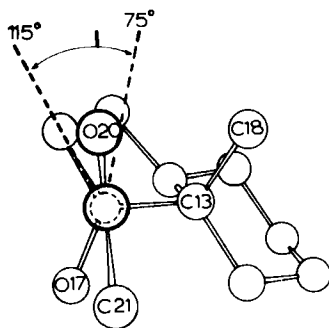


Fig. 71. The C(13)-C(17)-C(20)-O(20) torsion angles in pregnane 17β side chains having 20-keto substitutions are in the range 75-115 deg.

The crystal-structure data demonstrate that 17β sidechain orientation is influenced by 17α and 21 substitution. The average C(13)-C(17)-C(20)-O(20) torsion angles are 102 and 89 deg. in structures having 17α (H) and 17α (OH)

substitution, respectively (Fig. 72a). This difference

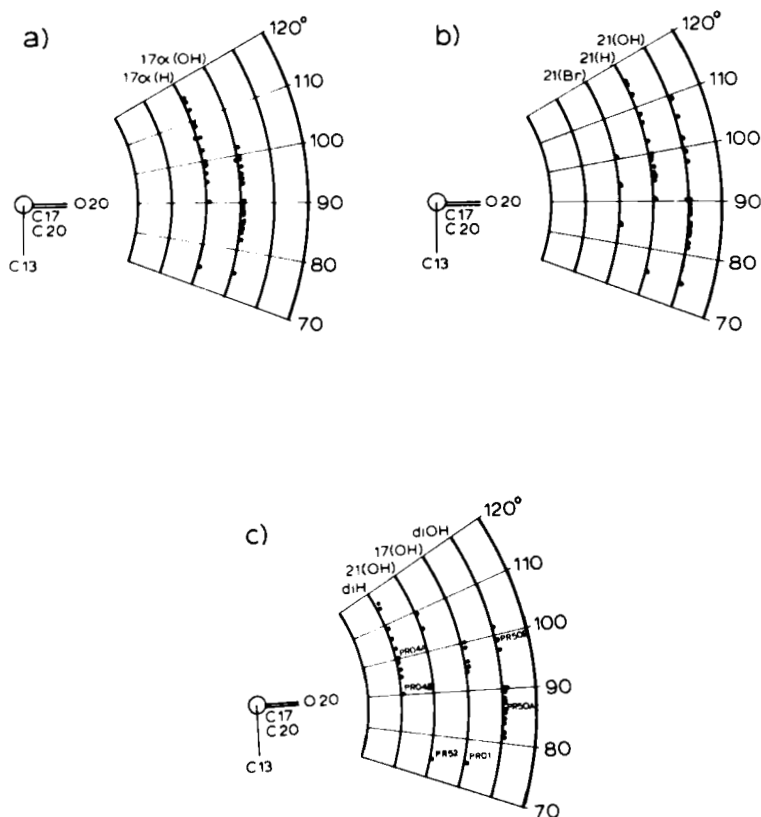


Fig. 72. Observed values of the torsion angle C(13)-C(17)-C(20)-O(20) that defines the 17β side chain orientation relative to the steroid skeleton are dependent upon 17α and 21 substituents. The range of this angle in 17α-hydroxy structures is contrasted with that in 17α-hydro structures in (a). The dependence of the side chain orientation upon 21 substitution is illustrated in (b) and 17α,21 disubstitution effects are shown in (c).

and the associated differences in the C(16)-C(17)-C(20)-O(20) torsion angle and the C(18)-O(20) distance are significant at the 99% level. C(21) oxygen and halogen substituents are all observed to be \pm synperiplanar relative to O(20). Substitution at the C(21) position restricts the rotational freedom of the 17β side chain (Fig. 72b). 17α,21-Dihydroxy-substituted molecules have

conformers in which the average C(13)-C(17)-C(20)-O(20) torsional angles are 85 and 100 deg., respectively. Molecules of each conformer are cocrystallized in PR50. These data indicate that the intramolecular control of side chain orientation is neither an artifact of, nor is it masked by, crystal-packing forces.[†]

The only observation in which an unrestricted sidechain is outside the plus clinal range occurs in one of the 16 β -brominated structures, PR02, and it is worth noting that the conformation observed in the other 16 β -brominated structure, PR01, is at one extreme of the range normally observed. The 16 β substitution crowds the 20-keto in PR01, and in PR02 the side chain adopts an alternative position in which the carbonyl nearly eclipses the C(13)-C(17) bond (Fig. 73).

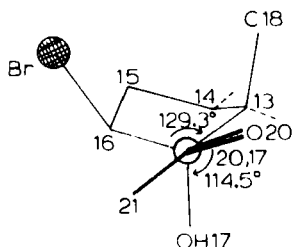


Fig. 73. The progesterone side chain in PR02 exhibits an unusual conformation due to crowding by 16 β -bromo substituent.

The introduction of groups that bridge the α face of the D ring (PR24, PR26, PR27, and PR30) has little effect upon the 17 β side chain conformation.

B. 17 β -Acetate and Benzoate Substituents

The data for 25 structures having 17 β -acetate substituents and eight structures having 17 β -benzoate substituents (Table 16) illustrate that the substituents are limited in flexibility of conformation. Their orientation relative to the D ring is defined by the

[†]The orientation of the side chain of 5 α -pregnan-20-one and progesterone in solution was determined by dipole moment measurements quite long ago, and the value found, C(16)-C(17)-C(20)-C(21) = 200-240 deg., is in the range of the values seen in crystal structures (76).

Table 15
Pregnane 17 β Side Chain Conformation

	C13-C17- C20-O20	C16-C17- C20-O20	C18...C20 (Å)	C18-C13 C17-C20	C14-C13- C17-C20	A (deg.)	ϕ_{max} (deg.)
a. 17 α -Hydroxy or Acetoxy							
	(deg.)	(deg.)		(deg.)	(deg.)		
PR02	-4.9	-129.3	2.955	-49.7	-168.1	3.83	47.93
PR01	75.2	-45.9	2.936	-49.5	-168.2	4.68	46.63
PR55a	81.6	-34.7	3.059	-53.1	-171.5	35.50	51.40
PR47a	82.2	-35.0	3.024	-53.6	-170.9	28.62	50.13
PR40b	83.9	-32.8	3.090	-50.8	-167.8	33.80	48.28
PR21b	84.7	-31.9	3.068	-49.3	-168.3	28.38	49.93
PR14a	84.8	-32.4	3.077	-51.2	-168.4	37.66	47.02
PR15a	85.3	-31.1	3.065	-49.7	-166.3	26.29	48.17
PR50A ^a	85.7	-32.1	3.060	-48.8	-165.5	15.43	48.92
PR19a	87.5	-28.1	3.023	-44.5	-163.5	10.94	47.86
PR49a	87.8	-29.8	2.999	-42.7	-160.4	14.61	44.32
PR20a	88.5	-28.9	3.054	-45.3	-163.6	12.45	47.03
PR23a	89.2	-27.8	3.057	-47.7	-165.5	17.70	48.06
PR22a	90.0	-26.6	3.108	-46.7	-164.7	11.18	48.22
PR17a	90.1	-26.7	3.033	-45.8	-163.9	13.52	47.48
PR29b	93.9	-21.7	3.129	-44.1	-163.8	19.82	47.44
PR12	94.8	-22.7	3.113	-41.8	-159.6	4.76	45.37
PR54	96.0	-21.2	3.114	-43.6	-162.1	5.67	46.61
PR18a	97.5	-18.4	3.213	-47.8	-165.7	25.89	47.49

Table 15 (Con't)

	C13-C17- C20-020	C16-C17 C20-020	C18...C20 Å	C18-C13- C17-C20(Å)	C14-C13- C17-C20	Δ(deg.)	φ _{max} (deg.)
PR37	99.2	-18.4	3.225	-50.0	-167.5	22.22	47.91
PR50B ^a	99.2	-16.4	3.141	-41.2	-160.1	11.75	46.39
PR03 ^b	100.3	-17.4	3.234	-49.7	-167.3	32.08	47.03
PR16	101.7	-16.0	3.163	-44.6	-160.8	3.82	45.72
b. 17α-Hydro	(deg.)	(deg.)		(deg.)	(deg.)		
PR52 ^a	74.4	-45.0	3.049	-51.0	-169.5	18.91	50.95
PR04B	90.3	-29.2	3.119	-47.5	-168.2	18.82	47.52
PR46	94.9	-24.2	3.198	-49.2	-167.4	17.14	47.64
PR33	97.3	-23.2	3.275	-51.5	-170.3	22.66	49.22
PR11	99.4	-22.0	3.219	-49.8	-166.3	12.09	46.01
PR04A	99.9	-19.7	3.286	-48.2	-166.4	18.12	47.51
PR32	102.6	-18.2	3.283	-44.7	-163.5	-0.28	47.73
PR38 ^a	105.6	-13.6	3.315	-46.2	-164.4	7.18	45.94
PR51	106.3	-14.4	3.359	-49.0	-166.6	13.26	47.04
PR31	108.5	-11.9	3.399	-46.4	-164.2	4.27	47.56
PR13 ^a	109.5	-11.1	3.390	-46.8	-164.1	13.28	44.78
PR34	112.8	-8.8	3.504	-46.1	-163.8	1.49	46.29
PR09	115.0	-6.4	3.464	-47.1	-165.5	11.77	45.43
PR08	115.8	-6.6	3.496	-46.3	-164.2	1.33	46.22

^a21-Hydroxy^b21-Halo, acetate, or benzoate.

torsion angle $C(13)-C(17)-O(17)-C(n)$, where $C(n)$ is the keto carbon. The observed values for these torsion angles in the 26 structures are plotted in Figure 74. The substituents are observed to fall in a 90 deg. range between positions antiperiplanar to the $C(13)-C(17)$ and the $C(16)-C(17)$ bonds. Observed conformations representative of the extremes of the range are superimposed in Figure 75.

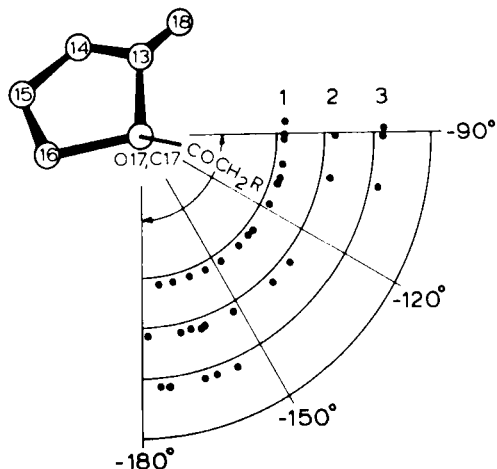


Fig. 74. Distribution of the conformations of 17β -acetate and 17β -benzoate substituents. Observed values of the torsion angle $C(13)-C(17)-O(17)-C(n)$, where $C(n)$ is the keto carbon, are plotted with 17β -acetates on Contour 1, 17β -haloacetates on Contour 2, and 17β -benzoates on Contour 3.

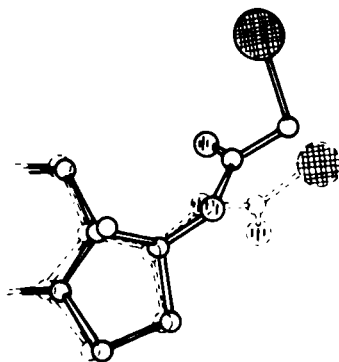


Fig. 75. A superposition diagram indicating the range in conformation observed for 17β -haloacetate substituents. The solid lines are ES02 and the dashed lines are ES11.

The 17 β -acetate conformations are observed to be distributed uniformly throughout this 90 deg. range. In contrast to this, the conformations of 17 β -benzoate substituents are clustered at either extreme of the range. Although there is some preference for the extremes of the range in the 17 β -haloacetate conformations as well, the more significant feature of their distribution is a correlation between the C(13)-C(17)-O(17)-C(n) torsion angle and the torsion angle defining the orientation of the carbon halogen bond relative to the keto oxygen. As the acetate orientation varies from antiperiplanar to clinal relative to the C(13)-C(17) bond the halogen position relative to the keto moves through 260 deg. from (-)antiperiplanar to (+)antiperiplanar passing through the synperiplanar position as illustrated in Figure 76.

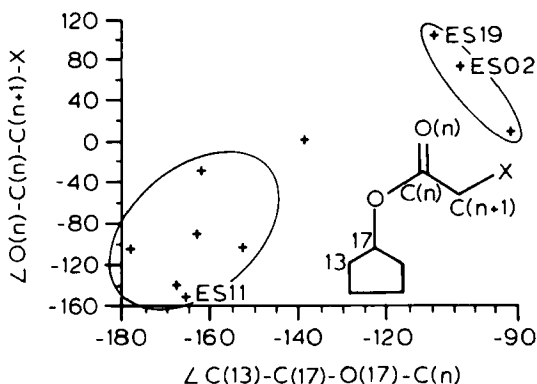


Fig. 76. The variation in the halogen orientation relative to the carbonyl is correlated with a change in the acetate orientation from antiperiplanar to clinal relative to the C(13)-C(17) bond.

Inspection of the Hodgkin packing notation (8) included in Table 16 reveals no perceivable pattern in crystal packing of the 17 β -acetate and benzoate derivatives. The fact that the 15 acetates and 10 haloacetates are observed in various modifications of eight basic patterns [0221, 0212, 0122, 0411, 0141, *Mabe*, *Mbea*, and *Meba*] indicates that the restriction of the acetate orientation to the observed 90 deg. range is independent of crystal packing. Furthermore, within this 90 deg. range there is no apparent correlation between crystal packing and conformation. For example, the acetate conformations in the four structures that are packed Obca 411 (AN64,

AN37, AN33, and ES33) cover most of the observed range. Finally the crystal packing is totally different in each of the 17 β -benzoate structures indicating that the limited range of observed conformations is not an artifact of molecular packing. The limited range of acetate orientations, the even greater conformational preference exhibited by benzoates, and the intramolecular correlations in the conformations of the 17-haloacetates further illustrate the intramolecular control of conformation largely undisturbed by and independent of variations in crystal packing.

C. 3 β -Acetate and Benzoate Substituents

The 13 structures having bulky 3 β substituents include the seven acetates and six benzoates listed in Table 17. The orientation of the substituent group relative to the A ring is defined by the torsion angles C(2)-C(3)-O(3)-C(n) and C(4)-C(3)-O(3)-C(n), in which C(n) is the keto carbon. The substituents are observed to fall into two conformational classes, and representative examples of conformers A and B are superimposed in Figure 77. In conformer A, the O(3)-C(n) bond is trans

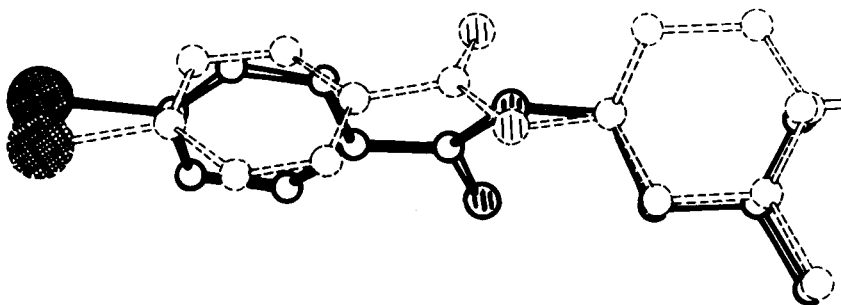


Fig. 77. Comparison of the two conformational isomers (A, dashed lines; B, solid lines) observed for 3 β -benzoate (and acetate) substituents on the steroid A ring.

to C(3)-C(4) and gauche to C(2)-C(3), and in conformer B, the O(3)-C(n) bond is gauche to C(3)-C(4) and trans to C(2)-C(3). It should be noted that a third conceivable conformer, one in which the O(3)-C(n) bond would be gauche to both C(3)-C(4) and C(2)-C(3), is not observed. A graph of torsion angles defining the orientation of the substituent relative to the A ring (Fig. 78) reveals a greater observed variability in conformers of type B.

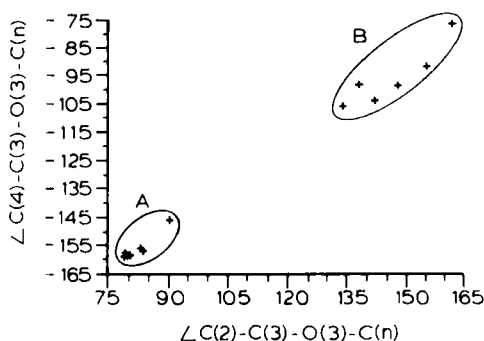


Fig. 78. The conformations of 3β -acetate and 3β -benzoate derivatives are clustered in two regions. Variance of conformer A is highly restricted. C(n) is the keto carbon.

The carbonyl conformation is also much more restricted in conformer A as illustrated in Figure 79. As inspection

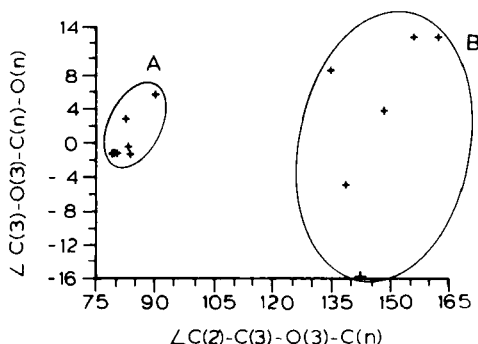


Fig. 79. The conformations of the carbonyl bond C(n)-O(n), relative to the C(3)-C(3) bond in thirteen acetate and benzoate derivatives are seen to be more restricted in conformers of type A than in type B.

of Table 17 reveals, this difference in flexibility of the two conformers is not a function of 3β substituent (acetates versus benzoates), C(5) configuration (5α versus 5-ene), or crystal packing. 3β -Acetate substituents are equally distributed between conformers A and B, as are the 3β -benzoate substituents. Conformers A include both 5α and 5-ene steroids, as do conformers B. Inspection of the packing notation reveals that the only similarity

in molecular packing is that in ten of the eleven crystals there are four molecules in the unit cell. There is no detectable difference in the packing patterns between structures of conformers A and conformers B. This conformational restriction observed in seven structures in variable crystal environments is an intramolecular property that is independent of crystal packing and probably related to the asymmetry of the steroid molecule.

Table 16
Conformations of 17 β -Acetate and 17 β -Benzoate Substituents

	1 ^a	2	3	4	5
a. 17 β -Haloacetates					
ES03	AP	-178.	AC	-107.1	Mb ₄₅ [°] c ₆₀ [°] a ₃₄ [°] 121
AN08	AP	-168.	AC	-142.7	Oc ₆ [°] b ₂₀ [°] a ₂₀ [°] 221
ES11	AP	-166.	AP	-151.6	Mc ₂₇ [°] b ₂₃ [°] a ₃₁ [°] 211
AN34	AP	-163.3	AC	-91.7	Oc ₂₈ [°] b ₃₇ [°] a ₂₄ [°] 221
ES20	AP	-162.	SP	-29.6	Oc ₁₂ [°] b ₂₄ [°] a ₂₁ [°] 141
AN22	AP	-152.7	AC	-105.6	Oc ₄₀ [°] a ₄₂ [°] b ₂₀ [°] 221
AN56	AC	-138.5	SP	-6	Ob ₁₈ [°] c ₁₇ [°] a ₁₆ [°] 212
ES19	AC	-109.	AC	103.9	Oa ₂₆ [°] c ₄₄ [°] b ₃₈ [°] 212
ES02	AC	-102.9	SC	72.	Ma ₅₀ [°] b ₃₆ [°] c ₃₂ [°] 112
AN20	AC	-91.4	SP	8.5	Oc ₃₉ [°] b ₅₁ [°] a ₄₀ [°] 221
b. 17 β -Acetates					
AN58	AP	-173.1			Oa ₄₂ [°] c ₄₅ [°] b ₁₉ [°] 212
AN64	AP	-168.6			Ob ₃₀ [°] c ₁₈ [°] a ₂₄ [°] 411
AN57	AP	-161.4			Oc ₄₂ [°] b ₄₁ [°] a ₁₆ [°] 141
AN37	AP	-154.4			Ob ₅₃ [°] c ₃₀ [°] a ₄₄ [°] 411
ES25	AC	-147.3			Oa ₁₃ [°] c ₈ [°] b ₁₂ [°] 212
AN19	AC	-137.7			Ma ₆ [°] c ₁₂ [°] b ₁₃ [°] 211
AN33	AC	-132.5			Ob ₁₈ [°] c ₂₂ [°] a ₁₃ [°] 411
AN51	AC	-130.			Oc ₃₇ [°] a ₄₅ [°] b ₃₁ [°] 221

Table 16 (Con't)

1 ^a	2	3	4	5
AN49	AC	-118.2		Mz ₁₂ [°] c ₁₂ [°] b ₁₃ [°] 211
AN59	AC	-109.5		Oe ₄ [°] b ₁₉ [°] a ₁₉ [°] 141
ES33	AC	-107.2		Ob ₂₂ [°] c ₂₂ [°] a ₁₉ [°] 411
AN41	AC	-102.1		Oe ₃₉ [°] a ₂₄ [°] b ₃₀ [°] 122
AN23	C	-91.4		Mb ₁₂ [°] c ₁₃ [°] a ₁₃ [°] 211
ES23	C	-90.		Oe ₂₁ [°] a ₂₅ [°] b ₃₂ [°] 122
AN68	SC	-84.8		Mz ₁₄ [°] b ₁₆ [°] a ₃₀ [°] (2) 1(2)
c. 17β-Benzozates				
ES28A2	AP	157.3		Oe ₄₂ [°] a ₃₉ [°] b ₄₄ [°] ; c ₄₅ [°] a ₃₂ [°] b ₄₅ [°] (4)
ES28A1	AP	162.5		
AN55	AP	-176.4		Mz ₄₄ [°] b ₁₅ [°] a ₄₈ [°] 121
AN52	AP	-174.1		Mz ₅₀ [°] c ₂₂ [°] b ₃ [°] 211
AN66	AP	-165.3		Ob ₂₄ [°] c ₂₄ [°] a ₆ [°] 411
AN60	AC	-103.3		Mz ₂₅ [°] c ₄₂ [°] b ₉ [°] 112
AN40	AC	-91.3		Oe ₂₇ [°] a ₃₆ [°] b ₂₅ [°] 122
AN48	SC	-89.8		Oa ₃₈ [°] c ₄₇ [°] b ₂₈ [°] 221

- ^a(1) Qualitative descriptor of substituent orientations (AP = antiperiplanar, SC = synclinal, etc.).
- (2) The torsion angle C(13)-C(17)-O(17)-C(n), where C(n) is the keto carbon.
- (3) Qualitative descriptor defining halogen orientations relative to the keto oxygen.

Table 16 (Con't)

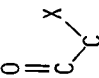
- (4) The torsion angle  where X is the halogen.
- (5) Modified Hodgkin packing notation. For purposes of calculation the steroid length is defined as parallel to the C(10)...C(13) direction, the width as parallel to the C(12)...C(14) direction, and the thickness is orthogonal to the other two. Examples:
 $Mb_{45}^{\circ}c_{60}^{\circ}a_{24}^{\circ}$ 121 means monoclinic, steroid thickness at 45° to b , steroid width at 60° to c , steroid length at 24° to a , packed one thick, two wide, and one long in the cell. $Or_{20}^{\circ}b_{20}^{\circ}a_{20}^{\circ}$ means orthorhombic, steroid thickness at 6° to c , steroid width at 20° to b , steroid length at 20° to a , packed two thick, two wide and one long in the cell. Notation of the form (2)1(2) indicates that steroid thickness and length are along diagonals of a cell face.

Table 17.
Conformational Parameters for 3 β -Acetate
and Benzoate Derivatives

	1 ^a	2	3	4	5	6
Conformer A						
PR02 A		α	79.5	-157.9	-1.3	$Oa_{35}^{\circ}c_{35}^{\circ}b_{10}^{\circ}$ 221
AN38 BrB		ene	79.9	-160.5	-1.3	$Ob_{29}^{\circ}c_{44}^{\circ}a_{37}^{\circ}$ (4)
AN58 A		α	80.8	-158.7	-1.3	$Oa_{42}^{\circ}c_{45}^{\circ}b_{19}^{\circ}$ 212
PR27 BrA		ene	82.8	-156.4	2.9	$Oa_{28}^{\circ}c_{10}^{\circ}b_{28}^{\circ}$ 212
PR28 BrB		ene	83.3	-156.3	-1.4	$Oa_{28}^{\circ}c_{30}^{\circ}b_{8}^{\circ}$ 221
PR07 BrB		α	83.6	-157.7	-1.4	$Ob_{44}^{\circ}a_{51}^{\circ}c_{23}^{\circ}$ 411
PR06 BrA		α	90.4	-145.9	5.7	$Oa_{27}^{\circ}c_{13}^{\circ}b_{29}^{\circ}$ 212
Conformer B						
PR26B A		ene	134.7	-105.7	8.5	$Ma_{52}^{\circ}a_{28}^{\circ}b_{23}^{\circ}; a_{43}^{\circ}c_{21}^{\circ}b_{22}^{\circ}$ (4) 1
AN26 A		ene	138.9	-98.3	-4.9	$Oe_{21}^{\circ}b_{28}^{\circ}a_{33}^{\circ}$ 141
PR05B BrB		α	142.6	-103.7	-15.9	$Mb_{43}^{\circ}c_{44}^{\circ}a_{7}^{\circ}; b_{37}^{\circ}c_{38}^{\circ}c_{5}^{\circ}$ 221
PR26A A		ene	148.5	-98.4	3.9	
PR05A BrB		α	156.1	-91.4	12.8	
AN27 BrB		ene	162.7	-75.7	12.6	$Mb_{21}^{\circ}c_{32}^{\circ}a_{40}^{\circ}$ 2(1)

(1) Substituent A = acetate, BrA = bromoacetate, B = benzoate,

BrB = bromobenzoate.

- (2) C(5) configuration.
- (3) The torsion angle $C(2)-C(3)-O(3)-C(n)$ where $C(n)$ is the keto carbon.
- (4) The torsion angle $C(4)-C(3)-O(3)-C(n)$, where $C(n)$ is the keto carbon.
- (5) $C(3)-O(3)-C(n)-O(n)$, where $C(n)-O(n)$ is the keto bond.
- (6) Modified Hodgkin packing notation.

D. C(19)-Substituents

Estrogen biosynthesis proceeds via a stepwise enzymic oxidation of the C(19) methyl of testosterone with the subsequent breaking of the C(10)-C(19) bond. Consequently, the conformations of C(19) oxygen-substituted androstanes are useful for the development of postulated mechanisms of estrogen biosynthesis.

The conformation about the C(10)-C(19) bond in structures having oxygen substitution at C(19) are illustrated in Figure 80. The aldehyde bond eclipses the C(1)-C(10) bond

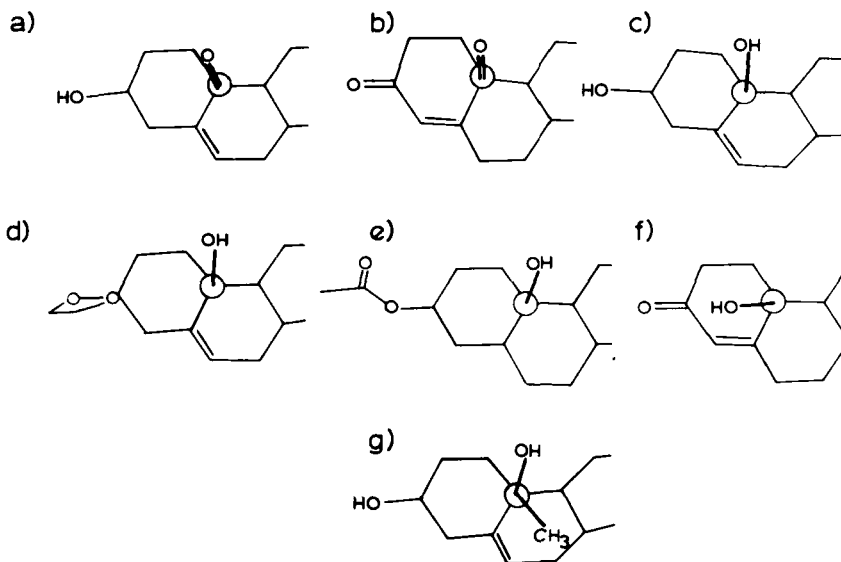


Fig. 80. The conformations of 19-oxo derivatives in (a) AN61, (b) AN48, (c) AN55, (d) AN60, (e) AN58, (f) AN54, and (g) AN65.

in AN61 and is nearly perpendicular to the C(9)-C(10) bond in AN48. In both cases, the oxygen is antiperiplanar to C(10)-C(5). The 19-hydroxyls are also positioned antiperiplanar to C(10)-C(5) in the saturated structure AN58 and in the 5-ene structures. In contrast, the 19-hydroxy in the Δ^4 -3-one structure (AN54) is oriented over the A ring. In the disubstituted 19-methyl-19-hydroxyl-5-ene structure the oxygen is again antiperiplanar to C(10)-C(5), and the methyl substituent is over the B ring. The fact that these observations indicate a highly preferred position for C(19) oxygen substituents in all but the Δ^4 -3-one case lends credence to the use of the crystallographic structures in postulating molecular level mechanisms.

VI. INTERMOLECULAR INTERACTION

A. Isomorphic and Polymorphic Forms

There are surprisingly few instances of identical crystal packing (isomorphism) despite the similarities in the molecular structures of the estranes, androstanes, and pregnanes and the fact that 85% of them crystallize in either the $P2_12_12_1$ or $P2_1$ space groups. On the contrary, there is an endless variety of packing patterns. Only through the use of the Hodgkin notation has it been possible to locate and define subsets of the packing patterns which are commonly found in many crystal structures (e.g., the 0212 subset where steroids are positioned two thick, one wide, and two long in an orthorhombic lattice). Patterns of extended structure (chains, coils, planes) are also detected in different crystal forms. However the total packing is seldom identical. The ten isomorphous pairs and one isomorphous triplet among the 164 crystal forms of Table 3 are listed in Table 18. In six of the isomorphous pairs, the hydrogen bonding observed in the two structures is different, indicating that there is no simple correspondence between hydrogen bonding and crystal packing.

Minor changes in molecular orientation greatly alter intermolecular contacts. A 15 deg. difference in the orientation of the steroid axis relative to one of the cell sides is so magnified by symmetry operations that closest intermolecular contacts differ substantially. A comparison of cell dimensions of two structures having similar gross packing but differing slightly in molecular orientation (Fig. 81) provides an example of the subtle differences in crystal packing that alter individual interatomic interactions. The intermolecular contacts less than 3.8 Å for the two structures are listed in Table

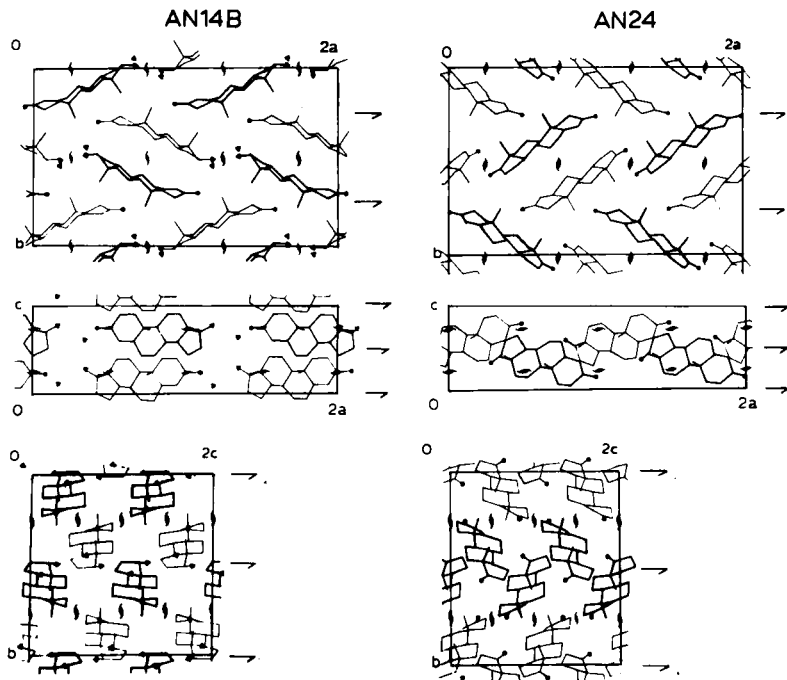


Fig. 81. Although the gross crystal packing in AN14B (left) is similar to that in AN24, the closest intermolecular contacts are totally dissimilar (Table 19).

19 and only three similar contacts are observed.

Another important facet of steroid crystal packing that should be stressed is the fact that flexible steroids such as estrone, testosterone, and progesterone have polymorphic forms differing completely in crystal packing (Fig. 19). It has already been pointed out that the conformations of the molecules in the polymorphs vary much less than the crystal packing. The greatest conformational differences are between independent molecules in crystals having a doubled asymmetric unit. Conformations observed in other polymorphs of the same molecules are observed to match one or the other of the molecules in the doubled unit.

Despite the similarity in the composition and hydrogen bonding potential of cortisol (PR15) and its three 9 α -halo derivatives (PR17, PR18, PR19), they have totally different crystal habits ranging through three crystal systems. Observations such as this further illustrate the absence of strong correlations between molecular composition and crystal packing.

Table 18.
Isomorphous Crystal Forms Among
164 Estrane, Androstane, and Pregnane Structures

Packing Type	Structure	Hodgkin Notation	Cell Dimensions				Hydrogen Bonding
			a (Å)	b (Å)	c (Å)	β (deg.)	
Mnbn	AN14A	$Mc_{14}^{\circ}b_{13}^{\circ}a_{14}^{\circ}$ 211	11.1	8.1	9.6	97.8	2D ^a
	AN07	$Mc_{12}^{\circ}b_{11}^{\circ}a_{14}^{\circ}$ 211	11.5	8.1	9.4	99.1	2D
	ES02	$Ma_{50}^{\circ}b_{36}^{\circ}c_{32}^{\circ}$ 211	12.6	7.0	10.9	92.3	None
	ES35	$Ma_{52}^{\circ}b_{36}^{\circ}c_{31}^{\circ}$ 211	12.9	7.0	10.6	95.1	None
	AN02	$Mc_{24}^{\circ}b_{21}^{\circ}a_{13}^{\circ}$ 211	12.3	7.2	10.3	114.1	2D
	AN30	$Mc_{24}^{\circ}b_{24}^{\circ}a_{21}^{\circ}$ 211	11.9	7.2	11.0	114.7	2D
	AN19	$Ma_6^{\circ}c_{12}^{\circ}b_{13}^{\circ}$ 211	9.8	14.0	7.8	90.8	None
	AN49	$Ma_{12}^{\circ}c_{12}^{\circ}b_{13}^{\circ}$ 211	9.8	12.5	7.3	96.8	None
Mbnn	PR25	$Mb_{14}^{\circ}c_8^{\circ}a_{18}^{\circ}$ 121	13.2	6.0	12.2	107.3	2D

Table 18 (Con't)

Packing Type	Structure	Hodgkin Notation	Cell Dimensions			Hydrogen Bonding
			a (Å)	b (Å)	c (Å)	β (deg.)
M212	PR45	$Mb_{20}c_{11}a_{11}^\circ$ 121	15.7	6.0	12.2	111.9
	AN01	$Mb_{15}c_{9}a_{19}^\circ$ 211	11.5	11.1	7.6	110.6
	PR01	$Mb_{16}c_{12}a_{15}^\circ$ 211	11.9	11.0	7.8	107.4
	PR13	$Mb_{30}c_{29}a_{41}^\circ$ 2(1)	8.7	12.5	8.5	98.0
	PR38	$Mb_{29}c_{27}a_{45}^\circ$ 2(1)	8.9	12.3	8.3	97.2
ES17	ES13	$Ma_{16}c_{15}b_{15}^\circ;$ $a_{6}c_{21}b_{13}^\circ$ 212	9.3	22.3	7.6	111.5
	ES17	$Ma_{19}c_{14}b_{15}^\circ;$ $a_{5}c_{23}b_{13}^\circ$ 212	9.3	23.0	7.6	111.0
	PR12	$Oa_{7}c_{6}b_{4}^\circ$ 212	9.8	23.5	7.8	
O212						1D

Table 18 (Con't)

Packing Type	Structure	Hodgkin Notation	Cell Dimensions			Hydrogen Bonding	
			a (Å)	b (Å)	c (Å)		β (deg.)
	PR17	$0a_4^{\circ}c_7^{\circ}b_6^{\circ}$	212	10.1	23.6	7.8	3D
	PR20	$0a_4^{\circ}c_8^{\circ}b_7^{\circ}$	212	10.1	23.7	7.7	3D
	PR47	$0c_{16}^{\circ}a_{43}^{\circ}b_{40}^{\circ}2(2)$		10.8	17.6	10.2	3D
	PR46	$0c_{12}^{\circ}a_{41}^{\circ}b_{39}^{\circ}2(2)$		10.6	17.0	10.1	1D
0221	AN22	$0c_{40}^{\circ}a_{42}^{\circ}b_{20}^{\circ}221$		13.5	16.6	10.8	None
	AN51	$0c_{37}^{\circ}a_{45}^{\circ}b_{31}^{\circ}221$		13.3	14.5	10.9	None

^a2D = two dimensional, etc.

Table 19.
Comparison of Intermolecular Contacts ($<3.8 \text{ \AA}$)
in the Structures AN14B and AN24

Hodgkin Notation	$Ob_{29^\circ}c_{6^\circ}a_{28^\circ}$	411	$Ob_{36^\circ}c_{21^\circ}a_{36^\circ}$	411
Cell dimensions (\AA)				
$a =$	13.6		13.0	
$b =$	15.9		17.0	
$c =$	7.9		7.4	
Contacts (\AA)	C(3) \rightarrow O(20)	3.55	C(1) \rightarrow C(6)	3.67
	C(4) \rightarrow C(18)	3.70	C(1) \rightarrow O(3)	3.76
	C(4) \rightarrow O(20)	3.71	C(2) \rightarrow O(17)	3.59
	C(6) \rightarrow C(18)	3.68	C(4) \rightarrow C(15)	3.79
	C(6) \rightarrow O(3)	3.69	C(4) \rightarrow C(18)	3.68
	C(12) \rightarrow O(20)	3.75	C(11) \rightarrow O(3)	3.53
	C(15) \rightarrow O(20)	3.59	C(16) \rightarrow O(3)	3.44
	C(16) \rightarrow O(3)	3.60	C(16) \rightarrow O(17)	3.49
	C(16) \rightarrow O(17)	3.68	C(18) \rightarrow O(17)	3.56
	C(16) \rightarrow O(20)	3.35	C(19) \rightarrow O(17)	3.49
	C(16) \rightarrow O(20)	3.58		
	C(17) \rightarrow O(20)	3.48		
	C(17) \rightarrow O(20)	3.72		
	C(19) \rightarrow O(17)	3.38		
	O(3) \rightarrow O(20)	2.90		
	O(17) \rightarrow O(20)	2.70		
	O(17) \rightarrow O(20)	2.77		

B. Gross Packing Features

As a result of the great variation in individual crystals, few generalizations can be drawn from analysis of the crystal packing patterns. However, some correlations between conformation and one and two-dimensional extended structures are observed. Estrane and androstane molecules having all trans junctions and the O(3) and O(17) atoms equatorially oriented pack in infinite chains aligned head to tail with adjacent chain links related by cell translation. The slight bowing of the A ring in 4-androsten-3-ones causes the chains to twist about an axis parallel to the molecular length. The increased α face bowing in structures such as 4-pregnen-3-ones and 1,4-pregnadienes produces coiled chains of molecules. Hydrogen bonding of steroids in monoclinic crystals forms one- or two-dimensional networks (chains and planes, respectively), whereas hydrogen

bonding in orthorhombic crystals forms three-dimensional networks as well. Consequently, a steroid having three or more potential hydrogen bond donors will tend to crystallize in an orthorhombic space group.

C. Hydrogen Bonding Patterns

The hydrogen bonding patterns of corticosteroid molecules and analogues indicate a high degree of directional specificity in the location of hydrogen bond donors and acceptors (Fig. 82). The 11β -hydroxy is

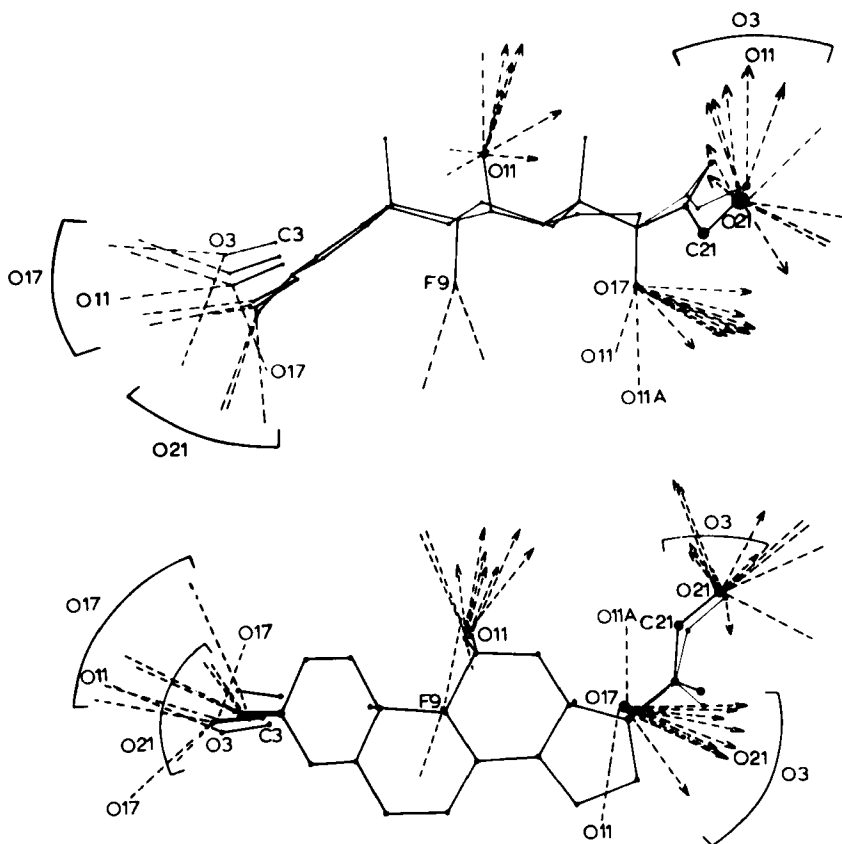


Fig. 82. The directionality of hydrogen bonding is observed to be dependent upon the conformation of hydroxyl hydrogen atoms when the steroid is the donor and overall molecular conformation when the steroid is acceptor.

consistently hydrogen bonded trans to the C(9)-C(11) bond and the 17 α -hydroxyl is consistently hydrogen bonded trans to the C(13)-C(17) bond. There is also a correlation between the orientation of the C(3)-O(3) bond and the location of hydrogen bond donors to that carbonyl. It is apparent that for a 0.5 Å change in the relative position of oxygen atom O(3), the optimum location for a hydrogen bond donor may vary by as much as 3.0 Å. The directionality of these hydrogen bonds is independent of the external hydrogen bond acceptor or donor identity. For example, the O(11) hydrogen bond acceptors in nine structures include the O(3), O(17), O(20), O(21), and F(9) atoms of adjacent molecules (Fig. 83). This consistency in the directionality

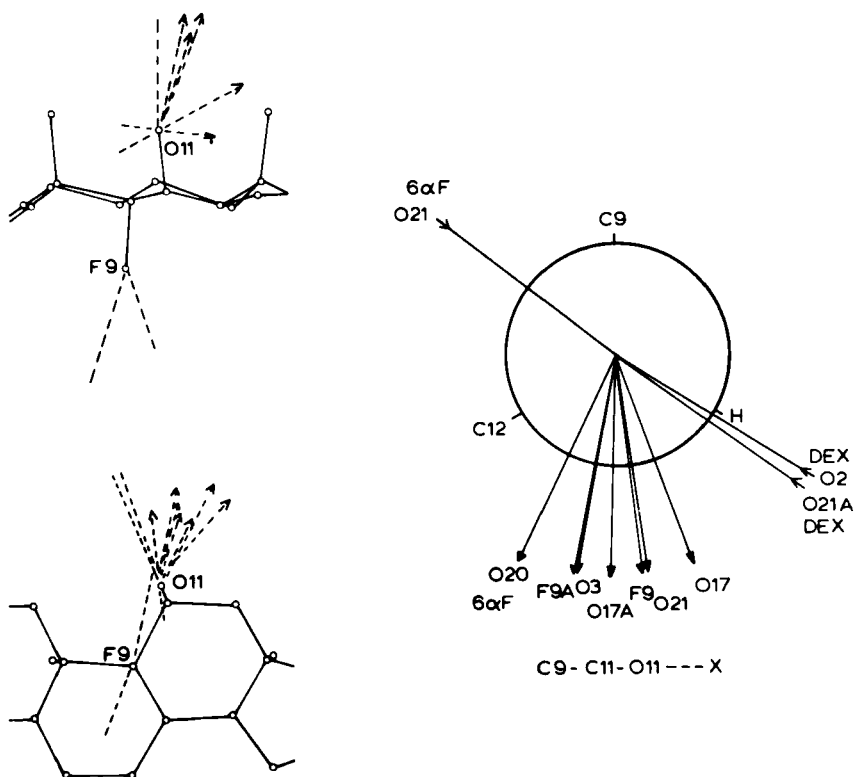


Fig. 83. The direction of hydrogen bonds involving O(11) atoms as donors is independent of the acceptor atoms.

of hydrogen bond donation and acceptance is perhaps the most important pattern to emerge from the analysis of intermolecular interactions in steroid crystal structures. Interaction with the immediate environment is shown to be independent of crystal packing arrangement and highly controlled by intramolecular forces.

VII. SUMMARY

The most important features brought to light by the comparative conformational analysis of steroids based upon X-ray observations are summarized below.

1. The conformations of steroids having flexible unsaturated rings and substituents are observed to have characteristic cluster patterns. These patterns of conformational isomerism are most apparent in 1,3,5(10)-estratriene structures; 17 β -benzoate, 3 β -acetate, and 3 β -benzoate derivatives; and Δ^4 -3-one structures having B- and C-ring substituents. In three observations estrone molecules have 7 α ,8 β half-chair conformations that are indistinguishable, whereas a fourth molecule of estrone is in the 8 β sofa conformation. A 2:1 ratio of conformers is observed for three molecules of each of the structures, 5 α -androsterane-3,17-dione and 17 β -hydroxy-5 α -androstan-3-one. The greatest differences in conformational isomers are found between two steroids in a crystal having a doubled asymmetric unit. This clustering of conformations of cocrystallization of significantly different conformers suggests equal population of the conformers in the crystallization medium and an appreciable barrier to interconversion.

2. Substitution will often remove, alter, or limit the flexibility of a steroid ring or side chain. Although the testosterone A ring ranges from 1 α ,2 β half-chair to 1 α sofa conformations, most B- and C-ring substitutions produce a clustering about one or the other of these symmetric forms. For example 9 α -halosubstitution stabilizes the 1 α ,2 β half-chair.

3. In contrast, the conformation of less flexible steroids will be indistinguishable despite changes in crystal habit. The conformation of the B ring of estradiol is a distorted 7 α ,8 β half-chair in complexes with water, propanol, and urea.

4. Specific substitutions are observed to have characteristic effects upon the conformations of flexible rings and side chains. The stabilization of a nearly perfect half-chair conformation brought about by 9 α -halo substitution and the 12 deg. shift in the relative orientation of the progesterone 17 β side chain caused by 17 α -hydroxy substitution are two of the best examples of these substituent effects that are clearly

illustrated by the crystal structure data.

5. Correlations between specific substitutions and changes in bond lengths and valency angles at points distant from the substituent are discernable in the data. The best example of these conformational transmission or long-range effects are illustrated in the significant difference in bond lengths and valency angles throughout the steroid nucleus observed when contrasting 4-androsten-3-ones with 4-pregnen-3-ones.

6. Definite patterns are observed in the directionality of hydrogen bonds. Clearly, the *trans* orientations of the 11 β -hydroxy and 17 α -hydroxy hydrogen bonds in cortisol derivatives relative to the C(9)-C(11) and C(13)-C(17) bonds, respectively, are intramolecularly controlled. Consequently, details of intermolecular interaction in the solid may have parallels at binding and reactive sites in the biological setting.

7. Molecular packing patterns vary so widely in the 164 crystals that no packing patterns can be associated with a particular hydrogen-bonding scheme, ring distortion, or sidechain orientation. This evidence suggests that conformational features are largely controlled by intramolecular forces rather than by crystal packing.

The intramolecular control of conformation, the crystallization of discrete conformational isomers, and the minimal influence of crystal packing upon conformation support the contention that the conformations observed in the solid closely approximate the most probable conformations regardless of environment. Therefore, crystal structure determinations provide precisely the information most useful for the development of models describing the action of steroids on a molecular level. The conformational features of steroids elucidated by X-ray analysis have already been used in a number of studies concerning steroid conformation and function *in vivo* and *in vitro*. Ambiguities in the interpretation of ORD and CD spectral data concerning the flexible Δ^4 -3-one A-ring of substituted testosterone derivatives have been resolved on the basis of crystallographically observed conformations (23,72,75). The detailed stereochemistry of the nucleus and 17 β sidechain conformations of glucocorticoid hormones required for optimum activity has been elucidated (140,181), and the structural requirements for estrogenic activity are being resolved through comparison of the structures of steroidal and nonsteroidal estrogens (180). Development of a molecular model for the mechanism of aromatization in which androgen is transformed to estrogen by human placental aromatase is being based upon X-ray structure studies (182).

Perhaps the most significant feature brought to light by this analysis is the existence of significantly different

conformational isomers of the most active natural steroid hormones. It is highly probable that this conformational isomerism facilitates interaction with a number of different proteins and that for a specific interaction a particular conformer may be optimal. Furthermore, many synthetic steroids may have an inflexible conformation that only competes for one of the protein molecules that interact with the natural hormone.

ACKNOWLEDGMENTS

This research was supported in part by USPH Grants CA-10906 and LM-02353.

Tables and graphs were prepared through interrogation of the steroid data stored in the NIH PROPHET system, an NIH interactive computer network. The authors express appreciation to C. DeVine, M. Erman, G. Sellers, and P. Strong for assistance in assembling and tabulating the data; to R. Dozoretz, A. Erman, G. Del Bel, D. Maracle, and M. Tugac for preparation of the figures; and to B. Giacchi, D. Hefner, V. Kamysz, and E. Robel for preparation of the manuscript. The authors are also grateful to V. Cody, G. DeTitta, J. Griffin, and H. Hauptman for helpful discussion of the manuscript.

REFERENCES

1. M. Hanach, *Conformation Theory*, Academic, New York, p. 225, 1965.
2. N. L. Allinger and G. A. Lane, *J. Amer. Chem. Soc.*, **96**, 2937 (1974).
3. R. T. Blickenstaff and K. Sophason, *Tetrahedron*, **28**, 1945 (1972).
4. V. V. Egorova, A. V. Zakhorychev, and S. N. Ananchenko, *Tetrahedron*, **29**, 301 (1973).
5. P. Morand, J. M. Lyall, and H. Sollar, *J. Chem. Soc., C*, 1970, 2117.
6. D. H. R. Barton, *Experientia*, Suppl. II, 1955, 121; D. H. R. Barton, A. J. Head, and P. J. May, *J. Chem. Soc.*, 1957, 935.
7. "IUPAC-IUB Revised Tentative Rules for Nomenclature of Steroids," *Biochemistry*, **8**, 2227 (1969).
8. J. D. Bernal, D. Crowfoot, and I. Fankuchen, *Phil. Trans. Roy. Soc., A*, **239**, 135 (1940).
9. H. Wieland, *Angew. Chem.*, **42**, 421 (1929).
10. C. H. Carlisle and D. Crowfoot, *Proc. Roy. Soc., A*, **184**, 64 (1945).

11. W. L. Duax and D. A. Norton, Eds., *Atlas of Steroid Structure*, Vol. I, Plenum, New York, 1975.
12. R. Bucourt, in *Topics in Stereochemistry*, E. L. Eliel and N. L. Allinger, Eds., Wiley-Interscience, New York, Vol. 8, p. 159, 1974.
13. J. D. Dunitz, *J. Chem. Ed.*, **47**, 488 (1970); J. D. Dunitz, *Tetrahedron*, **28**, 5459 (1972).
14. J. B. Hendrickson, *J. Amer. Chem. Soc.*, **83**, 4537 (1961).
15. C. Altona, H. J. Geise, and C. Romers, *Tetrahedron*, **24**, 13 (1968).
16. K. S. Pitzer and W. E. Donath, *J. Amer. Chem. Soc.*, **81**, 3213 (1959).
17. W. Klyne and V. Prelog, *Experientia*, **16**, 521 (1960).
18. W. D. S. Motherwell, L. Riva Di Sanseverino, O. Kennard, *Abstracts, First European Crystallographic Conference*, Bordeaux, France, Sept. 1973, group B₆.
19. C. Romers, C. Altona, H. J. C. Jacobs, and R. A. G. de Graaff, in *Terpenoids and Steroids*, The Chemical Society, London, Vol. 4, 1974.
20. R. R. Sobti, S. G. Levine, and J. Bordner, *Acta Crystallogr.*, **B28**, 2292 (1972).
21. J. Bordner, R. L. Greene, S. G. Levine, and R. R. Sobti, *Cryst. Struct. Comm.*, **2**, 55 (1973).
22. W. L. Duax, A. Cooper, and D. A. Norton, unpublished.
23. V. Cody and W. L. Duax, *Cryst. Struct. Comm.*, **1**, 439 (1972).
24. B. Busetta and M. Hospital, *Acta Crystallogr.*, **B28**, 560 (1972).
25. B. Busetta, C. Courseille, S. Geoffre, and M. Hospital, *Acta Crystallogr.*, **B28**, 1349 (1972).
26. W. L. Duax, *Acta Crystallogr.*, **B28**, 1864 (1972).
27. D. A. Norton, G. Kartha, and C. T. Lu, *Acta Crystallogr.*, **17**, 77 (1964).
28. V. Cody, F. DeJarnette, W. L. Duax, and D. A. Norton, *Acta Crystallogr.*, **B27**, 2458 (1971).
29. Y. Tsukuda, T. Sato, M. Shiro, and H. Koyama, *J. Chem. Soc.*, **B**, 1968, 1387.
30. Y. Tsukuda, T. Sato, M. Shiro, and H. Koyama, *J. Chem. Soc.*, **B**, 1969, 336.
31. J. N. Brown and L. M. Trefonas, *J. Amer. Chem. Soc.*, **94**, 4311 (1972).
32. B. Busetta, C. Courseille, and M. Hospital, *Acta Crystallogr.*, **B29**, 298 (1973); T. D. J. Debaerdemaeker, *Cryst. Struct. Comm.*, **1**, 39 (1972).
33. D. A. Norton, G. Kartha, and C. T. Lu, *Acta Crystallogr.*, **16**, 89 (1963).
34. R. Majeste and L. M. Trefonas, *J. Amer. Chem. Soc.*, **91**, 1508 (1969).

35. A. J. Olson, J. C. Hanson, and C. E. Nordman, *Acta Crystallogr.*, B31, 496 (1975).
36. A. Cooper, D. A. Norton, and H. Hauptman, *Acta Crystallogr.*, B25, 814 (1969).
37. H. P. Weber and E. Galantay, *Helv. Chim. Acta*, 55, 544 (1972).
38. C. M. Weeks and D. A. Norton, *J. Chem. Soc.*, B, 1970, 1494.
39. A. H. Joustra and H. Schenk, *Rec. Trav. Chim. Pays-Bas*, 89, 988 (1970).
40. J. G. H. de Jong, C. J. Dik-Edixhoven, and H. Schenk, *Cryst. Struct. Comm.*, 2, 33 (1973).
41. B. Busetta, C. Courseille, and M. Hospital, *Cryst. Struct. Comm.*, 1, 235 (1972).
42. J. N. Brown, R. L. R. Towns, and L. M. Trefonas, *J. Heterocycl. Chem.*, 8, 273 (1971).
43. C. F. W. van de Ven and H. Schenk, *Cryst. Struct. Comm.*, 1, 121 (1972).
44. J. C. Hanson and C. E. Nordman, *Acta Crystallogr.* B31, 493 (1975).
45. H. Schenk, W. M. B. Konst, W. N. Speckamp, and H. O. Huisman, *Tetrahedron Lett.*, 56, 4937 (1970).
46. D. Lednicer, D. E. Emmert, C. G. Chidester, and D. J. Duchamp, *J. Org. Chem.*, 36, 3260 (1971).
47. M. O. Chaney and N. D. Jones, *Cryst. Struct. Comm.*, 1, 197 (1972).
48. N. E. Taylor, D. C. Hodgkin, and J. S. Rollett, *J. Chem. Soc.*, 1960, 3685.
49. C. Courseille, B. Busetta, G. Precigoux, and M. Hospital, *Acta Crystallogr.* B29, 2462 (1973).
50. C. Courseille, F. Leroy, and J. Y. Lallemand, *Cryst. Struct. Comm.*, 3, 173 (1974).
51. G. Koyama, *Helv. Chim. Acta*, 57, 370 (1974).
52. R. A. G. de Graaff, C. A. M. van der Ende, and C. Romers, *Acta Crystallogr.*, B30, 2034 (1974).
53. N. Mandel and J. Donohue, *Acta Crystallogr.*, B28, 308 (1972).
54. G. Precigoux, B. Busetta, C. Courseille, and M. Hospital, *Cryst. Struct. Comm.*, 1, 265 (1972).
55. G. Kartha, C. T. Lu, and D. A. Norton, unpublished.
56. C. M. Weeks, A. Cooper, D. A. Norton, H. Hauptman, and J. Fisher, *Acta Crystallogr.*, B27, 1562 (1971).
57. D. F. High and J. Kraut, *Acta Crystallogr.*, 21, 88 (1966).
58. C. Courseille, G. Precigoux, F. Leroy, and B. Busetta, *Cryst. Struct. Comm.*, 3, 441 (1973).
59. B. Busetta, C. Courseille, J. M. Fornies-Marquina, and M. Hospital, *Cryst. Struct. Comm.*, 1, 43 (1972).
60. A. T. Christensen, unpublished.

61. J. S. McKechnie, L. Kubina, and I. C. Paul, *J. Chem. Soc., B*, 1970, 1476.
62. V. M. Coiro, E. Giglio, A. Lucano, and R. Puliti, *Acta Crystallogr. B29*, 1404 (1973).
63. D. Peck, D. A. Langs, C. Eger, and W. L. Duax, *Cryst. Struct. Comm.*, 3, 573 (1974).
64. J. R. Hanson, T. D. Organ, G. A. Sim, and D. N. J. White, *J. Chem. Soc., C*, 1970, 2111.
65. P. J. Roberts, R. C. Pettersen, G. M. Sheldrick, N. W. Isaacs, and O. Kennard, *J. Chem. Soc. Perkin II*, 1973, 1978.
66. B. Busetta, C. Courseille, F. Leroy, and M. Hospital, *Acta Crystallogr.*, B28, 3293 (1972).
67. G. Precigoux, M. Hospital, and G. Van Den Bosche, *Cryst. Struct. Comm.*, 3, 435 (1973).
68. A. Cooper, E. M. Gopalakrishna, and D. A. Norton, *Acta Crystallogr. B25*, 935 (1968).
69. A. Cooper, G. Kartha, E. M. Gopalakrishna, and D. A. Norton, *Acta Crystallogr.*, B25, 2409 (1969).
70. H. Koyama, M. Shiro, T. Sato, and Y. Tsukuda, *J. Chem. Soc., B*, 1970, 443.
71. C. M. Weeks, H. Hauptman, and D. A. Norton, *Cryst. Struct. Comm.*, 1, 79 (1972).
72. W. L. Duax, Y. Osawa, A. Cooper, and D. A. Norton, *Tetrahedron*, 27, 331 (1971).
73. H. Koyama, M. Shiro, T. Sato, and Y. Tsukuda, *J. Chem. Soc., B*, 1970, 443.
74. A. Cooper, C. T. Lu, and D. A. Norton, *J. Chem. Soc., B*, 1968, 1228.
75. W. L. Duax, C. Eger, S. Pokrywiecki, and Y. Osawa, *J. Med. Chem.*, 14, 295 (1971).
76. N. L. Allinger and M. A. Da Rooge, *J. Amer. Chem. Soc.*, 83, 4256 (1961).
77. B. Busetta, G. Comberton, C. Courseille, and M. Hospital, *Cryst. Struct. Comm.*, 1, 129 (1972).
78. C. M. Weeks, A. Cooper, and D. A. Norton, *Acta Crystallogr.*, B27, 531 (1971).
79. H. C. Mez and G. Rihs, *Helv. Chim. Acta*, 55, 375 (1972).
80. J. C. Portheine, C. Romers, and E. W. M. Rutten, *Acta Crystallogr.*, B28, 849 (1972).
81. W. L. Duax, D. A. Norton, S. Pokrywiecki, and C. Eger, *Steroids* 18, 525 (1971).
82. D. N. Peck, D. A. Langs, C. Eger, and W. L. Duax, *Cryst. Struct. Comm.*, 3, 451 (1974).
83. C. M. Weeks, A. Cooper, D. A. Norton, H. Hauptman, and J. Fisher, *Acta Crystallogr.*, B27, 1562 (1971).
84. C. Tamura and G. A. Sim, *J. Chem. Soc., B*, 1968, 8.
85. P. B. Braun, J. Hornstra, and J. I. Leenhouts,

- Philips Res. Rep.*, 24, 459 (1969)
86. P. B. Braun, J. Hornstra, and J. I. Leenhouts, *Philips Res. Rep.*, 24, 454 (1969).
87. W. E. Oberhansli and J. M. Robertson, *Helv. Chim. Acta*, 50, 53 (1967).
88. N. W. Isaacs, W. D. S. Motherwell, J. C. Coppola, and O. Kennard, *J. C. S., Perkin II*, 1972, 2335.
89. P. B. Braun, J. Hornstra, and J. I. Leenhouts, *Philips Res. Rep.*, 24, 436 (1969).
90. P. B. Braun, J. Hornstra, and J. I. Leenhouts, *Philips Res. Rep.*, 24, 450 (1969).
91. J. C. Portheine and C. Romers, *Acta Crystallogr.*, B26, 1791 (1970).
92. M. J. Green, N. A. Abraham, E. B. Fleischer, J. Molin-Case, and J. Fried, *Chem. Commun.*, 1970, 234.
93. H. Hope and A. T. Christensen, *Acta Crystallogr.*, B24, 375 (1968).
94. D. S. Savage, A. F. Cameron, G. Ferguson, C. Hannaway, and I. R. MacKay, *J. Chem. Soc., B*, 1971, 410.
95. J. S. McKechnie and I. C. Paul, *J. Amer. Chem. Soc.*, 90, 2144 (1968).
96. S. Neidle, D. Rogers, and M. B. Hursthouse, *J. C. S., Perkin II*, 1972, 760.
97. C. S. Yoo, J. Fletcher, and M. Sax, *Acta Crystallogr.*, B28, 2838 (1972).
98. G. Precigoux and J. Fornies-Marguina, *Cryst. Struct. Comm.*, 2, 287 (1973).
99. G. Weitz and E. Wolfel, *Acta Crystallogr.*, 15, 484 (1962).
100. A. Chiaroni and C. Pascard-Billy, *Acta Crystallogr.*, B28, 1085 (1972).
101. W. L. Duax and Y. Osawa, *Abstract, American Crystallographic Association Meeting*, Gainesville, Florida, Jan. 1973, p. 94.
102. W. L. Duax, unpublished.
103. W. L. Duax, T. F. Brennan, C. M. Weeks, and Y. Osawa, *Cryst. Struct. Comm.*, 4, 249 (1975).
104. D. C. Rohrer and W. L. Duax, *Cryst. Struct. Comm.*, 4, 265 (1975).
105. V. Cody, W. L. Duax, F. E. DeJarnette, D. A. Norton, and Y. Osawa, *Abstract, American Crystallographic Association Meeting*, Albuquerque, New Mexico, April 1972, p. 72.
106. W. L. Duax and M. Greiner, unpublished.
107. W. L. Duax and Y. Osawa, unpublished.
108. M. Greiner and W. L. Duax, unpublished.
109. C. M. Weeks, W. L. Duax, and Y. Osawa, *Cryst. Struct. Comm.*, 4, 97 (1975).

110. V. Cody, W. L. Duax, C. M. Weeks, and M. Wolff, *Acta Crystallogr.*, B31, 292 (1975).
111. G. I. Birnbaum, *Acta Crystallogr.*, B29, 1426 (1973).
112. P. B. Braun, J. Hornstra, and J. I. Leenhouts, *Acta Crystallogr.*, B26, 352 (1970).
113. C. M. Weeks, W. L. Duax, and Y. Osawa, *Cryst. Struct. Comm.*, 4, 417 (1975).
114. C. M. Weeks, D. C. Rohrer, W. L. Duax, Y. Osawa, and M. Soriano, *Acta Crystallogr.*, B31, 2525 (1975).
115. D. L. Ward, D. H. Templeton, and A. Zalkin, *Acta Crystallogr.*, B29, 2016 (1973).
116. M. Sax, E. Abola, C. S. Yoo, and J. Pletcher, *Acta Crystallogr.*, B29, 2247 (1973).
117. C. M. Weeks, W. L. Duax, and Y. Osawa, *Acta Crystallogr.*, B31, 1502 (1975).
118. D. Rohrer and W. L. Duax, unpublished.
119. K. Utsumi-Oda and H. Koyama, *J. C. S., Perkin II*, 1973, 1866.
120. A. Chiaroni, C. Riche, and C. Pascard-Billy, *Cryst. Struct. Comm.*, 3, 111 (1974).
121. D. S. Jones and I. L. Karle, *Acta Crystallogr.*, B30, 624 (1974).
122. R. A. G. de Graaff and C. Romers, *Acta Crystallogr.*, B30, 2029 (1974).
123. J. Bordner, S. G. Levine, Y. Mazur, and L. R. Morrow, *Cryst. Struct. Comm.*, 2, 59 (1973).
124. J. M. Ohrt, A. Cooper, and D. A. Norton, *Acta Crystallogr.*, B25, 41 (1969).
125. J. M. Ohrt, B. Haner, A. Cooper, and D. A. Norton, *Acta Crystallogr.*, B24, 312 (1968).
126. J. M. Ohrt, A. Cooper, G. Kartha, and D. A. Norton, *Acta Crystallogr.*, B24, 824 (1968).
127. E. M. Gopalakrishna, A. Cooper, and D. A. Norton, *Acta Crystallogr.*, B25, 2473 (1969).
128. H. Worch, E. Hohne, G. Adam, and K. Schreiber, *J. Prakt. Chem.*, 312, 1043 (1970).
129. D. R. Pollard and F. R. Ahmed, *Acta Crystallogr.*, B27, 1976 (1971).
130. A. T. Christensen, unpublished.
131. H. Campsteyn, L. Dupont, and O. Dideberg, *Acta Crystallogr.*, B28, 3032 (1972).
132. E. M. Gopalakrishna, A. Cooper, and D. A. Norton, *Acta Crystallogr.*, B25, 639 (1969).
133. G. I. Birnbaum, *Acta Crystallogr.*, B29, 54 (1973).
134. A. Cooper and D. A. Norton, *Acta Crystallogr.*, B24, 811 (1968).
135. J. P. Declercq, G. Germain, and M. Van Meerssche, *Cryst. Struct. Comm.*, 1, 9 (1972).
136. O. Dideberg, H. Campsteyn, and L. Dupont, *Acta*

- Crystallogr.*, B29, 103 (1973).
137. L. Dupont, O. Dideberg, and H. Campsteyn, *Acta Crystallogr.*, B29, 205 (1973).
138. P. J. Roberts, J. C. Coppola, N. W. Isaacs, and O. Kennard, *J. C. S., Perkin II*, 1973, 774,
139. W. L. Duax and D. A. Norton, *Abstract, ACS Northwest Regional Meeting*, Buffalo, New York, Oct. 1971, No. 208.
140. C. M. Weeks, W. L. Duax, and M. Wolff, *J. Amer. Chem. Soc.*, 95, 2865 (1973); L. Dupont, O. Dideberg, and H. Campsteyn, *Acta Crystallogr.*, B28, 3023 (1972).
141. C. M. Weeks and W. L. Duax, *Acta Crystallogr.*, B29, 2210 (1973).
142. C. M. Weeks, W. L. Duax, and M. E. Wolff, *Acta Crystallogr.*, B30, 2516 (1974).
143. J. P. Declercq, G. Germain, and M. Van Meerssche, *Cryst. Struct. Comm.*, 1, 13 (1972).
144. J. P. Declercq, G. Germain, and M. Van Meerssche, *Cryst. Struct. Comm.*, 1, 59 (1972).
145. W. L. Duax, A. Cooper, and D. A. Norton, *Acta Crystallogr.*, B27, 1 (1971).
146. J. P. Declercq, G. Germain, and M. Van Meerssche, *Cryst. Struct. Comm.*, 1, 5 (1972).
147. G. W. Krakower, B. T. Keeler, and J. Z. Gougoutas, *Tetrahedron Lett.*, 4, 291 (1971).
148. W. L. Duax and H. Hauptman, *J. Amer. Chem. Soc.*, 94, 5467 (1972).
149. A. J. Solo, B. Singh, E. Shefter, and A. Cooper, *Steroids*, 11, 637 (1968).
150. A. T. Christensen and E. Thom, unpublished.
151. E. Thom and A. T. Christensen, *Acta Crystallogr.*, B27, 794 (1971).
152. A. T. Christensen, *Acta Crystallogr.*, B26, 1519 (1970).
153. E. Thom and A. T. Christensen, *Acta Crystallogr.*, B27, 573 (1971).
154. P. B. Braun, J. Hornstra, and J. I. Leenhouts, *Philips Res. Rep.*, 24, 431 (1969).
155. P. B. Braun, J. Hornstra, and J. I. Leenhouts, *Philips Res. Rep.*, 24, 441 (1969).
156. P. B. Braun, J. Hornstra, and J. I. Leenhouts, *Philips Res. Rep.*, 24, 445 (1969).
157. C. Romers, B. Hesper, E. Van Heijkoop, and H. J. Geise, *Acta Crystallogr.*, 20, 363 (1966).
158. J. Guilhem, *Acta Crystallogr.*, B28, 291 (1972).
159. O. Dideberg and L. Dupont, *Acta Crystallogr.*, B28, 3014 (1972); *Cryst. Struct. Comm.*, 1, 99 (1972).
160. W. H. Watson, K. T. Go, and R. H. Purdy, *Acta Crystallogr.*, B29, 199 (1973).
161. H. Campsteyn, L. Dupont, and O. Dideberg, *Acta Crystallogr.*, B29, 1726 (1973).

162. C. Knobler, C. Romers, P. B. Braun, and J. Hornstra, *Acta Crystallogr.*, B28, 2097 (1972).
163. R. W. Kierstead, J. Blount, K. E. Fahrenholtz, A. Farone, R. A. Le Mahiere, and P. Rosen, *J. Org. Chem.*, 35, 4141 (1970).
164. I. Karle and J. Karle, *Acta Crystallogr.*, B25, 428 (1969).
165. I. L. Karle, *Proc. Nat. Acad. Sci., U. S.* 69, 2932 (1972).
166. C. M. Weeks, P. Strong, and W. L. Duax, *Cryst. Struct. Comm.*, 3, 515 (1974).
167. G. Lepicard, J. Delettre, and J. P. Mornon, *Acta Crystallogr.*, B29, 1723 (1973).
168. P. B. Braun, J. Hornstra, C. Knobler, E. W. M. Rutten, and C. Romers, *Acta Crystallogr.*, B29, 463 (1973).
169. C. M. Weeks, unpublished.
170. C. M. Weeks, unpublished.
171. A. Chiaroni, C. Riche, and C. Pascard-Billy, *Cryst. Struct. Comm.*, 3, 115 (1974).
172. H. Campsteyn, L. Dupont, and O. Dideberg, *Acta Crystallogr.*, B30, 90 (1974).
173. O. Dideberg, L. Dupont, and H. Campsteyn, *Acta Crystallogr.*, B30, 702 (1974).
174. H. P. Weber and E. Galantay, *Helv. Chim. Acta*, 57, 187 (1974).
175. L. Dupont, O. Dideberg, and H. Campsteyn, *Acta Crystallogr.*, B30, 514 (1974).
176. C. Romers, R. A. G. de Graaff, F. J. M. Hoogenboom, and E. W. M. Rutten, *Acta Crystallogr.*, B30, 1063 (1974).
177. R. J. Chandross and J. Bordner, *Acta Crystallogr.*, B30, 1581 (1974).
178. O. Dideberg, L. Dupont, and H. Campsteyn, *Acta Crystallogr.*, B30, 2064 (1974).
179. D. Rohrer and W. L. Duax, unpublished.
180. M. Hospital, B. Busetta, R. Bucourt, H. Weintraub, and E. Baulieu, *Mol. Pharmacol.*, 8, 438 (1972).
181. A. Cooper and W. L. Duax, *J. Pharm. Sci.*, 58, 1159 (1969).
182. Y. Osawa, Endocrinology Proceedings of 4th International Congress of Endocrinology, Washington, D. C., 1972, R. O. Scow, Ed., *Excerpta Medica*, Amsterdam, International Congress Series No. 273, p. 814, 1973.

SUBJECT INDEX

Abbreviations used: CONFO = conformation of

LIS = lanthanide induced shift in (or of)

MS = mass spectrum of

- A ring conformation in steroids, 310, 319, 323, 327, 330, 338, 359
 3 β -Acetate conformation, in steroids, 359-361
 2 β -Acetoxy-4-androsten-3-one, 325
 Acetylenes, 26
 Acetylnorbornane, MS, 69
 Adenosine isomers, trifluoroacetylated, MS, 65
 β -Adenosine-3',5'-phosphate, LIS, 177
 Affinity to LSRs, 140
 Agreement factor (R), in LIS, 126, 130, 168, 178, 181, 187, 188
 plot versus torsion angle, 168, 173-175, 180
 Alcohols, aliphatic, LIS, 163
 Aldehydes, α,β -unsaturated, LIS, 162
 Aldrindiol, 97
n-Alkanes, interconversion of conformers in, 204
 rotation in, 204
 Alkoxy radicals, MS, 43, 47
 2-Alkylcyclohexanones, conformational free energy difference in, 184
 Allenes, 1,3-disubstituted, 26
 Amides groups, *cis*, 240
 cis,trans-isomerization of, 200, 256
 trans, rotation, 257
 Amides, rotation in, 200, 256
 tertiary, LIS, 154
 α,β -unsaturated, LIS, 162
 Amines, aliphatic, LIS, 163
 inversion of, 200
 Ammonia, inversion of, 200
 Ammonia type, 15
 Ampère, A., 12
 Androgens, 296, 313
 5 α -Androstan-3,17-dione, 347, 348
 Androstane(s), 57, 290, 318, 330, 349
 Androstenes, 318
 4-Androsten-3-ones, 318, 320, 371
 Annulenes, CONFO, 240
 Appearance potential, 36, 47, 88
 Arago, D., 21
 Aromatic solvent-induced shift, 113
 Arrhenius, S., 2
 ASIS, 113
 Asymmetric carbon atoms, 26
 Asymmetric unit, multiple, 294
 Asymmetry parameters, 284
 Atomic heat rule, 7
 Atomic oscillations, theory of, 20
 Atomic theory, 3
 Atropisomers, MS, 89, 90
 Avogadro, A., 6
 Avogadro's hypothesis, 26
 Averaging of calculated LIS, 127
 Azabicycloalkenes, MS, 95
 6-Aza-bicyclo[3.2.1]octanes, 95
 1-Aza-bicyclo[3.3.3]undecane, CONFO, 263
 Azacycloalkanes, CONFO, 237
 8-Aza-9 β -estrene, 310
 Azetidines, LIS, 155

 B ring conformation, in steroids, 307-309, 334, 335, 339, 345
 Barriers, calculations of, 210
 Baudrimont, A., 11
 Benzaldehyde, elimination of the elements of, 65
 Benzene derivatives, structure of, 19
 Benzo group, annelated, 240
 3 β -Benzoate conformation, in steroids, 360, 361
 Benzocycloheptenes, CONFO, 242

- p*-Benzoquinone, adducts with bi-1-cycloalken-1-yls, MS, 80
- Berthollet, C., 2
- Berthollides, 2, 3
- Berzelius, J., 2
- Bicyclo[4.3.2]deca-2,4,4-trienes, LIS, 156
- 2-Bicyclo[4.3.1]decen-10-one, MS, 49
- Bicyclo[3.1.1]heptane, CONFO, 258
- Bicyclo[3.3.1]nonane, LIS, 179
- Bicyclo[4.2.1]nonane, LIS, 169
- Bicyclo[3.3.1]nonanols, MS, 47
- Bicyclo[6.1.0]nona-2,4,6-triene, conformation of (by LIS), 187
- Bicyclo[2.2.2]octane, CONFO, 263
- Bicyclo[3.3.3]undecane, CONFO, 263
- Bidentate complex, in LIS, 142
- Bidentate Eu(dpm) complex, 168
- Bidentate LSR-substrate complex, 138
- Bigeranyl tetrahydrochloride, conformational change in, 205
- Bile acids, MS, 55
- Binding constant of LSR complex, 144
- Biot's law, 21
- Biot, J., 21
- Bird's eye-view drawing, 203
- Bis-pentamethylene-*s*-tetrathiane, CONFO, 237
- Blomstrand, C., 28
- Boat-boat conformation of *trans*-decalin, 258
- Boat-chair conformation of cyclooctane, 229
- Boat conformation, in *cis*, *syn*, *cis*-perhydrophenanthrene, 260
- in [4.4.4]propellane, 261
- in saturated steroids, 342
- in tricyclo[4.4.4^{1,6}]tetradeca-3,8,12-triene, 263
- of cycloheptene, 242
- of cyclohexane, 200, 328
- of cyclohexene, 242
- of *cis*, *cis*-cycloocta-1,5-diene, 246
- of *cis*, *cis*, *cis*-cyclonona-1,4,7-triene, 249
- Bond angles, in steroids, variation of, 295
- Bond breaking fragmentations, 87
- Bond lengths, average, in steroids, 333, 336, 338-340
- variation of, 295
- Bound chemical shift, 143, 144
- Boyle's law, 6
- Broadening abilities of Gd(III), 135
- Broadening of nmr signals by LSR, 133
- 17 β -Bromoacetoxy-1 β ,2 β (1',1'-dichloro)-ethylene-5 α -androstane-3-one, 286
- 1-Bromo-2,3-dimethylcyclopropane, 87
- 5-Bromo-6 β ,19-epoxy-3 β -hydroxy-5 α -pregnan-20-one, 347
- 6 α -Bromo-17 β -hydroxy-17 α -methyl-4-oxa-androstane-3-one, 291
- 12 α -Bromo-11 β -hydroxyprogesterone, 315
- Bromomirestrol, 310, 311
- 6 β -Bromoprogesterone, 315
- Bunsen, R., 8
- 2,3-Butanedione, 98
- sec*-Butanol, MS, 92
- Butlerov, A., 18
- t*-Butylcyclohexanediol, MS, 52
- 3-*t*-Butylcyclohexanol, MS, 59
- 4-*t*-Butylcyclohexanol, MS, 46, 58, 61
- 4-*t*-Butylcyclohexyl methyl ether, MS, 61
- 4-*t*-Butylcyclohexyl chloride, MS, 61
- 5-*t*-Butylcyclooctanone, CONFO, 232
- C(19)-substituents, CONFO, 365
- Cacodyl, 8
- Caloric, 6
- Camphanediol, LIS, 114
- Cannizzaro, S., 19
- Carbomethoxy group, in MS, 74-77
- Carbon dioxide, elimination of, in MS, 77
- Carbon monoxide, elimination of, in MS, 90
- Carbon tetrabromide, 27
- Carbon tetraiodide, 27
- Carbonium ions, 36
- Carboxylic acids, MS, 71
- Carotenoids, 86
- Chain molecules, 204
- Chair conformation, of cyclohexane, 200, 236
- of cycloheptene, 242
- of *cis*, *cis*-cycloocta-1,5-diene, 247
- of *trans*-decalin, 258
- of [4.4.4]propellane, 262
- of spiro[5.5]undecane, 264
- Charles' law, 6
- Chemical ionization mass spectrometry, 98
- Chemical slide rule, 6
- 3-Chloroalkanoates, MS, 78
- 3-(*p*-Chlorophenyl)-3,5,5-trimethylcyclohexanone, LIS, 150
- Chlorophyll-a dimer, LIS, 188
- N*-Chloropiperidine, CONFO, 237

- 20-Chloro-5 α -pregnane-3 β ,16 β -diol di-*p*-promobenzoate, 348
- Chloroquine, LIS, 176
- 5 β -Cholan-3 α -ol, MS, 53, 56, 57
- 5 β -Cholanic acid, MS, 56
- Cholestan-3-ol, MS, 57
- Cholesterol, 278, 296
- Cholesteryl iodide, structure of, 279
- Circular birefringence, 21
- Circular dichroism, 26
- Circularly polarized light, 26
- Citraconic acid, 27
- Cleavage, in mass spectra, 41
simple, of ions, 39
- Coalescence temperature, 201
- Competition experiments in LIS, 140
- Complex binding constants, 183, 184
- Complex species, lanthanide, 143
- Complexation constant for LSR's, 139, 140, 143
- Complexes of 1,4,7,10-tetraoxacyclododecane, 218
- Complexing abilities of functionalities, LIS, 140
- Composition, definition of, 274
- Computer program, CHEMSHIFT, 125
LISHIFT, 125
MSEARCH, 178
PDIGM, 124, 168, 172, 181
PSEUDO, 125, 181
- Confidence level, 128
- Configuration, absolute, correlation of, by LIS, 154
definition of, 274
- cis,trans* configuration exchange between amide groups, 256
- Conformation, 203
by LIS analysis, 125, 130
definition of, 274
"ideal," 284
inverted, 203
molecular, 280
of acetylenic C₄ unit, 238
of *cis* double bond, 239
of *trans* double bond, 250
of steroids with bulky substituents, 289
pseudorotated, 203
s-cis, 163
s-trans, 163
- Conformational analysis, by LIS, 125, 158
- Conformational averaging, in MS, 37, 183
- Conformational change, caused by LSR, 158
in the solid state, 205
- Conformational dependence, of mass spectra, 42-44
- Conformational energy, 130
- Conformational energy minimum, 203
- Conformational equilibria, analysis of, by LIS, 160
- Conformational flexibility, 276, 280
in steroids, 342, 345, 374
- Conformational free-energy differences, by LIS, 183
- Conformational isomers, in crystals, 294, 359
- Conformational transmission, 277, 305, 374, 375
- Conformer, 203
a,a, 204
a,g⁺, 204
a,g⁻, 204
g⁺,a, 204
g⁺,g⁻, 204, 205
- Constitution, definition of, 274
- Contact interaction of lanthanide ions, 135
- Contact shift, 115, 117, 120, 123
- Coordination compounds, 28
- Correlation coefficients, 126
- Corticoids, 296, 313
- Cortisol, 291, 317, 323
- Cortisone, 291, 317
- Cortisone acetate, 317
- Cosmic dissymmetry, 22
- Couper, S., 1
- Coupling constants, 154
in conformational analysis, 179
in LSR-substrate complexes, 158
- Crown conformation, of cyclodecane, 223
of *cis,cis,cis*-cyclonona-1,4,7-triene, 249, 250
of cyclotetraeratriylene, 248
of cyclotrimeratriylene, 249
of *trans,trans*-cyclodeca-1,5-diene, 252
of *trans*-cyclodecene, 255
of *cis,trans,cis,trans*-cyclododeca-1,4,7,10-tetraene, 255
- Crum Brown, A., 2
- Crystal conformer, irreversible conversion of, 202
- Crystal packing, 366, 375
in steroids, 289, 366, 371
in steroid 17 β -acetates, 358

- in steroid 17 β -benzoates, 358
- Crystallographic disagreement factor, 126
- Crystallography, 10
- Cyclic tetrapeptides, conformation of, 255
- Cyclobutane, folding of ring in, 180
 - ring inversion in, 200
 - LIS structure of, 180
- Cyclobut-1-ene-3,4-dicarboxylic acids, 86
- Cyclodeca-1,5-diene, CONFO, 252
- Cyclodeca-1,6-diene, CONFO, 242, 243
- Cyclodecane, CONFO, 221
- Cyclodecanone, CONFO, 223
- Cyclodecene, CONFO, 253
- Cyclodecen-5-yl *p*-nitrobenzoate, crystal structure of, 254
- Cyclododecane, CONFO, 217
 - gem-dimethyl substituted, 218
- Cyclododecanone, CONFO, 219
- Cyclododeca-1,4,7,10-tetraene, CONFO, 248, 255
- Cyclododeca-1,5,9-triene, CONFO, 244, 245, 251
- Cycloglycylpropylglycylpropyl, CONFO, 257
- Cycloglycylsarcosylglycylsarcosyl, CONFO, 256
- Cycloglycyltrisarcosyl, CONFO, 256
- Cycloheptane, CONFO, 233
- Cycloheptene, CONFO, 240-242
- Cyclohexadecane, CONFO, 209
- Cyclohexa-1,4-diene, CONFO, 240
- Cyclohexane, CONFO, 236
 - ring inversion in, 200
 - substituted, equilibrium constant by LIS, 186
- 1,4-Cyclohexanediol, MS, 45, 51, 64
- Cyclohexanols, MS, 45, 46, 50
 - LIS, 138, 170, 171, 183
- Cyclohexanones, CONFO, 182
 - LIS, 170
- Cyclohexene, CONFO, 242
 - MS, 84
- Cyclohexyl chloride, MS, 61
- Cyclohexyl methyl ether, MS, 61
- Cyclononane, CONFO, 225
- Cyclononanone, CONFO, 228
- Cyclonona-1,4,7-triene, CONFO, 248, 249
- Cyclonona-1,4,7-trien-3-one, CONFO, 250
- Cyclooctadecane, CONFO, 207
- Cycloocta-1,5-diene, CONFO, 240, 246
- Cyclooctane, CONFO, 229
- Cyclooctane-1,5-diene, 233
- Cyclooctanone, CONFO, 232
- Cyclooctene, CONFO, 240
- Cyclooctene oxide, CONFO, 241
- Cyclopentadecane, 213
- Cyclopentane, CONFO, 237
 - conformational change in, 200, 201
- Cyclopentene, CONFO, 240
- Cyclotetradeca-1,8-diyne, CONFO, 238
- Cyclotetradecane, CONFO, 213
- Cyclotetrasarcosyl, CONFO, 256
- Cyclotetraveratrylene, CONFO, 248
- Cyclotridecane, CONFO, 215
- Cyclotrimeratrylene, CONFO, 249
- Cycloundecane, CONFO, 219
- Cycloundecanone, CONFO, 220, 223
- Cycloundeca-1,4,8-triene, CONFO, 252
- D ring conformation, in steroids, 349-351
- Dalton, J., 3
- Daltonides, 3
- Davy, H., 6
- Decalin, 258
 - framework, 64
 - olefins derived from, MS, 85
- 1,4-Decalindiol, MS, 62
- 1,5-Decalindiol, MS, 64
- Demarcation criterion, 23
- "Derived nuclei," 13
- Dessaigues, V., 23
- Deuterium labeling, in MS, 41
- "dfhd," 139
- Diamagnetic component to LIS, 114
- Diamagnetic shift, 123
- Diamond-lattice conformation, of cyclo-decane, 221
 - of cyclododecane, 217
 - of cyclooctadecane, 207
 - of cyclooctane, 229
 - of cyclotetradecane, 213
- Diastereoisomers, 22
 - assignment of configuration by LIS, 155
- Diastereotopic hydrogens, MS, 42
- Dibenzoycycloocta-1,5-diene, CONFO, 247
- 1,1-Dibromo-2,3-dimethylcyclopropane, 87
- Dicarboxylic acids, MS, 77
- Diels Alder reaction, 82
- 1,4-Diene-3-one steroids, 326, 327
- Diethyl ether, 12
- Diethylamine, LIS, 114
- 3,4-Diethylmuconates, MS, 76
- Diethylstilbesterol, 310, 311

- 3,3-Difluorocyclodecene, 254
2,2-Difluorodecalin, CONFO, 259
3,3-Difluoro[4.4.4] propellane, CONFO, 262
Dihydrotestosterone, 345
17 α ,21-Dihydroxyprogesterone, 317, 351
Dimerization of LSR, 134
Dimethoxybenzene, LIS, 141
1,3-Dimethoxycyclohexane, MS, 62
1,4-Dimethoxycyclohexane, MS, 62
1,4-Dimethoxydecalin, MS, 62
1,5-Dimethoxydecalin, MS, 64
N,N-Dimethylamides, barrier to rotation, 161
4,4-Dimethylandrostan-6-one, MS, 70
3,3-Dimethyl-1-butanol, 160
1,5-Dimethylcyclodeca-1,5-diene, CONFO, 253
1,1-Dimethylcyclodecane, CONFO, 224
1,1-Dimethylcycloheptane, CONFO, 234
1,1-Dimethylcyclononane, CONFO, 229
1,1-Dimethylcyclotetradecane, CONFO, 215
3,3-Dimethylthietane-1-oxide, LIS, 122
4,9-Dioxacyclodeca-1,6-diene, CONFO, 243
1,3-Dioxacyclooctane, CONFO, 232
1,5-Dioxacyclooctane, CONFO, 233
Dioxaphosphoranes, LIS, 160
2,4-Dioxaspiro[5.5] undecane, CONFO, 264
Diphenylsulfines, LIS, 159
Dipolar shift, *see* Pseudo-contact shift
Dipolar shift mechanism, 112
Dipyrromethenes, LIS, 142
Disalicyclides, cyclic, 247
Disrotatory ring opening, 87
Dissymmetry, 22
Distance relationship of LIS, 132
Distorted chairs, 286, 333
Diterpene epimers, elimination in, MS, 58, 59
4,9-Dithiacyclodeca-1,6-diene, CONFO, 243
DNMR (dynamic nmr spectroscopy), 201, 202
Double bonds, under electron impact, 76
DPM, 137
Drawing, bird's-eye view, 203
 perspective, 203
 side view, 203
 wedge type, 203
Dreiding models, 124
Dulong, P., 7
Dumas, J., 7
Duppa, B., 23
Eclipsing interactions, 42
Electrochemical series, 6
Electrochemical theory, 6
Electrochemistry, 10
Electrocyclic process, MS, 86
 concerted, 82
Elimination, *cis*, MS, 43
 of methanol, MS, 61
Enantiomorph, 21
Energy of activation, MS, 87
5-Enes, CONFO, 328, 332, 334, 335
Envelope conformation, 201, 282, 349
Epiaschantin, LIS, 179
Epitestosterone, 276
Epoxides, LIS, 175
Equilibrium binding constant, 144
Equilibrium constants, by LIS, 184
Equivalent weights, 7
Error function, 126
Esters, α,β -unsaturated, LIS, 162
Estradiol, 311
Estrane, 330, 349
Estratriene, conformational flexibility in, 302
 conformational transmission in, 305
 relative conformation of, 304
 substituent effects in, 309
1,3,5(10)-Estratriene, 290, 302, 303, 305, 312, 317, 330, 340, 374
1,3,5(10)-Estratriene, Δ^4 -3-ones, 333
8 α -Estrene, CONFO, 310-312
9 β -Estrene, CONFO, 312
5(10)-Estrenes, 310
4-Estren-3-ones, 320, 321
Estrogens, 296
Estrone, crystal forms of, 290, 292
Ethane, 1,2-disubstituted, rotation in, 200
Ethanol, LIS, 114
Ethyl alcohol, 12
"Ethylidene lactic acid," 24
Eu(dfhd)₃, 139
Eu(dpm)₃, 111, 112, 114, 121, 136, 140, 141, 148, 157, 163, 168, 170, 179, 187
Eu(fod)₃, 135, 136, 142, 148, 159, 187
"Facam," 139

- Fermi contact shift, *see* Contact shift
 Ferrocene derivative, LIS, 128
 Field desorption mass spectrometry, 52
 Field ionization kinetics, 84
 Flexibility of steroid structures, 309
 Fluorinated LSR, 136
 9 α -Fluorocortisol, 324
 1-Fluorocyclooctene, CONFO, 241
 3-Fluoropyridine-Eu(dpm)₃, contact shifts in, 119
 FOD, 137
 2-Formylfuran, LIS, 166
 Formylnorbornane, MS, 69
 2-Formylpyrrole, LIS, 166
 2-Formylthiophene, LIS, 166
 Fragment ion, 40
 Fragmentation, activation energy for, 39
 Frankland, E., 8
 Free energies of activation in complexes, 161
 Fresnel, A., 21
 Fumaric acid, 24
 "Fundamental nuclei," 13
- Gas laws, 3
 Gaudin, M., 12
 Gay-Lussac, J., 6
 Gem dimethyl substitution, in MS, 50
 Geminal exchange, 208, 213-215, 220, 224, 228, 230, 231, 233, 235, 236, 238, 247, 249, 250, 252, 254, 258, 262
 Geometric factors, in dipolar shift equation, 116
 Geometry optimization, by LIS, 131
 Gerhardt, C., 10
 Germacatriene, crystal conformation of, 252
 Gibberellins, MS, 72
 Glucocorticoid, 375
 activity, 325
 Graphic formula, 18
 Graphical methods for determination of LIS, 143, 145, 146, 151
- H-bonded hydroxyl groups, in MS, 98
 Half-chair conformation, 282, 283, 304, 307, 315-318, 321, 322, 328, 333, 334, 349
 of cyclohexene, 242
 Halogen substitution, 11
 Hamilton agreement factor, 126
 Häüy, R., 10
- Helix conformation, 245, 246
 Hemihedral faces, 21
 Herschel, J., 22
 Hetero-analogs of dibenzocycloocta-1,5-diene, CONFO, 247
 Heterocycles, MS, 95
 Heterosubstitution in steroids, 337
 Hexagon representation, 14
 $\Delta^{2,6}$ -Hexalin, CONFO, 261
 $\Delta^{2,6}$ -Hexalins, 9,10-disubstituted, CONFO, 261
n-Hexanol, LIS, 112
 1,4,7,10,13,16-Hexaoxacyclooctadecane, 208, 209
 2,5,7,10,11,14-Hexaoxa[4.4.4] propellane, CONFO, 262
 High resolution mass spectrometry, 73
 Highest occupied molecular orbital (HOMO), 86
 Hodgkin packing notation, 289, 358, 363, 366
 Ho(dpm)₃, 121
 Hofmann, A., 15
 HSAB theory, 140
 Humulene, CONFO, 252
 Hydrocarbons, MS, 91
 diastereomers in, MS, 88
 Hydrogen bonding, MS, 58
 directional specificity of, 372
 in steroids, 289, 373, 375
 Hydrogen scrambling, in MS of cyclohexene, 84
 Hydrophobic nature of molecular surfaces, 289
 Hydrophilic nature of molecular surfaces, 289
 17 β -Hydroxy-5 α -androstan-3-one, 345, 347
 3 α (and 6 α)-Hydroxy-5 β -cholanic acid, MS, 56
 4-Hydroxycyclohexyl bromide, MS, 99
 14-Hydroxy-D-homoestrones, MS, 53
 11-Hydroxyprogesterone, MS, 54
 16-Hydroxyprogesterone, MS, 54
 17 α -Hydroxyprogesterone, 317
 21-Hydroxyprogesterone, 317
 3 β -Hydroxy-20-thia-17 α (and β)-5-pregnene oxides, MS, 97
- Intermolecular contacts, 371
 Internal energy, of ion, 39
 Intraannular group, 215

- Intramolecular hydrogen transfer, MS, 43
Intrinsic LIS parameters, 143
 absolute values of, 151
Inversion, 203, 208, 209, 225, 261
 at nitrogen, in amines, 200
 in ammonia, 200
 in azacycloalkanes, 237
Ion cyclotron resonance, 98
Ion intensity and kinetics, 38
Ionization potential, 39
 of stereoisomers, 88, 89
 α -Ionones, MS, 79
de l'Isle, R., 10
Isoestrones, MS, 53
Isomorphism, 366
4-Isopropylcyclohexanol, MS, 51
Isoquinoline, contact shift in, 135
 Lis, 120

Japp, F., 28
"Job plot," 149, 150
Jørgensen, S., 28

Karlsruhe congress, 19
Kekulé, A., 1, 14
Keto compounds, α,β -unsaturated, LIS, 162
Ketones, α,β -unsaturated, LIS, 162
Kinetic energy release, MS, 86
Kolbe, H., 8
Körner, W., 19

 β -Lactams, stereoisomeric, MS, 94
Lactic acid, 24
Ladenburg, A., 20
La(dpm)₃, 114
Lanostenone, 277
Lanthanide complex equilibrium, 144
Lanthanide complex stoichiometry, 148, 149
Lanthanide induced shift value, definition of, 113
Lanthanide induced shifts, 112
 averaging of, 128, 170, 174
 parameters in, 143, 147, 151
Lanthanide shift reagents, 112, 133
 as hard acids, 140
 dimerization of, 134
 fluorinated, 136
 Lewis acidity of, 136
(LAOCN-3), 158
Laurent, A., 10

Lavoisier, A., 6
Law of combining volumes, 6
Law of isomorphism, 7
Law of partial pressures, 6
Le Bel, J., 1
Liebig, J., 3
Ligands used in LSR, 135
"Limiting" shifts, 143, 144
Line broadening, 178
LIS, *see* Lanthanide induced shift
LSR, *see* Lanthanide shift reagent
Lu(dpm)₃, 122

Magnetic axes, orientation of, 131
Maleic acid, 24
Malus, E., 21
Marsh-gas type, 16
Matridine, MS, 97
McConnell-Robertson equation, 116, 132, 162, 186
McLafferty rearrangement, 68, 70
Melsens, L., 12
Mercuric chloride complex of cyclononane, 228
Mesaconic acid, 27
Mesityl oxide, LIS, 163
Metastable ions, 41, 86, 92
Methanol, elimination of the elements of, MS, 71, 75
3-Methoxy-17-alkyl- $\Delta^{1,3,5,10}$ -D-homoelestatetraen-17-ol, MS, 58
Methoxybenzene, LIS, 141
4-Methoxy-3-*t*-butylcyclohexanol, MS, 50
Methyl bacteriopheophorbide a, 188
Methyl-20-conanine, MS, 93, 94
1-Methylcyclohexanol, conformational equilibrium in, 160, 183
4-Methylcyclohexanol, MS, 50
Methyl octadec-2-enoate, MS, 79
Methyl pheophorbide a, 188
6 α -Methylprednisolone, 291, 294, 324
Meyer, L., 19
Meyerson-Weitkamp hypothesis, 87-90
Minimum agreement factor, 130
Mitscherlich, E., 7
Molecular conformation, *see* Conformation
Molecular dissymmetry, 2
Molecular ion intensity, 39, 57, 60, 87
Molecular ion structure, 38
Molecular magnetic susceptibilities, 116
Morphine, MS, 96

- Multiple asymmetric unit, 294
Multiple complexation, 141
Multiple proportions, law of, 3, 4
- Naphthalene, 12
Newman projection, 203
Newton, I., 6
N-nitrosopiperidines, equilibrium constants for, 186
NMR signals, automatic sorting of, 154
NMR spectroscopy, dynamic, 201, 202
static, 201
Norborneal, MS, 91
Norbornyl bromide, MS, 91
Norbornyl cation, MS, 91
Nuclear Overhauser effect (NOE), 112
- Octahedral geometry, 28
Odling, W., 14
Olefinic carbonyl compounds under electron impact, 76
Olefins, unfunctionalized, MS, 80
1,2-disubstituted, 26
9 β ,10 α - Δ^4 -3-one, CONFO, 325
 Δ^4 -3-One 2 β -acetate structures, 324
One-step model in LIS, 147
 Δ^4 -3-Ones, conformational flexibility in, 313
conformational transmission in, 318
substituent effects in, 321, 323
Optical activity, 21
Optical purity of enantiomers, by LIS, 154
Orbital geometries, in MS, 92
Orbital symmetry arguments, in MS, 86
Organometalloid compounds, 8
Ostwald, W., 2
3-Oxacyclonona-1,4,7-triene, CONFO, 250
Oxacyclooctane, CONFO, 232
Oxetane, LIS, 181
Oximes, LIS, 156
Oxindole alkaloids, MS, 95
- Packing, *see* Crystal packing
Packing notation, *see* Hodgkin packing notation
Paramagnetic shift, 113, 117
Pasteur, L., 2, 22
Pattern recognition, 68
Pentane, CONFO, 204
2-Pentanol, MS, 42
2-Pentyl chloride, MS, 42
- Perhydroanthracene, CONFO, 259, 260
Perkin, W., 23
Perspective drawing, 203
Petit, A., 7
Phenyltetralins, MS, 97
Photoelectron spectroscopy, 39
Photoionization, 46
Phthalic acid, MS, 78
Piperidines, CONFO, 161
Piperidinone, CONFO, 237
Plot method (S_0 vs. $1/\Delta$), 146
Polyether complexes, 208
Polyfunctional molecules, LIS, 141, 143
Polygon representation, 14
Polymorphic forms, 294, 366
Population ratio, determined by LIS, 163
Pr(dpm)₃, 170, 177
1,4-Pregnadienes, 371
Pregnane, 291, 318, 330, 336, 349
5 α -Pregnanes substituted with hydroxyl and amino groups in ring A, MS, 98
5 α , 17 α -Pregnane-3 β , 20 α -diol, 348
Pregnane- Δ^4 -3-one, 291
Pregnane-20-one, CONFO, 288
Pregnenes, 318
4-Pregnen-3-ones, 318, 320, 371
Pr(fod)₃, 135, 163
Principal magnetic axis, 122
"effective," 122
Principle of inertia, 16
Principle of minimum structural change, 16
Principle of unripe time, 1
Progesterone, 317
Progestins, 288, 296, 313
[4.4.4] Propellane, CONFO, 261
Propeller conformation, 245, 246, 265
Proust, J., 3
de la Provostaye, F., 22
Pseudo-contact shift, 115, 121, 135
Pseudo-rotation parameters, 281
Pseudo-torsion angle, 280
Pseudorotation, 201, 203, 208, 209, 213, 225, 234, 247, 249
in boat-cycloheptane, 235
in cyclopentane, 237
in twist cyclohexane, 237
Puckering, in thietane-1-oxide, 181
of oxetanes, 182
Pyridine, LIS, 114, 118, 120, 127
Pyrrolinones, LIS, 156
Pyrromethanes, LIS, 172

- Pyromethenones, LIS, 172
- Quartz, 21
- Quinoline, MS, 95
LIS, 120
- R-factor, 126
ratio table, 129
- Racemic acid, 22
- Radical theory, 9
- Radicals, organic, 7
- Rational formulae, 17
- RDA fragment ions, *see* Retro-Diels-Alder reaction
- RDA reaction, *see* Retro-Diels Alder reaction
- Rearrangement in MS, 41
- Rearrangement fragmentation, 39
- Rearrangement loss of formaldehyde, 62
- Rearrangement reactions, MS, 87
- Regioselectivity in MS, 45
- Relaxation reagents, 112, 135
- Reliability factor, 126
diagram, 130
- Reliability of hypotheses, 128
- Resonance, assignment by LIS, 154
- Retro-Diels Alder reaction, 79, 83
fragment ions, 84
- Retro-steroids, 296
- Robinson, R., 2
- Rose, H., 8
- Rotation of *trans* double bond, 250
- Saccharide stereoisomers, 68
- Saccharides, derivatized, MS, 65
- Sarcosine cyclic tripeptide, CONFO, 250
- Scaling of calculated LIS values, 125
- Secondary isotope effect, LIS, 154
- Shifting power of lanthanide ions, 133
- Side chain conformations in steroids, 352-354
- Side-view drawing, 203
- Significance testing, 126, 129, 157, 174
- Silyloxy group, 65
- Simpson, M., 23
- Site exchange, full, 202
partial, 202
- Sofa conformation, 283, 304, 307, 315-318, 321, 322, 328, 330, 335, 351
of cyclotraveratrylene, 248
- Solid state, conformational change in, 205
- Solubility of LSR, 139
- Spin-spin couplings in presence of LSR, 113
- Spiro[5.5]undecane, CONFO, 264
- Square-planar geometry, 28
- Standard deviation of the mean, estimation of, 302
- Statistical in significance testing, *see* Significance testing
- Stereoselectivity, in MS, 42, 44
- Stereospecific *cis* requirement in fragmentation, 82
- Steroid alcohols, MS of, 53
diols, MS, 57
 Δ^{16} , MS, 92
function, 272
nomenclature, 277
- Steroidal 17β -acetates, 354, 358
 17β -benzoates, 354, 358, 359
olefins, MS, 84
- Steroids, conformation (overall) of, 287
crystal packing in, 289, 366, 377
crystal structures, list of, 295-302
hydrogen bonding in, 289, 371
saturated, MS, 97
boat conformation in, 342
conformations of, 330
twist conformation in, 331
- Stoichiometry, 3
of binding to LSR's, 143
of LSR complexes, 134, 148, 149
- Strain energies, calculations of, 202
- Succinic acid, 23, 24
- Symmetry, loss of by distillation, 333
of rings, 281-283
- Tartaric acid, 21-23
- Terpene alcohols, MS, 59
- Terpenes, LIS, 174
- Testosterone, 276, 315, 316, 321
- 2,4,6,8-Tetrabromocyclooctane, 1,5-dione, CONFO, 233
- 1,2,3,6-Tetrahydrophthalic anhydrides, MS, 90
- Tetralin, MS, 84
- 1,1,6,6-Tetramethylcyclodecane, CONFO, 224
- 1,1,4,4-Tetramethylcycloheptane, CONFO, 234
- 1,1,4,4-Tetramethylcyclononane, CONFO, 229
- 1,1,4,4-Tetramethylcyclotetradecane,

- CONFO, 215
- 1,1,5,5-Tetramethylcyclotetradecane, CONFO, 215
- 1,1,8,8-Tetramethylcyclotetradecane, CONFO, 215
- 1,1,4,4-Tetramethylcycloundecane, CONFO, 221
- 2,2,7,7-Tetramethoxydecalin, CONFO, 259
- 2,2,6,6-Tetramethoxyperhydroanthracene, CONFO, 260
- 1,4,7,10-Tetraoxacyclododecane, CONFO, 218
- Tetraoxacyclohexadecanes, CONFO, 209
- 1,3,9,11-Tetraoxacyclohexadecane, CONFO, 212
- 1,5,9,13-Tetraoxacyclohexadecane, CONFO, 212
- 1,3,5,7-Tetraoxacyclooctane, CONFO, 233
- Tetraphenylborate, 140
- Theory of types, 10
- Thietane-1-oxide, LIS, 181
- Torsion angle, average, in steroids, 333, 337-340
sign of, 203
- Torsional barrier, 203
- N-tosyl-3-aza-7-carbomethoxybicyclo-[3.3.1]-nonane, 97
- Triarylboranes, CONFO, 265
- Triarylcarbonium ions, CONFO, 265
- Triarylgermanes, CONFO, 265
- Triarylmethanes, CONFO, 265
- Triarylsilanes, CONFO, 265
- Tribenzocyclonona-1,4,7-triene, CONFO, 249
- Trichloroacetic acid, 12
- Tricyclo[4.4.4.0^{1,6}]tetradecane, CONFO, 261
- Tricyclo[4.4.4.0^{1,6}]tetradeca-3,8,12-triene, CONFO, 262
- Tridentate complex, in LIS, 142
- Trigonal prism benzene structure, 20
- 3 β ,12,17 β -Trihydroxy-5 α -androstane, MS, 56
- 1,3,5-Trimethoxycyclohexanes, MS, 62
- Trimethylcarbamate, barrier to rotation, 161
- Trimethylene sulfite, CONFO, 180
- 4-,Trimethylsiloxyhexyl benzyl ether, MS, 65
- 1,4,7-Trioxacyclononane, CONFO, 228
- Trisalicylides, cyclic, 246
- Triscyclopentadienyl(cyclohexylisonitrile)-praseodymium-(III), 185
- Tris(3,6-dimethylbenzo)-cyclodeca-1,5,9-triene, CONFO, 245
- Tris-3,6-dimethylsalicylide, 246
- Tris(dipivalomethanato)europium(III), *see* Eu(dpm)₃
- Tris(dipivalomethanato)lanthanum, *see* La(dpm)₃
- Twist-boat conformation, 201
of cyclohexane, 236
of cycloheptane, 235
of cycloheptene, 242
of *cis,cis*-cycloocta-1,5-diene, 247
- Twist-boat-chair conformation of cyclooctane, 229
- Twist-chair-chair conformation of cyclooctane, 231
- Twist-chair conformation of cycloheptane, 234
- Twist conformation, 283, 328, 334
in saturated steroids, 342
- Twist-envelope conformation, 201
of cyclopentane, 237
- Twist form of *cis,cis,cis*-cyclonona-1,4,7-trien-3-one, 250
- Twist-twist conformation of *trans*-decalin, 258
- Two-step mechanism in LIS, 149, 150
- Type theory, new, 15
- α,β -Unsaturated esters, MS, 78
- Valency angles, average, in steroids, 333, 337-340
- van't Hoff, J., 1
- Vapor densities, 12
- N-vinyl-1-pyrrolidone, LIS, 168
- Vitalism, 24
- Water type, 15
- Wedge-type drawing, 203
- Weighing factors, LIS, 126
- Werner, A., 28
- Williamson, A., 15
- Wislicenus, J., 24
- Wöhler, F., 8
- Wollaston, W., 5
- Woodward-Hoffmann rules, in MS, 86
- Wurtz, C., 15

- Xanthones, LIS, 168
X-ray crystal structure studies, 278
X-ray structure of LSR-substrate complexes, 121
Yb(dpm)₃, 119, 121, 163
Zinc alkyls, 8